TU Delft

Delft University of Technology

Integrated transport and energy systems based on hydrogen and fuel cell electric vehicles

Oldenbroek, V.D.W.M.

DOI
10.4233/uuid:f8f6566e-e50a-47e2-b1f9-67503ca1d021

Publication date
2021

Document Version
Final published version

Citation (APA)
Oldenbroek, V. D. W. M. (2021). *Integrated transport and energy systems based on hydrogen and fuel cell electric vehicles*. [Dissertation (TU Delft), Delft University of Technology].
https://doi.org/10.4233/uuid:f8f6566e-e50a-47e2-b1f9-67503ca1d021

Important note
To cite this publication, please use the final published version (if applicable).
Please check the document version above.

Copyright
Other than for strictly personal use, it is not permitted to download, forward or distribute the text or part of it, without the consent of the author(s) and/or copyright holder(s), unless the work is under an open content license such as Creative Commons.

Takedown policy
Please contact us and provide details if you believe this document breaches copyrights.
We will remove access to the work immediately and investigate your claim.

This work is downloaded from Delft University of Technology.
For technical reasons the number of authors shown on this cover page is limited to a maximum of 10.

Integrated transport and energy systems based on hydrogen and fuel cell electric vehicles

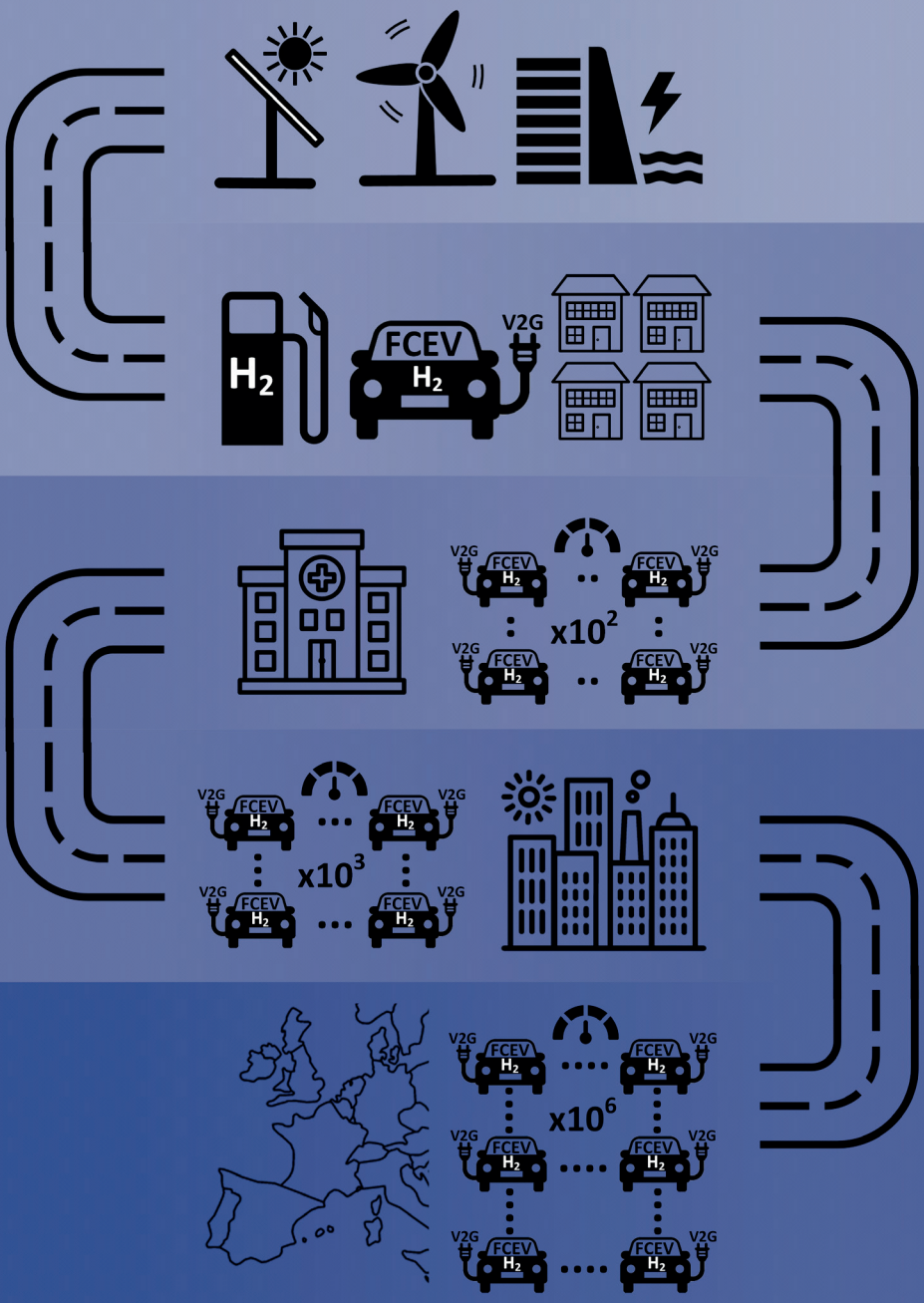

Vincent D.W.M.Oldenbroek

Integrated transport and energy systems based on hydrogen and fuel cell electric vehicles

Dissertation

for the purpose of obtaining the degree of doctor at
Delft University of Technology
by the authority of the Rector Magnificus Prof.dr.ir. T.H.J.J. van der Hagen,
chair of the Board for Doctorates
to be defended publicly on
Monday 4th October 2021 at 12:30 o'clock

by

Vincent Dirk Wichard Michiel OLDENBROEK
Master of Science in Mechanical Engineering, Delft University of Technology, the Netherlands
born in Kampen, the Netherlands

This dissertation has been approved by the promotors.

Composition of the doctoral committee:

Rector Magnificus,	chairperson
Prof. dr. A.J.M. van Wijk	Delft University of Technology, promotor
Prof. dr. K. Blok	Delft University of Technology, promotor
Prof. dr. A. Purushothaman Vellayani	University of Groningen / Delft University of Technology, promotor

Independent members:

Prof. dr. ir. Z. Lukszo	Delft University of Technology
Prof. dr. ir. D.M.J. Smeulders	Eindhoven University of Technology
Prof. dr. P. Leone	Politecnico di Torino, Italy
Prof. dr. K. Hirose	Kyushu University, Japan
Prof. dr. ir. S.A. Klein	Delft University of Technology, reserve member

TU Delft Delft University of Technology

NWO Nederlandse Organisatie voor Wetenschappelijk Onderzoek

Keywords: vehicle-to-grid, hydrogen, fuel cell electric vehicles, integrated transport and energy systems, techno-economic scenario modelling
Printed by: Gildeprint
Cover by: Vincent Dirk Wichard Michiel OLDENBROEK
Copyright © 2021 by Vincent Dirk Wichard Michiel OLDENBROEK
ISBN 978-94-6384-241-9
An electronic copy of this dissertation is available at http://repository.tudelft.nl/.

Acknowledgements

My PhD research program allowed me to explore and learn a tremendous amount of the so-called green and upcoming hydrogen economy, both from a technical, theoretical, economical, experimental and networking point of view. Also personally it challenged and confronted me from various angles. How to explore unknown territories, motivating and coaching students, keeping myself motivated, turning thoughts and results into academic texts, planning and (underestimating) workload. I value much testing ideas, as ideas itself are only stories but testing or executing them is what has value. During the PhD work I have seen that to test and start executing too many ideas, can result into an ever-growing workload and not finishing in time. “Kill your darlings” as once was taught in a writing course, should be also applied in testing ideas, even when successful sometimes should be stopped. Nevertheless, even though it took several years longer than expected, I am grateful for the opportunity.

This process of course would not be possible without the help of my first promotor, Professor Ad van Wijk. I was privileged to have him as my promotor and I would like to express my sincere gratitude to him. Always questioning on what fundamentals costs were based, be visionary, or just accept that others might think differently or call you overly optimistic. Also, I would like to thank him in sharing the same enthusiasm about new ideas, giving a lot of freedom, confidence and autonomy.

I would also like to thank my second promotor, Professor Kornelis Blok for all his help and guidance for finishing the thesis. Especially of improving the academic level of Chapter 7 and pushing me to improve it further and to convince publishing it, the last mile is definitely the longest. Nevertheless, it always feels very satisfying when a publication comes available online.

Also I would like to thank Professor Aravind to give me the opportunity to set-up an experiment with a single cell fuel cell, even though the results were not fruitful, it was an invaluable experience. Also without the help from Martijn Karsten, Michel van den Brink and Jaap van Raamt the set-up could not have been made safely.

Writing the first paper was hard and I would like to thank Leendert Verhoef for his time and joint writing sessions and patience for the endless revisions.

The Car as Power Plant multi-disciplinary research group and consortium partners, Shell, GasTerra, Stedin, Eneco, Q-Park, BAM, HyTruck, The Green Village made the project really lively and generated a lot of fruitful discussions and insights. I would like to thank in particular, Professor Zofia Lukszo, Professor Bart de Schutter, Professor Nathan van de Wouw, Carla, Samira, Rishabh, Reinier, Esther, Farid, Jaco, Henneke, Rene, Serge, Jaron, Willie and Aad for their kindness, help, collaboration, improving the English summary, joint experiments and publications.

Within this project many things have been tried and ideas explored. Some things also did not work out or parts which were not published because the lack of time. Nevertheless, often the things which did not work out, helped creating new insights or made conclusions firmer. Without the help and dedication of the

students Victor Hamoen, Samrudh Alva, Gilbert Smink, Tijmen Salet, Lennart Nordin, Siebren Wijtzes.

The experiments with the Hyundai FCEV and tracking of data from 3 other similar cars were really exciting. I would like to thank in particular Hub Cox, by then working at Rijkswaterstaat, to have introduced me to Menno Merts from HAN University of Applied Sciences who managed to get all the data out of the cars. Without the introduction by Hub and Menno's expertise, the experiments would never have generated the amount of data and insights gained. This showed me again that building up a network and discussing problems is essential. Sharing the data of the 3 other cars, the physical V2G setup and modifications to the car would not have been possible without the help of Ryu Chang Seok from Hyundai Motor Company, Frank Meijer and Soongil Kweon from Hyundai Motor Europe, Marco de Vos and John Luinen from Hyundai Motor Netherlands, Oriental Precision Industry, RDW, John and Martin Seiffers from Accenda, Bram Veenhuizen, Leo Buning, and Ben Pyman from HAN University of Applied Sciences, The Green Village – TU Delft and Peter Swart from the Gemeente Arnhem.

The designed systems and simulations rely on a lot of data which is not always easily and freely accessible. Without reliable data, results and conclusions become weak. I would like to thank in particular the following organizations for providing data and insights into their own modeling work, Reinier de Graaf Gasthuis, Energica b.v., SMAT S.p.A. di Collegno, Agencia Estatal de Meteorología (AEMET), Agora Energiewende, Dansk Energistyrelsen, Fraunhofer-Institut für Solare Energiesysteme ISE.

The last mile is often the longest one says, but the Dutch translation of the summary and propositions was an unexpected mile, that being Dutch. Over the years my written Dutch got rusty and I barely used it since high school, apart for some communication. Special thanks to Jaap, Lex, Tjeerd, Janneke, Martine, Berry, Eric to highlight the 'rusty' parts in the translations and providing proper Dutch suggestions.

Apart from all the work and direct colleagues, the department had a great amount of other PhDs and Post-docs working on other topics, but who contributed greatly to the working atmosphere, from coffees, to lunches, soccer games, borrels, parties, thanks a lot Nikos, Carla, Samira, Rishab, Gustavo, Reza, Johan, Karsten, Uttiya, Hassan, Ali, Pedro, Javier, Rumen, Jie, Rohit, Stephan, Tim, Lindert, Wei Wei, Noura, Marloes.

Special thanks to my parents, brother, family, family-in-law, grand-parents and friends for supporting me and showing also always an interest in the topic. But in particular also the past years in motivating me to finish the thesis work, no matter if it took longer.

Last but not least, I want to thank my wife Janneke. By being patient, unconditionally supporting in all my hydrogen activities and the thesis, pushing me from time to time, bearing my frustrations, stubbornness and while enjoying life, the African bush and adventures.

Vincent D.W.M. Oldenbroek
Harare, Zimbabwe, 2021

Summary

Introduction

This thesis presents the design and analysis of future 100% renewable integrated transport and energy systems based on electricity and hydrogen as energy carriers. In which Fuel Cell Electric Vehicles (FCEVs) are used for transport, distributing energy and balancing electricity demand. Passenger cars in Europe are parked on average 97% of the time. They are used for driving only 3% of the time (<300 hours per year). So passenger car FCEVs can be used for energy balancing and electricity generation when parked and connected to the electricity grid, in the so-called Vehicle-to-Grid (V2G) mode. In Europe around 15.3 million passenger vehicles were sold in 2019 [1]. Using the "Our Car as Power Plant" analogy of Van Wijk et al. [2], multiplying each vehicle by 100 kW of future installed electric power in it, this would equal to 1,530 GW of annual sold power capacity in passenger vehicles. This is more than the existing 950 GW installed power generation capacity in Europe in 2019 [3]. The theoretical potential to use passenger FCEVs for power production, with the present low usage for driving, seems to be large.

Commercially available FCEVs use proton exchange membrane fuel cells systems to generate electricity from oxygen from the air and the hydrogen stored in on-board tanks at 700 bar. In parallel to the fuel cell, a small high voltage (HV) battery pack is connected. The HV battery is used for regenerative braking and provides additional power for acceleration. This combination of fuel cell and HV battery can deliver almost every kind of electrical energy service, from balancing intermittent renewables to emergency power back-up. By using both the HV battery and fuel cell of a few up to tens of thousands of aggregated FCEVs in combination with large-scale hydrogen storage, kW to GW-scale power generation and energy storage from seconds to seasons can be achieved.

Method & Outline

The goal of this research is to explore the techno-economic potential of hydrogen, FCEVs and V2G in achieving affordable, reliable, scalable and 100% renewable integrated transport and energy systems. The main research question is: *"How can we design and analyze future 100% renewable integrated transport and energy systems, based on electricity and hydrogen as energy carriers, using fuel cell electric vehicles for transport, distributing and generating electricity?"* In this thesis an experimental, proof of principle approach, is presented to understand and to analyze the current available FCEV and V2G technologies and their limitations. Next, for three different aggregation levels from 500 up to more than 20 million FCEVs, 100% renewable integrated transport and energy systems are designed, including a hospital, a smart city and 5 countries. The system designs are focused on European regions. Abundant, low cost and widely available energy sources such as solar PV and wind form the basis to design the 100% renewable, integrated energy and transport systems.

In this research, integrated energy and transport systems are designed for exploring the maximum technical potential of individual technologies. There is a trade-off between the number of balancing and storage options considered, and the

ability to isolate and to explore the maximum technical potential of a specific technology within large, complex and integrated future energy systems. For that purpose, the research presented in this thesis is limited to the following balancing options: using FCEVs to convert stored hydrogen into electricity and using electrolyzers to convert electricity into hydrogen. The energy storage is in the form of compressed gaseous hydrogen. Here, only technologies that have a Technology Readiness Levels (TRL) of at least 7 in 2015, or preferably higher are considered. Also, cost projections based on future economies of scale are more readily available for technologies at TRL 7 and higher.

Proof of principle approach, current available FCEV and V2G technologies and limitations

In Chapter 2, titled "Fuel Cell Electric Vehicle-to-Grid: Experimental Feasibility and Operational Performance as a Balancing Power Plant", presents the results of an experimental, proof of principle approach. A commercially available hydrogen FCEV, a Hyundai ix35, was modified for Vehicle-to-Grid (V2G) purposes to be able to deliver a maximum of 10 kW direct current (DC) power. Electricity was supplied to the Dutch national electricity grid via an external inverter. The 10 kW DC V2G power was inverted to 9.5 kW three-phase alternating current (AC), constituting a partial load of 11-15% of the maximum fuel cell DC power of 100 kW. The experimental verification of this set-up shows that FCEVs can be used for mobility as well as for generating power when parked. Virtual power plants composed of multiple grid-connected FCEVs could perform with a higher part-load efficiency, faster power gradients and shorter cold start-up times than the existing fast-reacting thermal power plants, such as open cycle gas turbines or gas engines. At 10 kW V2G DC power, the measured maximum downward and upward power gradients of the fuel cell system were –47 kW/s (–470 %/s relative to 10 kW max. power) and +73 kW/s (+730 %/s), for the high voltage battery –76 kW/s (–760 %/s) and +43 kW/s (+430 %/s). In other words, within less than ¼ of second, both battery and fuel cell system can ramp up or down 10 kW. In the V2G tests, fast cold start-up times of less than 5 s at ambient temperatures were measured. Hydrogen consumption in 9.5 kW AC grid-connected mode was 0.55 kg/h, resulting in a Tank-To-Grid-AC efficiency of 43% on a Higher Heating Value basis (51% on a Lower Heating Value basis). Direct current to alternating current efficiency was 95%.

Chapter 3 presents the usage parameters related to driving and V2G services, which could be used to best predict the average fuel cell stack voltage degradation. The voltage degradation negatively impacts the fuel cell system efficiency and economic lifetime and so, increasing the cost of produced electricity. Measurements were conducted for four Hyundai ix35 FCEVs, where only one FCEV was used for both driving and V2G services. The FCEVs drove between 7,917 and 27,459 km in 531 up to 1,167 trips (one trip defined as a fuel cell system start-up and shut-down cycle). The fuel cell systems operated up to 872 hours and produced up to 5,610 kWh of electricity. During the period investigated, for the four FCEVs, the mean fuel cell stack voltage degradation relative to the beginning of measurements based on operating time was between 1.4-2.3% and based on total produced electricity it was between 1.4-2.4%. The type of usage before conducting measurements could have

had an impact on the degradation during the measurements. No consistent correlation was observed between the usage parameters of fuel cell operating time, distance driven, fuel cell stack produced electricity and the mean fuel cell stack voltage degradation. Using a durability indicator expressed solely in operating hours, or distance driven or produced energy is not relevant for an FCEV used for both driving and V2G services due to the potential large variation of usage. The operating and 'idling' hours, produced energy, driven distance, number of start-ups and shutdowns measured in this experiment, could be part of a multi-metric indicator for predicting fuel cell durability, since a single metric indicator does not adequately describe the combined driving and V2G operation.

System designs and techno-economic scenario analyses

In Chapter 4 to 7, three integrated, 100% renewable transport and energy system designs at increasing FCEV aggregation levels are presented:

1. a hospital,
2. an urban area,
3. an entire country.

The selection of a hospital and urban areas resulted after applying four design criteria, the designed integrated systems should be:

1. at locations where cars are naturally parked and in the proximity of demand centers,
2. scalable in number of FCEVs, i.e. not having any upper limit,
3. applicable in all European countries, i.e. not serving niche markets,
4. highly replicable in Europe, i.e., the system designs should be replicable at least 1,000 times.

All designed 100% renewable energy systems show that FCEVs can be integrated into current energy systems for driving and providing dispatchable balancing power. If scheduled smartly, providing dispatchable balancing power does not significantly limit the use of the FCEVs for driving. The integration of the hospital or urban area can be done on a piecemeal basis, partially, distributed and scaled over time.

Chapter 4 presents the results of a 100% renewable integrated transport and energy system for a 526-bed hospital, using only local energy sources; rooftop solar, wind energy as well as biogas. The electricity consumption profile of the hospital is based on the consumption data obtained from the all-electric Reinier de Graaf hospital in Delft. A heuristic approach is applied to the modeling and system design for a Mid Century energy scenario (approximately around 2050). The system is always balanced by electrolysis and converting hydrogen back into electricity by less than 250 grid connected FCEVs (2.5 MW total, 10 kW V2G power each).

Current hospitals have two emergency power systems. Here, the uninterruptable power supply system could be replaced by approximately 95 grid connected FCEVs. The emergency diesel generator system has an autonomy of six days. It could be replaced by the high-pressure hydrogen storage at the hospital hydrogen fueling station, providing 1 day autonomy and the power of 250 grid connected FCEVs. The on-board hydrogen in the tanks of the FCEVs could provide another day of autonomy. If required, an additional 4 days of autonomy can be guaranteed by trucking in 5-6 hydrogen tube trailers, carrying each up to 1,350 kg of hydrogen. In

this way the hospital's high requirements of reliability of energy supply in emergency situations are met. The designed integrated transport and energy system for the hospital is fully self-sufficient and 100% renewable with local energy sources only.

Chapter 5 presents a conceptual design framework for an integrated transport and energy system for an urban area based on average European statistics in a moderate climate, i.e. an average solar radiation, mild winter and moderate summer temperatures. The area is based on a European statistic average of residential and services sector buildings and considers all road transport vehicles are hydrogen fuel cell powered. 2,000 households with 4,700 inhabitants are an appropriate size for dimensioning the smart city area, as statistically there is one petrol station and one food-retail shop for this number of households. An annual energy balance and cost analysis are performed for a Near Future (towards 2025) and Mid Century (around 2050) technology cost development scenarios. For the smart city an integrated energy system, for power, heat, and transport is developed consisting of solar and wind electricity, hydrogen as energy storage and transport fuel and where FCEVs provide electricity generation, energy distribution and mobility. The smart city area energy supply is independent of other energy systems and networks. With 2,300 passenger cars FCEVs in the smart city area, each providing 10 kW power per car, this would translate into a fleet average capacity factor 13% and 4.7% in respectively the Near Future and Mid Century scenario.
Using FCEVs for driving and balancing power, integrated into renewable energy based smart city areas, can provide cost-effective energy and mobility. In the Near Future scenario, system levelized cost of hydrogen for transportation is 7.6 €/kg, system levelized cost of electricity is 0.41 €/kWh and the specific cost of hydrogen for passenger cars is 0.08 €/km. In the Mid Century scenario however, these costs are much lower resulting in2.4 €/kg, 0.09 €/kWh and 0.02 €/km, respectively.

In Chapter 6, and in contrast with Chapter 5 which uses European average statistics, treats two climatically different locations in Europe, being Hamburg in Germany and Murcia in Spain. Murcia has a high annual solar insolation, mild winters and one of the highest summer temperatures in Europe. In contrast, Hamburg has a low annual solar insolation, relatively cold winters and lower summer temperatures compared to Murcia. In Chapter 6 the model from Chapter 5 is expanded with underground large-scale hydrogen storage in salt caverns to overcome the seasonal differences in energy demand. The simulation is performed with an hourly time step, based on five consecutive years of climate and renewable energy data. Multi-annual and hourly modelling provide deeper insights about when FCEVs need to provide balance power. Based on national statistics, the 2,000 households in Hamburg and Murcia have respectively 2,360 and 1,850 passenger cars. Here it is assumed all these cars are FCEVs.
In Murcia there is a better match in time (daily and seasonal) between solar electricity production and building electricity consumption (dominated by space cooling in summer while having a high solar electricity production) than in Hamburg (dominated by space heating in winter while having low solar electricity production). This results in the need for a 40% smaller seasonal hydrogen storage and FCEV V2G (FCEV2G) balancing requirements in Murcia than in Hamburg, in all scenarios. In

Murcia, year-round, virtually no FCEV2G requirement occur during daylight hours. In Hamburg, this is only the case in the summer period in the Mid Century scenario, but not in the Near Future scenario.
In Murcia, the average annual cost (without taxes and levies) for power, heat and mobility in the Near Future is approximately 1,930 €/year per household and 520 €/year per household in the Mid Century scenario. In today's fossil-based energy systems this is on average 1,470 €/year per household in Murcia. In Hamburg, the average annual cost (without taxes and levies) for power, heat and mobility in the Near Future is approximately 2,610 €/year per household and 770 €/year per household in the Mid Century scenario. In today's fossil-based energy systems this is on average 1,510 €/year per household in Hamburg. This indicates that with the renewable based energy and transport systems have the potential to be lower in cost than today's fossil-based energy system. The reason for the lower average cost of energy for households (without taxes and levies) for Murcia compared to Hamburg, are the lower system levelized costs for hydrogen and electricity but also the lower energy consumption in Murcia per household. The system levelized energy costs in the Mid Century scenario are 71 and 104 €/MWh for electricity and 2.6 and 3.0 €/kg for hydrogen, for respectively Murcia and Hamburg.

In Chapter 7, future 100% renewable national electricity, heating and road transport energy systems of Denmark, Germany, France, Great Britain and Spain in 2050 are illustrated and analyzed. The total passenger car fleets range between 2.3 and 44 million, of which 50% are considered to be FCEVs and the other 50% being Battery Electric Vehicles (BEVs). BEVs are not used for V2G electricity production, they are only used for mobility. 0.5 to 8 million parked and grid connected, V2G, hydrogen fueled FCEV passenger cars have the potential to fully balance (5-80 GW power at 10 kW each) these integrated and 100% renewable national energy systems. Together with hydrogen production via electrolyzers (11-154 GW) and large-scale hydrogen storage (6.2-105 $TWh_{H2\ HHV}$, 160-2,700 million kg H_2), energy supply is always guaranteed.
At all times, there is sufficient FCEV2G power capacity available, the peak requirement never exceeds 43% of the capacity of the FCEV2G fleet and the usage, the capacity factor, is low (<6%). Therefore, the combined electric power capacity in FCEV passenger cars could be a reliable and full replacement for large scale stationary balancing plants.
The balancing power requirements and seasonal energy storage capacities in this study are of similar magnitude compared to other studies. The large range in the values found in other studies is the result of a multitude of different modeling inputs, percentage of intermittent renewables versus the percentage of fossil fueled electricity generation and the number and type of balancing and storage technologies used.

Comparison of aggregation levels and conclusions

Relatively larger systems with a more mixed type of electricity consumption (residential and commercial) face less peaks in power consumption (relative to the average power consumption), and so indirectly also less peaks in the required FCEV2G balancing power. Depending on the definition of the FCEV2G fleet

size and the technology development year modelled (2015, towards 2025 or around 2050), the FCEV2G capacity factors mostly range from 2% to 11% in the developed energy and transport systems. Here, the hospital case study presented in Chapter 4, represents the outliers of 0.15-15% and could also be considered as part of the smart city area. When comparing only the outcomes of systems modeled on an hourly basis and representing a technology development scenario of the year 2050, the FCEV2G annual utilization rate, called the capacity factor, ranges between 2.1-5.5%. This is in the same order of magnitude of the driving utilization rate or capacity factor of approximately 3%. A European passenger car drives on average 12,000 km per year at a speed of 45 km/h, resulting in a capacity factor of 3%.

Regions facing stronger seasonal effects in energy consumption and (solar) energy production will always need long-term, seasonal, energy storage. Systems having a larger share of solar energy compared to wind energy and having lower seasonal space heating requirements, require mostly FCEV2G balancing power during the night or early mornings and evenings. Aforementioned type of systems face lower FCEV2G capacity factors. For example, 2.1% and 3.7% in the national energy system of sunny Spain and smart city area in Murcia. This in comparison to 5.5% and 5.0% in the colder and windier national energy system of Denmark and smart city area in Hamburg, respectively. Simply said, the energy production and consumption match better in Murcia than in Hamburg. So, less FCEV2G balancing, seasonal hydrogen storage, hydrogen production, distribution and fueling station capacities are needed. A higher need of FCEV2G balancing during the night, in systems with higher shares of solar energy production, would also better match the regular driving usage of passenger cars.

As indicated, in this thesis the focus was predominantly on a limited set of balancing and storage technologies based on hydrogen. This gives the opportunity to explore the maximum potential of electrolyzers, underground hydrogen storage and grid-connected FCEVs within larger, complex and integrated energy and transport systems. The results show that these technologies have a large technical and economic potential for balancing energy consumption and production on a large scale within complex and integrated energy and transport systems. Nevertheless, future energy systems will use a variety of balancing and storage technologies and therefore total system cost optimizations should consider all relevant technologies available.

In conclusion, fully renewable integrated transport and energy systems based on hydrogen and fuel cell electric vehicles, where FCEVs can be used for both driving and V2G energy balancing, have a great potential to be highly reliable and to achieve similar or lower cost as today's, fossil fuel-based energy systems. This potential comes without much compromise on the vehicle's availability for driving, also there is a large overcapacity in passenger vehicles available and most balancing happens when vehicles are parked during the night.

Samenvatting

Introductie

Dit proefschrift behandelt het ontwerp en de analyse van toekomstige 100% hernieuwbare geïntegreerde transport- en energiesystemen met elektriciteit en waterstof als energiedragers. Waarin brandstofcel-elektrische voertuigen, ook wel Fuel Cell Electric Vehicles (FCEV's), worden ingezet voor transport, energiedistributie en het balanceren van de elektriciteitsvraag.

Personenauto's in Europa staan gemiddeld 97% van de tijd stil, slechts 3% van de tijd worden deze gebruikt (<300 uur per jaar). FCEV personenauto's kunnen dus gebruikt worden voor het balanceren van de elektriciteitsvraag en aanbod wanneer ze geparkeerd staan en aangesloten zijn op het elektriciteitsnet, in de zogenaamde Vehicle-to-Grid (V2G) modus. In 2019 werden in Europa ongeveer 15,3 miljoen personenauto's verkocht [1]. Analoog aan het concept "Our Car as Power Plant" van Van Wijk et al. [2], vermenigvuldigt men elk verkochte personenauto met 100 kW aan toekomstig geïnstalleerd elektrisch vermogen, zou dit gezamenlijk 1530 GW aan jaarlijks verkocht vermogen opleveren. Dit is meer dan de bestaande 950 GW totaal geïnstalleerde elecktriciteitsproductiecapaciteit in Europa in 2019 [3]. Uit theoretisch oogpunt lijkt er dan ook genoeg potentie om FCEV personenauto's te gebruiken voor elektriciteitsproductie.

Commercieel verkrijgbare FCEV's gebruiken brandstofcelsystemen met een protonenuitwisselingsmembraan om elektriciteit op te wekken, dit door middel van zuurstof uit de lucht en waterstof. Waterstof komt uit de in het voertuig aanwezige tanks met een opslagdruk van 700 bar. Parallel aan de brandstofcel is een kleine hoogspannings (HV) batterij aangesloten. De HV-batterij wordt gebruikt voor het regeneratief remmen en levert extra vermogen bij het accelereren. Deze combinatie van de brandstofcel en HV-batterij kan vrijwel alle soorten elektrische energie diensten leveren, uiteenlopend van het balanceren van variabele duurzame energiebronnen tot noodstroom. Door zowel de HV-batterij als de brandstofcel van enkele tot tienduizenden geaggregeerde FCEV's te gebruiken in combinatie met grootschalige waterstofopslag, kan elektriciteitsproductie van kW tot GW-schaal worden bereikt in combinatie met energieopslag van seconden tot aan seizoenen.

Methode & Overzicht

Het doel van dit onderzoek is om het techno-economische potentieel van waterstof, FCEV's en V2G te verkennen voor het realiseren van betaalbare, betrouwbare, schaalbare en 100% hernieuwbare geïntegreerde transport- en energiesystemen. De centrale onderzoeksvraag is: "Hoe kunnen we toekomstige 100% hernieuwbare geïntegreerde transport- en energiesystemen ontwerpen en analyseren, met elektriciteit en waterstof als energiedragers, met behulp van brandstofcel-elektrische voertuigen (FCEVs) voor transport, distributie en opwekking van elektriciteit?" In dit proefschrift wordt een experimentele, 'proof of principle'-methode toegepast om de huidige beschikbare FCEV- en V2G-technologieën te begrijpen en te analyseren. Daarbij worden ook de beperkingen van de technologieën inzichtelijk gemaakt. Vervolgens worden voor drie verschillende aggregatieniveaus van 500 tot meer dan 20 miljoen FCEV's, 100%

hernieuwbare geïntegreerde transport- en energiesystemen ontworpen. Waaronder een ziekenhuis, een slimme stad en vijf landen. De systeemontwerpen zijn gericht op Europese regio's. Goedkope en voldoende beschikbare energiebronnen zoals zon-PV en wind vormen de basis van de 100% hernieuwbare, geïntegreerde energie- en transport systeemontwerpen.

In dit onderzoek worden geïntegreerde energie- en transportsystemen ontworpen om het maximale technische potentieel van balancerings- en opslagtechnologieën op basis van waterstof in kaart te brengen. Het is moeilijk het maximale technische potentieel van deze balancerings- en opslagtechnologieën te verkennen binnen grote, complexe en geïntegreerde toekomstige energiesystemen als men gelijktijdig een groot aantal verschillende balancerings- en opslagtechnieken toepast. Daarom beperkt dit onderzoek zich tot het gebruik van de volgende balanceringstechnologieën: FCEV's voor zowel mobiliteit als elektriciteitsproductie en elektrolysers voor de waterstofproductie. Alle energieopslag is in de vorm van gecomprimeerde gasvormige waterstof. In dit onderzoek worden alleen technologieën overwogen die in 2015 een Technology Readiness Levels (TRL) van minimaal 7 hadden en bij voorkeur hoger. Voor technieken met een TRL 7 of hoger zijn er meer en betrouwbaardere kostenprognoses op basis van toekomstige schaalvoordelen beschikbaar.

Bewijs van principe-aanpak, huidige beschikbare FCEV- en V2G-technologieën en beperkingen

In hoofdstuk 2, getiteld "Fuel Cell Electric Vehicle-to-Grid: experimentele haalbaarheid en operationele prestaties als een balancerende energiecentrale", worden de resultaten gepresenteerd van een experimentele, 'proof of principle'-methode. Een commercieel verkrijgbare waterstof-FCEV, een Hyundai ix35, is aangepast voor Vehicle-to-Grid (V2G) doeleinden om maximaal 10 kW gelijkstroom (DC) te kunnen leveren. Zo kan elektriciteit via een externe omvormer aan het Nederlandse elektriciteitsnet worden geleverd. Het 10 kW DC V2G-vermogen is omgevormd naar 9,5 kW driefase wisselstroom (AC), dit staat gelijk aan 11-15% van het maximale gelijkstroomvermogen (100kW) van het brandstofcelsysteem. Door middel van een experimentele verificatie, laat de opstelling zien dat tijdens het parkeren FCEV's voor zowel mobiliteit als voor elektriciteitsproductie kunnen worden gebruikt. Virtuele energiecentrales bestaande uit meerdere aan het elektriciteitsnet gekoppelde FCEV's zouden een hoger deellastrendement, snellere vermogenswisselingen en een kortere koude start hebben dan de bestaande snel reagerende thermische energiecentrales, zoals open-cyclus gasturbines of gasmotoren. Bij 10 kW V2G DC-vermogen waren de gemeten maximale neerwaartse en opwaartse vermogenswisselingen van het brandstofcelsysteem –47 kW/s (–470 %/s ten opzichte van 10 kW max. vermogen) en +73 kW/s (+730 % /s), voor de HV batterij –76 kW/s (–760 %/s) en +43 kW/s (+430 %/s). Met andere woorden, binnen een kwart seconde kunnen zowel de HV-batterij als het brandstofcelsysteem 10 kW op- of af worden geregeld. In de V2G-tests werden snelle koude starttijden van minder dan 5 s gemeten bij omgevingstemperaturen. Het waterstofverbruik in de 9,5 kW AC-netgekoppelde modus was 0,55 kg/uur, wat resulteerde in een Tank-to-Grid-AC-efficiëntie van 43% op basis van de bovenste verbrandingswaarde (51% op

basis van de onderste verbrandingswaarde). De gemeten omvormerefficientië, van gelijkstroom naar wisselstroom, was 95%.

Hoofdstuk 3 presenteert de gebruiksparameters die het beste gebruikt zouden kunnen worden om de gemiddelde degradatie van het brandstofcelsysteem te voorspellen met betrekking tot rijden en V2G-diensten. De spanningsdegradatie heeft een negatieve invloed op de efficiëntie van het brandstofcelsysteem en zo dus ook op de economische levensduur, waardoor de kosten van de geproduceerde elektriciteit indirect kunnen stijgen. Metingen werden uitgevoerd bij vier Hyundai ix35 FCEV's, één FCEV werd gebruikt voor zowel rijden als V2G-diensten. De FCEV's reden tussen de 7.917 en 27.459 km in 531 tot 1.167 ritten (één rit gedefinieerd als een opstart- en uitschakelcyclus van het brandstofcelsysteem). Tijdens voorgenoemde inzet hebben de brandstofcelsystemen maximaal 872 uur aangestaan en produceerden tot 5.610 kWh aan elektriciteit.
Tijdens de onderzochte periode lag voor de vier FCEV's de gemiddelde degradatie van de brandstofcelstack ten opzichte van het begin van de metingen, op basis van bedrijfsuren en op basis van de totale geproduceerde elektriciteit respectievelijk tussen 1,4-2,3% en 1,4-2,4%. Het type gebruik voorafgaand aan het uitvoeren van metingen kan een impact hebben gehad op de degradatie tijdens de metingen. Er werd geen consistente correlatie waargenomen tussen de gebruiksparameters van de bedrijfstijd van de brandstofcel, de afgelegde afstand, de door de brandstofcelstack geproduceerde elektriciteit en de gemiddelde degradatie van de brandstofcelstack. Het gebruik van een degradatie indicator die uitsluitend wordt uitgedrukt in bedrijfstijd, afgelegde afstand of geproduceerde energie is niet relevant voor een FCEV die wordt gebruikt voor zowel rijden als V2G-diensten vanwege de mogelijk grote variatie in gebruik. De bedrijfs- en 'stationair'-uren, geproduceerde energie, gereden afstand, aantal starts en stops gemeten in dit experiment, zouden deel kunnen uitmaken van een samengestelde indicator voor het voorspellen van de levensduur van brandstofcellen, aangezien een enkelvoudige indicator de gecombineerde rij- en V2G-operatie onvoldoende beschrijft.

Systeemontwerpen en technisch-economische scenarioanalyses

In Hoofdstuk 4 tot 7 worden drie geïntegreerde, 100% hernieuwbare transport- en energiesysteemontwerpen in volgorde van toenemende FCEV-aggregatieniveaus gepresenteerd:

1. een ziekenhuis,
2. een stedelijk gebied,
3. een heel land.

De selectie van een ziekenhuis en het stedelijke gebied was het resultaat van vier ontwerpcriteria:

1. locaties waar auto’s vaak geparkeerd staan, in de nabijheid van energiegebruikers
2. schaalbaar in aantal FCEV's, d.w.z. zonder bovengrens,
3. toepasbaar in alle Europese landen, d.w.z. geen nichemarkten ,
4. repliceerbaar in Europa, d.w.z. de systeemontwerpen moeten minstens 1.000 keer repliceerbaar zijn.

Alle ontworpen 100% hernieuwbare energiesystemen laten zien dat FCEV's kunnen worden geïntegreerd in de huidige energiesystemen, voor zowel mobiliteit als het leveren van regelbaar balanceringsvermogen. Indien optimaal gepland, is er door het leveren van regelbaar balanceringsvermogen een minimale beperking in het gebruik van FCEV's voor mobiliteit. De integratie van het ziekenhuis of stedelijk gebied kan stukje bij beetje, gedeeltelijk, gedistribueerd en geschaald in de tijd gebeuren.

Hoofdstuk 4 presenteert de resultaten van een 100% hernieuwbaar geïntegreerd transport- en energiesysteem voor een ziekenhuis met 526 bedden, waarbij alleen lokale energiebronnen worden gebruikt; zonne-energie op het dak, windenergie en biogas. Het elektriciteitsverbruiksprofiel van het ziekenhuis is gebaseerd op de verbruiksgegevens van het volledig elektrische Reinier de Graaf ziekenhuis in Delft. Een heuristische benadering wordt toegepast op de modellering en systeemontwerp voor een Mid Century energiescenario (rond 2050). De vraag en het gebruik van energie wordt altijd in balans gehouden door middel van elektrolyse en het omzetten van waterstof in elektriciteit door minder dan 250 op het elektriciteitsnet aangesloten FCEV's (2,5 MW in totaal, 10 kW V2G-vermogen elk).

De huidige ziekenhuizen hebben twee verschillende noodstroomvoorzieningen. Hier zouden de zogenaamde 'Uninterruptable Power Supply (UPS)' systemen kunnen worden vervangen door ongeveer 95 netgekoppelde FCEV's. De noodstroomaggregaten hebben een autonomie van zes dagen. Deze zouden deels kunnen worden vervangen door het elektrisch vermogen van 250 op het net aangesloten FCEV's en de hogedruk waterstofopslag bij het waterstoftankstation van het ziekenhuis, dit zorgt voor een autonomie van 1 dag . De waterstof in de tanks van de FCEV's zou voor nog één dag autonomie kunnen zorgen. Indien nodig kan 4 dagen extra autonomie worden gegarandeerd door 5-6 waterstoftank opleggers, die elk tot 1.350 kg waterstof kunnen vervoeren. Er wordt hiermee voldaan aan de hoge eisen die het ziekenhuis stelt aan de betrouwbaarheid van de energievoorziening in noodsituaties. Het ontworpen geïntegreerde transport- en energiesysteem voor het ziekenhuis is volledig zelfvoorzienend en 100% hernieuwbaar met alleen lokale energiebronnen.

Hoofdstuk 5 presenteert een conceptueel ontwerpkader voor een geïntegreerd transport- en energiesysteem voor een stedelijk gebied op basis van gemiddelde Europese statistieken in een gematigd klimaat, d.w.z. een gemiddelde zonnestraling, milde winters en gematigde zomertemperaturen. Het stedelijk gebied is gebaseerd op een Europees statistisch gemiddelde van gebouwen in de woon- en dienstensector en veronderstelt dat alle wegvoertuigen worden aangedreven door brandstofcellen op waterstof. 2.000 huishoudens met 4.700 inwoners zijn een geschikte grootte voor het dimensioneren van een slim stedelijk gebied. Statistisch gezien is er namelijk één tankstation en één supermarkt voor dit aantal huishoudens. Een jaarlijkse energiebalans en kostenanalyse worden uitgevoerd voor een scenario op basis van de geschatte technologieontwikkeling en technologie kosten in de nabije toekomst, een 'Near Future scenario' (tegen 2025) en halverwege de 21ste eeuw, een 'Mid Century scenario' (rond 2050). Voor een slim stedelijke gebied is een geïntegreerd energiesysteem voor elektriciteit, warmte en

mobiliteit ontworpen op basis van zonne- en windelektriciteit, samen met waterstof voor energieopslag en transport brandstof waarbij FCEV's zorgen voor elektriciteitsproductie, energiedistributie en mobiliteit. De energievoorziening van een slim stedelijke gebied is onafhankelijk van andere energiesystemen en netwerken. Met 2.300 FCEV's voor personenauto's in het slimme stadsgebied, die elk 10 kW vermogen per auto kunnen leveren, zou de vlootgemiddelde capaciteitsfactor 13% en 4,7% worden in respectievelijk het Near Future en het Mid Century-scenario.
Het gebruik van FCEV's voor mobiliteit en regelbaar balanceringsvermogen, geïntegreerd in door hernieuwbare energie voorziene slimme stedelijke gebieden, kunnen een kosteneffectieve energie- en mobiliteitsvoorziening bieden. In het Near Future scenario bedragen de werkelijke systeemkosten van waterstof voor transport 7,6 €/kg, de werkelijke systeemkosten van elektriciteit 0,41 €/kWh en de specifieke kosten van waterstof voor personenauto's 0,08 €/km. In het Mid Century scenario zijn deze kosten echter veel lager, resulterend in respectievelijk 2,4 €/kg, 0,09 €/kWh en 0,02 €/km.

In hoofdstuk 6, in tegenstelling tot hoofdstuk 5 dat gebruikmaakt van Europese gemiddelde statistieken, worden twee klimatologisch verschillende locaties in Europa behandeld, Hamburg in Duitsland en Murcia in Spanje. Murcia heeft een hoge jaarlijkse zonnestraling, milde winters en een van de hoogste zomertemperaturen in Europa. Hamburg heeft daarentegen een lage jaarlijkse zonnestraling, relatief koude winters en lagere zomertemperaturen in vergelijking met Murcia. In hoofdstuk 6 is het model uit hoofdstuk 5 uitgebreid met een ondergrondse grootschalige opslag van waterstof in zoutkoepels om de seizoensverschillen in de energievraag te overbruggen. De simulatie wordt uitgevoerd met een tijdstap van één uur, gebaseerd op vijf opeenvolgende jaren aan klimaat- en hernieuwbare energiegegevens. Meerjarige en uurlijkse modellering verschaffen beter inzicht in wanneer van FCEV's balanceringvermogen gevraagd wordt. Op basis van nationale statistieken hebben de 2.000 huishoudens in Hamburg en Murcia respectievelijk 2.360 en 1.850 personenauto's. Er wordt aangenomen dat al deze auto's FCEV's zijn.
In Murcia is er een betere afstemming op zowel dag- als seizoensbasis, tussen de productie van zonne-elektriciteit en het elektriciteitsverbruik van gebouwen (gedomineerd door gebouwkoeling in de zomer ten tijde van een hoge opwekking van zonne-elektriciteit) dan in Hamburg (gedomineerd door gebouwverwarming in de winter ten tijde van een lage opwekking van zonne-elektriciteit). In alle scenario's resulteert dit in een 40% kleinere seizoensgebonden waterstofopslag en FCEV V2G (FCEV2G) balanceringsvereisten in Murcia dan in Hamburg. In Murcia is overdag vrijwel geen FCEV2G balancering nodig. In Hamburg is dit alleen in de zomerperiode van het Mid Century scenario het geval, maar niet in het Near Future scenario.
In Murcia bedragen de gemiddelde jaarlijkse kosten (zonder belastingen en heffingen) voor elektriciteit, warmte en mobiliteit in het Near Future scenario ongeveer 1.930 €/jaar per huishouden en in het Mid Century scenario 520 €/jaar per huishouden. In het huidige fossiele energiesysteem is dit gemiddeld 1.470 €/jaar per huishouden in Murcia. In Hamburg bedragen de gemiddelde jaarlijkse kosten (zonder belastingen en heffingen) voor elektriciteit, warmte en mobiliteit in het

Near Future scenaro ongeveer 2.610 €/jaar per huishouden en in het Mid Century scenario 770 €/jaar per huishouden. In het huidige fossiele energiesysteem is dit gemiddeld 1.510 €/jaar per huishouden in Hamburg. Dit laat zien dat hernieuwbare energie- en transportsystemen in de toekomst goedkoper kunnen zijn dan de huidige fossiele energie- en transportsystemen. De reden voor de lagere gemiddelde energiekosten voor huishoudens (zonder belastingen en heffingen) in Murcia in vergelijking met Hamburg, zijn de lagere werkelijke systeemkosten voor waterstof en elektriciteit, maar ook het lagere energieverbruik in Murcia per huishouden. De werkelijke systeemkosten voor energie in het Mid Century scenario zijn 71 en 104 €/MWh voor elektriciteit en 2,6 en 3,0 €/kg voor waterstof, voor respectievelijk Murcia en Hamburg.

In hoofdstuk 7 worden toekomstige 100% hernieuwbare nationale elektriciteits-, verwarmings- en wegtransport energiesystemen van Denemarken, Duitsland, Frankrijk, Groot-Brittannië en Spanje voor het jaar 2050 geïllustreerd en geanalyseerd. Het totale wagenpark varieert van 2,3 tot 44 miljoen personenauto's. Hiervan wordt aangenomen dat 50% FCEV's en de andere 50% batterij elektrische voertuigen, Battery Electric Vehicles (BEV's), zijn. BEV's worden niet gebruikt voor V2G elektriciteitsproductie, maar enkel voor mobiliteit. Gezamenlijk hebben 0,5 tot 8 miljoen geparkeerde en door V2G op het elektriciteitsnet aangesloten FCEV-personenauto's (5-80 GW vermogen, bij 10 kW per FCEV), het potentieel om de geïntegreerde en 100% hernieuwbare nationale energiesystemen volledig te balanceren. Samen met waterstofproductie via elektrolyzers (11-154 GW) en grootschalige waterstofopslag (6,2-105 $TWh_{H2\ HHV}$, 160-2.700 miljoen kg H_2) is de energievoorziening altijd gegarandeerd.

Ten alle tijde is er voldoende FCEV2G-capaciteit beschikbaar, de piekbehoefte is nooit hoger dan 43% van de capaciteit van het FCEV2G wagenpark en is de bezettingsgraad, de zogenaamde capaciteitsfactor, laag (<6%). Daarom zou het gecombineerde elektrisch vermogen van de FCEV-personenauto's een betrouwbare en complete vervanging kunnen zijn van grootschalige stationaire balancerings elektriciteitscentrales.

De benodigde balanceringsvermogens en seizoensgebonden energieopslagcapaciteiten in dit onderzoek zijn vergelijkbaar met andere onderzoeken. De grote variatie in balanceringsvermogens en energie opslagcapaciteiten gevonden in andere onderzoeken is het resultaat van een veelheid aan verschillende invoergegevens voor de modellen. Bijvoorbeeld het percentage variabele hernieuwbare elektriciteitsproductie in verhouding tot het percentage fossiele elektriciteitsporductie of het aantal en type toegepaste balancerings en opslagtechnologieën.

Vergelijking van aggregatieniveaus en conclusies

Grotere systemen met een gevarieerder elektriciteitsverbruik (residentiële en diensten sector) hebben te maken met minder pieken in het elektriciteitsverbruik (ten opzichte van het gemiddelde elektriciteitsverbruik). Indirect hebben deze systemen ook minder pieken in het benodigde FCEV2G-balanceringsvermogen. Afhankelijk van de grootte van het FCEV2G wagenpark en het gemodelleerde technologie ontwikkelingsscenario (2015, tegen 2025 of rond 2050), variëren de

FCEV2G capaciteitsfactoren meestal van 2% tot 11% in de ontwikkelde energie- en transportsystemen. Uitschieters van 0,15-15% komen voor bij het energie en transportsysteem van het ziekenhuis in hoofdstuk 4. Daarentegen zou dit systeem ook kunnen worden beschouwd als een onderdeel van een slim stadsgebied. Als alleen de resultaten van systemen worden vergeleken die op uurbasis zijn gemodelleerd in een techniek ontwikkelingsscenario rond 2050, dan varieert de jaarlijkse capaciteitsfactor van het FCEV2G wagenpark, tussen de 2,1-5,5%. Dit ligt in dezelfde orde van grootte als de capaciteitsfactor voor mobiliteitsgebruik van circa 3%. Een Europese personenauto rijdt gemiddeld 12.000 km per jaar met een snelheid van 45 km/u, wat resulteert in een capaciteitsfactor van 3%.

Regio's die sterkere seizoenseffecten in het energieverbruik en (zonne)energieproductie ondervinden, zullen in de toekomst altijd behoeftehebben aan langdurige, seizoensgebonden, energieopslag. Systemen met een groter aandeel zonne-energie dan windenergie en met een lagere seizoensgebonden behoefte aan gebouwverwarming, vereisen meestal alleen FCEV2G balanceringsvermogen tijdens de nacht of vroege ochtenden en avonden. Dit sluit ook beter aan bij het reguliere mobiliteitsgebruik van personenauto's. De hiervoor genoemde type systemen hebben te maken met lagere FCEV2G capaciteitsfactoren. Bijvoorbeeld 2,1% en 3,7% in het zonnige nationale systeem van Spanje en het stadsgebied in Murcia. Tegenover 5,5% en 5,0% in het respectievelijk koudere en winderigere nationale systeem van Denemarken en het stadsgebied in Hamburg. Kortgezegd, de energieproductie en het energieverbruik komen beter overeen in Murcia dan in Hamburg. Daardoor is er dus minder FCEV2G balancering, seizoensgebonden waterstofopslag, waterstof productie, distributie en tankstation capaciteit nodig.

De focus van dit proefschrift is gericht op een beperkte set van balancerings- en opslagtechnologieën op basis van waterstof. Dit biedt de mogelijkheid om het maximale potentieel van elektrolysers, ondergrondse waterstofopslag en netgekoppelde FCEV's binnen grotere, complexe en geïntegreerde energie- en transportsystemen te verkennen. De resultaten tonen aan dat deze technologieën een groot technisch en economisch potentieel hebben voor het op grote schaal balanceren van energieproductie en consumptie binnen complexe en geïntegreerde energie- en transportsystemen. Desalniettemin zullen toekomstige energiesystemen een verscheidenheid aan balancerings- en opslagtechnologieën gebruiken en daarom moet bij de optimalisatie van de totale systeemkosten rekening worden gehouden met alle relevante beschikbare technologieën.

Kortom, volledig hernieuwbare geïntegreerde transport- en energiesystemen op basis van waterstof en elektrische brandstofcelvoertuigen, hebben het potentieel om zeer betrouwbaar te zijn met vergelijkbare of lagere kosten als de huidige, op fossiele brandstoffen gebaseerde energiesystemen. De potentie om FCEV’s te gebruiken voor zowel mobiliteit als energiebalancering is groot. De beschikbaarheid van het voertuig voor mobiliteitsgebruik wordt vrijwel niet beperkt door het V2G gebruik. Daarbovenop komt dat er een grote overcapaciteit is in het vermogen van de aanwezige personenauto's en de meeste balancering nodig is wanneer het voertuig 's nachts geparkeerd staat.

Contents

Acknowledgements i
Summary iv
Samenvatting x
Contents x
List of Figures xx
List of Tables xxvi
1 Introduction and background 1
1.1 Research motivation and background 1
1.2 Research goal and questions 12
1.3 Thesis outline, methodology, scope and boundaries 12
2 Fuel Cell Electric Vehicle-to-Grid: Experimental Feasibility and Operational Performance as Balancing Power Plant 19
2.1 Abstract 19
2.2 Introduction 19
2.3 Experimental 21
2.4 Results and Discussion 27
2.5 Conclusions 38
3 Hyundai ix35 fuel cell electric vehicles: degradation analysis for driving and vehicle-to-grid usage 41
3.1 Abstract 41
3.2 Introduction 41
3.3 Materials and Method 42
3.4 Results and Discussion 47
3.5 Conclusion 51
4 Fuel cell electric vehicle-to-grid: emergency and balancing power for a 100% renewable hospital 53
4.1 Abstract 53
4.2 Introduction 53
4.3 Methodology 55
4.4 Energy balance results and discussion 65
4.5 Feasibility replacement emergency power system by V2G FCEVs 69
4.6 Conclusions 70
5 Fuel cell electric vehicle as a power plant: fully renewable integrated transport and energy system design and analysis for smart city areas 71
5.1 Abstract 71
5.2 Introduction 71
5.3 Methodology 74
5.4 Design of a fully autonomous renewable and reliable energy system for a smart city area 78
5.5 Energy demand and production in two scenarios 80
5.6 Technology choices, sizing, characteristics and development 84
5.7 Energy balance results 95
5.8 Cost of energy results and allocation methodology 98

5.9 Discussion 109
5.10 Conclusion 111
6 Fuel Cell Electric Vehicle as a Power Plant: Techno-Economic Scenario Analysis of a Renewable Integrated Transportation and Energy System for Smart Cities in Two Climates 113
6.1 Abstract 113
6.2 Introduction 113
6.3 Materials and Methods 116
6.4 Energy Balance Results and Discussion 126
6.5 Cost of Energy Results and Discussion 133
6.6 Discussion 139
6.7 Conclusions 142
7 Fuel cell electric vehicles and hydrogen balancing 100 percent renewable and integrated national transportation and energy systems 145
7.1 Abstract 145
7.2 Introduction 145
7.3 Materials and methods 148
7.4 Energy balance results 159
7.5 Discussion 168
7.6 Conclusion 173
8 Conclusions and Recommendations for future research 175
8.1 Conclusions 175
8.2 Recommendations for future research 184
Appendices 193
A Fuel Cell Electric Vehicle as a Power Plant: Techno-Economic Scenario Analysis of a Renewable Integrated Transportation and Energy System for Smart Cities in Two Climates 193
A.1 Locations Selection, System Design, Dimensioning, and Components 194
A.2 Detailed Description and Background Data of the Calculation Model and Hourly Simulation 199
A.3 Calculating Cost of Energy 206
A.4 Energy Balance Figures 208
A.5 Total System Cost Table 211
A.6 Background Figures Cost of Energy for a Household 213
B Fuel cell electric vehicles and hydrogen balancing 100 percent renewable and integrated national transportation and energy systems 215
B.1 Hourly electricity generation and consumption figures 215
B.2 Annual energy balance figures 218
B.3 Hourly distribution of Fuel Cell Electric Vehicle to Grid electricity production figures 221
Nomenclature 223
References 225
List of publications 290

List of Figures

Figure 1-1 The hydrogen cycle, lowest cost electricity can be produced far away from the demand, converted into to hydrogen via water electrolysis for low cost transport of electricity on an inter-regional, -national and intercontinental scale [20,21]. 2
Figure 1-2 Indirect electrification via hydrogen gas is a very versatile option as it can facilitate the coupling between electricity and buildings, transport and industry. Where hydrogen can balance energy production and use in location and time, and decarbonise end uses [78]..... 7
Figure 1-3 The “Car as a power plant” by Van Wijk et al. [2] 9
Figure 1-4 Hydrogen Fuel Cell Electric Vehicle powertrain components [183]. 10
Figure 1-5 Electricity storage technologies, balancing services and applications, adapted from IEA [126]. 11
Figure 1-6 – Structure of this thesis, giving an overview between the 6 chapters, 3 research methods, and the aggregation level of cars in the chapters. The arrows and chapter numbers indicate the preferred reading order. 16
Figure 2-1 Experimental Fuel Cell Electric Vehicle-to-Grid (FCEV2G) set-up at The Green Village, Delft University of Technology, Delft, The Netherlands. 21
Figure 2-2 Scheme of electrical architecture of the FCEV and V2G modification. .. 22
Figure 2-3 V2G Type 1 Socket integrated in the front bumper. 22
Figure 2-4 New dashboard V2G activation button also initiates Cold Shut Down. . 23
Figure 2-5 V2G-DCAC unit connected to the FCEV. 24
Figure 2-6 Simplified electrical architecture of the V2G-DCAC connecting the FCEV to the AC grid. 24
Figure 2-7 Coolant temperatures and pump angular velocity at 9.5 kW AC V2G for the entire test duration of 6 hours and 5 minutes on February 13, 2017. 29
Figure 2-8 Pump angular velocity and coolant temperature difference for the 7000 to 8000 seconds period for the test on February 13, 2017. 29
Figure 2-9 FC and HV battery gross electrical power for the entire test duration of 6 hours and 5 minutes on February 13, 2017. 30
Figure 2-10 FC and HV battery gross electrical power for the 7000 to 8000 seconds period for the test on February 13, 2017. 31
Figure 2-11 Hydrogen mass in tanks and HV battery state of charge (SOC) cycling for the 7000 to 8000 seconds period for the test on February 13, 2017. 31
Figure 2-12 Downward and upward power gradients of the FC and HV battery for the entire test duration of 6 hours and 5 minutes on February 13, 2017. 32
Figure 2-13 Downward and upward power gradients of the FC and HV battery for the 7000 to 8000 seconds period for the test on February 13, 2017. 32
Figure 2-14 Hydrogen mass in tanks and HV battery state of charge (SOC) cycling for the entire test duration of 6 hours and 5 minutes on February 13, 2017. 34
Figure 3-1 Fuel Cell stack voltage vs. current for FCEV1. The blue and green data points represent the analysed and excluded data respectively. 43
Figure 3-2 Cumulative percentage of voltage data points for each measured current before and after applying the <250V filtering condition for the data of FCEV1 including the approximate data loss for filtering conditions. The plotted

cumulative percentage without the <250V filtering (red) condition is underneath the cumulative percentage with <250V filtering condition (blue). 43
Figure 3-3 Number of voltage data points for each measured current after applying the <250V filtering condition for FCEV1. 44
Figure 3-4 Weibull distribution of the number of voltage data points for all measured currents after applying the <250V filtering condition for FCEV1. 44
Figure 3-5 Fuel Cell stack voltage vs. current for FCEV1 zoomed into 0-29 A region. The blue and green data points represent the analysed and excluded data respectively. The selected voltage data points at 15 A are displayed in red. 46
Figure 3-6 L.l.s. and r.l.s. regression analysis applied to Fuel Cell stack voltage vs. operating time at 15A for FCEV1. 46
Figure 3-7 L.l.s. and r.l.s. regression analysis applied to Fuel Cell stack voltage vs. cumulative produced electricity at 15A for FCEV1. 47
Figure 3-8 Cumulative percentage of voltage data points for each measured current after applying the <250V filtering condition. 50
Figure 4-1 Key elements and functional energy performance of the fully autonomous hospital integrated transport and energy system 57
Figure 4-2 Reinier de Graaf Gasthuis hospital and its car parking area with a total potential surface area of 13,070 m^2 to place solar panels. 58
Figure 4-3 Hourly energy consumption and production profiles for a Mid Century scenario. 59
Figure 4-4 Electricity production of a 4.2 MW wind turbine in a Mid Century scenario based on the combined wind profile of Rotterdam and Hoek van Holland. 62
Figure 4-5 Annual energy balance of the integrated transport and energy system. 66
Figure 4-6 Load duration curve electricity surplus (+, electrolyzer operation) and electricity shortage (-, FCEVs V2G operation). Due to the cable limitation for about 1800 hours both electrolyzer and FCEVs are running simultaneously. 67
Figure 4-7 Number of FCEVs required for balancing during the day. The blue box represents the 25th and 75th percentile (50%). The whiskers represent 1.5 times the interquartile range (49.7%). Outliers are marked with a red plus, medians with a red horizontal line in the blue boxes and the averages by a black asterisk. 67
Figure 4-8 Net hydrogen production profile shows that the net import and export of hydrogen over a year is zero. 68
Figure 5-1 Smart City Area key elements and functional energy performance. 79
Figure 5-2 Generated solar electricity in each scenario compared to the building and transport final energy consumption categories. 83
Figure 5-3 The relevant conversion processes in the smart city area. 85
Figure 5-4 Smart City Final Energy Consumption and Production 95
Figure 5-5 Energy Balance Near Future (left) and Mid Century scenario (right). 96
Figure 5-6 Near Future (left) and Mid Century (right) Smart City Area annual capital cost and O&M cost distribution. 98
Figure 5-7 Near Future (left) and Mid Century (right), cost distribution (outer) of 1 kWh final electricity consumption (SLCoEe) & energy distribution (inner) of 1 kWh primary electricity input. 105

Figure 5-8 Specific Cost of Energy for Buildings ($SCoE_B$ in €/m^2/year) and Transport ($SCoE_T$ €/km) per sector (Services sector upper diagram, Residential sector lower left diagram) and Smart City Area Total System Cost of Energy ($TSCoE_{SCA}$ in M€/year) (lower right diagram).....106
Figure 5-9 Cost of Energy distribution for the Residential and Services sector for buildings and transportation in the Near Future and Mid Century scenario. 106
Figure 5-10 Relative change in Smart City Area Total System Cost of Energy compared to the Mid Century base scenario. 108
Figure 6-1 Location selection steps and criteria resulted in the urban area of Hamburg in Germany and Murcia in Spain.....117
Figure 6-2 Smart city area components, electricity, water, hydrogen flows, and transportation. fuel cell electric vehicles (FCEV), fuel cell electric vehicle; V2G, vehicle-to-grid.....119
Figure 6-3 Simplified hourly simulation scheme. 124
Figure 6-4 Annual energy balance for Hamburg for the Near Future scenario (left) and Mid Century scenario (right).....129
Figure 6-5 Annual energy balance for Murcia for the Near Future scenario (left) and the Mid Century scenario (right). 130
Figure 6-6 Boxplots showing the hourly average FCEVs needed for producing V2G electricity (# left y-axis, % of all cars right y-axis) throughout the day during the colder winter period (in blue, left, 1 October–31 March) and the warmer "summer" period (in orange, right, 1 April–30 September) in the Near Future and Mid Century scenarios for, respectively, Hamburg and Murcia. The black crosses represent the mean values, the red lines represent the medians, and the green triangles represent the maxima. Based on a normal distribution, the bars represent the interquartile range, IQR, the difference between the first and third quartiles (Q1 and Q3), approximately 50%. The upper and lower whiskers represent the data points within the ranges [Q1–(Q1-1.5×IQR)] and [Q3+(Q3+1.5×IQR)], approximately 44%. Dots indicate outliers, outside aforementioned ranges, the remaining approx. 1%.....132
Figure 6-7 Total system cost of energy (TSCoE) for the component categories in the Near Future and Mid Century scenarios for Hamburg and Murcia. The subsystems are grouped into "Hydrogen" and "Electricity".....134
Figure 7-1 Generic 100% renewable system design applied to the national electricity, heating, cooling and transport systems of Denmark, Germany, Great Britain, France and Spain. Fuel cell electric vehicle to grid (FCEV and V2G), electrolyzers and hydrogen storage provide all of the necessary balancing requirements.....150
Figure 7-2 Schematic and simplified overview of the model. 153
Figure 7-3 Relative hourly hydrogen fueling (orang) and BEV charging (blue) profile during a week based on [58,147]. 157
Figure 7-4 Annual energy balance (TWh/year) for Denmark in 2050 based on 2017 renewable energy data.....160
Figure 7-5 Annual energy balance (TWh/year) for Spain in 2050 based on 2017 renewable energy data.....161
Figure 7-6 Average annual hourly FCEV2G balancing expressed as a percentage of the total annual FCEV2G balancing in each country.....163

Figure 7-7 Average annual hourly electrolyzer balancing as a percentage of the total annual electrolyzer balancing in each country.....164
Figure 7-8 Boxplot showing the hourly distribution of FCEV2G electricity production in Spain (million vehicles, left y-axis; % of all FCEV passenger cars, right y-axis) throughout the day (based on 2016-2017 input data). The black crosses represent the mean values, the medians are indicated by the red horizontal lines in the blue bars. The blue bars represent the range of 50% of the data points. The whiskers represent approximately 49% of the data points. The red pluses indicate the outliers, outside the above-mentioned ranges, and represent less than 1%. 165
Figure 7-9 Boxplot showing the hourly distribution of FCEV2Gs needed for producing V2G electricity in Denmark (million vehicles, left y-axis; % of all FCEV passenger cars, right y-axis) throughout the day (based on 2016-2017 input data). The black crosses represent the mean values, the medians are indicated by the red horizontal lines in the blue bars. The blue bars represent the range of 50% of the data points. The whiskers represent approximately 49% of the data points. The red pluses indicate the outliers, outside the above-mentioned ranges, and represent less than 1%.....166
Figure 7-10 Average monthly FCEV2G balancing as a percentage of total FCEV2G balancing in each country.....166
Figure 7-11 Normalized hydrogen storage capacity requirements for all five countries, based on varying years of input data ranging from 2015 to 2018. 168

Figure A 1 Load duration curves for the simulation, based on 2016 weather data for Hamburg (top) and Murcia (bottom) for the Near Future (left) and Mid Century scenarios (right). Direct solar use (purple), FCEV2G electricity (red), combined FCEV2G and direct solar use (blue), and the solar electrolyzer power consumption (green). 208
Figure A 2 Hourly electricity balances for an entire year based on 2016 weather data. From top to bottom, Hamburg in the Near Future and Mid Century and Murcia in the Near Future and Mid Century. 209
Figure A 3 Seasonal hydrogen storage content over the year (black line), from top to bottom Hamburg Near Future and Mid Century and Murcia Near Future and Mid Century. The annual maximum and minimum are indicated by an upward (orange) and downward (green) facing triangle. For every month, the bars on the left side (in) represent the monthly inflow of hydrogen from either solar (yellow) or wind (blue), and the bar on the right (out) shows the monthly outflow to the hydrogen fueling station.....210

Figure B1 Hourly electricity consumption (orange) versus the renewable electricity generation (blue) for Denmark.....215
Figure B2 Hourly electricity consumption (orange) versus the renewable electricity generation (blue) for Germany.....215
Figure B3 Hourly electricity consumption (orange) versus the renewable electricity generation (blue) for Great Britain.....216
Figure B4 Hourly electricity consumption (orange) versus the renewable electricity generation (blue) for France.....216

Figure B5 Hourly electricity consumption (orange) versus the renewable electricity generation (blue) for Spain. 217
Figure B6 Annual energy balance (TWh/year) for Germany in 2050 based on 2017 renewable energy data. 218
Figure B7 Annual energy balance (TWh/year) for France in 2050 based on 2017 renewable energy data. 219
Figure B8 Annual energy balance (TWh/year) for Great Britain in 2050 based on 2017 renewable energy data. 220
Figure B9 Boxplot showing the hourly distribution of FCEV2G electricity production in Germany (million vehicles left y-axis, % of all FCEV passenger cars right y-axis) throughout the day (based on 2014-2017 input data). The black crosses represent the mean values, the medians are indicated by the red horizontal lines in the blue bars. The blue bars represent the range of 50% of the data points. The whiskers represent approximately 49% of the data points. The red pluses indicate the outliers, outside the above-mentioned ranges, and represent less than 1%. 221
Figure B10 Boxplot showing the hourly distribution of FCEV2G electricity production in France (million vehicles left y-axis, % of all FCEV passenger cars right y-axis) throughout the day (based on 2014-2017 input data). The black crosses represent the mean values, the medians are indicated by the red horizontal lines in the blue bars. The blue bars represent the range of 50% of the data points. The whiskers represent approximately 49% of the data points. The red pluses indicate the outliers, outside the above-mentioned ranges, and represent less than 1%. 221
Figure B11 Boxplot showing the hourly distribution of FCEV2G electricity production in Great Britain (million vehicles left y-axis, % of all FCEV passenger cars right y-axis) throughout the day (based on 2015-2017 input data). The black crosses represent the mean values, the medians are indicated by the red horizontal lines in the blue bars. The blue bars represent the range of 50% of the data points. The whiskers represent approximately 49% of the data points. The red pluses indicate the outliers, outside the above-mentioned ranges, and represent less than 1%. 222

List of Tables

Table 1-1 Relation between sub-questions and chapter topics. 15
Table 2-1 Maximum downward (↓) and upward (↑) power gradients of the FC and HV battery expressed in kW s-1 and % s-1 of maximum power output. Eight tests at 9.5 kW AC V2G conditions were performed and the values averaged..... 28
Table 2-2 Test durations with hydrogen consumption rates and corresponding AC and DC system efficiencies. 35
Table 2-3 Results from 'spinning reserve' tests. 37
Table 3-1 Total excluded current and voltage data points after applying all filtering conditions. 45
Table 3-2 Measurements and results of FCEV use indicators versus average % stack voltage drop compared to the b-o-m voltage for the considered current range using an l.l.s and r.l.s. regression analysis method. 49
Table 3-3 Estimated durabilities expressed in hours, distance driven and electricity produced. Using the average voltage drops from the time based l.l.s. regression analysis and assuming a linear degradation trend at a maximum allowable mean voltage drop of 10% [313]. 51
Table 4-1 Characteristics of the hospital transport and energy system scaling the Reinier de Graaf Gasthuis hospital parameters with European statistics 58
Table 4-2 Main installed component sizes of the integrated transport and energy system. 68
Table 5-1 Characteristics of a smart European city area. 80
Table 5-2 Specific energy consumption (kWh/m^2/year) per consumption category for the residential sector. 81
Table 5-3 Average annual distance driven and Near Future and Mid Century specific energy consumption for van, lorry, road tractor and bus type FCEVs..... 82
Table 5-4 Specific energy consumption (kWh/m^2/year) per energy consumption category for the services sector. 82
Table 5-5 Electricity and water production parameters. 92
Table 5-6 Specific electricity consumption (kWh/kg H2) of the conversion processes in the smart city for both scenarios. 93
Table 5-7 Economical parameters of the Smart City Area components for the Near Future and Mid Century scenario. IC_i = installed capital cost, OM_i = annual operational and maintenance cost expressed as an annual percentage of the installed investment cost, LT = Lifetime. 94
Table 5-8 Calculated installed capacities, capital, O&M and total costs for the components in the Smart City Area. 99
Table 5-9 Calculated (System) levelized cost parameters for the Near Future and Mid Century scenarios. 104
Table 5-10 Sensitivity parameters for a pessimistic and optimistic scenario of the Mid Century case. 107
Table 6-1 Components, energy, and water flow in the smart city area (Figure 6-2). 120
Table 6-2 Characteristics of the modeled smart city areas. 121

Table 6-3 Key energy balance parameters for FCEVs through vehicle-to-grid (FCEV2G), solar electrolyzer, and SHS usage for Hamburg and Murcia in the Near Future and Mid Century scenarios. 128
Table 6-4 Levelized (LCoE) and system levelized cost of energy (SLCoE) parameters for Hamburg and Murcia in the Near Future and Mid Century scenarios. 136
Table 6-5 The annual cost of energy for households (CoE_{hh}) without taxes and levies for the Present, Near Future, and Mid Century scenarios in Hamburg and Murcia. 138
Table 7-1 Key figures for the selected countries 2015. 149
Table 7-2 Road transport vehicle types and the share of annual distance traveled and specific energy consumption per vehicle type and technology in 2050 152
Table 7-3 Renewable electricity installed capacity mixes in 2050 for Denmark (DK), Germany (DE), Great Britain (GB), France (FR) and Spain (ES) based on existing studies [37,58–64]. 154
Table 7-4 Assumed road transport vehicle use in 2050. 156
Table 7-5 Key energy balancing parameters for the energy system, FCEV2G and electrolyzer usage for all five countries. 162
Table 7-6 Seasonal Hydrogen Storage key parameters for the five countries analyzed. 167
Table 8-1 FCEV2G fleet average full load hours (hours/car/year) or expressed as capacity factor (%) of systems modelled on an hourly basis and representing a technology development scenario of the year 2050. 183

Table A1 Key figures, characterizing the climate of the two locations, Hamburg and Murcia. 194
Table A2 Specific energy consumption SEC or production SEP ($kWh_e/kg\ H_2$) of the energy conversion processes in the smart city area for both scenarios and locations. 196
Table A3 Economic parameters of the smart city area components for the Near Future and the Mid Century scenario. IC_i = installed capital cost; OM_i = annual operational and maintenance cost expressed as an annual percentage of the installed investment cost; LT = lifetime. 197
Table A4 Specific annual energy consumption SEC_B ($kWh/m^2/year$) per energy consumption category and total annual energy consumption E_B (MWh/year) in buildings for the residential and the services sector for the Hamburg- and Murcia-based smart city areas at Present and the Near Future and Mid Century scenarios. 201
Table A5 Specific energy consumption savings for the Near Future and Mid Century scenarios compared to the Present Situation. 202
Table A6 The average annual distance driven d and Near Future and Mid Century scenario-specific energy consumption of transport (SECT) for van, truck, tractor-trailer, and bus type FCEVs. 204
Table A 7 Installed component capacities (Q) and component total annual costs (TC_i) in the smart city area Hamburg and Murcia in the Near Future and Mid Century scenario, 2012–2016 average (μ) and coefficient of variation (CV) 211

1 Introduction and background

1.1 Research motivation and background

1.1.1 Climate goals, clean air, energy consumption

The urgency to significantly reduce the impacts of climate change is felt around the globe. The 'Paris Agreement' was adopted by virtually all of the 195 countries of the United Nations on December 12, 2015 [4]. 195 governments agreed on a long-term goal of keeping the increase in global average temperature to well below 2°C above pre-industrial levels and aim to limit the increase to 1.5°C [4]. Air pollution, climate change, human health and the environment are intertwined [5]. Climate change and air pollution are two major global challenges, the causes and solutions of which are closely linked. Europe's air is getting cleaner but persistent pollution, especially in cities, still damages people's health and the economy [6,7]. As greenhouse gases and air pollutants share the same emission sources, benefits can arise from limiting emissions of one or the other [6].

At the same time, there have been some positive developments over the past decade. Many countries have enacted climate policies; currently 121 countries and 454 cities have committed to achieve net zero CO_2 emissions by 2050 [8]. Europe aims to become the world's first climate-neutral continent by 2050. To achieve this, the European Commission presented the European Green Deal. This new growth strategy aims to transform the EU into a fair and prosperous society, with a modern, resource-efficient and competitive economy where there are no net emissions of greenhouse gases in 2050 and where economic growth is decoupled from resource use [9].

Currently in the European Union (EU) the sectors contributing more than half of the anthropogenic greenhouse gas emissions are the residential and commercial (13%), energy supply (28%) and transport (20%, excluding international shipping and aviation) sectors [10]. Gross inland energy consumption in the EU-28 in 2017 was 1 675 Mtoe (19480 TWh, 70.13 EJ) [11], where 14% was provided by renewables. The biggest share of the gross inland energy consumption was used in energy conversion (25.8%), for example refining crude oil into fuels for transport or coal and natural gas into electricity and heat. Final energy consumption in EU-28 in 2017 was 1 060 Mtoe (12328 TWh, 44.38 EJ), the majority consumed by the transport (31%), households (27%) and services (15%) sectors [11]. Most used energy carriers for final energy are electricity (22.7 %) and fossil fuels (60%), primarily oil, petroleum products and natural gas [11]. Approximately 80% of all oil and petroleum products are consumed by the transport sector [12] and transport activity is still expected to grow [13]. Estimates indicate passenger transport will increase by 42% by 2050 and freight transport by 60% [13]. If no significant change happens, this will result into additional pressure on the environment.

In view of climate change and air pollution, both transport and energy systems need to change rapidly into zero emission systems. These systems need to become clean while remaining reliable and affordable. This will require major technological, organizational and social changes in the energy and the transport system. Major transitions in and integration of both systems via direct electrification [14] and as a

second step indirect [15,16] electrification (i.e. electricity to hydrogen, heat), are foreseen according to the hydrogen and energy system integration strategies [17,18] of the European Union. Hydrogen is regarded to play a major role among the indirect electrification strategies and energy carriers [17,19].

1.1.2 Global sustainable energy system based on low-cost renewable electricity, need of storage and transportation of energy via hydrogen

A global sustainable energy system can address aforementioned global challenges. Such a system can be constructed by using low-cost renewable electricity combined with low-cost storage and transportation of energy via hydrogen or other hydrogen carrier. Where useful and cost effective, the electricity produced is directly consumed. However, lowest cost electricity is often not sufficiently and not year-round available in the vicinity of demand centers. The lowest cost electricity can also be produced far away from the demand, converted into to hydrogen via water electrolysis for low-cost transport and storage of electricity. Electricity transportation via hydrogen could be applied on an inter-regional, -national and intercontinental scale. Hydrogen can be used directly as a feedstock or fuel but also converted back into electricity and heat via a fuel cell, hydrogen gas turbine or boiler and so close the 'hydrogen cycle' [20,21], see Figure 1-1.

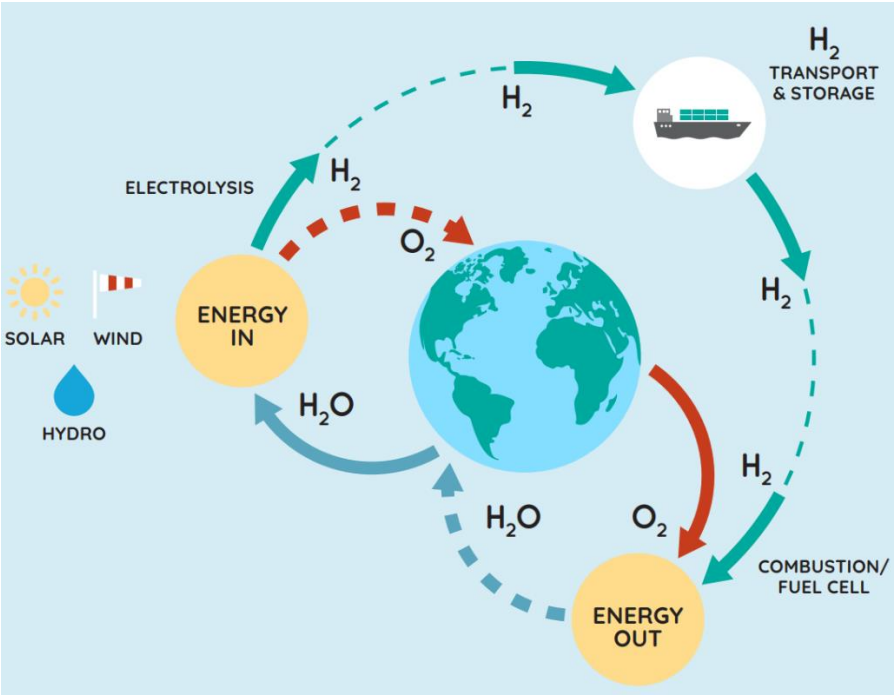

Figure 1-1 The hydrogen cycle, lowest cost electricity can be produced far away from the demand, converted into to hydrogen via water electrolysis for low cost transport of electricity on an inter-regional, -national and intercontinental scale [20,21].

The lower electricity production cost can compensate for the introduced storage, transport and energy conversion losses (e.g. fuel cell or hydrogen gas turbine) and investments compared to local solar electricity production and consumption in regions with less strong solar irradiation [20]. Above all, this would make renewable electricity available on demand, day and night, summer and winter.

Low-cost renewable electricity

In many parts of the world including Europe, the cheapest source of new bulk electricity generation on an LCOE (Levelized Cost Of Electricity) basis is onshore wind and utility scale solar PV, without subsidies [22–25]. Auctions worldwide including Europe have reached LCOEs below 20€/MWh for solar [26,27] and below 50€/MWh for off-shore wind [28,29]. Especially in sunny regions, solar PV in combination with short term 4-hour battery electric storage start even to outperform gas peaker plants[30–32], as the cost of battery storage systems have fallen significantly [33–36]. The availability of large scale and low cost renewable electricity together with direct and indirect electrification technologies such as hydrogen for storage and transport of energy [14,37–41], make it possible to decarbonize the largest energy consuming sectors (power, transport, heating and cooling). The decarbonization will cause the electricity generation and consumption to more than double by 2050 according to the European Commission [42]. Electrification of the energy generation also reduces the use of biomass and biofuels to sustainable levels [43–47].

Storage of electricity via hydrogen

The share of renewable energy sources (RES) in the total energy supply will have to increase to more than 80% by 2050. RES have a volatile production profile. Hence, a massive increase in flexibility measures in all energy consuming sectors are needed for a secure energy system [42,48]. Demand response side management can increase flexibility significantly but has its limitations too [49–52]. Matching demand and supply for all sectors, therefore, requires versatile, affordable, scalable (from distributed to large-scale), reliable and sustainable energy storage. A broad range of thermal, mechanical, chemical, electrical and electrochemical storage technologies covering all characteristics regarding power, capacity, duration and response is available, and several of them will be needed to have a reliable energy system [53–56]. There will not only be a need for short-term storage of seconds, minutes, hours or days, but also large-scale seasonal storage over months up to years [14], similar as with today's natural gas storage [57,58]. In particular decarbonizing the space heating demand with primarily wind and solar energy will require large amounts of long-term energy storage, as Europe's annual solar generation profile is close to opposite to the space heating demand profile [59–61]. On top of that in the winter season so-called 'dark doldrums' [62–65] might occur, combined low solar and wind production for several weeks.

Electrical and electrochemical energy storage technologies such as batteries (lithium, redox-flow) are more suitable for short term (microseconds to weeks) and high cyclic (e.g. once per day or more) energy storage [66]. Although they remain relatively expensive for large scale and long-term energy storage [67]. Mechanical storage technologies such as flywheels, pumped hydro and compressed air energy

storage [68] or thermal energy storage have a low storage density. Next to that, pumped hydro energy storage is geographically limited [69,70]. These aspects remain a drawback to large-scale implementation, especially for seasonal storage [68]. In the case of thermal energy storage, the heat loss at higher temperatures remains a barrier [69] for seasonal energy storage. Whereas combining thermal and chemical energy storage with Power-to-Heat and Power-to-Hydrogen (ammonia or other e-gases and e-liquids) technologies are promising for long-term and large-scale energy storage and connecting the electricity, heat transport and chemical sectors [71,72].

Transportation of electricity via hydrogen

As it is the case today for oil, natural gas and biofuels, hydrogen and e-fuels could actually become globally traded commodities and imported from regions with comparatively cheaper, abundant renewables [17,73–75], often called the 'new oil or LNG' [76,77]. Imports could help reduce the cost of the transition [20,78] as well as possible pressure on domestic resources (land and sea) linked to large-scale deployment of renewables [79,80]. When determining the overall economics of future energy infrastructure, transportation costs of energy are important [81]. Currently, most of the long-distance energy transport occurs via merchant ships and pipelines carrying oil or natural gas. Transporting renewable electricity via hydrogen gas in pipelines can be several times more cost-effective than via electricity and cables [82–85]. Moreover, the existing natural gas transport and distribution infrastructure, connecting the majority of homes in Europe, can be reused for hydrogen gas transport [86]. Concluding, low-cost renewable electricity in the form of hydrogen, can be cost effectively stored and transported on a regional, national and intercontinental scale.

1.1.3 Transport sector

The transport sector in 2017 in Europe was responsible for 31% of the final energy consumption, 326 Mtoe (3797 TWh, 13.67 EJ). The energy consumption in transport remains dominated by oil products as only 8.9% renewable energy is used for transport in 2019 [87]. It will require significant efforts to decarbonize the transport sector. 24% of the total EU-28 GHG and 21% of the CO_2 emissions, can be attributed to the transport sector [10,88]. Here 72% of the total transport CO_2 emissions originate from road transport [89], of which passenger cars account for 61%.

About a decade ago, biofuels were generally seen as the only feasible route for near-term decarbonization of ground transport. However, in the wake of cheap renewables, electric powertrains [90–92], lower battery costs [93], "Dieselgate" [94], technical maturity and foreseen cost reductions of hydrogen tanks and fuel cells (via economies of scale and platinum content reduction) [95–102], decarbonization in the entire transport sector is shifting towards direct electrification and indirect electrification [103] via so-called 'e-fuels', of which the main focus is on hydrogen [17], where the Total Cost of Ownership (TCO) is quickly reaching break-even with Battery Electric Vehicles (BEVs) and Internal Combustion Engine Vehicles (ICEVS) [104]. Biofuel combustion still emits other unwanted

emissions, e.g. NO_x. The availability of sustainable biomass feedstock [43–47] is limited and is in competition with other uses of bio-energy and for bio-based materials [105], justifies moving towards electrification of transport. About 16 countries have banned sales of new fossil fueled cars and other vehicles in the period of 2030-2050 and more than 40 cities have banned the use of them completely or in certain areas [106,107]. A joint statement signed by seven truck manufacturers state that all by 2040 all new commercial vehicles sold must be fossil free and have a clear focus on hydrogen [108]. Which is in line with the EU-wide CO_2 emission standards for heavy duty vehicles [109].

All kinds of battery electric transport vehicles are becoming increasingly available. From motorbikes, forklifts, passenger cars, vans, buses and trucks [110,111] in the road transport sector, electric ferries [112] in the maritime [113] and rail sectors [111] and small electric airplanes [114]. Indirect electrification is an important option in areas where direct electrification runs into technical difficulties. For example, transport dealing with large freights, large distances, long operational hours, weight limitations or when there is a limited electric grid capacity for charging batteries [73,115]. Here hydrogen or hydrogen-based fuels such as ammonia or synthetic jet fuel can decarbonize material handling [73,115], light commercial vehicles and taxis [73,116] or heavy duty road freight [117], shipping [118], rail [119] and aviation [120,121].

Passenger cars represent one of the largest energy consumers among all energy-demand technologies in the EU [122,123]. For passenger cars, either battery electric, or for the larger passenger vehicles, SUVs and mid-size long range cars, hydrogen fuel cell electric is likely the preferred technology to decarbonize [73,116]. Currently Europe has registered 0.90 million Battery Electric Vehicle (BEV) type passenger cars, 0.38% of the total passenger car vehicles stock [124]. In 2020, 1,492 Fuel cell Electric Vehicle (FCEV) passenger cars are registered in Europe [124]. In 2019, globally an estimated 18,900 FCEV passenger cars were operational [125]. Although currently numbers of registered BEVs are significantly higher than FCEVs in Europe, long term scenarios estimate that the distribution between BEV and FCEVs for passenger cars ranges between 90:10 and 15:85 [14,73,116,126–132], depending on the usage and passenger car vehicle segment [73,116].

In contrast to space heating demand, transport fuel demand is relatives constant throughout the year (disregarding the Covid-19 impact) [59,61,133]. The daily road transport fuel demand (primarily petrol and diesel) is 1-1.3 times the daily electricity demand [60,133,134]. With the weekly and seasonal fluctuations of solar and wind energy, long term decarbonized energy storage would be needed to secure transport energy supply.

1.1.4 Decarbonizing the energy system via sector coupling and integration: Hydrogen and its applications

Energy system integration – the coordinated planning and operation of the energy system 'as a whole', across multiple energy carriers, infrastructures and consumption sectors – is the pathway towards an effective, affordable and deep decarbonization of the European economy according to the European Commission [18]. Energy technologies, infrastructures and sectoral systems can further optimize their contribution to decarbonization when coupled and integrated [14]. Think of opportunities allowing the best possible or multiple use of the available resources and assets.

Sector coupling involves the increased integration of energy end-use and supply sectors with one another [135]. This can improve the efficiency and flexibility of the energy system as well as its reliability and adequacy. Additionally, sector coupling can reduce the costs of decarbonization. Furthermore, a more integrated approach to energy systems planning is needed. This integration includes production, conversion, storage, and demand [136]. Coupling also means that action in one sector is heavily dependent on other sector(s) [14]. For example, decarbonization of hydrogen production via electrification will not happen unless power generation decarbonizes.

Two major approaches contributing to sector coupling are large-scale electrification of energy use in the end-use sectors and the indirect electrification by using electricity to produce heat, gaseous or liquid energy carriers for use in the end-use [15].

Indirect electrification via hydrogen gas is a very versatile option as it can facilitate the coupling between electricity and buildings, transport and industry [137,138], see Figure 1-2 [78]. Besides its versatility, hydrogen is a clean and safe energy carrier [138]. Hydrogen produced from renewable electricity and water can enable large-scale efficient renewable energy integration, provide storage and so act as a buffer in times of high energy demand or low energy production. Hydrogen can be stored and distributed in the pure form, compressed, liquid or cryo-compressed. Furthermore, it can be chemically stored in ammonia (NH_3), methanol (CH_3OH), formic acid (HCOOH), synthetic methane (CH_4) or bound to methylcyclohexane (MCH) based liquids, often also called 'Liquid Organic Hydrogen Carriers' (LOHCs). Aforementioned hydrogen storage technologies are very complementary and together they can provide the required electrical energy storage and transport (section 1.1.2) for the long term and on large scale for all sectors and various types of end use, including chemical feedstock [126]. In addition to storage, fuel cells or gas turbines can convert hydrogen or its chemically stored version back into electricity, on a small and large scale.

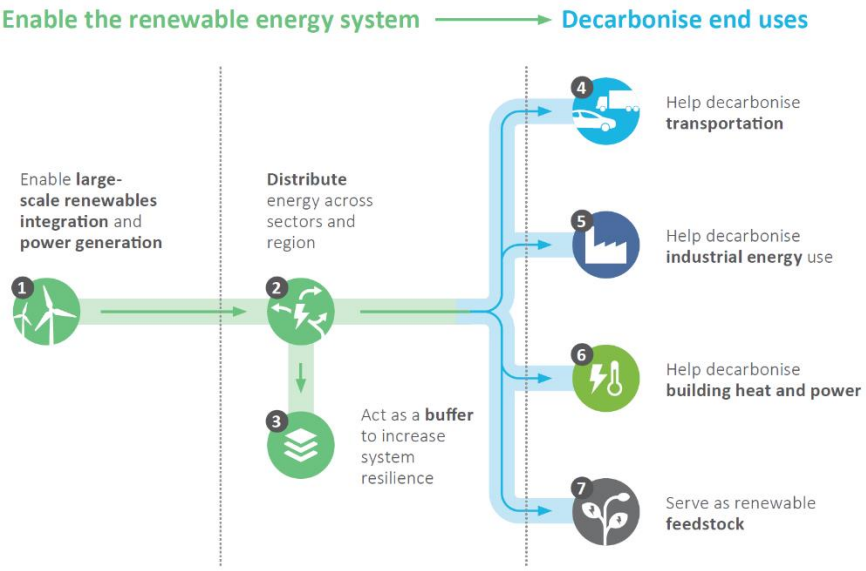

Figure 1-2 Indirect electrification via hydrogen gas is a very versatile option as it can facilitate the coupling between electricity and buildings, transport and industry. Where hydrogen can balance energy production and use in location and time, and decarbonise end uses [78].

Hydrogen storage for power production also creates synergies with the transport sector, where hydrogen can be used as clean transport fuel. The long-term large-scale hydrogen storage would have a similar function for the transport sector as the current strategic storage of crude oil and petroleum products referred to in section 1.1.3.

The European Union, China, USA, Germany, Japan, the Republic of Korea, Australia and more and more regions are embracing hydrogen as a new energy carrier [139]. Mainly because of the technical and operational advantages over batteries in the long-range transport sector and ability to decarbonize hard to abate sectors [138]. In addition to these advantages, green hydrogen and its applications are expected to become competitive with fossil derived hydrogen [73,140–143]. Hydrogen technology is maturing and being scaled-up [144,145] and costs of production, storage and (fuel cell) applications [73,143] being reduced. More and more electrolyser systems are being built and planned [146,147]. The electrolyser capital cost are expected to decrease with scaling up electrolyser production facilities and system scale [148–150]. Most important, the cost of hydrogen will become cheaper with the ongoing reduction of renewable electricity cost [73,78,148].

1.1.5 Large scale seasonal energy and fuel storage, hydrogen and "Car as Power Plant"

As shares of intermittent renewable energy sources increase [151], stationary back-up power plants [152–154] will face even lower utilization factors in coming years

and result into expensive back-up or balancing power [153,155–157]. Present research on high renewable European energy scenarios for 2050 use open cycle gas turbines (OCGTs) for balancing the electricity grid, fueled by (synthetic) methane or hydrogen [37,58,67,158–164]. These research studies indicated large central and stationary power plants will have low capacity factors, with estimates of less than 5% [162,164] and so contributing to a higher total system cost [153,155].

In the EU-28 in 2018 the primary energy consumption was 18050 TWh [165] of which 5077 TWh of natural gas consumption [166] and 7235 TWh of oil and petroleum products (excluding biofuels) [165]. Current operational underground gas storage facilities have a capacity of 1131 TWh [57]. Underground natural gas storage serves mainly as seasonal energy storage [167], for heating demand and electricity generation [168]. Also, the concept of large storage of transport fuel is not something new. European Member States have an obligation to maintain minimum stocks of crude oil and/or petroleum products. Either 90 days of average daily net imports or 61 days of average daily inland consumption [169,170], which in September 2020 storage was 140 days [171]. For the EU-28, this would correspond to about 1200 TWh of crude oil and petroleum products storage. The combined underground gas and petroleum products storage capacity is approximately 13% of the EU-28 primary energy consumption in 2018, which is in the upper range (2-14%) of what Blanco et. Al [48] indicate as storage for future 100% renewable energy systems.

In several European long term energy strategy scenarios, the gross and final energy consumption will be dominated by electricity [14]. The estimated amount of electricity storage ranges from 300-450 TWh, of which 100-200 TWh battery storage and 75-175 TWh hydrogen storage [14]. Although studies for Germany, France and Spain combined indicate a storage requirement of 24-282 TWh hydrogen [172–174]. Sector coupling and energy system integration focuses on the best possible use of available assets [14]. Currently passenger cars face low utilization factors and could be put to better use while parked. On average, passenger cars drive 12,000 km per year at an average annual speed of 45 km/h [175]. They are parked 97 % of the time. One promising alternative to stationary back-up and balancing power plants is parked and grid-connected electric vehicles (EVs). EVs are able to provide power to the grid while parked, which is known as a ‘‘Vehicle-to-Grid‘‘ (V2G) system [176,177]. The combined installed power capacity of passenger cars is enormous, every year more than 80 million new cars are sold worldwide [2]. In the work of Van Wijk et al. [2] “Car as a Power Plant”, the number of cars sold annually is multiplied by 100 kW of future installed electric power per car and calculated that 8,000 GW of power capacity in cars would be sold each year, see Figure 1-3. The installed power plant capacity worldwide is only around 5,000 GW [2]. In Europe around 15.3 million passenger cars were sold in 2019 [1]. Using the similar “Car as Power Plant” analogy as Van Wijk et al. [2], this would equal to 1530 GW of annual sold power capacity in passenger cars. Which is more than the 946 GW installed power generation capacity in Europe in 2018 [3]. Where this only relates to the amount of passenger cars sold per year, not considering commercial vehicles. One car could produce electricity for dozens of houses, or thousands could be grouped together and replace entire powerplants (Figure 1-3).

Figure 1-3 The "Car as a power plant" by Van Wijk et al. [2]

There are three types of EVs that are suitable for delivering power while parked: plug-in hybrid electric vehicles (PHEVs), battery electric vehicles (BEVs) and fuel cell electric vehicles (FCEVs) [176,177], where the latter two are more suitable to provide silent, decarbonized electricity with zero tail pipe emissions. In the EU-28 in 2018 271.5 million passenger cars are in use [1]. In case all would become BEVs with a battery of 100 kWh each, they would represent a combined electricity storage of 27.15 TWh. That amount is similar to 1-1.5 days of average EU final energy consumption in 2050 [14,178]. Hydrogen and derived 'e-fuels' are widely considered to be more suitable for large scale and seasonal storage, similar to natural gas [14,126], see Figure 1-5. In particular, underground salt caverns already in use for natural gas [57], could be used for large scale seasonal hydrogen storage. The technical potential of underground seasonal hydrogen storage for Europe is enormous, 84.8 PWh [179]. Instead of using large scale MW size OCGTs for converting the stored hydrogen gas into electricity, parked FCEVs could be used.

1.1.6 Hydrogen FCEV, Vehicle to Grid (V2G), Scientific contribution

Commercially available FCEVs use proton exchange membrane (PEM) fuel cells (FCs) to generate electricity from oxygen from the air and on-board stored hydrogen in tanks at 700 bar. In parallel to the fuel cell a high voltage (HV) battery pack is connected [180–182], see Figure 1-4 [183]. The battery is used for regenerative braking and provides additional power for acceleration. This combination of FC and battery is capable of delivering almost every kind of electrical energy service [184], from balancing to emergency power back-up [185], primary reserve [176,186,187], see Figure 1-5.

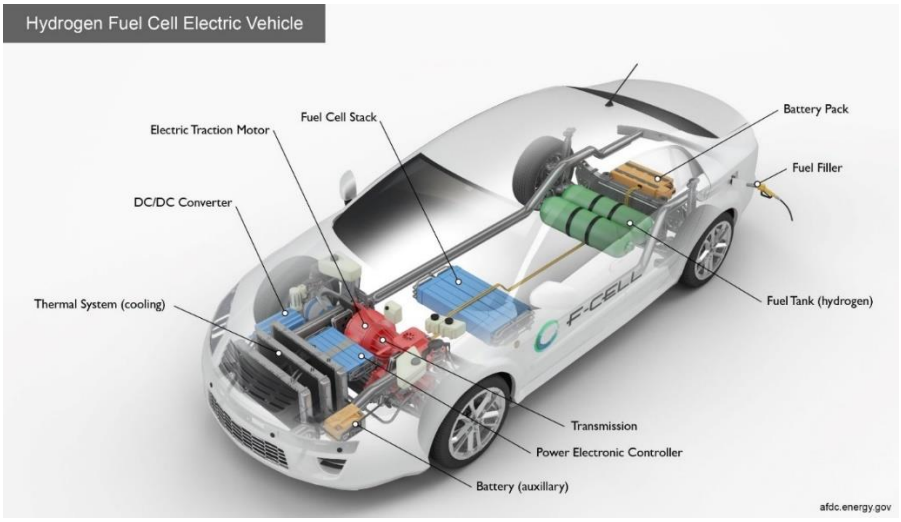

Figure 1-4 Hydrogen Fuel Cell Electric Vehicle powertrain components [183].

The power output of V2G equipment is in the range of 1-100 kW [188] and the fuel cell maximum power in a single FCEV is approximately 100 kW and traction battery up to 40kW [189]. By using one or several FCEVs in parallel, hydrogen as seasonal storage would not only be feasible at a MW scale but also at smaller powers down to 1kW. See the red lined box in Figure 1-5, where FCEVs could distribute seasonal stored hydrogen to end-user and distribution level (T&D). Due to the quick refueling of less than 5 minutes [190], together with the hydrogen from large scale underground storage, electricity could be produced for weeks or months and so for example overcome the so-called 'dark doldrums' [62–65]. By converting seasonally stored hydrogen into electricity close to the demand, there is an opportunity to be independent of the electricity grid. Figure 1-5, adapted from [126], displays the various electricity storage technologies, balancing services and applications on time and power scales from microseconds to seasons and kWs to GWs. Currently, the power and discharge duration capacities of battery systems, range from kWs up to hundred MW and from sub-minute to multiple hours. Electrolysers, hydrogen storage and reconversion to electricity via gas turbines, engines or fuel cells, are currently regarded as useful storage and balancing technologies in the range from several MWs up to GWs with discharge durations of days to seasons. By using actively the battery and fuel cell of a few or tens of thousands of aggregated FCEVs in combination with seasonally stored hydrogen, kW to GW-scale power generation and energy storage from seconds to seasons could be achieved, see the black dashed outlined section in Figure 1-5. V2G with a few up to hundreds of FCEVs also could provide new services, electricity storage from days to seasons from MW- to kW-scale down to the End-user level, which often is the owner of a passenger car, indicated via the red outlined section in Figure 1-5.

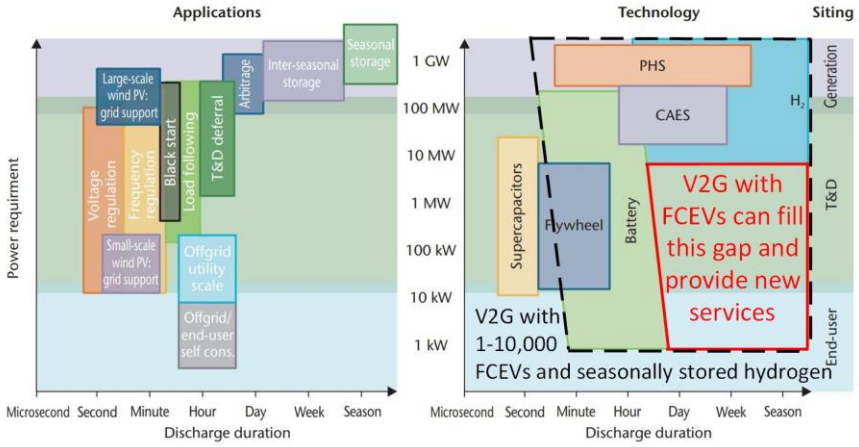

Figure 1-5 Electricity storage technologies, balancing services and applications, adapted from IEA [126].

Manufacturers are preparing mass production of automotive fuel cell systems [191,192], which has the potential to reduce costs to 40-60 US$/kW [96,98]. These costs are approximately ten times lower than the OCGT 2050 installed capital costs of 400-600 EUR/kW, at economic lifetimes of 25-35 years [58,159,163,164,193]. With ultimate durability targets of 8,000 hours of automotive fuel cells [194], economic lifetimes could be over 20 years (400 operational hours per year).

More than 60 V2G projects with BEVs have already been executed worldwide [195] and the V2G concept with BEVs has been researched extensively [196–199], in contrast to V2G with FCEVs. In particular there is a lack of research on the design and analysis of fully renewable integrated energy and transport systems based on V2G with FCEVs. A number of FCEV manufacturers [181,200,201] are developing FCEVs capable of providing power to electric appliances (Vehicle-to-Load, V2L), small grids or homes (Vehicle-to-Home, V2H) [202], although none claim to have connected a FCEV to a national electricity grid. Many studies and pilot projects investigate stand-alone and national grid-connected renewable energy systems using hydrogen as energy storage and stationary fuel cells for the reconversion of the stored hydrogen [203–206]. Some studies use the produced hydrogen for transportation [103,207–212] or solely use the fuel cell in the vehicle as an electric generator [213–217] without considering hydrogen production. Integration of FCEVs through V2G into a local electricity network for operating in island mode, emergency power, or balancing local renewables has been done mostly on a smaller or a very large scale [218–222]. Some studies include a cost analysis [223,224], but then do not compare with a future scenario with improved cost and efficiency (scenario and trend analysis) [225], are dependent on the grid electricity, or do not include seasonal hydrogen storage [225]. The authors of [226] focus on a small-scale system in a specific region without considering hydrogen transportation, although includes a future cost scenario. The authors of [227] look into urban areas and road transportation in different regions in different Japanese climate zones, but the

described system is not 100% renewable and does not include economics or consider V2G electricity services with FCEVs. This indicates there is a lack of techno-economic studies looking into 100% renewable integrated transport and energy system designs, based on electricity and hydrogen energy carriers, where V2G connected FCEVs can provide transport and energy services.

1.2 Research goal and questions

The goal of this research is to explore the techno-economic potential of hydrogen, FCEVs, V2G and how these technologies can be integrated into the design of affordable, reliable, scalable and 100% renewable integrated transport and energy systems. The main research question is:

"How can we design and analyze future 100% renewable integrated transport and energy systems, based on electricity and hydrogen as energy carriers, using fuel cell electric vehicles for transport, distributing and generating electricity?"

The research sub-questions addressed in this thesis are:

1. Are commercially available FCEVs suitable to act as balancing power plants?
2. How can we integrate FCEVs, used for transport, distributing and generating electricity, into future energy systems?
3. What impact do European regional characteristics have on the techno-economic system performance and the usage of FCEVs for transport, distributing and generating electricity?

1.3 Thesis outline, methodology, scope and boundaries

1.3.1 Thesis outline and methodology

The organization of this thesis and the relation between the six chapters and the three sub-questions, as well as the research methods used, are presented in Table 1-1 and Figure 1-6. To answer the three sub-questions, six topics are formulated and treated in chapters two to seven, see Table 1-1. In Figure 1-6, the arrows and chapter numbers indicate the preferred reading order. This thesis uses three research methods to design and analyze future 100% renewable integrated transport and energy systems based on electricity and hydrogen as energy carriers, where fuel cell electric vehicles are used for energy balancing. See Figure 1-6, the first research method is an experimental, proof of principle approach (Chapters 2 and 3), the second method is the combination of system design, a heuristic modeling approach and simulation (Chapters 4 to 7), and third, a techno-economic scenario analysis (Chapters 5 and 6). Aggregating the power of cars make it possible to serve different levels of power requirement. Therefore Figure 1-6 also indicated the level of aggregated cars in the chapters.

After the introduction and background in section 1.1, Chapter 2 titled Fuel Cell Electric Vehicle-to-Grid: Experimental Feasibility and Operational Performance as Balancing Power Plant, starts with an experimental, proof of principle approach. The aim of this chapter is to analyze whether current commercially available FCEVs and V2G technology, are technically suitable for providing balancing power in renewable energy systems and to highlight integration aspects. Here a commercially available hydrogen FCEV from the brand Hyundai, type ix35 FCEV forms the basis of the experimental set-up. Vehicle-to-Grid Modifications have been made to the vehicle and a variable power discharger connected to the Dutch national electric grid has been built. The discharger can simulate various loads to analyze the performance, internal power management and component behavior of the FCEV in V2G mode. Performance of the FCEV is analyzed while simulating several electricity balancing services such as spinning reserve, continuous power, power gradients, start-up time. Impact of basic parameters such as hydrogen fuel cost, electrical efficiency on the cost of generated electricity is discussed. Gaps in development and research, are highlighted such as dedicated power management strategies for V2G services as well as the degradation of fuel cell in V2G mode and its impact on the cost of generated electricity.

Chapter 3, Hyundai ix35 fuel cell electric vehicles: degradation analysis for driving and vehicle-to-grid usage, dives further into the topic of fuel cell degradation and is based on an experimental approach. Three Hyundai ix35 FCEVs are used for driving only and one Hyundai ix35 FCEV is used for both driving and V2G services. Fuel cell stack and vehicle usage data is gathered and analyzed. Then the relevance of several durability indicators is discussed with respect to the combined driving and V2G usage of FCEVs.

FCEVs can be integrated at a range of aggregation levels, for meeting various needs, in different environments and distinct geographic locations facing other renewable energy patterns and load demands. Integration of vehicles into energy systems and designing future concepts requires first a thorough analysis of the usage of vehicles and other energy and hydrogen generating, handling and consuming equipment. In addition to insights in energy use in the various sectors, technology trends, cost and development of new (hydrogen) technologies, operational aspects of end-users, are just a grasp of subjects related to future energy and transport systems. Once future integrated systems are designed, simulations can be run to analyze both the designed future energy system performance and the role of the integrated cars in the designed systems.

Chapter 4, titled Fuel cell electric vehicle-to-grid: emergency and balancing power for a 100% renewable hospital, adopts a heuristic approach to the modeling and system design. Hospitals are one of the most energy demanding buildings and require a high reliability of energy supply. A 100% renewable and reliable integrated transport and energy system for a hospital is designed using only urban energy sources. The car park at the hospital with 500 places can easily host the FCEVs providing balancing electricity. In addition to that, it is analyzed whether the FCEVs via V2G connections can replace the hospital's uninterruptable power supply (UPS) and emergency diesel power generator system. To analyze the system performance,

an hourly simulation is performed using local renewable energy and demand data as an input.

From an aggregation level of 500 cars in Chapter 4, Chapter 5, Fuel cell electric vehicle as a power plant: Fully renewable integrated transport and energy system design and analysis for smart city areas, aggregates around 2300 cars. The chapter describes a conceptual design framework based on a heuristic approach and covers the future energy consumption of the residential, services and road transport sectors in Europe. The chapter starts with an extensive gathering of European statistics of vehicle and energy use in urban environments. Integrated system requirements are formulated and result into a system design and technology choice. The technical and cost data of the chosen technology is gathered for a so-called 'Near Future' (around 2020) and 'Mid Century' (around) 2050 technology development scenario. This data serves as an input to the annual energy balance and is used to estimate the operational system performance and component systems sizing. Based on the technical analysis a levelized cost of energy analysis method is applied to the integrated system and performed for the two scenarios.

Chapter 6 is a detailed and a more extensive continuation of the conceptual design work of Chapter 5. Fuel Cell Electric Vehicle as a Power Plant: Techno-Economic Scenario Analysis of a Renewable Integrated Transportation and Energy System for Smart Cities in Two Climates, focuses on two specific locations: Murcia in Spain and Hamburg in Germany. The model design of Chapter 5 is extended by including seasonal hydrogen storage technology. Whereas here the simulation is performed with an hourly time step, based on five consecutive years of local climate and renewable energy data. This also allows to perform an inter-annual variability analysis of wind and solar energy production on the cost of energy. In contrast to Chapter 5 where long-term annual average European climate and renewable energy production and consumption data was used. The technical and cost data of the chosen technology in Chapter 5 for the so-called 'Near Future' scenario, are in Chapter 6 adjusted with cost estimations from literature for the period around 2025 instead of 2020.

The highest aggregation level is reached in Chapter 7, Fuel cell electric vehicles & hydrogen balancing national 100% renewable integrated transportation & energy systems, which explores the feasibility of systems with 1-20 million cars. An energy system is designed and modeled for five European countries adopting a heuristic approach. The energy systems are fully self-sufficient and 100% renewable and consist of the national electricity, space heating and road transport sectors. Existing country renewable energy scenarios for the year 2050 serve as an input for the simulation or are adapted to 100% renewable energy scenarios in case of not being 100% renewable. Hourly simulations of all energy flows for all five countries are done. The simulations are run for multiple consecutive years and will address, if any, inter-annual variability effects of renewable energy production on the seasonal hydrogen storage and balancing with FCEV2Gs.

Table 1-1 Relation between sub-questions and chapter topics.

		Sub-questions		
Chapter	**Topic**	**1**	**2**	**3**
2	Fuel Cell Electric Vehicle-to-Grid: Experimental Feasibility and Operational Performance as Balancing Power Plant	X		
3	Hyundai ix35 fuel cell electric vehicles: degradation analysis for driving and vehicle-to-grid usage	X		
4	Fuel cell electric vehicle-to-grid: emergency and balancing power for a 100% renewable hospital		X	
5	Fuel cell electric vehicle as a power plant: Fully renewable integrated transport and energy system design and analysis for smart city areas		X	X
6	Fuel cell electric vehicle as a power plant: Techno-economic scenario analysis of a renewable integrated transportation and energy system for smart cities in two climates		X	X
7	Fuel cell electric vehicles & hydrogen balancing national 100% renewable integrated transportation & energy systems		X	X

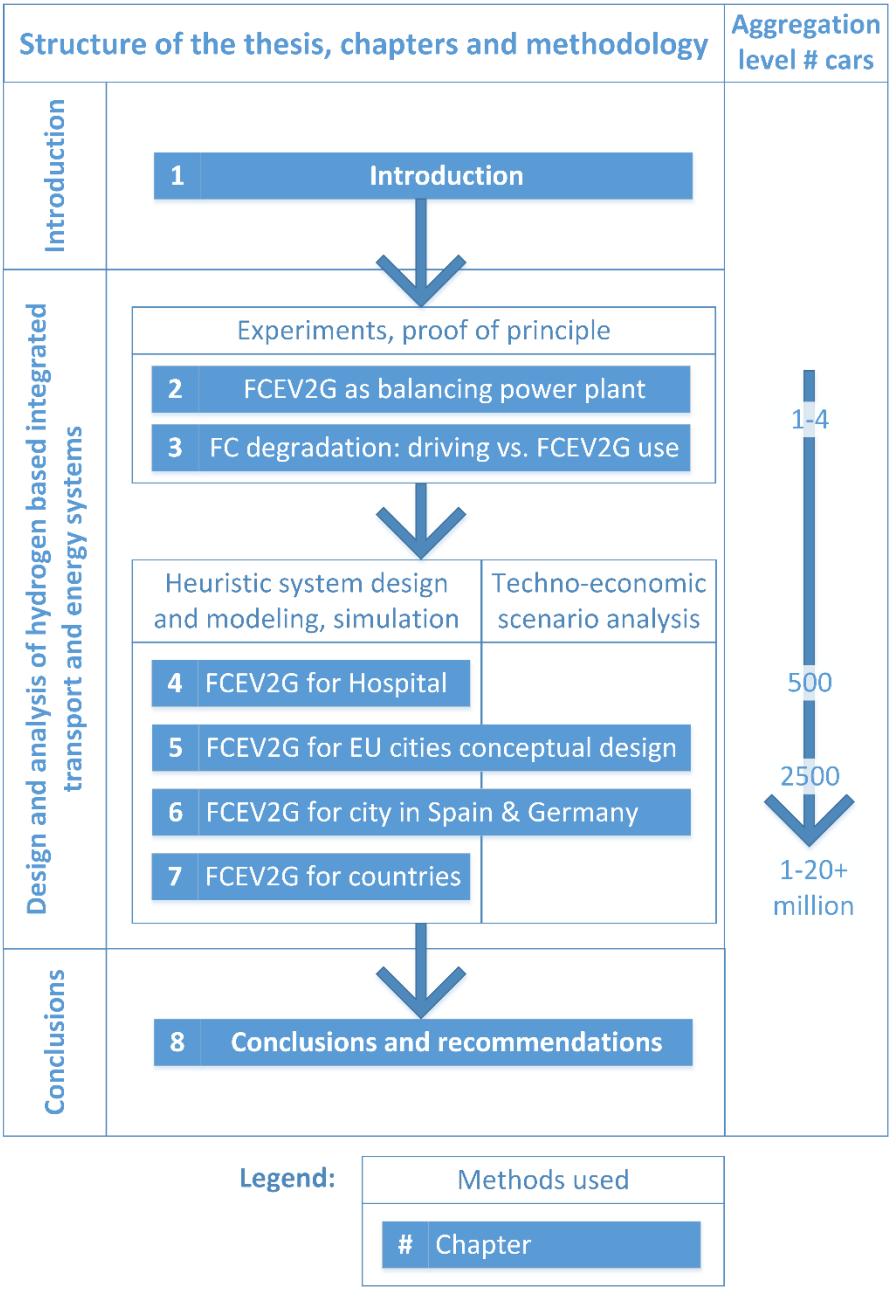

Figure 1-6 – Structure of this thesis, giving an overview between the 6 chapters, 3 research methods, and the aggregation level of cars in the chapters. The arrows and chapter numbers indicate the preferred reading order.

1.3.2 Scope and boundaries

System integration or sector coupling impacts the energy system at several levels: physical and communications (i.e. technologies, infrastructures), functions and services (e.g. for business, for consumers), market (regulation, transactions) [14], this thesis is limited to physical level and will relate outcomes to possible functions or services. The main focus is to explore the technical potential of V2G with FCEVs and to highlight any potential operational restrictions or integrations aspects.

The systems designs are focused on regions in Europe only. Hence, European statistics on energy consumption, vehicle usage, renewable energy sources, climate related data etc. are used. Abundant and widely available energy sources such as solar PV and wind form the basis to design the 100% renewable energy and transport systems on the different aggregation levels. Depending on the aggregation levels, other renewable energy sources such as hydropower or biomass have a minor role and their role in the energy mix are assumed not to expand compared to today's share.

Any storage of energy is in the form of hydrogen. There is a trade-off between number of balancing and storage options, and the ability to isolate and to explore the maximum technical potential of a specific technology within larger, complex and integrated energy systems. For that purpose, this thesis limits itself to use only FCEVs to convert stored hydrogen into electricity, even though a large variety of commercially proven technologies able to convert hydrogen into electricity exist (e.g. gas turbines).

As several hydrogen and fuel cell technologies are still in the early stages of development, here only technologies which had a Technology Readiness Levels of at least 7 (as defined by the European Commission) in 2015 or preferably higher are considered [228]. Quoting the European Commission's TRL 7 definition; " TRL 7 – system prototype demonstration in operational environment". In addition to the TRL requirement, in case of hydrogen technologies serving the same purpose, technologies being commercially more attractive or available at large power scales, have a preference. For example hydrogen production from electricity and water, only PEM or alkaline electrolyser technologies are considered, e.g. not solid oxide or alkaline membrane electrolysis technology. In a similar manner, only hydrogen fuel cell electric vehicles with proton exchange membrane fuel cells are considered, not solid oxide or any other type of future fuel cell being in early stages of development.

2 Fuel Cell Electric Vehicle-to-Grid: Experimental Feasibility and Operational Performance as Balancing Power Plant

The research presented in this chapter has been published in [229]. The work in this chapter tries to address research sub-question 1 "Are commercially available FCEVs suitable to act as balancing power plants?" and use an experimental, proof of principle method.

2.1 Abstract

The world's future energy supply will include intermittent renewable sources, such as solar and wind power. To guarantee reliability of supply, fast reacting, dispatchable and renewable back-up power plants are required. One promising alternative is parked and grid-connected hydrogen-powered Fuel Cell Electric Vehicles (FCEVs) in 'Vehicle-to-Grid' systems. We modified a commercial FCEV and installed an external 9.5 kW three-phase alternating current (AC) grid connection. Our experimental verification of this set-up shows that FCEVs can be used for mobility as well as generating power when parked. Our experimental results demonstrate that present-day grid-connected FCEVs can respond to high load gradients in the range of -760 % s^{-1} to +730 % s^{-1}, due to the parallel connection of the high voltage battery and the fuel cell stack. Virtual power plants composed of multiple grid-connected FCEVs could perform higher power gradients than existing fast-reacting thermal power plants with typical power gradients of 1.67 % s^{-1}. Hydrogen consumption in 9.5 kW AC grid-connected mode was 0.55 kg h-1, resulting in a Tank-To-Grid-AC efficiency of 43% on a Higher Heating Value basis (51% on a Lower Heating Value basis). Direct current to alternating current efficiency was 95%.

2.2 Introduction

As shares of intermittent renewable energy sources increase [152], stationary back-up power plants [152–154,230,231] will face even lower utilization factors in coming years and require expensive back-up power [152,153,155,156,232]. Passenger cars also face low utilization factors and could be put to better use while parked. On average, passenger cars drive 12,000 km per year [175] at an average annual speed of 45 km h-1 [175]. They are parked 97% of the time. One promising alternative to stationary back-up power plants is parked and grid-connected Electric Vehicles (EVs). EVs are able to provide power to the grid while parked, which is known as a 'Vehicle-to-Grid' (V2G) system [176,177]. The combined installed power capacity of passenger cars is enormous [2]. Every year, more than 80 million new cars are sold worldwide. Van Wijk et al. [2] multiplied the number of cars sold annually by 100 kW of future installed electric power per car and calculated that 8,000 GW of power capacity in cars would be sold each year. The installed power plant capacity worldwide is only around 5,000 GW [2].

There are three types of EVs that are suitable for delivering renewable power while parked: Battery Electric Vehicles (BEVs), Plug-in Hybrid Electric Vehicles (PHEVs) and Fuel Cell Electric Vehicles (FCEVs) [176,177]. This article focuses on FCEVs for V2G use. Commercially available FCEVs use Proton Exchange Membrane Fuel Cells (PEMFCs) to convert hydrogen into electricity and have a high voltage (HV) [233] battery connected in parallel [180–182]. The battery is used for regenerative braking and provides additional power for acceleration. This combination of FC and HV battery is capable of delivering almost every kind of electrical energy service [184], from balancing to emergency power back-up [185], primary reserve [177,186,187] or reconverting hydrogen from seasonal hydrogen energy storage in underground salt caverns [185]. Hundreds of grid-connected FCEVs sitting in parking lots could function as local power plants [221] and balance entire cities and countries [234], resulting in cost-effective balancing power for intermittent power sources [235].
Brauner et al. [153] identified the following operational requirements for balancing power plants in the future, once high shares of intermittent renewables have been achieved, and particularly in cases where large-scale pumped storage is limited or unavailable:

1. ability to perform high power gradients (≥ 0.05 % s^{-1} of all plants in the grid combined);
2. ability to be operated at low minimal generation (e.g. 15–20% instead of 40%);
3. high efficiency under partial load as well as nominal load (e.g. 25% instead of 50% partial load);
4. high number of start-ups and shutdowns (e.g. 0.5 start-ups and shutdowns per day instead of 0.25 start-ups and shutdowns per day);
5. ability to schedule cars in the face of an insecure day ahead energy prognosis.

Brauner et al. stated [153] that, for a load gradient of 15 GW h^{-1} in the grid, approximately 25 GW of flexible power plants with 0.0167 % s^{-1} of power capacity must be available for the German electricity system in 2020. However, the available capacity could be reduced to 8 GW if an ability of 0.05 % s^{-1} could be achieved. Aeroderivative open-cycle gas turbines and gas engines can reach 1.67 % s^{-1} under hot start conditions [236–239], reducing the available capacity to 0.25 GW – this amount corresponds to 25,000 cars at a rated capacity of 10 kW. Increasing the ability to perform high power gradients reduces the number of power plants in hot standby and economizes energy [153].
The question therefore arises as to whether grid connected FCEVs can fulfil these requirements. In order to gain insight and answers to this question, in this study, we analyzed the feasibility and operational performance of a commercial Hyundai ix35 FCEV [180] modified for V2G purposes combined with a 9.5 kW three-phase AC (Alternating Current) grid connection [240].

2.3 Experimental

A number of FCEV manufacturers [181,200,201] are developing FCEVs capable of providing power to electric appliances (Vehicle-to-Load, V2L), small grids or homes (Vehicle-to-Home, V2H) [202], although none claim to have connected an FCEV to a low-voltage national AC grid. At the Car as Power Plant project at The Green Village in The Netherlands, we modified a Hyundai ix35 FCEV to include a power outlet plug and designed a discharge unit that connects the car to the Dutch national electricity grid (see Figure 2-1).

Figure 2-1 Experimental Fuel Cell Electric Vehicle-to-Grid (FCEV2G) set-up at The Green Village, Delft University of Technology, Delft, The Netherlands.

We have conducted experiments with the car in idling mode (simulated 'spinning reserve' mode) since January 2016. Since July 2016, we have carried out further experiments with the car connected to the grid and delivering 9.5 kW three-phase AC power. We measured the performance of the FCEV in both V2G and idling mode by analyzing the data obtained from various sensors, the discharge unit, and a data logger installed in the car in MATLAB®.

The experimental set-up consisted of three main components:

1. a modified commercially available Hyundai ix35 FCEV [180,241] with a V2G DC (Direct Current) outlet plug;
2. a Vehicle-to-Grid DC-AC discharge unit (V2G-DCAC) that converts DC power in the range of 300-400V received from the FCEV into three-phase AC power at 380V. The power discharge setting can be manually defined in the V2G-DCAC. DC switching safety and grounding was incorporated in the V2G-DCAC unit;
3. a three-phase 380V AC grid connection including fuses and kWh meter.

2.3.1 Modified Hyundai ix35 FCEV for V2G Purposes

The modified Hyundai ix35 FCEV [180,241,242] has a 100 kW FC on board. In parallel, we connected an HV battery with Bi-directional High-voltage DC-DC Converter (BHDC) to the HV Junction Box (HVJB) [241,242]. These components and connections are illustrated in Figure 2-2, which provides a scheme of the electrical architecture of the FCEV and the modifications.

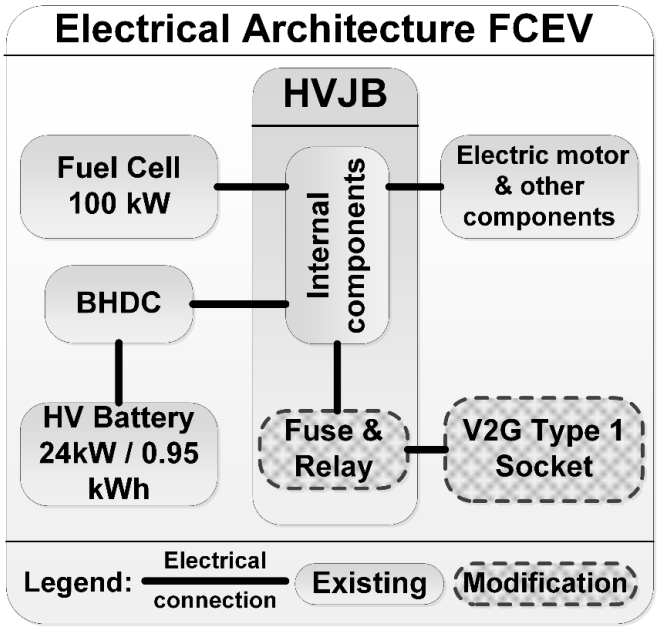

Figure 2-2 Scheme of electrical architecture of the FCEV and V2G modification.

The battery has an energy capacity of 0.95 kWh and a maximum power output and input of 24 kW [242]. The electric motor that powers the wheels has a maximum power of 100kW. The modifications consisted of an extra parallel connection in the HVJB for the DC outlet protected by a fuse [243] and activated by a relay switch [244]. We replaced the front bumper of the car with an adapted version to accommodate a Type 1 SAE J1772 [245] socket (see Figure 2-3).

Figure 2-3 V2G Type 1 Socket integrated in the front bumper.

We used the socket for the DC connection to the V2G-DCAC discharge unit. Finally, we installed a software update for the car along with a dashboard activation button (see Figure 2-4) that also activates the Cold Shut Down procedure (CSD).

Figure 2-4 New dashboard V2G activation button also initiates Cold Shut Down.

We made no further adaptions to the FCEV. We maintained the vehicle's road access permit, in accordance with the requirements of the Dutch National Vehicle and Driving License Registration Authority (RDW). We logged the FC and HV battery operating voltage, current, and other power system-related parameters at a frequency of 1 to 5 Hz using a CAN bus data logger [246].

2.3.2 Vehicle-to-Grid DC-AC Discharge Unit

We fitted every component of the V2G-DCAC unit in a weather-proof enclosure, see Figure 2-5.

Figure 2-6 illustrates the simplified electrical architecture of the V2G-DCAC and its main components. We connected the FCEV with the V2G-DCAC via a Type 1 socket and cable with plugs. We mounted a red-colored combined start-up and shutdown button that must be unlocked with a key. Cooling fins on the back of the enclosure enhanced possible heat dissipation for the three-phase grid-tie inverter [247]. The DC input and AC output voltages and currents were monitored every five minutes by the inverter and sent to an internet server. We programmed an Arduino shield [248] to establish a connection between the FCEV power outlet and the three-phase AC grid connection. The proximity detection and control pilot [245] and the lockable start button served as inputs for the control logic. The Arduino shield controlled the inverter, the DC relay, the three-phase switches, the relay and the Red-Blue-Green (RGB) LED strip indicating the current status. We installed a galvanic isolation transformer between the three-phase switches and the AC grid connection to prevent any stray voltage incidents [249].

Figure 2-5 V2G-DCAC unit connected to the FCEV.

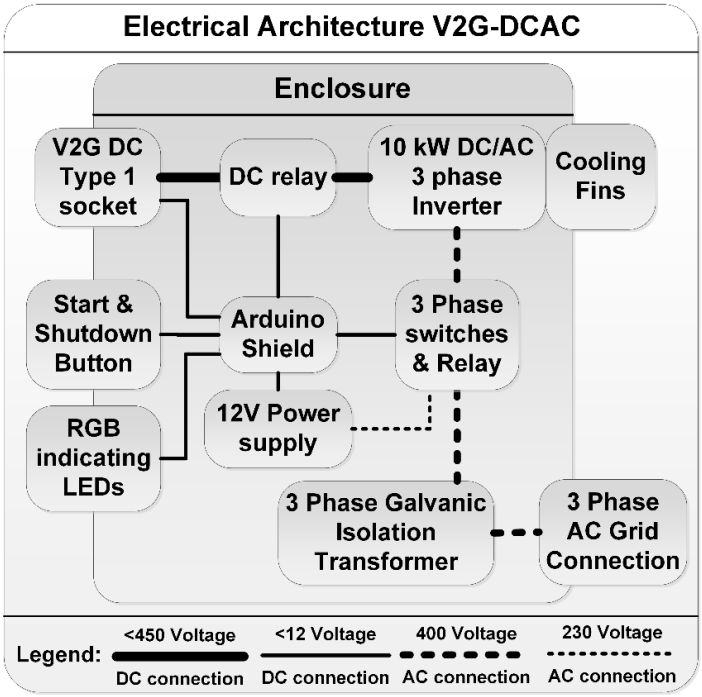

Figure 2-6 Simplified electrical architecture of the V2G-DCAC connecting the FCEV to the AC grid.

2.3.3 AC Grid Connection

The three-phase 400 V AC grid connection included a C-characteristic circuit breaker, a Class B ground fault circuit interrupter and an electricity meter.

2.3.4 Operation and Safety Fuel Cell Electric Vehicle-to-Grid

To commence delivering power to the grid, we start the inverter and synchronize with the electric grid upon activating the combined start-up and shutdown button. The inverter can be started up either before or after connecting the V2G cable and starting up the FCEV. To stop delivering power to the grid, we first switch off the AC load, in this case by switching off the inverter. The FCEV is programmed such that the V2G DC HV relay [244] opens the instant we switch the FCEV in V2G mode off or disconnect a load. This strict switch-off sequence could be avoided by applying DC arc suppression and contact protection [233,250,251].

2.3.5 Test Time, Start-up Time and Power Gradient Measurements

We drove the FCEV prior to performing each test and therefore only examined 'warm starts' in V2G mode. During the V2G tests, we elected to start the FCEV up before applying any load (switching on the inverter), which enabled us to monitor load-switching behavior. The data logger in the FCEV was actively monitoring before any load was applied; therefore the time during which the FCEV was switched on, t_{test}, was always somewhat longer than the grid connection time, t_{grid}. We calculated this as the difference between the end time and start time of the V2G tests using Equation (2.1):

$$t_{test} = t_{end} - t_{start} \tag{2.1}$$

This difference in test time with respect to the grid connected time is called the Grid Connect/Disconnect time, $t_{GC/D}$. The Grid Connect/Disconnect time was partly defined by the inverter start-up and grid frequency synchronization time (approximately 1 minute) and the user's lingering time. We calculated this using Equation (2.2):

$$t_{GC/D} = t_{test} - t_{grid} \tag{2.2}$$

We calculated the gross electric power, $P_{component,e,gross}$, of the component, either the FC or the HV battery, by the product of the voltage, $U_{component}$, and gross current, $I_{component,gross}$, of the FC stack and battery every 0.2 s (5 Hz sample frequency) using Equation (2.3):

$$P_{component,e,gross} = U_{component} \cdot I_{component,gross} \tag{2.3}$$

We measured the upward and downward power gradients of the FC and HV battery in V2G mode. The power gradients, $\Delta P\ \Delta t^{-1}$, are expressed in kW s^{-1} and were calculated using Equation (2.4):

$$\Delta P\ \Delta t^{-1} = \left(P_{component,e,gross\ @\ t+0.2s} - P_{component,e,gross\ @\ t} \right) / \ 0.2\ s \quad (2.4)$$

The power gradients are also expressed in % change of maximum power per second % s^{-1}, negative for downward gradients and positive for upward gradients, as shown in Equation (2.5):

$$\Delta P\ \Delta t^{-1} = \Delta P\ \Delta t^{-1} / P_{V2G\ DC\ max} \quad (2.5)$$

The maximum V2G DC power, $P_{V2G\ DC\ max}$ was 10 kW. Electric powers were measured every 0.2 seconds (5 Hz sample frequency).

2.3.6 Efficiency FCEV2G and Hydrogen Consumption

The efficiency of the combined FCEV and V2G-DCAC system is called Tank-To-Grid AC (T2G-AC) efficiency, $\eta_{TTG\text{-}AC}$, was calculated using Equation (2.6):

$$\eta_{T2G-AC} = \left(E_{AC} + \Delta E_{HV\ Bat} \right) / E_{\mathrm{H2}} \quad (2.6)$$

where E_{AC} is the three-phase AC electrical energy delivery to the grid. $\Delta E_{HV\ Bat}$ is the difference in HV battery energy. E_{H2} is the hydrogen energy consumption, which we calculated using Equation (2.7):

$$E_{\mathrm{H2}} = \Delta m_{\mathrm{H2}} \cdot HHV \quad (2.7)$$

based on the hydrogen HHV of 39.41 kWh kg^{-1}. We calculated the difference in HV battery energy by multiplying the difference in State Of Charge, ΔSOC, of the HV battery at the start and the end of the test with the maximum energy capacity, $E_{HV\ Bat,\ max}$, of 0.95 kWh [242], using Equation (2.8):

$$\Delta E_{HV\ Bat} = \Delta SOC \cdot E_{HV\ Bat,\ max} \quad (2.8)$$

This is a simplification of the HV battery characteristics since capacity according to C-rate and temperature [252,253], but we were unable to take a more accurate approach due to lack of battery-specific information. We therefore included the charging and discharging efficiency of the HV battery in the $\eta_{T2G\text{-}AC}$, as well as the BHDC conversion efficiency. We calculated the hydrogen consumption, Δm_{H2}, by the difference in hydrogen density at the start and end of the test, ρ_{start} and ρ_{end},

multiplied by the fixed volume capacity of 0.144 m^3 [180] of the hydrogen tanks, V_{tanks}, on board as shown in Equation (2.9):

$$\Delta m_{H2} = V_{tanks} \cdot \left(\rho_{start} \left[p_{tanks,start}, T_{tanks,start} \right] - \rho_{end} \left[p_{tanks,end}, T_{tanks,end} \right] \right) \quad (2.9)$$

We calculated hydrogen density using measured hydrogen tank pressures, $p_{tanks,start}$ and $p_{tanks,end}$, and temperatures, $T_{tanks,start}$ and $T_{tanks,end}$, at the start and end of the test and REFPROP software [254]. We calculated inverter efficiency, η_{DCAC}, by dividing the delivered AC Energy, E_{AC}, by the incoming DC energy, E_{DC}, as shown in Equation (2.10):

$$\eta_{DCAC} = E_{AC} / E_{DC} \quad (2.10)$$

We calculated the Tank-to-Grid DC efficiency, $\eta_{T2G\text{-}DC}$, which may be considered an approximation of the efficiency of the FC and HV Battery system, as per Equation (2.11):

$$\eta_{T2G-DC} = \eta_{T2G-AC} / \eta_{DCAC} \quad (2.11)$$

We calculated the hydrogen consumption rate, $\Delta m_{H2}\, \Delta t^{-1}$, by dividing the hydrogen consumption obtained in Equation (2.9) by the duration of the test obtained in Equation (2.1), as shown in Equation (2.12):

$$\Delta m_{H2} \Delta t^{-1} = \Delta m_{H2} / t_{test} \quad (2.12)$$

We obtained the hydrogen consumption in 'spinning reserve' mode [186] by keeping the FCEV in idling mode. In the spinning reserve case, no power was delivered to either the grid or the electric motor. The cabin heating and cooling, entertainment and navigation devices and lighting were all switched off. During the V2G tests, in addition to delivering power to the grid, the FC and HV battery also deliver power to the on-board devices which cannot be switched off manually, such as FC auxiliary components and instruments. All of the calculated efficiencies include any hydrogen and HV battery energy use by the FCEV during the Grid Connect/Disconnect time.

2.4 Results and Discussion

2.4.1 Selection of Tests

We have carried out experiments with the car in idling mode (simulated 'spinning reserve' mode) since January 2016. The duration of all 'spinning reserve' tests was over nine hours, which equates to more than 0.35 kg of hydrogen consumption. Since July 2016, we conducted tests with the car connected to the grid and delivering three-phase 9.5 kW AC power. Although ambient conditions such as

temperature, wind speed, wind direction and solar radiation can all influence the cooling of the FC in 9.5 kW AC V2G mode, we did not investigate these factors for the purposes of this study. We selected tests based on similar coolant temperature and pump angular velocity behavior during the test. From the period between July 2016 and April 2017 (see Table 2-1), we selected eight V2G tests.

Table 2-1 Maximum downward (↓) and upward (↑) power gradients of the FC and HV battery expressed in kW s-1 and % s-1 of maximum power output. Eight tests at 9.5 kW AC V2G conditions were performed and the values averaged.

	Date	t_{test}	$t_{GC/D}$	↓ $\Delta P_{FC}\,\Delta t^{-1}$		↑ $\Delta P_{FC}\,\Delta t^{-1}$		↓ $\Delta P_{HV\,BAT}\,\Delta t^{-1}$		↑ $\Delta P_{HV\,BAT}\,\Delta t^{-1}$	
#	**DD-MM-YY**	**h:mm**	**h:mm**	**kW s^{-1}**	**% s^{-1}**	**kW s^{-1}**	**% s^{-1}**	**kW s^{-1}**	**% s^{-1}**	**kW s^{-1}**	**% s^{-1}**
1	15-08-16	5:51	0:05	-43	-430	73	730	-77	-770	32	320
2	16-08-16	7:05	0:05	-48	-480	72	720	-76	-760	30	300
3	13-02-17	6:05	0:05	-47	-470	73	730	-78	-780	51	510
4	14-02-17	5:59	0:05	-53	-530	72	720	-74	-740	38	380
5	15-02-17	6:06	0:04	-47	-470	73	730	-76	-760	41	410
6	17-02-17	6:06	0:04	-46	-460	74	740	-77	-770	57	570
7	11-04-17	5:56	0:03	-48	-480	73	730	-77	-770	54	540
8	12-04-17	6:26	0:19	-42	-420	72	720	-76	-760	39	390
Mean				-47	-470	73	730	-76	-760	43	430
Sample standard deviation				3	34	1	5	1	11	10	100

The results of the V2G test conducted on February 13, 2017 are used as an illustrative example throughout this paper. Figure 2-7 shows the coolant temperature entering and leaving the radiator during the entire duration of the February 13, 2017 test.

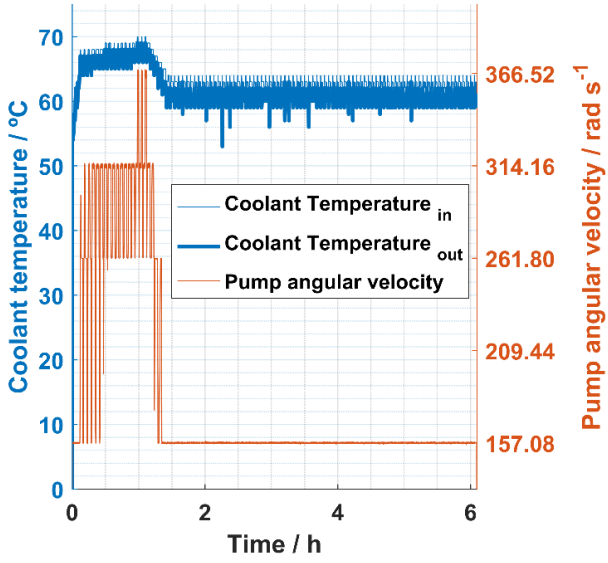

Figure 2-7 Coolant temperatures and pump angular velocity at 9.5 kW AC V2G for the entire test duration of 6 hours and 5 minutes on February 13, 2017.

Figure 2-8 shows a more detailed pattern for the period between 6000 to 7000 seconds for the coolant temperature difference and pump angular velocity.

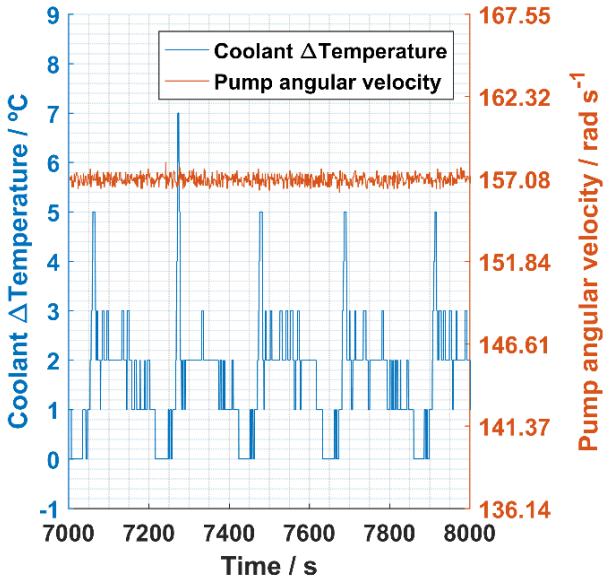

Figure 2-8 Pump angular velocity and coolant temperature difference for the 7000 to 8000 seconds period for the test on February 13, 2017.

All eight V2G tests selected showed similar coolant temperature and pump angular velocity behavior and were characterized by a period of an elevated pump angular velocity of up to 367 rad s^{-1} and temperatures of up to 70 °C. Subsequently, the coolant temperatures and pump angular velocity decreased and stabilized to 60-64 °C and 157 rad s^{-1}, respectively. The exceptions were tests 5 and 8, in which there was a short period at the end of the test with elevated coolant pump angular velocity and temperatures.

2.4.2 Power Gradients

As an example, Figure 2-9 shows the gross electric power of the FC and HV battery over a period of 6 hours and 5 minutes of the test on February 13, 2017.

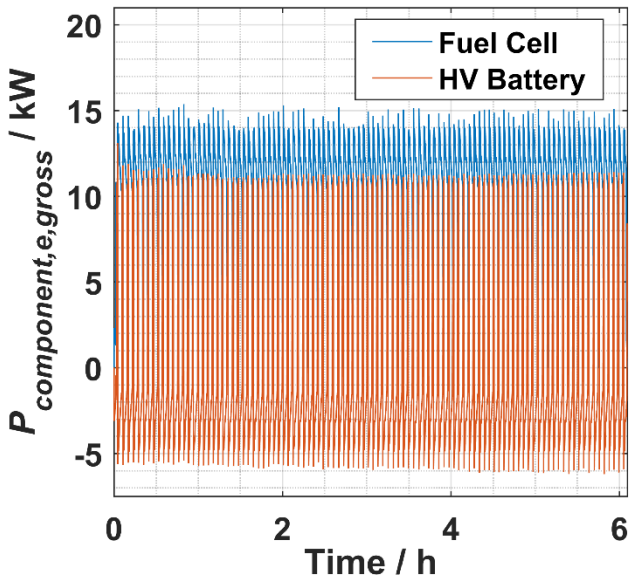

Figure 2-9 FC and HV battery gross electrical power for the entire test duration of 6 hours and 5 minutes on February 13, 2017.

Figure 2-10 zooms into the period from 7000-8000 seconds (1 hour 56 minutes to 2 hours 13 minutes). Although the V2G AC output was fixed at a constant 9.5 kW, the FCEV power management alternated between FC and HV battery power. The FC delivered power to the grid and recharged the HV battery. Figure 2-10 and Figure 2-11 show that once the HV battery reached an *SOC* of 57.5%, the FC was switched off and HV battery was discharged to an *SOC* of 42.5%.

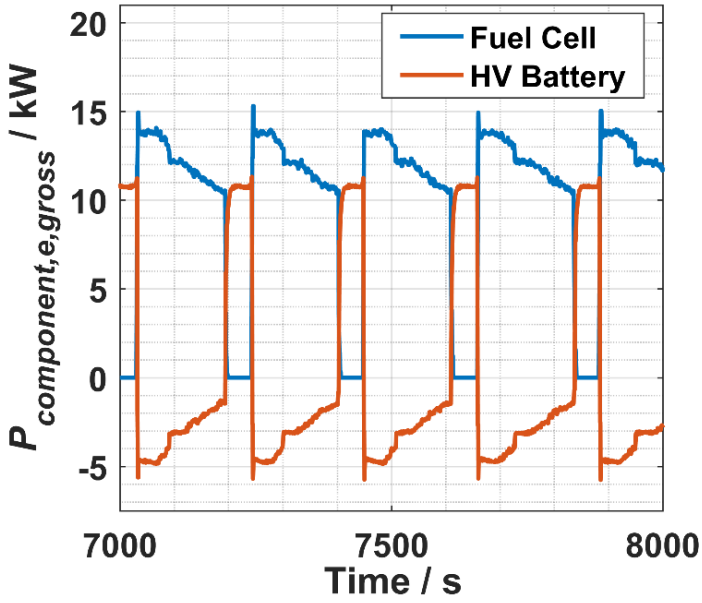

Figure 2-10 FC and HV battery gross electrical power for the 7000 to 8000 seconds period for the test on February 13, 2017.

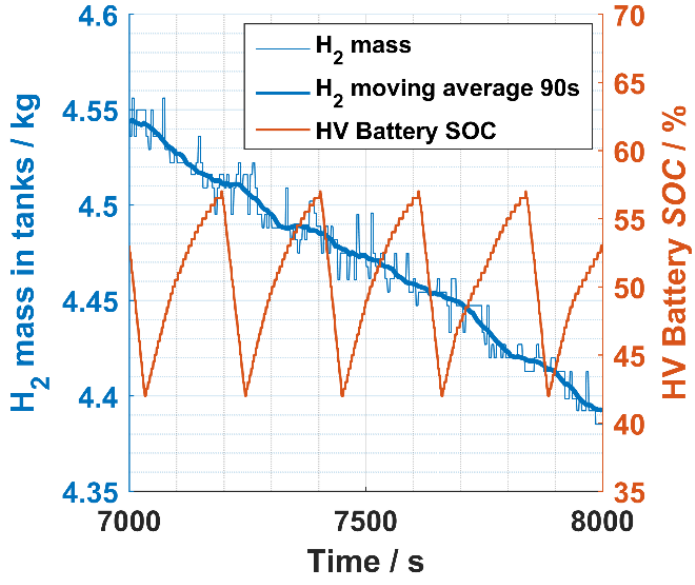

Figure 2-11 Hydrogen mass in tanks and HV battery state of charge (SOC) cycling for the 7000 to 8000 seconds period for the test on February 13, 2017.

The power management switched between FC and HV battery power. The executed V2G measurements can therefore also be used to analyze the power gradients of the FC and HV battery. The results of the power gradient analysis are set out in Figure 2-12, Figure 2-13 and Table 2-1.

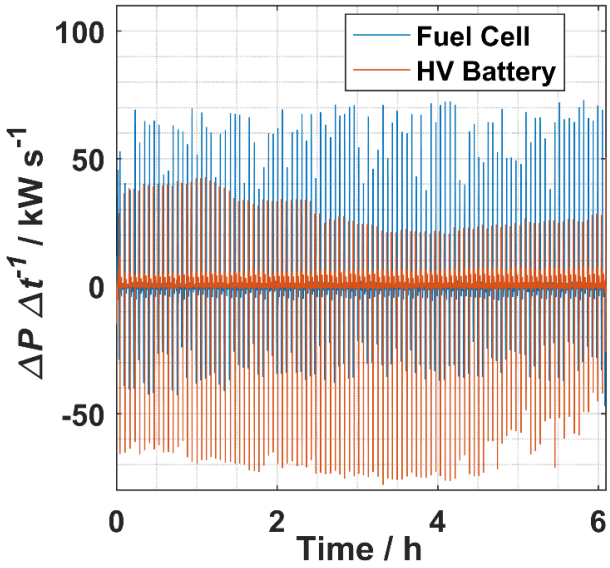

Figure 2-12 Downward and upward power gradients of the FC and HV battery for the entire test duration of 6 hours and 5 minutes on February 13, 2017.

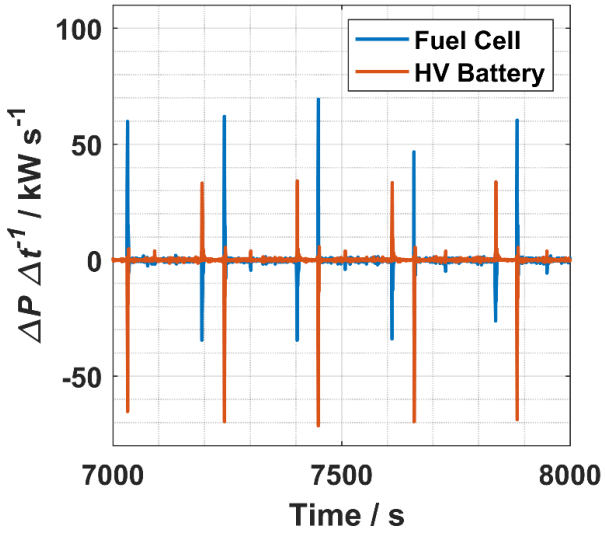

Figure 2-13 Downward and upward power gradients of the FC and HV battery for the 7000 to 8000 seconds period for the test on February 13, 2017.

The mean maximum downward and upward power gradients of the FC were -47 kW s^{-1} (-470 % s^{-1}) and +73 kW s^{-1} (+730 % s^{-1}) respectively, at the sample frequency of 5 Hz. Sample standard deviations are 3 and 1 respectively. The mean maximum downward and upward power gradients of the HV battery are -76 kW s^{-1} (-760 % s^{-1}) and +43 kW s^{-1} (+430 % s^{-1}) respectively, at the sample frequency of 5 Hz. Sample standard deviations are 1 and 10 respectively. From these results, we concluded that the FC and the battery in particular are capable of responding many times faster than fast-reacting small-scale (< 60MW) aeroderivative open-cycle gas turbines and gas engines, with respective maximum values of 0.3% s^{-1} for cold start and 1.67 % s^{-1} for hot start [236–239]. General Electric's LM6000 Hybrid Electric Gas Turbine combines a fast-reacting gas turbine with a large battery [255], which could be viewed as a forerunner of even faster-reacting combined FC battery balancing power plants. Combining the output of millions of grid connected FCEVs would create so-called Virtual Power Plants [198,256] with – in theory – unlimited capacities and could balance entire cities [235] and national electricity grids. If the FC and HV battery power were combined, even higher absolute downward and upward power gradients of -123 kW s^{-1} and +116 kW s^{-1} respectively could be achieved (taking into account the 5Hz sample frequency). Relative power gradients in % s^{-1} can be tailored to the requirements of energy services [184,186,187] by selecting different FC and battery power capacities.

The impact of additional V2G load ramps and different power management strategies on the durability of the combined FC and battery system is yet to be quantified. Many studies focus primarily on V2G impact [257–262] on batteries in BEVs, but little is known about how the V2G mode will impact FC degradation in FCEVs.

It is estimated that, during a vehicle's lifetime, the powertrain faces 300,000 full load power gradients (0-100% rated power) [263]. Several studies show that start-ups/shutdowns and high load cycles can reduce FC durability [264,265]. In the V2G mode experiments performed in this study, load ramps were limited to approximately 10 kW, corresponding to only 10% rated power of the FC in the car, which is relatively small in comparison to the full load ramps in driving mode.

Approximately 38,500 start-up/shutdown cycles take place during the 5,500 hour life of an FCEV [263]. If FCEVs were never switched off and instead continuously used for either driving or V2G energy services, start-up/shutdowns would be eliminated. Additional degradation due to V2G load cycles (less than 10% rated power) could possibly be compensated for by a reduction in start-ups/shutdowns. Furthermore, a smarter power management system of both FC and HV battery could be applied or ultra-capacitors introduced [266].

2.4.3 Start-up Time

FCEVs are already capable of cold start-up time to 50% of their rated power within ten seconds at an ambient temperature of 20 °C and within 20 seconds at -20 °C [267]. In our V2G tests using the modified Hyundai ix35, we measured cold start-up times of less than 5 s at ambient temperatures. Driving to cruising speed can already be achieved within 11 seconds at -20 °C [268], which is comparable to V2G power

of 10 kW (10% of the rated FC power). The newer model Toyota Mirai FCEV is even able to provide full stack power of 114 kW at -30 °C within 70 seconds [181].
In conclusion, today's FCEVs have extremely fast start-up times for providing V2G services to full rated power even at very low ambient temperatures. If FCEVs were never switched off and continuously used for either driving or V2G energy services, cold start-up temperature could even become irrelevant.
As described in Section 2.3, the way we started our V2G tests incurred additional start-up and grid frequency synchronization time. To further reduce grid connection times, the inverter could also be switched on before connecting and turning on the FCEV, eliminating additional start-up and grid frequency synchronization time from the inverter. Moreover, inductive discharging instead of conductive discharging (by cable) could reduce any further grid connection time [269–272], and likewise specialized FCEV V2G inverters with reduced reaction time and tailored Maximum Power Point Tracking or combining the V2G inverter with solar photo-voltaic inverters [273].

2.4.4 System Efficiencies & Hydrogen Consumption in V2G Mode

The hydrogen content in the two tanks and HV battery state of charge during the illustrative test on February 13, 2017 are shown in Figure 2-11, Figure 2-14 and further V2G test results are presented in Table 2-2. Fluctuations and 1 °C accuracy of the tank temperature sensors have an impact on the hydrogen density calculations (Equation (2.9)), therefore we applied a 90-second moving average to the hydrogen mass calculation and used this in our hydrogen consumption calculations.

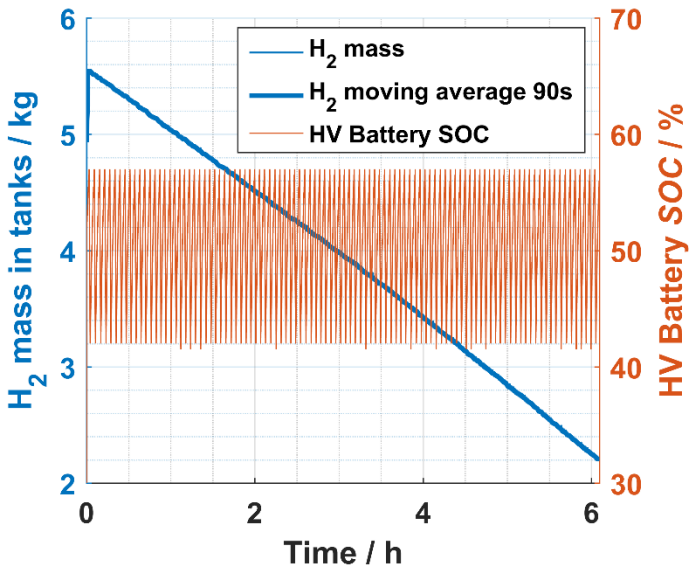

Figure 2-14 Hydrogen mass in tanks and HV battery state of charge (SOC) cycling for the entire test duration of 6 hours and 5 minutes on February 13, 2017.

Table 2-2 Test durations with hydrogen consumption rates and corresponding AC and DC system efficiencies.

	Date	t_{test}	$t_{GC/D}$	Δm_{H2}	$\Delta m\ \Delta t^{-1}$	η_{T2G-AC}	η_{DCAC}	η_{T2G-DC}
#	**DD-MM-YY**	**h:mm**	**h:mm**	**kg**	**kg h^{-1}**	**%**	**%**	**%**
1	15-08-16	5:51	0:05	3.28	0.56	42	95	44
2	16-08-16	7:05	0:05	3.96	0.56	42	95	45
3	13-02-17	6:05	0:05	3.34	0.55	43	95	45
4	14-02-17	5:59	0:05	3.33	0.56	42	95	45
5	15-02-17	6:06	0:04	3.39	0.56	43	95	45
6	17-02-17	6:06	0:04	3.38	0.55	43	95	46
7	11-04-17	5:56	0:03	3.33	0.56	43	95	46
8	12-04-17	6:26	0:19	3.51	0.54	42	95	44
Mean				3.44	0.55	43	95	45
Sample standard deviation				0.22	0.01	1	0	1

The average V2G test duration was approximately six hours with a mean hydrogen consumption of 3.44 kg and consumption rate of 0.55 kg h^{-1} per test. The maximum capacity of the hydrogen tank is 5.6 kg, with a minimum operating pressure of approximately 2.5 MPa; 5 kg for V2G energy services and the remaining hydrogen is enough to fulfill average European daily driving [175] requirements and reach a hydrogen filling station before using the car in V2G mode again. At a consumption rate of 0.55 kg h^{-1}, approximately nine hours of AC power can be delivered to the grid on a full tank, resulting in 86 kWh. The mean η_{T2G-AC}, η_{DCAC} and η_{T2G-DC} efficiencies were 43% (51% on an LHV basis), 95% and 45% (53% on an LHV basis) respectively. The values of the efficiencies we calculated were consistent throughout all the tests. As discussed in Section 2.4.2, η_{T2G-DC} is an approximate value of the efficiency of the FC and HV battery system. η_{T2G-DC} is in line with the 43-51% FC system efficiencies of FCEVs in driving mode at 10-15% rated power reported in the literature [269,274,275]. The η_{T2G-DC} of 45% (53% on an LHV basis) is close to the reported Hyundai ix35 FCEV FC system DC efficiency of 46.8% (55.3% on an LHV basis) [276]. Current automotive FC stacks with power ranges of 80-100 kW, used as primary power source in FCEVs (not in a fuel cell range extender configuration), show highest FC system efficiency at 10-15% rated power [274,275]. Future automotive FC system developments aim for higher system efficiencies at even lower rated powers, as driving cycles, such as the NEDC, consist of high power frequencies below 10% rated power [277,278]. As mentioned in our introduction, the ability to operate balancing plants at low minimal generation (e.g. 15–20% instead of 40%) is important. In the performed V2G tests, the PEMFC was operating at only 10-15% of its maximum generation capability, see Figure 2-10. It is possible for FCEVs to generate more power, although this would require a better understanding of the cooling capacity of the radiator [279] when parked and the maximum operating temperature of the PEMFC. Tests at different DC powers in the range of 0-10 kW done with the same set-up, show that 10 kW gives the highest V2G efficiency [280]. Conducting further tests at DC powers above 10 kW would provide full insight into the partial load and optimum V2G efficiency.

At relative low FC rated power of 10-15%, there is less water production on the cathode side of the FC. Depending on the amount of air supplied by the air-blower membrane humidification problems can occur with different and opposite effects [281]. A relative low air stoichiometry or sometimes called cathode stoichiometric factor, a relative low air flow rate is sent to the cathode channel and can result in a reduced removal of produced water [281,282]. Whereas at a high air stoichiometry, an increase of the water removal rate can result in membrane dehydration and higher membrane resistance [281]. When delivering 10 kW DC power to the grid and the fuel cell is producing power, see Figure 2-10, calculated average FC stack air stoichiometry is in the range of 2 up to 6 According to Heuer et al. [283] air stoichiometry above 3 can be considered high and increase the probability of accelerated degradation. Air stoichiometry at individual cells and within individual cells [284] can differ significantly from the calculated FC stack average, for example for individual cells at the inlet there is a probability of too low membrane humidification whereas for cells at the outlet there is a probability of too high membrane humidification [281–283].

Idling, low load and low current density are associated with cell potentials of 0.87-0.90 V and can result in accelerated degradation [285–291]. When delivering 10 kW DC power to the grid, average single cell potential calculated from the total FC stack voltage is in the range of 0.75-0.84V, based on the total number of 434 cells [292]. Although average calculated cell potential is lower than 0.87 V, cell potentials of individual cells can differ from the calculated average and possibly face higher potentials. Extended periods at high cell potentials resulting into accelerated degradation, can be reduced by smart hybridization between HV battery and FC [286,293], especially if the V2G power production profile is known upfront it could be incorporated in the power management. The influence of the V2G power production on the degradation of the FC is still a relatively uncovered topic in literature.

The mean $\eta_{T2G\text{-}AC}$ of 43% (51% on an LHV basis) gives a specific electricity production of 17 kWh kg^{-1} H2. With current hydrogen prices of \$10-\$14 kg^{-1} at hydrogen fueling stations in California [294,295] and 9.5€ kg^{-1} in Germany [296], this would result in an V2G electricity price of respectively 590-825 \$ MWh-1 and 560 € MWh^{-1}, when considering the price of dispensed hydrogen only. Hydrogen fueling infrastructure is still at a development stage, so the cost of hydrogen fuel for fuel cell powered road transport is not yet comparable to conventional transportation fuels [296]. The current hydrogen prices are initial, politically motivated prices jointly determined by the project partners [296]. There is a high potential of lower hydrogen prices at fueling stations with economies of scale [103,297–299], i.e. when the number of FCEVs (including vans, buses and trucks) increase, hydrogen production and refueling infrastructure costs decrease and result in a dispensed hydrogen price of 2-4 € kg^{-1} [297–301]. Combined with a future expected maximum FC system efficiencies of 60% (70% on an LHV basis) [126,267] and similar $\eta_{T2G\text{-}AC}$ or $\eta_{T2G\text{-}DC}$, V2G electricity price would become 85-170 € MWh^{-1}, when considering the price of dispensed hydrogen only.

In the period of 2015-2017 in the Californian electricity market, the 5-minute and 15-minute positive imbalance prices rose above 250 \$ MWh^{-1} for respectively 0.9%

and 0.3% of the year, with some periods above 1000 $ MWh^{-1} [302,303]. In 2017 in the German electricity market, imbalance prices above 85, 170, 250 and 560 € MWh^{-1} occurred respectively for 8.8%, 0.9%, 0.3% and 0.1% of the year [304,305]. Future business models for FCEV2Gs participating in electricity imbalance markets rely on future FC system efficiency, imbalance and hydrogen prices. Other relevant business model parameters need additional research. For example the future costs of V2G infrastructure, FC systems and FC system additional degradation, operation and maintenance due to the V2G load cycles.

2.4.5 Hydrogen Consumption in Spinning Reserve Mode

Table 2-3 shows the hydrogen consumption in the 'spinning reserve' (or idling mode) tests. Tests conducted for varying durations on different dates throughout the year revealed a relatively constant hydrogen consumption rate of approximately 0.040 kg h^{-1}. Taking the 5 kg hydrogen mass available for V2G purposes mentioned in Section 2.4.4, the maximum running time in spinning reserve mode is projected to be 125 hours – a little over five days. A hydrogen consumption rate of 0.040 kg h^{-1} corresponds to an average hydrogen power flow of 1.6 kW (on an HHV basis). At an estimated FC stack gross efficiency of 40 %, approximately 0.6 kW electrical power is produced to power the FCEV's auxiliary devices. This long-term idling power consumption could possibly be reduced in a purpose-built V2G FCEV.

Table 2-3 Results from 'spinning reserve' tests.

	Date	t_{test}	Δm_{H2}	$\Delta m\ \Delta t^{-1}$
#	**DD-MM-YY**	**h:mm**	**kg**	**kg h^{-1}**
1	19-01-16	11:02	0.52	0.047
2	07-04-16	09:00	0.39	0.043
3	08-04-16	09:03	0.37	0.041
4	21-07-16	10:00	0.39	0.039
5	25-07-16	09:14	0.35	0.037
6	27-07-16	46:30	1.76	0.038
7	01-08-16	45:28	1.59	0.035
8	03-08-16	49:03	2.04	0.041
Mean			0.92	0.040
Sample standard deviation			0.73	0.004

During the 'spinning reserve' tests, the FCEV is in idling mode and the HV battery and FC are only powering the FC auxiliary components and instruments, see Section 2.3.6. Because the FC power production is low, so is the water production. High calculated average FC stack air stoichiometry values above 10 occur for more than 70% of the time during the 'spinning reserve' tests. This could result in a high removal rate of produced water, low humidification of the membrane and therefore higher probability of accelerated degradation [283]. Additional research focused on the conditions at individual cells could provide more insight into the effects of prolonged 'spinning reserve' operation on the rate of degradation.

Cell potentials higher than 0.87V and up to 1.5 V can cause accelerated degradation and are associated with operating conditions such as idling, no load, prolonged periods of no use, start-up and shutdown [286,290]. For an FCEV not used for V2G purposes (driving only) and depending on the usage profile, idling time at cell potentials of approximately 0.9 V could amount up to 1000h over a vehicle's 5500h of operational life [306]. Time spent at open circuit voltage (OCV) of approximately 0.95 V during no load conditions could be over 100h [306]. Yu et al. show there is a significant lower durability for an equal number of hours spent at OCV than at idle conditions [307]. For 25% of the time spent during the 'spinning reserve' tests, the average calculated cell potential from the total FC stack voltage was higher than 0.87V and could cause accelerated degradation. The impact of extended periods of time at high potentials during the 'spinning reserve' tests and their impact on degradation need to be investigated further. Also smarter hybridization between HV battery and FC and V2G operation integrated in a flexible power management can possibly reduce operating time at high potentials [286,293].

Apart from taking part in the imbalance market as described in Section 2.4.4, Poorte et al. show that FCEV2Gs are able take part in the Frequency Containment Reserves (FCR) and automatic Frequency Restoration Reserves (aFRR) markets [308]. E.g. Hundred FCEV2Gs each providing 10 kW V2G power would represent 1 MW and have a hydrogen consumption rate of 4 kg h^{-1}. With the current hydrogen prices of \$10-\$14 kg^{-1} at hydrogen fueling stations in California [294,295] and 9.5€ kg^{-1} in Germany [296], this would result in an 'spinning reserve' fuel price of respectively 40-56 \$ MW^{-1} h^{-1} and 38 € MW^{-1} h^{-1}, when considering the price of dispensed hydrogen only. Annual mean prices of ancillary services markets in 2014 in the United States of America range from 1-40 \$ MW^{-1} h^{-1} [309] and FCR and aFRR prices in 2017 in Germany range from 1-23 € MW^{-1} h^{-1} [304].

Future business models for FCEV2Gs participating in FCR and aFRR imbalance markets rely on future FC system efficiency, FCR, aFRR and hydrogen prices. Other relevant business model parameters need additional research. For example the future costs of V2G infrastructure, FC systems and FC system additional degradation, operation and maintenance due to the V2G load cycles.

2.5 Conclusions

We performed a series of V2G tests in which a modified commercially available FCEV delivered 9.5 kW of AC power to the grid. This paper is the first to report the performance results of this kind of system. Our results show that the FCEV can be used for mobility and to generate power when parked. We contend that grid-connected FCEVs are indeed capable of meeting the requirements for future balancing power plants identified by Brauner et al. [153]. With a maximum V2G DC power output of 10 kW, the maximum downward and upward power gradients of the FC were -47 kW s^{-1} (-470 % s^{-1}) and +73 kW s^{-1} (+730 % s^{-1}) respectively, at the sample frequency of 5 Hz. The maximum downward and upward power gradients of the HV battery were -76 kW s^{-1} (-760 % s^{-1}) and +43 kW s^{-1} (+430 % s^{-1}) respectively, at the sample frequency of 5 Hz. Thus the FC and HV battery in the FCEV have the ability to perform high power gradients (≥ 0.05 % s^{-1} of all power

plants in the electricity grid combined). Also the FC and HV battery in the FCEV respond faster than conventional fast-reacting thermal power plants, which have maximum values of 1.67 % s^{-1} for hot starts [236–239]. Increasing the ability to perform high power gradients reduces the number of power plants in hot standby. Virtual power plants [198,256] composed of many grid-connected FCEVs do indeed have this ability.

We have demonstrated that the FC in the FCEV have the ability to efficiently operate at 10-15 % of its total generation capacity in V2G mode. Whereas existing thermal power plants often can be operated at a low minimal generation of 40%. If all cars were capable of delivering 100 kW (the same as when in driving mode) to the grid via a virtual power plant arrangement, 15-20% minimal generation could be achieved without any problem. If the maximum possible amount of power delivered were limited to 10 kW per car, further tests would need to be performed in the range of 0-10 kW to evaluate FCEV performance and determine whether they can deliver such low power generation values.

The grid-connected FCEV has an AC electric power efficiency of 43% on a HHV basis (51% on an LHV basis) when feeding 9.5 kW AC power to the electricity grid. This corresponds to a low partial load of 11-15% of the maximum FC DC power of 100 kW. The measured AC efficiency is close to the reported FC system DC efficiency of 46.8% on a HHV basis by Hyundai Motor Company [276]. These high efficiencies at low partial load are higher than efficient gas engines under low partial loads, although hydrogen production efficiency is not considered here. The V2G power in this work was limited to 10 kW DC and is examined as 100% V2G output. In a virtual power plant composed of many grid-connected FCEVs, reducing V2G output for every FCEV from 10 kW to 5kW DC could also be avoided by switching more FCEVs off instead of running them at lower power. Further tests at different V2G powers will provide more insight into the partial load and optimum V2G efficiency.

Approximately 38,500 startup/shutdown cycles take place during the life of automotive FC systems. Up to several startup/shutdown cycles can occur during a day due to driving usage of the FCEV. If the V2G usage would be combined with the driving usage, so either occur before or after driving usage, then the V2G usage would not result into additional startup/shutdown cycles. If FCEVs were never switched off and continuously used for either driving or providing V2G energy services, start-ups/shutdowns would be eliminated. Additional degradation due to V2G load cycles (less than 10% rated power) could possibly be compensated for by reducing start-up/shutdown cycles, in combination with smarter power management of both the FC and the HV battery. Furthermore, inductive discharging instead of conductive discharging (by cable) could possibly reduce any further grid connection time.

We did not investigate the ability to schedule cars for this paper. However, the prospect of self-driving, cloud- and grid-connected cars [310,311] with inductive charging and discharging [270–272] technologies in the future could facilitate scheduling of cars when faced with an insecure day ahead prognosis. Data pertaining to car parking locations, parking durations and tank fuel levels for a large number of cars, in combination with local grid imbalance data, could throw light on the problem of scheduling cars.

3 Hyundai ix35 fuel cell electric vehicles: degradation analysis for driving and vehicle-to-grid usage

The research presented in this chapter has been published in [312]. The work in this chapter tries to address research sub-question 1 "Are commercially available FCEVs suitable to act as balancing power plants?" and use an experimental, proof of principle method.

3.1 Abstract

How can we analyse fuel cell stack voltage degradation with transient phenomena and are existing durability indicators as distance driven or operating hours still relevant in commercial FCEVs, used for driving and vehicle-to-grid (V2G) purposes? The mean stack voltage drop is measured over fuel cell operating time and produced electricity in 4 commercial Hyundai ix35 FCEVs. The experiments show that a durability indicator expressed solely in operating hours, distance or produced energy is not relevant for combined driving, V2G and idling load profiles. An indicator consisting of several usage parameters is recommended.

3.2 Introduction

The United States Department of Energy (DOE) increased recently the automotive fuel cell ultimate durability target to 8,000 hours at 10% voltage degradation [313], comparable to 150,000 miles on a lower average speed drive cycle [313]. Cumulative produced energy is suggested as durability indicator [314] for automotive fuel cells operating under highly variable loads affecting durability [315,316].

Variable load profiles can be categorized in transient loadings, zero-current ('idling/spinning reserve'), high and low power and number of startup/shutdowns [315,316].

Fuel Cell Electric Vehicles (FCEVs) with a 100kW fuel cell [241] can also be used for power supply to the electricity grid up to 10 kW when parked, so called 'Vehicle-to-Grid' (V2G) [229] (Figure 2-1). In V2G mode, durability expressed as driven distance is not relevant as the car is parked. Durability expressed as cumulative produced energy when functioning as so called 'spinning reserve', is also not relevant as no power is produced. Questionable is if the number of operating hours or distance driven still is a useful durability indicator.

Real stack voltage is measured from four commercial FCEVs used for driving and V2G purposes. Real usage data contains transient phenomena. Filtering, noise removal and fitting algorithms could help in defining voltage degradation [315]. Summarizing, how can we analyze fuel cell stack voltage degradation with transient phenomena and are existing durability indicators as distance driven or operating hours still relevant in commercial FCEVs, used for driving and vehicle-to-grid purposes?

3.3 Materials and Method

Fuel Cell (FC) operating voltage, current, driving speed and other parameters in four commercial Hyundai ix 35 FCEVs [241] are measured at a frequency in the range of 1 to 5 Hz by CAN bus data loggers. Three FCEVs (labelled FCEV1 to FCEV3) are used solely for driving and one FCEV (labelled FCEV2G) is used for driving and V2G purposes (Figure 2-1). MATLAB ® was used to analyse the recorded data. It is assumed all FCEVs are built during the same period and have the same age.

The data loggers were installed after a certain driven distance, therefore a linear degradation trend is assumed [317]. The voltage drop is measured over fuel cell operating time and produced electricity. The mean stack voltage drop is expressed in percentages relative to the fitted begin-of-measurement (b-o-m) voltage at measured zero operating time or zero cumulative produced electricity. This also explains that the measured voltage drop is relative to the begin-of-measurement (b-o-m) voltage, instead of the begin-of-life (b-o-l) voltage. This method is based on [317], together with filtering conditions, data exclusion and two types of linear least squares regression analysis and applied to all 4 FCEVs.

3.3.1 Filtering conditions and excluded data

Figure 3-1 to Figure 3-4 serve as an illustrative example for the voltage and current data filtering and exclusion for FCEV1.

The voltage measurements recorded at currents below 3 A and above 150 A are excluded (Figure 3-1). The lower threshold of 3 A is equal to the maximum global offset current of the fuel cell stack current sensor [318]. Voltage measurements at the upper threshold of 150 A result mainly from infrequent, irregular and transient phenomena. Fuel Cell gross electric power at 150 A is at least 40 kW. Power above 40 kW mainly occurs in harsh acceleration and lasts only several seconds. 40 kW of continuous power corresponds to cruising speeds of 130 km/h or higher on a flat road, which is allowed in the Netherlands. As the cars are primarily used on flat Dutch roads, where the speed limit is 130 km/h on a limited number of highways, often only during night time. The < 3 A and > 150 A filtering conditions results in an approximately 8.0 % data loss (Figure 3-2) for FCEV1.

Voltages below 250V for currents of 0-150A are excluded, as they originate from transient phenomena, specific idling and shutdown routines (Figure 3-1). The <250 V filtering condition together with the < 3 A and >150 A filtering condition combined result in an approximately 8.0 % data loss (Figure 3-2) for FCEV1. Due to overlap of both filtering conditions the data loss has not significantly increased by applying the <250V filtering condition.

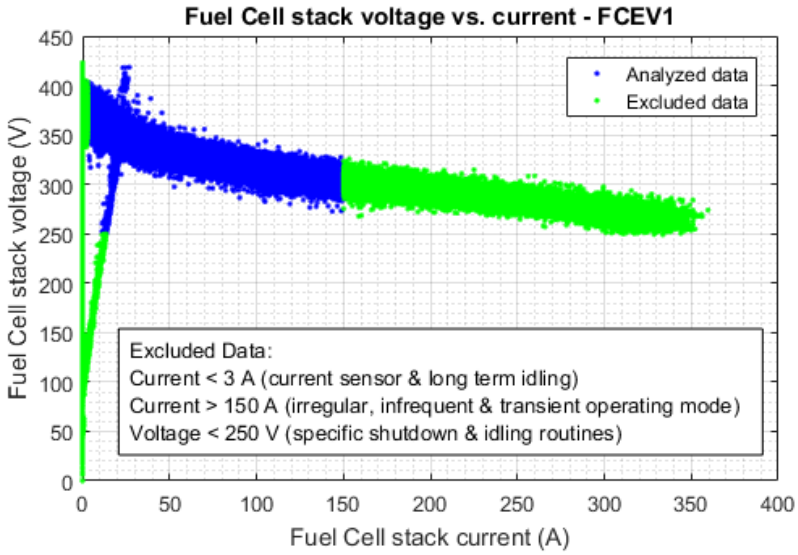

Figure 3-1 Fuel Cell stack voltage vs. current for FCEV1. The blue and green data points represent the analysed and excluded data respectively.

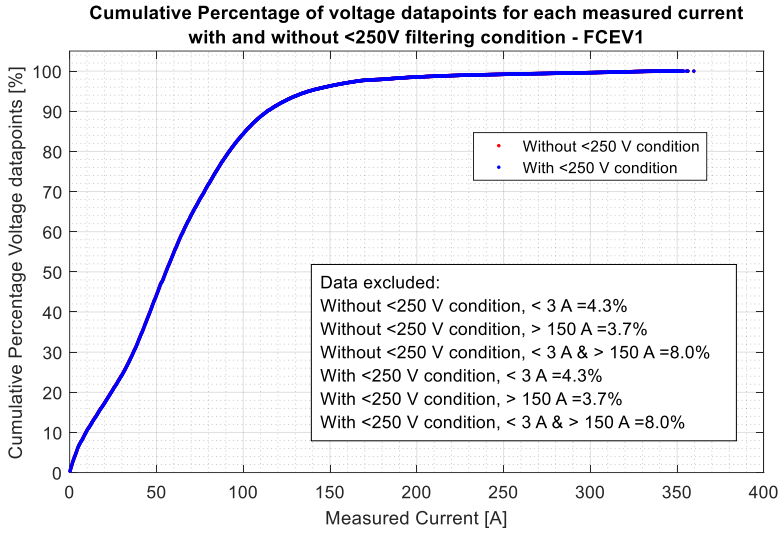

Figure 3-2 Cumulative percentage of voltage data points for each measured current before and after applying the <250V filtering condition for the data of FCEV1 including the approximate data loss for filtering conditions. The plotted cumulative percentage without the <250V filtering (red) condition is underneath the cumulative percentage with <250V filtering condition (blue).

Figure 3-3 shows the number of voltage data points for each measured current after applying the <250V filtering condition for FCEV1. Currents higher than 150A contain relatively low number of voltage data points. Figure 3-4 shows the Weibull distribution of the number of voltage data points for all measured currents after

applying the <250V condition for FCEV1 data. All measured currents with less than 10 voltage data points are discarded from the analysis, for the FCEV1 data this is approximately 3.3 % (Figure 3-4). The aforementioned filtering conditions have some overlap and the total percentage excluded data for all four analysed FCEVs is listed in Table 3-1. The total excluded current data points is approximately 60% for all 4 FCEVs. Total excluded voltage data points for FCEV1, FCEV3 and FCEV2G is approximately 8%. Whereas for FCEV2 this is 34%. Figure 3-8 in the results and discussion section shows that FCEV2 has relatively more data points in the low current region than the other cars.

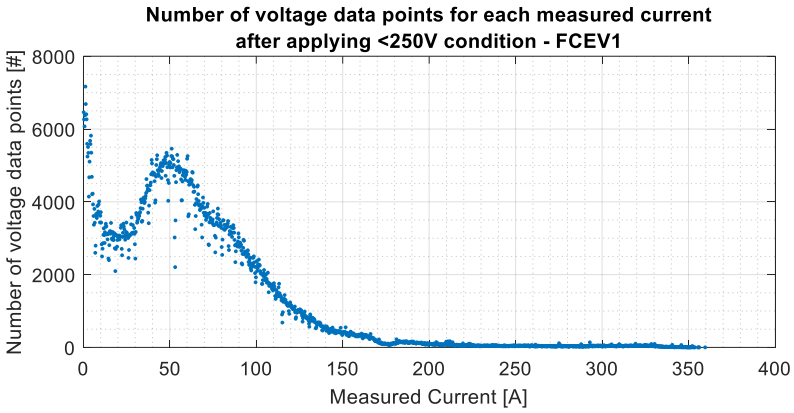

Figure 3-3 Number of voltage data points for each measured current after applying the <250V filtering condition for FCEV1.

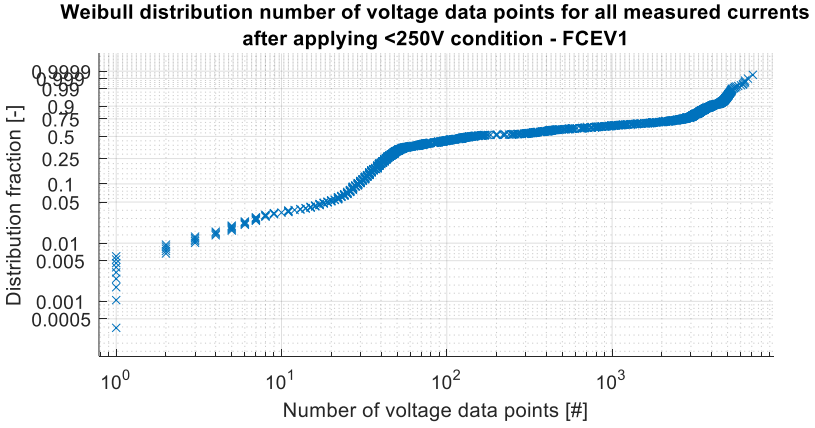

Figure 3-4 Weibull distribution of the number of voltage data points for all measured currents after applying the <250V filtering condition for FCEV1.

Table 3-1 Total excluded current and voltage data points after applying all filtering conditions.

Total Excluded data points	FCEV1	FCEV2	FCEV3	FCEV2G
Current (%)	58	58	58	59
Voltage (%)	8	34	8	8

3.3.2 Regression analysis and mean stack voltage drop

A linear least squares (l.l.s.) and robust linear least squares (r.l.s.) regression analysis is used [319]. The latter aims to reduce the influence of outliers resulting from measurements in transient phenomena [319]. For every considered and measured current, the corresponding voltage data points (Figure 3-5) are plotted versus fuel cell operating time (Figure 3-6) and cumulative produced electricity (Figure 3-7). Figure 3-5 to Figure 3-7 serve as an illustrative example for the voltage data regression analysis at 15 A for FCEV1. Both linear least squares regression methods are applied and a first order polynomial, Equations (3.1) and (3.2), are used to fit the data [317].

$$V_{XXA@t}\left(t\right) = V_{XXA@t=0} - a_{XXA@E} \times t\left(h\right) \tag{3.1}$$

Where $V_{XXA@t}(t)$ is the Fuel cell stack voltage as a function of operating time in hours, t(h), at a specific current. $a_{XXA@t}$ is the fuel cell stack degradation in voltage per hour (V/h) at a specific current. $V_{XXA@t=0}$ is the fitted fuel cell stack voltage at operating time zero h at a specific current.

$$V_{XXA@E}\left(E\right) = V_{XXA@E=0} - a_{XXA@E} \times E\left(kWh\right) \tag{3.2}$$

Where $V_{XXA@E}(E)$ is the Fuel cell stack voltage as a function of cumulative produced electricity in kWh, E(kWh), at a specific current. $a_{XXA@E}$ is the fuel cell stack degradation in millivoltage per kWh (mV/kWh) at a specific current. $V_{XXA@E=0}$ is the fitted fuel cell stack voltage at zero cumulative produced electricity at a specific current.

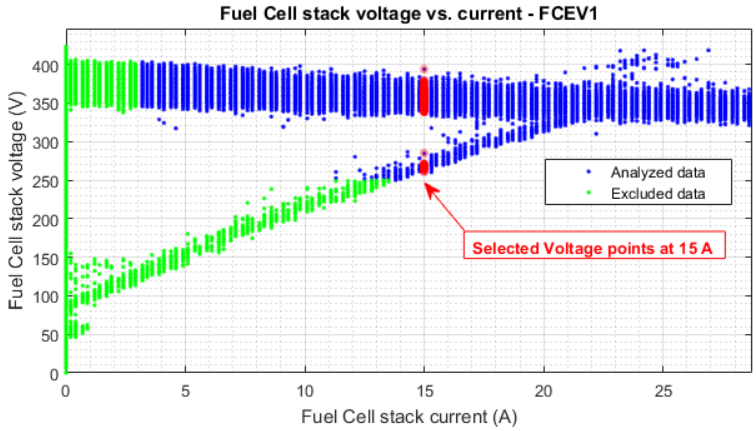

Figure 3-5 Fuel Cell stack voltage vs. current for FCEV1 zoomed into 0-29 A region. The blue and green data points represent the analysed and excluded data respectively. The selected voltage data points at 15 A are displayed in red.

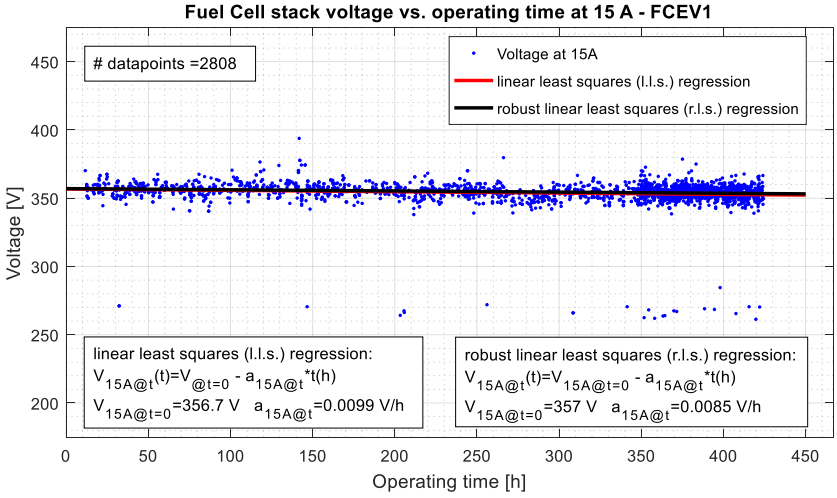

Figure 3-6 L.l.s. and r.l.s. regression analysis applied to Fuel Cell stack voltage vs. operating time at 15A for FCEV1.

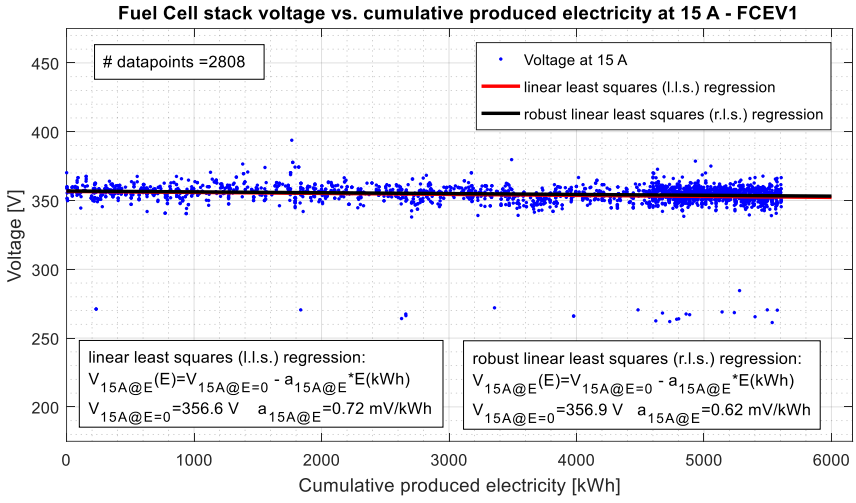

Figure 3-7 L.l.s. and r.l.s. regression analysis applied to Fuel Cell stack voltage vs. cumulative produced electricity at 15A for FCEV1.

The measured voltage drop is expressed in percentages relative to the fitted begin-of-measurement (b-o-m) voltage at zero operating time $\Delta V_{XAA@t}$, Equation (3.3), or zero cumulative produced electricity $\Delta V_{XAA@E}$, Equation (3.4).

$$\Delta V_{XXA@t}(\%) = \frac{a_{XXA@t} \times \max(t(h))}{V_{XXA@t=0}} \tag{3.3}$$

$$\Delta V_{XXA@E}(\%) = \frac{a_{XXA@E=0} \times \max(E(kWh))}{V_{XXA@E=0}} \tag{3.4}$$

3.4 Results and Discussion

Table 3-2 displays FCEV use indicators versus average % stack voltage drop compared to the b-o-m voltage for the considered current range using an l.l.s and r.l.s. regression analysis method based on fuel cell operating time and produced energy. The bold underlined values represent the maximum value in each row and could be an indicator for a relatively higher average % stack voltage drop. Table 3-2 displays results up till the 2nd quarter of 2017 for FCEV1, FCEV2 and FCEV2G, and up till 1st quarter of 2017 for FCEV3.

The percentage stack voltage drop relative to the begin-of-measurement is between 1.4% and 2.6% for all cars throughout all types of regression methods on a fuel cell operating time basis as well as produced electricity basis. For every FCEV the mean, standard deviation and relative standard deviation show consistent values throughout all types of regression methods on a fuel cell operating time basis as well as produced electricity basis.

Average stack voltage drop is the largest for FCEV2G and also shows the largest difference for the two regression analysis algorithms applied, 2.3% and 2.5% on an operating hour basis and 2.4% and 2.6% on a produced electricity basis. This can be an indication that a relative larger number of measurements were performed in transient phenomena [319]. FCEV2G shows low average speed and FC Power, resulting from several long term 'spinning reserve' tests with minimal or no power production, also highly contributing to the total zero current time. Possible reason for the highest average stack voltage drop could be the high number of operating and zero current hours [315,316]. Also FCEV2G has the 2nd highest Gross (Total) FC produced electricity and number of start-up-shutdowns. Average stack voltage drop for FCEV1 and FCEV3 is approximately 1.6% and 1.4%. The measured driven kilometres, operating hours and produced electricity is higher for FCEV1 than for FCEV3 and could be an explanation. FCEV3 has significantly more start-ups and shutdowns. FCEV2 show a relative high mean stack voltage drop when comparing the driven kilometres, operating hours, produced electricity and start-ups and shutdowns.

Table 3-2 Measurements and results of FCEV use indicators versus average % stack voltage drop compared to the b-o-m voltage for the considered current range using an l.l.s and r.l.s. regression analysis method.

Indicators	**FCEV 1**	**FCEV 2**	**FCEV 3**	**FCEV2G**
Distance driven before data-logger installation (km)	16276	4924	**22875**	6299
Distance driven after data-logger installation (km)	**27459**	7917	18004	12649
Number of Trips or number startup-shutdowns (#)	676	531	**1167**	1095
Operating time (h) (incl. zero current)	424	184	314	**872**
Total zero current time and 'idling/spinning reserve' (h)	138	28	98	**457**
Gross (Total) FC produced electricity (kWh) incl. V2G	**5610**	1970	4230	4487
Electricity delivered for V2G purposes (kWh)	0	0	0	**1620**
Average speed (km/h)	**65**	43	57	15
Standard deviation speed (km/h)	42	**42**	41	32
Average speed excluding idling time (km/h)	**76**	60	68	61
Standard deviation speed excluding idling time (km/h)	35	**38**	36	36
Average FC Power (kW)	13	11	**13**	5
Standard deviation FC Power (kW)	14	14	**15**	10
Average FC power excluding idling time (kW)	20	13	**20**	11
Standard deviation FC power exluding idling time (kW)	13	14	**14**	12
% Stack voltage drop relative to b-o-m based on:				
Operating time (l.l.s) - Mean	1.7%	2.0%	1.4%	**2.3%**
Operating time (l.l.s) - Standard deviation	0.5%	0.7%	0.3%	**0.8%**
Operating time (l.l.s) - Relative standard deviation	27%	**35%**	21%	34%
Operating time (r.l.s) - Mean	1.7%	2.0%	1.4%	**2.5%**
Operating time (r.l.s) - Standard deviation	0.5%	0.7%	0.3%	**0.8%**
Operating time (r.l.s) - Relative standard deviation	27%	**35%**	21%	34%
Cumulative electricity (l.l.s) - Mean	1.6%	2.1%	1.4%	**2.4%**
Cumulative electricity (l.l.s) - Standard deviation	0.4%	0.8%	0.3%	**0.9%**
Cumulative electricity (l.l.s) - Relative standard deviation	27%	37%	21%	**38%**
Cumulative electricity (r.l.s) - Mean	1.6%	2.1%	1.4%	**2.6%**
Cumulative electricity (r.l.s) - Standard deviation	0.4%	0.8%	0.3%	**1.0%**
Cumulative electricity (r.l.s) - Relative standard deviation	27%	**37%**	20%	37%

Both FCEV2 and FCEV2G have high standard deviations compared to FCEV1 and FCEV3. This can possibly be explained by the different fuel cell use when compared to FCEV1 and FCEV3. Figure 3-8 shows the cumulative percentage of voltage data points for each measured current after applying the <250V filtering condition. Both FCEV1 and FCEV2G have relatively a lot more data points in the low current region. For FCEV1 65% of the voltage data points are for currents lower than 50A, for FCEV2G this is 80%. Obviously for FCEV2G this is due to the V2G electricity production, which is limited at 10kW, corresponding to currents lower than 50A. The majority of V2G tests were performed at 10kW and in a lesser extent at 3 kW, this is indicated clearly by the sharp increase in the 25-40A region. FCEV2 is only used for driving and has no V2G option. The average speed of FCEV2 is lower than

FCEV1 and FCEV3, which explains the high number of voltage data points below 50A region.

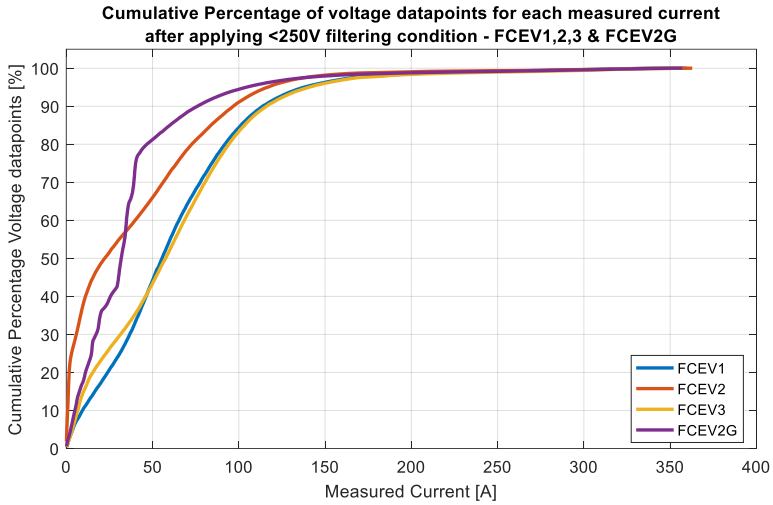

Figure 3-8 Cumulative percentage of voltage data points for each measured current after applying the <250V filtering condition.

Both FCEV2 and FCEV2G have relatively higher standard deviations, 0.7% and 0.9%, when compared to FCEV1 and FCEV3 0.4% and 0.3%. The relative standard deviation for FCEV2 and FCEV2G is between 34% and 38% whereas for FCEV1 and FCEV3 this is between 21% and 27% respectively. Aforementioned high share of data points in the low current region could be a reason for this. FCEV2 has the lowest usage compared to all cars and so has also generated the fewest data points, of which the majority is in the 0-50 current region. Further analysis at higher usage or comparing a partial dataset of FCEV1 and FCEV3 could provide more insight on the effect of the total number of data points or the effect of data points in specific current regions. Applying a weight factor to the voltage data points based on the number of data points per current could possibly reduce the standard deviation and relative standard deviation of the calculated mean voltage drop. Also increasing the minimum voltage data points of 10 or changing the upper current threshold of 150 A could have an effect on the standard and relative standard deviation.
Using the mean stack voltage drops from the time based l.l.s. regression analysis and assuming a linear degradation trend at a maximum allowable mean voltage drop of 10% [313], the durabilities expressed in kilometers, hours and electricity produced can be estimated (Table 3-3). This would result in estimated durabilities of 2550h, 920h, 2250h and 3710h for respectively FCEV 1-3 and FCEV2G (Figure 3-3), of which FCEV 1, FCEV2 and FCEV2G are comparable with DOE results when compared on an fuel cell operating time basis [313]. For FCEV1 the estimated durability of 920 is very low but is also based on the mean stack voltage drop with high standard and relative standard deviation. The durability indicator driven distance, only makes sense for driving only cars. Also, the durability indicator fuel cell produced electricity seems relatively consistent for FCEV1 and FCEV3 but is

approximately 50% lower for FCEV2G due to the high total zero current time and 'idling/spinning reserve' where the fuel cell system is operating but not producing any electricity. A durability indicator expressed solely in operating hours, distance or produced energy is not relevant for combined driving and V2G load profiles. An indicator consisting of several usage parameters is recommended but could require extensive and long-term testing under real circumstances or other measurement techniques. Some suggested combination of parameters, but not limited to, are the operating and 'idling' hours, produced energy, driven distance, number of start-ups and shutdowns.

Table 3-3 Estimated durabilities expressed in hours, distance driven and electricity produced. Using the average voltage drops from the time based l.l.s. regression analysis and assuming a linear degradation trend at a maximum allowable mean voltage drop of 10% [313].

Estimated durability in:	**FCEV 1**	**FCEV 2**	**FCEV 3**	**FCEV2G**
Fuel cell operating time (h)	2550	920	2250	3710
Distance driven (km)	164700	39800	129000	53900
Fuel cell produced electricity (kWh)	35000	9500	30900	18600

3.5 Conclusion

How can we analyse fuel cell stack voltage degradation with transient phenomena and are existing durability indicators as distance driven or operating hours still relevant in commercial FCEVs, used for driving and vehicle-to-grid (V2G) purposes? The mean stack voltage drop is measured over fuel cell operating time and produced electricity in 4 commercial Hyundai ix35 FCEVs. Using only voltage data in the 3-150 A current range at voltages above 250V and with a minimum of 10 datapoints per analysed current. Both a linear and robust linear least squares regression analysis are applied to the voltage data.

Fuel cell stack current and voltage are recorded in three FCEVs used for driving only and one FCEV used in both driving as well as V2G mode. Between 7900 and 27500 kilometers, 184 and 872 fuel cell operating hours, 1970 and 5610 kWh fuel cell produced electricity and 530 and 1170 startup and shutdowns are recorded in all 4 FCEVs during the analysed period.

For every FCEV the mean, standard deviation and relative standard deviation show consistent values throughout all types of regression methods on a fuel cell operating time basis as well as produced electricity basis. The percentage stack voltage drop relative to the begin-of-measurement is 1.4% and 2.6% for all FCEVs for all types of regression methods, both on a fuel cell operating time basis as well as produced electricity basis. For two FCEVs driven 18000 and 27500 km (314 and 424 operating hours), the mean stack voltage drop is 1.4% and 1.7% with a standard deviation of 0.3% and 0.4%. The relative standard deviation is 21% and 27%. For the less driven FCEV, 7900km (184 operating hours), the mean stack voltage drop with 2.0% is relatively high compared to the other driven only FCEVs. The same FCEV also has a relatively high standard deviation of 0.7% and relative standard deviation of 38%, which could be attributed to the relative low usage. Also, the relatively high usage

in the low fuel cell current range (0-50A) compared to the high current range (150-350A) could have an impact on the higher standard deviations. A similar trend is seen for the FCEV used for both driving and vehicle-to-grid purposes.
Applying a weight factor to the voltage data points based on the number of data points per current could possibly reduce the standard deviation and relative standard deviation of the calculated mean voltage drop. Also increasing the minimum threshold of number of voltage data points per analysed current (now 10) or changing the upper current threshold of 150 A could influence the standard and relative standard deviation.
For two driving only FCEVs and the FCEV used for both driving and vehicle-to-grid purposes the average voltage drops compared to the operating hours are comparable with the DOE measured durability in hours. The durability indicator driven distance, only makes sense for driving only cars. The durability indicator produced electricity is extremely sensitive to the number of 'idling' or fuel cell zero current operating hours, as there is no electricity production during these operating hours.
A durability indicator expressed solely in operating hours, distance or produced energy is not relevant for combined driving and V2G load profiles. As for neither operating hours, driven distance nor produced energy, no clear correlation with average voltage drop is seen amongst all four FCEVs. An indicator consisting of several usage parameters is recommended but could require extensive and long-term testing under real circumstances or other measurement techniques. Some suggested combination of parameters, but not limited to, are the operating and 'idling' hours, produced energy, driven distance, number of start-ups and shutdowns.

4 Fuel cell electric vehicle-to-grid: emergency and balancing power for a 100% renewable hospital

The research presented in this chapter has been published in [320]. The work in this chapter tries to address research sub-question 2 “How can we integrate FCEVs, used for transport, distributing and generating electricity, into future energy systems?” and use a combined approach of system design, heuristic modeling and simulation.

4.1 Abstract

Hospitals are one of the most energy demanding buildings and require high reliability of energy supply. This work answers the question whether for an all-electric hospital, (urban) solar, wind and municipal wastewater biogas together with grid connected FCEVs and hydrogen as an energy carrier, can provide a 100% renewable and reliable energy system for power, heat and transport in a Mid Century (~ 2050) scenario. An integrated transport and energy system for a 530-bed hospital is designed based on European statistics and real energy consumption data of a newly built hospital. Year-round energy supply is guaranteed by biogas from the city wastewater treatment plant (WWTP), wind turbines at the WWTP location and rooftop solar panels on the hospital building and car park. Temporary surplus electricity is converted via water electrolysis into hydrogen. Less than 250 V2G connected FCEVs are required to balance the system at all times by generating electricity from the produced hydrogen in times of low energy supply by the intermittent renewables. The 500-place counting car park can easily host these cars. Hydrogen also serves as a fuel for the hospital vehicle fleet, consisting of only FCEVs. Seasonal imbalance of hydrogen is solved by exchange with other hydrogen consumers and producers. The emergency power system of the hospital could be replaced by grid connected FCEVs, a high-pressure hydrogen storage tank at the hydrogen fueling station and hydrogen tube trailers providing an autonomy of six days during an electricity outage.

4.2 Introduction

The healthcare sector contributes to approximately 5% of the European Union’s Green House Gas (GHG) emissions [321–324]. The urgency to significantly reduce the impacts of climate change is felt around the globe, agreed by 195 governments [325]. In view of these goals both the energy and transport systems need to change into zero emission systems by 2050. Several projects and studies are aimed to reduce the carbon footprint and increase the energy self-sufficiency (energy independency) of the healthcare sector [326–328]. In Europe there are approximately 15,000 hospitals [326,329–331]. Common factors amongst hospitals are:

1. 24/7 operation [329]
2. high reliability of energy supply
3. high specific building energy use per square meter compared to other buildings (kWh/m^2/year) [328,332,333]
4. situated in congested urban areas with limited space for renewable energy development.

Large challenges arise when combining these common factors with the aim to reduce the carbon footprint and increase the energy self-sufficiency [326,329]. Especially as a 100% zero carbon hospital is not just about building energy, up to 10% of the hospital total energy can be accounted to transport [334]. Abundantly available renewable energy sources such as solar and wind power do not provide 24/7 reliable energy and require energy storage and balancing. Due to the high specific building energy per square meter and high rise buildings, relatively low amount of rooftop areas are available for solar energy [335,336]. Being situated in congested urban area's also limits the possibility of having additional solar panels or other renewable energy sources close by to increase self-sufficiency.

The Energy Performance of Buildings Directive [337], requires all new buildings to be nearly zero energy by the end of 2020, for new public buildings by 2018. Electrification [338] and reduction in final energy consumption [336,339–341], application of sustainable energy sources and efficient technologies such as heat pumps are promising technical solutions [326,328]. Most recommended and used sources are solar thermal and PV systems and ground source heat pumps [326,329,333,337]. In case of no underground parking, additional solar panels could be placed on the multilevel car parking area at hospitals [326,342]. Parked electric vehicles (EVs), such as commercial available and so called 'Vehicle-to-Grid' (V2G) [202] connected Fuel Cell Electric Vehicles (FCEVs) [181,182,229], could be aggregated in the car park [221] and used to provide balancing power during night [214,235] or even emergency power for hospital electric appliances [200].

Northern European countries have limited solar energy potential [343,344] and other sources are needed such as wind or biomass [333,337]. Biogas from waste water treatment plants (WWTP) are often already today cost-effective renewable urban energy sources [345–348] and could also be a viable source for zero carbon transport [349]. WWTPs can become net energy producers [350–356] through efficient treatment technologies [357] and anaerobic digesters [358] Additional renewable electricity can be generated as well at the WWTP site such as solar or wind [359–365].

The question arises, for an all-electric hospital, can (urban) solar, wind and municipal wastewater biogas together with grid connected FCEVs and hydrogen as an energy carrier, provide a 100% renewable and reliable energy system for power, heat and transport in a Mid Century (~2050) scenario?

4.3 Methodology

The research is performed in four steps:

1. Design and dimensioning of a fully autonomous renewable and reliable integrated transport and energy system for a hospital, based on the Reinier de Graaf Gasthuis hospital in Delft, the Netherlands [366].
2. Technology selection for the components of the hospital energy system. Establishing hourly consumption and production profiles using Mid Century (~2050) technology efficiency status of today's commercial available hydrogen technologies.
3. Calculating the annual and hourly energy balance by matching demand with local solar, wastewater biogas, wind energy and hydrogen production and reconversion by grid connected FCEVs.
4. Feasibility hospital emergency power system replacement by grid V2G FCEVs.

4.3.1 System functional design

By applying the design requirements, the integrated energy system design of the hospital has 2 locations with each 3 major elements (Figure 4-1):

City Hospital location

- Hospital building and car park: are all electric in end-use, without any natural gas connection and have rooftop solar systems. Every parking place has an V2G connection. The hospital car fleet and the visiting cars are all FCEVs.
- Smart electric grid: managed by a controller, which connects all buildings, cars and city WWTP components through a 2 MW limited electricity cable connection.
- Hydrogen Fueling Station (HFS): includes a high pressure storage, hydrogen chiller and dispenser. The hydrogen is imported via hydrogen tube trailers.

City Wastewater treatment plant

- Wastewater treatment plant: includes waste water treatment system and a heat pump required for the biogas production unit.
- Hydrogen production: contains a biogas steam reformer for hydrogen production. An electrolyser converts temporary surplus electricity from solar and wind into hydrogen. A compressor pumps the produced hydrogen into tube trailers.
- Wind turbines.

Functional energy performance of the system comprises of the following conversion steps:

- Electricity is generated by solar modules on all roofs at the hospital location.
- Wastewater treatment requires electricity and heat for anaerobic digestion of the sludge into biogas. Heat is supplied via an electric powered heat pump.
- Hydrogen is produced via steam methane reforming of the biogas.
- The wind turbine provides additional electricity for the hospital and WWTP site through a 2 MW limited electricity cable connection.
- Surplus electricity is converted via water-electrolysis into pure hydrogen. All produced hydrogen is compressed and stored into tube trailer modules.
- Full tube trailer modules are transported by a trailer tractor to the Hydrogen Fueling Station (HFS) or exported to/imported from other hydrogen consumers or seasonal storage.
- At the HFS, the hydrogen is further compressed and dispensed on demand. Electric energy is required for hydrogen compression and dispensing at the HFS.
- The hydrogen is used as a transport fuel for the hospital vehicle fleet.
- In case of a temporary shortage in electricity production, the fuel cells in grid-connected cars in the car park provide the necessary electricity by converting hydrogen from the on-board hydrogen storage tanks fueled at the HFS.

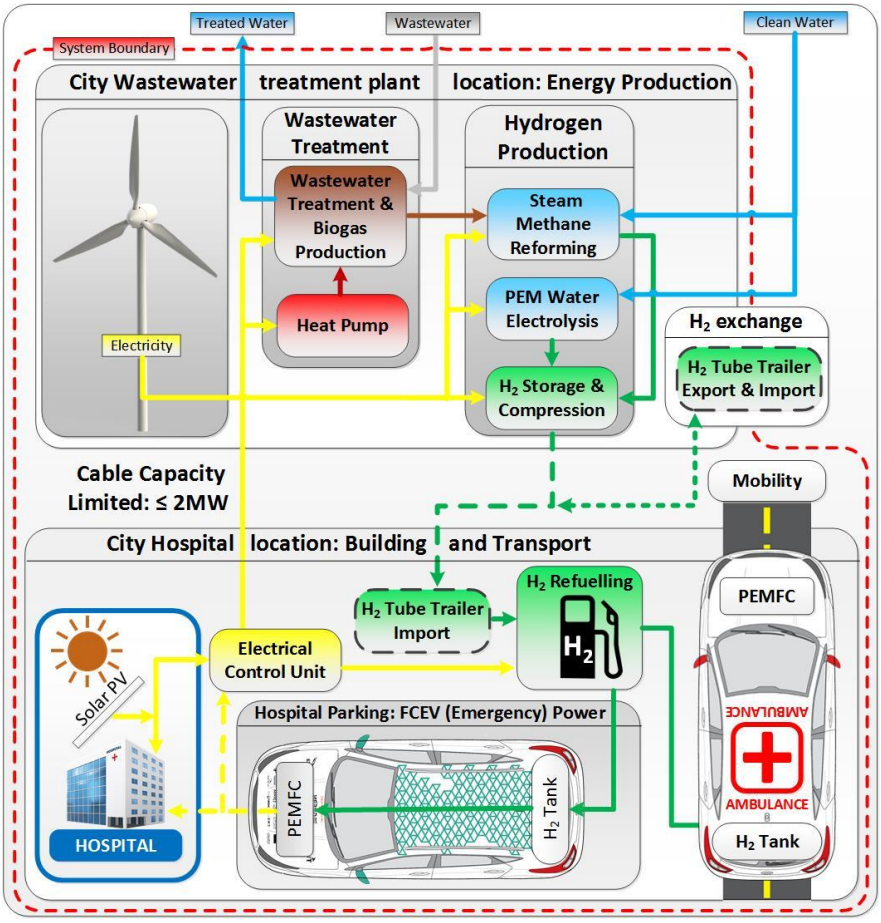

Figure 4-1 Key elements and functional energy performance of the fully autonomous hospital integrated transport and energy system

4.3.2 Dimensioning

The hospital energy system is based on the Reinier de Graaf Gasthuis 475-bed hospital and it's 450-place car parking area in Delft, the Netherlands [367,368]. The hospital has two buildings and car parking area with a total potential roof surface area of 13,070 m^2 to place solar panels (Figure 4-2).

Figure 4-2 Reinier de Graaf Gasthuis hospital and its car parking area with a total potential surface area of 13,070 m^2 to place solar panels.

The existing hospital vehicle fleet consists of several fossil fueled cars, small vans and ambulances, in this study it is assumed they are all hydrogen fuel cell powered. In Europe there are on average 526 hospital beds for every 100,000 citizens [331]. In this study the Reinier de Graaf Gasthuis 475-bed hospital, its number of parking places, potential solar surface and floor area [55], hospital vehicle fleet and all other parameters are scaled proportionally to the European average 526 hospital beds per 100,000 citizens. The scaled numbers are summarized in Table 4-1.

Table 4-1 Characteristics of the hospital transport and energy system scaling the Reinier de Graaf Gasthuis hospital parameters with European statistics

Parameters	**Quantity**
Citizens	100,000
Number of hospital beds per 100,000 citizens	526
Total floor area hospital buildings (m^2)	62,570
Total potential roof area for solar panels (m^2)	14,470
Parking places	500
Annual driven distance hospital passenger cars (km/year)	124,800
Annual driven distance small vans and ambulances (km/year)	132,000

4.3.3 Technology selection and production and consumption profiles

The technology selection only uses today's commercial available hydrogen technologies and uses estimated efficiencies for the Mid Century scenario (~2050) based on literature research.

4.3.3.1 Hospital Building technology

The hospital is 'near' all electric in its end-use. For space heating & cooling and warm water heating heat pumps in combination with thermal aquifer storage are used. The heat pumps are of brand Carrier [369] and have a measured Coefficient of Performance (COP) of 4. In cold periods an additional gas boiler is used for space heating and warm water heating. In this study the gas boiler is replaced by an electric boiler.

The hospital has its own combined wastewater and special hospital waste treatment system. This treatment system's electricity consumption is displayed in Figure 4-3, having a net annual consumption of 438 MWh/year.

End of 2015 the new hospital opened and hourly energy consumption data from October 2015 up to March 2016 was available at the time of modelling. A full year energy consumption profile is based on the energy consumption profiles of the old hospital for space heating and electrical appliances and scaled to a 526-bed hospital. A 20% reduction in electricity consumption in the Mid Century scenario is assumed from today's annual electricity consumption, resulting in 13,900 MWh/year. The hourly consumption profile is displayed in Figure 4-3.

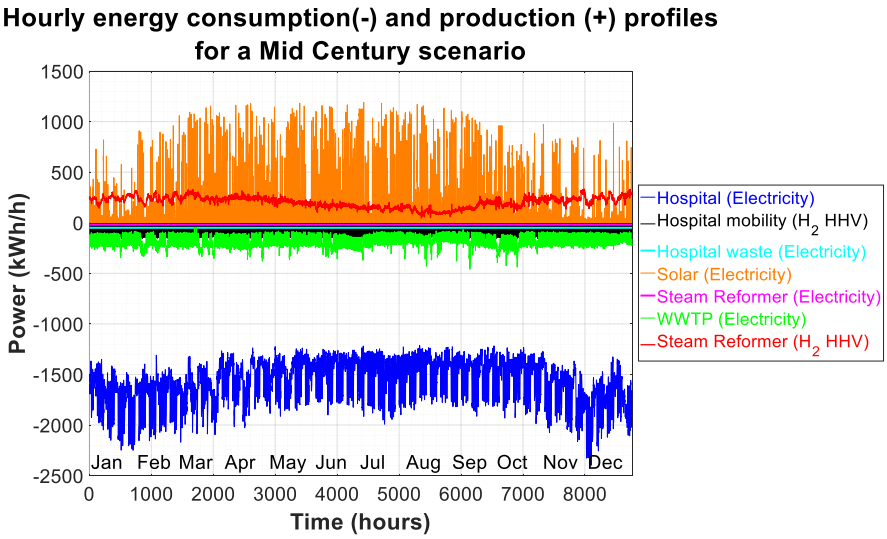

Figure 4-3 Hourly energy consumption and production profiles for a Mid Century scenario.

4.3.3.2 Fuel Cell Electric Vehicles and Vehicle-to-Grid Connection

The FCEVs have an on-board fuel cell has a maximum power output of 100kW [58], but in V2G mode its power output is limited to 10kW. Commercial FCEVs all have a high voltage battery on-board and has a maximum power output of 24kW and capacity of 0.95 kWh [180]. Foreseen Mid Century hydrogen tank content is 6.5 kg [126]. In this study it is assumed maximum 6kg is available for electricity production, at a conversion efficiency of 60 % Higher Heating Value (HHV) based [126]. The hospital vehicle fleet's passenger cars, small vans and ambulances consume respectively 0.6 kg/100km and 1.2 kg/100km [126,235], resulting in 2400 kg/year (95 MWh/year on an HHV basis).

4.3.3.3 Solar system

Using a solar panel inclination of 39.6°, inter-row spacing of 3.2m, it is assumed 2150 solar panels can be placed, resulting in a total solar panel surface area of 3655 m^2. The performance ratio and solar module efficiency are 0.90 and 0.35 kWp/m^2 [370], resulting in an installed peak power of 1280 kWp. For the RDGG location no solar radiation data was available, therefore data of the Rotterdam weather station is used [371] in combination with the NREL solar position algorithm [372]. Hourly production profile is displayed in Figure 4-3, with an annual production of 1395 MWh/year.

4.3.3.4 Wastewater treatment plant

The annual electricity and heat consumption of the wastewater treatment is respectively 13.9 kWh [373,374] and 10 kWh [375] per person equivalent (PE) annual wastewater production. When using heatpumps with a COP of 4 [369], 2.5 kWh/PE electricity is required for heat production. Which for 100,000 citizens results in a total annual electricity consumption of 1640 MWh/year by the WWTP.
1 PE annual wastewater production is defined as 0.15m^3/day/person, for 100,000 citizens this results in 5,475,000 m^3 wastewater. Approximately 370,000 m^3 biogas is produced with a HHV of 7.3 kWh/m^3 (60% CH_4 and 40% CO_2) [375], resulting in 2700 MWh/year biogas energy.
Hourly total electricity consumption and biogas production are scaled proportionally with the incoming wastewater flow, based on a normalized wastewater flow from the SMAT Collegno wastewater treatment plant in Turin, Italy [376], see also Figure 4-3.

4.3.3.5 Hydrogen Production: Steam Methane Reformer

The steam methane reformer is based on [377] and its size is proportionally scaled to the maximum biogas production of 70 m^3/h. The assumed increased reforming efficiency of 76% is based on [59,65] for Hydrogen 5.0 grade (99.999%) on a HHV basis at 7.5 bar. The scaled parasitic electric load of 20 kW includes a reverse osmosis system for clean water production [377]. The hydrogen production profile is directly related to the biogas production profile, see Figure 4-3. Annual hydrogen production is 45,080 kg/year (1780 MWh/year HHV).

4.3.3.6 Hydrogen Production: Electrolysis

The PEM electrolyzer's size is proportionally scaled to the surplus electricity. The part-load efficiency curve is used from [378] and its maximum efficiency point is adjusted to 86%, according [126]. Hydrogen outlet pressure is 20 bar. Hydrogen specific electricity consumption ranges from 46-54 kWh/kg hydrogen including hydrogen purification to 5.0 grade and clean water production through reverse osmosis.

4.3.3.7 Hydrogen compression

The compressor at the WWTP is a medium-pressure compressor. Maximum flow rate of the medium-pressure compressor is equal to the maximum hydrogen production flow rate from the electrolyzer and steam methane reformer.
The compressor at the HFS is a high-pressure compressor. The maximum flow rate of the high-pressure compressor is equal to the maximum hydrogen dispensing flow rate for refueling the hospital fleet and the grid connected balancing FCEVs.
Energy consumption for the pressure compressors are calculated using [379–382], taking into account a variable inlet pressure from the emptying tube trailer. Average specific compression energy for respectively the medium and high-pressure compressor is 2.0 kWh/kg and 0.9 kWh/kg hydrogen compressed.

4.3.3.8 Hydrogen tube trailers

Hydrogen tube trailers [379,383,384] with compressed hydrogen are used for exchange between the WWTP location and hospital and low pressure storage during production at the WWTP location. Roundtrip distance for transport hydrogen between WWTP and hospital is assumed 100km. Tube trailer tractors consume 5.5 kg/100km [235]. For every 2 tube trailers 1 tractor is needed, which can transport a full tube trailer while the other is being filled at the production site. Minimum number of tube trailers and tractors in the system therefore is respectively 2 and 1. In the Mid Century scenario tube trailers can store an effective mass of 1350 kg of hydrogen at a pressure of 540 bar [379,383,384]. Tube trailers are also used to export to and import hydrogen from other consumers in the urban area, such as the chemical industry or it is stored into salt caverns as seasonal storage [385].

4.3.3.9 Hydrogen Fueling Station (HFS)

Hydrogen is chilled and dispensed from the 875 bar high pressure storage scaled to the normalized fueling profile defined [386]. The high-pressure storage tanks are dimensioned such that it can hold sufficient hydrogen to power the hospital 24 hours by hydrogen only. Resulting in 1650 kg of hydrogen, which would fit in less than 2 cylindrical tanks with a diameter of 2.6 meter and 7.5 meter length as proposed in [387]. Specific chiller energy is 0.15 kWh/kg hydrogen chilled [388]. Maximum hydrogen dispensing rate is 2.0 kg/min per dispenser [389].

4.3.3.10 Wind turbines

From Figure 4-3 it can be seen that the hospital's 24/7 operation and continuous energy demand is higher than the hydrogen energy from wastewater and solar electricity. Therefore, annual wind energy production must close the annual energy balance, by installing a sufficient number of wind turbines. No wind profile of the hospital's location was available therefore the used wind profile is an average of the wind profile from the Hoek van Holland and Rotterdam weather stations [371,390]. The power curve of the 4.2MW wind turbine is based on [391]. A 3% capacity factor increase is assumed in a Mid Century scenario [392] by adjusting the power curve for the used wind profile. This results in a capacity factor of 43% (15,300 MWh/year per turbine) and the electricity production profile in Figure 4-4.

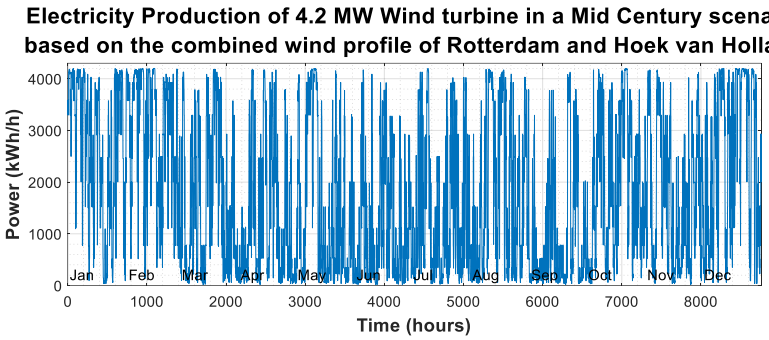

Figure 4-4 Electricity production of a 4.2 MW wind turbine in a Mid Century scenario based on the combined wind profile of Rotterdam and Hoek van Holland.

4.3.4 Energy balance equations

4.3.4.1 Annual energy balance

The annual energy balance consists of the summation (1 year consists of 8760 hours) of the hourly average consumption ($\bar{E}_{cons}$), production ($\bar{E}_{prod}$) and electricity-hydrogen-electricity and wastewater-to-hydrogen conversion losses ($\bar{E}conv.loss$), Equation (4.1).

$$\sum_{h=1}^{8760} \bar{E}_{cons}(h) = \sum_{h=1}^{8760} \bar{E}_{prod}(h) - \sum_{h=1}^{8760} \bar{E}_{conv.loss}(h) \quad (4.1)$$

The annual electricity consumption, Equation (4.2), is the summation of the hourly average consumption of the hospital ($\bar{E}_{hosp}$), hospital waste system ($\bar{E}_{hosp.waste}$), hospital car fleet ($\bar{E}_{car\ fleet}$), WWTP ($\bar{E}_{WWTP}$) and auxiliary components of the steam methane reformer ($\bar{E}_{ref,aux}$).

$$\sum_{h=1}^{8760} \bar{E}_{cons}(h) = \sum_{h=1}^{8760} \left[\begin{array}{c} \bar{E}_{hosp}(h) + \bar{E}_{hosp.waste}(h) + \bar{E}_{car\ fleet}(h) + \bar{E}_{WWTP}(h) \ldots \\ + \bar{E}_{ref,aux}(h) \end{array} \right] \quad (4.2)$$

Annual electricity production, Equation (4.3), consists of the summation of the hourly average solar ($\bar{E}_{solar}$), wind ($\bar{E}_{wind}$) and hydrogen production from wastewater ($\bar{E}_{ref,H_2}$). The annual solar energy is related to the fixed roof area and the hydrogen production is limited by the annual wastewater inflow and its energy content. From Figure 4-3 it can be clearly seen that the hospital's 24/7 operation and continuous energy demand is higher than the hydrogen energy from wastewater and solar electricity. Therefore annual wind energy production has to close the annual energy balance, by installing sufficient wind turbines (N_{Turb}).

$$\sum_{h=1}^{8760} \bar{E}_{prod}(h, N_{Turb}) = \sum_{h=1}^{8760} \left[\bar{E}_{solar}(h) + \bar{E}_{wind}(h, N_{Turb}) + \bar{E}_{ref,H_2}(h) \right] \quad (4.3)$$

The conversions losses, Equation (4.4), consist of the hourly average steam methane reforming losses ($\bar{E}_{ref,loss}$) and the losses in the electrolyzer's electricity to hydrogen conversion ($\bar{E}_{el,loss}$) and fuel cell's hydrogen to electricity conversion ($\bar{E}_{FCEV2G,loss}$) and hydrogen compression and cooling energy consumption ($\bar{E}_{H_2\ compr\&cool}$). Except the reforming losses, all other losses are dependent on the hourly imbalance, either shortage or surplus electricity.

$$\sum_{h=1}^{8760} \bar{E}_{conv.loss}(h) = \sum_{h=1}^{8760} \left[\bar{E}_{ref,loss}(h) + \bar{E}_{el,loss}(h) + \bar{E}_{FCEV2G,loss}(h) + \bar{E}_{H_2\ compr\&cool}(h) \right] \quad (4.4)$$

4.3.4.2 Hourly electricity balance

The hourly electricity balance, Equation (4.5), consists of the hourly average production, $\bar{E}_{prod}$ in Equation (4.6), consumption, $\bar{E}_{cons}$ in Equation (4.7), and electricity balancing by the grid connected FCEVs ($\bar{E}_{FCEV2G}$) and electrolyser ($\bar{E}_{el}$).

$$\bar{E}_{prod}(h) - \bar{E}_{cons}(h) = \bar{E}_{FCEV2G}(h) - \bar{E}_{el}(h) \quad (4.5)$$

Solar ($\bar{E}_{solar}$) and wind ($\bar{E}_{wind}$) produce electricity, Equation (4.6).

$$\bar{E}_{prod}(h) = \bar{E}_{solar}(h) + \bar{E}_{wind}(h) \quad (4.6)$$

Electricity is consumed by the hospital ($\bar{E}_{hosp}$), hospital waste system ($\bar{E}_{hosp.waste}$), WWTP ($\bar{E}_{WWTP}$), auxiliary components of the steam methane reformer ($\bar{E}_{ref,aux}$) and compressors and hydrogen cooling ($\bar{E}_{H_2\ compr\&cool}$), Equation (4.8).

$$\bar{E}_{cons}(h) = \bar{E}_{hosp}(h) + \bar{E}_{hosp.waste}(h) + \bar{E}_{WWTP}(h) + \bar{E}_{ref,aux}(h) + \bar{E}_{H_2\ compr\&cool}(h) \quad (4.7)$$

4.3.4.3 Hourly hydrogen balance

The hourly hydrogen balance, Equation (7.11), consists of hydrogen produced via electrolysis ($\bar{E}_{el,H_2}$), in case of temporary surplus electricity, together with the hydrogen leaving the reformer ($\bar{E}_{ref,H_2}$) which is stored in tube trailers ($\Delta\bar{E}_{tube,H_2}$). Filled tube trailers can be transported to the HFS or exported to other hydrogen consumers. The hospital car fleet ($\bar{E}_{car\ fleet}$) is fueled at the HFS with hydrogen from the tube trailers. In case of a temporary electricity shortage, grid connected FCEVs convert hydrogen ($\bar{E}_{FCEV2G,H_2}$) from the tube trailers into electricity to balance the system, Equation (4.5), after being fuelled at the HFS.

$$\Delta\bar{E}_{tube,H_2}(h) = \bar{E}_{el,H_2}(h) + \bar{E}_{ref,H_2}(h) - \bar{E}_{FCEV2G,H_2}(h) - \bar{E}_{car\ fleet,H_2}(h) \quad (4.8)$$

4.4 Energy balance results and discussion

4.4.1 Annual energy balance

The integrated transport and energy system is supplied by 100% renewable energy sources. Annual total primary energy supply is 24.1 GWh/year, see Figure 4-5. Solar and biogas from municipal wastewater are responsible for respectively 6% and 4% of the primary energy supply. Wind provides the remaining 90%. The annual energy balance is closed by the energy from the wind turbines. The roof area of the high-rise hospital buildings and car park is not sufficient to cover the hospital building demand. Even considering a Mid Century solar panel efficiency of 35% and building energy consumption reduction of 20%. Hydrogen energy from wastewater

Combined electricity and hydrogen consumption of the hospital buildings (96%), vehicle fleet (1%) and its special and normal waste treatment system (3%) is 14.4 GWh/year. Daytime power consumption of the hospital's building and waste treatment system is always higher than the maximum solar electricity production (Figure 4-3). Therefore, all solar electricity can be used directly, providing 10% of the final energy consumption of the hospital building and its waste treatment system. Direct wind electricity supplies 45% as well as 45% electricity from the grid connected FCEVs in the car park.

Total annual hydrogen production is 286,100 kg/year (11.3 GWh/year), of which 84% is produced from temporary wind surplus electricity. Hydrogen for both the hospital vehicle fleet as the tube trailer tractors is 4,800 kg/year (0.2 GWh/year) of which 50% is for the hospital vehicle fleet and 50% for the hydrogen tube trailers. 430 number of roundtrips are made by the tube trailer tractors to either hospital or external hydrogen consumers and producers or seasonal storage.

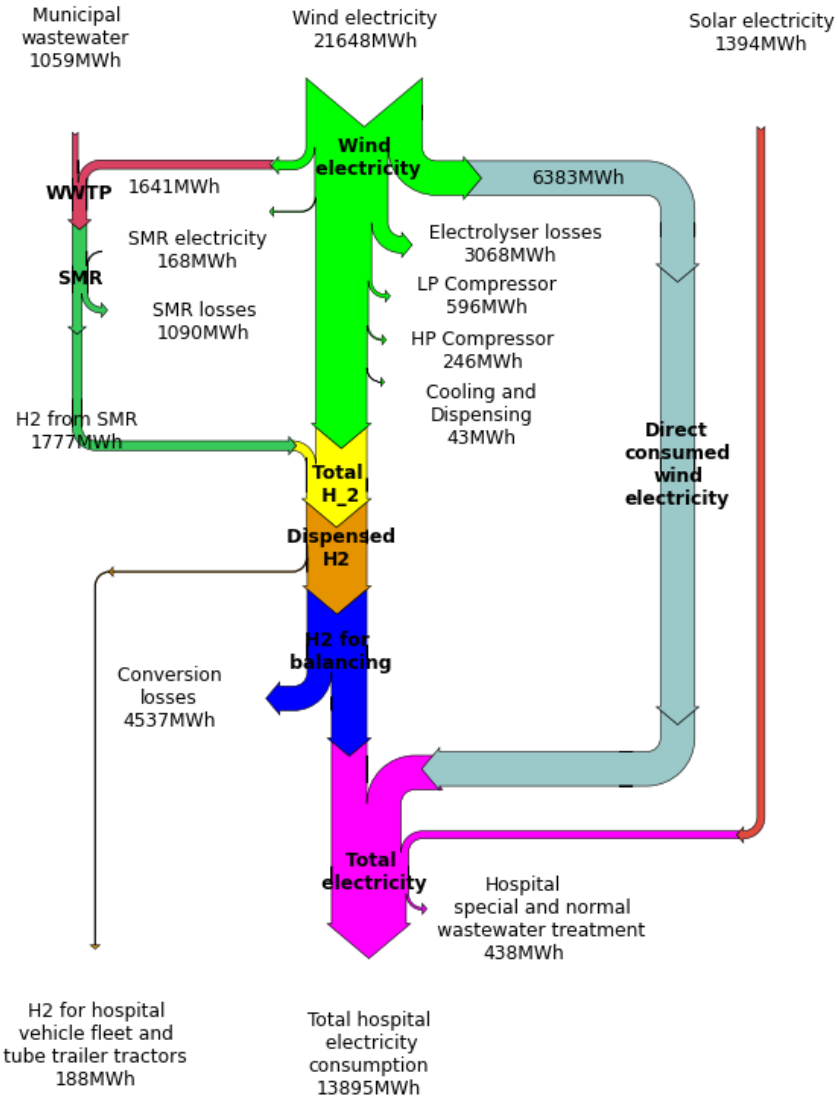

Figure 4-5 Annual energy balance of the integrated transport and energy system.

4.4.2 Hourly electricity balance and FCEV balancing

The hourly electricity balance is maintained at all times, by either converting surplus electricity into hydrogen via the electrolyzer or converting hydrogen into electricity by grid connected FCEVs when there is a shortage of electricity, see Figure 4-6. The electrolyzer maximum capacity is 4.8 MW with a capacity factor of 25%. Maximum shortage power is 2.50 MW, which corresponds to 250 FCEVs at 10kW V2G power, with a capacity factor of 30%. For about 1900 hours, both electrolyzer and FCEVs are in operation. This is due to the cable limitation of 2MW between the hospital and WWTP location.

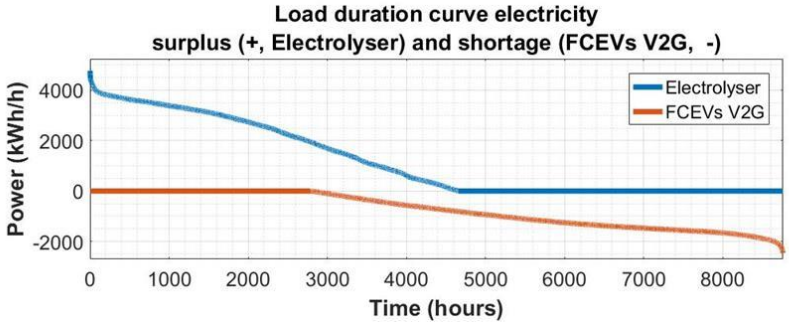

Figure 4-6 Load duration curve electricity surplus (+, electrolyzer operation) and electricity shortage (-, FCEVs V2G operation). Due to the cable limitation for about 1800 hours both electrolyzer and FCEVs are running simultaneously.

Figure 4-7 shows the number of FCEVs required for balance over the course of a year for every hour of the day. On average during nighttime, more FCEVs are required as during daytime, due to the absence of solar power. The whiskers, representing 1.5 times interquartile range are smaller during nighttime, due to the lower power consumption during night. During daytime, interquartile range is larger and also outliers (red plus sign) occur, this can be explained by fluctuating solar energy due to moving clouds at windy days. Maximum number of 250 FCEVs occurs in the beginning of December at 15h. On average during the year 75 FCEVs can provide all balancing, occupying only 15% of the 500 parking places available.

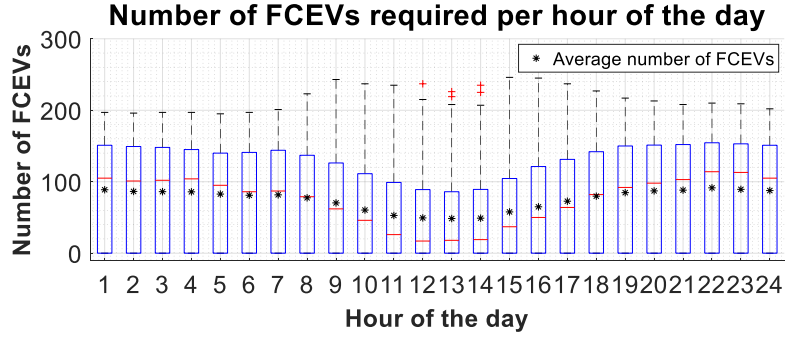

Figure 4-7 Number of FCEVs required for balancing during the day. The blue box represents the 25th and 75th percentile (50%). The whiskers represent 1.5 times the interquartile range (49.7%). Outliers are marked with a red plus, medians with a red horizontal line in the blue boxes and the averages by a black asterisk.

4.4.3 Hourly hydrogen balance

Figure 4-8 shows the net hydrogen production during the year, with a net import/export of zero. A seasonal effect can be observed showing more hydrogen production during the winter months, due to the higher wind production in this period. In case of seasonal storage, storage size should be approximately 70,000 kg of hydrogen with a start filling of 20,000 kg for the analyzed year. A storage size of 70,000 kg corresponds to 24% of the total annual hydrogen production.

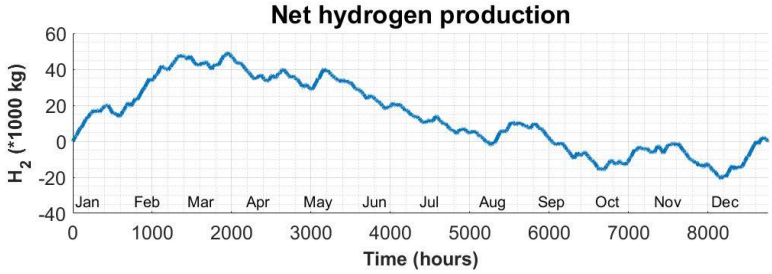

Figure 4-8 Net hydrogen production profile shows that the net import and export of hydrogen over a year is zero.

4.4.4 Component sizing

Table 4-2 shows the main component sizes of the integrated transport and energy system. Maximum required wind turbine power of 5.8 MW, representing approximately 1.4 wind turbines of 4.2 MW, is about 1 MW smaller than the maximum required electrolyser power. This is because of the base load of more than 1MW of the hospital. In practice 2 wind turbines or more will be installed, so either surplus electricity will be sold to other consumers in the region or more hydrogen will be produced. 1 dispenser is sufficient to fuel the hospital car fleet and the parked FCEVs used for balancing. 2 tube trailers and 1 tractor are required for all hydrogen transport between hospital and WWTP site and for importing and exporting temporary surplus and shortage hydrogen.

Table 4-2 Main installed component sizes of the integrated transport and energy system.

Main components	**Installed sizes**
Solar system (MWp)	1.3
Wind turbine (MW)	5.8
Electrolyser (MW)	4.8
Steam methane reformer (kg/h H_2)	8.5
Compressor at WWTP (kg/h)	120
Compressor at HFS (kg/h)	110
Dispensers	1
Tractors	1
Tube Trailers	2

4.5 Feasibility replacement emergency power system by V2G FCEVs

4.5.1 Replacement Uninterruptable Power Supply (UPS) systems

During the first 15 seconds of an electricity outage the Uninterruptable Power Supply systems provide the necessary power. After 15 seconds the emergency power diesel generators should take over. The hospital's dispersed UPS systems have a combined power output of approximately 500kW and capacity of 95 kWh. Power output can be matched with 50 FCEVs, taking into account the V2G connection limitation of 10kW. To match the energy capacity approximately 95 FCEVs would be required. The high voltage battery in the grid connected FCEVs can respond within a second to any load.

4.5.2 Replacement emergency power diesel generators

The maximum power capacity of the existing emergency power diesel generators is 150% of the hospital peak power (3.6 MW), so including 50% redundancy. The emergency generators consist of 3 subsystems each able to provide 50% of the peak power. To match this power output including redundancy, 360 FCEVs are required, taking into account the V2G connection limitation of 10kW. Questionable is if a 50% redundancy is required at all times in case of replacement by 360 grid connected FCEVs. The probability of failure on demand of 120 FCEVs at once is likely lower than 1 out of 3 systems. As FCEVs are mobile, sizing the emergency power system for only the hospital base load could be an option as well, resulting in 120 FCEVs. As within short periods of time additional FCEVs could be driven into the car park.

The hospital has approximately 2200 full-time appointed employees. Assuming three shifts a day, with a night-shift occupation of 50% of a day-time shift, would result in the presence of 440 employees during night-time. If 50% of the 440 employees would have an FCEV provided by the hospital, including V2G capabilities, 220 FCEVs would be present at all times. Although this is still somewhat lower than the hospital peak power, by switching off a heat pump this could be lowered temporarily.

6 days of autonomy at average hospital power demand (1.6MW) is guaranteed by the diesel tanks of the emergency generators. This can be achieved as well with hydrogen as following. The high-pressure hydrogen storage at the HFS is dimensioned such that it provides 1 day of autonomy (Section 4.3.3.9). Combined autonomy of using hydrogen from the on-board tanks of the 220 FCEVs present, results in another 20h of autonomy. If required, after the first day, an additional 4.5 days of autonomy can be guaranteed by trucking in 5-6 additional tube trailers (about 20h of autonomy per tube trailer). In this way a total of 6 days of autonomy or more can be achieved during an electricity outage.

Keeping in mind that the system is designed for a Mid Century scenario (~2050), self-driving cars and trucks could facilitate the replacement of the emergency diesel power system by grid connected FCEVs and tube trailers. FCEVs could connect themselves in the car park via inductive discharging.

Partial replacement of the emergency power system could be an option as well. Base load power could be provided by a stationary UPS and smaller emergency power system. Additional peak power and days of autonomy could be provided by grid connected FCEVs and hydrogen tube trailers.

4.6 Conclusions

An 100% renewable and reliable integrated transport and energy system for a 526-bed hospital is designed using only urban energy sources. The hospital energy system is dimensioned using European statistics, based on 100,000 inhabitants. Rooftop solar and biogas from municipal wastewater of 100,000 inhabitants, together with estimated energy savings in building of 20% in a Mid Century energy scenario, is not sufficient to provide year round renewable energy supply. Therefore, additional wind energy, installed at the wastewater treatment plant site closes the energy balance. Rooftop solar energy provides 6% of the required energy. Due to the high specific building energy per square meter and high-rise buildings, a relatively low amount of rooftop area is available for solar energy. Biogas from municipal wastewater wind energy provide respectively 4% and 90% of the primary energy supply. Temporary surplus electricity can be converted into hydrogen via electrolysis and stored for temporary shortages. Seasonal imbalance is solved by exchanging hydrogen with other local hydrogen consumers and producers or by using salt caverns as hydrogen storage. The system is balanced at all times, by converting stored hydrogen into electricity by less than 250 grid connected FCEVs. The car park at the hospital with 500 places can easily host the FCEVs.

The existing emergency power system consist of two subsystems: an uninterruptable power supply and emergency diesel power generators including diesel tanks providing 6 days of autonomy during an electricity outage. The uninterruptable power supply system could be replaced by approximately 95 grid connected FCEVs. The high-pressure hydrogen storage at the hydrogen fueling station provides sufficient hydrogen for 1 day of autonomy. 220 grid connected FCEVs could provide sufficient power and another 20hours of autonomy. If required, after the first day, an additional 4.5 days of autonomy can be guaranteed by trucking in 5-6 additional tube trailers (about 20h of autonomy per tube trailer). In this way a total of 6 days of autonomy and even more can be achieved during an electricity outage. Partial replacement of the emergency power system by grid connected FCEVs and tube trailers could be an option as well.

5 Fuel cell electric vehicle as a power plant: fully renewable integrated transport and energy system design and analysis for smart city areas

The research presented in this chapter has been published in [235]. The work in this chapter tries to address research sub-questions 2 “How can we integrate FCEVs, used for transport, distributing and generating electricity, into future energy systems?” and 3 “What impact do European regional characteristics have on the techno-economic system performance and the usage of FCEVs for transport, distributing and generating electricity?”. A combined approach of system design, heuristic modeling, simulation and techno-economic scenario analysis is used.

5.1 Abstract

Reliable and affordable future zero emission power, heat and transport systems require efficient and versatile energy storage and distribution systems. This paper answers the question whether for city areas, solar and wind electricity together with fuel cell electric vehicles as energy generators and distributors and hydrogen as energy carrier, can provide a 100% renewable, reliable and cost-effective energy system, for power, heat, and transport. A smart city area is designed and dimensioned based on European statistics. Technological and cost data is collected of all system components, using existing technologies and well-documented projections, for a Near Future and Mid Century scenario. An energy balance and cost analysis are performed. The smart city area can be balanced requiring 20% of the car fleet to be fuel cell vehicles in a Mid Century scenario. The system levelized cost in the Mid Century scenario is 0.09 €/kWh for electricity, 2.4 €/kg for hydrogen and specific energy cost for passenger cars is 0.02 €/km. These results compare favorably with other studies describing fully renewable power, heat and transport systems.

5.2 Introduction

The urgency to significantly reduce the impacts of climate change is felt around the globe. December 12, 2015, 195 governments agreed on a long-term goal of keeping the increase in global average temperature to well below 2°C above pre-industrial levels and aim to limit the increase to 1.5°C [325].

In view of these goals both the energy and transport systems need to change into zero emission systems. Both systems need to become clean while remaining reliable and affordable. This will require major technological, organizational and social changes in both the energy and the transport system. We envisage major transitions in and integration of both systems.

The transition in the electricity system will be from fossil fueled power plants to renewables. However, the intermittent nature of many renewables such as wind and solar require a more flexible electricity system, which may be provided by

flexibility in demand, electricity storage, electricity conversion into fuels, chemicals or heat and (distributed) smart grids [345].

The major technological transition in the transport system will be from combustion engines to electric engines. The electricity will be provided by batteries or fuel cells that can produce electricity with high efficiencies from a fuel such as hydrogen. In addition, an electricity charging infrastructure and/or hydrogen fueling infrastructure is needed to accommodate the introduction of electric vehicles.

Until today both the electricity and transport system have developed independently from each other. However, the integration of these two systems may solve major problems related to the separate transitions described above, and create synergies benefiting both systems [218,220,223,225,393–395]. To our knowledge, no such comprehensive study has been performed up to now. Many studies and pilot projects investigate (stand-alone) renewable energy systems using hydrogen as energy storage and stationary fuel cells for re-conversion of the stored hydrogen [203,204,403–412,205,413,396–402]. Some studies use the produced hydrogen for transport [207,393,421,398,414–420] or solely use the fuel cell in the vehicle as an electric generator [214,215,422] without considering hydrogen production. None of the aforementioned studies integrates grid connected hydrogen fuel cell powered transport, renewable electricity and hydrogen production and hydrogen reconversion on the scale of a smart city area, analyzing energy demand and cost of energy in different time frames.

Balancing excess and shortage of electricity can be handled in three ways:

1. Power to Power. At moments of excess electricity generated by renewables, the electricity can be stored in batteries of electric vehicles which are connected to the grid. When there is a shortage of power production by renewables, the stored electricity in car batteries could be used to feed into the grid. At present the electricity stored in batteries of a car is between 10 and 90 kWh.
2. Power to Gas and Power to Chemicals [413]. At moments of excess electricity by renewables the electricity can be converted into hydrogen. The hydrogen can be stored under pressure and transported by boat and/or truck to car fueling stations as a clean fuel. Hydrogen has a high energy density, 39 kWh/kg (HHV). Pressurized hydrogen tanks in present fuel cell cars contain 5 to 6 kg hydrogen [423]. Hydrogen can also be used as a feedstock to produce chemicals and other fuels such as ammonia, methanol, methane, and formic acid.
3. Gas to Power. At moments of electricity shortage, the fuel cells in vehicles could supply electricity to the grid [181,200,214–216,221,424–427], using the hydrogen stored in their tank. Fuel cells can produce electricity from hydrogen with a high efficiency. Peak energy efficiencies of the present PEM fuel cells in the cars are about 51.5% (HHV) in part load, with United States (US) Department of Energy (DOE) targets of 60.0% (HHV) [126,194]. One kilogram of hydrogen can therefore supply between 20 and 25 kWh to the electricity system.

Cars have sufficient power to influence the energy system world-wide. Summarizing an analysis done by [2]: Worldwide power plant capacity is about 5.000 GW. At present the typical fuel cell of a car has a capacity of about 100 kW, sufficient to power on average 100 European homes. Every year worldwide more than 80 million new cars are sold. The number of new cars multiplied by 100 kW capacity per fuel cell per car, would amount to 8.000 GW new power production capacity on the road every year. In a renewable electricity production system, fuel cell cars can therefore provide all necessary flexible electricity production capacity.

Hydrogen can be produced from all kind of renewable energy sources, such as biogas, biomass, direct sunlight or renewable electricity [428–432]. Also hydrogen can be produced far from load centers [433]. It can be stored and transported by boat and truck to these load centers, mainly associated with urbanized areas [434]. For example floating wind turbines far in the ocean at very high wind speed locations, can produce electricity which is converted into hydrogen by electrolysis and shipped to the load centers [435,436]. This creates flexibility in supply and demand for renewable energy production both geographically and in time and avoids huge investments in electricity transmission lines between renewable energy generation sites and demand centers [437].

Market introduction of Fuel Cell Electric Vehicles (FCEVs) is gaining momentum [182,438–440]. Many scenarios show substantial penetration of fuel cell vehicles in the coming decades [126,441–448]. The Japanese government wants to create a market for hydrogen and fuel cell cars, with projected annual market size increasing to 800,000 fuel cell electric vehicles sold in 2030 [449]. Similar in Germany, a program is initiated to build 400 hydrogen fueling stations in the coming years in Germany, combined with car fleet development [450,451].

Studies [452] show strong evidence of achievable cost reductions for hydrogen technologies, to approx. 30 USD/kW for automotive PEM fuel cell systems in production volumes of 500,000/year; with comparable cost reduction for hydrogen generation cost [452]. But also hydrogen storage tank costs, electrolyzer costs and compressor costs will decrease considerably in the coming decades, based on technology improvements but primarily on increasing production volumes [126].

Inspired by the concept of a “Hydrogen Economy” [279,414,453–459], the question arises: Can solar and wind electricity together with fuel cell electric vehicles and hydrogen as energy carrier, provide a 100% renewable, reliable and cost effective energy system, for power, heat, and transport for smart city areas? To get insights and answers to this question, this study performs the design, energy balance, and cost analysis of an integrated electricity and transport system, based on renewable electricity production, hydrogen as an intermediate energy carrier and fuel cell electric vehicles for transport and providing all the necessary flexibility for the electricity system, in two time frames: Near Future and Mid Century.

5.3 Methodology

5.3.1 Approach

The research is performed in five steps:

1) Design and dimensioning of a fully autonomous renewable and reliable integrated transport and energy system for a smart city area based on European statistics. Requirements are listed in section 5.3.2.
2) Analyzing annual energy demand for the designed smart city area in two time frames: a Near Future (around 2020) and Mid Century scenario (around 2050), see section 5.3.3.
3) Calculating the annual energy balance by matching energy demand with solar and wind electricity production, energy storage in the two scenarios, see section 5.3.4. Selection of technologies for the components of the energy system in the smart city area and analyzing their technological and economical characteristics in two time frames.
4) Calculating cost of energy for the two time frames, by calculating in section 5.3.5
    a) Smart city area total system cost of energy
    b) System levelized cost of energy
    c) Specific cost of energy
5) Sensitivity analysis for the cost of energy in the Mid Century scenario for a wide range of key assumptions and parameters used, see section 5.3.6.

5.3.2 System design requirements and dimensioning

A fully autonomous renewable and reliable energy and transport system is designed for a smart city area. The smart city area energy and transport system is designed in such a way that it fulfills the following design requirements:

- uses only electricity and hydrogen as energy carriers and is all electric in end use
- uses only hydrogen to power all road transport vehicles
- is an average European city area.
- is integrated into existing infrastructure and buildings
- does not require a new-build underground infrastructure, for example an underground hydrogen pipeline network
- uses abundant renewable energy sources in Europe: solar and wind only
- is independent of High and Medium Voltage electricity grids, natural gas and district heating grids or expansion of these.

Section 5.4 describes the design and dimensioning of such an energy system starting by a statistical analysis of the European characteristics for an average city area. The dimensioning includes a wide range of aspects defining a city area, for example the number of inhabitants and households, floor and roof area of buildings, road transport vehicles and refueling stations.

5.3.3 Analyzing energy demand

The annual energy demand of such an integrated transport and energy system for a smart city area started by a statistical analysis of the European Union (EU) energy consumption in buildings and for road transport, see section 5.5. Building energy consumption consists of heating, cooling and electrical appliances in the residential sector and the services sector. Road transport energy consumption analysis looks into average transport kilometers per vehicle type and its energy consumption. For such an average city area, the Near Future and Mid Century energy demand in buildings and for transport, are based on statistical historical data and studies about future energy efficiency improvement in end use, use of different technologies such as heat pumps for heating and by replacing conventional internal combustion powered road vehicles by hydrogen powered fuel cell electric vehicles.

The two scenarios can be characterized as follows:

- The Near Future scenario uses *current state of the art* renewable and hydrogen technology and current energy demand for buildings and transport. It is already an all-electric energy system in the end use, which means space heating is done via heat pumps fulfilling present heat demand for houses and buildings. Only commercially available hydrogen technologies are used. For all systems, including hydrogen technologies, present technology characteristics and cost figures are used. The near future scenario presents a system that could be implemented around 2020.
- In the Mid Century scenario a *significant reduction of end-use energy* consumption is assumed. Hydrogen and fuel cell technology *has become mature with mass production* and performing on the cost and efficiency targets projected for 2050. Also for all the other technologies, such as solar, wind, electrolyzers the learning curves are taken into account.

In both scenarios it is assumed that the number of vehicles and the annual kilometers driven per vehicle are the same as nowadays.

5.3.4 Calculating the energy balance

The maximum amount of generated solar electricity in the smart city is calculated with the available roof area on buildings, based on the statistical analysis of the average European city area in section 5.4. Due to the possible insufficient solar electricity production and mismatch with building and transport energy consumption (see section 5.5.4), additional wind electricity and energy storage is required.

A technology choice is performed and an assessment is conducted for, efficiencies, sizes, cost and development in time for all involved components of the smart city area energy system, see section 5.6. Component sizes are determined using calculation methods from other studies or are based on average day patterns.

Once the technology choice and assessment are performed, the energy balance is calculated. In both scenarios wind electricity closes the annual energy balance of energy demand and local solar electricity generation, taking into account all efficiencies of the different conversion and storage technologies.

5.3.5 Calculating cost of energy

Three components for the cost of energy (CoE) will be calculated.

- Smart City Area Total System Cost of Energy, $TSCoE_{SCA}$ in Euro per year.
- System Levelized Cost of Energy for electricity $SLCoE_e$ in Euro per kWh and for hydrogen $SLCoE_H$ in Euro per kg Hydrogen.
- Specific Cost of Energy for Buildings $SCoE_B$ in Euro per m^2 per year and for Transport $SCoE_T$ in Euro per km.

5.3.5.1 Smart city area total system cost of energy

The $TSCoE_{SCA}$ in Euro per year, Equation (7.11), is the sum of the Total annual capital and operation and maintenance Costs TC_i (€/year) of the total number of components (n) in the Smart City Area:

$$TSCoE_{SCA}\left(€/year\right) = \sum_{1}^{n} TC_i \tag{5.1}$$

The TCi of an individual component, Equation (7.11), are calculated with the annual Capital Cost CC_i (€/year) and Operation and Maintenance Cost OMC_i (€/year):

$$TC_i\left(€/year\right) = CC_i + OMC_i \tag{5.2}$$

The CC_i (€/year) of a component is calculated with the annuity factor AF_i (%), installed component capacity Q_i (component specific capacity) and Investment Cost IC_i (€ per component specific capacity):

$$CC_i\left(€/year\right) = AF_i \times Q_i \times IC_i \tag{5.3}$$

Where the annuity factor AF_i [460,461], Equation (7.11), is based on the weighted average cost of capital WACC (%) and the economic lifetime of a component LT_i (years):

$$AF_i = \frac{WACC \times \left(1+WACC\right)^{LT_i}}{\left[\left(1+WACC\right)^{LT_i}\right]-1} \tag{5.4}$$

The annual operation and maintenance costs OMC_i (€/year), Equation (7.11), are expressed as an annual percentage OM_I (%) of the Q_i and IC_i:

$$OMC_i\left(€/year\right) = OM_i \times Q_i \times IC_i \tag{5.5}$$

The cost analyses are in constant 2015 euros. An exchange rate of 0.88 USD to EUR is used. The website [462] is used to convert all USD values to USD_{2015} values. A WACC of 3% is used.

5.3.5.2 System levelized cost of energy

The system levelized cost of energy, for either electricity $SLCoE_e$ (€/kWh) in Equation (5.6) or hydrogen $SLCoE_H$ (€/kg H_2) in Equation (7.11), are calculated by allocating a share of the $TSCoE_{SCA}$ related to either electricity $TSCoE_{SCA,e}$ or hydrogen consumption $TSCoE_{SCA,H}$. These shares are then divided by either the annual electricity EC_e (kWh/year) or hydrogen consumption EC_H (kg H_2/year) and resulting in respectively the $SLCoE_e$ or $SLCoE_H$:

$$SLCoE_e\left(€/kWh\right) = \frac{TSCoE_{SCA,e}}{EC_e} \tag{5.6}$$

$$SLCoE_H\left(€/kg\ H_2\right) = \frac{TSCoE_{SCA,H}}{EC_H} \tag{5.7}$$

5.3.5.3 Specific cost of energy

The specific cost of energy is defined as the energy cost per physical unit [463]. For transportation services, the Specific Cost of Energy for transport $SCoE_T$ is defined as the energy cost for driving a vehicle over a distance of 1 km. For FCEVs the $SCoE_{T,veh}$ in Equation (5.8), is the Specific Energy Consumption of hydrogen per hundred kilometer for each type of vehicle, $SEC_{T,veh}$ (kg H_2/100 km), times the $SLCoE_H$ and divided by 100 kilometer:

$$SCoE_{T,veh}\left(€/km\right) = \frac{SLCoE_H \times SEC_{T,veh}}{100\,km} \tag{5.8}$$

For building energy consumption, the Specific Cost of Energy for Buildings $SCoE_B$ (€/m^2/year) in Equation (7.11) is defined as the cost of the annual Specific Energy Consumption SEC_B (kWh/m^2/year) by all energy-consuming equipment within that building per square meter:

$$SCoE_B\left(€/m^2/year\right) = SLCoE_e \times SEC_B \tag{5.9}$$

5.3.6 Sensitivity analysis

A sensitivity analysis for the Mid Century scenario is performed for the parameters that have a large impact on the $TSCoE_{SCA}$. Amongst others the specific energy consumption of FCEVs, cost of hydrogen technologies, specific energy consumption of buildings and annual solar irradiation.

5.4 Design of a fully autonomous renewable and reliable energy system for a smart city area

5.4.1 Smart integrated energy and transport city functional design

Main energy consumers in cities are buildings and transportation vehicles and account for 67% of the final energy consumption in the EU [464]. Buildings in cities belong to either the residential or services sector, as industrial buildings are often located outside city areas. Energy consumption of road transportation vehicles energy accounts for 80% of the EU final energy consumption for transportation [464]. The road transportation vehicles are owned by either the residential or services sector and energy is consumed in or between smart city areas. By applying the design requirements from section 5.3.2, the integrated system design of the smart city area has the following 6 major elements (Figure 5-1):

- The residential and services sector buildings. All buildings have rooftop solar electricity systems and water collection systems. The buildings are all electric, without any natural gas connection. Industrial and agricultural buildings are excluded from the analysis.
- Hydrogen production & purification, and storage system.
- Smart electric grid, managed by a controller, which connects all buildings and cars.
- A hydrogen tube trailer transporter and a Hydrogen Fueling Station (HFS).
- A fleet of hydrogen fuel cell cars and other road transportation vehicles.
- An off-site wind turbine park, not located near or in the smart city area, with water collection, purification and hydrogen production and storage system, with no electrical grid connection

The functional energy performance of the smart city area comprises of the following conversion steps:

- Electricity is generated by solar modules on all roofs.
- Rainwater is collected from the roofs of buildings and is demineralized and purified and used in the electrolysis process. Purification is needed for good operation of the electrolyzer.
- Surplus solar electricity is converted via water-electrolysis into pure hydrogen. The hydrogen is compressed and stored into tube trailer modules. Full tube trailer modules are transported by a trailer tractor to the nearby Hydrogen Fueling Station (HFS).
- At the HFS, the hydrogen is further compressed depending on vehicle demand. Electric energy required for hydrogen compression at the HFS comes from the city area.
- The hydrogen is used as a transport fuel for all types of fuel cell powered electric vehicles; passenger cars, vans, motorcycles, buses and trucks.
- In case of a temporary shortage in production of solar electricity, the fuel cells in grid-connected passenger cars provide the necessary electricity by converting hydrogen from the on-board hydrogen storage tanks. At parking places at home or at the local shopping area, vehicle-to-grid points connect the cars to the smart city electrical grid.

- All wind-electricity produced is converted at the wind turbine park into hydrogen via water-electrolysis. These wind turbines are located either on-shore or off-shore. The produced hydrogen from wind is transported via tube trailers to a hydrogen fueling station.
- Surface or seawater in the vicinity of the wind turbines is purified and used in the water-electrolysis process.

The system design configuration is flexible to use other renewable energy sources if present, for example as biomass or hydropower to hydrogen, but is not analyzed in this study.

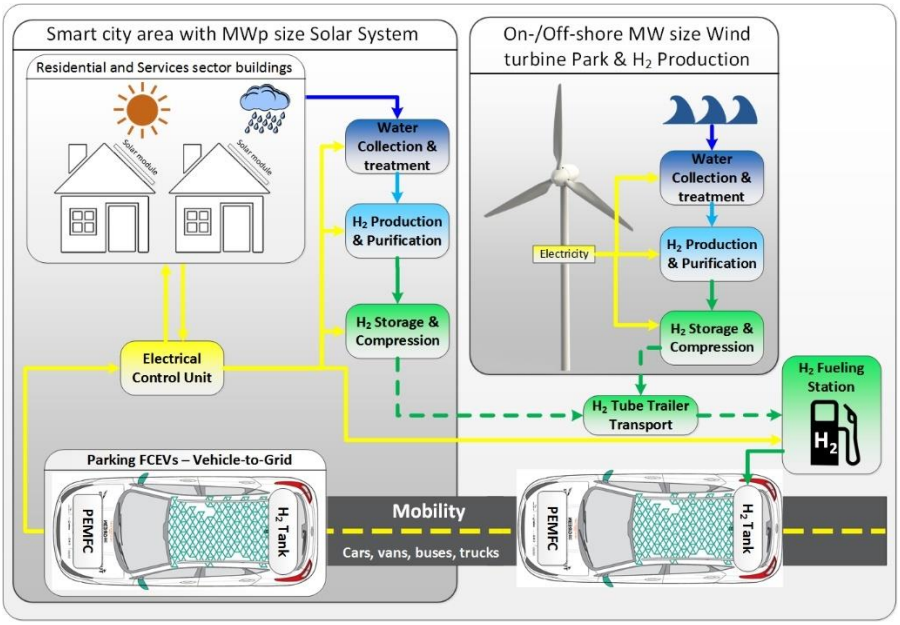

Figure 5-1 Smart City Area key elements and functional energy performance.

5.4.2 Dimensioning of smart integrated city area

The size of a European city area for this study is determined using the dispersion of supermarkets and petrol stations. In the EU 28, for every 1,900 households there is one petrol station [465,466] and for every 2,100 households there is an medium-sized supermarket so 2,000 households is a good indicator for dimensioning the smart integrated city area. This hydrogen fueling station will serve a similar vehicle population as current gasoline stations [386]. Total capital cost per capacity for large HFS (≥ 1,500 kg/day) is lower than for smaller HFS [467]. Also in the future with lower specific energy consumption for transport the hydrogen fueling station will still dispense sufficient amount of hydrogen [467] with the benefits of lower total capital cost per capacity.

On average 2,000 households correspond to 4,700 persons, with in total 2,300 cars, 190 motorcycles and some 320 other vehicles and each household using 89.75 m^2 of built area, according to European statistical data [465,466,468–474], see Table 5-1. Of the lorries and vans, approximately 10% are lorries [475–481].

Table 5-1 Characteristics of a smart European city area.

Parameter	Quantity
Petrol stations	1
Food retail shop	1
Households and dwellings[1] in smart integrated city	2,000
Persons	4,680
Floor area buildings residential (m^2)	179,500
Floor area buildings services (m^2)	57,200
Passenger cars	2,300
Motorcycles	190
Lorries and Vans	300
Large Trucks with trailers (road tractors)[2]	18
Buses	8

[1] Assumed that only 1 household lives in a dwelling.
[2] The number of large trucks with trailers includes the number of tractors used for transporting hydrogen tube trailers.

5.5 Energy demand and production in two scenarios

5.5.1 Residential Sector

The building-related energy demand of the residential sector accounts for 27% of the total EU final energy consumption [464]. The present European residential building floor space of 18.95 million m^2 and present-day energy consumption was, 3,493 TWh/year [464,472]. For the Near Future scenario, all electric buildings are assumed, where heat pumps with an estimated annual average COP of 3.5 replace conventional heating & cooling [482–485]. In the Mid Century scenario, buildings are also all-electric, and significant energy savings will be achieved: 95% savings on space heating and cooling and 50% on water heating [486]. It is assumed cooking energy consumption [472] in the Mid Century scenario will be the same as in the Near Future scenario. Although lighting energy savings will be significant by LED technologies, electrical consumption will increase due to an increased number and use of electrical appliances and home-automation. Therefore, it is assumed that the combined electricity consumption for electrical appliances, lighting and cooking is the same as in the Near Future scenario.

Road transport energy accounts for 26% of the total EU final energy consumption [464], of which 1,959 TWh/year (59%) is due to passenger cars [470]. For the Near Future and Mid Century scenario, 100% hydrogen powered FCEVs are foreseen, with a $SEC_{T,car}$ of 1.0 and 0.6 kg H_2/100 km, respectively [126]. The final energy consumption for motorcycles is not included as it represents only 1.3% [429] of the total road transport final energy consumption.

In both scenario's, the present European passenger cars average annual driven distance of 11,940 km [470] is used. With the specific energy consumption and energy content of 39.41 kWh/kg of hydrogen (on a HHV basis), the annual final energy consumption of a FCEV passenger car, equivalent to 62 respectively 37 kWh per square meter residential floor area per year.
Summarizing: the total specific energy consumption in the residential sector for transport and buildings is calculated using data from Table 5-1, [126,464,466,469,470,472,473], and results in 288, 142, and 89 kWh/m^2/year at Present, Near Future, and Mid Century, respectively, see Table 5-2. The specific energy consumption in buildings is comparable with the values in [487].

Table 5-2 Specific energy consumption (kWh/m^2/year) per consumption category for the residential sector.

	SEC [kWh/m^2/year]		
Energy consumption category	**Present**	**Near Future**	**Mid Century**
Space heating & cooling	126.3	27.4	6.3
Water heating	23.3	19.6	11.7
Electrical appliances, lighting, cooking	34.7	33.4	33.4
Total in buildings ($SEC_{B,residential}$)	184.3	80.4	51.4
Passenger cars relative to floor surface	103.4	62.0[1]	37.2[1]
Total transport and buildings	287.7	142.4	88.6

[1] Specific energy consumption on a HHV basis.

5.5.2 Services Sector

The building-related energy consumption of European services sector accounts for 1,850 TWh per year (with climatic corrections) [471], equal to 14% of the total EU final energy consumption [464]. For the Near Future scenario a combined energy saving of 50% is assumed compared to the present situation, by virtue of application of heat pumps [232,488–492] for all thermal energy demands [493]. For the Mid Century scenario energy saving of 50% is assumed for hot water and 85% for other thermal demands compared to the present situation, based on [486].
Road transport of the services sector, excluding passenger cars, accounts for 10 % of the total EU final energy consumption, 1,302 TWh/year [464,470]. In both scenarios, all vehicles are powered by hydrogen fuel cells. Table 5-3 shows the average annual distance driven [475,476,497,498,477–481,494–496] and the $SEC_{T,veh}$ (kg H_2/100km) for vans, lorries, road tractor and buses for both scenarios. The specific energy consumption in the Near Future of vans is based on the average of [187] and [499] with an assumed average fuel cell system Tank-To-Wheel (TTW) efficiency of 51.5% (HHV) [126]. For lorries and road tractors it is based on the specific energy use of Battery Electric Vehicle (BEV) type lorries and road tractors [187] and the fuel cell system Tank-To-Wheel (TTW) efficiency [126]. FCEV bus specific energy use for the Near Future is taken from [500]. An efficiency improvement of 30% for vans (somewhat lower than the 40% expected for cars [126] and 20% for FCEV buses, lorries and road tractors [500], is assumed in Mid Century scenario.

Table 5-3 Average annual distance driven and Near Future and Mid Century specific energy consumption for van, lorry, road tractor and bus type FCEVs.

Vehicle type	EU average annual distance driven [km/year]	Near Future $SEC_{T,veh}$ [kg H_2/100km]	Mid Century $SEC_{T,veh}$ [kg H_2/100km]
Van	20,725	1.3	0.9
Lorry	46,176	4.6	3.7
Road tractor	87,152	6.9	5.5
Bus	47,611	8.6	6.9

With the specific energy consumptions given in Table 5-3 and the energy content of 39.41 kWh/kg of hydrogen (HHV basis), the annual final energy consumption of FCEVs is calculated. In Near Future as well in Mid Century the average annual distance driven remains constant. The number of tube trailer trucks for hydrogen transport and their driven kilometers are assumed to be included in the number of road tractors and their annual driven kilometers. Using the data from [126,464,470,471,473,493], Table 5-1 and Table 5-3, total specific energy consumption for the service sector area is calculated, see Table 5-4. The total specific energy consumption is 522, 411, and 307 kWh/m^2/year at present, Near Future, and Mid Century, respectively. The specific energy consumption in buildings is comparable with the values in [487].

Table 5-4 Specific energy consumption (kWh/m^2/year) per energy consumption category for the services sector.

	SEC [kWh/m^2/year]		
Energy consumption category	**Present**	**Near Future**	**Mid Century**
Space heating & cooling, process heating & cooling (with climatic corrections)	166.1	83.1	25.0
Water Heating	27.0	13.5	13.5
Electrical appliances, lighting	113.4	113.4	113.4
Total in buildings ($SEC_{B,services}$)	306.6	210.0	152.7
Road vehicles (vans, lorries, buses, road tractors) relative to floor surface	215.7	198.8[1]	154.1[1]
Total transport and buildings	522.3	411.7	306.7

[1] Specific energy consumption on a HHV basis.

5.5.3 Local energy production by solar electricity systems

Residential and service sector roofs will be used for solar electricity systems and for rainwater collection [501–503]. Solar electricity systems are installed on all technically suitable roof areas: 9 m^2 per person on residential buildings and 4 m^2 per person on service sector buildings area [504,505]. Façades are not considered. In the Near Future scenario the performance ratio and solar module efficiency are 0.75 and 0.20 kWp/m^2, and in the Mid Century scenario these are 0.90 and 0.35 kWp/m^2 [370,506–510]. Thus 12.4 and 21.3 MWp are installed in Near Future and Mid Century scenario, respectively. The electricity generated is calculated using a typical global irradiation on optimally inclined modules in European urbanized areas of 1,300 kWh/m^2/year [343,511,512].

5.5.4 Overview energy consumption and production

The final energy consumption for each category and solar electricity production for the two scenarios is shown in Figure 5-2. The total final energy consumption for the smart city is 48 and 33 GWh/year in the Near Future and Mid Century scenario, respectively. The solar electricity production is 12 respectively 25 GWh/year.

In the Near Future scenario, demand exceeds supply, and solar electricity systems are insufficient to cover the residential and service sector demand nor the transport energy demand in the Near Future scenario. To balance demand and supply, additional energy has to be generated or imported. Exchange between residential and service sector does not solve this imbalance. In the Mid Century scenario, demand still exceeds supply, but for the residential sector there is a small net surplus of energy, and additional energy is still required. No attention has been given yet to temporal mismatch between solar electricity production and electricity consumption, and storage losses. The next section will address this.

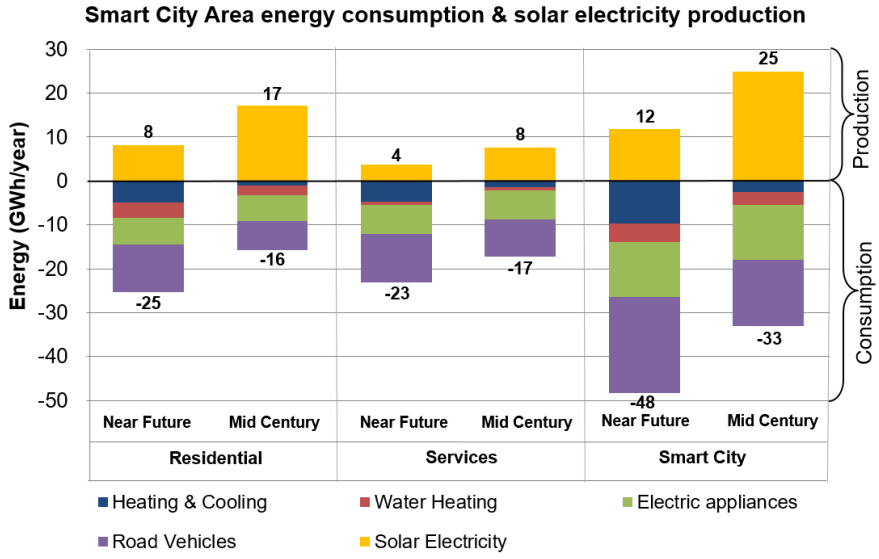

Figure 5-2 Generated solar electricity in each scenario compared to the building and transport final energy consumption categories.

5.6 Technology choices, sizing, characteristics and development

5.6.1 Data structuring

The relevant conversion processes in the smart city, as shown schematically in Figure 5-3, are:

- hydrogen production and purification,
- hydrogen compression, storage and transport,
- hydrogen fueling station (compression, storage, dispensing and cooling)
- fuel cell electric vehicle power production,
- water collection and storage,
- water treatment,
- solar electricity production,
- wind electricity production

In both scenarios, the most appropriate, commercially available technologies are selected. The size of the components can be deducted from the energy balance. That requires meticulous evaluation of system component characteristics and calculation of the intermediate conversion efficiencies (and losses) especially from electricity to hydrogen production and the partial re-conversion to electricity. Cost characteristics of all these components are determined for both scenarios, using present-day technologies, discarding technologies with Technology Readiness Levels less than 7.

For the system cost calculations, the energy producing equipment, solar modules and wind-turbines including their installation, connection, maintenance and auxiliary component costs are included in this study. Energy saving measures and appliances and equipment, such as heat pumps, LED lights, washing machines, building automation and improved insulation are *not* taken into account.

All hydrogen related equipment including their installation, connection, maintenance and auxiliary component costs are included. Amongst hydrogen related equipment we consider the electrolyzers, hydrogen purification, compressors, tube trailers and tractors, high pressure compressors, high pressure stationary storage, hydrogen chillers and dispensers.

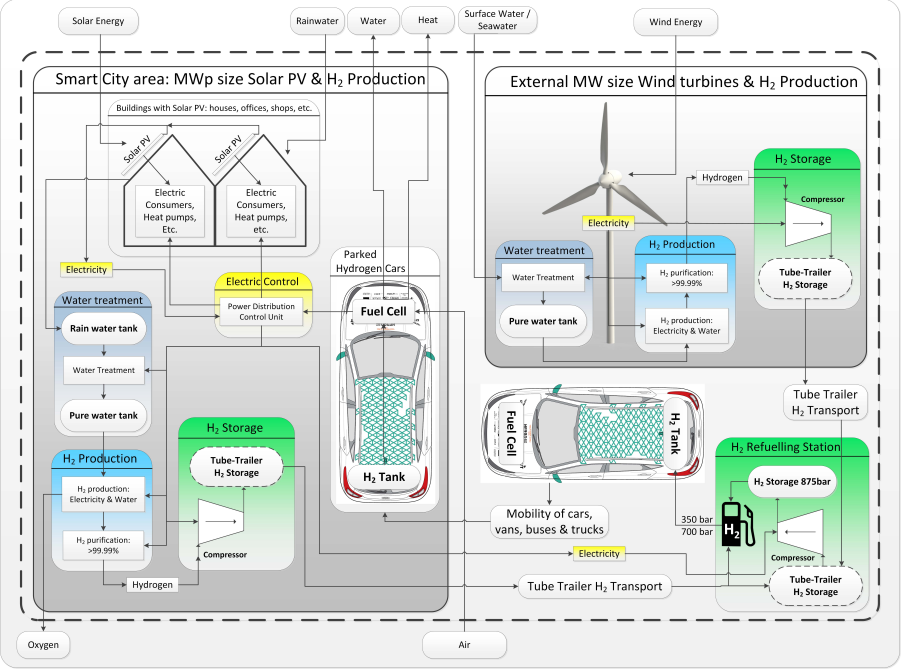

Figure 5-3 The relevant conversion processes in the smart city area.

5.6.2 Hydrogen production and purification: PEM water electrolysis

Technology

The most mature and commercial available technologies in MW-scale systems are alkaline and PEM type electrolyzers [513]. Hydrogen from electrolyzers is not sufficiently pure [514] for FCEV use and needs to be purified [515,516]. PEM electrolyzers are used, because are more suitable to couple with intermittent renewable electricity sources as wind and solar electricity [513,517,518]. Also PEM electrolysis has a higher cost reduction potential and efficiency improvement potential compared to alkaline electrolysis [126,519]. The electrolyzer and purifier energy requirements [126,520–522] are assumed constant over the entire operating range and are listed in Table 5-6. The purifier hydrogen output pressure is 30 bar in both scenarios [513,514,516,521,522].

To calculate the required peak capacity of the electrolyzer connected to the solar system, it is assumed that all hydrogen is produced from the surplus solar electricity within 5 full-load hours per day. Here we assume that if the electrolyzer produces hydrogen, the purification module and compressor run simultaneously and also consume a part of the surplus electricity. The actual operational hours, which determine the stack degradation, are assumed to be 10 hours per day.

The capacity of the electrolyzer connected to the wind turbine park is the wind-turbine capacity minus the electric power requirement of the hydrogen purification module and compressor. The actual operational hours are assumed to be 24 hours per day. It is assumed that the calculated electrolyzer size is available in the market, or larger size electrolyzers are cost-shared with other smart cities.

Cost

Installed capacity capital cost for the PEM electrolyzer is based on an extensive, detailed analysis in power to gas applications [519,523], which concludes 300-350 Euro/kW for a single produced 100MW system in 2030. For the smart city electrolyzer, cost reductions are possible because of higher volume production, economies of scales for membrane production [524] and component reduction, thus coming to 250 Euro/kW for the Mid Century scenario. Other sources have less detail in system size, production volume and components used in 2050 [126] or only have estimations for 2025 [520]. System lifetime is 20 to 30 years, but lifetime of the PEM stack and major components are 80,000 hours in the Near Future scenario and 90,000 in the Mid Century scenario [513,514].

The OM can be found in Table 5-7 for both scenarios for both electrolyzer locations. The OMC consist of a fixed part dependent on electrolyzer size [513] and a variable part due to stack and major component replacement. Replacement costs occur in case operational hours during system lifetime exceed the stack lifetime. The variable part is 15% of the installed electrolysis system cost in the Near Future and 12% in Mid Century [522,525].

5.6.3 Hydrogen storage and transport

Technology

Several types of hydrogen storage exist [526–528], but compressed hydrogen storage is selected, because it is the most mature and commercially available technology in mobile and stationary applications [389,529]. Using tube trailers [379,383,384] for exchange between wind site and urban area. In the Near Future scenario tube trailers can store 720 kg an effective mass of hydrogen at a pressure is 250 bar. In Mid Century scenario this will be 1350 kg of hydrogen at 500 bar [379,383]. At the hydrogen fueling station hydrogen is stored at 875 bar in variable storage sizes [379,389,530–532].

Storage capacity of the hydrogen tube trailers is two times the average daily hydrogen production at each electrolyzer location. The high-pressure stationary storage is sized to contain the average daily dispensed hydrogen. Both types of storage (tube trailer and stationary storage) are not rounded off to the closest available storage tank or tube trailer capacity. The calculated storage capacity is used directly to calculate the (installed) costs. Either a larger or smaller fueling station will be built and shared with a smaller or larger vehicle fleet, as this smart city is based on an illustrative number of vehicles.

The number of tractors for trucking in the tube trailers to the fueling station are calculated using the amount average daily dispensed hydrogen, the capacity of a tube trailer, average driving speed (50km/h), roundtrip distance (100km), loading and unloading time (2 hours) and working hours per day (8 hours) [533], coming to approx. 1 respectively 3.5 tractors in Mid Century versus Near Future scenario. The tractor driver also executes the charging operations so that no further personnel is required [533].

Cost

Economic parameters of the tube trailers, tractors and stationary storage [383,384,530–534] are listed in Table 5-7. Especially tube trailer have long lifetimes of 30 year and an OM of 2% [533]. The OMC consist of the tractor maintenance costs (12% of IC), fuel costs and labor costs (35€/hour) [533]. Fuel efficiency of the tractor is listed Table 5-3. Sea transport costs of hydrogen produced off-shore are not included.

5.6.4 Hydrogen Compression

Technology

Compressors used in hydrogen production and fueling stations selected are of reciprocating multi-stage piston and diaphragm [379]. The electrolyzer and storage pressures define the operating pressures ranges of the compressors. The maximum flow per compressor is assumed to be 250kg/h. If a larger flow is required, multiple compressors will be installed.

The compressor at the solar system and at the wind-turbines are medium-pressure compressors. Maximum flow rate of the medium-pressure compressors is equal to the maximum hydrogen production flow rate from the electrolyzers. Energy consumption of the low pressure compressors is calculated according [380,386].

The compressor at the hydrogen fueling station is a high-pressure compressor. The maximum flow rate of the high-pressure compressor is the average daily dispensed hydrogen compressed in 12 hours [380,381,386]. Energy consumption for the high pressure compressor(s) at the fueling station are calculated using [382], taking into account a variable inlet pressure from the emptying tube trailer.

Specific compression electric energy is assumed constant over the entire operating range of the compressors and can be found in Table 5-6. It is assumed that equal work is done by all three compression stages with intercooling between stages back to original feed temperature. Isentropic compressor efficiency is 60% in the Near Future and assumed 80% in Mid Century [379]. Using the specific compression electric energy with the flow rate of the compressor, the compressor electric power is calculated. The motor rating of the compressor is defined according [380,382,386].

Cost

For the Near Future scenario compressor costs are taken from [535], using the calculated motor power of the compressor for medium- and high-pressure compressors at low production volumes. For the Mid Century scenario compressor costs are calculated with the formulas for high production volumes. Economic

parameters of the compressors for both scenarios can be found in Table 5-7, reflecting OM of 4% and 2% in Near Future and Mid Century [536].

5.6.5 Hydrogen dispensing and cooling

Technology

Hydrogen fueling at 700 bar requires cooling [379] to reduce the temperature increase caused by the gas expansion, done by a chiller. Specific cooling electric energy [388,537] is assumed constant over the entire operating range of the chiller and can be found in Table 5-6.

Sizing

Most vehicles are fueled between 6a.m. and 12p.m. [380]. About $1/12^{th}$ of the average daily dispensed fuel is refueled during peak hour [380,382,386]. The filling rate for dispensers in the Near Future is 0.65 kg/min [538] and 2.0 kg/min [389] assumed in the Mid Century scenario. Therefore, hydrogen chiller capacity needs to be matched with the peak fueling capacity. An average lingering time of 0.5 min per kg fueled is assumed. The average filling hose occupancy during peak hour is estimated to be 50% [522,525]. The chiller capacity is sized with the number of dispensers, dispenser filling rate and average filling hose occupancy during peak hour.

Cost

Economic parameters of the dispensers and chillers [379,535] for both scenarios can be found in Table 5-7.

5.6.6 Fuel Cell Electric Vehicles

Technology

The FCEVs have a fuel cell and a battery for regenerative braking. The combination of fuel cell and battery makes it possible to deliver almost every kind of energy service [184,186], from balancing to emergency power back-up or primary reserve. Batteries in present FCEVs for regenerative braking have capacities of approximately 1 kWh with 24kW power [439]. Tank-To-Wheel efficiency (η_{TTW}) of 51.5% (HHV) for the Near Future scenario and 61.0% HHV for the Mid Century scenario [126,194]. In Vehicle-To-Grid (V2G) mode, the efficiency of converting hydrogen from the FCEV tank to electricity is assumed equal to the Tank-To-Wheel efficiency (η_{TTW}).

Cost

For the Near Future scenario a durability of 4,100 hours in automotive drive cycle is assumed [275], 53 USD/kW (47.6€/kW) [452] at a production rate of 500,000 units per year. For the Mid Century scenario, US DOE targets for a passenger car fuel cell system are assumed: durability of 8,000 hours in automotive drive cycle, fuel cell system cost of 30 USD/kW (26.9 €/kW) [194] at a production rate of 500,000 units per year.

A Fuel Cells Dynamic Load Cycle (FC-DLC) [539] based on the New European Driving Cycle (NEDC) [540] is defined. With an average speed of 44.8 km/h excluding idling

time [541]. Maximum fuel cell power in the FC-DLC is approx. 34 kW [542] for constant speed driving at 120 km/h. The average load level calculated over the FC-DLC cycle is 29.02% [539], corresponding to 9.9 kW. A study [314] recommends to use cumulative produced energy as degradation indication/parameter for dynamic operated fuel cells instead of power or voltage loss over time. Annual driven distance for a passenger car is 11,940 km, see section 5.5.1, resulting in 267 operational hours and producing 2630 kWh. At 9.9 kW, a fuel cell system of a passenger car could produce 78,950 kWh during its lifetime in automotive driving cycle in the Mid Century scenario and 40,460 kWh in the Near Future. These values would correspond to respectively 30.0 and 15.4 years of operational lifetime in automotive drive cycle only for the Mid Century and the Near Future scenario.

It can be deducted from [130,188] that approximately 14-16 hours of balancing power is required on an average day basis, during the no/low solar electricity hours. The largest share of this balancing energy is condensed in 6-8 hours, therefore we assume an average of 6 full-load hours of balancing per day at 10 kW per passenger car. This corresponds to 21,900 kWh of annual balancing energy per car in both scenarios. The required number of passenger cars for balancing is calculated in section 5.7.2. It is assumed every produced kWh for electricity balancing is causing 50% of the degradation as a produced kWh in driving mode. So the production of 21,900 kWh of balancing equals 10,950 kWh degradation by driving. 10,950 kWh out of 13,580 kWh per year driving and balancing represents 81%. If fuel cell durability is larger or degradation by balancing is lower, degradation due to balancing is smaller.

Durability depends on the type of load; constant load, load changing or start-stop [264,265,288,543–545]. Different US DOE durability targets are set for fuel cells; 25,000 for fuel cell transit buses, 10,000 hours for fuel cell back-up power systems and 60,000-80,000 hours for fuel cell CHP units [194]. The assumption for lower degradation rate per produced kWh in balancing mode is made because we expect the load ramps, one of the main degradation factors, are smaller in balancing mode than in driving mode. This is due to the limitation of 10 kW for balancing, whereas in driving mode load ramps can be up too 100kW. Also the load ramps can be divided amongst the connected cars resulting in even smaller load ramps.

An OM of 5% [126] is included, proportional to the degradation share of electricity balancing to the total degradation for driving and electricity balancing. It is assumed the battery and other components present in the FCEV are not degraded due to electricity balancing or included in the OMC. Furthermore, it is also assumed that the actual replacement is included in the capital cost of the replacement fuel cell. The V2G output plug on the FCEVs is assumed to be a standard feature at no further cost. The cost of other fuel cell powered transport vehicles (vans, buses, trucks) are not included either, as in principle the transport vehicles are bought for the transporting services.

5.6.7 Electric Infrastructure, control and Vehicle-to-Grid (V2G) connection

Technology

An electric grid and an IT infrastructure are present in the smart city. A central electrical control unit is in charge of managing all the power flows, measuring and predicting power consumption and production from the solar modules and power to the hydrogen production and storage and required power from the FCEVs. For FCEVs, only a V2G connection is required. Here the technology selected is based on a solar power converter technology [370]. Discharging poles will have 4 connections points of each 10kW and 1 power converter with 40kW rating. The amount of V2G connections is approximately half the amount of passenger cars in the smart city.

Cost

The costs of V2G connections is calculated using mass production and installation of 4-point 40 kW poles, consisting of 30 Euro/kW [370] in the Mid Century and 110 Euro/kW [370], for both scenarios an installed cost of 2,000 Euro/pole is assumed. The installed poles include all intelligence and interconnections between buildings and vehicles. The electrical connection cost for the solar modules and hydrogen production and compression equipment is already included in those component specific installed cost. The electrical connection cost of the buildings is assumed included in the building.

5.6.8 Water Collection and Storage

Technology

Urban rainwater is collected in a rainwater tank and then demineralized and stored in a pure water tank. Interconnecting tubing, filters and transfer pumps complete the system. Energy consumption by the rainwater collection system [546] is presented in Table 5-6. It is assumed that the ground floor area taken from [504] is equal to the roof area suitable for rainwater collection. The roof area potential for rainwater collection for residential buildings is 105,200 m^2 and for buildings of the services sector 44,500 m^2.

Maximum collected rainwater from roofs is calculated by assuming a roof run-off coefficient of 0.95 [547]. No first flush volume is accounted [547]. Average European precipitation is 785 L/m^2/year [548,549]. Maximum rainwater collection potential on a year basis by using the roofs of the residential buildings is 78,490 m^3 and 33,140 m^3 when using the roofs of the services buildings. Only the water required for electrolysis is collected and the size of the system is determined from the energy balance.

At the wind turbine site surface water or sea water is used, assuming sufficient supply at all times. The holding tank capacity for demineralized water is equal to 7 days of average daily demineralized water consumption from the electrolyzer.

Cost
For rainwater collection the piping to and related equipment of the reverse osmosis system are included. The CC and OMC for all components are deducted from [501,550] and presented in Table 5-7.

5.6.9 Water treatment: Reverse Osmosis

Technology
Reverse Osmosis systems can demineralize rain- or seawater for use in electrolyzer systems [551] using electric energy [552]. Energy use is listed in Table 5-6, for rainwater, surface water or seawater [546,552,553]. Capacities of reverse osmosis systems in the smart city are small compared to large drinking water treatment plants [514,552,554], and relatively low recovery rates of only 50% [552,554–556] are assumed. The capacity of the reverse osmosis equipment is equal to the maximum water requirement by the electrolyzer.

Cost
The installed cost includes piping and connections, pre-treatment of the water such as basic filtration and infrastructure-related costs. Cost parameters [552] are listed in Table 5-7.

5.6.10 Solar modules

Technology
Technical parameters of the solar electricity system are given in section 5.5.3. The share of direct self-consumed electricity of new-built solar electricity systems in both scenarios is assumed 38%, as given for 40kW to MW systems in [187].

Cost
Utility scale solar system cost parameters [370] are assumed and listed in Table 5-7. The installed system cost includes the module cost, balance of system and inverter cost. Balance of system includes all other cost components: Mounting system, installation, DC cables, infrastructure, transformer, grid connection, and planning and documentation.

5.6.11 Wind Power

Technology
Wind power on- or offshore is used to balance demand and supply. For the Near Future all wind power is assumed to be located onshore. For the Mid Century scenario, half of the wind turbine power will be installed off-shore and half on-shore. The averaged capacity factor for the wind turbines installed is 35% and 46% in the Near Future scenario and the Mid Century scenario, respectively [392]. The installed wind power is calculated by completing the energy balance.

Cost

The wind turbines are connected directly to the electrolyzers. Therefore, grid connection costs are not applicable. For on-shore wind turbines grid connection costs are on average 11.5% and for off-shore wind turbines 22.5% [557,558]. Other cost parameters [559–562] can be found in Table 5-7. It is assumed that wind parks are cost-shared with other smart cities, thus not requiring rounding of wind capacities to turbine sizes.

Table 5-5 shows the specific electricity and water production parameters. Solar and wind specific electricity production are higher in the Mid Century scenario due to the increase in solar system efficiency (section 5.5.3) and wind power capacity factor (section 5.6.11). The pure water production from collected rainwater per square meter of roof area includes the reverse osmosis recovery factor of 50% (section 5.6.9). The conversion of hydrogen to electricity by the FCEV is respectively 20.3 and 23.6 kWh/kg H_2 in the Near Future and Mid Century scenario, corresponding to the Tank-To-Wheel efficiency (η_{TTW}) given in section 5.6.6.

Table 5-5 Electricity and water production parameters.

Component	Specific production parameters	
	Near Future	Mid Century
Solar electricity system [kWh/(kWp × year)] [343,370,506–511]	975	1,170
Wind Power [kWh/(kW × year)] [392]	3,065	4,030
Pure water production [m^3/(m^2 roof × year)] [504,547–549,552,556]	0.37	0.37
FCEV hydrogen to electricity [kWh/kg H_2] [232,265]	20.3	23.6

Table 5-6 list the specific electricity consumption in the Near Future and Mid Century scenario for the different conversion processes, from rainwater collection to hydrogen fueling at 700 bar. The specific electricity consumption for PEM electrolysis, hydrogen purification and specific cooling electric energy decrease in the Mid Century scenario compared to the Near Future, due to an increase in efficiency. The specific electricity consumption for the compressors in the smart city area and at the wind turbines increase in the Mid Century due to the higher pressure of the tube trailers in the Mid Century. Total specific electricity consumption of the compressors decreases from 3.3 kWh/kg H_2 in the Near-Future to 3.0 kWh/kg H_2 in the Mid Century. In this study no reduction of specific electricity consumption is foreseen in the Mid Century for reverse osmosis and the transfer of rainwater from the buildings to the reverse osmosis unit. From electricity to fueled hydrogen at 70 bar, is respectively 68% and 79% efficient in the Near Future and Mid Century scenario. The roundtrip efficiency from electricity via fueled hydrogen at 700 bar to electricity is respectively 35% and 47% efficient in the Near Future and Mid Century scenario.

Table 5-6 Specific electricity consumption (kWh/kg H2) of the conversion processes in the smart city for both scenarios.

Conversion processes	Specific electricity consumption	
	Near Future [kWh/kg H_2]	Mid Century [kWh/kg H_2]
PEM Electrolysis [126,520]	53.4	45.8
Hydrogen Purification [155,156]	1.3	1.1
Compressor in smart city area [379–382,386]	1.5	1.9
Compressor at wind turbines [379–382,386]	1.5	1.9
Compressor at hydrogen fueling station [379–382,386]	1.8	1.1
Specific cooling electric energy [388,537]	0.20	0.15
Reverse Osmosis – seawater [546,552,555]	0.0405	0.0405
Reverse Osmosis – rainwater [546,552,555]	0.0056	0.0056
Rainwater transfer [546]	0.0028	0.0028

Table 5-7 Economical parameters of the Smart City Area components for the Near Future and Mid Century scenario. IC_i = installed capital cost, OM_i = annual operational and maintenance cost expressed as an annual percentage of the installed investment cost, LT = Lifetime.

Subsystems and components	Near Future			Mid Century		
	IC_i	OM_i [%/year]	LT_i [years][1]	IC_i	OM_i [%/year]	LT_i [years][1]
Hydrogen Production, Storage and Transport						
PEM electrolyzer at solar system [513,514,519,522,523,525]	1,790 €/kW	2.8%	20	250 €/kW	2.3%	30
PEM electrolyzer at wind turbines [513,514,519,522,523,525]	1,790 €/kW	2.7%	20	250 €/kW	3.2%	30
Tube trailers at solar system [383,384,530–534]	730 €/ kg H_2	2.0%	30	510 €/ kg H_2	2.0%	30
Tube trailers at wind turbines [383,384,530–534]	730 €/ kg H_2	2.0%	30	510 €/ kg H_2	2.0%	30
Trailer tractors [383,384,530–534]	160,000 €/tractor	109%	8	160,000 €/tractor	91%	8
Compressor at solar system [535,536]	8,170 €/ kg H_2/h	4.0%	10	3,650 €/ kg H_2/h	2.0%	10
Compressor at wind turbines [535,536]	5,890 €/ kg H_2/h	4.0%	10	4,200 €/ kg H_2/h	2.0%	10
Hydrogen Fueling Station (HFS)						
Compressor at HFS [535,536]	11,090 €/kg H_2/h	4.0%	10	4,940 €/ kg H_2/h	2.0%	10
Stationary storage at HFS 875 bar [383,384,530–534]	1,100 €/ kg H_2	1.0%	30	575 €/ kg H_2	1.0%	30
Dispensers units [379,535]	91,810 €/unit	0.9%	10	72,890 €/unit	1.1%	10
Chiller units [379,535]	143,880 €/kg H_2/min	2.0%	15	118,520 €/kg H_2/min	2.0%	15
Fuel Cell system in FCEV for balancing only [126,264,541–545,564,265,267,275,288,314,452,539,540]	3,830 €/100 kW	5.0%	4,100h	2,170 €/100 kW	5.0%	8,000 h
Smart grid, Control and V2G infrastructure [370]	6,400€/ 4 dischargers	5%	15	3,200€/ 4 dischargers	5.0%	15
Water collection, storage and purification						
Rainwater collection and storage [501,550]	21,030 €/m^3/day	0.33%	50	21,030 €/m^3/day	0.33%	50
Pure water tank at wind turbines [501,550]	120 €/m^3	0.33%	50	120 €/m^3	0.33%	50
Reverse Osmosis at solar system [552]	1.20 €/L/day	4.8%	25	1.20 €/L/day	4.8%	25
Reverse Osmosis at wind turbines [552]	1.20 €/L/day	4.8%	25	1.20 €/L/day	4.8%	25
Energy Production						
Solar electricity system [370]	995 €/kWp	2.0%	25	440 €/kWp	2.3%	30
Wind Turbines onshore [557–562]	1,110 €/kW	2.8%	20	800 €/kW	3.2%	25
Wind Turbines off-shore [557–562]	1,880 €/kW	4.5%	20	1040 €/kW	4.7%	25

[1]Lifetime = Economic lifetime of components in years, except for the fuel cell system in the FCEV for which the lifetime is expressed in operating hours.

5.7 Energy balance results

5.7.1 Energy balance results

Figure 5-4 shows the calculated energy balance in the smart city system in the Near Future and Mid Century scenario. The consumption of 48 GWh/year in the Near Future can be covered fully by 106 GWh renewable electricity production. Consisting of 12 GWh/year rooftop solar electricity and 95 GWh/year distant wind electricity. The difference between production and consumption is due to hydrogen conversion efficiencies. In the Mid Century scenario, consumption of 33 GWh/year is covered by 48 GWh/year production, more than two-third (69%) of the production reaches final energy consumption or 57% final energy. In the Mid Century scenario renewable electricity supply consists of 24 GWh/year rooftop solar electricity and 23 GWh/year distant wind electricity.

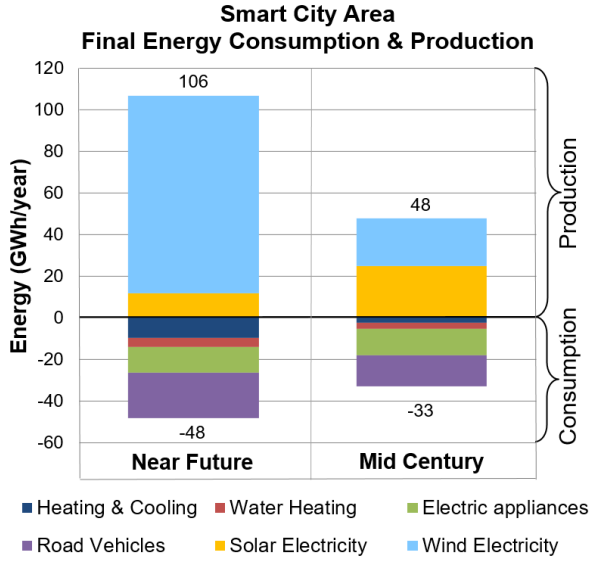

Figure 5-4 Smart City Final Energy Consumption and Production.

Figure 5-5 shows all energy flows in the smart city, for both scenarios. In the Near Future scenario, the amount of wind energy is 89% of all energy needed, solar electricity provides the remaining 11%. In the Mid Century scenario, solar and wind electricity provide approximately 50% of the required energy each. In the Mid Century scenario, direct use of solar electricity is 9.5 GWh/year, 53% of all building energy used. Respectively 72 GWh/year and 31 GWh/year hydrogen is produced from surplus solar and wind electricity in the Near Future and Mid Century scenario. The hydrogen used for energy balancing is of similar magnitude as for driving in the Mid Century scenario, whereas the majority of hydrogen is for balancing the electricity demand, in the Near Future scenario. In this balancing, 48% of the energy is lost due to conversion in the Near Future scenario, whereas in the Mid Century scenario this is 40%, due to the higher fuel cell efficiency, see section 5.6.6.

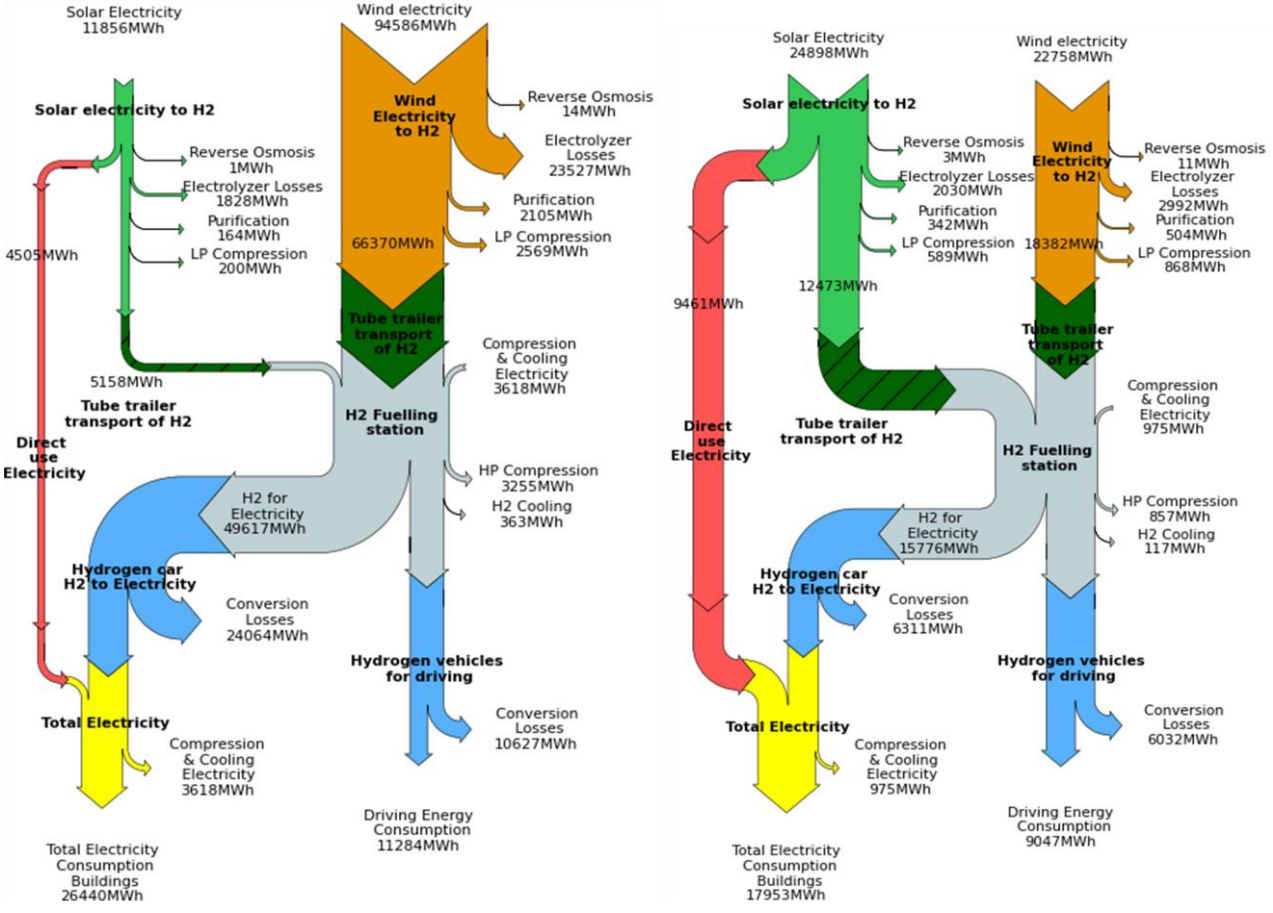

Figure 5-5 Energy Balance Near Future (left) and Mid Century scenario (right).

5.7.2 Energy balance discussion & evaluation

Balancing by FCEVs and H_2 transport

Electricity generated from V2G connected FCEVs is 25,553 MWh/year in the Near Future scenario and in the Mid Century scenario, 9,465 MWh/year are needed. These amounts of electricity can be produced by respectively 1,167 and 423 FCEVs, 51% and 19% of the car fleet, assuming each car generating 60 kWh per day, at max power 10 kW. It can be deducted from [563,564] that approximately 14-16 hours of balancing power is required per day, during the no/low solar electricity hours. The largest share of back-up power is condensed in 6-8 hours peak hours, assuming 6 hours in this study. With 430-1170 cars, it can be managed to provide the required power at all times. If the cars can generate 20 kW (20% of the installed power) [565,566], halve the required amount of passenger cars would suffice. If more hours of balancing per car per day are assumed, proportionally less cars are needed.

When using all cars in the fleet, the average daily amount of hydrogen used for re-electrification per car is 1.5 kg for the Near Future scenario and 0.5 kg for the Mid Century scenario. With hydrogen tank storage of 5 kg [181,182,439] for the Near Future and 6.5 kg [126] for the Mid Century scenario, the average daily amount of hydrogen for re-electrification would be respectively 30% and 7% of the usable hydrogen tank content, requiring one extra tank stop per 2.7 days and 9.7 days, respectively. The normal use of the cars (home-work commuting) arranges presence of cars at demand centers: during the day at office / service sector buildings, and in the evening and at night at home [175].

Share of direct solar electricity consumption

In the Mid Century scenario solar electricity generation is larger than in the Near Future scenario due to higher solar module efficiency. In Near Future, 17% of consumption is directly generated by the solar electricity system, whereas in Mid Century this is 53%. Because of the larger installed power and a significant demand reduction, in the Mid Century the share of direct solar electricity consumption has risen so much. It is also based on the assumption that demand response technology is well developed [567].

Water balance

In the Mid Century and Near Future scenario rainwater use for hydrogen production in the urban area is 6,000 respectively 2,500 m^3/year. Rain water collection from roofs far exceeds this water consumption, and only 2-5 % of the roofs are really required for collection.

5.8 Cost of energy results and allocation methodology

5.8.1 Smart city area total system cost of energy overview

Installed capacities, annual capital and O&M costs of all components, are presented in Table 5-7. Total annual costs, $TSCoE_{SCA}$, are 15.2 million Euro in the Near Future and 2.5 million Euro in the Mid Century scenario. In the Mid Century scenario costs are due to significant energy demand reduction, increased conversion efficiencies and cost reduction in the hydrogen cycle and renewable energy production.
Distribution of these costs are shown in Figure 5-6. In the Near Future scenario, PEM electrolyzer and wind energy account for more than half of both annual capital and O&M costs of the Smart City Area. In the Mid Century scenario, PEM electrolyzer costs are reduced considerably, and wind energy and solar energy account for approximately half of both annual capital and O&M costs.

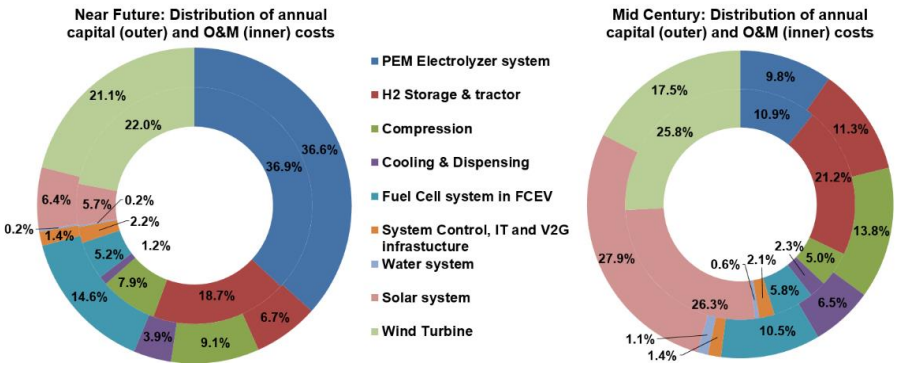

Figure 5-6 Near Future (left) and Mid Century (right) Smart City Area annual capital cost and O&M cost distribution.

Table 5-8 Calculated installed capacities, capital, O&M and total costs for the components in the Smart City Area.

		Near Future				Mid Century			
Subsystems and components	**i**	**Q_i**	**CC_i [k€/year]** Eq. (5.3)	**OMC_i [k€/year]** Eq. (5.5)	**TC_i [k€/year]** Eq. (5.2)	**Q_i**	**CC_i [k€/year]** Eq. (5.3)	**OMC_i [k€/year]** Eq. (5.5)	**TC_i [k€/year]** Eq. (5.2)
Hydrogen Production, Storage and Transport									
PEM electrolyzer at solar system	S4	3,740 kW	450	190	640	7,760 kW	100	45	140
PEM electrolyzer at wind turbines	W5	29,330 kW	3,530	1,390	4,930	5,310 kW	68	43	110
Tube trailers at solar system	S6	720 kg H_2	27	10	37	1735 kg H_2	45	18	63
Tube trailers at wind turbines	W7	9,230 kg H_2	340	130	480	2555 kg H_2	66	26	92
Trailer tractors	HFS1	3.45 tractors	79	600	680	0.80 tractors	18	120	130
Compressor at solar system	S5	72 kg H_2/h	69	23	92	173 kg H_2/h	74	13	87
Compressor at wind turbines	W6	550 kg H_2/h	380	130	510	116 kg H_2/h	57	10	67
Hydrogen Fueling Station (HFS)									
Compressor at HFS	HFS2	415 kg H_2/h	540	180	720	179 kg H_2/h	104	18	120
Stationary storage at HFS 875 bar	HFS3	4,980 kg H_2	280	55	330	2145 kg H_2	63	12	75
Dispensers units	HFS4	29 # units	310	23	340	6 # units	51	4.8	56
Chiller units	HFS5	9.2 kg H_2/min	110	26	140	6.0 kg H_2/min	59	14	73
Replacement cost of Fuel Cell systems (100kW) in FCEVs for balancing	FCEV2	1167# systems	1,590	220	1,810	432# systems	180	47	230
Smart grid, Control and V2G infrastructure	FCEV1	292 4-point dischargers	160	93	250	108 4-point dischargers	23	17	41
Water collection, storage and purification									
Rainwater collection and storage	S2	6.5 m^3/day	5.3	0.5	5.7	15.6 m^3/day	13	1.1	14
Pure water tank at wind turbines	W3	290 m^3	1.3	0.1	1.4	80 m^3	0.4	0.03	0.4
Reverse Osmosis at solar system	S3	15.5 m^3/day	1.6	0.9	2.5	37.5 m^3/day	3.8	2.2	6.0
Reverse Osmosis at wind turbines	W4	118.7 m^3/day	12.0	6.9	18.9	25.0 m^3/day	2.5	1.4	4.0
Energy Production									
Solar electricity system	S1	12,160 kWp	690	240	940	21,280 kWp	470	210	690
Wind Turbines onshore	W1	30,850 kW	2,290	940	3,240	2,825 kW	130	72	200
Wind Turbines off-shore	W2	0 kW	0.0	0.0	0.0	2,825 kW	170	140	300
Total			10,880	4,280	15,150		1,700	810	2,500

5.8.2 Cost of energy allocation methodology

In a fully renewable and autonomous city area, electricity is produced by solar systems on the roofs of the houses and buildings. Electricity is also produced by fuel cell cars when there is a shortage of electricity from solar, which is during the night and in winter. So the system levelized cost of electricity is determined by both the levelized cost of electricity from solar and the levelized cost of electricity by fuel cell cars.

Hydrogen is produced by a wind farm which is located outside the city area and from surplus solar electricity. So the levelized cost of hydrogen is determined by both the wind farm cost and the surplus solar electricity cost.

The question is how to allocate these costs to both the system levelized cost of energy for electricity and the system levelized cost of energy for hydrogen.

5.8.2.1 Levelized cost of energy

First the levelized cost of energy for solar electricity and wind electricity is calculated.

The Levelized Cost of Energy for Solar electricity $LCoE_{e,S}$ (€/kWh) in Equation (7.11) is calculated by dividing the TC_{S1} (see Table 5-8 for component numbering), with the annual Energy Production of solar electricity $EP_{e,S}$ (kWh/year) from Figure 5-5:

$$LCoE_{e,S}\left(€/kWh\right) = \frac{TC_{S1}}{EP_{e,S}} \tag{5.10}$$

The levelized cost of energy for electricity from onshore wind $LCoE_{e,W\text{-}onshore}$ (€/kWh) or off-shore wind $LCoE_{e,W\text{-}onshore}$ (€/kWh), Equations (5.11) and (7.11), is calculated by dividing the TC_{W1} or TC_{W2} (€/year) of the on- or offshore wind turbines, with the annual Energy Production of on- or off-shore wind electricity, $EP_{e,W\text{-}onshore}$ or $EP_{e,W\text{-}offshore}$ (kWh/year):

$$LCoE_{e,W\text{-}onshore}\left(€/kWh\right) = \frac{TC_{W1}}{EP_{e,W\text{-}onshore}} \tag{5.11}$$

$$LCoE_{e,W\text{-}offshore}\left(€/kWh\right) = \frac{TC_{W2}}{EP_{e,W\text{-}offshore}} \tag{5.12}$$

The wind electricity is partly from onshore and offshore wind farms. In Equation (5.13) the levelized cost of energy for wind electricity $LCoE_{e,W}$ (€/kWh) is calculated by dividing both the TC_{W1} and TC_{W2} of the on- and offshore wind turbines (€/year) with the total annual Energy Production of wind electricity $EP_{e,W}$ (kWh/year) from Figure 5-5):

$$LCoE_{e,W}\left(€/kWh\right) = \frac{TC_{W1} + TC_{W2}}{EP_{e,W}} \tag{5.13}$$

Now the levelized cost of energy for hydrogen from wind and solar surplus electricity is calculated, $LCoE_{H,W}$ (€/kg H_2) and $LCoE_{H,S\text{-}surp}$ (€/kg H_2). In both on- and off-shore wind cases it means that besides the cost for electricity production by on- or off-shore wind, the TC for pure water production by reversed osmosis TC_{W3} and storage TC_{W4}, hydrogen production and purification by electrolysis TC_{W5}, low

pressure compression TC_{W6} and tube trailer storage TC_{W7} needs to be included. The sum of aforementioned costs is divided by the Energy Production of hydrogen $EP_{H,W}$ (kg H_2/year). For wind onshore hydrogen production this results in the following levelized cost of energy $LCoE_{H,W\text{-}onshore}$ (€/kg H_2), Equation (5.14):

$$LCoE_{H,W\text{-}onshore}\left(€/kg\ H_2\right) = \frac{TC_{W1} + \left(\sum_{W3}^{W7} TC_i\right) \times \left(\frac{EP_{e,W\text{-}onshore}}{EP_{e,W}}\right)}{EP_{H,W\text{-}onshore}} \tag{5.14}$$

For wind offshore hydrogen production the levelized cost of energy $LCoE_{H,W\text{-}offshore}$ (€/kg H_2) is calculated in Equation (7.11) a similar way:

$$LCoE_{H,W\text{-}offshore}\left(€/kg\ H_2\right) = \frac{TC_{W1} + \left(\sum_{W3}^{W7} TC_i\right) \times \left(\frac{EP_{e,W\text{-}offshore}}{EP_{e,W}}\right)}{EP_{H,W\text{-}offshore}} \tag{5.15}$$

The Levelized Cost of Energy of hydrogen from wind $LCoE_{H,W}$ is calculated as follows, Equation (7.11):

$$LCoE_{H,W}\left(€/kg\ H_2\right) = \frac{\sum_{W1}^{W7} TC_i}{EP_{H,W}} \tag{5.16}$$

The levelized cost of energy for hydrogen produced by the solar surplus electricity is calculated $LCoE_{H,S}$ (€/kg H_2). The solar surplus electricity is that part of the solar electricity that cannot directly used as electricity in the smart city area $EP_{e,S\text{-}surp}$ (kWh/year), see Figure 5-5. The fraction of the solar modules costs TC_{S1} that is responsible for generating the surplus electricity and the total cost of the hydrogen production components, divided by the hydrogen production $EP_{H,S}$ (kg H_2/year), results in the $LCoE_{H,S}$ Equation (7.11). The TC of the hydrogen production components consists of the costs for the rainwater collection and storage TC_{S2}, reverse osmosis TC_{S3}, hydrogen production and purification TC_{S4}, low pressure compressor TC_{S5} and tube trailer storage TC_{S6}.

$$LCoE_{H,S}\left(€/kg\ H_2\right) = \frac{\left(\frac{EP_{e,S\text{-}surp}}{EP_{e,S}}\right) \times TC_i + \sum_{S2}^{S6} TC_i}{EP_{H,S}} \tag{5.17}$$

Because only solar surplus electricity is converted into hydrogen, the capacity factor of the hydrogen production and storage equipment is relatively low and implies a relatively high price per kg hydrogen produced from surplus solar.

5.8.2.2 System levelized cost of energy

For transportation energy only hydrogen from wind is used. Electricity for buildings is supplied, directly from the solar system and from conversion of hydrogen from surplus solar and wind by FCEVs. Therefore first the system levelized cost of energy for electricity from wind hydrogen $SLCoE_{e,W}$ (€/kWh) needs to be calculated.
Hydrogen produced from wind and surplus solar electricity needs to be transported, compressed to 875 bar, stored at the hydrogen fueling station, cooled and dispensed, before it can be reconverted into electricity by FCEVs. The components

involved by these additional steps are used for both hydrogen produced from wind and surplus solar electricity. Therefore, the term system is added to the levelized cost of energy term. The energy consumption of the tube trailer tractor is included in the OMC of the tube trailer tractor. The energy consumption of the compressor and chiller at the HFS $EC_{H,HFS}$ (kg H_2/year), is supplied by FCEVs converting hydrogen from wind into electricity. A fraction of; the energy consumption of the compressor and chiller at the HFS $EC_{H,HFS,H\text{-}W}$ (kg H_2/year), the HFS cost of energy $CoE_{HFS,H\text{-}W}$ (€/year) and HFS cost $TC_{HFS,H\text{-}W}$ (€/year) are allocated to the system levelized cost of dispensed hydrogen from wind $SLCoE_{H,W}$ (€/kg H_2), Equation (7.11):

$$SLCoE_{H,W}\left(€/kg\ H_2\right)=\frac{\left(LCoE_{H,W}\times EP_{H,W}\right)+CoE_{HFS,H\text{-}W}+TC_{HFS,H\text{-}W}}{EP_{H,W}} \tag{5.18}$$

Where the cost of energy for compressing and cooling the hydrogen from wind $CoE_{HFS,H\text{-}W}$ (€/year) consist of; the hydrogen cost used for electricity consumption at the HFS $EC_{e,HFS,H\text{-}W}$ (kWh/year), a fraction of the costs for the smart grid, control, V2G infrastructure TC_{FCEV1} and the replacement of fuel cell systems in FCEVs TC_{FCEV2}, relative to the electricity production by FCEVS $EP_{e,FCEV}$ (kWh/year), Equation (7.11):

$$CoE_{HFS,H\text{-}W}\left(€/year\right)=\left(EC_{H,HFS,H-W}\times LCoE_{H,W}\right)+\ldots$$
$$\ldots\left[\left(\frac{EC_{e,HFS,H\text{-}W}}{EP_{e,FCEV}}\right)\times\left(TC_{FCEV1}+TC_{FCEV2}\right)\right] \tag{5.19}$$

The fraction of the HFS cost for hydrogen from wind, $TC_{HFS,H\text{-}W}$ Equation (7.11), is calculated with costs of the tube trailer tractors TC_{HFS1}, compressor TC_{HFS2}, stationary storage TC_{HFS3}, dispenser TC_{HFS4} and chiller TC_{HFS5} units.

$$TC_{HFS,H\text{-}W}\left(€/year\right)=\left(\frac{EP_{H,W}}{EP_{H,W}+EP_{H,S}}\right)\times\sum_{HFS1}^{HFS5}TC_i \tag{5.20}$$

In a similar way, a fraction of; the energy consumption of the compressor and chiller at the HFS $EC_{H,HFS,H\text{-}S}$ (kg H_2/year), the HFS cost of energy $CoE_{HFS,H\text{-}S}$ (€/year) in Equation (5.22) and HFS cost $TC_{HFS,H\text{-}S}$ (€/year) in Equation (7.11), are allocated to the system levelized cost of dispensed hydrogen from surplus solar $SLCoE_{H,S}$ (€/kg H_2) in Equation (5.21):

$$SLCoE_{H,S}\left(€/kg\ H_2\right)=\frac{\left(LCoE_{H,S}\times EP_{H,S}\right)+CoE_{HFS,H\text{-}S}+TC_{HFS,H\text{-}S}}{EP_{H,S}} \tag{5.21}$$

$$CoE_{HFS,H\text{-}S}\left(\frac{€}{year}\right)=\left(EC_{H,HFS,H-S}\times LCoE_{H,S}\right)+\ldots$$
$$\ldots\left[\left(\frac{EC_{e,HFS,H\text{-}S}}{EP_{e,FCEV}}\right)\times\left(TC_{FCEV1}+TC_{FCEV2}\right)\right] \tag{5.22}$$

$$TC_{HFS,H\text{-}S}\left(€/year\right)=\left(\frac{EP_{H,S}}{EP_{H,W}+EP_{H,S}}\right)\times\sum_{HFS1}^{HFS5}TC_i \tag{5.23}$$

The dispensed hydrogen from wind and surplus solar is then distributed by the FCEVs and converted into electricity. The system levelized cost of electricity from wind hydrogen $SLCoE_{e,W}$, Equation (5.24), or surplus solar hydrogen $SLCoE_{e,S}$,

Equation (5.25), depends on five factors; system levelized cost of dispensed hydrogen from surplus solar $SLCoE_{H,W}$ or wind $SLCoE_{H,W}$, the Tank-To-Wheel efficiency of the FCEV η_{TTW} (%) from section 5.5.1, Higher Heating Value of hydrogen HHV_H (kWh/kg H_2), the relative costs of the smart grid, control, V2G infrastructure TC_{FCEV1} and replacement cost of fuel cell systems in FCEVs TC_{FCEV2}:

$$SLCoE_{e,W}\left(€/kWh\right)=\left(\frac{SLCoE_{H,W}}{HHV_H\times\eta_{TTW}}\right)+\left(\frac{TC_{FCEV1}+TC_{FCEV2}}{EP_{e,FCEV}}\right) \quad (5.24)$$

$$SLCoE_{e,S}\left(€/kWh\right)=\left(\frac{SLCoE_{H,S}}{HHV_H\times\eta_{TTW}}\right)+\left(\frac{TC_{FCEV1}+TC_{FCEV2}}{EP_{e,FCEV}}\right) \quad (5.25)$$

Electricity for buildings is supplied via three routes, directly from the solar system $EP_{e,S\text{-}dir}$ (kWh/year), see Figure 5-5, electricity from the conversion of hydrogen from surplus solar $EC_{e,B,H\text{-}S}$ (kWh/year) and wind $EC_{e,B,H\text{-}W}$ (kWh/year). Therefore the system levelized cost of energy for electricity $SLCoE_e$ (€/kWh), see section 5.3.5.2, is a weighted average of the aforementioned electricity supply routes:

$$SLCoE_e\left(€/kWh\right)=\ldots$$
$$\ldots\frac{LCoE_{e,S}\times EP_{e,S-dir}+SLCoE_{e,S}\times EC_{e,B,H\text{-}S}+SLCoE_{e,S}\times EC_{e,B,H\text{-}W}}{EP_{e,S-dir}+EC_{e,B,H\text{-}S}+EC_{e,B,H\text{-}W}} \quad (5.26)$$

This system levelized cost of energy for electricity includes all the cost to supply electricity to the area at all moments, so all storage and balancing cost are taken into account.

5.8.2.3 *Specific cost of energy*

Equation (5.8), $SCoE_T$, can be re-written into Equation (5.27) as only hydrogen from wind is used for transportation:

$$SCoE_{T,veh}\left(€/km\right)=\frac{SLCoE_{H,W}\times SEC_{T,veh}}{100\,km} \quad (5.27)$$

For building energy consumption, the Specific Cost of Energy for Buildings $SCoE_B$ (€/m^2/year), Equation (5.9) can be made specific for each sector, either residential or services, Equation (7.11):

$$SCoE_{B,sector}\left(€/m^2/year\right)=SLCoE_e\times SEC_{B,sector} \quad (5.28)$$

5.8.3 Cost of energy results

5.8.3.1 *System levelized cost of energy*

The (system) levelized cost parameters are presented in Table 5-9 for the Near Future and Mid Century scenarios.

A levelized cost of energy of wind and solar electricity of respectively 0.034 ($LCoE_{e,S}$) and 0.079 ($LCoE_{e,W}$) €/kWh in the Near Future scenario results in a system levelized cost of energy for electricity ($SCLoE_e$, equation (5.26)) of 0.41 €/kWh. Converting solar electricity into hydrogen and back into electricity again, electricity price increases from 0.079 €/kWh ($LCOE_{e,S}$) to 0.70 €/kWh ($SLCoE_{e,S}$) for the Near Future.

For re-electrified hydrogen from wind electricity in the Near Future, price increases from 0.034 €/kWh ($LCoE_{e,W}$) to 0.45 €/kWh ($SLCoE_{e,W}$).
For the Mid Century $LCoE_{e,S}$ and $LCoE_{e,W}$ of respectively 0.028 and 0.022 €/kWh result in an $SCLoE_e$ of 0.088 €/kWh. Converting solar electricity into hydrogen and back into electricity again, electricity price increases from 0.028 €/kWh ($LCOE_{e,S}$) to 0.70 €/kWh ($SLCoE_{e,S}$) for the Mid Century. For re-electrified hydrogen from wind electricity in the Near Future, price increases from 0.034 €/kWh ($LCoE_{e,W}$) to 0.45 €/kWh ($SLCoE_{e,W}$).

Table 5-9 Calculated (System) levelized cost parameters for the Near Future and Mid Century scenarios.

(System) Levelized Cost parameter	Equation	Near Future	Mid Century
$LCoE_{e,S}$ [€/kWh]	(5.10)	0.079	0.028
$LCoE_{e,W}$ [€/kWh]	(5.13)	0.034	0.022
$LCoE_{H,S}$ [€/kg H_2]	(5.17)	10.4	2.3
$LCoE_{H,W}$ [€/kg H_2]	(5.16)	5.4	1.7
$SLCoE_{H,S}$ [€/kg H_2]	(5.21)	12.5	3.1
$SLCoE_{H,W}$ [€/kg H_2]	(5.18)	7.6	2.4
$SLCoE_{e,S}$ [€/kWh]	(5.25)	0.70	0.16
$SLCoE_{e,W}$ [€/kWh]	(5.24)	0.45	0.13
$SLCoE_e$ [€/kWh]	(5.26)	0.41	0.088

It has to be kept in mind that other allocation principles will result in different System levelized cost of electricity and system levelized cost of hydrogen for transport. If for example all the hydrogen cost from the surplus electricity from solar is allocated to transport, the system levelized cost of electricity will be lower and the system levelized cost of hydrogen for transport will be higher (Table 5-9). Therefore in all renewable integrated energy systems, it is important to compare total energy cost for buildings and transport with these total cost for other fully renewable and reliable integrated energy systems.
Figure 5-7 shows the Near Future (left) and Mid Century (right), cost distribution (outer) of 1 kWh final electricity consumption ($SLCoE_e$) & energy distribution (inner) of 1 kWh primary electricity input. The outer ring shows the cost distribution of the System levelized cost of energy for electricity $SLCoE_e$, which in the Near Future is 0.41 €/kWh and in the Mid Century 0.088 €/kWh (Table 5-9). In the Near Future the two largest cost contributors for the $SLCoE_e$ are the Electrolysis and water production equipment (Purple, 34.5%) and the Low- and High-Pressure Compression, Storage and Transport equipment (Cyan, 20.2%). For the Mid Century the two largest cost contributors are the share of the cost of solar electricity which is not used directly but converted into hydrogen (Red, 27.0%) and the Low- and High-Pressure Compression, Storage and Transport equipment (Cyan, 24.9%).
The inner ring represents the primary input energy distribution for the consumed electricity in Buildings. The final electricity consumption consists of Electricity Solar direct use (Blue, 6.1% and 33.7%), Electricity Solar H_2 re-electrification (Red, 3.6% and 26.7%) and Electricity Wind H_2 re-electrification (Green, 26.2% and 4.3%), together respectively 35.9% and 64.0% in the Near Future and Mid Century scenario

of the primary input energy. The remainder part of respectively 64.1% and 36% in the Near Future and Mid Century represent the energy losses. The energy losses are primarily dominated by the hydrogen to electricity conversion in the grid connected FCEVs (Orange, 31.2% and 21.3%), into a lesser extent the hydrogen production via electrolysis (Purple, 27.1% and 10.6%) and the Low- and High-Pressure Compression, Storage and Transport equipment (Cyan, 5.7% and 4.2%).

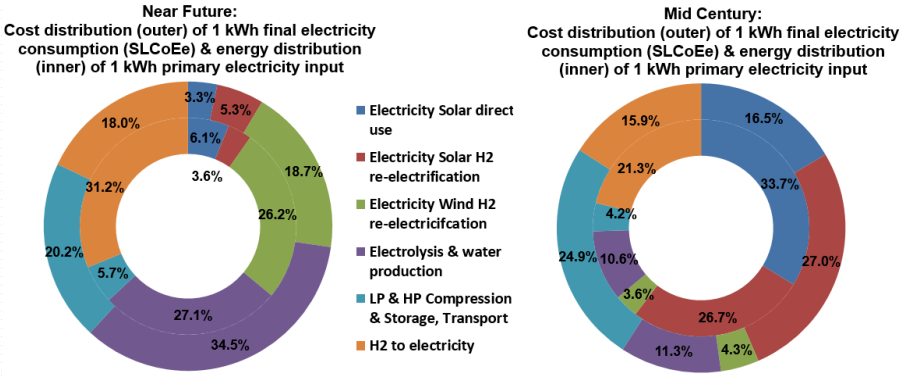

Figure 5-7 Near Future (left) and Mid Century (right), cost distribution (outer) of 1 kWh final electricity consumption (SLCoEe) & energy distribution (inner) of 1 kWh primary electricity input.

5.8.3.2 Specific cost of energy

Figure 5-8 shows the $SCoE_B$ and $SCoE_T$ for the residential and the services sector. For the residential sector, the $SCoE_B$ is 33.3 €/m^2/year and 4.5 €/m^2/year in the Near Future and Mid Century scenario. The $SCoE_T$ is 0.076 €/km and 0.015 €/km in the Near Future and Mid Century scenario (Table 5-7).

For the services sector, the $SCoE_B$ is 87.0 €/m^2/year and 13.4 €/m^2/year in the Near Future and Mid Century scenario. The $SCoE_T$ is ranging between 0.10-0.65 €/km and 0.022-0.17 €/km in the Near Future and Mid Century scenario (Table 5-7). The large reduction in specific costs of energy for either transport or buildings occur due to the combined decrease of system levelized cost of energy for electricity and hydrogen as well as the specific energy consumption for transport and buildings.

5.8.3.3 Smart city area total system cost of energy

Figure 5-8 shows the $TSCoE_{SCA}$ (M€/year) in the Near Future and Mid Century scenario. The $TSCoE_{SCA}$ decreases from 15.2 M€/year in the Near Future scenario to 2.5 M€/year in the Mid Century scenario.

The large reduction in smart city area total system cost of energy and costs of energy per sector are due to the reduction of total capital and O&M costs of all components as well as the specific energy consumption for transport and buildings.

Figure 5-9 shows the annual cost of buildings and transport energy distribution for residential and services sectors. The largest cost share is due to energy consumption in residential and services sector buildings: in the Near Future scenario 72%, in the

Mid Century scenario 63%. Using the number of households 2,000 (Table 5-1), it can be calculated that the household annual energy costs for transport and household energy decreased from 4,030 €/year in the Near Future to 605 €/year in the Mid Century.

Figure 5-8 Specific Cost of Energy for Buildings ($SCoE_B$ in €/m²/year) and Transport ($SCoE_T$ €/km) per sector (Services sector upper diagram, Residential sector lower left diagram) and Smart City Area Total System Cost of Energy ($TSCoE_{SCA}$ in M€/year) (lower right diagram).

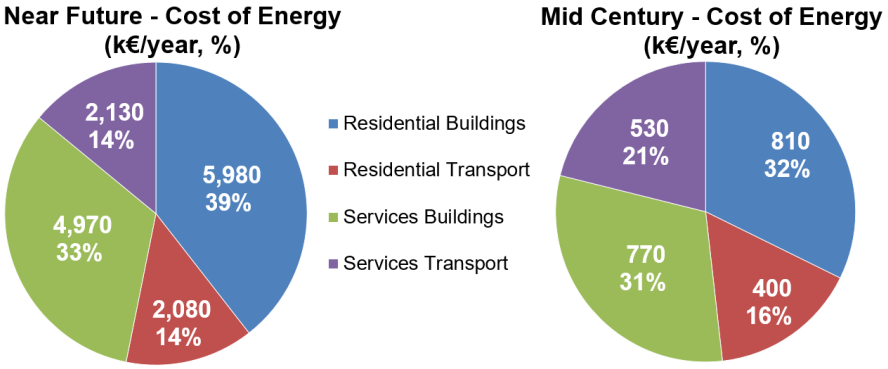

Figure 5-9 Cost of Energy distribution for the Residential and Services sector for buildings and transportation in the Near Future and Mid Century scenario.

5.8.4 Cost sensitivity results

A cost sensitivity analysis is performed for the Smart City Area Total System Cost of Energy ($TSCoE_{SCA}$ in M€/year) by changing key input parameters and assumptions for the Mid Century scenario for 'pessimistic' and 'optimistic' deviations from the baseline, see Table 5-10. The pessimistic values result in a higher costs ($TSCoE_{SCA}$), the optimistic values in lower costs ($TSCoE_{SCA}$).

A higher or lower WACC has a direct impact on the $TSCoE_{SCA}$. The assumed range of the WACC in the sensitivity study is based on [562,568]. External factors such as (national) economic and market conditions or interest rate can have influence on the WACC [568,569]. As hydrogen technologies are still in development, future costs can deviate from predictions made today. If the learning rate or the rate of installed capacities deviates from what is expected, Mid Century costs could deviate by 30% [126,570,571]. Fuel cell cost still decreases [571,572]. In a Mid Century scenario, apart from cost, also future fuel cell efficiency and degradation rate can vary from predictions made and so influence the $TSCoE_{SCA}$. Application of new materials or fuel cell types, improved balance of plant or smart power management strategies could increase fuel cell system efficiency and durability. Therefore a relative increase of 7.5% in fuel cell system efficiency (η_{TTW}) and specific energy consumption for transport ($SEC_{T,veh}$) is assumed in the optimistic scenario. 7.5% relative increase would result in an efficiency of 64.5% HHV, less than the maximum theoretical fuel cell efficiency of 83% [573,574]. Direct solar electricity consumption [187,567], fuel cell efficiency or energy consumption reduction in buildings [575], all have a direct impact on the energy balance. Any deviation of these parameters results in more or less imported hydrogen from wind, or smaller or larger hydrogen equipment size and so influences the $TSCoE_{SCA}$. A wide range of building energy consumption as well as the global irradiation on optimal inclined modules in urban areas is included. These wide ranges represent the entire European continent.

Table 5-10 Sensitivity parameters for a pessimistic and optimistic scenario of the Mid Century case.

Sensitivity parameter	**Mid Century Baseline**	**Optimistic Scenario relative change**	**Pessimistic Scenario relative change**
Weighted Average Cost of Capital (WACC)	3%	-30%	+30%
Hydrogen equipment cost	1.1M€	-30%	+30%
Share of direct solar electricity consumption	38%	+30%	-30%
FCEV η_{TTW} and vehicle specific energy consumption for transport ($SEC_{T,veh}$)	60.0% HHV and $SEC_{T,veh}$	+7.5%	-7.5%
Fuel cell degradation factor V2G Mode	50%	-30%	+30%
Energy consumption in buildings	18.0 GWh/year	-30%	+30%
Global irradiation on optimal inclined modules in urban areas	1,300 kWh/m^2/year	+30%	-30%

Figure 5-10 shows the results of the sensitivity analysis. The four sensitivity parameters with the largest impact on the $TSCoE_{SCA}$ are the estimated energy savings in buildings, global irradiation on optimal inclined modules in urban areas, hydrogen equipment costs and share of direct solar electricity consumption. The sensitivity parameters impact is in the range of -2% to -27% and +2% to +27% on the Smart City Area relative change in the $TSCoE_{SCA}$. The optimistic cases for the share of direct solar electricity consumption, energy consumption in buildings and global irradiation on optimal inclined modules in urban areas result in situation where the buildings energy balance is positive and do not require hydrogen from wind for electricity production. Therefore a part of the hydrogen from sun can be used for driving. A relatively higher surplus solar hydrogen price therefore results in higher transportation costs, despite the decrease of the $TSCoE_{SCA}$ and the smart city area system levelized cost of electricity $SLCoE_e$.

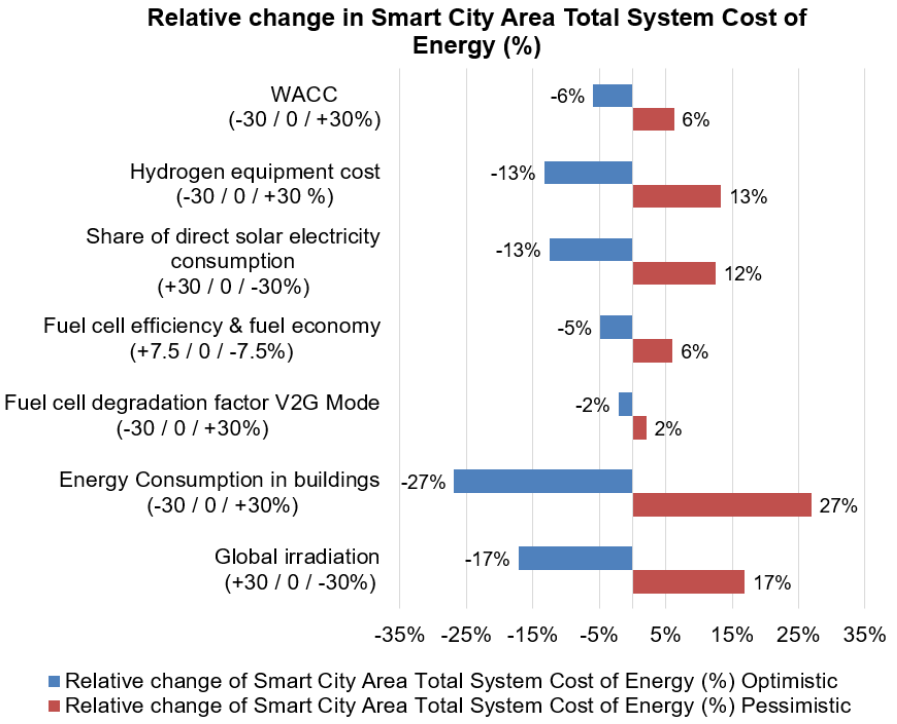

Figure 5-10 Relative change in Smart City Area Total System Cost of Energy compared to the Mid Century base scenario

5.9 Discussion

It was concluded that the smart city design can provide the required energy at all times without any grid connection to a medium or high voltage grid. However, the potential of the smart city area with fuel cell electric cars depends on several aspects, the most important of which are discussed here.

5.9.1 Car availability and developments

The V2G electricity can be supplied by 1,170 cars for the Near Future and 430 cars in the Mid Century scenario, during 6 hours on an average day basis. For a day without any solar power, for the Near Future and Mid Century scenario, the cars can still supply all power, requiring respectively 1,375 and 865 cars, representing 60% and 38% of the car fleet.

The normal car use profiles arranges that cars are present at demand centers: during the day at office/service sector buildings and in the evening and at night at home [175] or at a car park in the smart city area [221,342]. A high degree of monitoring and automation, e.g. self-connecting and driving cars, and incentives for car owners to participate will help assuring car availability and energy security at all times at the desired locations.

New developments, such as free-floating car sharing-fleets [576] combined with autonomous driving [577,578] could provide mobility and power on demand. Due to car sharing initiatives, the number of cars per person will decrease. Most balancing electricity from FCEVs is required during night [579]. So even if car sharing spreads widely, most likely with heavy use during day time, during night time FCEVs will still be available to provide power.

The system uses only hydrogen fuel cell powered vehicles. In future it is likely to have a mix of electric powered vehicles: battery, fuel cell and hybrids of these [440], all zero emission technologies. These technologies could complement each other and could share facilities, for example the possibly future wireless V2G infrastructure [580].

5.9.2 Local climate and population density

In the sensitivity analysis a wide range of building energy consumption as well as the global irradiation on optimal inclined modules in urban areas is included. These wide ranges represent the entire European continent and its widely available solar and wind energy sources. Not included in the sensitivity analysis, is the available solar rooftop area per capita in cities, which varies as a function of population density [505].

The system size based on 2,000 households and one hydrogen fueling station results in a cost-effective system. Smaller system sizes could result in slightly higher costs, as certain components are relatively more expensive at lower capacities.

5.9.3 Technology synergy effects and development

A fully autonomous smart city area is considered. However, in reality these smart city areas will be interconnected with other city areas and industry sites, rural areas, etc. Therefore, system integration will result in more complex systems, with

synergies leading to lower costs and higher reliability. For example if surplus electricity from solar in the summer time could be directly used for cooling at cold stores, less electricity conversion into hydrogen is needed in the smart city area, which will reduce cost. Or producing hydrogen from hydropower or biogas from agricultural residues, manure and waste water treatment plants could lead to lower prices for hydrogen. Smart integration with local heat grids and heat storage [395,581] can reduce system cost and affect economies of scale of hydrogen technologies.

The levelized cost of energy of wind or solar electricity is less than 0.03€/kWh in the Mid Century scenario, but balancing fluctuating renewable energy with energy storage and additional generators comes at a price. The hydrogen related components account for half of the total annual cost of the Smart City Area. Solar annual irradiation, energy savings measures in buildings and the share of direct solar electricity consumption have a large impact on the hydrogen equipment size and thus system cost.

For most of the hydrogen technologies used in the calculations, other technologies are being developed which are likely to be more energy efficient and/or cost effective. Examples are high temperature solid oxide or proton conducting electrolyzers [517,582], alkaline membrane [583–585] electrolyzers and direct solar to hydrogen technologies replacing solar panels and electrolyzers [586–591]. Ionic liquid piston compressors [592] and electrochemical hydrogen compression and purification [593,594] could replace compressors and purification systems. Several types of hydrogen storage methods are being investigated [526–528], but in particular liquid organic hydrogen carriers could be a cost effective alternative [595–597] and (partly) avoid the need for compressors. Also some research is performed in the field of reversible unitized (PEM) fuel cells, combining an electrolyzer and fuel cell in one device [598–601].

5.9.4 Comparing system costs with other power and transport systems

A comparison with other integrated power and transport systems is not straightforward due to combination of an integrated design, scale of the system, technologies used and projections in two technology and cost development scenarios. Balancing is commonly done using fossil resources, unlike the presented system.

The levelized cost results of the Near Future scenario can be compared with present day levelized costs of electricity. The levelized costs of electricity from wind and solar for the two scenarios are comparable with other studies, 0.02-0.08 €/kWh [370,562,564,602]. The levelized cost of dispensed hydrogen from wind or solar electricity in the Mid Century scenario is in a similar range as other studies, 2-4 €/kg H_2 [126,519,523]. Specific Costs of Energy for Transportation for the Near Future scenario for passenger cars is lower than the hydrogen cost per kilometer of 0.10-0.31€/km calculated by NREL [393] for a smaller integrated power and transport system with electricity grid connection. The levelized cost of electricity including storage and reconversion of 0.40€/kWh as calculated by NREL [393] is comparable

with the Near Future $SLCoE_e$ of 0.41€/kWh. The Mid Century $SLCoE_e$ of 0.09€/kWh is of similar magnitude as the 100% renewable system electricity cost 0.10€/kWh in 2050-2055 in [603]. In conclusion, the designed system has equivalent costs for the parameters where comparison with other studies could be performed.
System levelized electricity costs are very hard to compare to other studies, and in this discussion we focus on some methodological observations. The $SLCoE_e$ cannot be compared directly with any future conventional or fossil based electricity cost [603]. For example conventional electricity cost projections do not integrate transportation, power and heating/cooling. Conventional calculations do not account for a multitude of avoided costs, such as health and climate related savings [604,605], possible avoidance of electric grid congestion problems [606–609] or using different energy carriers than electricity and hydrogen. Avoided costs are more complex to estimate than levelized costs because it requires information about how a similar system would have operated without the described system changes [610]. Therefore attempts are made to include these in cost calculations, such as the methodology of the Levelized Avoided Cost of Electricity [611]. The designed system is independent of any future fuel costs or High and Medium Voltage electricity grids, natural gas and district heating grids or expansion of these, and including these as avoided costs seems reasonable, hard to quantify, and for various stakeholders arguable.

5.10 Conclusion

It is concluded that for smart city areas, solar and wind electricity together with fuel cell electric vehicles as energy generators and distributors and hydrogen as energy carrier, can provide a 100% renewable, reliable and cost-effective energy system, for power, heat, and transport.
A smart city area is designed and dimensioned based on European statistics. The smart city area consists of 180,000 m^2 floor area of residential and 57,000 m^2 floor area services sector buildings and 2,800 fuel cell powered road transport vehicles. 2,000 households with 4,700 inhabitants are an appropriate size for dimensioning the smart city area as statistically there is one petrol station and one food-retail shop.
All electricity and hydrogen can be supplied by solar and wind to fulfill the energy demand for power, heat and transport. Electricity is generated by solar modules on all roofs. Surplus solar electricity is converted via water-electrolysis with rainwater into pure hydrogen. The hydrogen is compressed and transported by tube trailer modules to the nearby Hydrogen Fueling Station. At the Hydrogen Fueling Station, the hydrogen is further compressed to fuel all types of fuel cell powered electric vehicles; passenger cars, vans, motorcycles, buses and trucks. In case of a temporary shortage in production of solar electricity, the fuel cells in grid-connected passenger cars provide the necessary electricity by converting hydrogen from the on-board hydrogen storage tanks. At parking places at home, office or at the local shopping area, vehicle-to-grid points connect the cars to the smart city electrical grid. To provide year-round energy supply, distant on-shore or off-shore wind-electricity is converted at the wind turbine park into hydrogen via water-electrolysis with surface

or seawater. The produced hydrogen from wind is transported via tube trailers to a hydrogen fueling station.
An energy balance and cost analysis are performed for a Near Future and Mid Century scenario. Technological and cost data is collected of all system components, using existing technologies and well-documented technology and cost development projections. In the Near Future, renewable electricity supply consists of 12 GWh/year rooftop solar electricity and 95 GWh/year distant wind electricity producing hydrogen. 4.5 GWh/year of solar electricity is used directly and 72 GWh/year hydrogen is produced from surplus solar and wind electricity. In the Mid Century scenario renewable electricity supply consists of 24 GWh/year rooftop solar electricity and 23 GWh/year distant wind electricity producing hydrogen. 9.5 GWh/year of solar electricity is used directly and 31 GWh/year hydrogen is produced from surplus solar and wind electricity. This lower renewable electricity production is possible due to savings in final energy consumption in buildings and transport, higher use of direct solar energy due to demand side management and efficiency increase in hydrogen production and fuel cell technologies.
The smart city area energy supply is reliable at all times and independent of other energy systems and grid connections. Reliability of energy supply is guaranteed by converting temporary surplus solar and distant wind electricity into hydrogen and through electricity supply with grid-connected fuel cell electric passenger cars providing 10 kW each (10% of installed power). The balancing electricity can be supplied by 1,170 cars for the Near Future and 430 cars in the Mid Century scenario, during 6 hours on an average day basis. For a day without any solar power, for the Near Future and Mid Century scenario, the cars can still supply all power, requiring respectively 1,375 and 865 cars, representing 60% and 38% of the car fleet. If the cars can generate 20 kW (20% of the installed power) halve the required of amount passenger cars would suffice. If more hours of balancing per car per day are assumed, proportionally less cars are needed.
In conclusion, the fuel cell electric vehicle and renewable energy based smart city area can provide a future cost-effective energy supply, as the annual total system cost of energy demand for power, heat and transport is 15 M€/year in the Near Future and 2.5 M€/year in the Mid Century scenario for the entire smart city area. This corresponds to an average annual cost for power, heat and mobility of 600 €/year per household for the Mid Century scenario. In the Near Future scenario system levelized cost of hydrogen for transportation is 7.6 €/kg, system levelized cost of electricity is 0.41 €/kWh and the specific cost of energy for passenger cars is 0.08 €/km. In the Mid Century scenario however, this is only 2.4 €/kg, 0.09 €/kWh and 0.02 €/km. System levelized cost of energy and specific energy costs compare favorably with other scenario studies describing fully renewable energy and transport systems.
Future dynamic simulations and tailoring to geographical demand and climate conditions is needed to calculate system cost, and FCEV fleet deployment for specific city areas in Europe. Also, other configurations using different renewable energy sources and different storage and conversion technologies is of interest for future research.

6 Fuel Cell Electric Vehicle as a Power Plant: Techno-Economic Scenario Analysis of a Renewable Integrated Transportation and Energy System for Smart Cities in Two Climates

The research presented in this chapter has been published in [612]. The work in this chapter tries to address research sub-questions 2 “How can we integrate FCEVs, used for transport, distributing and generating electricity, into future energy systems?” and 3 “What impact do European regional characteristics have on the techno-economic system performance and the usage of FCEVs for transport, distributing and generating electricity?”. A combined approach of system design, heuristic modeling, simulation and techno-economic scenario analysis is used.

6.1 Abstract

Renewable, reliable, and affordable future power, heat, and transportation systems require efficient and versatile energy storage and distribution systems. If solar and wind electricity are the only renewable energy sources, what role can hydrogen and fuel cell electric vehicles (FCEVs) have in providing year-round 100% renewable, reliable, and affordable energy for power, heat, and transportation for smart urban areas in European climates? The designed system for smart urban areas uses hydrogen production and FCEVs through vehicle-to-grid (FCEV2G) for balancing electricity demand and supply. A techno-economic analysis was done for two technology development scenarios and two different European climates. Electricity and hydrogen supply is fully renewable and guaranteed at all times. Combining the output of thousands of grid-connected FCEVs results in large overcapacities being able to balance large deficits. Self-driving, connecting, and free-floating car-sharing fleets could facilitate vehicle scheduling. Extreme peaks in balancing never exceed more than 50% of the available FCEV2G capacity. A simple comparison shows that the cost of energy for an average household in the Mid Century scenario is affordable: 520–770 €/year (without taxes and levies), which is 65% less compared to the present fossil situation. The system levelized costs in the Mid Century scenario are 71–104 €/MWh for electricity and 2.6–3.0 €/kg for hydrogen—and we expect that further cost reductions are possible

6.2 Introduction

The Paris Agreement, which pledges to keep global warming well below 2 degrees Celsius above pre-industrial levels and to limit the increase to 1.5 degrees Celsius, needs a boost [613]. The highest emitting 100 cities, or so-called urban areas, account for 18% of the global carbon footprint [614,615]. Therefore, cities are increasingly focusing on and shaping the trajectory and impacts of climate change and air quality [616–621]. The C40 Cities Climate Leadership Group connects more than 90 of the world’s largest cities, representing over 650 million people and one-

quarter of the global economy [622]. C40 is focused on tackling climate change and driving urban action that reduces greenhouse gas emissions and climate risks.
More than 54% of the world's population lives in urban areas (cities, towns, or suburbs) [623]; in Europe, this is almost 75% [624]. Energy consumption is growing rapidly in urban areas [619]. A smart, integrated, and combined centralized and decentralized approach is essential for creating sustainable urban energy systems [345,624–627]. By coupling energy sectors through electrification and hydrogen [603,628–630], major problems related to the intermittent nature of many renewables, such as wind and solar, can be solved, and synergies benefiting all sectors can be created [393,395,631–634]. Both the Hydrogen Council and the World Energy Council support and leverage the enabling role of hydrogen and fuel cell solutions around the world [138,635].
Inspired by the concept of a "Hydrogen Economy" [20,161,279,636–639], the authors designed a 100% renewable, reliable, and cost-effective energy system for power, heat, and transportation for smart urban areas in Europe [235]. The system covers the annual energy consumption of the main energy functions in urban areas, namely road transportation and, in residential and services buildings, space heating and cooling, hot water, lighting, and electrical appliances. The heating and transportation system is all-electric in its final energy use. Heating is by means of electric powered heat pumps and transportation by hydrogen fuel cell-powered electric vehicles; no other technologies are used for these applications. Local solar and large-scale wind electricity provide all renewable energy, together with hydrogen and electricity, as intermediate energy carriers. Fuel cell electric vehicles (FCEVs) provide transportation and energy distribution and balance the intermittent solar and wind electricity production by converting renewable hydrogen into electricity. This concept of grid-connected FCEVs providing grid services when parked—also known as vehicle-to-grid (V2G)—has already been demonstrated on a small scale with one V2G-ready commercial Hyundai ix35 FCEV and an all-electric house [229,640]. FCEVs providing power to electric appliances (also referred to as vehicle-to-load, V2L), small grids, or homes (vehicle-to-home, V2H) [202] are being developed by several FCEV manufacturers [181,200,201,641], although none of them have reported connecting an FCEV to a low-voltage national AC grid.
European regions have different climatic conditions [642](including supplement of [642]), which have an impact on the energy consumption of buildings [643–645], especially for space heating and cooling [469,646–649]. In addition, the different average building and household types, sizes, and compositions in European countries also impact the energy consumption in buildings [471,472,650]. Vehicle ownership and the average number of kilometers driven per year determine the final road transportation energy consumption, which varies among European countries [470,473]. The regional availability and magnitude of solar and wind energy differ significantly across Europe [343,344,512,651,652]. Wind and solar power generation across European regions exhibits hourly, diurnal, and strong seasonal behavior [653,654], as well as intra-annual [655–657] or decadal/multi-decadal variability [658–662].
Average European statistics, average hourly energy consumption, and production profiles for an average day during an average year were used to calculate system

component sizes, including safety margins [235]. Rough estimations, such as several days without sun or wind power, were used to define the required back-up and balancing power and energy storage sizes [235]. Hourly modeling will capture the biggest variations for larger systems and is, therefore, more adequate to dimension flexibility requirements [663]. Modeling on an hourly basis and tailoring to geographical energy demand and climatic conditions will give a better insight into hourly, diurnal, and seasonal energy production and consumption mismatch, in other words, the energy storage requirements, and the system design and its related cost.

The question is: can solar and wind electricity, together with fuel cell electric vehicles and hydrogen as an energy carrier, provide year-round 100% renewable, reliable, and affordable energy for power, heat, and transportation for smart urban/city areas in two different European climates?

To address this question, this study performed a techno-economic scenario analysis and design for a 100% renewable, reliable, and cost-effective energy system. The energy systems provide year-round power, heat, and transportation for smart urban areas. The total system cost and energy performance are compared for two different technology development scenarios and two European climate zones for five years (2012–2016). Analyzing the system over five years will give insight into the inter-annual variability of the cost and energy performance. To our knowledge, no such comprehensive study has been performed up to now. Many studies and pilot projects investigate stand-alone and national grid-connected renewable energy systems using hydrogen as energy storage and stationary fuel cells for the reconversion of the stored hydrogen [203–206,664]. Some studies use the produced hydrogen for transportation [103,207–209,211,665] or solely use the fuel cell in the vehicle as an electric generator [213–217] without considering hydrogen production. Integration of FCEVs through V2G into a local electricity network for operating in island mode, emergency power, or balancing local renewables has been done mostly on a smaller or a very large scale [218–222]. Some studies include a cost analysis [223,224,234], do not compare with a future scenario with improved cost and efficiency (scenario and trend analysis) [225], are dependent on the grid electricity, do not compare different climate zones nor include inter-annual variability [666], or do not include seasonal hydrogen storage [225]. The authors of [226] focus on a small-scale system in a specific region without considering hydrogen transportation, although includes a future cost scenario. The authors of [227] look into urban areas and road transportation in different regions in different Japanese climate zones, but the described system is not 100% renewable and does not include economics or consider V2G electricity services with FCEVs. A study [667] performs a future techno-economic 100% renewable energy analysis, including multi-annual variability for multiple large national and trans-national regions. Various energy sectors are coupled, where hydrogen is used as energy storage and road transportation fuel along with several other energy carriers and storage techniques. However, here too, but also here V2G electricity services with FCEVs are not considered.

6.3 Materials and Methods

6.3.1 Approach

The techno-economic scenario analysis of a fully autonomous renewable and reliable integrated transportation and energy system for a smart city area is performed in four steps:

1. Location selection, system design and dimensioning, technological and economic characterization for the system components in two technology development scenarios (Section 6.3.2).
2. Developing a calculation model for hourly simulation of all energy flows for multiple years and sizing of system components, for two different European climates zones in two technology development scenarios (Section 6.3.3).
3. Calculating the cost of energy for the two technology development scenarios in two climate zones based on the sizing and economic characterization of the system components (Section 6.3.4).
4. Inter-annual variability analysis of wind and solar energy production on the cost of energy (Section 6.3.5).

6.3.2 Location Selection, System Design and Dimensioning, System Components, and Scenarios

6.3.2.1 Location Selection

The following criteria apply to the selection of two locations in different European climate zones. They are listed in order of significance (Figure 6-1):

1. Close to a large European functional urban area [624] or city with at least 50,000 inhabitants, preferably in one of Europe's five most populous countries [668].
2. Located in different European climate zones, as defined by the Köppen–Geiger climate classification [642] and supplement of [642].
3. Located in a region with underground salt formations suitable for underground gas storage [385].
4. One location should have a relatively high, and one location should have a relatively low solar global irradiation compared to European measurements [343,344,512].
5. One location should have a relatively low annual precipitation compared to European measurements [669].
6. All required statistical and hourly modeling data should be available for the selected locations (wind velocity, solar irradiation, precipitation, building energy consumption, etc.).

The urban area of Hamburg in Germany and Murcia in Spain were selected, see Figure 6-1. Hamburg is the cooler, windier, and rainier area; Murcia is the warmer, sunnier, and dryer area. In Appendix A.1.1, Table A1 shows key figures characterizing Hamburg in Germany and Murcia in Spain and their climates.

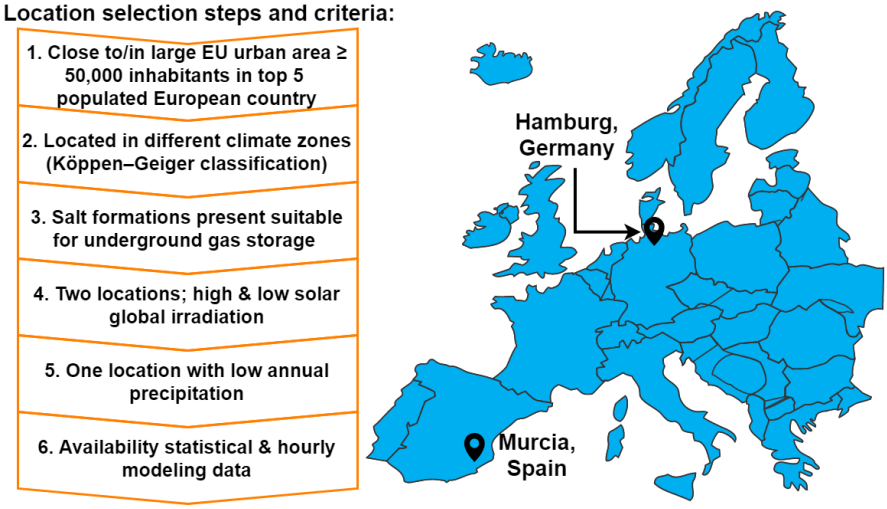

Figure 6-1 Location selection steps and criteria resulted in the urban area of Hamburg in Germany and Murcia in Spain.

6.3.2.2 System Design and Dimensioning

The smart city area energy and transportation system is designed in such a way that it fulfills the following design requirements:

- uses only electricity and hydrogen as energy carriers and is all-electric in end-use
- uses only hydrogen as seasonal energy storage and fuel to power all road vehicles
- can be applied to an average European city area and is a scalable design
- can be operated in a network of multiple smart city areas and renewable hydrogen and electric energy hubs or centers [459,638,670–673]
- can be integrated into existing infrastructure and buildings
- is not dependent on an in-urban area underground hydrogen pipeline transportation network
- uses abundant renewable energy sources in Europe: local solar and large-scale wind only
- is independent of high and medium voltage electricity grids, natural gas, and district heating grids or the expansion of these.

By applying the design requirements, the integrated system design of the smart city area has the following seven major elements and functional energy performance and conversion steps (Figure 6-2 and Table 6-1):

1. *Local solar electricity and hydrogen production (orange)*: Local rooftop solar electricity and rainwater collection, purification, and storage systems (S1–S3) produce solar electricity (E_S) and pure water (H_2O_S). A part of the solar electricity is directly consumed (E_{DC}) in buildings and other sub-systems. The remaining surplus solar electricity (E_S) is used with purified water (H_2O_S) in the hydrogen

production, purification, and compression system (S4–S6) for filling tube trailers (TT1) with hydrogen (H_S).

2. *Fuel cell electric vehicle-to-grid, building electricity consumption, and smart grid control (yellow)*: The smart electric grid is managed by a controller, which connects all buildings, grid-connected FCEVs (FCEV1and2), the hydrogen fueling station (HFS1-HFS4), solar electricity and hydrogen production (S1–S6), and the tube trailer filling station (SHS2) at the seasonal hydrogen storage (SHS1). The directly consumed solar electricity (E_{DC}) is divided amongst the all-electric residential and services sector buildings (E_B), HFS (E_{HFS}), and SHS (E_{SHS}) electricity consumption. Any shortage of electricity is met by the electricity produced from hydrogen (E_{V2G}) through parked (at home or in public or commercial spaces) and V2G connected FCEVs (FCEV1and2).
3. *Hydrogen tube trailer transportation (grey)*: Tube trailers (TT1) towed by tube trailer tractors (TT2) transport hydrogen from either the local solar hydrogen production or the SHS to the HFS, or from the local solar hydrogen production to the SHS.
4. *Hydrogen fueling station (blue)*: Hydrogen from tube trailers is further compressed (HFS1) and stored at high pressure (HFS2). A chiller (HFS3) cools the dispensed hydrogen (H_{HFS}), including sufficient dispensers (HFS4) to provide hydrogen for both road transportation (H_{road}) and V2G (H_{V2G}) use.
5. *Road transportation (purple)*: A fleet of road transportation FCEVs, namely passenger cars, vans, buses, trucks, and tractor-trailers.
6. *Large-scale and shared wind hydrogen production (green)*: A large-scale wind turbine park (W1) that is not located near or in smart city areas is shared with other smart city areas and renewable hydrogen hubs and consumers. All wind electricity (E_W) is used with purified water (H_2O_W) from local surface water or seawater in hydrogen production (W4), purification (W5), and compression system (W6), which includes a water collection and purification system (W2 and W3). The hydrogen produced (H_W) is stored in a large-scale underground seasonal hydrogen storage (SHS1).
7. *Large-scale and shared seasonal hydrogen storage (red)*: Large-scale underground seasonal hydrogen storage (SHS1), including a tube trailer filling and emptying station (SHS2).
8. The system design configuration is sufficiently flexible to allow other renewable energy sources, if present, to be used (e.g., offshore wind, biomass, or hydropower). However, this was not analyzed in this study. The smart urban area operates in a network of multiple smart urban areas, hydrogen fueling stations, other renewable hydrogen and electric energy hubs, and other hydrogen and electricity consumers (not part of this study). Hydrogen is produced within the smart urban areas from local surplus solar electricity and at large-scale wind parks. These large-scale wind parks, as well as the large-scale seasonal underground hydrogen storage, are jointly owned by the smart urban areas and other hydrogen consumers. Hydrogen is transported via tube trailers from the smart urban areas to hydrogen fueling stations, or the large-scale and shared underground seasonal hydrogen storage [385,674].

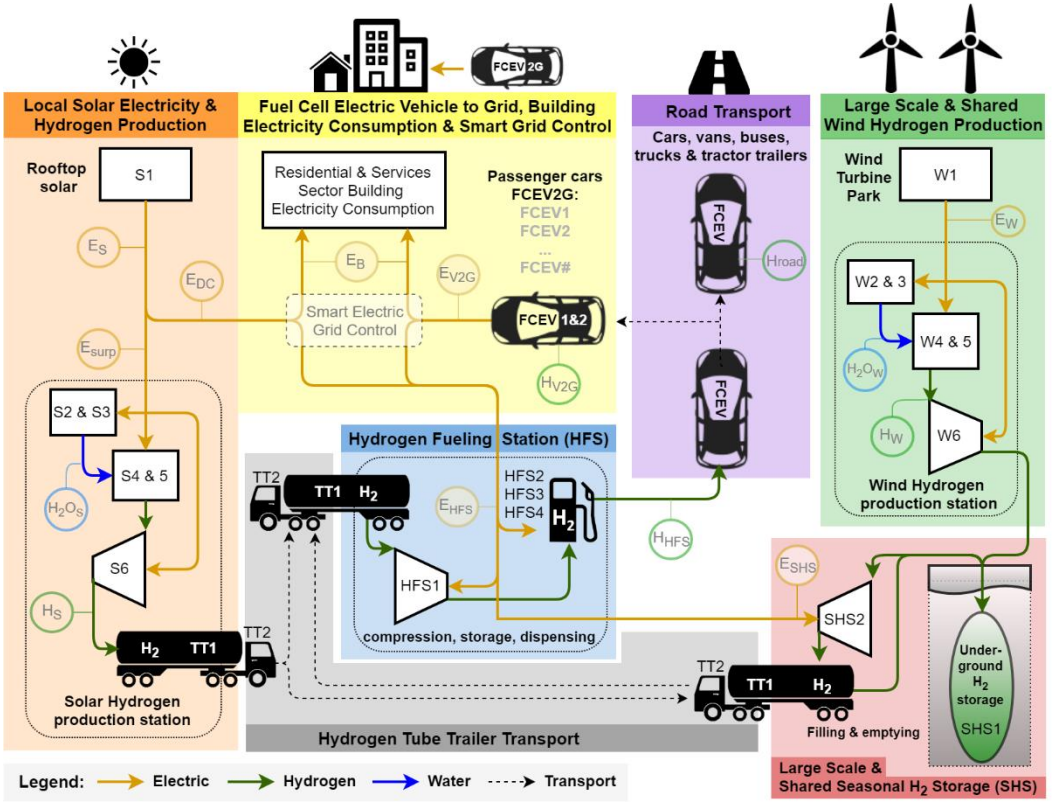

Figure 6-2 Smart city area components, electricity, water, hydrogen flows, and transportation. fuel cell electric vehicles (FCEV), fuel cell electric vehicle; V2G, vehicle-to-grid.

Table 6-1 Components, energy, and water flow in the smart city area (Figure 6-2).

Label	Components	Label	Components
S	*Local solar electricity and hydrogen production*	*TT*	*Hydrogen tube trailer transportation*
S1	Solar electricity system	TT1	Tube trailers
S2	Water purification (reverse osmosis)	TT2	Trailer tractors
S3	Pure-water tank	FCEV	Fuel cell electric vehicle-to-grid (V2G)
S4	Electrolyzer	FCEV1	Fuel cell in fuel cell electric vehicle (FCEV) for V2G use
S5	Hydrogen purifier	FCEV2	V2G infrastructure
S6	Low-pressure compressor		*Energy and water flows*
W	*Large-scale and shared wind hydrogen production*	*E*	*Electricity*
W1	Shared wind turbine park	E_W	Electricity from wind
W2	Water purification (reverse osmosis)	E_S	Electricity from solar
W3	Pure water tank	E_{DC}	Direct consumption solar electricity
W4	Electrolyzer	E_{surp}	Surplus solar electricity
W5	Hydrogen purifier	E_B	Electricity consumption in buildings
W6	Low-pressure compressor to SHS	E_{V2G}	Electricity from hydrogen via V2G
HFS	*Hydrogen fueling station (HFS)*	E_{HFS}	Electricity consumption HFS
HFS1	High-pressure compressor	E_{SHS}	Electricity consumption SHS
HFS2	High-pressure stationary storage	*H*	*Hydrogen*
HFS3	Chillers	H_W	Hydrogen from wind electricity
HFS4	Dispensers	H_S	Hydrogen from surplus solar electricity
SHS	*Large-scale and shared seasonal hydrogen storage (SHS)*	H_{HFS}	Dispensed hydrogen at HFS
SHS1	Shared seasonal hydrogen storage (SHS)	H_{Road}	Hydrogen consumed by road vehicles
SHS2	Low-pressure compressor	H_{V2G}	Hydrogen consumed for V2G electricity
		H_2O	*Water*
		H_2O_W	Water for hydrogen production via wind
		H_2O_S	Water for hydrogen production via solar

The size of a Hamburg- or Murcia-based illustrative smart city area for this study was determined using the dispersion of supermarkets and gas stations in Europe, Germany, and Spain. In the EU 28 countries, for every 2000 households, there is one medium-sized supermarket and one gas station [465,468,471,675]. In Germany and Spain, there is one gas station per 2600 and 1700 households, respectively [465,471,675]. Thus, 2000 households are a good indicator for dimensioning the smart integrated city area; see Table 6-2 (common parameters). This hydrogen fueling station will serve a similar vehicle population as current gasoline stations [386,676]. Total capital cost per capacity for large HFS (≥1500 kg/day) is lower than

for smaller HFS [467], thus also defining the minimum size of this scalable and illustrative smart city area.

On average, 2000 households in Germany and Spain correspond to, respectively, 4310 and 5083 people, with 2364 and 1846 passenger cars and 156 and 410 other vehicles, according to German and Spanish national statistical data [470,471,675,677–679]. See Table 6-2 (local parameters).

The floor area of residential and services buildings is derived from national statistical data and scaled to 2000 households: German and Spanish average household floor area S_{hh} is, respectively, 91.60 and 91.78 m^2 [471,472]. Residential and service sector roofs will be used for solar electricity systems and rainwater collection [501–503,550]. Solar electricity systems are installed on all technically suitable roof areas: 9 m^2 per person on residential buildings and 4 m^2 per person on service sector buildings area [504,505]. Façades are not considered.

For ease of comparison between Hamburg and Murcia, the roof area available for solar electric modules and rainwater collection in Murcia is based on the Hamburg parameters.

Table 6-2 Characteristics of the modeled smart city areas.

Characteristics	**Quantity**	
	Hamburg, Germany	**Murcia, Spain**
Common parameters (based on European statistics)		
Gas stations (#) [465]	1	1
Retail food shops (#) [468]	1	1
Households and dwellings [1] in smart integrated city (#) [472]	2000	2000
Local parameters (based on national statistics)		
People (#) [677]	4310	5083
Passenger cars (#) [470,678,679]	2364	1846
Vans (#) [2] [470,678,679]	115	356
Trucks (#) [470,678,679]	27 [3]	31 [4]
Tractor-trailers [470,678,679]	10	12 [4]
Buses (#) [470,678,679]	4.1	4.5
Floor area of residential buildings (m^2) [5,6] [472]	183,200	183,550
Floor area of services buildings (m^2) [6] [471]	92,940	38,330
Roof area available for solar electric modules (m^2) [504,505]	56,000	56,000 [7]

[1] Assuming that only one household lives in a dwelling. [2] German data [678,679] *defines a van as a vehicle with a weight of less than 3.5 tons; the Odyssee database* [470] *used for Spain defines a van as a vehicle with a weight of less than 3 tons. [3] Including commercial vehicles of 3.5–6.0 tons. [4] No distinction is made between trucks and tractor-trailers in* [470]*; therefore, the same relation between the number of trucks and tractor-trailers as in Germany is used. [5] Based on the surface area of permanently occupied dwellings* [472]*. [6] The floor area represents the floor space that needs to be heated, cooled, or illuminated* [680]*. [7] For ease of comparison, the value is kept equal to the Hamburg case.*

6.3.2.3 *Technological and Economic Characterization of System Components in Two Scenarios*

The technological and economic characteristics of the selected components will be listed according to the latest available figures in two technology development scenarios. The two scenarios, in different time frames, can be characterized as follows:

- The Near Future scenario uses current state-of-the-art renewable and hydrogen technology and current energy demand for buildings and transportation. It is an all-electric energy system, which means space heating is done using heat pumps, meeting the present heat demand for houses and buildings. Only commercially available hydrogen technologies are used. For all systems, including hydrogen technologies, current technology characteristics and cost figures are used. The Near Future scenario presents a system that could be implemented in 2020–2025.
- In the Mid Century scenario, a significant reduction in end-use energy consumption is assumed. Hydrogen and fuel cell technologies have become mature with mass production and performing on the cost and efficiency targets projected for 2050. Also, for all the other technologies, such as solar, wind, and electrolyzers, the learning curves are taken into account.

The detailed technical and cost-related parameters of the system components are presented in Appendix A.2 Table A2 and Table A3. The technology selection for the system components and sizing methods is based on the component description in [235].

6.3.3 Calculation Model and Hourly Simulation

Figure 6-3 shows the simplified simulation scheme of the calculation model, consisting of five major steps that are executed hourly for an entire year. A detailed description and input data are described in Appendix A.2.

1. Electricity consumption and production (yellow; see description in Appendix A.2.1)
2. Road transport hydrogen demand (blue; see description in Appendix A.2.2)
3. Electricity and hydrogen hourly balance (red; see description in Appendix A.2.3)
4. Hydrogen tube trailer and tractor fleet (grey; see description in Appendix A.2.4)
5. Wind hydrogen production and seasonal storage balance (green; see description in Appendix A.2.5)

Two sets of energy balances are calculated on both an hourly and an annual basis (Figure 6-3 in red and green) for both hydrogen and electricity energy carriers. Energy consumption takes place in buildings and for mobility. Energy production is by roof-top solar and wind turbines and covers all energy consumption needs, taking into account all efficiencies of the different energy conversion and storage processes.

The amount of rooftop area available for solar electricity systems is fixed in both scenarios and locations for ease of comparison of the system performance between the two climates. The amount of installed wind capacity is the degree of freedom in the calculation model and completes the annual energy balance.

The system is simulated for five years using weather data from 2012 to 2016, which results in varying hourly electricity production consumption profiles, as well as electricity production per installed capacity. For ease of comparison between the years, the annual building electricity demand is kept constant.

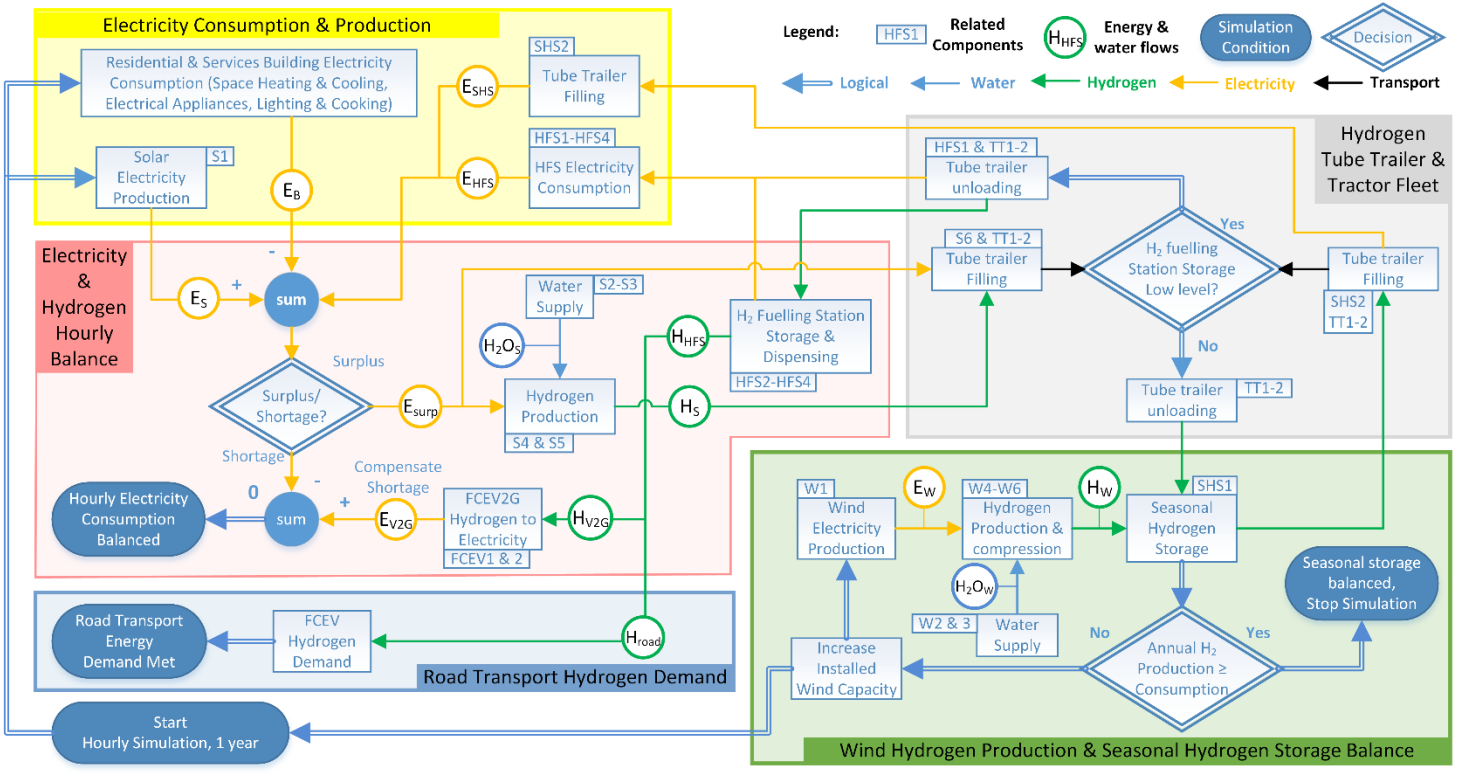

Figure 6-3 Simplified hourly simulation scheme.

6.3.4 Calculating the Cost of Energy

Three components of the cost of energy (CoE) will be calculated for each location in both scenarios.

1. Smart city area total system cost of energy ($TSCoE_{SCA}$) in euros per year (Appendix A.3.1).
2. System levelized cost of energy for electricity ($SLCoE_e$) in euros per kWh and for hydrogen ($SLCoE_H$) in euros per kg of hydrogen (Appendix A.3.2).
3. Cost of energy for households (CoE_{hh}) in euros per household per year (Appendix A.3.3).

6.3.4.1 Smart City Area Total System Cost of Energy

The $TSCoE_{SCA}$ in euros per year is the sum of the total annual capital and operation and maintenance costs TC_i (€/year) of the total number of components (n) in the smart city area. The TC_i of an individual component is calculated using the annual capital cost CC_i (€/year) and operation and maintenance cost OMC_i (€/year); cost formulas used are listed in Appendix A.3.1.

The cost analyses are in constant 2015 euros. An exchange rate of 0.88 USD to 1 EUR is used as in [235]. The website [681] is used to convert all USD values to USD_{2015} values. A weighted average cost of capital WACC of 3% is used from Appendix 0 of [667].

6.3.4.2 System Levelized Cost of Energy

The system levelized cost of energy, for either electricity $SLCoE_e$ (€/kWh) or hydrogen $SLCoE_H$ (€/kg H_2), is calculated by allocating a share of the $TSCoE_{SCA}$ (€/year) related to either electricity $TSCoE_{SCA,e}$ (€/year) or hydrogen consumption $TSCoE_{SCA,H}$ (€/year). These shares are then divided by either the annual electricity consumption EC_e (kWh/year) or the annual hydrogen consumption EC_H (kg H_2/year), resulting in, respectively, the $SLCoE_e$ (€/kWh) or the $SLCoE_H$ (€/kg H_2). The cost formulas used are listed in Appendix A.3.2.

6.3.4.3 Cost of Energy for Households (Without Taxes and Levies)

Cost of Energy for a single household CoE_{hh} (€/hh/year), here calculated without taxes and levies, consists of the cost of energy for the building energy $CoE_{hh,B}$ (€/hh/year) and the transportation energy $CoE_{hh,T}$ (€/hh/year). The cost formulas used are listed in Appendix A.3.3.

6.3.5 Inter-Annual Variability Analysis

Multiple years of hourly solar global irradiation data and hourly average wind speed data recorded at both locations will be used to analyze the inter-annual variability and its impact on the smart city area total system cost of energy ($TSCoE_{SCA}$).

6.4 Energy Balance Results and Discussion

6.4.1 Annual Energy Balance Results

Key energy balance parameters for FCEV2G, solar electrolyzer, and SHS usage for Hamburg and Murcia in the Near Future and Mid Century scenarios are summarized in Table 6-3. Detailed background figures that serve as input to Table 6-3 can be found in Appendix A.4 (Figure Figure A 1, load duration curves, Figure A 2, hourly electricity balance for an entire year, Figure A 3, SHS storage level, and monthly hydrogen flows).

The annual energy balances of Hamburg and Murcia in the Near Future and Mid Century scenarios are shown in Figure 6-4 and Figure 6-5.

The key energy balance parameters and annual energy balances of the years 2012–2015 show similar outcomes. Several major trends can be seen when looking at the FCEV2G, wind and solar electricity production, direct consumption of solar electricity, and seasonal hydrogen storage.

- *Reliable electricity supply can be realized at all times, as extreme FCEV2G peaks never exceed 50% of the car fleet*. Maximums of 760 and 772 cars, 32% and 42% of the car fleet in Hamburg and Murcia in the Near Future scenario, are reduced to 391 and 275 cars, 17% and 15% of the car fleet in the Mid Century scenario. The above maximums are extreme outliers, and values close to these occur for only a few hours per year (Figure A 1).
- *In the Mid Century scenario, FCEV2G usage is comparable to driving*. In the Near Future scenario, the fleet average FCEV2G hours are 880 h/year compared to 440 h in Mid Century scenario at 10 kW/car output for Hamburg. For Murcia, this is 670 h and 330 h. The Mid Century scenarios' FCEV2G hours are similar to the average driving hours for passenger cars: 310 and 280 h/year for, respectively, Hamburg and Murcia.
- *The 87% higher solar electricity output in the Mid Century scenario* in both locations results in less required external wind-to-hydrogen production to close the energy balance. This, together with more than a 30% reduction in building and road transportation energy consumption, and improvements in energy conversion processes, results in reductions of 70% and 90% of wind electricity production for, respectively, Hamburg and Murcia.
- *The 490% higher solar hydrogen production* in the Mid Century scenario in both locations compared to the Near Future scenario. Due to lower building electricity consumption and higher solar electricity production, there is more solar surplus electricity for hydrogen production. In Hamburg, solar electrolyzer power consumption always peaks in the summer's time, whereas, in Murcia, solar electrolyzer power consumption peaks in winter (Figure A 2).
- *The 40% and 56% higher coverage of electricity consumption with direct solar electricity production* in the Mid Century scenario in, respectively, Hamburg and Murcia compared to the Near Future scenario. Due to higher solar radiation and lower building and system electricity consumption, a higher percentage can be met directly with solar electricity. Nighttime electricity consumption has to be met with FCEV2G electricity production.

- *The 15%–25% lower seasonal hydrogen storage requirements in the Mid Century scenario* due to a better match of higher solar electricity production and lower building electricity demand compared to the Near Future scenario. For Hamburg, the maximum storage content of hydrogen occurs in the fall for both scenarios, whereas, in Murcia, this period shifts from spring to fall. The minimum storage content occurs in winter for both locations and scenarios. In the Mid Century scenario, a typical salt cavern [385] (Table A3) could serve approximately 23 similarly operating smart city areas in Hamburg and 40 Murcia smart city areas.
- *The 40% lower seasonal hydrogen storage and FCEV2G requirements in Murcia* compared to Hamburg, in all scenarios. In the Mid Century scenario, solar electricity alone is almost able to supply all of Murcia's energy needs for buildings and road transportation (despite its 21% higher consumption of road transportation hydrogen; Appendix A.2.2). If approximately 15% more solar panels were to be installed, either on facades, in public spaces, or nearby solar fields, the entire energy demand could be met with solar energy. The reason for the lower SHS and FCEV2G requirements in Murcia compared to Hamburg is the better match in time (daily and seasonal) between solar electricity production and building electricity consumption. In addition, Murcia also has a relatively higher solar electricity output and lower building demand compared to Hamburg. In the Mid Century scenario in Murcia, the same solar system produces 73% more electricity than in Hamburg.
- *Relatively, 70% and 30% more seasonal hydrogen storage is needed in the Mid Century scenario* for, respectively, Hamburg and Murcia. Even though absolute hydrogen and electricity production, energy consumption, and seasonal hydrogen storage decrease in the Mid Century scenario, the higher dependency on solar electricity production increases the seasonal effect. Hence, there is an increase in relative seasonal hydrogen storage compared to the annual hydrogen and electricity production in the Mid Century scenario.

Table 6-3 Key energy balance parameters for FCEVs through vehicle-to-grid (FCEV2G), solar electrolyzer, and SHS usage for Hamburg and Murcia in the Near Future and Mid Century scenarios.

Location	**Hamburg**		**Murcia**	
Scenario	**Near Future**	**Mid Century**	**Near Future**	**Mid Century**
FCEV2G				
Fleet average FCEV2G hours at 10 kW (hours/year)	880	440	670	330
Annual electricity production (MWh)	20,794	10,388	12,247	6112
Max. power (MW)	7.60	3.91	7.72	2.75
Date max. power (dd-mm)	3 January	4 January	12 June	3 September
Max. FCEV2Gs (#) / Max fleet percentage (%)	760/32.1	391/16.5	772/41.8	275/14.9
FCEV Driving				
Average driving time passenger car (hours/year)	310	310	280	280
Solar electrolyzer				
Capacity factor (%)	4.1	8.6	7.8	15.5
Annual electricity consumption (MWh)	2680	12,428	5658	7648
Max. absorbed power (MW)	7.43	16.47	8.26	19.05
Date max. power (dd-mm)	27 July	27 July	23 February	23 February
SHS				
Max. H_2 storage (×1000 kg H_2)	191	163	122	92
Max. H_2 storage relative to typical SHS 3733 ton H_2 (%)	5.1	4.4	3.2	2.5
No. similar smart city areas served by one typical SHS (#)	20	23	30	40
Date max. storage (dd-mm)	4 September	29 September	29 May	6 October
Date min. storage (dd-mm)	24 January	15 March	3 February	17 February
Annual hydrogen production (×1000 kg H_2)	1504	753	1149	640
Max. H_2 storage relative to annual H_2 production (%)	13	22	11	14
Max. H_2 storage relative to annual electricity production (%)	8.9	15	6.7	9.3

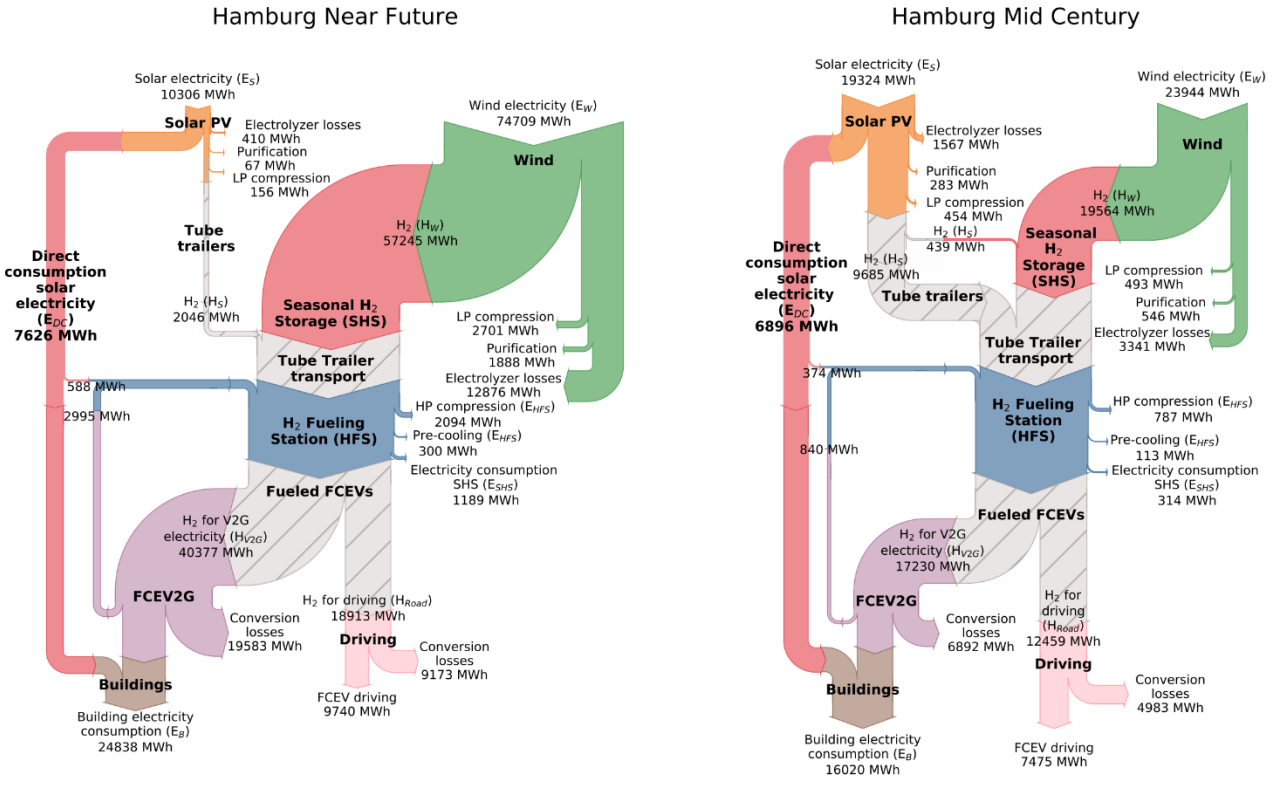

Figure 6-4 Annual energy balance for Hamburg for the Near Future scenario (left) and Mid Century scenario (right).

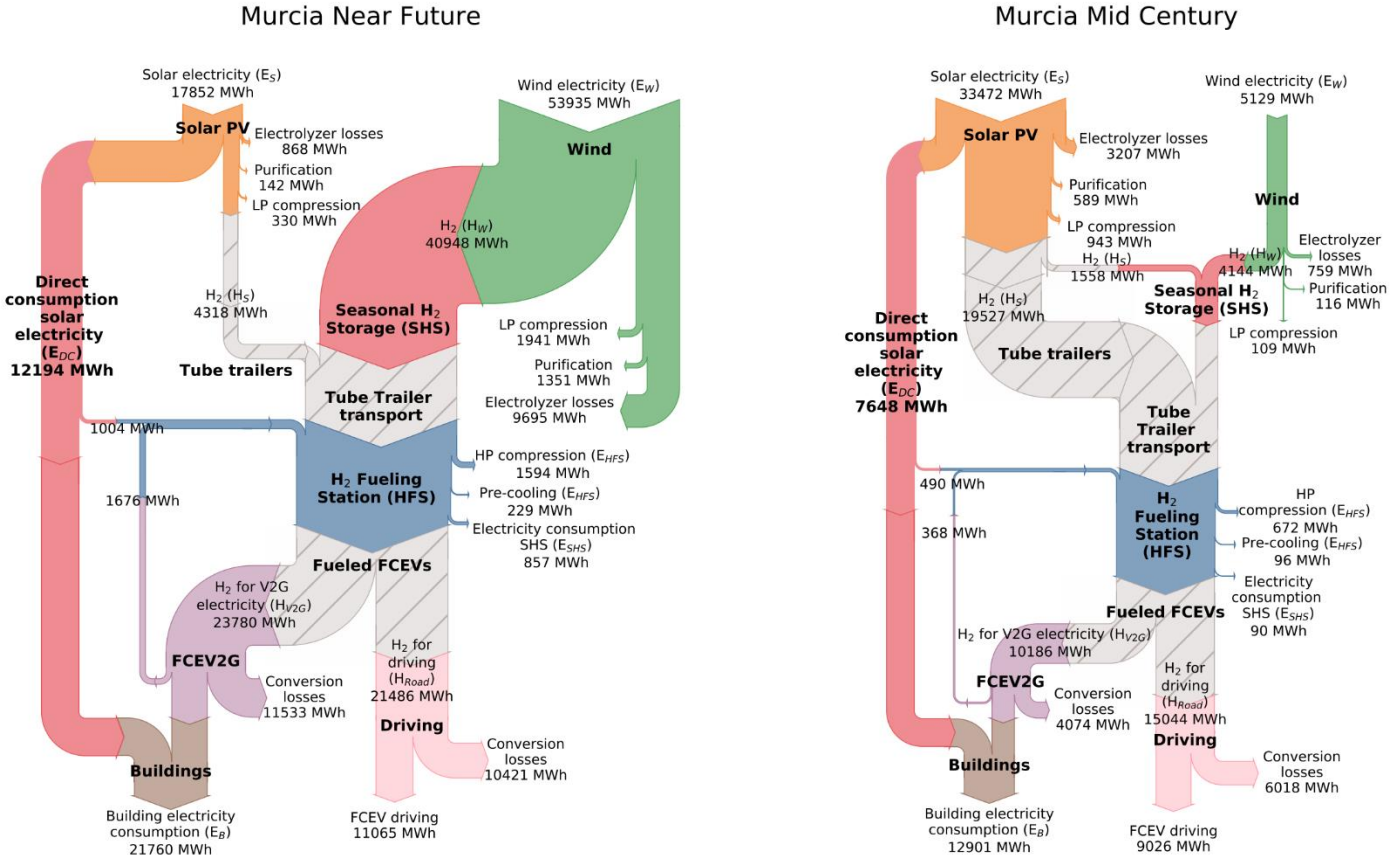

Figure 6-5 Annual energy balance for Murcia for the Near Future scenario (left) and the Mid Century scenario (right).

6.4.2 FCEV2G Usage and Electricity Balance Discussion and Results

Figure 6-6 provides further insight into seasonal and hourly FCEV2G usage. The FCEVs needed for producing V2G electricity (# cars left *y*-axis, % of car fleet right *y*-axis) are shown by means of boxplots for every hour of the day. For both locations and scenarios, usage is shown separately for both the colder winter period (in blue, left, 1 October–31 March) and the warmer summer period (in orange, right, 1 April–30 September).

- *Reliable electricity supply can be realized at all hours of the day,* as extreme FCEV2G peaks never exceed 50% of the total car fleet. The number of cars needed to balance the system peaks in the morning (06:00–09:00) and the late afternoon/early evening (16:00–20:00) and correspond to driving rush hours. These peaks are extreme outliers, and values close to these occur for only a small number of hours per year (Figure A 1).
- *In Murcia, virtually no cars are required during daylight hours*. This is valid in all scenarios and seasons, except for some moments. In Hamburg, this is only the case in the summer period, for both scenarios.
- *Hamburg faces a greater seasonal, and Murcia a greater day-night storage challenge*, particularly in the Mid Century scenario. In Hamburg, peak FCEV2G electricity production occurs in the winter period, whereas, in Murcia, the production is highest in both the summer and the winter period (see also Figure A 2).
- *On average, less than 22% and 13% of all cars are required during peak hours (17:00–19:00),* in, respectively, the Near Future and the Mid Century scenario (black crosses).
- *In Murcia, the mean FCEV2G usage is highest in summer. In Hamburg, the mean FCEV2G usage is highest in winter*. Electricity demand in Murcia is dominated by space cooling, whereas, in Hamburg, it is dominated by space heating. In the Mid Century scenario, the mean daily FCEV2G usage in the winter period in Hamburg is 7.3% of all cars, whereas, in Murcia, the figure is 4.6%. In summer, this is 3% of all cars in Murcia and 2.7% of all cars in Hamburg.
- *Relatively more FCEV2G electricity is produced outside regular driving hours* (20:00–06:00) [175] than during regular driving hours (06:00–20:00). In the Mid Century scenario, up to 60% of all FCEV2G electricity production in Murcia takes place during the 10 night hours (20:00–06:00); the remaining 40% FCEV2G electricity is produced during the 14 regular driving hours (06:00–20:00). In Hamburg, in the Mid Century scenario, the figures are 50% during the 10 regular driving hours and 50% during the 14 regular driving hours.

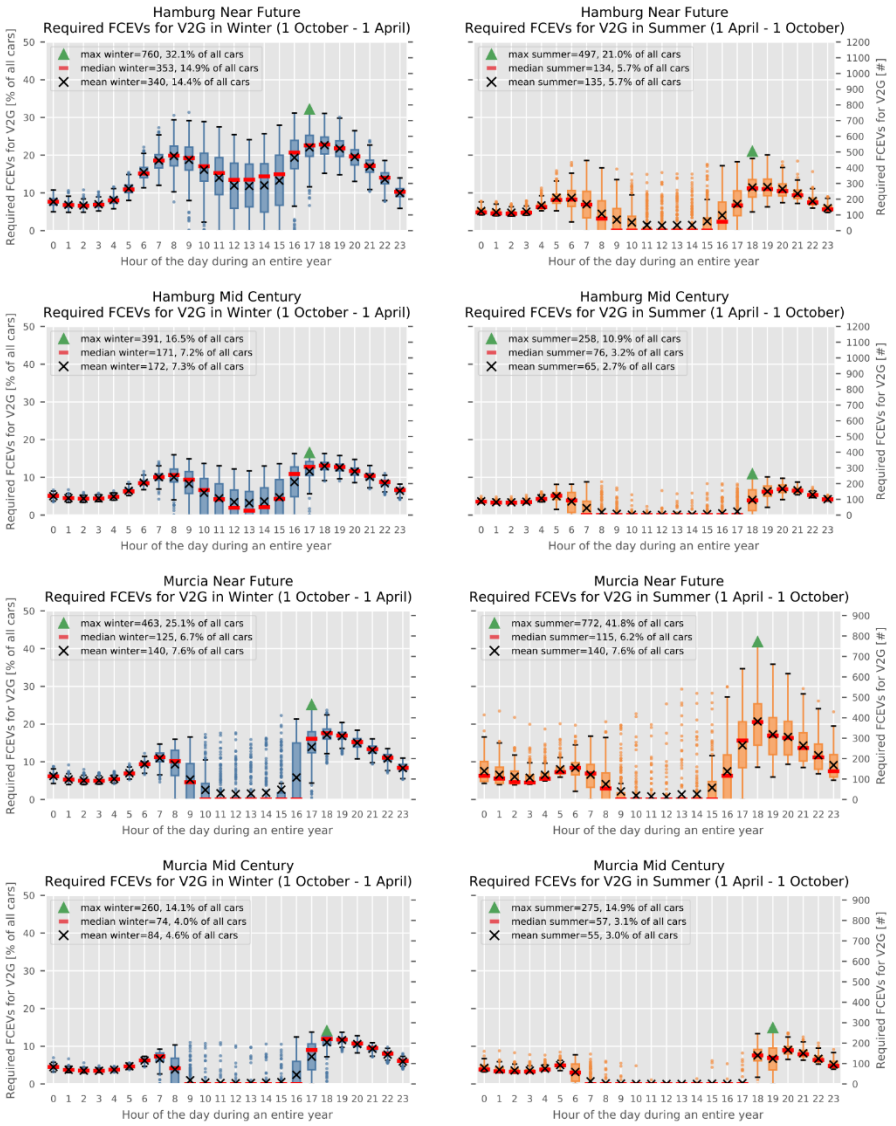

Figure 6-6 Boxplots showing the hourly average FCEVs needed for producing V2G electricity (# left y-axis, % of all cars right y-axis) throughout the day during the colder winter period (in blue, left, 1 October–31 March) and the warmer "summer" period (in orange, right, 1 April–30 September) in the Near Future and Mid Century scenarios for, respectively, Hamburg and Murcia. The black crosses represent the mean values, the red lines represent the medians, and the green triangles represent the maxima. Based on a normal distribution, the bars represent the interquartile range, IQR, the difference between the first and third quartiles (Q1 and Q3), approximately 50%. The upper and lower whiskers represent the data points within the ranges [Q1–(Q1-1.5×IQR)] and [Q3+(Q3+1.5×IQR)], approximately 44%. Dots indicate outliers, outside aforementioned ranges, the remaining approx. 1%.

6.5 Cost of Energy Results and Discussion

6.5.1 Total System Cost of Energy

The total system cost of energy per year TSCoE (k€/year) in the Near Future and Mid Century scenarios for Hamburg and Murcia is shown in Figure 6-7. The subsystems are grouped into hydrogen and electricity. The average component installed capacities and their total annual costs (TC_i) are listed in Appendix A.5 and serve as input for Figure 6-7. The following major trends can be observed when comparing both locations and scenarios.

- *The 70% reduction in TSCoE in the Mid Century* compared to the Near Future scenario for both locations. Higher efficiencies, lower final energy consumption, and increased favorable match between solar electricity production and final energy consumption significantly reduce installed capacities, thus costs. Economies of scale also reduce both installed capital and operation and maintenance costs.
- *The 20–30% lower TSCoE for Murcia* compared to Hamburg for both scenarios. For Murcia, the TSCoE is 1.9 million euros/year in the Mid Century scenario, whereas, for Hamburg, it is 2.6 million euros/year. The reason for this is the lower final transportation and building electricity demand and lower storage and reconversion requirements.
- *Variations in TSCoE from year to year are very small*, 2.2–4.0% (coefficient of variation CV in Table A 7 in Appendix A.5). This can be explained by the variations in daily and annual wind and solar electricity production, as well as the varying mismatch between solar electricity production and consumption. Seasonal hydrogen storage has relatively higher cost variations (8–12%) in comparison to other components, as the SHS is responsible for coping with all the above-mentioned variations.
- *The cost of hydrogen components in the Mid Century scenario drops up to 75%.* For both locations, in the Near Future scenario, the hydrogen components represent about 70% of the TSCoE; this reduces to 63% on average. As hydrogen technology is relatively new, economies of scale have a bigger impact on future cost reductions than on solar and wind electricity technology. In addition, the increase in solar output reduces storage requirements.
- *Hydrogen transportation, seasonal hydrogen storage, and the solar system are the only components that share in the total costs' relative increase compared to all other components.* This is because the cost reductions for these components are relatively lower compared to the other components. The relatively higher use of seasonal hydrogen storage in the Mid Century scenario compared to the annual hydrogen production (see Section 6.4.1) is another contributing factor.

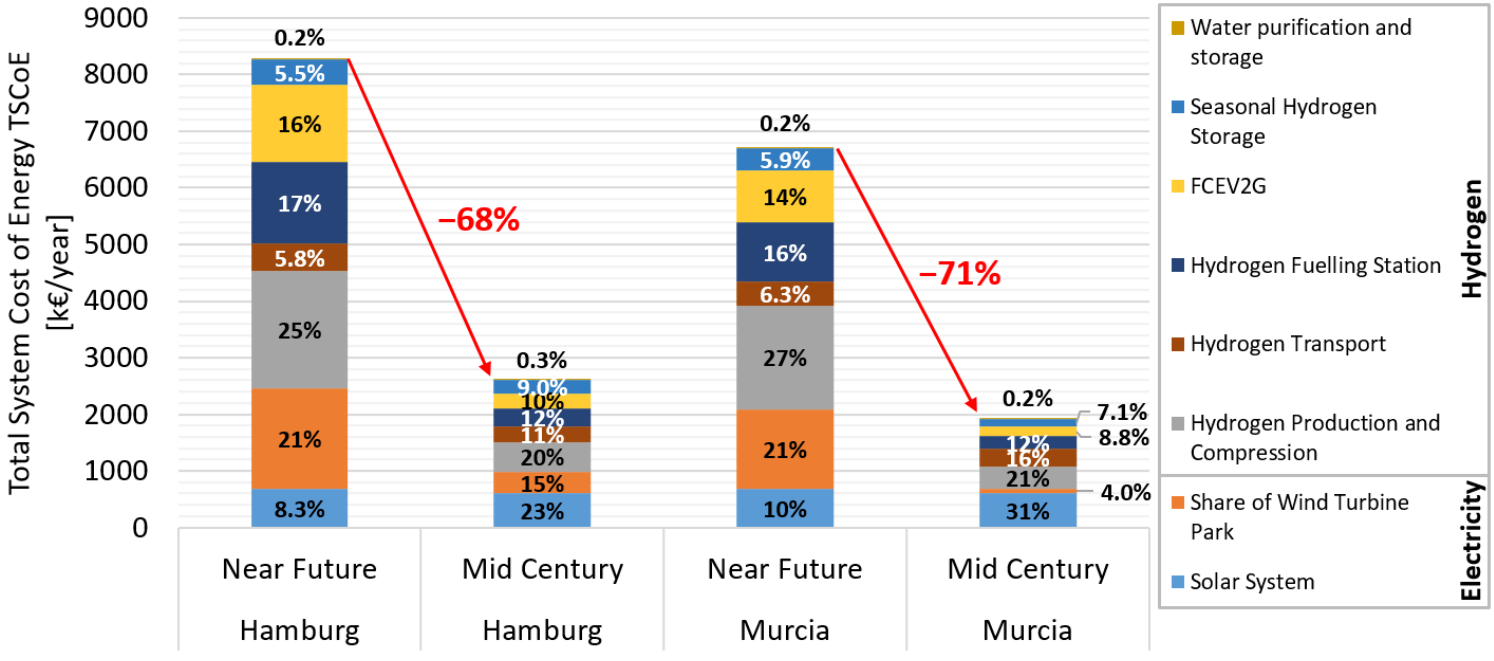

Figure 6-7 Total system cost of energy (TSCoE) for the component categories in the Near Future and Mid Century scenarios for Hamburg and Murcia. The subsystems are grouped into "Hydrogen" and "Electricity".

6.5.2 System Levelized Cost of Energy

The levelized and system levelized cost of electricity and hydrogen for Hamburg and Murcia in the Near Future and the Mid Century scenario are listed in Table 6-4. The values represent the average of the five simulated years. The levelized cost of energy (LCoE) and SLCoE parameters are calculated using the total costs (TC_i, Appendix A.5) of the various components and the corresponding energy flows (Figure 6-4 and Figure 6-5). Detailed calculation methods can be found in Appendix A.3 and [235].

- *The system levelized cost of energy of electricity ($SLCoE_e$) is 239 and 176 €/MWh in the Near Future scenario for, respectively, Hamburg and Murcia, and 104 and 71 €/MWh in the Mid Century scenario.* The $SLCoE_e$ is calculated by summing the costs of solar and FCEV2G electricity for buildings and dividing it by the total building electricity consumption. The total costs of solar electricity for buildings are calculated by multiplying the solar electricity consumption of buildings (Figure 6-4 and Figure 6-5) by the levelized cost of energy of solar electricity ($LCoE_{e,S}$). The total FCEV2G electricity costs are calculated by multiplying the FCEV2G electricity for buildings by the system levelized cost of energy of FCEV2G electricity ($SLCoE_{e,V2G}$).
- *All $SLCoE_e$ reduce by approximately 60% in the Mid Century scenario compared to the Near Future scenario.* Also, in Murcia, the $SLCoE_e$ is about 30% lower compared to Hamburg. In Murcia, a larger part of the building load can be directly covered by cheap and abundant solar electricity (even for hydrogen production) in both scenarios. As a result, less hydrogen production, storage, dispensing, and FCEV2G electricity are required.
- *The levelized cost of energy of hydrogen from surplus solar electricity ($LCoE_{H,S}$ in €/kg H_2) in this system is always higher than the levelized cost of energy of hydrogen from wind electricity ($LCoE_{H,W}$ in €/kg H_2).* The levelized cost of energy of hydrogen ($LCoE_{H,W\&S}$) before transportation and storage is based on hydrogen from both wind and solar. Even in Murcia, in the Mid Century scenario, the cost of solar electricity ($LCoE_{e,S}$) is lower than the cost of wind electricity $LCoE_{e,W}$. The reason for this is that a significantly higher capacity factor is achieved when the electrolyzer is connected to the wind turbine than to the solar electricity system, which only uses surplus solar electricity peaks.
- *The system levelized cost of energy of hydrogen ($SLCoE_H$) is 70–80% higher than the combined levelized cost of energy of hydrogen from solar and wind ($LCoE_{H,W\&S}$).* The $SLCoE_H$ includes the costs of hydrogen transportation by tube trailers, seasonal and fueling station storage, and dispensing on top of the solar and wind electricity costs, and the electrolyzers and low-pressure compressors, which is only the case for the $LCoE_{H,W\&S}$.

Table 6-4 Levelized (LCoE) and system levelized cost of energy (SLCoE) parameters for Hamburg and Murcia in the Near Future and Mid Century scenarios.

		Hamburg		Murcia	
Levelized Cost Parameter	**Involved Cost (TC_i) of Components (i) (Table A 7 Appendix A.5)**	**Near Future**	**Mid Century**	**Near Future**	**Mid Century**
$LCoE_{e,S}$ [€/MWh]	S1	68	31.7	37.6	17.5
$LCoE_{e,W}$ [€/MWh]	W1	23.5	16	26.5	18.2
$LCoE_{H,S}$ [€/kg H_2]	S1–6	13.7	2.9	6.5	1.5
$LCoE_{H,W}$ [€/kg H_2]	W1–6	2.3	1.2	2.7	1.4
$LCoE_{H,W\&S}$ [€/kg H_2]	W1–6 and S1–6	2.7	1.7	3	1.5
System levelized cost parameter					
$SLCoE_H$ [€/kg H_2]	W1–6, S1–6 (surplus), TT1 and 2, SHS1 and 2, HFS1–4,	4.9	3	5.2	2.6
$SLCoE_{e,V2G}$ [€/MWh]	W1–6, S1–6 (surplus), TT1 and 2, SHS1 and 2, HFS1–4, FCEV1 and 2	307	154	332	139
$SLCoE_e$ [€/MWh]	W1–6, S1–6, TT1 and 2, SHS1 and 2, HFS1–4, FCEV1 and 2	239	104	179	71.2

6.5.3 LCoE and SLCoE Comparison with Other Studies

Studying "100% renewable energy systems" is relatively new [682], and no integrated transportation and energy systems are the same. Comparing the $SLCOE_e$ with other 100% renewable energy systems should be taken as a general indication since there are many differences; for example, differences in geographical locations, renewable energy sources, energy carriers, storage technologies, and simulation criteria, such as energy self-sufficiency ratios or cost input parameters. Despite such differences, we can, to a certain extent, compare some subsystem costs, onshore wind and solar electricity, stored and dispensed hydrogen, and all-time available system electricity costs, including daily and seasonal storage.

- *Onshore wind electricity costs ($LCoE_{e,W}$) are relatively low in comparison with other studies.* Near Future scenario 24–27 €/MWh compared to 30–50 €/MWh for 2025 [683], and Mid Century scenario 16–18 €/MWh with 20–35 €/MWh for 2050 [683]. There are three reasons for this. First, the exclusion of grid connection costs of 11.5% [557,558] in this study, because of the direct coupling between the wind turbine and the electrolyzer. Second, the use of a lower WACC (3%) compared to other studies (3.5–10%) [683]. Third, the placement of wind turbines on sites with good wind conditions, resulting in good onshore wind capacity factors (33–38%).
- *Rooftop solar electricity costs ($LCoE_{e,S}$) are comparable to the average small rooftop and utility-scale solar electricity costs*, also known as community-scale or large rooftop. Near Future scenario costs of 38–68 €/MWh are similar to 20–90 €/MWh [370,684] in 2025, and Mid Century scenario costs of 18–32 €/MWh to 15–44 €/MWh [370] in 2050. The aforementioned values from the literature

have similar global horizontal irradiation, although higher WACC (4–5%) [370,684].

- *Stored and dispensed hydrogen costs ($SLCoE_H$) are similar or lower compared to other studies.* Near Future scenario costs of 4.9–5.2 €/kg H_2 are similar to the 4–7 €/kg H_2 according to studies by the Fuel Cell Hydrogen Joint Undertaking (FCH JU) and United States Department of Energy (US DoE) [298,516,685,686]. The $SLCoE_H$ in the Mid Century scenario of 2.6–3.0 €/kg H_2 is slightly lower than the US DoE targets of dispensed hydrogen (3.3–3.9 €/kg H_2) [687]. The major reasons for this are the higher electricity and expensive electrolyzer costs assumed by the US DoE.
- *System electricity costs ($SCLoE_e$) are similar to or lower than those in other studies* on 100% renewable energy systems, including energy and transportation. The Near Future scenario $SCLoE_e$ of 179–239 €/MWh is lower compared to the transportation and energy system of the United States National Renewable Energy Laboratory (NREL) [3]. The difference can be explained by the system's smaller scale, higher, and older component cost figures, and the use of stationary fuel cells instead of FCEV2G technology. The Mid Century scenario $SLCoE_e$ of 71–104 €/MWh is close to the $SLCoE_e$ of 88 €/MWh for an average European smart city area, excluding seasonal hydrogen storage [235]. Several hydrogen electricity reconversion pathways in the north of Germany have been designed and evaluated for the year 2050, including underground seasonal hydrogen storage [688]. The study reports higher values of 176–247 €/MWh, although it confirms that the costs are dominated in all pathways by the costs of purchasing electricity [688]. The authors of [667] and [689] report similar values of 75–85 €/MWh and 100 €/MWh for 100% renewable and self-sufficient energy systems in 2050. Although they have similar system electricity costs, there are several differences: [667] and [689] use different storage technologies simultaneously, include more sectors (industry, agriculture, fishing, and forestry) and renewable energy sources, and either simulate for entire countries (Germany and Spain) [667] or cities in a different continent (North America) [689].

6.5.4 Cost of Energy for Households (Without Taxes and Levies)

Total system costs or system levelized energy costs do not represent the combined effect of energy-saving measures, higher efficiencies, and decreased costs. Therefore, the cost of energy for an average household CoE_{hh} (€/hh/year) is introduced as an example. To put the designed system into perspective, a comparison with today's household energy costs would be interesting to make. This, however, is not as straightforward as it seems.

The developed system and the technologies used are very different from today's fossil-based energy and transportation system. Cities today are not self-sufficient: They import energy from both the national and the international power and fuel network. These national and international electricity and fuel supply chain networks also come at a cost. This, however, falls outside the scope of this study.

The analyzed size of this system is very small; one could compare it to a neighborhood within these big urban areas or a very small village. In addition, only the building and the road transportation sector are analyzed and integrated here. Increasing the system size and combining several different sectors would create more integration opportunities and reduce costs. For example, the equipment could be shared to avoid underutilization.

Environmental and health savings and welfare creation (e.g., jobs) [690] compared to the present fossil system are difficult to express in costs for this specific and small-scale system. In the present situation, taxes and levies on energy can represent a great part of the energy costs for household consumers, but future estimates of taxes and levies are not within the scope of this study.

Summarizing, it is very difficult to make a fair cost comparison. Nevertheless, a very simple energy cost comparison for an average household is shown below, without any taxes or levies. The present fossil situation is compared with the designed 100% renewable system in the Near Future and the Mid Century scenarios. Additional background data for the present situation can be found in Appendix A.6.

The cost of energy for a single household CoE_{hh} (€/hh/year) consists of the cost of energy for the building energy $CoE_{hh,B}$ (€/hh/year) and the transportation energy $CoE_{hh,T}$ (€/hh/year); see Table 6-5. The Near Future scenario CoE_{hh} shows an increase compared to the present situation, although not by several magnitudes. For Murcia, the increase is only 30% in the Near Future scenario. This shows that even though new hydrogen technologies are used, Near Future scenario costs can come close to the present situation costs and thus give reason to explore further. We should bear in mind that the Near Future scenario only changes technologies (e.g., electric water heating and heat pumps for heating) and has no significant energy savings as in the Mid Century scenario. However, in reality the installation of a heat pump often goes hand in hand with energy-saving measures like insulation. What's more, any further integration with other sectors and increasing the system size could also further reduce costs.

The cost of energy for households (without taxes and levies) in the Mid Century scenario is significantly lower (up to 65%) compared to the present situation—namely 770 and 520 €/year per household for Hamburg and Murcia, respectively.

Therefore, the designed system is not only renewable and reliable but also affordable.

Table 6-5 The annual cost of energy for households (CoE_{hh}) without taxes and levies for the Present, Near Future, and Mid Century scenarios in Hamburg and Murcia.

	Hamburg			Murcia		
Annual Cost of Energy for Households (Without Taxes and Levies)	**Present**	**Near Future**	**Mid Century**	**Present**	**Near Future**	**Mid Century**
Building $CoE_{hh,B}$ [€/hh/year]	1050	1820	480	1120	1360	340
Transportation $CoE_{hh,T}$ [€/hh/year]	460	790	290	350	570	180
Total CoE_{hh} [€/hh/year]	1510	2610	770	1470	1930	520

6.6 Discussion

The designed and analyzed integrated transportation and energy system is an extreme hypothetical scenario, because:

1. The city area is not connected to any national electricity or natural gas grid or a transportation fuel network. It is self-sufficient and stand-alone.
2. Only the residential, services, and road transportation sectors have been taken into account as energy consumers (e.g., not industry, agriculture, rail, or air transportation sectors).
3. Space heating and hot water production are all-electric.
4. It uses a single set of technologies for road transportation, transportation fuel, energy storage, and balancing, namely hydrogen, hydrogen production, and fuel cells (FCEVs), (no batteries or Battery Electric Vehicles, BEVs).
5. The city area is relatively small, based on approximately 5000 people.

In the future, a mix of multiple energy carriers, storage methods, and energy technologies could all work together. Cities in Europe already have connections to national electricity and sometimes natural gas grids. In addition, all sectors should be considered, not only the residential, services, and road transportation sectors. Increasing the system size and combining several different sectors would create more integration opportunities and could reduce costs.
However, the calculated energy costs of the designed system are affordable and in line with other studies. This gives reason to explore whether variations in system designs and balancing methods can reduce total system costs even further. The system designs and balancing methods discussed below are a non-exhaustive selection of possible options.

6.6.1 Other System Designs

- *A national electricity grid connection* would make it possible to import electricity or export peaks of solar electricity to other cities or electricity consumers in different sectors, such as industry, for example, by importing lower-cost onshore or offshore wind electricity during periods of insufficient solar electricity production (e.g., at night). This would reduce the need for hydrogen storage and FCEV2G electricity. High solar output at midday in the Mid Century scenario results in high surplus peaks to be absorbed by the solar electrolyzer. Exporting these high peaks of solar electricity to, for example, industrial cooling warehouses would reduce solar electrolyzer installed capacity and costs. Using only one electrolyzer connected to the national grid and placed next to the hydrogen station could reduce hydrogen transportation. Smart placement of electrolyzers in the electricity grid could obviate electricity grid congestion and reduce or avoid the need for expensive capacity expansion [691].
- *A hydrogen pipeline network* [638,692–696] could reduce hydrogen transportation via tube trailers and fueling station capacity. Multiple electrolyzers and hydrogen fueling stations could be interconnected via a

pipeline network [697]. In this way, tube trailer hydrogen transportation could be replaced, and hydrogen transportation costs reduced. Furthermore, the partial re-compression of hydrogen when emptying a tube trailer could also be reduced or avoided altogether. The compressor could even be omitted, provided the electrolyzer hydrogen output pressure is higher than the pipeline pressure. In the case of parked FCEVs delivering V2G electricity, the fuel cell could be connected directly to the hydrogen distribution pipeline network, instead of using hydrogen from the on-board hydrogen tank [698]. Not using hydrogen from the 700 bar tank eliminates the need for refueling for V2G purposes, which in turn reduces the required capacity of hydrogen fueling stations.

- *Import of low-cost renewable hydrogen could partially replace, possibly costlier, local hydrogen production and seasonal hydrogen storage, and thus total system costs.* Locally and at certain times of the year, there could be insufficient solar and onshore wind sources available to produce hydrogen. Regions with abundant and low-cost hydro, solar, or wind power [699–705] could produce low-cost hydrogen for export. This hydrogen could be imported at demand centers instead of being produced and stored on-site. Several ideas already exist, for example, producing hydrogen (far) offshore [706] from fixed or floating wind [435,436,638,707] and solar structures [708,709], or wave energy [433] and bringing the hydrogen onshore via existing natural gas or newly built pipelines [638] or ships [710,711]. The onshore pipeline network would then distribute the hydrogen to the consumers.
- *Using a lower-cost mix of renewable energy sources.* In this study, the rooftop solar surface area was kept equal in both locations, even though solar electricity is more expensive in Hamburg than in Murcia. Therefore, using the lowest cost renewable energy source locally available could reduce total system costs even further. For example, hydropower, offshore wind, biomass, concentrated solar power, by-product hydrogen, or tidal or wave energy could result in lower-cost electricity than onshore wind or solar Photovoltaic (PV).
- *Tailor electricity mix and its supply pattern to local demand.* In Murcia, solar electricity production has a better time match with electricity consumption on both a daily and a seasonal basis. During the day, solar electricity production in summer aligns well with electricity demand in buildings for space cooling. Therefore, a lower total system cost can be achieved by tailoring the renewable energy mix to allow for a better match between the production pattern and the demand pattern [652,653,717–721,655,667,689,712–716]. This would result in lower hydrogen production, storage, transportation, fueling, and FCEV electricity production costs.

6.6.2 Other Balancing Methods

- *Using a mix of FCEVs, BEVs, or fuel cell plug-in hybrid electric vehicle (FCPHEV) and stationary batteries* [103,215,722–724]. Instead of only using hydrogen and FCEV2G for both daily and seasonal energy balancing, other technologies could be used in parallel. For example, batteries in BEVs or FCPHEV, as well as stationary batteries, could be used for storing or releasing peak surplus or shortage of electricity [725] for day-to-day storage. Especially in Murcia, this could result in lower total system costs, as the day-to-day storage is more prevalent in Murcia [726]. Capacity factors of electrolyzers could be improved, and so decrease costs. FCEVs and hydrogen production and storage could subsequently be used for energy balancing for longer periods, up to entire seasons [726].
- *Using other CO_2-free hydrogen carriers for energy transportation, short and long-term energy storage.* There are several other proven and available carriers today, such as liquefied hydrogen [68,727–730], ammonia (NH_3) [731], or liquid organic hydrogen carriers (LOHC) [533,732]. Transporting liquid hydrogen can be less costly compared to compressed hydrogen when volumes and distances are larger. Ammonia storage and LOHC storage are becoming commercial applications at scale, and both represent reasonable alternatives in the absence of salt caverns.
- *Increase passenger car FCEV2G power output, use other FCEVs and stationary fuel cells for combined heat and power*. At the moment, only passenger cars with an output of 10 kW/car while having a 100 kW fuel cell system on-board are used for FCEV2G electricity. This limitation is mainly because of potential insufficient cooling radiator capacity when parked and providing FCEV2G electricity [229]. If V2G output could be increased by enhancing cooling capacity, then proportionally fewer passenger cars would be needed. Cooling capacity could be enhanced by installing, for example, a bigger radiator and cooling fans, or by using two-phase cooling fluids with a higher cooling capacity [733]. Commercial vehicles (vans, trucks, buses) are more widely used than passenger cars, although often not during the night. By also using commercial for V2G purposes [734], the number of passenger cars would be reduced. In the case of an underground hydrogen pipeline network, stationary fuel cells [735–740] could provide heat and power to buildings, and when necessary, FCEV2Gs could provide peak power.
- *Internet Technology (IT) usage for demand response forecasting, scheduling, virtual power plants, and autonomous driving*. Weather and electricity demand forecasting [741–750] in combination with demand response [631,634,751–753] could potentially avert peaks in temporal surplus or shortage of electricity. This would reduce installed capacity cost. Combining the output of thousands of grid-connected FCEVs would create so-called virtual power plants [198,256] with potentially large capacities. Similar to mobility as a service (MaaS) [577,578,754–756], power or electricity as a service (PaaS or EaaS) could be introduced. To create these markets, additional pricing structures, contract types, and aggregators scheduling and operating the cars will be required [757–

760]. Upcoming technologies could facilitate the scheduling of cars, for example, self-driving, free-floating, cloud-connected car-sharing fleets [310,311,576], together with inductive (wireless) self-connecting V2G infrastructure [270–272,580,761]. As mentioned earlier, most FCEV2G electricity is required at night, whereas most people travel and work during the day. So, even if car-sharing spreads widely and the total number of cars decreases, at night, car-sharing fleets will be used less and, therefore, will be available to provide power.

6.7 Conclusions

The designed and modeled system for smart urban areas is based on wind, solar, and hydrogen, where fuel cell electric vehicles provide year-round 100% renewable, reliable, and affordable energy for power, heat, and transportation in two different European climates.

The two locations in different climate zones—namely Murcia in Spain and Hamburg in Germany—were selected based on several criteria. Both are close to or in a large European urban area in one of the five most populated countries. Located in a different climate zone according to the Köppen–Geiger classification, Hamburg has a temperate oceanic climate (Cfb), and Murcia a hot semi-arid climate (BSh). Both locations have salt formations suitable for underground hydrogen gas storage. One location has a high level of solar radiation (Murcia), while the other has a low level (Hamburg).

The two designed smart city areas have the climate characteristics of Hamburg and Murcia; the dimensions are based on, respectively, German and Spanish statistical data. The smart city areas consist of 185,000 m^2 floor area of residential sector buildings, and for Hamburg and Murcia, respectively, 93,000 m^2 and 38,000 m^2 floor area services sector buildings. Hamburg and Murcia have, respectively, a total of 2500 and 2250 fuel cell electric vehicles (FCEVs), of which 2360 and 1850 are passenger cars that can be used for producing electricity via vehicle-to-grid (V2G), so-called fuel cell electric vehicle to grid (FCEV2G). Two thousand households with a total of approximately 4300–5000 inhabitants are the minimum viable economic size for dimensioning the smart city area, as statistically, there is one gas station and one retail food shop per 2000 households. Smaller capacity fueling stations are relatively costlier.

The designed smart city area system is 100% renewable. All electricity and hydrogen can be supplied by solar and wind to fulfill the energy demand for power, heat, and transportation. The transportation and energy sectors are fully integrated, and their final energy use is all-electric. Electricity is generated by solar modules on all roofs. Surplus solar electricity is converted via water-electrolysis with rainwater into pure hydrogen. The hydrogen is compressed and transported by tube trailer modules to the nearby hydrogen fueling station (HFS) or underground seasonal hydrogen storage (SHS). At the HFS, the hydrogen is further compressed to fuel all types of FCEVs, from passenger cars, vans, buses to trucks, and tractor-trailers. In the case of a temporary shortage of solar electricity, the fuel cells in the parked and grid-connected passenger cars provide the necessary electricity (FCEV2G) by converting hydrogen from the on-board hydrogen storage tanks. At parking places at home, the

office, or the local shopping area, vehicle-to-grid points connect the cars to the smart city electrical grid. The SHS is filled with hydrogen from surplus solar electricity and via a very short pipeline with hydrogen produced from wind electricity from an onshore wind turbine park. The stored hydrogen in the SHS is transported via tube trailers to the hydrogen fueling station.

The designed smart city area system is reliable at all times and independent of other energy systems and grid connections. The energy balance is simulated on an hourly basis for an entire year for a Near Future and a Mid Century scenario. Five years are simulated using climate data input from the years 2012–2016, although no significant differences in the energy balance are observed.

Reliable electricity supply can be realized at all times, as extreme peaks in the FCEV2G electricity supply never exceed 50% of the car fleet. Maximums of 32% and 42% of all cars (760 and 772 cars) in Hamburg and Murcia in the Near Future scenario drop to 17% and 15% of all cars (391 and 275 cars) in the Mid Century scenario. These maximums are extreme outliers, and values close to these only occur for a few hours per year. On average, less than 13% of all cars are required during peak hours (17:00–19:00) in the Mid Century scenario. FCEV2G usage is comparable to driving in the Mid Century scenario. There is an average of 440 FCEV2G hours per year per car compared to 310 driving hours per year for Hamburg. For Murcia, there are about 330 FCEV2G hours per year and 280 driving hours. The average number of FCEV2G hours could be reduced significantly by increasing the output per car or using other vehicles, such as buses, trucks, or vans. The passenger cars are limited to 10% (10 kW) of their maximum output (100 kW).

The underground seasonal hydrogen storage (SHS) guarantees year-round storage of hydrogen for driving and electricity production. A typical size SHS can serve around 20 smart city energy and transportation systems based on Hamburg in both scenarios, the equivalent of 86,000 people and 50,000 vehicles (passenger cars, vans, trucks, buses, and tractor-trailers). In the case of Murcia, this is about 30 smart city systems in the Near Future and 40 in the Mid Century scenarios. For the Near Future and Mid Century scenarios in Murcia, this is, respectively, the equivalent of 153,000 and 203,000 people with 68,000 and 90,000 vehicles (passenger cars, vans, trucks, buses, and tractor-trailers).

The designed smart city area system is affordable, and further cost reductions are possible. It is very difficult to make a fair cost comparison between today's energy system and the one proposed in this study in the Mid Century scenario. Nevertheless, a very simple energy cost comparison for an average household shows that the cost of energy for households (without taxes and levies) in the Mid Century scenario can be 65% lower compared to the present situation—namely 770 and 520 €/year per household for, respectively, Hamburg and Murcia.

The developed system and the technologies used are very different from today's fossil-based energy and transportation system. The designed and analyzed integrated transportation and energy system is an extreme hypothetical scenario because:

1. The city area is not connected to any national grid; it is self-sufficient and stand-alone.

2. Only the residential, services, and road transportation sectors have been taken into account as energy consumers.
3. Space heating and hot water production are all-electric.
4. It uses a single set of technologies for road transportation, transportation fuel, energy storage, and balancing; hydrogen, hydrogen production, and fuel cells (FCEVs and no batteries or BEVs).
5. The city area is relatively small, based on approximately 5000 persons.

Increasing the system size and combining several different sectors would create more integration opportunities and could reduce costs. Environmental and health savings and welfare creation (e.g., jobs) compared to the present fossil system are difficult to express in costs for this specific and small-scale system. In the future, multiple energy carriers, storage methods, and energy technologies could work in parallel. The system levelized costs in the Mid Century scenario are 71–104 €/MWh for electricity and 2.6–3.0 €/kg for hydrogen. These results compare favorably with other studies describing fully renewable power, heat, and transportation systems. This gives reason to explore whether variations in system designs and balancing methods and technologies can further reduce total system costs.

7 Fuel cell electric vehicles and hydrogen balancing 100 percent renewable and integrated national transportation and energy systems

The research presented in this chapter has been published in [762]. The work in this chapter tries to address research sub-questions 2 “How can we integrate FCEVs, used for transport, distributing and generating electricity, into future energy systems?” and 3 “What impact do European regional characteristics have on the techno-economic system performance and the usage of FCEVs for transport, distributing and generating electricity?”. A combined approach of system design, heuristic modeling and simulation is used.

7.1 Abstract

Future national electricity, heating, cooling and transport systems need to reach zero emissions. Significant numbers of back-up power plants as well as large-scale energy storage capacity are required to guarantee the reliability of energy supply in 100 percent renewable energy systems. Electricity can be partially converted into hydrogen, which can be transported via pipelines, stored in large quantities in underground salt caverns to overcome seasonal effects and used as electricity storage or as a clean fuel for transport. The question addressed in this paper is how parked and grid-connected hydrogen-fueled Fuel Cell Electric Vehicles might balance 100 per cent renewable electricity, heating, cooling and transport systems at the national level in Denmark, Germany, Great Britain, France and Spain? Five national electricity, heating, cooling and transport systems are modeled for the year 2050 for the five countries, assuming only 50 percent of the passenger cars to be grid-connected Fuel Cell Electric Vehicles, the remaining Battery Electric Vehicles. The grid-connected Fuel Cell Electric Vehicle fleet can always balance the energy systems and their usage is low, having load factors of 2.1-5.5 percent, corresponding to an average use of 190-480 hours per car, per year. At peak times, occurring only a few hours per year, 26 to 43 percent of the grid-connected Fuel Cell Electric Vehicle are required and in particular for energy systems with high shares of solar energy, such as Spain, balancing by grid-connected Fuel Cell Electric Vehicles is mainly required during the night, which matches favorably with driving usage.

7.2 Introduction

The future energy and transport system in Europe will and must become 100% renewable, with zero emissions [14,325]. Three major aspects dominate the transition toward this goal:

- A high share of electricity in generation but also in final energy consumption, as heating and transport shift to all-electric
- High shares of (low cost) intermittent electricity generation mainly from solar and wind
- Reliability of energy supply

Significant numbers of back-up power plants, as well as balancing and large-scale energy storage capacity are required to guarantee the reliability of energy supply in a fully renewable European energy and transport system. Additional back-up generation, energy storage and transmission requirements are driven by two key issues [158]. First, the shortage of dispatchable generation due to high shares of solar and wind energy. Second, the surplus or deficit in overall generation. Many studies have demonstrated that the integration of high shares of renewable energy (up to 95%) into the European electricity sector is both technically feasible and affordable [58]. The literature [58,159] mentions two solutions to the above-mentioned key issues: 1) the coupling of electricity to other energy sectors, such as transport and heating, known as "sector coupling" [14]; and 2) the expansion of the power transmission network and its capacity; for example, through more and larger transnational [763] and transcontinental [764,765] power connections.

These solutions are limited to 100% renewable energy systems in a European context. In this respect, the impact of various hydrogen applications, in particular, have not been comprehensively researched in the design of 100% renewable energy systems [160,766]. However, hydrogen could play an important role in the industry and transport sectors, as well as in the provision of electricity, heat and energy storage [14,161]. Hydrogen can couple energy sectors and offer another solution in realizing 100% renewable energy systems by converting power to hydrogen, which can be used as a transport fuel and for energy storage in back-up power plants [160]. Recent research shows that in a system with more than 70% intermittent renewable electricity, 10% or more needs to be converted into hydrogen [116].

Renewable hydrogen production will be cost competitive with fossil fuels in the near future, as renewable electricity and electrolyzer costs have reduced significantly [143,767]. Today, hydrogen is already being stored on a large scale in underground salt caverns [768], and this is a proven and cost-effective [385,769] storage method applicable in many countries [179,770,771]. Large-scale seasonal hydrogen storage also occurs in the form of ammonia, liquid hydrogen, Liquid Organic Hydrogen Carriers (LOHC) [772], or in depleted gas fields.

Present research on highly renewable European energy scenarios for 2050 use open cycle gas turbines (OCGTs) to balance the electricity grid [55,67], fueled by synthetic methane [58,162], bio-methane [164] or hydrogen [160,161]. These large, central and stationary power plants have low capacity factors of approximately 3.5% [162,164], thus contributing to higher total system costs [153,155]. The quick refueling of hydrogen, taking less than 5 minutes [190], makes FCEVs dispatchable generators similar to hydrogen-fueled OCGTs. An FCEV powertrain consists of a hydrogen-fueled Proton Exchange Membrane (PEM) fuel cell system and a traction battery. This combination makes it possible to outperform an OCGT (hydrogen fueled) on several parameters, such as maximum upward and downward ramp rate; hot, warm and cold start-up times [184,229,773]; and electrical efficiency, especially in part load [229].

Interest in the field of 100% renewable energy systems is growing [682], and no integrated transportation and energy systems are the same. Blanco et al. [48] reviewed more than 60 renewable energy system studies and made a clear distinction between "transition energy systems" (30-90% renewable energy) and

"100% renewable energy system" studies. Current research agrees that the need for storage and balancing will increase significantly, with higher shares of variable renewable power sources (e.g., > 80%) [67]. Increasing the share of variable renewable power sources beyond 90% will result in a sharp increase in balancing requirements [48,774,775]. Few studies have focused specifically on power to gas (P2G) or power to hydrogen (P2H) from an energy modeling perspective [48], and even fewer specifically look into V2G from a large system point of view. Most of the studies to date have included P2H [67,775], P2G [14,48,132,157] and/or V2G with BEVs [58,173,174] as one of the balancing or storage options, but they primarily focus on the energy system as a whole (or part), its transition pathways or overall system cost optimization.

Research by Oldenbroek et al. [229] has demonstrated that a hydrogen Fuel Cell Electric Vehicle (FCEV), the Hyundai ix35 FCEV [180], can be modified and connected to the electricity grid, so-called Vehicle-to-Grid (V2G). The same set-up also has been used to power a single house [280]. In this way, an FCEV can function as a rapid-reacting balancing and back-up power plant, known as a Fuel Cell Electric Vehicle to Grid (FCEV2G). As one car could power several houses [280], thousands could be grouped together to power entire cities [235,612] and act as Virtual Power Plants (VPP) [256]. Millions of cars could likely replace large stationary balancing power plants in countries.

Mass production of automotive fuel cell systems will reduce costs to 40-60 USD/kW [96]. This is approximately ten times lower than the OCGT 2050 installed capital costs of 400 [58] to 600 [164] EUR/kW, with economic lifetimes of 25 [55,164,193] to 30 [58,159] years. With ultimate durability targets of 8,000 hours of automotive fuel cells [194], the economic lifetimes of these VPPs could also be over 20 years (400 operational hours per year).

The power capacity sold in passenger cars is enormous, with approximately 15 million passenger cars sold annually in Europe [776,777]. Imagine 50% of these cars being FCEVs and having only a V2G outlet power of 10 kW (10% of the rated fuel cell system power of an average FCEV). This would be the equivalent of an annual sold power capacity of 75 GW, much more than the total currently installed capacity of gas turbine power plants in Europe (approximately 15 GW [778]). Large fleets of future FCEV passenger cars with V2G outlet power have the potential to fully replace gas turbine power plants, especially because passenger cars in Europe are parked on average 97% of the time. In other words, they are used for driving only 3% of the time which, based on an estimate of the average annual driven distance of 12,000 km per year at an average speed of approximately 45 km/h [175], is less than 300 hours per year.

Inspired by the concept of a green hydrogen economy [453,637,638,670], the question addressed in this paper is:

How might parked and grid-connected (Vehicle-to-Grid, V2G) hydrogen-fueled FCEVs balance 100% renewable electricity, heating, cooling and transport systems at the national level in Denmark, Germany, Great Britain, France and Spain?

To find an answer to this question for each of the five countries, this study designed integrated national electricity, road transport and heating systems based on renewable electricity production and hydrogen as an intermediate energy carrier. The energy balances were calculated for each of these countries. Both hydrogen fuel cell and battery electric vehicles were considered to be in use for road transport. In the energy systems designed, only fuel cell electric vehicle to grid (FCEV2G), electrolyzers and hydrogen storage were used for balancing.
In this article, first the methods and data used will be explained (Section 7.3), then the results and energy balances will be presented (Section 7.4). Subsequently, the results will be discussed (Section 7.5) and then the conclusions are drawn (Section 7.6).

7.3 Materials and methods

To analyze how grid-connected (Vehicle-to-Grid, V2G) hydrogen-fueled FCEVs could balance 100% renewable national electricity, space heating and road transport systems, energy systems are designed for several European countries that would be fully self-sufficient and 100% renewable. The systems are hypothetical in the sense that energy exchange with other countries is excluded, and to balance the energy systems, only fuel cell electric vehicle to grid is used, electrolyzers and hydrogen storage. First, several countries were selected and an analysis and synthesis of their existing energy scenarios for 2050 was undertaken. Data and insights gathered served as input for the adapted system design and the simulations; for example, any partial renewable energy mix in the existing energy scenarios was converted to a 100% renewable energy mix.
The adapted system designs consist of the electricity, heating and road transport sectors, with the road transport sector only consisting of battery and fuel cell electric vehicles, the heating sector relying on heat pump electric and solar thermal heating, and with all energy storage in the form of hydrogen. To address inter-annual variability effects of renewable energy production on seasonal hydrogen storage and balancing using FCEV2G, several years were simulated, as recommended by [779].
The design and analysis were performed in four steps:

1. Selection of countries, analysis and synthesis of their existing energy scenarios for 2050 (Section 7.3.1).
2. Adapted system design for a 100% renewable national electricity, heating and road transport system (Section 7.3.2).
3. Selection of the system components and technological characterization in a mid-century scenario ~2050 (Section 7.3.3).
4. Hourly simulation of all energy flows for multiple years for the selected European countries and sizing of the system components (Section 7.3.4).

7.3.1 Selection of countries

To verify the applicability of this concept to Europe, the analysis was applied to five European countries: Denmark (DK), Germany (DE), Great Britain (GB), France (FR) and Spain (ES). These countries already have power-to-hydrogen sites in operation [116]; they have large-scale underground natural gas storage facilities [57]; and they have significant technical potential for hydrogen storage in salt caverns [179]. All five countries have energy scenarios for 2050 [132,172,232,780–784], and the required input data and the current hourly renewable electricity generation profiles were readily available [472,677,793,785–792]. Table 7-1 presents key figures for the five selected countries. These countries combined represent approximately 52% of the EU-28 population in 2015, 53% of the final energy consumption, 50% of passenger cars and 64% of petrol stations.

Table 7-1 Key figures for the selected countries 2015.

	DK	**DE**	**GB**	**FR**	**ES**	**EU-28 total**
Population (million) [794]	5.66	81.52	65.84[1]	66.81	46.53	508.52
Final energy consumption (TWh) [795]	157	2568	1429	1824	912	13042
Passenger cars (million) [470,679,777,796–798]	2.27	43.96	30.25[1]	31.90	16.93	251.92
Number of petrol fueling stations [465]	2007	14531	8494	11269	10947	109041

[1] *Figure for the entire United Kingdom (UK).*

In this research, only the future energy demand is considered of the electricity, road transport, residential and commercial heating sectors. Which today represent approximately 75% of final energy consumption in the five countries [795]. Road transport in these countries represents, on average, 27%, residential and commercial heating 26%, and the electricity sector 22% [795]. Sectors such as industry and agriculture were not included, due to a lack of detailed information about energy use throughout the year, which makes it difficult to construct hourly consumption profiles.

7.3.2 System design

Figure 7-1 presents an overview of the generic 100% renewable national electricity, heating, cooling and transport system design applied to each of the five countries modeled. In summary, in each system:

- Power is generated by renewable sources alone, the electricity generation mix is country specific but may consist of onshore and offshore wind power, solar photovoltaic (PV), Concentrated Solar Power (CSP), hydropower, biomass and waste Combined Heat and Power (CHP).
- Generated electricity is either directly consumed and transmitted via the electricity grid or used to produce hydrogen (H2) via water electrolysis.

- Road transport consists of passenger cars, motorcycles, vans, trucks, tractor trailers and buses. A combination of technologies is foreseen, including: Fuel Cell Electrical Vehicles (FCEVs) and Battery Electric Vehicles (BEVs) or Fuel Cell Hybrid Electric Vehicles (FCHEV).
- Only FCEVs connected to the grid (FCEV2G) are considered to provide balancing power to compensate electricity shortages.
- The hydrogen produced is either transported directly to the hydrogen fueling stations for road transport and re-electrification, or hydrogen is stored in seasonal hydrogen storage, such as underground salt caverns.
- From the seasonal storage, hydrogen can be transported through pipelines (converted natural gas pipelines or newly built pipelines, or via the road with tube trailer trucks).
- Heating in the residential and commercial sectors is supplied by solar thermal systems and electric heat pumps.

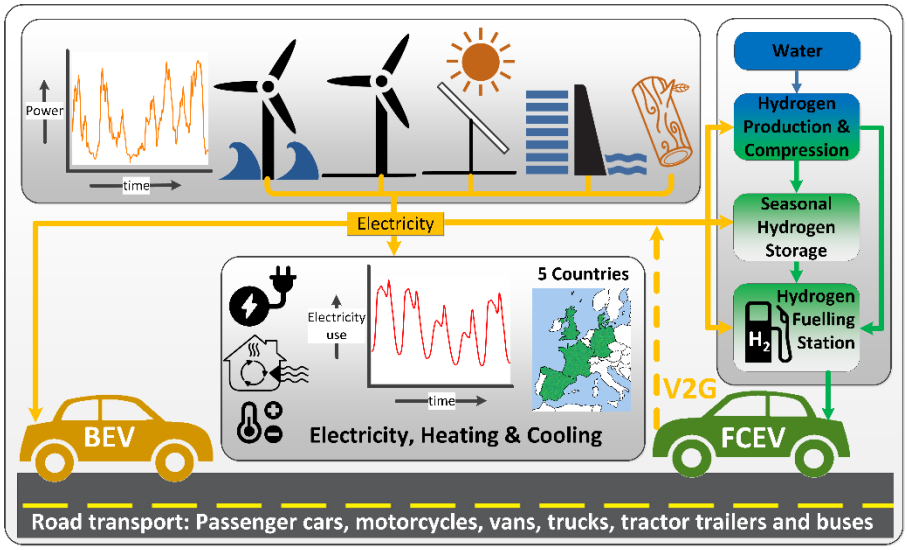

Figure 7-1 Generic 100% renewable system design applied to the national electricity, heating, cooling and transport systems of Denmark, Germany, Great Britain, France and Spain. Fuel cell electric vehicle to grid (FCEV and V2G), electrolyzers and hydrogen storage provide all of the necessary balancing requirements.

7.3.3 Technological characterization of system components

Renewable electricity is converted into hydrogen (H_2) through the electrolysis of water, which may be groundwater, surface or seawater, all demineralized through reverse osmosis. The energy use for the latter is included in the electricity consumption of the electrolyzer. Several manufacturers have designs available for large-scale alkaline electrolysis plants of up to 400 MW [799]. The electricity consumption on the basis of a produced kilogram of hydrogen for water demineralization [235,546,552,800], hydrogen production [126,801], drying and

purification [522] at 30 bar is taken to be 47 kWh/kg H_2 and is assumed to be constant in this model. Further compression to 120 bar for either pipeline transport or underground hydrogen storage requires approximately 0.9 kWh of electricity per compressed and transported kilogram of hydrogen [536]. Further compression from the underground hydrogen storage pressure to the hydrogen fueling station storage pressure of 880 bar [536], including pre-cooling for hydrogen dispensing of 700 bar [388,537], requires about 1.4 kWh of electricity per kilogram of hydrogen. Summarizing, to produce hydrogen from water, approximately 49.3 kWh of electricity is required per kilogram of hydrogen dispensed at 700 bar. This includes the purification and demineralization of water and the production, drying, compression, storage, pre-cooling and dispensing of hydrogen. With hydrogen having an HHV of 39.41 kWh/kg [802], the estimated HHV energy efficiency in this study in 2050 of producing hydrogen from water and dispensing hydrogen at 700 bar is 80%.

Fuel cell systems in part-load have higher efficiencies than at full-load [274]. The 10 kW output per passenger car in FCEV2G mode corresponds to only a 10% load of the approximate 100 kW fuel cell system and results in high efficiency. In 2050, fuel cell system efficiencies of up to 60% on a Higher Heating Value basis (HHV) are foreseen [126]. This fuel cell system efficiency, to convert hydrogen back into electricity, results in 23.6 kWh of electricity production per kilogram of hydrogen consumed.

Salt caverns can have geometric volumes of up to 1,000,000 m^3, with operating pressures of up to 20 MPa and cushion gas ratios of approximately 30–50% [385]. For example, a salt cavern with geometric volume of 500,000 m^3 has a net useable hydrogen storage of approximately 3,733 ton H_2 (corresponding to 147 GWh, HHV based) [385].

There are various predictions of the vehicle technologies that will be in use in a zero or low emission 2050 road transport scenario [38,126,128,129,132,157,174,442,803,804]. For zero emission transport scenarios where only BEV and FCEV technologies are considered, and when reaching tens of millions of vehicles, a hydrogen fueling infrastructure demonstrates some clear advantages over a battery charging infrastructure [103]. Due to the widespread use of all vehicle types, a hydrogen fueling infrastructure is comparable to today's conventional system. Such infrastructure offers quick vehicle fueling and long refueling intervals, combined with the relatively cost-effective and high fueling capacity of hydrogen stations, which all contribute to lower infrastructure costs [103]. A hydrogen fueling infrastructure would also match well with large-scale seasonal energy storage in the form of hydrogen gas [78,179,385] and the re-use of natural gas infrastructure [78,86,160,805–807]. Robinius et al. [103] concluded that a hybrid strategy for the roll-out of both infrastructures would help to maximize energy efficiency and optimize the use of renewable energy resources, while eliminating CO2 emissions over a broad range of purposes and transportation modes.

The distribution of annual distance traveled per vehicle type and technology in 2050 is presented in Table 7-2. The same distribution is used for all five countries. Table

7-2 also lists the estimated specific energy consumption per vehicle type and technology in 2050.

Table 7-2 Road transport vehicle types and the share of annual distance traveled and specific energy consumption per vehicle type and technology in 2050

	Distribution of annual distance traveled per vehicle type and technology in 2050		**Estimated specific energy consumption vehicle type and technology in 2050**	
Vehicle type	**BEV**	**FCEV**	**BEV (kWh/km)**	**FCEV (kg H_2/100km)**
Passenger cars	50%	50%	0.15 [808]	0.60 [126]
Motorcycles	50%	50%	0.056 [809,810]	0.28 [126,809,810]
Vans	40%	60%	0.206 [187,810]	0.90 [126,269,810–812]
Trucks	20%	80%	0.818 [187,810]	3.70 [126,810,813]
Tractor trailers	0%	100%	-	5.50 [104,126,814–816]
Buses	30%	70%	1.61 [810]	6.90 [500,817–819]

7.3.4 Calculation model and hourly simulation

Figure 7-2 displays the simplified simulation scheme of the calculation model and consists of four major steps, executed hourly for an entire year:

1. Renewable electricity generation (grey, see description in Section 7.3.4.1)
2. Electricity consumption (green, see description in Section 7.3.4.2)
3. Road transport hydrogen and electricity demand (red, see description in Section 7.3.4.3)
4. Balancing electricity and hydrogen demand (blue, see description in Section 7.3.4.4)

As mentioned, the simulation is based on an hourly resolution performed for an entire year. The simulations were also repeated for several years to gain some insight into the annual variation of renewable electricity sources. At the time this study was conducted, four years of renewable electricity generation and electricity consumption data were available and simulated for Germany and Denmark, (2014-2017), three years for France and Great Britain (2015-2017) and two years for Spain (2016-2017). It is assumed that the road transport demand remains constant throughout the years and independent of weather influences. Both an hourly and annual hydrogen and electricity balance were calculated. The future 2050 total installed capacity of renewable energy sources was calculated in several iterations, such that both hourly and annual electricity and hydrogen balances were met (in blue and Section 7.3.4.4).

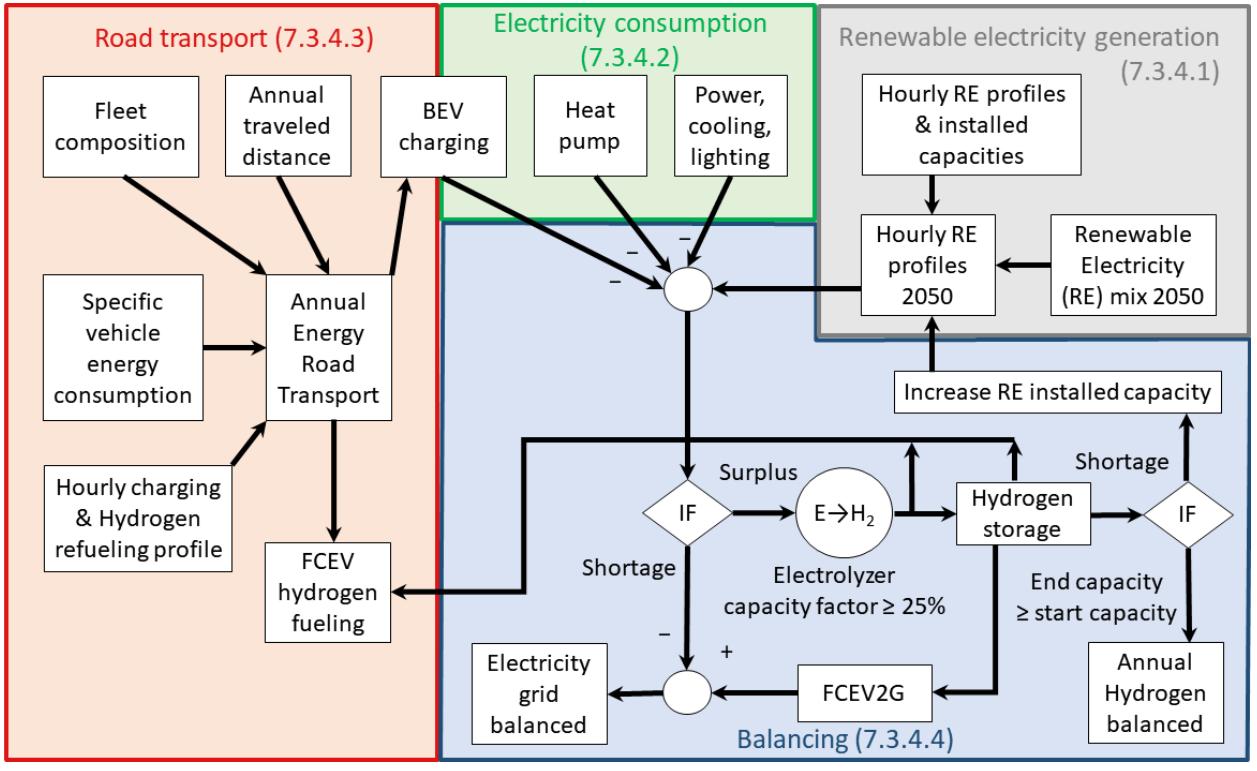

Figure 7-2 Schematic and simplified overview of the model.

7.3.4.1 Renewable electricity generation

The grey section in Figure 7-2 represents the renewable energy generation in simplified form. Table 7-3 shows the renewable electricity installed capacity mixes in 2050 per country. It was only in the case of Denmark that this could be taken directly from the available scenario studies [232,780,781]. For the other countries, a 100% renewable energy mix was constructed by omitting the fossil-fuel powered electricity generation capacity from low carbon energy scenarios and replacing this amount of electricity with an increase of renewable energy generation by wind and solar energy, according to the shares in the projected remaining electricity mix [132,172,782–784,820]. The hourly electricity generation profiles for every renewable energy source were collected from the Transmission System Operators (TSOs) and affiliated organizations and normalized with the installed capacity for each respective year [472,677,793,785–792]. These normalized hourly electricity generation profiles of solar PV, CSP, and onshore and offshore wind were then scaled with the installed capacity required. The installed capacity of hydropower, geothermal and biomass and waste-fired Combined Heat Power (CHP) should not exceed the values from the country scenario studies, as these energy sources are limited. In several iteration steps, the required installed capacity is the result of the annual energy balance calculation (see and Section 7.3.4.4).

Table 7-3 Renewable electricity installed capacity mixes in 2050 for Denmark (DK), Germany (DE), Great Britain (GB), France (FR) and Spain (ES) based on existing studies [37,58–64].

Renewable electricity installed capacity share	**DK**	**DE**	**GB**	**FR**	**ES**
Solar PV	8%	52%	42%	33%	52%
Solar CSP	0%	0%	0%	0%	6%
Onshore Wind	14%	37%	20%	50%	37%
Offshore Wind	71%	8%	28%	5%	0%
Hydropower	0%	1%	3%	12%[1]	5%
Geothermal	0%	0%	0%	0%	0%
Biomass Combined Heat and Power (CHP)	5%	2%	7%	0%	0%
Waste Combined Heat and power (CHP)	2%	0%	0%	0%	0%

[1] *5% run of the river and 7% reservoir.*

7.3.4.2 Electricity consumption

The green sections in Figure 7-2 display the electricity consumption in simplified form, consisting of "classic electricity consumption," heat pump electric heating and BEV charging.

The country-specific electricity consumption data, as provided by the TSOs and affiliated organizations, is the "classic" electricity consumption. This consists of aggregated electricity consumption data from various sectors; for example, the services and residential building sectors (lighting, appliances, space heating and cooling and hot water), industry, rail, agriculture, public lighting and other sectors. In the case of France, the classic electric consumption profile [793] was corrected [820] for the share of about 18% of electric space heating [472,795]. It was assumed that there will be no net increase or reduction of classic electricity consumption in 2050 compared to today. Despite efficiency increases in lighting and electrical

appliances, the increased number and use of these would not result in a reduction of total electricity consumption.
Currently, hot water and space heating demand in most countries still heavily relies on fossil fuels. To decarbonize this demand, most future 2050 scenarios envisage a large increase in electric heat pumps and solar thermal collectors, either per household or coupled to a district heating network [821]. These district heating networks could also facilitate the use of geothermal power, community solar thermal, and waste or biomass-fired CHPs [822–825]. Alternatively, existing natural gas distribution networks could also be used for the transport of hydrogen [638,692,693,826–828] and use in hydrogen boilers [828–830] or CHP fuel cell systems [161,735]. In the scenario studies by other institutions used in this work [132,172,232,780–784], heat supply from electric heat pumps predominates, and therefore it was used in the generic model here.
For each country, the annual total heating demand for space heating (sh) and hot water (hw), ($E_{shhw,total}$), [132,172,232,780–784,820], which cannot be met by solar thermal ($E_{shhw,solar}$) or geothermal energy ($E_{shhw,\ geo}$), is provided by electric heat pumps (ehp), $E_{shhw,ehp,h}$ in equation (7.11).

$$E_{shhw,ehp,h} = E_{shhw,total} - E_{shhw,solar} - E_{shhw,geo} \quad (7.1)$$

The electricity required by the electric heat pumps ($E_{shhw,ehp,el}$) is calculated in equation (7.11) by dividing the remaining heating demand with a seasonal coefficient of performance (SCOP) of 3.5, based on [482–485].

$$E_{shhw,ehp,el} = \frac{E_{shhw,ehp,h}}{SCOP} \quad (7.2)$$

The fraction of electricity for heating demand for domestic hot water (f_{hw}), compared to the total electricity for heating demand, if not specified in the scenario studies used, was calculated with historical data from the Odyssee database [471,472], see equation (7.11).

$$E_{hw,ehp,el} = E_{shhw,ehp,el} \times f_{hw} \quad (7.3)$$

The fractions for domestic hot water use are 15.3% for Denmark, 14.9% for Germany, 22.2% for Great Britain, 12.0% for France and 13.0% for Spain. The aggregated electricity demand for hot water is assumed to be constant for every hour of the year, similar to [58].
The aggregated hourly heat pump electricity profile for space heating electricity demand is dependent on the outside temperature and estimated with the use of Heating Degree Days (HDD). The daily (d) HDDs are calculated using equation 2.4. Where the daily mean temperature (T_{mean}) data of the five countries [820,831] serves as an input. With increased insulation in 2050, a reference temperature (T_{ref}) of 16ºC was used [832].

$$HDD(d)=\begin{Bmatrix} 0 & T_{mean}(d)>T_{ref} \\ T_{ref}-T_{mean}(d) & T_{mean}(d)<T_{ref} \end{Bmatrix} \quad (7.4)$$

The daily heat pump electricity demand for space heating, $E_{sh,ehp,el}(d)$, was assumed to be constant over a day. In equation (7.11), the heat pump electricity demand per day profile throughout the year is calculated by multiplying the normalized daily HDD profile over a year with the annual heat pump electricity demand for space heating and hot water ($E_{shhw,ehp,el}$, equation (7.3)) and the fraction of the electricity for space heating ($1-f_{hw}$).

$$E_{sh,ehp,el}(d)=\frac{HDD(d)}{\sum_{1}^{365} HDD(d)}\times E_{shhw,ehp,el}\times(1-f_{hw}) \quad (7.5)$$

7.3.4.3 Road transport electricity and hydrogen demand

The red section in Figure 7-2 displays the road transport energy consumption in simplified form, consisting of the FCEVs and BEVs.

No increase in annual kilometers driven in 2050 was assumed in calculating the road transport energy demand. Some studies predict a growth in kilometers driven due to increasing population; other studies expect a decrease in vehicle kilometers driven due to car-sharing or increased use of public transport [128,833,834].

Total annual road transport electricity and hydrogen demand was calculated using the distribution of annual distance traveled per vehicle type and technology (Table 7-2), the estimated specific energy consumption vehicle type and technology (Table 7-2), a charging efficiency for BEVs of 95% [132], 49.3 kWh of electricity required per kilogram of hydrogen produced and dispensed at 700 bar (Section 7.3.3), and the annual distance traveled per vehicle type (Table 7-4).

Table 7-4 Assumed road transport vehicle use in 2050.

	Annual distance traveled per vehicle type (millions of km)				
Vehicle type/Country	**DK**	**DE**	**GB**	**FR**	**ES**
Passenger cars	38,489	618,719	398,600	414,600	212,203
Motorcycles	457	9,612	4,500	16,394	7,428
Vans	7,221	42,569	75,000	97,455	121,154
Trucks	977	16,366	12,060	7,960	59,378
Tractor trailers	1,068	18,702	14,740	8,976	
Buses	612	4,378	4,300	3,420	6,132

The annual amount of hydrogen dispensed for both driving and FCEV2G electricity consumption was based on the relative hourly profile for one week (orange line in Figure 7-3) and was repeated and normalized for an entire year. The relative weekly profile was based on the pattern used by the US DoE in their simulations [835]. The BEV charging profile, Figure 7-3, remains constant throughout the day, similar to the

scenario by the Danish Energy Agency [780]. According to Ekman [836], simple day and night charging schemes do not significantly contribute to balancing, and smart charging requires more insight into usage and charging of BEVs, and therefore they were not applied here.

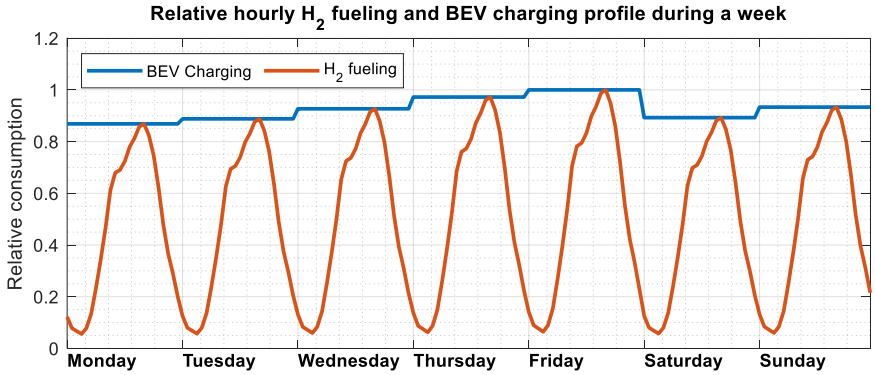

Figure 7-3 Relative hourly hydrogen fueling (orang) and BEV charging (blue) profile during a week based on [58,147].

7.3.4.4 Balancing electricity and hydrogen

The blue section in Figure 7-2 displays the hourly electricity balance and hourly and annual hydrogen balance calculations in simplified form.

In the system proposed, the hourly (h) electricity balance, $E_{Balance}$ equation (7.11), always has to be zero: a perfectly balanced electricity grid, subtracting total electricity consumption ($E_{consumption}$) from renewable electricity production ($E_{production}$). Deficits are compensated for with passenger FCEVs in V2G mode that convert the hydrogen produced earlier into electricity (E_{FCEV2G}). Surplus electricity is converted into hydrogen, the electrolyzer electricity consumption ($E_{electrolyzer}$), for both transport FCEV fueling and FCEV2G. The hydrogen produced is either used directly or stored seasonally. The total aggregated installed electrolyzer capacity is such that it operates with a minimum capacity factor of 25%. A lower capacity factor would result in higher hydrogen costs [837]. Remaining electricity production is utilized in sectors other than those dealt with in this article or it is curtailed.

$$\begin{aligned} &E_{balance}\left[MWh\right](h)=E_{production}\left[MWh\right](h)+E_{FCEV2G}\left[MWh\right](h)... \\ &-E_{consumption}\left[MWh\right](h)-E_{electrolyser}\left[MWh\right](h)=0 \end{aligned} \tag{7.6}$$

The hourly electricity production, $E_{production}$, equation 2.7, is the product of the estimated required installed renewable electricity capacity ($P_{estimated}$) for each hour.

$$E_{production}\left[MWh\right](h)=P_{estimated}\left[MWh/h\right]\times t\left[1h\right] \tag{7.7}$$

Here, FCEV2G electricity production, E_{FCEV2G} equation (7.11), is the product of the hydrogen fueling for FCEV2G ($H_{fueling,FCEV2G}$), the fuel cell system FCEV2G efficiency (η_{FCEV2G}) of 60% (Section 7.3.3) and the HHV of hydrogen (Section 7.3.3).

$$E_{FCEV2G}\left[\frac{MWh}{h}\right](h) = \eta_{FCEV2G}[\%] \times H_{fueling,FCEV2G}[kg\,H_2] \times \ldots$$
$$\ldots HHV_{Hydrogen}\left[\frac{kWh}{kg\,H_2}\right] \times \frac{1}{1000}\left[\frac{MWh}{kWh}\right] \quad (7.8)$$

The hourly hydrogen storage capacity ($H_{storage}$) at hour h, is determined in Equation (7.11), where hydrogen production ($H_{production}$), is added and hydrogen fueling ($H_{fueling}$), is subtracted from the hydrogen storage capacity ($H_{storage}$) of the previous hour (h-1). Hydrogen fueling consists of both hydrogen for transportation and FCEV2G electricity production.

$$H_{storage}[kg\,H_2](h) = H_{storage}[kg\,H_2](h-1) + H_{production}[kg\,H_2](h) - H_{fueling}[kg\,H_2](h) \quad (7.9)$$

Hydrogen production ($H_{production}$, equation 3.0) results from the absorbed power by the hydrogen production equipment ($E_{H2\ production}$) multiplied by the hydrogen production efficiency ($\eta_{electrolyzer}$, Section 7.3.3) and the HHV of hydrogen (Section 7.3.3).

$$H_{production}[kg\,H_2](h) = \frac{\eta_{H2\ Production}[\%] \times E_{H2\ Production}[MWh](h)}{HHV_{Hydrogen}\left[\frac{kWh}{kg\,H_2}\right] \times \frac{1}{1000}\left[\frac{MWh}{kWh}\right]} \quad (7.10)$$

The seasonal storage of hydrogen must also be balanced over the course of a year, see equation (7.11). If the storage capacity at the end of the year is lower than at the start of the year, the estimated installed capacity in the generation mix is increased in a subsequent iteration step, until the hydrogen storage capacity is equal to or higher than at the beginning of the year (8760 hours). In some case studies, the installed capacity of some renewable energy sources is limited (e.g., due to land space or hydropower). If the limit is reached, the installed capacity of the constrained energy source will increase no further, and only the installed capacities of the other sources increase.

$$\text{if}\begin{pmatrix} H_{storage}[kg\,H_2](h{=}8760) \geq H_{storage}[kg\,H_2](h=1) \Rightarrow \text{simulation end} \\ H_{storage}[kg\,H_2](h{=}8760) < H_{storage}[kg\,H_2](h=1) \Rightarrow \text{increase } P_{estimated} \end{pmatrix} \quad (7.11)$$

7.4 Energy balance results

Section 7.4.1 presents the annual energy balance results and the key energy balancing parameters and energy flows. Balancing on an hourly resolution is done by the FCEV2Gs and electrolysers and the hydrogen storage. These results are presented in section 7.4.2 and 7.4.3.

7.4.1 Annual energy balance results

No energy balancing would be needed if renewable electricity generation always exactly matched electricity consumption; however, this is not the case. Table 7-5 summarizes the key energy balancing parameters for the energy system, FCEV2G and electrolyzer usage for all five countries based on several years of energy data. Appendix B.1 shows hourly electricity consumption versus electricity generation for all five countries for an entire year. The annual energy balances (Sankey diagrams) for Denmark and Spain are shown in Figure 7-4 and Figure 7-5, respectively. The annual energy balances (Sankey diagrams) for Germany, Great Britain and France are shown in Appendix 0.

- *For all five countries, more than 88% of primary electricity generation originates from solar and wind*. Spain has the highest share of solar electricity generation (54%, 46% solar PV and 8% solar CSP) and Denmark has the highest share of wind electricity generation (87%, 78% wind offshore and 9% onshore).
- *In all five countries, more than 87% of electricity consumption can be directly met with renewable electricity generation.* FCEV2G generates the remaining electricity, where the highest values are seen in Denmark, at 13%. Spain has the lowest share of FCEV2G electricity production relative to annual electricity consumption, at 6%.
- *There is a significant share of unused FCEV2G capacity, up to 74%.* At peak times, occurring only a few hours per year, 26% (France) to 43% (Denmark) of the FCEV2Gs are required (the FCEV2Gs only make up 50% of all passenger cars).
- *FCEV2G fleet usage is low, with load factors of 2.1-5.5%*. Denmark has the highest FCEV2G fleet capacity factor of 5.5%, corresponding to an average of 480 FCEV2G hours per car, per year. Spain has the lowest, at 2.1%, corresponding to an average of 190 FCEV2G hours per car, per year. The range of 190-480 FCEV2G hours per car has the same order of magnitude as average driving hours per year of approximately 300 hours per car, per year (see Section 7.2, Introduction). Section 7.4.2 will shed more light on FCEV2G use during the day.

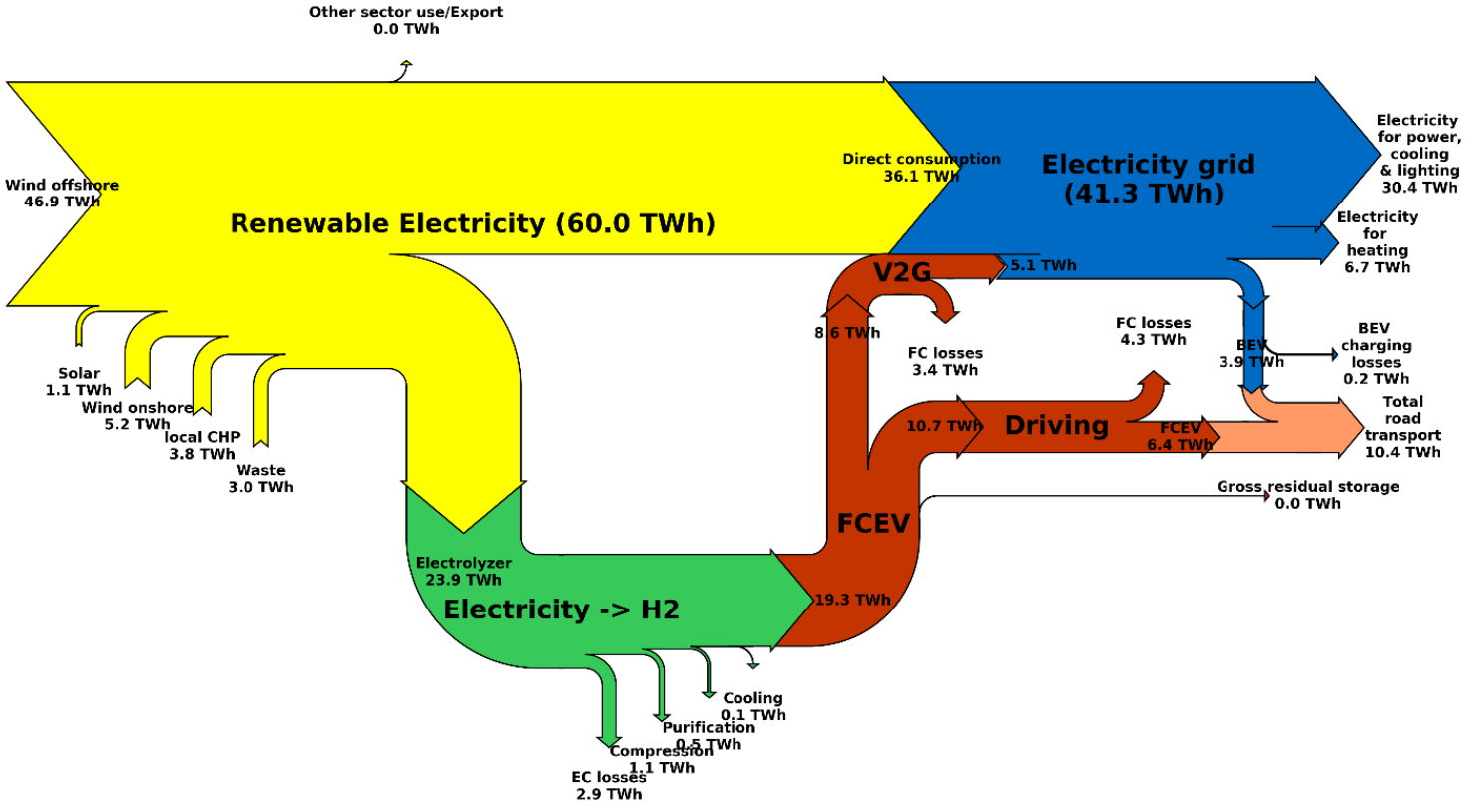

Figure 7-4 Annual energy balance (TWh/year) for Denmark in 2050 based on 2017 renewable energy data.

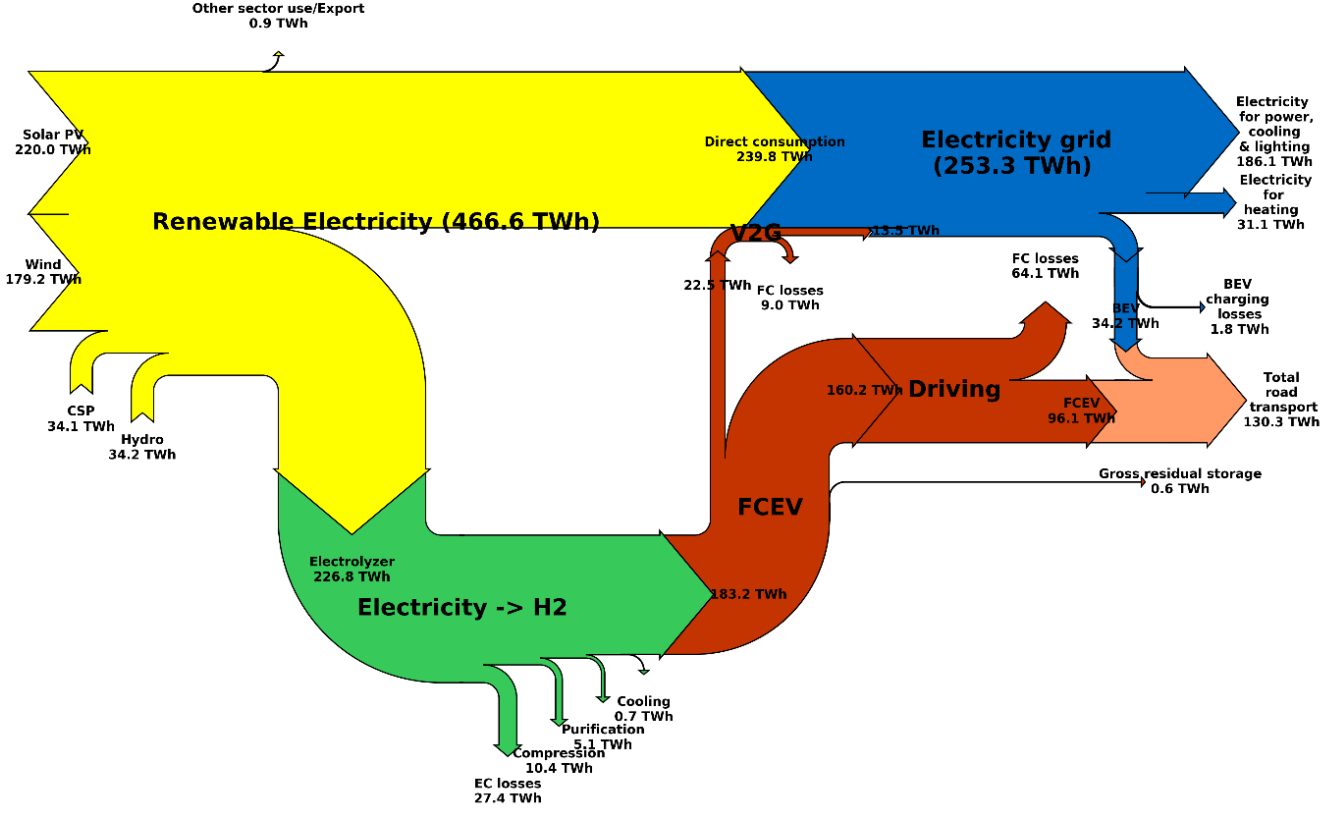

Figure 7-5 Annual energy balance (TWh/year) for Spain in 2050 based on 2017 renewable energy data.

Table 7-5 Key energy balancing parameters for the energy system, FCEV2G and electrolyzer usage for all five countries.

Country	**Denmark**	**Germany**	**Great Britain**	**France**	**Spain**
Years of electricity production data	2014-2017	2014-2017	2015-2017	2014-2017	2016-2017
Energy system					
Annual renewable electricity production (TWh)	61	822	541	619	471
Final annual electricity consumption incl. road transport (TWh)	47.5	637	428	503	348
Peak power "classic electricity consumption" (GW)	5.5	62.3	42.5	54.9	30.3
Peak power "classic", heating and BEV charging electricity consumption (GW)	10.6	170	107	112	62.9
Pearson's correlation coefficient total production vs. total demand	0.39	0.40	0.42	0.43	0.52
Installed renewable electricity capacity (GW)	17.5	569	281	391	249
Share of solar electricity generation (%) (PV and CSP[1])	2%	34%	22%	25%	54%[1]
Share of wind electricity generation (%) (onshore/offshore)	87%	61%	76%	64%	39%
FCEV2G					
Annual FCEV2G electricity production (TWh)	5.4	63.9	30.7	36.4	15.7
Peak capacity FCEV2G (GW)	4.8	79.8	44.4	41.9	25.0
FCEV2G electricity production relative to total annual electricity consumption (%)	13.2%	11.6%	8.5%	8.2%	6.2%
Peak FCEV2G fleet percentage (%)	42%	36%	29%	26%	30%
Capacity factor FCEV2G fleet (%)	5.5%	3.3%	2.3%	2.6%	2.1%
Average FCEV2G hours per car (hours/year/car at 10kW V2G) ("full-load hours")	480	290	200	230	190
Electrolyzer					
Electrolyzer installed capacity (GW)	11.1	154	92.2	93.8	97.4
Electrolyzer load factor (%)	28%	25%	27%	26%	27%

[1]*Only Spain uses solar CSP electricity generation: 7% of the 54% solar electricity generation originated from solar CSP, 47% from solar PV*

7.4.2 Fuel Cell Electric Vehicle to Grid and electrolyzer balancing results

Large differences in the FCEV2G fleet load factors in Spain and Denmark were observed on an annual basis and an hourly basis. Also, here the large differences in wind and solar electricity generation shares are contributing to this difference in FCEV2G fleet load factors.

Figure 7-6 shows average annual hourly FCEV2G balancing, expressed as a percentage of total annual FCEV2G balancing in the respective countries. All countries except Denmark show a lower percentage of FCEV2G balancing between 10:00-18:00 compared to 18:00-10:00. This effect is also often referred as the "duck curve" [838]. In other words, during daylight hours, less FCEV2G balancing is required. This would match favorably with the usage of passenger cars, as they are mostly driven during the day. In particular for Spain, on average, almost no FCEV2G balancing is needed between 12:00-16:00. However, at the same time, Spain has peaks of 8.9% and 6.9% around 07:00 and 22:00, although there is still sufficient capacity that can easily follow the power ramps [229]. In Denmark, on average, FCEV2G balancing is almost constant throughout the entire 24 hours, at 3.5% to 4.7%.

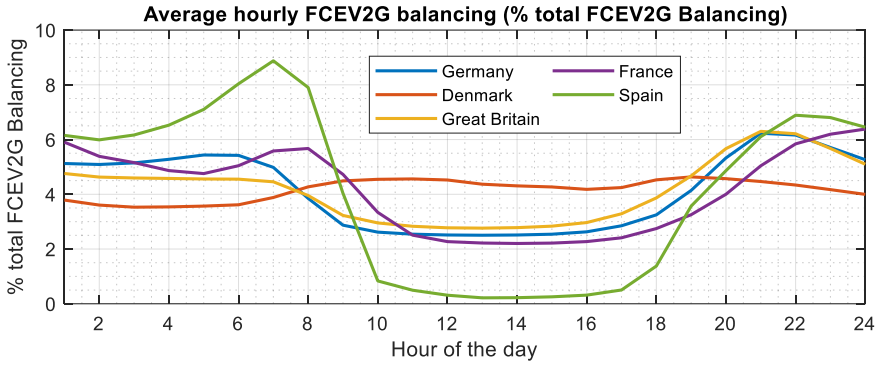

Figure 7-6 Average annual hourly FCEV2G balancing expressed as a percentage of the total annual FCEV2G balancing in each country.

Opposite patterns to the duck curve can be seen in Figure 7-7, which presents average annual hourly electrolyzer use as a percentage of total annual electrolyzer use in the respective countries. In Denmark, average hourly electrolyzer balancing is relatively constant throughout the day, at 3.9-4.5%. In contrast, in Spain, a clear pattern can be seen of approximately 1% between 22:00-08:00 and a clear peak of 10.6% at 14:00. The pattern for Spain, resulting from the large share of solar electricity generation, is very similar to other studies with high solar electricity generation [839–841]. The other countries in this study, having lower shares of solar electricity generation, show a similar but milder pattern than the Spanish one. Currently, the average hourly BEV charging pattern is assumed to be fixed throughout the 24 hours (see Figure 7-3). Charging more BEVs during the solar/daylight hours, except for Denmark, would reduce the electrolyzer balancing peak [842,843], provided BEVs are available for charging during the day.

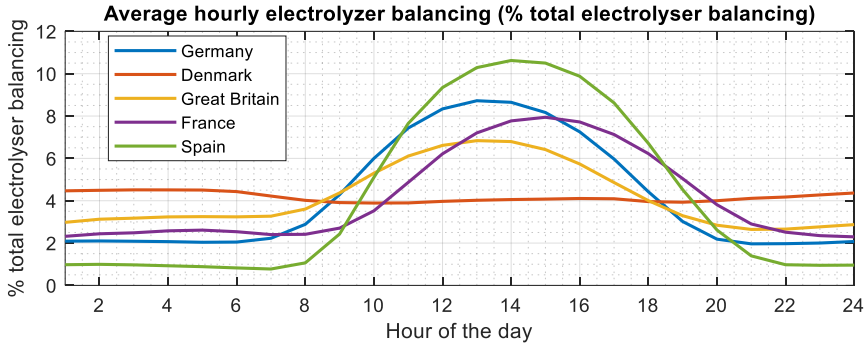

Figure 7-7 Average annual hourly electrolyzer balancing as a percentage of the total annual electrolyzer balancing in each country.

The boxplots in Figure 7-8 and Figure 7-9 provide more insight into the hourly distribution of FCEV2G electricity production in Spain and Denmark over the course of the simulated years (million vehicles, left y-axis; % of all FCEV passenger cars, right y-axis). The black crosses represent the mean values. Based on a normal distribution, the blue bars represent the interquartile range (IQR), the difference between the first and third quartiles (Q1 and Q3), at approximately 50%. The upper and lower whiskers represent the data points within the ranges [Q1-(Q1-1.5xIQR)] and [Q3-(Q3+1.5xIQR)], at approximately 49%. The red pluses indicate the outliers, which are outside the above-mentioned ranges, and represent less than 1%. Appendix B.3 also contains the boxplots for Germany, France and Great Britain.

Figure 7-8 also confirms the strong solar effect for Spain. During the daytime, only some outliers higher than zero occur (red pluses, approximately 1% of the time). These outliers could originate from temporal low solar [844–852] or wind generation [853–855], a combination of both [718,856–858], called “dark doldrums” [62–65], or peak loads [853,854,859,860]. Most of the FCEV2Gs are required between 18:00-09:00, with averages ranging between 0.7%-4.5% of the FCEVs (0.6-3.8 GW). The two-year peak in Spain of 29.6% of the FCEVs (25 GW, red plus) occurs at 22:00 (during the simulation with 2017 input data). The peak among the hourly averages (black cross) occurs at 07:00, at 4.5% of the FCEVs (3.8 GW).

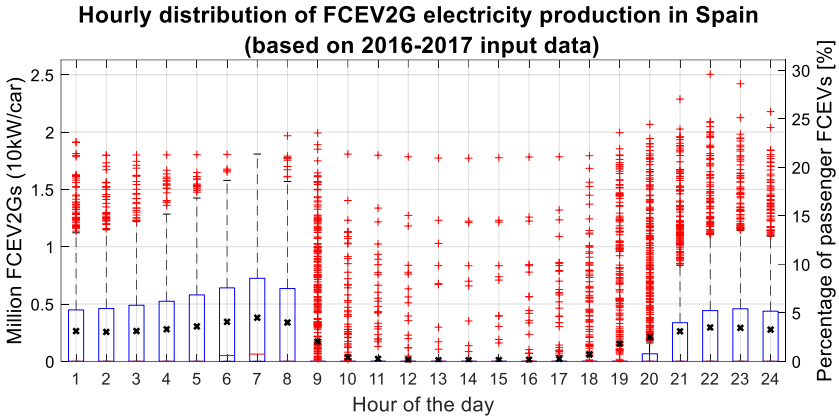

Figure 7-8 Boxplot showing the hourly distribution of FCEV2G electricity production in Spain (million vehicles, left y-axis; % of all FCEV passenger cars, right y-axis) throughout the day (based on 2016-2017 input data). The black crosses represent the mean values, the medians are indicated by the red horizontal lines in the blue bars. The blue bars represent the range of 50% of the data points. The whiskers represent approximately 49% of the data points. The red pluses indicate the outliers, outside the above-mentioned ranges, and represent less than 1%.

The boxplot in Figure 7-9 shows the hourly distribution of FCEV2G electricity production in Denmark throughout the day. The hourly average over the modeled years (black crosses) is relatively constant and ranges between 4.6%-6.1% of the FCEV2Gs (0.05-0.07 million FCEV2Gs, 0.5-0.7 GW). A clear night (01:00-07:00) and day plus evening (08:00-24:00) pattern can be recognized when looking at the interquartile range (blue bars representing 50% of the FCEV2G hours) and the whiskers (49% of the FCEV2G hours). Of the FCEV2G hours (blue bars plus whiskers) during the night, 99% remain below 20% of the FCEV2G fleet. For 99% of the FCEV2G hours during the day plus evening (blue bars plus whiskers), this remains below 28% of the FCEV2G fleet. The four-year peak of 42.1% occurred over a period of 24 hours during a period of consecutive low wind electricity generation.

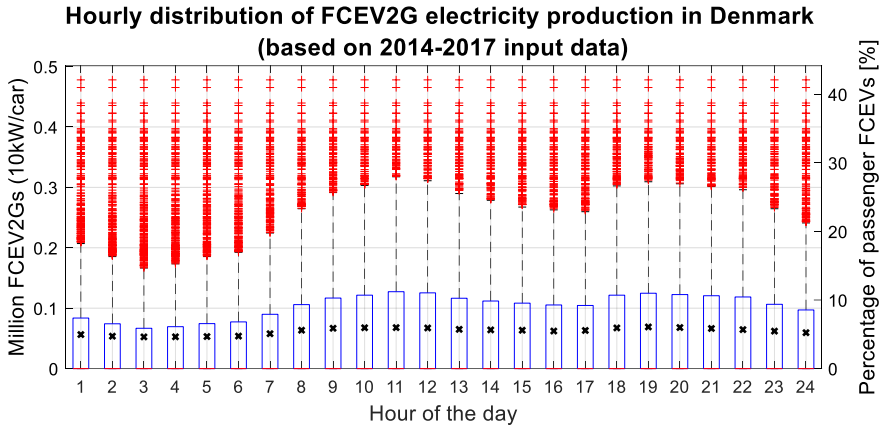

Figure 7-9 Boxplot showing the hourly distribution of FCEV2Gs needed for producing V2G electricity in Denmark (million vehicles, left y-axis; % of all FCEV passenger cars, right y-axis) throughout the day (based on 2016-2017 input data). The black crosses represent the mean values, the medians are indicated by the red horizontal lines in the blue bars. The blue bars represent the range of 50% of the data points. The whiskers represent approximately 49% of the data points. The red pluses indicate the outliers, outside the above-mentioned ranges, and represent less than 1%.

Average monthly FCEV2G balancing, expressed as a percentage of total FCEV2G balancing in each country, is displayed in Figure 7-10. Once again, Denmark differs from the other countries. There is no clear seasonable pattern for Denmark; throughout the year, monthly balancing ranges between 6.2% and 13%. For Germany, France and Great Britain, and to a lesser extent Spain, there are clear peaks in January and December of up to 20%, while all are below 5% in May. In the case of Spain, there is relatively low combined electricity production and relatively higher electricity consumption for space heating during the period October-December. The seasonal solar impact on the demand side for space heating and cooling, as well as solar electricity generation, is clearly reflected in hourly/diurnal and seasonal FCEV2G balancing.

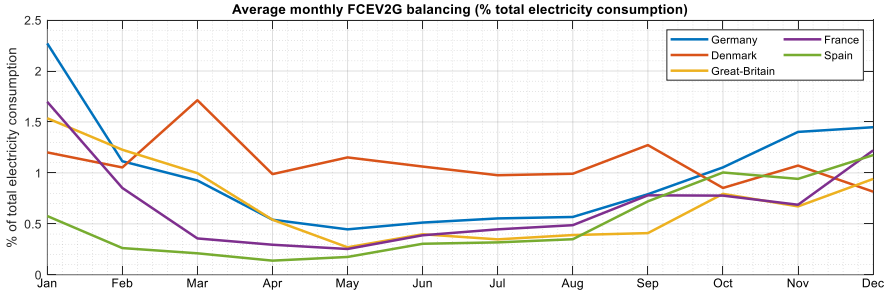

Figure 7-10 Average monthly FCEV2G balancing as a percentage of total FCEV2G balancing in each country.

7.4.3 Hydrogen storage and balance results

Hydrogen could be seasonally stored in underground salt caverns or empty gas fields. Table 7-6 shows the Seasonal Hydrogen Storage key parameters for the five countries analyzed. Germany has relatively large hydrogen storage requirements compared to the other countries. Germany has the highest hydrogen storage relative to annual average hydrogen production, at 40%, while Spain has the lowest, at 26%. Great Britain has the lowest hydrogen storage relative to annual average electricity production, at 8.5%, while Germany again has the highest, at 12.8 %. Germany has the second highest share of solar PV electricity generation (34%), with most of the solar PV electricity generation concentrated during the summer months, while consumption is highest in the winter months (see Figure B2 in Appendix B.1). The current operational, under construction and planned underground gas storage [57] is comparable to the peak hydrogen storage modeled for all countries. It is noted that the volumetric density of natural gas (primarily methane) at any pressure is approximately three times higher than that of hydrogen gas [861]. From an energy point of view, as the modeled hydrogen storage is comparable to current and planned gas storage, one must consider that this study only includes the power, transport and space heating sectors. However, there are indications that the total dedicated underground cavern technical hydrogen storage potential, onshore and offshore, is several magnitudes higher [179].

Table 7-6 Seasonal Hydrogen Storage key parameters for the five countries analyzed.

Seasonal Hydrogen Storage	**DK**	**DE**	**GB**	**FR**	**ES**
Peak hydrogen storage (million kg H_2)	157	2668	1162	1564	1226
Average annual hydrogen production (million kg H_2)	504	6632	4287	4234	4741
Peak hydrogen storage relative to average annual hydrogen production (%)	31%	40%	27%	37%	26%
Peak hydrogen storage (TWh_{HHV})	6.2	105	46	62	48
Maximum hydrogen storage relative to annual electricity production (%)	10.3%	12.8%	8.5%	10.0%	10.3%
Natural gas storage					
Operational, under construction and planned underground natural gas storage (TWh) [57]	10.4	270	60.4	137	32.0

Figure 7-11 clearly shows strong fluctuations in the total hydrogen storage capacity requirements for Germany (blue) based on four years of meteorological input data from 2014 to 2018. Germany (blue), Great Britain (yellow), France (purple) and Spain (green) show similar trends for most of the simulated years. A low storage content is observed between February and May and a high storage content is seen around September-October. During the summer period, energy consumption is relatively low and solar electricity contribution is high. This allows surpluses to be converted to hydrogen and stored for the winter period, during which the opposite occurs: high energy consumption and low solar energy contribution. For Denmark (orange, thicker line), no distinct seasonal pattern can be recognized in the storage content. Due to the large share of wind, mostly offshore, there is a better seasonal match between electricity generation and consumption. Both onshore and offshore

wind generate more electricity during the winter period, which favorably matches the higher winter energy consumption.

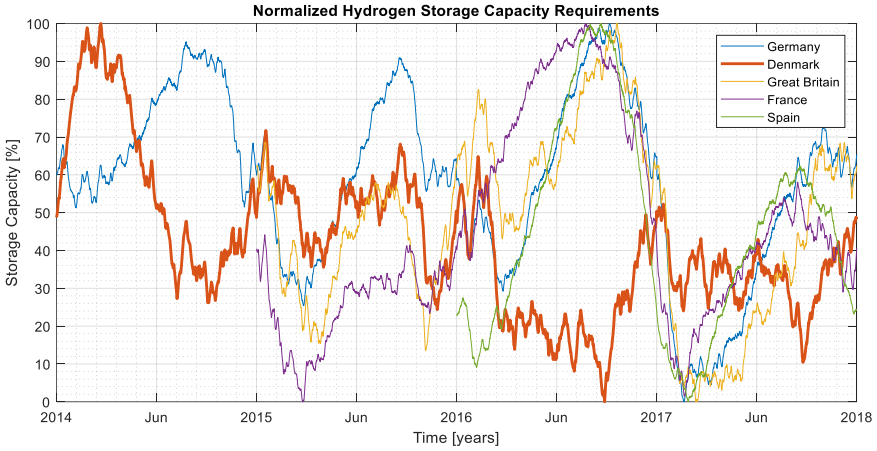

Figure 7-11 Normalized hydrogen storage capacity requirements for all five countries, based on varying years of input data ranging from 2015 to 2018.

7.5 Discussion

The focus of this study was on the role of balancing national 100% renewable energy systems with V2G using hydrogen-fueled FCEVs. Having this specific hydrogen focus, seasonal hydrogen storage and hydrogen production using downward balancing with electrolyzers were a logical and natural choice from an energy system modeling point of view. In a techno-economic energy system optimization study, Brown et al. [58] considered hydrogen for seasonal energy, but concluded that its role is limited. However, this was due to the fact that they assumed costly above-ground hydrogen storage, whereas underground hydrogen storage in depleted salt caverns may be 10-30 times cheaper [58,71,862–864].

The above example shows there is a trade-off between a number of balancing and storage options, various dimensions (e.g., time, cost), model complexity (regions, interconnections, integration, energy vectors, networks and their capacity constraints) and the ability to isolate and explore the maximum technical potential [179,865] of a specific technology within large energy systems. In this study, model complexity was relatively low. By not including the capacity of the electricity network or gas network, being “unlimited” or “copperplate,” and with no international connections or other balancing options, the required balancing and storage might be overestimated, as other studies [48,866] have also indicated. The focus of this study was an exploration of the technical potential of V2G with FCEVs (at 50% of passenger cars) and to highlight any potential operational restrictions or overcapacity. Both FCEV2G capacity as well as underground hydrogen storage potential are significantly greater than what is required, according this study, even if this study overestimates the requirements.

The results show that it is technically possible to undertake all hourly and seasonal balancing with FCEV2G, electrolyzers and hydrogen storage in a 100% renewable electricity, heating, cooling and transport system. As no integrated transportation and energy systems are the same, it is not possible to straightforwardly compare results. Many studies look to Europe as a whole, or parts of Europe [14,58,67,775,867], with some focusing on the same countries analyzed in this study. As the systems developed are sometimes difficult to compare, the comparison here is limited to balancing and long-term storage. The majority of the 100% renewable energy systems analyzed in [48] include the power sector, and some include heating and mobility. The storage size expressed as a percentage of annual demand ranges between 1.5% and 5%, with some studies reporting 14% [48]. In this study, the analysis is made for Denmark, Germany, Great Britain, France and Spain, with results for the countries varying; however, the hydrogen storage relative to annual hydrogen and electricity consumption ranges between 9% and 13% for all countries. Compared to [48], it could be concluded that the results might overestimate the storage required, due to the fact that not all possible flexibility options are included in the model. Moreover, in this study, FCEV2Gs were used for upward balancing in cases where there is a shortage of electricity and downward balancing with electrolyzers when electricity consumption is met. Below, the findings here are compared with other studies for each country separately.

Case studies of Germany [132,173,174] have found that its upward and downward balancing capacities range between 40-103 GW and 23-274 GW, excluding interconnections to other countries. In this study, respectively 80 GW and 154 GW is found for Germany for upward balancing with FCEV2G and downward balancing with electrolyzers. In relation to long-term large-scale storage, other studies found 24-154 TWh [132,173,174] compared to 105 TWh in this study.

Case studies of Denmark [157,232,579] have found that upward and downward balancing ranges between 4.6-6.0 GW and 7.2-9.0 GW, while this study found 4.8 GW and 11.1 GW, respectively. Seasonal long-term storage was not further specified in the other studies of Denmark [157,232,579], despite synthetic natural gas (SNG) and hydrogen production and consumption being part of the applied technologies. These studies [157,232,579] on the case of Denmark used approximately 60 TWh of biomass for primary energy use and included the industrial, aviation and shipping sectors. In this study, the electricity generation from CHPs and waste was fixed at 6.8 TWh and required 6.2 TWh of hydrogen storage capacity.

Case studies of the UK have concluded that there is not yet consensus across the industry about the necessary level of hydrogen storage, nor the preferred solutions [868]. One study found that the necessary upward balancing would be 73 GW [868], with 47 GW from natural gas turbine power plants with carbon capture, use and storage (CCUS). This study found 44 GW for FCEV2G balancing.

In the case of France [172–174], 28-57 GW of upward and 23-177 GW of downward balancing were found, excluding interconnections to other countries. In comparison, this study found 42 GW of FCEV2G and 94 GW of electrolyzer capacity. Furthermore, while 3-92 TWh of hydrogen and/or SNG storage was reported by the other case studies of France [172–174], this study found 62 TWh.

Finally, case studies of Spain [173,174] have reported 14-23 GW for upward and 12-117 GW for downward balancing. In comparison, this study found 25 GW FCEV2G and 97 GW electrolyzer capacity. The two studies of Spain [173,174] also reported a range of 3-92 TWh of storage. In comparison this study found 32 TWh hydrogen storage.

In summary, the results of this study are of similar magnitude to other studies. The large range in the findings across studies is the result of a multitude of different modeling and technology choices. These range from the level of renewable energy sources and fossil energy resources used, interconnections, import of energy, energy mix, parallel use of balancing and storage technologies and the number of sectors included, which all make it difficult to draw detailed comparisons.

This study assumed a “copperplate” electric grid within each country: an electric grid with unlimited capacity, with all renewable electricity sources, FCEV2Gs and electrolyzers coupled to the electric grid. In reality the electric grid has a limited capacity, locations have to be selected carefully according to the local grid capacity. The usage of a gas (hydrogen) pipeline grid for energy or hydrogen transportation was not considered, nor any synergies between the electric grid and gas grid.

The designed country systems are hypothetical in the sense that energy exchange with other countries is excluded. Currently European countries are connected to each other via electric cables and gas pipelines. Renewable energy supply deficits in one country can be balanced with surpluses in other countries. The current EU interconnection targets for 2030 aim that each country should have in place electricity cables that allow at least 15% of the electricity produced by its power plants to be transported across its borders to neighboring countries [763]. Increased interconnection will in certain times with favorable renewable electricity and consumption patterns reduce the balancing volumes and peaks by the FCEV2Gs and electrolyzers. At the same time, increased interconnection, also means that grid-connected FCEVs in one country could provide balancing for another country in case their cars would not be available. Instead of a regional or national pool of FCEV2Gs, there could be a European pool of FCEV2Gs balancing the European electricity grid and fully replace balancing power plants on a large scale.

Instead of transporting the renewable electricity via cables, also hydrogen could be produced first and transported via hydrogen pipelines. Eleven gas grid operators have recently published their plans in the “European Hydrogen Backbone” study, outlining how a dedicated hydrogen infrastructure can be created [869]. The study also highlights potential connections to North Africa for the import of green hydrogen [78]. Having such a hydrogen pipeline network in place, it would create the possibility for countries without large underground gas storage facilities, but with large renewable energy sources, to produce hydrogen and export it via pipeline to a neighboring country. The hydrogen then can be stored in underground facilities in other countries and transported back to the country of origin when needed for balancing.

Instead of domestic hydrogen production, the importation of hydrogen might also be considered [173,174,704]. In the current energy system, most energy for transport is imported. The imported hydrogen could be distributed via the gas

pipeline grid for electricity generation and refueling. In this way, it could avoid energy transport via the electric grid [638,693].
FCEV2Gs could be distributed close to load centers and help to reduce peak load on electricity transmission and distribution grids. In contrast to large stationary gas turbine plants located far from load centers. Hydrogen fueling stations supply hydrogen for both driving and FCEV2G, with hydrogen for FCEV2G potentially requiring large peak capacities. A hydrogen pipeline distribution network (e.g., converted natural gas distribution network) close to demand centers would avoid large dispensing peaks at hydrogen stations due to FCEV2G. FCEV2Gs could be supplied directly with low pressure hydrogen from a hydrogen pipeline distribution network. This would also avoid emptying the on-board hydrogen tank during FCEV2G electricity generation and thus the driving range would not be affected. Smart placement and dedicated hydrogen production at renewable energy sources close to gas storage and the gas pipeline grid also have the potential to reduce the load and further capacity expansion of the electricity grid.
Looking further into FCEV2G, electrolyzer and hydrogen storage usage in this study, several methods could improve their use. For example, although the peak FCEV2G capacity required never exceeded 43% of the FCEV2G passenger car fleet, lower capacity peaks will ease operational aspects, such as scheduling, and improve the guaranteed supply of electricity, as well as potentially reduce costs (not considered in this study). Based on the findings of this study, a 100% renewable power, heating and road transport energy system is possible, but there remain various opportunities for further optimization, outlined below:

Reducing total produced FCEV2G electricity and changing the time of FCEV2G use, which could be achieved:

- By a better match of renewable electricity generation with electricity consumption. A carefully selected mix of solar PV and wind electricity generation, combined with (partially) dispatchable renewable energy sources such as hydropower, solar CSP and CHP, could more favorably match the seasonal and daily patterns of consumption. As cars are mostly used during the day for driving, large amounts of solar energy (duck curve) could almost completely shift FCEV2G to the night hours. With some other renewable energy sources, such as wind, solar CSP and hydropower, FCEV2G balancing during the early morning and late afternoon driving peak hours could also be avoided almost completely.
- Through the demand response of electrical devices, space heating or BEV charging, such that the consumption pattern better matches electricity generation and thus impacts the time of use of FCEV2G.
- Through the importation of electricity from other countries at times of shortage; although, when relying on wind and solar energy, shortages and surpluses might occur at similar times. However, other research mentions that interconnecting large areas reduces this effect.

Reducing the number of participating FCEV2G, which could be possible:

- By reducing FCEV2G electricity generation. Several ways have been mentioned above in this section.
- By increasing the FCEV2G output per car, which is now limited to 10 kW of the 100 kW on-board capacity. Currently, the limitation is due to the cooling capacity of the fuel cell system radiator when the vehicle is parked. Increasing FCEV2G output per car would require a better understanding of the cooling capacity of the parked radiator [229].
- By increasing capacity through the use of other vehicles, such as FCEV vans, buses or trucks, in addition to passenger cars. Although these commercial vehicles might be used more during the day, at night they could also provide FCEV2G electricity.
- By using the batteries in BEVs for (short-term) storage and upward and downward balancing.

Increasing the electrolyzer capacity factor and reducing peak capacity, which could be possible:

- Through electricity consumption by other sectors not included in this study, such as industry and agriculture.
- By exporting temporary surplus electricity to other countries.
- Through the demand response of electrical devices, space heating or BEV charging, such that the consumption pattern better matches electricity generation.

Reducing the hydrogen storage capacity, which could be achieved:

- By reducing FCEV2G electricity generation and thus hydrogen consumption and storage. Several ways were mentioned above under "Reducing total produced FCEV2G electricity."
- By (temporarily) importing or exporting low-cost renewable hydrogen from or to other regions, or only at times when storage requirements would otherwise be high. Import or export of hydrogen could involve distant or neighboring countries and use tankers or hydrogen pipelines.
- By producing hydrogen for driving with renewable energy sources that have relatively constant output during the year. This would mean that a minimal amount of hydrogen needs to be stored, as hydrogen consumption for driving has no distinct seasonal patterns.

Similar to other studies, the five country cases were analyzed here as greenfield models [866], which generate a perfect outcome from a specific foresight [870]. V2G infrastructure and the use of BEVs are increasingly expanding [195,871]. Here, V2G with FCEVs could piggyback on BEV V2G infrastructure developments and standards. The specific role of V2G and how large it will become in balancing energy systems should be addressed in future work. Questions about the development path – for example, will it be incremental versus disruptive, distributed versus central – remain open and depend on whether or when widespread adoption of passenger car FCEVs occurs.

There is an ever-increasing interest in the role of hydrogen in renewable energy system studies, as the cost of hydrogen technology is decreasing faster than expected [73]. Therefore, thorough cost analysis should be addressed in future work. Also cost optimizations of using FCEV2G for balancing versus other upward balancing technologies, like hydrogen fueled gas turbines, distributed or large-scale fuel cell based CHP systems could be investigated to shed light on the optimal mix of technologies in relation the balancing needs. As well as the influence of several parameters and others designs such as the use of BEVs for V2G purposes, distributed and large-scale stationary batteries, the distribution between the number of BEVs and FCEVs, type of renewable energy sources could be of further interest in analyzing future cost of similar type of energy systems.

7.6 Conclusion

The future energy and transport system in Europe will and must move to zero emissions. Significant numbers of back-up power plants, as well as balancing and large-scale energy storage capacity are required to guarantee the reliability of energy supply. Here, hydrogen can offer a solution in highly renewable systems by converting power to hydrogen to be used as a transport fuel and in energy storage for back-up power plants.

Parked and grid-connected (Vehicle-to-Grid, V2G) hydrogen-fueled FCEV passenger cars (FCEV2G) can fully balance a 100% renewable national electricity, heating and transport system. Combined with hydrogen production using electrolyzers and large-scale hydrogen storage, energy supply can be guaranteed at all times. There is more than sufficient power capacity available from FCEV passenger cars, with no more than 43% of the FCEV passenger car fleet required, even with a restricted output of 10 kW per car and with 50% of passenger cars considered to be FCEVs. This applied to all five countries modeled: Denmark, Germany, France, Great Britain and Spain.

FCEV2G fleet usage is low and matches favorably with driving usage. For example, especially in systems with larger shares of solar electricity, FCEV2G balancing is required during the night. As cars are mostly driven during the day, they will generally be parked at night when this balancing capacity is needed. Moreover, the large overcapacity, in combination with the low usage of already purchased electric power capacity in passenger cars, would make it possible to fully replace large-scale stationary balancing plants. The capacity of millions of distributed FCEV2G can be combined into Virtual Power Plants.

In the five countries modeled, 88% or more of the electricity generation originated from solar and wind, where Denmark has the highest share of wind electricity generation (87%) and the lowest share of solar electricity generation (2%) and Spain has the highest solar (54%) and lowest wind electricity generation (39%). The FCEV2G fleet capacity factor is highest in Denmark, at 5.5% (average of 480 hours per car, per year) and lowest in Spain, at 2.1% (190 hours per car, per year). Nevertheless, these capacity factors are both very low and comparable to driving usage (European average, 300 hours per car, per year).

Spain and Denmark also showed the most contrasting patterns in daily average FCEV2G and electrolyzer balancing. In Denmark, FCEV2G and electrolyzers may be needed at any time of the day during the year. FCEV2G is needed somewhat more during daylight hours and electrolyzers slightly more during nighttime hours. In Spain, however, FCEV2G balancing, on average, is mainly required outside daylight hours (17:00-10:00) and electrolyzers during daylight hours (08:00-20:00). By producing hydrogen from solar electricity during daylight hours, the duck curve phenomenon can be reduced. Especially in summertime, hydrogen can be produced and contained in large-scale gas storage for the winter period in, for example, underground salt caverns or empty gas fields. The calculated hydrogen storage capacities ranged between 6-105 TWh and were not more than 76% of the existing, under construction and planned underground gas storage capacity. Other research has reported that the total dedicated underground cavern technical hydrogen storage potential onshore and offshore is several magnitudes higher.

8 Conclusions and Recommendations for future research

8.1 Conclusions

The main research question addressed in this thesis is: "How can we design and analyze future 100% renewable integrated transport and energy systems, based on electricity and hydrogen as energy carriers, using fuel cell electric vehicles for transport, distributing and generating electricity?". The main question is answered through the three research sub-questions in sections 8.1.1, 8.1.2 and 8.1.3. Section 8.1.4 describes the impact of the different sizes and types of systems on the usage of FCEVs providing balancing electricity.

8.1.1 Suitability of commercially available FCEVs to act as balancing power plants

In Chapter 1 and 1, the experimental work was carried out to answer the first sub-question: *"Are current commercially available FCEVs suitable to act as balancing power plants?".* The results show that the FCEV can be used for mobility and to generate power when parked. Grid-connected FCEVs are capable of functioning as balancing power plants. Virtual power plants composed of many grid-connected FCEVs can provide both small and large balancing power requirements at different aggregation levels. In this way they could reduce the number of large-scale stationary balancing power plants in hot standby and reduce overall system costs.

Chapter 1 describes the experimental set-up and tests of a connected commercially available Hyundai ix35 FCEV (production year 2013, available in the Netherlands 2015) to the Dutch national electric grid via a Vehicle to Grid connection on the car and a variable power discharger.

Tests in the range of 0–10 kW DC power (0-9.5 kW AC power) with the same set-up, show that 10 kW gives the highest V2G efficiency [280]. At a hydrogen consumption rate of 0.55 kg/h at 10 kW DC power, on a full tank, approximately 10 hours of power can be delivered to the grid. The grid-connected FCEV has an AC electric power efficiency of 43% on a HHV basis (51% LHV). The measured AC efficiency is close to the reported FC system DC efficiency of 46.8% on a HHV basis (55.3% LHV) by Hyundai Motor Company [68]. Operating at 10 kW DC power in V2G mode, results in 0-15 kW delivered by the fuel cell system or 0-10kW by the High Voltage (HV) battery. To recharge the High-Voltage (HV) battery (depending on the state of charge of the HV battery) and power the balance of plant components from the fuel cell system while delivering 10 kW DC power in V2G mode, requires up to 15kW power of the fuel cell system. This corresponds to 10–15 % of the fuel cell system maximum power capacity of 100 kW.

The fuel cell and high voltage battery systems in the FCEV respond faster than conventional fast-reacting thermal power plants, which have maximum values of 1.67 %/s for hot starts [236–238] . At 10 kW V2G DC power, the measured maximum

downward and upward power gradients of the fuel cell system were –47 kW/s (–470 %/s relative to 10 kW max. power) and +73 kW/s (+730 %/s), for the high voltage battery 76 kW/s (–760 %/s) and +43 kW/s (+430 %/s). In other words, within less than ¼ of second, both battery and fuel cell system can ramp up or down 10kW. In our V2G tests, we measured fast cold start-up times of less than 5 s at ambient temperatures. Driving to cruising speed can already be achieved within 11 s at –20 °C [60], which is comparable to V2G power of 10 kW (10 % of the rated FC power). The combination of power sources of the FCEV, the fuel cell system and the HV battery, would be suitable to offer fast frequency reserve services [773]. Such as upward and downward Automatic Frequency Restoration Reserve (aFRR) and Frequency Containment Reserve (FCR). This was investigated in experiments with the same set-up by other researchers from the same research group [759].
Further research done with the same set-up [280] looks into the power supply for a grid connected house in the Netherlands with an electric heat pump and solar panels. A modelling study based on the experimental results is performed and simulates 10 houses and 5 FCEVs during the course of a year. The load-following mode is the most cost-efficient operation, here the 5 FCEVs produce on a year basis 32,690 kWh and 13,137kWh is imported from the electricity grid. If also the imported electricity would be provided by the 5 FCEVs (10kW per car), this would result in an average capacity factor of 11%. According to European statistics (Chapter 1), 10 houses would on average own 11.5 cars. If all 11.5 cars would be FCEVs with V2G functionality, then the fleet capacity factor would be reduced to 5%.

Chapter 1 investigates which usage parameters related to driving and V2G services could be used to establish a correlation between them and the average fuel cell stack voltage degradation. The voltage degradation negatively impacts the fuel cell system efficiency and economic lifetime and so increasing the cost of produced electricity. Measurements have been conducted for four Hyundai ix35 FCEVs, where only one is used for both driving and V2G services. The FCEVs have driven between 7917 and 27459 km in 531 up to 1167 trips (one trip defined as a fuel cell system start-up and shut-down cycle). Both driving and V2G services resulted in 184 up to 872 hours of operation, of which the fuel cell system was idling (producing no power) for 28 up to 457 hours. The total produced fuel cell stack electricity was between 1970 and 5610 kWh. The mean fuel cell stack voltage degradation relative to the beginning of measurements based on operating time was between 1.4-2.3% and based on total produced electricity was between 1.4-2.4%. The FCEVs were already driven between 4924-22875km before the measurements were conducted. The impact of the type of usage before conducting measurements could have had an impact on the degradation during the measurements. There is no consistent correlation observed between the usage parameters such as fuel cell operating time, distance driven, fuel cell stack produced electricity and the mean fuel cell stack voltage degradation. Prolonged testing with a larger number of FCEVs without any usage before the start of measurements could potentially provide sufficient and complete data to establish such a correlation. A durability indicator expressed solely in operating hours, or distance driven or produced energy is not relevant for an FCEV used for both driving and V2G services due to the large variation of usage. A durability indicator consisting of several usage parameters is recommended, such

as the operating and 'idling' hours, produced energy, driven distance, number of start-ups and shutdowns. Alternatively, using the same data, an approach by analyzing the frequency of specific voltages, currents and voltage transient cycles, a better comparison between the different types of usage could be established [872]. A better correlation between usage and performance degradation could be established, provided the impact of these specific voltages, currents and voltage transient cycles on the performance degradation can be measured.

8.1.2 Integration of FCEVs into future energy systems

Chapter 1 and 1 treat the sub-question *"How can we integrate FCEVs, used for transport, distributing and generating electricity, into future energy systems?"*. Two integrated, 100% renewable, transport and energy systems where designed. Four design criteria were applied. First, systems where cars are naturally parked near demand centers. Second, these systems should be scalable. Third, applicable in all European countries, i.e. not serving niche markets. Fourth, having a large replicability in Europe, i.e., the system designs should be replicable at least 1,000 times.

The first designed future energy system is a hospital, the second an urban area. Both 100% renewable energy systems show that FCEVs can be integrated into current energy systems for driving and providing dispatchable balancing power without significant change to end-user energy patterns. If scheduled smartly, providing dispatchable balancing power does not significantly limit the use of the FCEVs for driving. The integration can be done on a piecemeal basis, partially, distributed and scaled over time.

Chapter 1 describes a 100% renewable integrated transport and energy system for a 526-bed hospital is designed using only local energy sources. A heuristic approach is applied to the modeling and system design for a Mid Century energy scenario (approximately around 2050). A Rooftop solar, wind energy at the municipal wastewater treatment plant (WWTP) site as well as biogas from the municipal WWTP, together with future estimated energy savings of a hospital compared to today's state of the art, closes the annual energy balance. Via electrolysis, temporary surplus electricity is converted into hydrogen for energy storage and transport fuel. The system is always balanced, by converting stored hydrogen into electricity by less than 250 grid connected FCEVs (2.5 MW, 10 kW V2G power each). The car park at the hospital with 500 places can easily host the FCEVs if needed.

According to European statistics, for every community of 100,000 inhabitants there is a 526-bed hospital and approximately 49,000 passenger cars. If all these cars in the community together would provide the 6556 MWh/year of required balancing power for the hospital, that would result in a fleet average capacity factor of 0.15%. Assuming the car park (500 places, each 10kW) would be operated as a power plant with maximum output of 5 MW with a dedicated fleet of 500 cars, it would operate at a capacity factor of 15%.

Current hospitals have two emergency power systems. Here, the uninterruptable power supply system could be replaced by approximately 95 grid connected FCEVs.

The diesel power generator system provides 6 days of autonomy. The high-pressure hydrogen storage at the designed hospital hydrogen fueling station provides sufficient hydrogen for 1 day of autonomy. Additionally, 250 grid connected FCEVs could provide sufficient peak power and enough energy for another day of autonomy. If required, an additional 4 days of autonomy can be guaranteed by trucking in 5-6 hydrogen tube trailers, carrying each up to 1350 kg of hydrogen [383].

Chapter 1 describes a conceptual design framework for an average urban smart city area in Europe having an average solar radiation, mild winter and moderate summer temperatures. The area is sized based on a European statistic average of residential and services sector buildings and fuel cell powered road transport vehicles. 2000 households with 4700 inhabitants are an appropriate size for dimensioning the smart city area as statistically there is one petrol station and one food-retail shop.

An energy balance and cost analysis are performed for a Near Future (towards 2025) and Mid Century (around 2050) technology cost development scenarios. Solar and wind electricity together with fuel cell electric vehicles as energy generators and distributors and hydrogen as energy carrier, can provide a 100% renewable, reliable and cost-effective energy system, for power, heat, and transport. The smart city area energy supply is independent of other energy systems and grid connections. Reliability of energy supply is always guaranteed by dispatchable electricity supply from hydrogen fuel cell electric passenger cars. Electricity produced from V2G connected FCEVs is 25,553 MWh/year in the Near Future scenario and 9,465 MWh/year in the Mid Century scenario. With 2,300 passenger cars FCEVs in the smart city area, each providing 10kW power per car, this would translate into a fleet average capacity factor 13% and 4.7% in respectively the Near Future and Mid Century scenario. Hydrogen is stored and generated from temporary surplus solar and wind electricity. For a day without any solar power in the Mid Century scenario, only 865 cars providing 10 kW each (10% of the fuel cell system maximum power of 100kW) would be required, representing 38% of the car fleet.

The fuel cell electric vehicle and renewable energy based smart city area can provide a future cost-effective energy supply, as the average annual cost (without taxes and levies) for power, heat and mobility is 600 €/year per household in the Mid Century scenario. In the Near Future scenario system levelized cost of hydrogen for transportation is 7.6 €/kg, system levelized cost of electricity is 0.41 €/kWh and the specific cost of hydrogen for passenger cars is 0.08 €/km. In the Mid Century scenario however, this is 2.4 €/kg, 0.09 €/kWh and 0.02 €/km. System levelized electricity costs are difficult to compare to other studies as system boundaries and type differ. Nevertheless, the hydrogen cost per kilometer for the Near Future scenario for passenger cars is lower than the 0.10-0.31€/km calculated by NREL [393] for a smaller integrated power and transport system with electricity grid connection. The levelized cost of electricity including storage and reconversion of 0.40€/kWh as calculated by NREL [393] is comparable with the 0.41€/kWh in the Near Future scenario in this work. The Mid Century system levelized cost of electricity of 0.09€/kWh is of similar magnitude as the 100% renewable system electricity cost 0.10€/kWh in 2050-2055 in [873].

8.1.3 Impact of European regional characteristics on the techno-economic system performance, where FCEVs are used for transport, distributing and generating electricity?

Chapter 1 and 1 address the third sub-question: *"What impact do European regional characteristics have on the techno-economic system performance and the usage of FCEVs for transport, distributing and generating electricity?"*.

Chapter 1 treats, in contrast to Chapter 1 which uses European average statistics, two climatically different locations in Europe, being Hamburg in Germany and Murcia in Spain. Murcia has a high solar global horizontal irradiation (1855 kWh/m^2/year), very mild winter (854 Heating Degree Days) and one of the highest average daily high temperatures (25.5 °C) in Europe. In contrast, Hamburg has a low solar global irradiation (1020 kWh/m^2/year), relatively cold winters (3066 Heating Degree Days) and lower average daily high temperatures (13.4°C). Also, in the model of Chapter 1 underground seasonal hydrogen storage in salt caverns is added. The simulation is performed with an hourly time step, based on five consecutive years of climate and renewable energy data, whereas in Chapter 1 only an annual energy balance is made. Multi-annual and hourly modelling provides a greater insight into when FCEVs need to provide balance power. Based on national statistics, the 2000 households in Hamburg and Murcia have respectively 2360 and 1850 passenger cars, here it is assumed all cars are FCEVs.

In Murcia there is a better match in time (daily and seasonal) between solar electricity production and building electricity consumption (dominated by space cooling in summer) than in Hamburg (dominated by space heating in winter). This results in a 40% lower seasonal hydrogen storage and FCEV2G requirements in Murcia than in Hamburg, in all scenarios. In Hamburg in respectively the Near Future and Mid Century scenario, the fleet average FCEV2G capacity factors are 10% and 5.0%, for Murcia these are 7.6% and 3.7%. These numbers are comparable to the average capacity factor of driving of 3.5 and 3.2% for passenger cars in Germany and Spain (310 and 280 hours/year/car). The peak seasonal underground hydrogen storage for Hamburg is in the Mid Century scenario up to 70% higher than in Murcia (163,000 kg versus 92,000 kg).

In the Mid Century scenario in Murcia, if next to the rooftop solar approximately 15% more solar panels were to be installed, the entire system energy demand could be met with solar energy. In Murcia, year-round, virtually no cars are required during daylight hours. In Hamburg, this is the case in the summer period in the Mid Century scenario, but not in the near future scenario.

The system levelized energy costs in the Mid Century scenario are 71 and 104 €/MWh for electricity and 2.6 and 3.0 €/kg for hydrogen, for respectively Murcia and Hamburg. Due to the higher solar radiation in Murcia and better match between solar electricity generation and consumption, system levelized costs for electricity and hydrogen are lower than in Hamburg. Murcia also benefits lower average cost of energy for households (without taxes and levies) in the Mid Century scenario than in Hamburg, respectively 520 and 770 €/year per household. Here, also the lower energy consumption in Murcia per household contributes.

Further research based on the same system looks into the optimal mix of using both Battery Electric Vehicles (BEVs) and FCEVs for V2G services for both locations and the solar-wind supply ratio versus the total system cost [726]. Systems operating in sunnier regions in Europe with low space heating needs during the winter are likely to have lower total systems costs compared to colder regions in the North of Europe. Applying more solar energy capacity and using more BEVs compared to FCEVs and hydrogen storage. The research also indicates complete elimination of hydrogen storage for systems in sunny and warm regions in Europe might not results in the lowest total system cost.

In Chapter 1, future 100% renewable national electricity, heating and transport systems of Denmark, Germany, France, Great Britain and Spain in 2050 are designed and analyzed. The total passenger car fleets range between 2.3 and 44 million, of which 50% are considered to be FCEVs and the other 50% being BEVs. BEVs are not used for V2G electricity production. 0.5 to 8 million (5-80 GW at 10kW each) parked and grid connected (Vehicle-to-Grid, V2G) hydrogen fueled FCEV passenger cars (FCEV2G) have the potential to fully balance these integrated and 100% renewable national energy systems. Together with hydrogen production via electrolyzers (11-154 GW) and large-scale hydrogen storage (6.2-105 $TWh_{H2\ HHV}$, 160-2700 million kg H_2), energy supply is always guaranteed. There is sufficient FCEV2G power capacity available, the peak requirement never exceeds 43% of the car fleet. Considering the restricted output of 10kW per car and 50% of the passenger cars being FCEVs.

In systems with larger shares of solar electricity systems, FCEV2G balancing is primarily required during the night when cars are parked, whereas mostly cars are driven during the day. The FCEV2G fleet capacity factor is highest in Denmark, 5.5% and lowest in Spain 2.1%. The large overcapacity in combination with the low usage of already being purchased electric power capacity in passenger cars, would make it possible to fully replace large scale stationary balancing plants.

8.1.4 Impact of system size and type on the usage of FCEVs providing balancing electricity

Via the concept of so-called Virtual Power Plants or Car Park Power Plants as described in the 'car as a power plant' vision [2] and in work done by others [773,874], the capacity of tens, hundred, thousands or millions of distributed FCEV2Gs could be combined and used.

When introducing 100% renewable integrated transport and energy systems based on hydrogen and FCEV2G, the minimum technical and commercially viable size of subsystems have to be taken into account. The minimum technically viable size theoretically of FCEV2G is one FCEV providing at least 5-10kW power. When assuming one commercially available FCEV with a fuel cell of 100 kW. Below 5 kW the 100kW fuel cell system efficiency drops significantly due to the balance of plant power consumption, i.e. parasitic losses. Although introducing one FCEV2G could work, an integrated transport and energy system also requires a refueling system for the FCEV. The minimum commercially viable size then will be larger than just one FCEV. Refueling systems containing small scale hydrogen production via

electrolysis and refueling systems for one car per day exist but are on a capacity basis relatively costly, compared to a larger station serving, for example, 2000 cars per day. The same applies to the cost of electricity from solar or wind electricity production, larger systems result in a lower cost of electricity and so lower cost of hydrogen. Underground seasonal hydrogen storage systems have storage capacities of 3,000-6,000 ton hydrogen and so demand even larger volumes of hydrogen to be commercially viable. Although not modeled in this work, the overseas import of hydrogen could reduce or eliminate the local production of hydrogen and required solar and wind farms. Nevertheless, also then large-scale infrastructure such as pipelines or tankers, off-loading terminals in ports and hydrogen distribution infrastructure are required or adapted. The minimum size of these infrastructures demands even larger volumes of hydrogen to reach commercially viability.

The designed and analyzed integrated transportation and energy systems are greenfield models showing a perfect outcome of a specific foresight. The cases studied are hypothetical scenarios. As they use a single set of technologies for energy storage and balancing, namely hydrogen, hydrogen production, and fuel cells (FCEVs) and are based on a significant share of FCEV passenger cars (50%) or exclusively FCEVs. There is a trade-off between a number of balancing and storage options, various dimensions (e.g., time, cost), model complexity (regions, interconnections, integration, energy vectors, networks and their capacity constraints) and the ability to isolate and explore the maximum technical potential [179,865] of a specific technology within large energy systems. In this study, model complexity was relatively low. By not including the capacity of the electricity network or gas network, being “unlimited” or “copperplate,” and with no international connections or other balancing options, the required balancing and storage might be overestimated, as other studies [48,866] have also indicated. The focus of this study was an exploration of the technical potential of V2G with passenger car FCEVs and to highlight any potential operational restrictions or overcapacity.

Nevertheless, a comparison of the capacity factor outcomes of the designed and analyzed systems is made. Relatively larger systems with a more mixed type (residential and commercial) electricity consumption face less peaks in power consumption (relative to the average power consumption) and so less peaks in FCEV2G balancing power. Depending on the definition of the FCEV2G fleet size and the technology development year modelled (2015/2020/2025), the capacity factors mostly range from 2% to 11%. Here the hospital case study in Chapter 1 represents the outliers of 0.15-15% and could also be considered as part of the smart city area. When comparing only the outcomes of systems modeled on an hourly basis and representing a technology development scenario of the year 2050, the FCEV2G capacity factor ranges between 2.1-5.5%, see Table 8-1. This is in the same order of magnitude of the driving capacity factor of approximately 3%, as a European passenger car drives on average 12,000 km per year at a speed of 45 km/h (3% capacity factor).

In the range of 2% to 11%, the numbers above 5.5%, originate from integrated systems based on state-of-the-art technology of 2015, 2020 or 2025. Meaning end-users such as buildings have higher energy consumption and

technologies such as solar panels, fuel cells, electrolyzers, compressors having lower efficiencies compared to estimated efficiencies of state-of-the-art technology in 2050. Due to the higher energy consumption, lower load factors of solar panels, the degree of solar energy self-sufficiency is lower and more balancing and energy storage is required. But regions facing stronger seasonal effects in energy consumption and (solar) energy production will always need long term, seasonal, energy storage. Systems having a larger share of solar energy compared to the wind energy and less seasonal space heating requirements, require mostly FCEV2G balancing power during the night or early mornings and evenings and face lower FCEV2G capacity factors (2.1 and 3.7% in sunny Spain or Murcia versus 5.5 and 5.0% in colder and windy Denmark or Hamburg). Simply said, the energy production and consumption match better and so less FCEV2G balancing as well as seasonal hydrogen storage and energy conversion steps are needed. A higher FCEV2G balancing need during the night in systems with higher shares of solar energy production, would also better match the regular driving usage of passenger cars.

Table 8-1 FCEV2G fleet average full load hours (hours/car/year) or expressed as capacity factor (%) of systems modelled on an hourly basis and representing a technology development scenario of the year 2050.

Chapter	System analyzed	Fleet size (cars)	Percentage FCEV passenger cars	Fleet average full load hours (hours/car/year)	Capacity factor (%)
4	Hospital	49,000	100%	14	0.15%
6	Smart city Murcia/ Hamburg	1850 - 2360	100%	330 / 400	3.7% / 5.0%
7	Countries	2.3 – 44 million	50%	480-190	5.5-2.1 %

The available FCEV2G capacity in all case studies is significantly greater than what is required. The FCEV2G fleet average capacity factor or full load hours is an outcome of specific chosen model inputs and is highly dependent on several inputs, which all can significantly reduce the capacity factor:

1. Fleet size. The more vehicles participating the lower the capacity factor. Next to passenger cars other vehicles such as vans, buses, trucks, and trains could also be used. With 35 million commercial vehicles and buses in Europe next to the 243 million passenger cars [875], the capacity factor could be reduced substantially.
2. Power output per vehicle. Now the capacity factors are calculated based on 10 kW per passenger FCEV, which is only 10% of the 100kW available power. Running at higher powers means often lower efficiencies but could reduce the capacity factor by a factor 10. Assuming the 28 million vans in Europe [875] could provide 100kW V2G power each, this would total a power of 2800 GW, being more than 243 million passenger cars at 10kW (2430 GW).
3. Usage of other balancing methods like for example stationary or automotive batteries could eliminate or significantly reduce the usage of vehicles for V2G balancing.

8.2 Recommendations for future research

This work has been a first exploration of the techno-economic potential of the 'Car as a Power Plant' concept, Vehicle-to-Grid with hydrogen fueled Fuel Cell Electric Vehicles (FCEVs). Socio-economic [876] and control [877] aspects have been explored in other work part [666] of the same 'Car as a Power Plant' project.
Renewable energy generation and other storage and mobility technologies next to hydrogen related technologies and applications are currently being improved, expanded, scaled up and costs being reduced. These parallel developments of clean energy technologies will spur new system designs, increase synergies and accelerate the deployment.
This work treats experimental, techno-economic system design and analysis aspects of the 'Car as a Power Plant'. The recommendations for future research are combined into three sections, in-line with the three sub-questions. Section 8.2.1 gives recommendations with respect to the suitability of commercially available FCEVs acting as balancing power plants. Section 8.2.2 provides further suggestions regarding the integration of FCEVs used for transport, distributing and generating electricity in future energy systems. Section 8.2.3 highlights several recommendations for future research on the impact of European regional characteristics on the techno-economic system performance and FCEVs providing balancing power.

8.2.1 Suitability of commercially available FCEVs acting as balancing power plants

The Hyundai ix35 FCEV used in this research was a first-generation commercial FCEV from Hyundai, which was not designed for V2G purposes, but for driving use only. Via a relatively simple V2G modification, to maintain the road access permit, the behavior with various V2G loads was analyzed. This first-generation commercial FCEV from Hyundai was suitable to act as a balancing power plant. Nevertheless, several recommendations with respect to the powertrain its efficiency, management, operation, and performance degradation are listed next.

Mapping optimal FCEV efficiency point in V2G power production
Tests at different constant DC powers in the range of 0–10 kW done with the same set-up, show that 10 kW gives the highest V2G efficiency. Conducting further tests at DC powers above 10 kW would provide full insight into the partial load and optimum V2G efficiency. Efficiency of specific V2G profiles could be of interest too.

Impact of Vehicle to Grid power production on Fuel cell performance degradation
The impact of additional V2G power production in combination with driving usage on the durability of the combined fuel cell and battery system is yet to be quantified. Many studies focus primarily on V2G impact on batteries in BEVs, but little is known about how the V2G mode will impact fuel cell degradation in FCEVs and maintenance cycles. Different power management and performance degradation mitigation strategies might need to be developed to minimize additional performance degradation and maintenance.

Dynamic FCEV power management tailored to V2G power production profiles and driving use

The current FCEV power management system of both the fuel cell and high voltage battery system is developed for driving usage and uses a 'feed forward' control. In other words, once the brake or accelerator pedal is used, the FCEV power management responds to it. Whereas in V2G mode in the built set-up in this work, the FCEV power management is 'blind' to what load it will need to serve and so reacts on the load, 'feedback' controlled. Dynamic power management strategies are relevant future research topics, think of smart hybridization between HV battery and FC in response to V2G loads. Especially if the V2G power production profile is known upfront it could be included in the FCEV power management. Also the FCEV power management could be incorporated and operated from the energy system where it is integrated in.

Tailored powertrains and components, hybrid V2G and G2V

The FCEV used in the experiments performed uses the fuel cell system as main power supplier and the high voltage batter as an auxiliary support for acceleration when driving or storing a small amount of braking energy. The size and capacity of the fuel cell, hydrogen tank and battery could be optimized for the combined usage of driving and V2G power production. Instead of the battery or next to the battery, also a so-called supercapacitor could be used [878,879]. Then depending on the duration and power ramp, either the supercapacitor, battery or fuel cell could be activated. Also the option of charging the on-board high voltage battery via the electricity grid (Grid to Vehicle, G2V), similar to the Mercedes Benz GLC F-Cell [723], might be worth researching.

Increase of V2G power output of commercially available FCEVs

It is possible for FCEVs to generate more than 10 kW DC V2G power as the fuel cell system maximum output is 100 kW. Although this would require a better understanding of the cooling capacity of the radiator when parked and the maximum operating temperature of the fuel cell system. This V2G power is currently limited because of potential insufficient cooling radiator capacity when parked and producing power at elevated ambient temperatures. V2G output could be limited depending on the heat dissipation to the environment. Alternatively, the cooling capacity could be increased by installing a bigger radiator and cooling fans, by using two-phase cooling fluids with a higher cooling capacity or by an increased fuel cell system operating temperature.

V2G equipment improvements and shared usage

Inductive discharging instead of conductive discharging (by cable as in the set-up in this work) and could automate and reduce any further grid connection time. The current V2G discharger as-built uses a DC-AC grid-tie inverter designed for small scale wind turbines. Here a specialized FCEV V2G inverter with reduced reaction time and tailored Maximum Power Point Tracking/pre-loaded battery and fuel cell current-voltage curves could be integrated. Also combining the V2G inverter with

on-site available solar photo-voltaic inverters could maximize utilization of existing assets (night or cloudy day usage by V2G, solar during the day).

Establishing a correlation between combined driving and V2G usage and performance degradation

As commercial FCEVs have not been sold on a large scale, durability data and correlations between driving usage and performance degradation of the fuel cell system in specific FCEV models is extremely scarce in literature. To express the usage of the fuel cell system in a FCEV, the indirect durability indicator driven distance only makes sense for cars used for driving only. The electricity produced by the fuel cell seems a relevant durability indicator for FCEVs in V2G mode, but also has its limitations in 'idling/spinning reserve' mode. Where the fuel cell system is operating but not producing any electricity. Therefore, a durability indicator expressed solely in operating hours, distance or produced energy is not relevant for combined driving and V2G services. An indicator consisting of several usage parameters is recommended. A combination of parameters, but not limited to, are the operating and 'idling' hours, produced energy, driven distance, number of start-ups and shutdowns. To establish usable correlations could require extensive and long-term testing under real circumstances with multiple FCEVs or would require other measurement techniques than used in this work.

8.2.2 Integration of FCEVs used for transport, distributing and generating electricity in future energy systems

Hydrogen, fuel cell and V2G technologies are still relatively new and have not deployed much yet, in particular not yet for passenger cars. The designed and analyzed integrated transportation and energy systems specifically focus on the potential with V2G with FCEVs. How the technology development scenarios and the deployment of these technologies in the future will look like still has to be seen.

The systems are not connected to any national electricity or natural gas grid or a transportation fuel network. They are self-sufficient and stand-alone and they only consider the residential, services, and road transportation sectors (e.g., not industry, agriculture, rail, or air transportation sectors).

When considering the hydrogen technologies used in the models and calculations, other hydrogen technologies are existing or being developed which could have the potential to be more energy efficient and/or cost effective.

Integration into other case studies and integration of other vehicles than passenger cars

A fully autonomous hospital, smart city area and countries are only considering the road transport and building energy sectors, where wind and solar energy are the dominant energy sources. Other integrated case studies as farms, datacenters, airports, bus depots, offices, (cooling) warehouses, distribution centers, mines or a combination of these and using other vehicles than passenger car FCEVs, such as buses, trucks, vans, trains, construction and other purpose-built work vehicles, are worthwhile to explore.

V2G infrastructure, development pathways, integration and adoption of FCEVs
Like other studies, the developed models in Chapters 1 to 1 are greenfield models showing a perfect outcome of a specific foresight. V2G infrastructure and the use of BEVs is increasingly being built out. Here, V2G with FCEVs could piggyback on BEV V2G infrastructure developments and standards. What specific and how large the role of V2G will become in balancing energy systems, is something which should be addressed in future work. Questions as what the development paths will be, e.g. incremental versus disruptive, distributed versus central are open questions and depend on whether or when widespread adoption of (passenger car) FCEVs will take place. The potential success of FCEVs (for passenger cars) will depend much more on the overall success of the broader so-called 'green hydrogen economy'. Creating the demand, the fueling infrastructure and the availability of cost competitive green hydrogen, either produced locally or imported from outside Europe.

Availability and scheduling of cars and other upcoming technologies regarding the integration of cars
This work only investigated the technical potential and with some qualitative checks on the realizable potential. In other words, we only simulated when V2G balancing power would be needed and verified if the required number of cars did not exceed the assumed fleet size. Some additional checks have been done, such as sufficient overcapacity and whether V2G usage was not conflicting too much with the average hours and times of driving. We did not investigate how to schedule the cars nor checked or estimated the (future) availability. We limited ourselves to the physical integration only, assuming instant availability, perfect communication, regulations, markets and infrastructures. However, the prospects of shared mobility, self-driving, cloud- and grid-connected cars with inductive charging and discharging technologies in the future could facilitate the scheduling of cars. Data pertaining to car parking locations, parking durations and tank fuel levels for a large number of cars, in combination with local grid imbalance data, could throw light on the problem of scheduling cars and shed some lights on the realizable potential.

Hydrogen pipeline network for hydrogen fuelling stations and V2G via FCEV
A hydrogen pipeline network could reduce hydrogen transportation via tube trailers and fueling station capacity. Multiple electrolyzers and hydrogen fueling stations could be interconnected via a pipeline network. In this way, tube trailer hydrogen transportation could be replaced, and hydrogen transportation costs reduced. Furthermore, the partial re-compression of hydrogen when emptying a tube trailer could also be reduced or avoided altogether. The compressor could even be omitted, provided the electrolyzer hydrogen output pressure is higher than the pipeline pressure.
In the case of parked FCEVs delivering V2G electricity, the fuel cell in the car could be connected directly to the hydrogen distribution pipeline network, instead of using hydrogen from the on-board hydrogen tank. Not using hydrogen from the 700 bar tank eliminates the need for refueling for V2G purposes.

Integration of other sectors, energy networks and renewable energy sources

The designed and analyzed integrated transportation and energy systems are hypothetical scenarios with limited model complexities and focused to explore the maximum technical potential of FCEVs balancing renewable energy. A fully autonomous hospital, smart city area and countries are only considering the road transport and building energy sectors, where wind and solar energy are the dominant energy sources. However, in reality these developed energy systems will be interconnected with other countries, city and rural areas, industrial and agricultural sites and other transport sectors. Demand patterns and peak use will vary and in certain cases deviate from the national or regional averages.

Currently as well as in future, several other factors could influence the use and integration of FCEVs. In contrast to this study, electricity networks do have limited capacities. In addition to that, new purpose-built, or if present natural gas grids, could be re-used for hydrogen transport. Smart integration of renewables with present heat grids and heat storage are just another factor to consider. Larger system integration involving more sectors, sources and energy carriers will result in more complex systems, but likely with higher synergies leading to lower system costs and higher reliability.

Integration with upcoming hydrogen technologies

In the developed and analyzed systems, electricity and hydrogen are the only energy carriers considered with a limited set of technologies with high Technology Readiness Levels (TRLs >7). In the future, a mix of multiple hydrogen energy carriers, storage methods, and conversion technologies could all work together and have an influence on the integration and use of FCEVs and the total system cost of energy.

When considering the hydrogen technologies used in the models and calculations, other hydrogen technologies are existing or being developed which could have the potential to be more cost efficient.

For example, research being performed in the field of reversible unitized PEM and solid oxide fuel cells, combining an electrolyzer and fuel cell in one device, or direct ammonia and LOHC fuel cells.

Storing and distributing gaseous hydrogen will always require compressors. Here, electrochemical hydrogen compression with purification could (partially) replace mechanical compressors and purification systems.

Several types of hydrogen storage technologies applications and technologies are being investigated next to gaseous hydrogen. From liquid hydrogen and metal hydrides to ammonia and liquid organic hydrogen carriers. All having their specific cost and integration advantages and disadvantages.

When it comes to electrolyzers, high temperature solid oxide or proton conducting electrolyzers and alkaline membrane electrolyzers have the potential to become cheaper or more efficient than current alkaline or proton exchange membrane electrolyzers. Direct solar to hydrogen technologies could even replace solar panels and electrolyzers.

How fast, at what scale and how generally applicable these technologies will become or what niches they will serve, still must be seen.

8.2.3 Impact of European regional characteristics on the techno-economic system performance and FCEVs providing balancing power

The designed and analyzed integrated transportation and energy systems are not connected to any national electricity or natural gas grid or a transportation fuel network. They are self-sufficient and stand-alone, where also today many regions rely on the import of energy. They use a single set of technologies for energy storage, and balancing, namely hydrogen, hydrogen production, and fuel cells (FCEVs). For road transportation and transportation fuel in Chapter 1 50% BEV passenger cars are considered, although do not participate in V2G services.
In the future, a mix of multiple energy carriers, storage and balancing methods and energy technologies could all work together. Alternatively, depending on the European regional characteristics, only the most cost-effective methods and technologies could be applied.
The calculated energy costs of the designed system in this work are affordable and in line with other studies. This gives reason to explore whether variations in system designs and balancing methods technologies can reduce total system costs even further. The system designs and balancing methods discussed below are a non-exhaustive selection of possible options.

Optimum ratio of BEVs and FCEVs, stationary batteries, hydrogen and fuel cells

Depending on the climate, the energy demand and chosen energy mix, a more day-to-day or season-to-season energy storage is needed in integrated transport and energy systems. could reduce total system costs In systems with a more profound day-to-day short term energy storage requirement, total system costs could be lowered by a larger share of BEVs than FCEVs participating into V2G energy and storage services. Also charging BEVs during the solar/day-light hours for their daily driving consumption would reduce the midday balancing peak by electrolyzers in solar dominated energy systems (reducing the 'duck curve' [838,840,852]). Provided BEVs would be available for charging during the day. As BEVs might be in use during the day, also stationary batteries could be charged during the day and discharged during the night, here BEVs only would be charged or discharged when stationary batteries are full/empty, in other words avoid peaks and increase capacity factors of stationary batteries.
Hydrogen storage is more suitable for large scale seasonal energy storage. Depending on the ratio between the required electricity or heat and the profile of the required electricity and /or heat in time, a mix of different hydrogen conversion technologies could be applied. Stationary Combined Heat and Power (CHP) units, either fuel cell, turbine or combustion engines are more suitable to use the waste heat if needed. Turbines and combustion engines provide relatively more heat than electricity in comparison to fuel cells, so could be better suited for end-users with higher heat demands. Combustion engines, turbines and solid oxide fuel cells operate at higher temperatures than PEM fuel cells and could provide high temperature heat.

End-users with a high electricity and or heat base load demand might also consider a hybrid-solution of both stationary (fuel cell) based CHP systems where FCEVs provide peak electricity demand.
Summarizing, depending on the requirements and available assets, the most operational, secure and cost-efficient solution most likely consists of a tailored combination of FCEVs, BEVs, or fuel cell plug-in hybrid electric vehicles (FCPHEVs), stationary batteries and CHP systems providing heat and electricity.

Energy sources, storage and carriers
In this study the number of storage technologies and energy sources is limited. The choice is fixed irrespective of the climate related type of energy demand (heating, cooling, power, transport fuel) and pattern. Other renewable energy sources, (e.g. biomass, hydro and geothermal power, solar thermal) and natural energy storage possibilities (aquifer thermal energy storage, pumped hydro storage) could better match specific climate related energy storage and demand patterns. Choosing different energy carriers than electricity and hydrogen, such as other thermal and chemical energy carriers and storage methods could potentially result in a more operational, secure and cost-effective energy systems.

International hydrogen import and pipeline network
Instead of generating and storing hydrogen in European countries or in Europe as a region, hydrogen could be imported from regions with other hydrogen demand and generation patterns. Via this way, large scale hydrogen storage could be reduced to a level of strategic hydrogen storage only. Hydrogen could be produced in regions with the lowest-cost renewable electricity and imported to Europe via international pipelines or vessels. Like today's international natural gas and oil trade. Either in the form of gaseous hydrogen, liquid hydrogen, ammonia or liquid organic hydrogen carriers. For example, via pipelines from the sunny regions in Southern Europe to Northern Europe or even from Northern Africa and the Middle-East. Alternatively, via vessels from Iceland, South or Central America, Africa or Australia.

Demand response, storage, autonomous driving and Internet of Things
In this work hourly and daily demand patterns are based on the current energy demand patterns. Considering a future estimated higher efficiency and reduced building energy use. Sophisticated weather and electricity demand forecasting in combination with demand response could potentially avert or reduce temporal surplus or shortage of electricity. With an increasing presence of various forms of energy storage (e.g. electricity in batteries, hot water reservoirs) on various levels (e.g. domestic, neighborhood), connectivity of devices (e.g. Internet of Things, IoT), market triggers (time of use and capacity based pricing schemes), demand and supply could be better matched and existing assets better used. This could reduce the need for balancing by FCEVs, depending on the scale, type and climatic region of the energy system.
Self-driving, cloud controlled [310,311,576], wireless power transfer [271,272,580] and V2G self-connecting [761] cars would facilitate the use and scheduling of them

[424,880]. The distribution of hydrogen via road transport could benefit from self-driving and cloud connected trucks.

Appendices

A Fuel Cell Electric Vehicle as a Power Plant: Techno-Economic Scenario Analysis of a Renewable Integrated Transportation and Energy System for Smart Cities in Two Climates

A.1 Locations Selection, System Design, Dimensioning, and Components

A.1.1 Location Selection

Table A1 shows some key figures characterizing Hamburg in Germany and Murcia in Spain and their climates. Respectively, 1.8 and 1.5 million inhabitants live in urban areas [881–883]. Hamburg has a temperate oceanic (Cfb), and Murcia a hot semi-arid (BSh) climate, according to the Köppen–Geiger climate classification [642,884–887]. Local weather station data from 2012 to 2016 [888–890] are used to calculate the five-year average (μ) and annual coefficient of variation (CV, also known as the relative standard variation) of the average annual wind speed, solar global horizontal irradiation, precipitation, air temperature, daily maximum and minimum air temperatures, heating degree days (HDD) [680,891], and cooling degree days (CDD) [647,648].

Table A1 Key figures, characterizing the climate of the two locations, Hamburg and Murcia.

Key Figures	**Locations**	
	Hamburg, Germany	**Murcia, Spain**
No. of inhabitants of urban area (# x 1,000,000) [881–883]	1.8	1.5
Climate zone (Köppen–Geiger) (-) [642,884–887]	temperate oceanic (Cfb)	hot semi-arid (BSh)
Weather station data		
Weather station height above sea-level (m) [1] [888,889]	11	61
Weather station location [1] [888,889]	53°38′ N, 9°59′ E	38°0′ N, 1°10′ W
Weather data 2012–2016 means and standard deviations	**μ (CV)**	**μ (CV)**
Wind speed at 10 m above ground (m/s) [1] [888,892]	4.1 (4.3%)	3.9 (4.3%)
Solar global horizontal irradiation (kWh/m^2/year) [888,890]	1020 (4%)	1855 (1.8%)
Precipitation (l/m^2/year) [888,890]	735 (4.9%)	255 (24%)
Air temperature (°C) [888,890]	9.9 (5.9%)	19.1 (2.8%)
Daily maximum air temperature (°C) [888,890]	13.4 (5.1%)	25.5 (2.2%)
Daily minimum air temperature (°C) [888,890]	6.3 (8.7%)	13.7 (4.4%)
Heating Degree Days (°C·day/year) [2] [888,890]	3066 (6.5%)	854 (16%)
Cooling Degree Days (°C·day/year) [2] [888,890]	101 (24%)	1245 (6.9%)

[1] *Wind speeds measured at the nearby Almeria Airport weather station are used* [892,893] *because, at the Murcia weather station* [889,890]*, wind speeds are economically less favorable for wind turbines. The non-wind weather data of the Murcia weather station is more complete than that of the Almeria Airport weather station. The Almeria Airport weather station is 21 m above sea-level and has the following coordinates: 36°50′ N, 2°21′ W. The Murcia weather station five-year average (2012–2016) and coefficient of variation of the average annual wind speed at 10 m above ground are 2.4 m/s and 2.8%, respectively.* [2] *Calculated with a base temperature of 18 °C as in* [647,648,680].

A.1.2 Technological and Economic Characterization of System Components in Two Scenarios

Table A2 lists the specific energy consumption and production (SEC and SEP) ($kWh_e/kg\ H_2$) in the Near Future and Mid Century scenarios for the different energy conversion processes, from rainwater collection to hydrogen production, fueling, and reconversion to electricity. Alkaline water electrolysis technology is chosen as, at the moment, it is cheaper than Proton Exchange Membrane (PEM) electrolysis technology [298,518]. The electrolyzer is coupled directly to the direct current renewable energy source, so there is no AC/DC conversion needed at the electrolyzer [894]. Current state-of-the-art alkaline electrolysis technology can respond sufficiently fast [298,895,896] to short-term solar and wind power fluctuations [897–903]. The alkaline water electrolysis part-load efficiency curve is used from [519], and its maximum efficiency point (higher heating value (HHV)-based) is 88.8% [904–906] for the Near Future and 92.6% for the Mid Century scenario [906,907]. SEC for hydrogen purification is, respectively, 1.3 and 1.1 $kWh_e/kg\ H_2$ in the Near Future and the Mid Century scenario [521,522]. After purification, drying, and oxygen removal, the hydrogen meets the purity required for FCEVs [245] at a pressure of 15 bar and 30 bar in, respectively, the Near Future and the Mid Century scenario [298,904,905,907]. Compression SEC for all compressors (S6, W6, HFS1, and SHS2) in the Near Future scenario is in the range of 0.5–3.1 $kWh_e/kg\ H_2$, and in the Mid Century scenario 0.4–2.5 $kWh_e/kg\ H_2$ [379–382,386]. The reduction in SEC in the Mid Century scenario is due to the increase in isentropic efficiency from 60% to 80% [379] and, for compressors S6 and W6, also the higher hydrogen output pressure of the electrolyzers. The compressor at the wind park (W6) has an outlet pressure of 180 bar, the maximum SHS operating pressure [385], which is assumed to be constant in this study. The operating pressure range of hydrogen tube trailers in both scenarios is 30–500 bar with an effective storage capacity of 1014 kg H_2 [298,536,908,909]. By applying a smart consolidation strategy for emptying and filling tube trailers at the SHS [379,380,910,911], the net electricity consumption is simplified as compressing hydrogen from 180 bar to 500 bar (SHS2). The electricity consumption of compressor S8 is modeled as the compression of hydrogen from the hydrogen purification output pressure of 30 bar to 500 bar. The combined compressor capacity at the HFS (HFS1) is the largest of all compressors and is modeled with a variable inlet pressure of 30–500 bar (emptying the tube trailers) and fixed outlet pressure of 875 bar of the storage (HFS2). Hydrogen cooling SEC for fueling at 700 bar is 0.20 and 0.15 $kWh_e/kg\ H_2$ in, respectively, the Near Future and the Mid Century scenario [177,178], and is assumed to be constant over the entire operating range of the chiller. In this study, no reduction in specific electricity consumption is foreseen in the Mid Century scenario for reverse osmosis [546,552,800]. The specific energy production SEP by the FCEV is, respectively, 20.3 and 23.6 $kWh_e/kg\ H_2$ in the Near Future and the Mid Century scenario. These values correspond to a tank-to-grid efficiency, η_{TTG}, [640] (analogous to tank-to-wheel, η_{TTW}, efficiency when driving) of, respectively, 51.5% and 60% (HHV) [126,194]. Furthermore, it is assumed that the SEC and SEP of the conversion processes are location independent.

Table A2 Specific energy consumption SEC or production SEP ($kWh_e/kg\ H_2$) of the energy conversion processes in the smart city area for both scenarios and locations.

Label (See Figure 2 and Table 2)	Energy Conversion Processes	Specific Energy Consumption/Production (SEC/SEP)	
		Near Future [$kWh_e/kg\ H_2$]	Mid Century [$kWh_e/kg\ H_2$]
W4 and S4	Alkaline water electrolysis [519,895,904–907]	44.4–50.0 [1,2]	42.6–47.7 [1,2]
S5 and W5	Hydrogen purification [521,522]	1.3	1.1
S6	Compressor at local solar (500 bar) [379–382,386]	3.0 [3]	1.8 [3]
W6	Compressor at wind turbine park to SHS (180 bar) [379–382,386]	1.9 [3]	1.0 [3]
HFS1	Compressor at HFS ([30–500]–875 bar) [379–382,386]	0.5–3.1 [1]	0.4–2.5 [1]
SHS2	Compressor at SHS (180–500 bar) [379–382,386]	0.8	0.6
HFS3	Chiller [388,537]	0.20	0.15
S2 and W2	Reverse Osmosis—rainwater/surface water [546,552,800]	0.006	0.006
FCEV1	FCEV hydrogen to electricity [126,194,912]	20.3	23.6

[1] Direct current electrical consumption [907] *at 15–100% load in the Near Future scenario and 10–100% load in the Mid Century scenario. [2] 15 and 30 bar hydrogen outlet pressure in, respectively, the Near Future and the Mid Century scenario. [3] 15 and 30 bar hydrogen inlet pressure in, respectively, the Near Future and the Mid Century scenario.*

Table A3 Economic parameters of the smart city area components for the Near Future and the Mid Century scenario. IC_i = installed capital cost; OM_i = annual operational and maintenance cost expressed as an annual percentage of the installed investment cost; LT = lifetime.

Label	Subsystems and Components	Near Future			Mid Century		
		IC_i	OM_i [%/year]	LT_i [years]	IC_i	OM_i [%/year]	LT_i [years]
	Solar and wind electricity production						
S1	Solar electricity system [370,936,937]	725 €/kWp	2.8%	25	440 €/kWp	2.3%	30
W1	Wind turbine park [557,558,560–562,936,937]	975 €/kW	2%	25	800 €/kW	1%	25
	Hydrogen production and compression						
S4 and S5	Alkaline electrolyzer, including H_2 purification at solar system [298,513,774,799,938]	575 [1] €/kW	2.5% [2]	20[3]	200 €/kW	2.5% [2]	30 [3]
W4 and W5	Large-scale alkaline electrolyzer, including H_2 purification at wind turbines [298,513,774,799,938]	480 [1] €/kW	4.2% [2]	20[3]	200 €/kW	4.4% [2]	30 [3]
S6	Compressor at solar system [535,536]	10,030/9630 €/kg H_2/h [4]	4%	15	3445/3325 €/kg H_2/h [4]	2%	15
W6	Compressor at wind turbine park to SHS [535,536]	8250/8915 €/kg H_2/h [4]	4%	15	3515/6260 €/kg H_2/h [4]	2%	15
	Hydrogen transport						
TT1	Tube trailer storage [298,533,536]	830 €/ kg H_2	2%	30	510 €/ kg H_2	2%	30
TT2	Trailer tractors [298,533,536]	160,000 €/ tractor	61/65% [5]	8 [6]	160,000 €/tractor	63/62% [5]	8 [6]
	Hydrogen fueling station (HFS)						
HFS1	Compressor at HFS [535,536]	8375/8820 €/kg H_2/h [4]	4%	10	3630/3670 €/kg H_2/h [4]	2%	10
HFS2	Storage HFS 875 bar [379,387,939]	920 €/kg H_2	1%	30	575 €/ kg H_2	1%	30
HFS3	Chiller units [379,535]	143,875 €/kg H_2/min	2%	15	118,520 €/kg H_2/min	2%	15
HFS4	Dispensers units [379,521,522,535]	91,810 €/unit	1.1%	10	72,890 €/unit	0.9%	10

	Fuel cell electric vehicle to grid (FCEV2G)						
FCEV1	Replacement of fuel cell system in FCEV for V2G use [96,126,314,539–545,564,940,194,229,235,264,265,275,285,288]	3970 €/100 kW	5%	4100 h [7]	2650 €/100 kW	5%	8000 h [7]
FCEV2	Smart grid, control, and V2G infrastructure [370]	6400 €/4-point dischargers	5%	15	3200 €/4-point dischargers	5%	15
	Seasonal hydrogen storage (SHS)						
SHS1	SHS plant (3733 ton H_2 cavern) [385]	107,000,000 €/plant	0.5%	30	107,000,000 €/plant	0.5%	40
SHS2	Compressor at SHS [535,536]	3470/3825 €/kg H_2/h [4]	4%	15	1560/1665 €/kg H_2/h [4]	2%	15
	Water purification and storage						
S2 and W2	Water purification [552]	1,200 €/m^3/day	4.8%	25	1,200 €/m^3/day	4.8%	25
S3 and W3	Pure-water tank [501–503,550]	120 €/m^3	0.33%	50	120 €/m^3	0.33%	50

[1] The size of the electrolyzer at the solar system is smaller than 10 MW and, therefore, still has a higher IC in the Near Future scenario than the wind connected electrolyzer. [2] The OM includes stack replacement [235]*, which is calculated based on an average of 13 and 24 operating hours per day for, respectively, solar and wind-powered electrolyzers. [3] System LT is 20 and 30 years, and stack economic operating lifetime is 80,000 and 90,000 h in, respectively, the Near Future and the Mid Century scenario. [4] Figures for, respectively, Hamburg/Murcia. The compressor IC costs are dependent on, for example, mass flow capacity, discharge pressure, and pressure ratio* [235]*. [5] Figures for, respectively, Hamburg/Murcia. The OM is defined by the amount of hydrogen transported* [235] *and differs per location and scenario. [6] Lifetime of 8 years based on approximately 75,000 km/year; for the cost calculation* [235]*, only the required driven kilometers are included, i.e., there are no "idling" costs. [7] Lifetime = economic lifetime in driving operating hours. The economic lifetime calculation when using the FCEV for both driving and V2G is explained in* [235].

A.2 Detailed Description and Background Data of the Calculation Model and Hourly Simulation

A.2.1 Electricity Consumption and Production

The yellow rectangle in Figure 6-3 includes the electricity consumption of the services and residential buildings (E_B), the HFS compressor and chiller (E_{HFS}), the SHS compressor (E_{SHS}), and the solar electricity production (E_S). E_{HFS} and E_{SHS} are calculated by multiplying the hourly hydrogen throughputs by the specific energy consumption component values SEC ($kWh_e/kg\ H_2$) from Table A2.

The electricity consumption of the services and residential buildings (E_B) in the Near Future and the Mid Century scenario is based on the energy consumption at present, called the Present Situation. Therefore, first, the Present annual specific energy consumption of the residential and services buildings SEC_B ($kWh/m^2/year$) is defined for each location. The method described is applicable to any location within Europe.

Building energy consumption is divided into six energy consumption categories:

1. Space heating
2. Space cooling
3. Water heating
4. Cooking
5. Lighting
6. Electrical appliances

Space heating and cooling depend on the ambient temperature, which is reflected in the number of annual heating and cooling degree days (HDD and CDD; see Table A1). Hamburg and Murcia differ greatly in this regard. Also, within the respective countries (Spain and Germany), locally, the number of HDDs and CDDs [647,648,913] can differ greatly from the national weighted average [677]. Due to a lack of recent and complete studies on building energy demand relations with respect to climatic parameters, a similar method is developed as in [647,648]. For space heating for both the residential and the services sector, a relation between the specific thermal heating demand and the number of HDDs per country is established using [471,472,677]. The specific thermal heating demand is derived from the used fuel mix, useful thermal energy per fuel type, fuel demand, and floor space [471,472,677,680]. The value used as specific thermal demand for space heating in Murcia and Hamburg is taken from countries with a similar number of HDDs as Murcia and Hamburg. For Murcia, the specific thermal demand is based on the specific thermal heating demand of Cyprus, Malta, and Portugal of the available years 2010–2015. For Hamburg, it is based on the specific thermal demand of Germany, Sweden, Finland, and Lithuania.

For space cooling, the relations between CDDs, specific thermal cooling demand, and specific electricity demand from [647,648] are used. For water heating, cooking, lighting, and electrical appliances, it is assumed the local consumption in the Murcia and Hamburg regions does not differ from the national average values [471,472].

Table A4 shows the specific annual energy consumption for buildings SEC_B ($kWh/m^2/year$) per energy consumption category, and annual electricity

consumption in buildings E_B (MWh/year) for the residential and services sector for the Hamburg- and Murcia-based smart city areas in the Present Situation and in the Near Future and Mid Century scenarios. For the Present Situation in Hamburg and Murcia, this is 194 and 173.6 kWh/m^2/year and 98.6 and 223.5 kWh/m^2/year for the residential and the services sector, respectively. Combining the SEC_B values with the floor areas from Table A4 results in total annual energy consumption of 51,617 MWh and 26,672 MWh for Hamburg and Murcia, respectively.

SEC_B values in the Near Future and the Mid Century scenario are fully electric in its end-use and are defined by applying specific energy consumption savings (Table A5) to the Present SEC_B. Space heating SEC_B in the Near Future scenario for both residential and services buildings is a conversion of the Present Situation SEC with its fuel mix [471,472] and corresponding useful thermal energy fractions [680] and a heat pump Coefficient of Performance (COP) of 3.5 [482–485] into the electrical equivalent energy. For the Mid Century scenario, savings for, respectively, the residential and the services sector of 95% and 85% are achieved, based on [486]. Space cooling SEC_B in the Near Future remains equivalent to the Present SEC [647,648], whereas, in the Mid Century scenario, savings of 70% are realized for both sectors [482,483,486]. In the Near Future scenario, water heating and cooking SEC is realized by electrification of the Present SEC fuel mix [471,472], with the useful thermal energy fractions [680] into the electrical equivalent energy [680]. Only for water heating, savings of 50% are used in the Mid Century [486], due to the combined application of electrification, heat pump usage, solar thermal heating, and other heat recuperation techniques. By extensive use of LED technology for lighting and LED efficiency increase, savings of 20% and 80% are assumed for, respectively, the Near Future and the Mid Century scenario in both sectors [914–916]. A total of 0% of net savings are assumed for the SEC_B of electrical appliances. Although energy savings will be significant, the net savings will be zero due to an increased number and use of electrical appliances, home automation, and IT services [917–919].

Hamburg residential and services total SEC_B values in the Near Future are 83.2 and 103.3 kWh/m^2/year, respectively, resulting in total energy consumption of 24,838 MWh/year. In the Mid Century scenario, SEC_B values decrease to 49.8 and 74.2 kWh/m^2/year, and the energy consumption to 16,020 MWh/year. Murcia residential and services total SEC_B values in the Near Future are 82.9 and 170.5 kWh/m^2/year, resulting in total energy consumption of 21,760 MWh/year. In the Mid Century scenario, SEC_B values decrease to 51.3 and 90.8 kWh/m^2/year, and the energy consumption to 12,901 MWh/year.

Table A4 Specific annual energy consumption SEC_B (kWh/m²/year) per energy consumption category and total annual energy consumption E_B (MWh/year) in buildings for the residential and the services sector for the Hamburg- and Murcia-based smart city areas at Present and the Near Future and Mid Century scenarios.

Energy Consumption Category	Specific Energy Consumption Buildings SEC_B [kWh/m²/Year]					
	Hamburg, Germany			Murcia, Spain		
	Present Situation	Near Future	Mid Century	Present Situation	Near Future	Mid Century
Residential sector						
Space heating [472]	131.1 [1]	29.2	6.6	13.8 [1]	2.7	0.7
Space cooling [648]	0.9 b	0.9	0.3	30.2 [2]	30.2	9.1
Water heating [472]	32.3 [1]	24.5	16.2	16.4 [1]	13.7	8.2
Cooking [472]	7.8 [1]	7.4	7.4	7.7 [1]	6.7	6.7
Lighting [472]	2.9 [2]	2.3	0.6	4.9 [2]	3.9	1.0
Electrical appliances [472]	18.9 [2]	18.9	18.9	25.7 [2]	25.7	25.7
Total	194.0	83.2	49.8	98.6	82.9	51.3
Services sector						
Space heating [471]	80.3 [1]	18.3	12.1	48.3 [1]	11.4	7.2
Space cooling [647]	3.4 [2]	3.4	1.0	43.0 [2]	43.0	12.9
Water heating [471]	8.3 [1]	7.3	4.1	7.7 [1]	6.4	3.8
Cooking [471]	13.1 [1]	11.5	11.5	4.1 [1]	3.5	3.5
Lighting [3] [471]	28.8 [2]	23.0	5.8	71.5 [2]	57.2	14.3
Electrical appliances [471]	39.7 [2]	39.7	39.7	49.0 [2]	49.0	49.0
Total	173.6	103.3	74.2	223.5	170.5	90.8
	Total annual Energy consumption buildings E_B [MWh/year]					
	Hamburg			**Murcia**		
	Present Situation	**Near Future**	**Mid Century**	**Present Situation**	**Near Future**	**Mid Century**
Residential	35,541	15,241	9127	18,105	15,225	9422
Services	16,130	9597	6893	8567	6535	3479
Total	51,671	24,838	16,020	26,672	21,760	12,901

[1] Fuel mix [471,472] *and useful thermal energy fractions, electricity: 0.97, heat: 0.95, gas: 0.80, oil: 0.72, coal: 0.65, wood 0.55* [680]. *[2] electrical energy. [3] Including the electricity used for public lighting* [920].

Table A5 Specific energy consumption savings for the Near Future and Mid Century scenarios compared to the Present Situation.

Energy Consumption Category	**Specific Energy Consumption Savings Compared to Present Situation**	
Residential Sector	**Near Future**	**Mid Century**
Space heating [482–486]	71% [1]	95%
Space cooling [482,483,486,648]	0%	70%
Water heating [471,472,484,486,680]	24/16% [2]	50%/50% [3]
Cooking [471,472,680]	5/13% [2]	5/13% [2]
Lighting [914]	20%	80%
Electrical appliances [917–919]	0% [4]	0% [4]
Services sector		
Space heating [482–486]	71% [1]	85%
Space cooling [482,483,486,647]	0%	70%
Water heating [471,472,486,680]	12/17% [2]	50%/50% [3]
Cooking [471,472,680]	12/15% [2]	12/15% [2]
Lighting [914–916]	20%	80%
Electrical appliances [917–919]	0% [4]	0% [4]

[1] *Savings due to heat pump usage, conversion of the Present Situation fuel mix* [471,472] *with the useful thermal energy fractions (electricity: 0.97, heat: 0.95, gas: 0.80, oil: 0.72, coal: 0.65, wood 0.55)* [680] *and a heat pump COP of 3.5* [482–485] *into the electrical equivalent energy.* [2] *Hamburg/Murcia savings due to the electrification of existing primary fossil energy demand for thermal purposes. Conversion of the Present Situation fuel mix* [471,472] *with the useful thermal energy fractions (electricity: 0.97, heat: 0.95, gas: 0.80, oil: 0.72, coal: 0.65, wood 0.55)* [680] *into the electrical equivalent energy for the thermal demand* [680]. [3] *Hamburg/Murcia combined savings due to the application of electrification, heat pump usage, solar thermal heating, and other heat recuperation techniques.* [4] *Although energy savings will be significant, the net savings will be zero due to an increased number and use of electrical appliances, home automation, and IT services* [917–919].

Hourly profiles for an entire year are constructed for each energy consumption category, type of building sector, modeled location, and scenario by multiplying the SEC_B values from Table A4 by normalized profiles:

1. Space heating SEC_B is multiplied by the normalized hourly profile of aggregated natural gas consumption profiles for space heating, only in the residential [921] and the services sector [922], and the daily HDD profile with base temperature 18 °C [832]. The natural gas consumption profiles for space heating only are made by subtracting the natural gas consumption for water heating from the total natural gas consumption profiles.
2. Space cooling SEC_B is multiplied by the hourly CDD profile with base temperature 21 °C [832,891].
3. Water heating SEC_B is multiplied by the normalized hourly profile of the aggregated gas consumption profiles for water heating only. The natural gas consumption for water heating is extracted from the total aggregated natural gas consumption profiles during the period of 3 summer weeks (day 205 of the year onwards) with ambient temperatures above 18 °C, where it is assumed no space heating is taking place [921,922]. As the profiles are based on aggregated values, it is assumed that holiday effects are excluded.
4. Cooking, lighting, and electrical appliances SEC_B values are multiplied by the normalized aggregated electricity consumption profiles for residential [923] and services sector buildings [924].

The solar electricity production (E_S) is calculated [925,926] using the hourly global horizontal irradiation values from both Murcia and Hamburg [888–890]. The irradiation values are assumed to be equal in both scenarios. With the given fixed roof area available for solar electric modules (Table 6-2) and the solar electricity system performance ratio and efficiency of, respectively, 0.80 and 0.20 kWp/m^2 in the Near Future scenario and 0.90 and 0.33 kWp/m^2 in the Mid Century scenario [370,507–509,927,928], 11.20 and 18.67 MWp of solar power is installed in the Near Future and Mid Century for Hamburg and Murcia. The solar system inclination is 34° and 39° for, respectively, Murcia and Hamburg [929], both with an azimuth of 0°.

A.2.2 Road Transportation Hydrogen Demand

Annual hydrogen consumption for road transportation H_{road} (kg H_2/year) (blue rectangle in Figure 6-3) of the passenger cars, vans, trucks, tractor-trailers, and buses is calculated in Table A6 using the German and Spanish national average annual distance driven d [470,678,679] and the estimated vehicle fuel economy, specific energy consumption SEC_T (kg H_2/100 km), in the Near Future and the Mid Century scenario [235]. For Hamburg, this results in H_{road} of 479,909 kg H_2/year in the Near Future scenario and decreases to 316,129 kg H_2/year in the Mid Century scenario. For Murcia, this results in H_{road} of 545,192 kg H_2/year in the Near Future scenario and decreases to 381,732 kg H_2/year in the Mid Century scenario. H_{road} is then multiplied by a normalized repeating weekly fueling profile [521].

In the Near Future and the Mid Century scenario, the average annual distance driven is assumed to remain constant. The number of tube trailer tractors for hydrogen

transportation and their driven kilometers are assumed to be included in the number of road tractors and the number of kilometers they are driven each year. The road vehicles are owned by either the residential or the services sector, and the road transportation energy is consumed in or between smart city areas. The final energy consumption for motorcycles is not included as it currently represents only about 1% of the total road transportation final energy consumption.
At an average annual speed of 45 km/h for passenger cars [175] in Europe and the average annual distance driven d (Table A6), there are only about 305 and 280 driving hours per year per car for, respectively, Hamburg and Murcia, mostly occurring during daylight hours [175]. For most of the non-driving time, passenger cars are mostly parked at home, the office, or close to a services sector building like a supermarket or hospital [175,342].

Table A6 The average annual distance driven d and Near Future and Mid Century scenario-specific energy consumption of transport (SECT) for van, truck, tractor-trailer, and bus type FCEVs.

	Specific Energy Consumption Transportation SEC_T [kg H_2/100 km]		**Average Annual Distance Driven d [km/year/vehicle]**	
Vehicle Type	**Near Future** [235]	**Mid Century** [235]	**Hamburg, Germany** [678,679]	**Murcia, Spain** [470]
Passenger car	1.0	0.6	13,728	12,535
Van	1.3	0.9	19,388	17,704 [a]
Truck	4.6	3.7	31,870 [b]	37,077
Tractor-trailer	6.9	5.5	96,211	151,513
Bus	8.6	6.9	55,883	147,398
	Hamburg, Germany		**Murcia, Spain**	
Annual hydrogen consumption H_{road}	**Near Future**	**Mid Century**	**Near Future**	**Mid Century**
Hydrogen [kg H_2 /year]	479,909	316,129	545,192	381,732
Hydrogen Energy [c] [MWh_{HHV}/year]	18,913	12,459	21,486	15,044

[a] No data is present for vans in [470]*; therefore, the same relation between the average annual distance driven of cars and vans as in Germany is used. [b] Including commercial vehicles 3.5–6.0 tons. [c] Based on a higher heating value (HHV) of 39.41 kWh/kg H_2.*

A.2.3 Electricity and Hydrogen Hourly Balance

The red rectangle, in Figure 6-3, includes both the electricity and the hourly balance. First, the electricity consumption of the services and residential buildings (E_B), the HFS compressor and chiller (E_{HFS}), SHS compressor (E_{SHS}) is subtracted from the solar electricity production (E_S). Any surplus solar electricity (E_{surp}) is converted via electrolysis and water (H_2O_S) into "solar" hydrogen (H_S). If there is a shortage of electricity, this is compensated for by electricity from the FCEV2Gs (E_{V2G}) by converting hydrogen (H_{V2G}). The amount of hydrogen consumed for V2G (H_{V2G}) is added the next day to the hydrogen fueling profile for road transportation (H_{road})

and follows the same hourly pattern. H_{V2G} and H_{road} combined make up the total hydrogen dispensed at the HFS (H_{HFS}).

A.2.4 Hydrogen Tube Trailer and Tractor Fleet

The grey rectangle, in Figure 6-3, shows the hydrogen tube trailer transportation. Once a tube trailer (TT1) is filled with "solar" hydrogen (H_S), tube trailer tractors (TT2) transport the tube trailers to the HFS and unload them if the high-pressure storage tank (HFS2) is not full. If HFS2 is full, the tube trailer is emptied at the seasonal hydrogen storage (SHS1). If there is insufficient H_S, and HFS2 is not full, tube trailers are filled at the SHS with the compressor (SHS2) and transported to the HFS.

Transportation of the tube trailers is modeled as one hour of unavailability; tube trailer tractor averages driving speed of 50 km/h with a single trip distance of 50 km. With a 2-h loading and unloading time [533] and 8 working hours per shift, one tractor can make two roundtrips per shift. The number of tube trailers at the three locations (solar hydrogen production, HFS, and SHS), together with the maximum number of tube trailers transported at the same time, defines the total number of tube trailers needed.

A.2.5 Wind Hydrogen Production and Seasonal Hydrogen Storage Balance

Wind hydrogen production and the seasonal hydrogen storage balance is shown in the green rectangle in Figure 3. As the amount of solar electricity consumption variation is limited due to the limited amount of suitable roof area, the amount of installed wind capacity, together with energy storage, closes both the hourly and the annual energy balance. The large-scale wind turbine park shared with other smart urban areas produces electricity (E_W) and is directly connected to a water electrolysis and compression system (W2–W6) and has no connection with any other electricity grid. The wind energy production is sized such that the net amount of consumed hydrogen from the seasonal hydrogen storage in underground salt caverns is zero on a yearly basis. There is no curtailment of wind electricity (E_W), and all electricity produced is used for the production and compression of "wind" hydrogen (H_W) from water (H_2O_W).

The wind turbine park performance is based on the 4.2 MW land-based Enercon E-141 EP4 [391] for the Near Future scenario, and, for the Mid Century, it includes future power curve improvements based on [392]. In both scenarios, the hub height is 159 m, and the rotor diameter 141 m. The wind electricity production (E_W) is calculated using the hourly wind speed values from both Almeria (see Table A1, footnote 1) and Hamburg [179–182]. The wind speeds are assumed to be equal in both scenarios and are scaled [930] to the aforementioned hub height with a roughness factor z_0 of 0.13 m [931].

A.3 Calculating Cost of Energy

A.3.1 Smart City Area Total System Cost of Energy

The $TSCoE_{SCA}$ in euros per year, Equation (A.1), is the sum of the total annual capital and operation and maintenance costs TC_i (€/year) of the total number of components (n) in the smart city area:

$$\mathrm{TSCoE_{SCA}}\left(€/\mathrm{year}\right)=\sum_{1}^{n}\mathrm{TC_i} \tag{A.1}$$

The TCi of an individual component is calculated in Equation (A.2) using the annual capital cost CC_i (€/year) and operation and maintenance cost OMC_i (€/year):

$$\mathrm{TC_i}\left(€/\mathrm{year}\right)=\mathrm{CC_i}+\mathrm{OMC_i} \tag{A.2}$$

The CC_i (€/year) of a component is calculated in Equation (A.3) using the annuity factor AF_i (%), installed component capacity Q_i (component-specific capacity), and investment cost IC_i (€ per component-specific capacity):

$$\mathrm{CC_i}\left(€/\mathrm{year}\right)=\mathrm{AF_i}\times\mathrm{Q_i}\times\mathrm{IC_i} \tag{A.3}$$

Where the annuity factor AF_i [460,461], Equation (A.4), is based on the weighted average cost of capital WACC (%) and the economic lifetime of a component LT_i (years):

$$\mathrm{AF_i}=\frac{\mathrm{WACC}\times\left(1+\mathrm{WACC}\right)^{\mathrm{LT_i}}}{\left[\left(1+\mathrm{WACC}\right)^{\mathrm{LT_i}}\right]-1} \tag{A.4}$$

The annual operation and maintenance costs OMC_i (€/year), Equation (A.5),are expressed as an annual percentage OM_i (%) of the Q_i and IC_i:

$$\mathit{OMC_i}\left(€/\mathrm{year}\right)=\mathrm{OM_i}\times\mathrm{Q_i}\times\mathrm{IC_i} \tag{A.5}$$

A.3.2 System Levelized Cost of Energy

The system levelized cost of energy, for either electricity $SLCoE_e$ (€/kWh) or hydrogen $SLCoE_H$ (€/kg H_2), is calculated by allocating a share of the $TSCoE_{SCA}$ related to either electricity $TSCoE_{SCA,e}$ or hydrogen consumption $TSCoE_{SCA,H}$. These shares are then divided by either the annual electricity consumption EC_e (kWh/year) or the annual hydrogen consumption EC_H (kg H_2/year), resulting in, respectively, the $SLCoE_e$, Equation (A.6), or the $SLCoE_H$, Equation (A.7):

$$SLCoE_e\left(€/kWh\right)=\frac{TSCoE_{SCA,e}}{EC_e} \quad \text{(A.6)}$$

$$SLCoE_H\left(€/kg\,H_2\right)=\frac{TSCoE_{SCA,H}}{EC_H} \quad \text{(A.7)}$$

A.3.3 Cost of Energy for Households (Without Taxes and Levies)

Cost of energy for a single household CoE_{hh} (€/hh/year), Equation (A.8), here calculated without taxes and levies, consists of the cost of energy for the building energy $CoE_{hh,B}$ (€/hh/year) and the transportation energy $CoE_{hh,T}$ (€/hh/year).

$$CoE_{hh}\left(€/year\right)=CoE_{hh,T}+CoE_{hh,B} \quad \text{(A.8)}$$

The cost of energy for transportation energy $CoE_{hh,T}$ (€/hh/year), Equation (A.9), is calculated by multiplying the $SLCoE_H$ by the average annual distance driven by passenger cars $d_{passenger\ car}$ (km/year/vehicle), the number of passenger cars per household $n_{hh,passenger\ cars}$ (#/hh), divided by the $SEC_{T,passenger\ cars}$ (kg H_2/100 km).

$$CoE_{hh,T}\left(€/year\right)=SLCoE_H\times\frac{d_{passenger\ car}}{SEC_{T,passenger\ car}}\times n_{hh,passenger\ cars} \quad \text{(A.9)}$$

The cost of energy for building energy $CoE_{hh,B}$ (€/hh/year) is calculated in Equation (A.10) by multiplying the $SLCoE_e$ by the residential building $SEC_{B,residential}$ (kWh/m^2/year) and the German and Spanish average household floor area S_{hh} from Section 6.3.2.2.

$$CoE_{hh,B}\left(€/year\right)=SLCoE_e\times SEC_{B,residential}\times S_{hh} \quad \text{(A.10)}$$

A.4 Energy Balance Figures

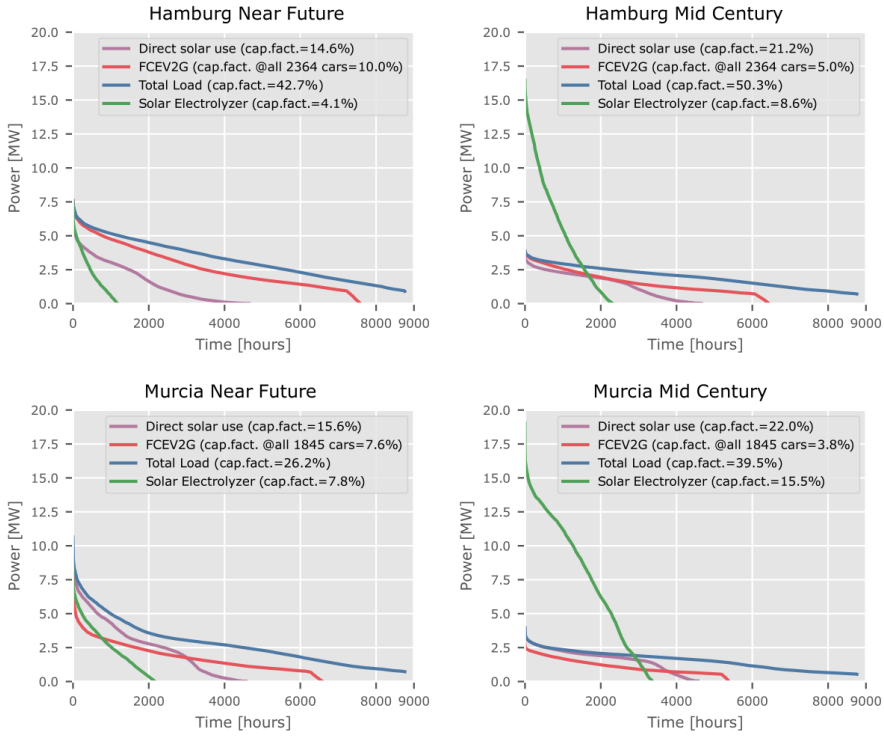

Figure A 1 Load duration curves for the simulation, based on 2016 weather data for Hamburg (top) and Murcia (bottom) for the Near Future (left) and Mid Century scenarios (right). Direct solar use (purple), FCEV2G electricity (red), combined FCEV2G and direct solar use (blue), and the solar electrolyzer power consumption (green).

Figure A 2 Hourly electricity balances for an entire year based on 2016 weather data. From top to bottom, Hamburg in the Near Future and Mid Century and Murcia in the Near Future and Mid Century.

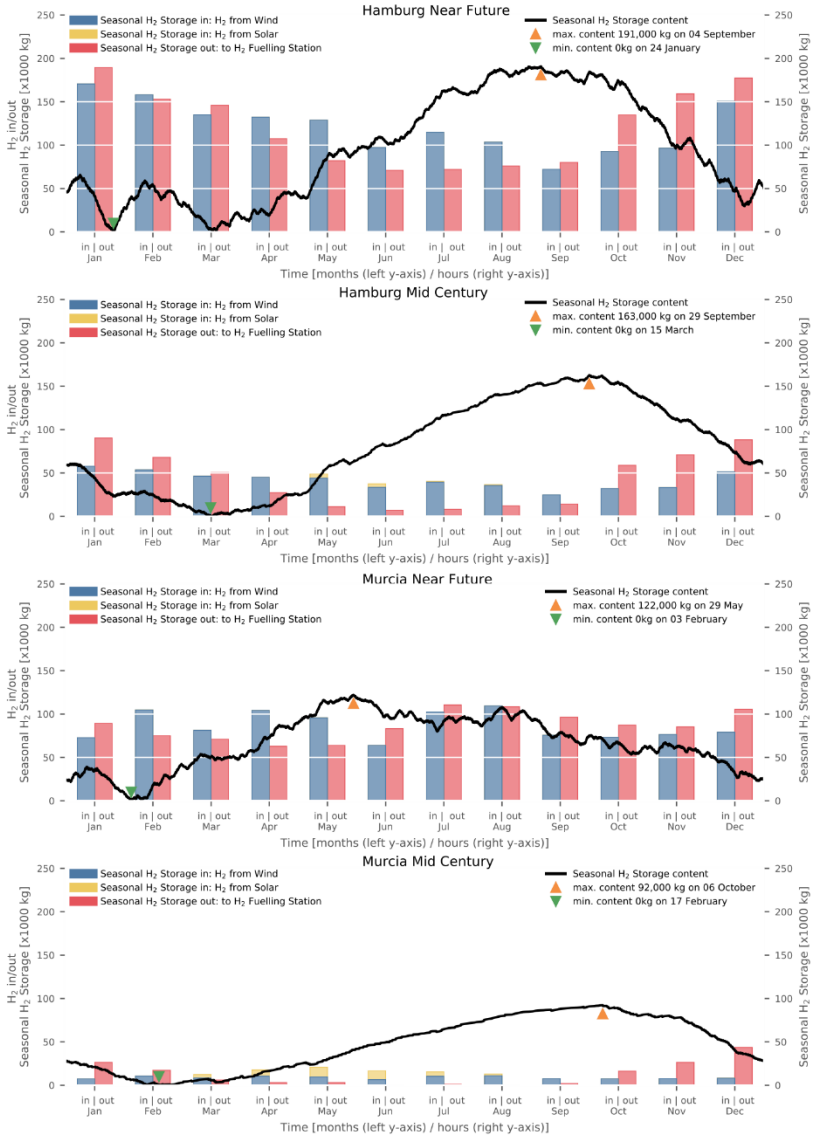

Figure A 3 Seasonal hydrogen storage content over the year (black line), from top to bottom Hamburg Near Future and Mid Century and Murcia Near Future and Mid Century. The annual maximum and minimum are indicated by an upward (orange) and downward (green) facing triangle. For every month, the bars on the left side (in) represent the monthly inflow of hydrogen from either solar (yellow) or wind (blue), and the bar on the right (out) shows the monthly outflow to the hydrogen fueling station.

Table A 7 Installed component capacities (Q) and component total annual costs (TC_i) in the smart city area Hamburg and Murcia in the Near Future and Mid Century scenario, 2012–2016 average (μ) and coefficient of variation (CV).

		Hamburg								Murcia							
		Near Future				Mid Century				Near Future				Mid Century			
		Q_i		TC_i		Q_i		TC_i		Q_i		TC_i		Q_i		TC_i	
Label	**Subsystems and Components**	**μ**	**CV [%]**	**μ [k€/yr]**	**CV [%]**	**μ**	**CV [%]**	**μ [k€/yr]**	**CV [%]**	**μ**	**CV [%]**	**μ [k€/yr]**	**CV [%]**	**μ**	**CV [%]**	**μ [k€/yr]**	**CV [%]**
	Electricity production																
S1	Solar electricity system [MWp]	11.20	-	690		18.67	-	600	-	11.20	-	690	-	18.67	-	600	-
W1	Wind turbines park share [MW]	23.36	8.3	1760	8.3	7.26	10.1	390	10.1	18.60	6.5	1400	6.5	1.43	16.4	80	16.4
	Hydrogen production and compression																
S4 and S5	Alkaline electrolyzer—solar [MW]	6.20	5.7	330	4.5	14.63	4	220	3.7	6.97	4.8	360	3.8	16.23	5.5	240	4.9
W4 and W5	Alkaline electrolyzer share—wind [MW]	21.95	8.3	1150	8.3	6.95	10.1	130	10.1	17.48	6.5	920	6.5	1.36	16.4	30	16.4
S6	Compressor—solar [kg H_2/h]	125	5.7	150	3.7	308	4	110	2.6	140	4.8	170	3.1	342	5.5	120	3.6
W6	Compressor share—wind [kg H_2/h]	441	8.3	450	5.5	146	10.1	50	6.7	351	6.5	390	4.3	29	16.4	20	10.5
	Hydrogen transport																
TT1	Tube trailer storage [kg H_2]	4620	9.5	270	9.5	4400	0	160	0	4400	-	260	0	4400	-	160	-
TT2	Tractor-trailers [#]	1.9	6.6	200	1.7	1.1	9.5	120	2.3	1.4	8.7	160	1.9	1.3	-	140	0.6

	Hydrogen fueling station (HFS)																
HFS1	Compressor [kg H_2/h]	489	4	640	4.6	240	3.4	120	2.4	343	9.6	480	8.3	172	5.1	90	8.4
HFS2	Stationary storage 875 bar [kg H_2]	5705	4.6	320	4.6	2715	3.2	100	3.2	4051	10.7	230	10.7	1954	5.5	70	5.5
HFS3	Chiller capacity [kg H_2/min]	9.5	4.6	140	4.6	4.5	3.2	60	3.2	6.7	10.7	100	10.7	3.3	5.5	40	5.5
HFS4	Dispensers units [#]	29.2	4.6	340	4.6	4.5	3.2	40	3.2	20.7	10.7	240	10.7	3.3	5.5	30	5.5
	FCEV2G																
FCEV1	Replacement of FC system in FCEV due to V2G use only [#100 kW systems]	755	7.5	1190	1.2	389	3.3	230	0.8	774	4.3	750	1.7	265	2.2	140	1.2
FCEV2	Smart grid, Control, and V2G infrastructure [# 4-point dischargers]	189	7.5	160	7.5	97	3.2	40	3.2	193	4.3	170	4.3	66	2.2	30	2.2
	Seasonal hydrogen storage (SHS)																
SHS1	Share of SHS plant (3733 ton H_2 cavern) [%]	4.1	14.7	250	14.7	3.8	7.9	200	7.9	3.9	12.9	230	12.9	2.1	12.2	110	12.2
SHS2	Tube trailer filling (compressor) at SHS [kg H_2/h]	488	4.2	210	8.5	239	3.4	40	12.5	341	9.7	160	6.3	171	5	30	3.2
	Water purification and storage																
S2	Reverse osmosis—solar [m^3/day]	95	8.3	12	8.3	31	10.1	4	10.1	75	6.4	10	6.4	6.2	16.4	1	16.4
W2	Reverse osmosis—wind [m^3/day]	6.7	3.8	0.8	3.8	20	4.5	2.6	4.5	7.6	5.7	1	5.7	21	2.1	2.6	2.1
S3	Pure-water tank—solar [m^3]	13	3.8	0.1	3.8	41	4.5	0.2	4.5	15	5.7	0.1	5.7	42	2.1	0.2	2.1
W3	Pure-water tank—wind [m^3]	189	8.3	1	8.3	63	10.1	0.3	10.1	150	6.4	0.8	6.4	12	16.4	0.1	16.4
	Total			8290	4			2620	2.2			6710	3.7			1920	2.7

A.6 Background Figures Cost of Energy for a Household

Results from previous sections serve as input for the cost of energy for a single household CoE_{hh} (€/hh/year) in Table 6-5 in Section 6.5.4 the SEC_T and average annual distance driven d from Table A6, the specific energy consumption in buildings (SEC_B) from Table A4, the number of passenger cars and households from Table 6-2, the average household floor area (S_{hh}) from Section 6.3.2.2, and the $SLCoE_e$ and $SLCoE_H$ from Table 6-4.

For the Present scenario, additional parameters are used as given in the previous sections. An average gasoline fuel consumption of a passenger car in the European Union is approximately 5.6 L/100 km [932]. Gasoline prices without taxes and levies in Germany and Spain in 2017 were 0.500 €/L and 0.544 €/L [933]. For this comparison, it is assumed that natural gas is used for space heating, water heating, cooking, and electricity for space cooling, lighting, and appliances. Average electricity prices without taxes and levies for households in Germany and Spain in 2017 were 164 €/MWh (1000–2500 kWh annual consumption) and 150 €/MWh (5000–15,000 kWh annual consumption), and natural gas prices without taxes and levies were 45 €/MWh (20–200 GJ annual consumption) and 80 €/MWh (<20 GJ annual consumption) [934,935].

B Fuel cell electric vehicles and hydrogen balancing 100 percent renewable and integrated national transportation and energy systems

B.1 Hourly electricity generation and consumption figures

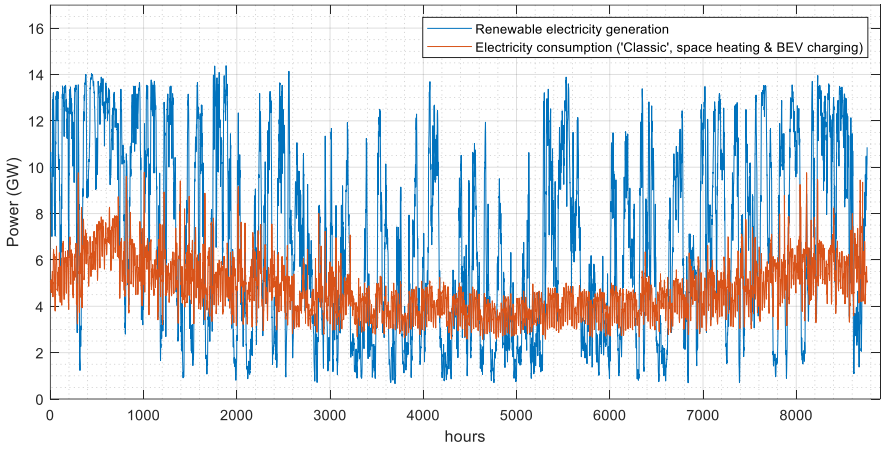

Figure B1 Hourly electricity consumption (orange) versus the renewable electricity generation (blue) for Denmark.

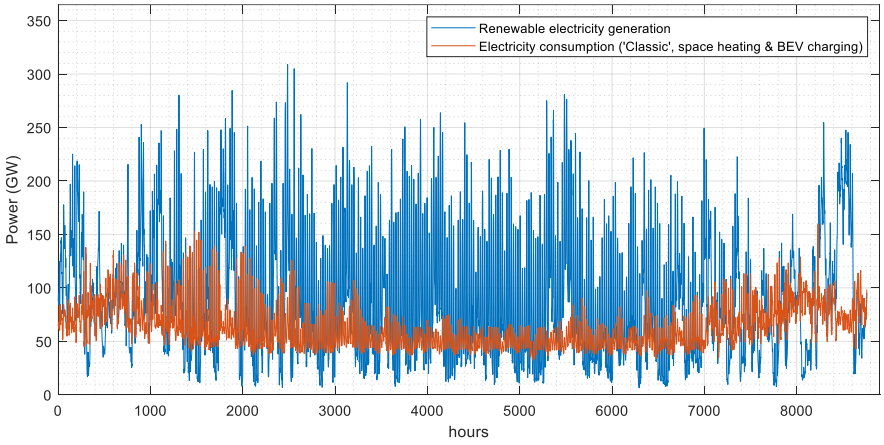

Figure B2 Hourly electricity consumption (orange) versus the renewable electricity generation (blue) for Germany.

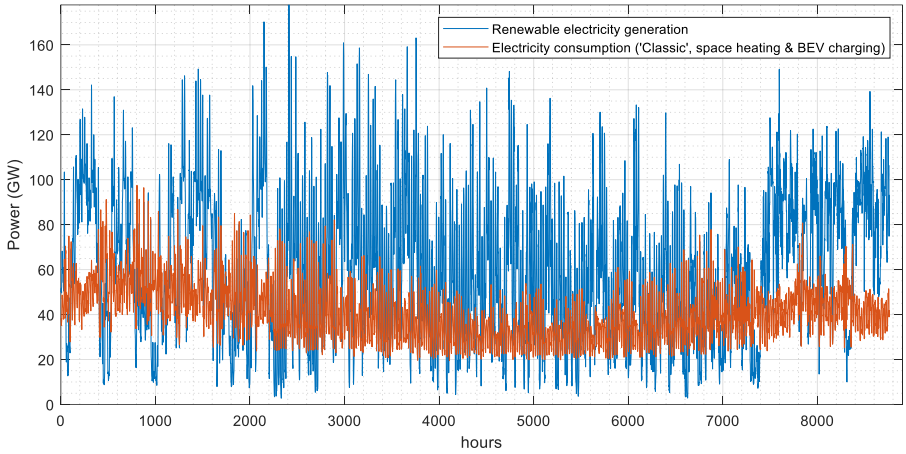

Figure B3 Hourly electricity consumption (orange) versus the renewable electricity generation (blue) for Great Britain.

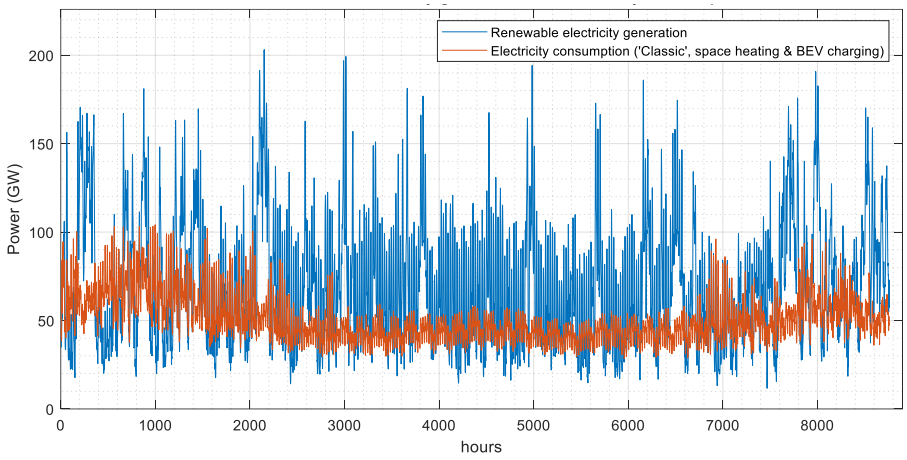

Figure B4 Hourly electricity consumption (orange) versus the renewable electricity generation (blue) for France.

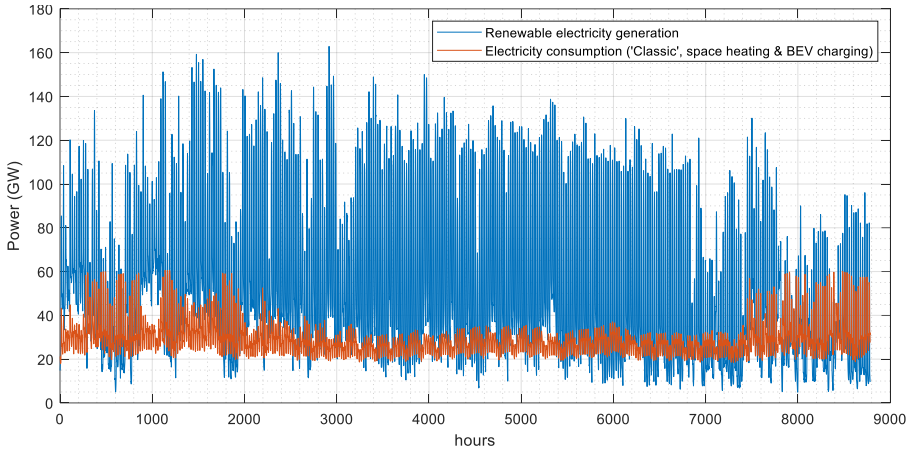

Figure B5 Hourly electricity consumption (orange) versus the renewable electricity generation (blue) for Spain.

B.2 Annual energy balance figures

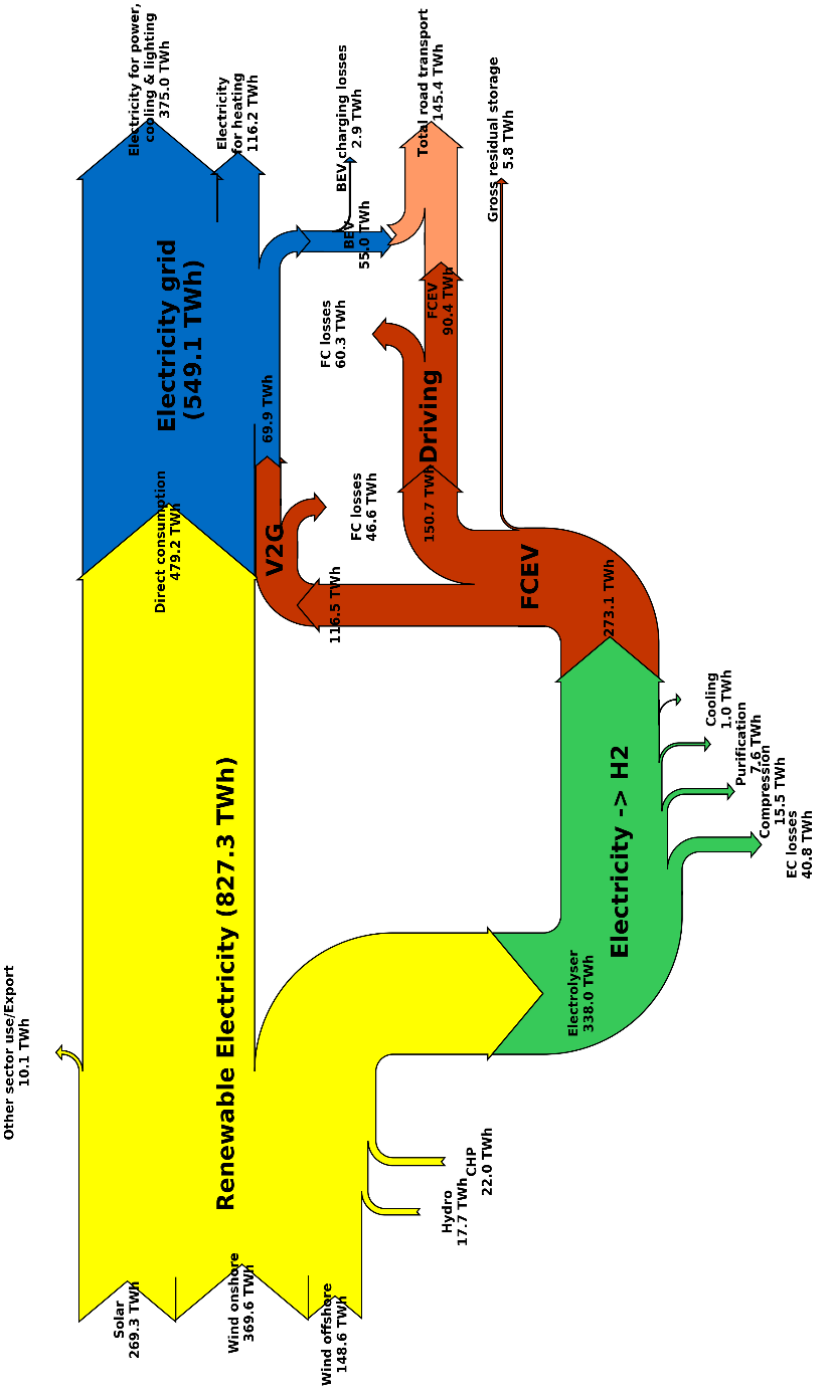

Figure B6 Annual energy balance (TWh/year) for Germany in 2050 based on 2017 renewable energy data.

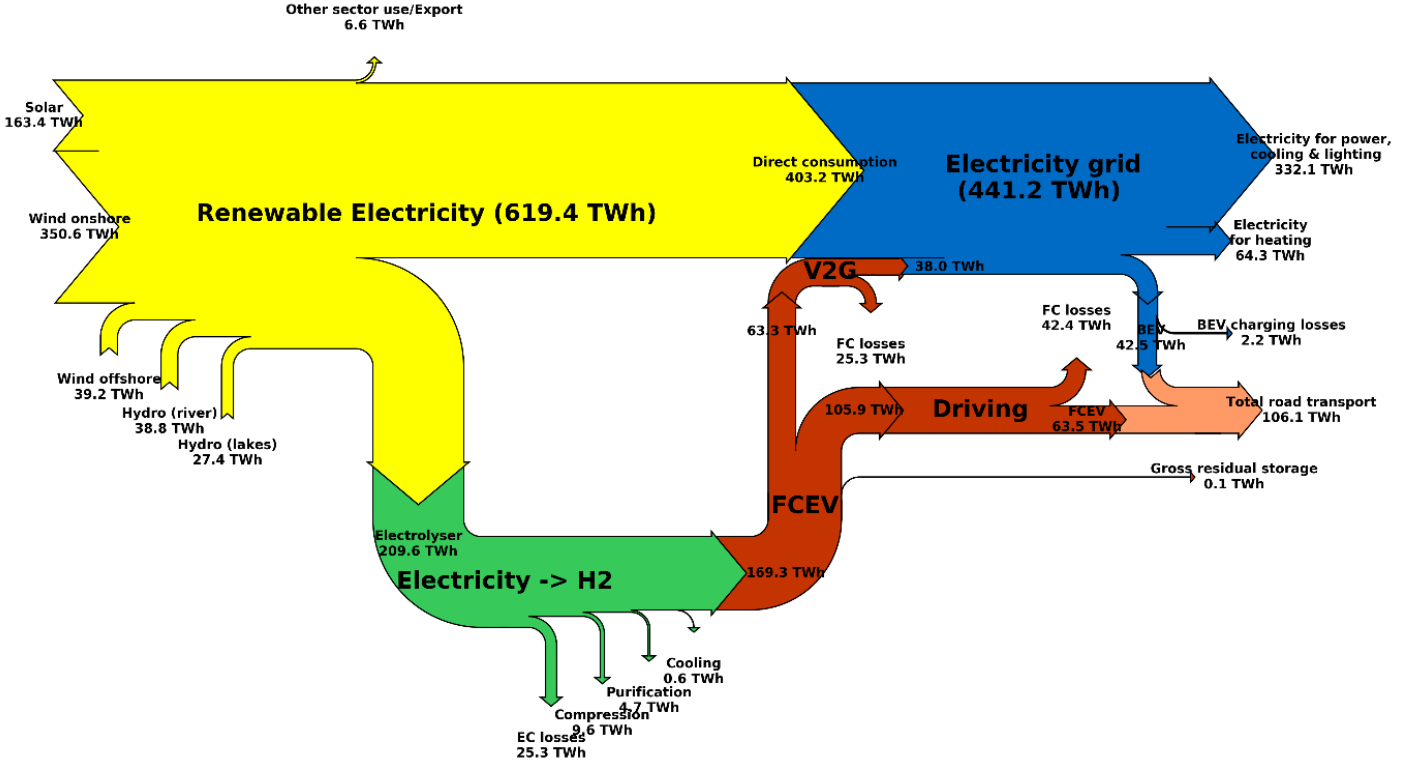

Figure B7 Annual energy balance (TWh/year) for France in 2050 based on 2017 renewable energy data.

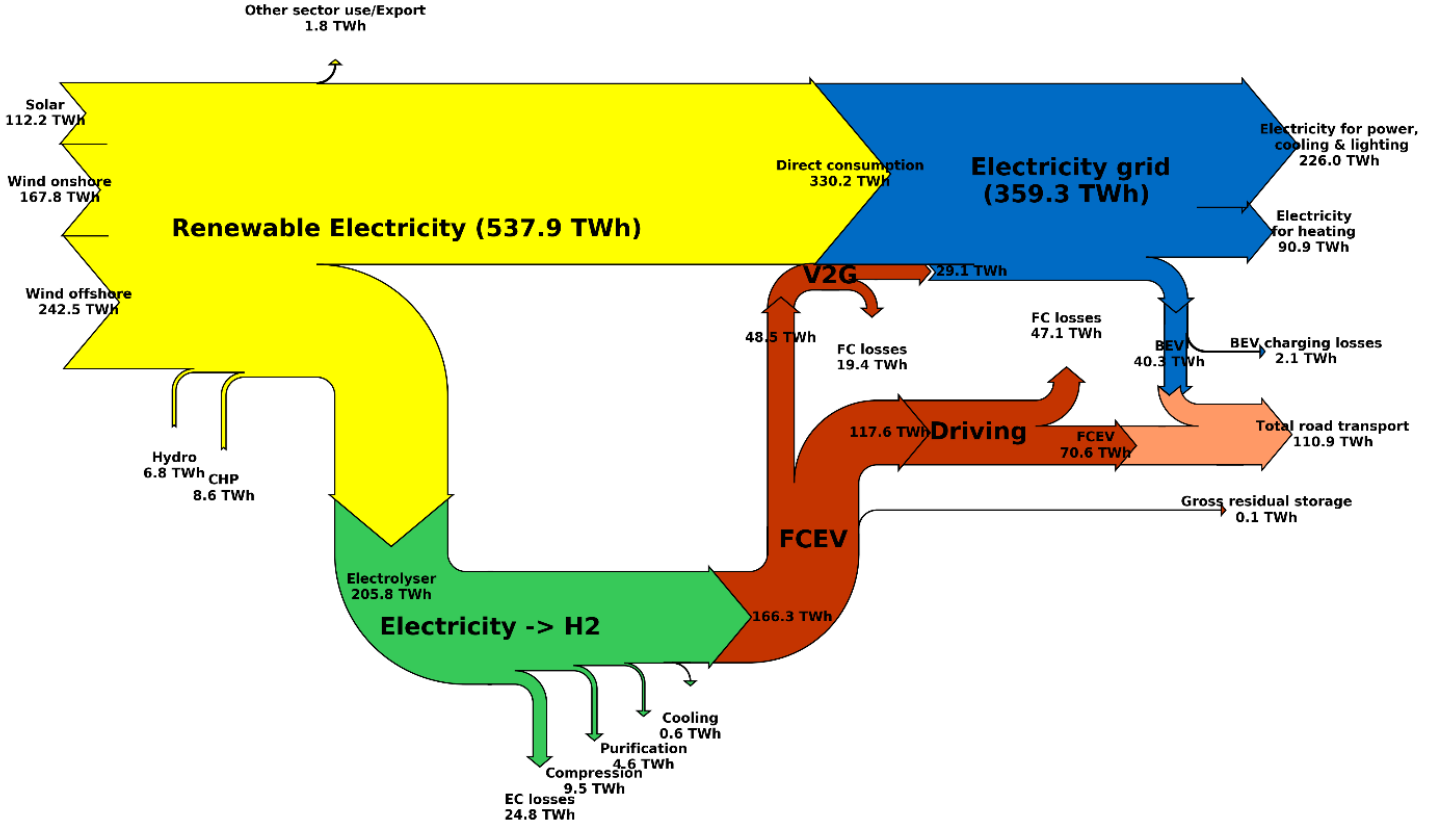

Figure B8 Annual energy balance (TWh/year) for Great Britain in 2050 based on 2017 renewable energy data.

B.3 Hourly distribution of Fuel Cell Electric Vehicle to Grid electricity production figures

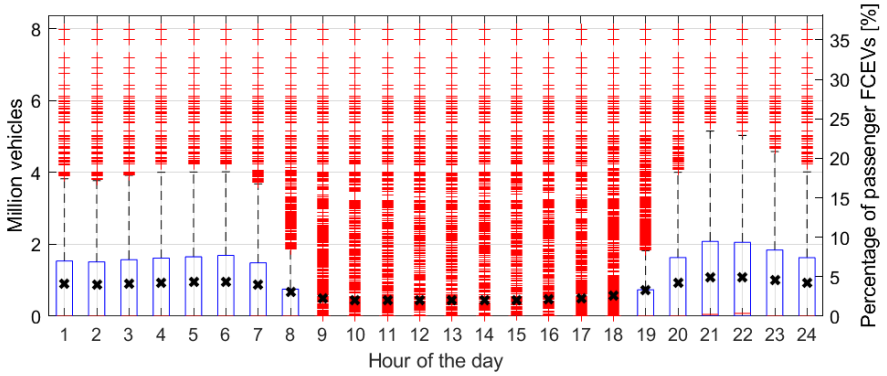

Figure B9 Boxplot showing the hourly distribution of FCEV2G electricity production in Germany (million vehicles left y-axis, % of all FCEV passenger cars right y-axis) throughout the day (based on 2014-2017 input data). The black crosses represent the mean values, the medians are indicated by the red horizontal lines in the blue bars. The blue bars represent the range of 50% of the data points. The whiskers represent approximately 49% of the data points. The red pluses indicate the outliers, outside the above-mentioned ranges, and represent less than 1%.

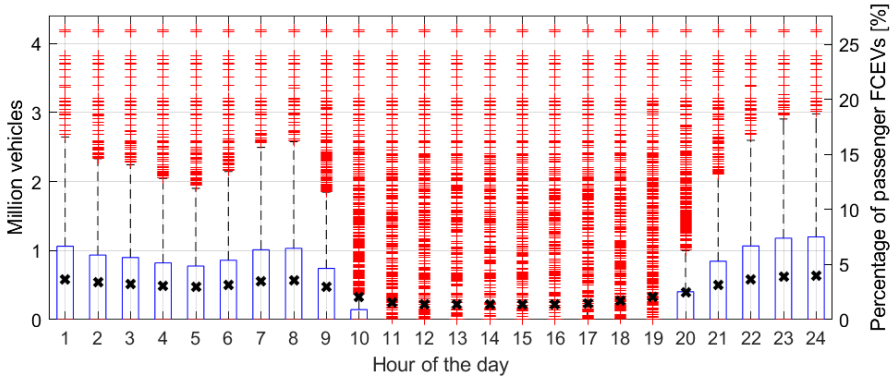

Figure B10 Boxplot showing the hourly distribution of FCEV2G electricity production in France (million vehicles left y-axis, % of all FCEV passenger cars right y-axis) throughout the day (based on 2014-2017 input data). The black crosses represent the mean values, the medians are indicated by the red horizontal lines in the blue bars. The blue bars represent the range of 50% of the data points. The whiskers represent approximately 49% of the data points. The red pluses indicate the outliers, outside the above-mentioned ranges, and represent less than 1%.

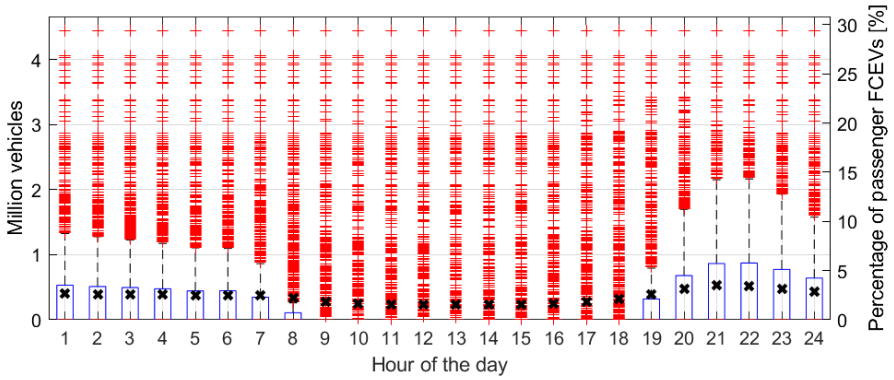

Figure B11 Boxplot showing the hourly distribution of FCEV2G electricity production in Great Britain (million vehicles left y-axis, % of all FCEV passenger cars right y-axis) throughout the day (based on 2015-2017 input data). The black crosses represent the mean values, the medians are indicated by the red horizontal lines in the blue bars. The blue bars represent the range of 50% of the data points. The whiskers represent approximately 49% of the data points. The red pluses indicate the outliers, outside the above-mentioned ranges, and represent less than 1%.

Nomenclature

AC	Alternating Current
aFRR	automatic Frequency Restoration Reserves
BEV	Battery Electric Vehicle
BHDC	Bi-directional High-voltage DC-DC Converter
CAN	Controller Area Network
CSD	Cold Shut Down
Δm_{H2}	Hydrogen Consumption / kg
$\Delta m_{H2}\, \Delta t^{-1}$	Hydrogen Consumption Rate / kg h^{-1}
$\Delta P\, \Delta t^{-1}$	Upward or Downward Electric Power Gradient / kW s^{-1} or % s^{-1}
ΔSOC	Difference State of Charge High Voltage Battery / %
DD	Day
DC	Direct Current
η	Efficiency / %
η_{DCAC}	Direct Current to Alternating Current Efficiency / %
$\eta_{T2G\text{-}AC}$	Higher Heating Value Tank-to-Grid Alternating Current Efficiency / %
$\eta_{T2G\text{-}DC}$	Higher Heating Value Tank-to-Grid Direct Current Efficiency / %
E_{AC}	Alternating Current Electrical Energy / kWh
E_{DC}	Direct Current Electrical Energy / kWh
$E_{HV\ Bat,\ max}$	High Voltage Battery Maximum Electrical Energy / 0.95 kWh
EV	Electric Vehicle
EU	European Union
EUR	Euro
FC	Fuel Cell
FCEV	Fuel Cell Electric Vehicle
FCEV2G	Fuel Cell Electric Vehicle to Grid
FCR	Frequency Containment Reserves
h	hours
H_2	Hydrogen
HHV	Higher Heating Value of Hydrogen / 39.41 kWh kg^{-1}
HV	High Voltage
HVJB	High Voltage Junction Box
$I_{component,gross}$	Gross Current of Component (Fuel Cell or High Voltage Battery) / A
LED	Light Emitting Diode
LHV	Lower Heating Value of Hydrogen / 33.3 kWh kg^{-1}
MM	Month
NEDC	New European Driving Cycle
OCV	Open Circuit Voltage
p	Pressure / Pa
$P_{component,e,gross}$	Gross Electric Power of Component (Fuel Cell or High Voltage Battery) / kW
$P_{V2G\ DC\ max}$	Maximum Vehicle to Grid Direct Current Electric Power / 10 kW
PEM	Proton Exchange Membrane

PEMFC	Proton Exchange Membrane Fuel Cell
PHEV	Plug-in Hybrid Electric Vehicle
ρ	Density / kg m^{-3}
RDW	Dutch National Vehicle and Driving License Registration Authority
RGB	Red-Blue-Green
SAE	Society of Automotive Engineers
SOC	State Of Charge High Voltage Battery / %
t_{end}	Test End Time / h
$t_{GC/D}$	Grid Connect/Disconnect Time / h
t_{grid}	Grid connection time / h
t_{start}	Test Start Time / h
t_{test}	Test Start Time / h
T	Temperature / °C
T2G	Tank-to-Grid
T2G-AC	Tank-to-Grid Alternating Current
T2G-DC	Tank-to-Grid Direct Current
$U_{component}$	Voltage of Component (Fuel Cell or High Voltage Battery) / V
USD	United States Dollar
V2G	Vehicle-to-Grid
V2G-DCAC	Vehicle-to-Grid Direct Current to Alternating Current
V2L	Vehicle-to-Load
V2H	Vehicle-to-Home
V_{tanks}	Volume Capacity Hydrogen Tanks / 0.144 m^3
YY	Year

References

[1] European Automobile Manufacturers Association (ACEA). The Automobile Industry Pocket Guide 2020/2021 2020.

[2] van Wijk AJM, Verhoef LA. Our Car as Power Plant. Amsterdam: Ios Press; 2014. doi:10.3233/978-1-61499-377-3-i.

[3] Eurostat. Electricity production capacities by main fuel groups and operator [nrg_inf_epc] - 2019 2021.

[4] UNFCCC. Historic Paris Agreement on Climate Change. UN Clim Chang Newsroom 2015:8. doi:10.1017/CBO9781107415324.004.

[5] Kinney PL. Interactions of Climate Change, Air Pollution, and Human Health. Curr Environ Heal Reports 2018;5:179–86. doi:10.1007/s40572-018-0188-x.

[6] European Environment Agency. Air quality in Europe — 2020 report - EEA Report No 9/2020. Publ Off Eur Union 2020.

[7] European Environment Agency. Cutting air pollution in Europe would prevent early deaths, improve productivity and curb climate change 2020.

[8] UNFCCC. Climate Ambition Alliance: Net Zero 2050. Glob Clim Action 2020.

[9] European Commission. The European Green Deal - COM(2019) 640 final. Commun from Comm to Eur Parliam Eur Counc Counc Eur Econ Soc Comm Comm Reg 2019.

[10] European Environment Agency. GHG emissions by sector in the EU-28, 1990-2016 2018.

[11] Eurostat. Energy statistics - an overview, statistics explained 2020.

[12] European Environment Agency. Final energy consumption of petroleum products by sector 1990-2016 2018.

[13] European Commission. Transport in the European Union - Current Trends and Issues 2019.

[14] European Commission. A Clean Planet for all. A European long-term strategic vision for a prosperous, modern, competitive and climate neutral economy. Com(2018) 773 2018:393.

[15] Erbach G. Energy storage and sector coupling - Towards an integrated, decarbonised energy system. Eur Parliam Res Serv 2019.

[16] BloombergNEF, Eaton, Statkraft. Sector Coupling in Europe: Powering Decarbonization - Potential and Policy Implications of Electrifying the Economy 2020.

[17] European Commission. A hydrogen strategy for a climate-neutral Europe COM(2020) 301 final. Commun from Comm to Eur Parliam Eur Counc Counc Eur Econ Soc Comm Comm Reg 2020.

[18] European Commission. Powering a climate-neutral economy: An EU Strategy for Energy System Integration COM(2020) 299 final. Commun from Comm to Eur Parliam Eur Counc Counc Eur Econ Soc Comm Comm Reg 2020.

[19] European Commission. European Clean Hydrogen Alliance - declaration. New Ind Strateg 2020.

[20] Van Wijk AJM, van der Roest E, Boere J. Solar Power to the People.

Nieuwegein, The Netherlands: Allied Waters; 2018.
[21] David B. Session: NH3 Fuel Use - Hydrogen Cycle. 2016 NH3 Fuel Conf 2016.
[22] BloombergNEF. Scale-up of Solar and Wind Puts Existing Coal, Gas at Risk 2020.
[23] International Renewable Energy Agency (IRENA). Renewable Power Generation Costs in 2019 2020.
[24] Vartiainen E, Masson G, Breyer C, Moser D, Román Medina E. Impact of weighted average cost of capital, capital expenditure, and other parameters on future utility-scale PV levelised cost of electricity. Prog Photovoltaics Res Appl 2020;28:439–53. doi:10.1002/pip.3189.
[25] Luther-Jones N. Europe's Subsidy-free Transition – the road to grid parity. DLA Piper 2019.
[26] Weaver JF. Top ten list of lowest solar power prices in the world – updated November 23, 2020. CommercialSolarGuyCom 2020.
[27] Evans S, Gabbatiss J. Solar is now 'cheapest electricity in history', confirms IEA. Carbon Br 2020.
[28] Komusanac I, Brindley G, Fraile D, Walsh C. Wind energy in Europe in 2019 - Trends and statistics. Wind Bus Intell 2019.
[29] Department for Business Energy & Industrial Strategy (BEIS). Electricity Generation Costs 2020. UK Gov 2020.
[30] Carden K, Dombrowsky AK, Winkler C. 2020 Joint IOU ELCC Study Report 1 - Decision Adopting Modeling Requirements to Calculate Effective Load Carrying Capability (ELCC) Values for Renewables Portfolio Standard Procurement. Astrapé Consult South Calif Edison Company, Pacific Gas Electr Company, San Diego Gas Electr Co 2020.
[31] Lazard. Lazard's Levelized Cost of Energy Analysis - Version 14.0 2020.
[32] Lazard. Lazard's Levelized Cost of Storage Analysis - Version 6.0 2020.
[33] Bloch C, Newcomb J, Shiledar S, Tyson M. Breakthrough Batteries: Powering the Era of Clean Electrification. Rocky Mt Inst 2019.
[34] Irany R, Kumar A, Gnoth D, Guesmi A. Energy Storage Monitor Latest trends in energy storage | 2019. World Energy Counc 2019.
[35] International Energy Agency (IEA). Capital cost of utility-scale battery storage systems in the New Policies Scenario, 2017-2040 2019.
[36] Ralon P, Taylor M, Ilas A, Diaz-Bone H, Kairies K. Electricity storage and renewables: Costs and markets to 2030. Int Renew Energy Agency Abu Dhabi, UAE 2017.
[37] Eurelectric. Decarbonisation pathways Full study results 2018. https://cdn.eurelectric.org/media/3558/decarbonisation-pathways-all-slideslinks-29112018-h-4484BB0C.pdf (accessed November 1, 2019).
[38] Teske S, Sawyer S, Schäfer O. energy [r]evolution a sustainable world energy outlook 2015 - 100% renewable energy for all. Greenpeace Int Glob Wind Energy Counc Sol Power Eur 2015.
[39] Buck M, Graf A, Graichen P. European Energy Transition 2030: The Big Picture. Ten Priorities for the next European Commission to meet the EU's 2030 targets and accelerate towards 2050. Agora Energiewende 2019.

[40] International Renewable Energy Agency (IRENA). Global Renewables Outlook: Energy transformation 2050 (Edition: 2020) 2020.
[41] Baldino C, O'Malley J, Searle S, Zhou Y, Christensen A. Hydrogen for heating? Decarbonization options for households in the United Kingdom in 2050. Int Counc Clean Transp (ICCT), Three Seas Consult 2020.
[42] Gamon C. Report on a comprehensive European approach to energy storage (2019/2189(INI)). Comm Ind Res Energy, Eur Parliam 2020.
[43] European Commission. Sustainability criteria for biofuels specified 2019.
[44] Mortensen AW, Mathiesen BV, Hansen AB, Pedersen SL, Grandal RD, Wenzel H. The role of electrification and hydrogen in breaking the biomass bottleneck of the renewable energy system – A study on the Danish energy system. Appl Energy 2020. doi:10.1016/j.apenergy.2020.115331.
[45] Olsson O, Bailis R. Electrification and the bioeconomy: three sides to the story - Discussion brief. Stock Environ Inst 2019.
[46] Prussi M, O'Connell A, Lonza L. Analysis of current aviation biofuel technical production potential in EU28. Biomass and Bioenergy 2019. doi:10.1016/j.biombioe.2019.105371.
[47] Ghosh P, Westhoff P, Debnath D. Biofuels, food security, and sustainability. Biofuels, Bioenergy Food Secur., 2019. doi:10.1016/b978-0-12-803954-0.00012-7.
[48] Blanco H, Faaij A. A review at the role of storage in energy systems with a focus on Power to Gas and long-term storage. Renew Sustain Energy Rev 2018. doi:10.1016/j.rser.2017.07.062.
[49] Quiggin D, Buswell R. The implications of heat electrification on national electrical supply-demand balance under published 2050 energy scenarios. Energy 2016;98:253–70. doi:10.1016/j.energy.2015.11.060.
[50] Märkle-Huß J, Feuerriegel S, Neumann D. Large-scale demand response and its implications for spot prices, load and policies: Insights from the German-Austrian electricity market. Appl Energy 2018. doi:10.1016/j.apenergy.2017.08.039.
[51] Kohlhepp P, Harb H, Wolisz H, Waczowicz S, Müller D, Hagenmeyer V. Large-scale grid integration of residential thermal energy storages as demand-side flexibility resource: A review of international field studies. Renew Sustain Energy Rev 2019;101:527–47. doi:10.1016/j.rser.2018.09.045.
[52] Lindberg CF, Zahedian K, Solgi M, Lindkvist R. Potential and limitations for industrial demand side management. Energy Procedia, 2014. doi:10.1016/j.egypro.2014.11.1138.
[53] Gracceva F, Zeniewski P. A systemic approach to assessing energy security in a low-carbon EU energy system. Appl Energy 2014. doi:10.1016/j.apenergy.2013.12.018.
[54] Deane JP, Gracceva F, Chiodi A, Gargiulo M, Gallachóir BPÓ. Assessing power system security. A framework and a multi model approach. Int J Electr Power Energy Syst 2015. doi:10.1016/j.ijepes.2015.04.020.
[55] Victoria M, Zhu K, Brown T, Andresen GB, Greiner M. The role of storage technologies throughout the decarbonisation of the sector-coupled

European energy system. Energy Convers Manag 2019. doi:10.1016/j.enconman.2019.111977.
[56] Bussar C, Stöcker P, Cai Z, Moraes L, Magnor D, Wiernes P, et al. Large-scale integration of renewable energies and impact on storage demand in a European renewable power system of 2050-Sensitivity study. J Energy Storage 2016. doi:10.1016/j.est.2016.02.004.
[57] Gas Infrastructure Europe (GIE). STORAGE MAP 2018 - existing & planned infrastructure 2018. https://www.gie.eu/download/maps/2018/GIE_STOR_2018_A0_1189x841_FULL_FINAL.pdf (accessed November 2, 2019).
[58] Brown T, Schlachtberger D, Kies A, Schramm S, Greiner M. Synergies of sector coupling and transmission reinforcement in a cost-optimised, highly renewable European energy system. Energy 2018. doi:10.1016/j.energy.2018.06.222.
[59] Wilson G. Multi-vector energy diagram Great Britain - daily resolution 2014-2019. Energy-Charts Dot Org 2020.
[60] (EBN) EN. Energy in Numbers 2020 2020.
[61] Bundesverband der Energie- und Wasserwirtschaft (BDEW). Monatlicher Erdgasverbrauch in Deutschland 2020 - Vorjahresvergleich 2020.
[62] Boblenz K, Frank V, Meyer B. Energy system analysis for evaluation of sector coupling technologies. Fuel 2019. doi:10.1016/j.fuel.2019.115658.
[63] Matsuo Y, Endo S, Nagatomi Y, Shibata Y, Komiyama R, Fujii Y. Investigating the economics of the power sector under high penetration of variable renewable energies. Appl Energy 2020. doi:10.1016/j.apenergy.2019.113956.
[64] Huneke F, Perez Linkenheil C, Niggemeier M. Kalte Dunkelflaute Robustheid des Stromsystems bei Extremwetter. Energy Brainpool 2017.
[65] Diesendorf M, Elliston B. The feasibility of 100% renewable electricity systems: A response to critics. Renew Sustain Energy Rev 2018. doi:10.1016/j.rser.2018.05.042.
[66] Argyrou MC, Christodoulides P, Kalogirou SA. Energy storage for electricity generation and related processes: Technologies appraisal and grid scale applications. Renew Sustain Energy Rev 2018. doi:10.1016/j.rser.2018.06.044.
[67] Cebulla F, Naegler T, Pohl M. Electrical energy storage in highly renewable European energy systems: Capacity requirements, spatial distribution, and storage dispatch. J Energy Storage 2017. doi:10.1016/j.est.2017.10.004.
[68] Reuß M, Grube T, Robinius M, Preuster P, Wasserscheid P, Stolten D. Seasonal storage and alternative carriers: A flexible hydrogen supply chain model. Appl Energy 2017;200:290–302. doi:10.1016/j.apenergy.2017.05.050.
[69] Shah SK, Aye L, Rismanchi B. Seasonal thermal energy storage system for cold climate zones: A review of recent developments. Renew Sustain Energy Rev 2018. doi:10.1016/j.rser.2018.08.025.
[70] Lanahan M, Tabares-Velasco PC. Seasonal thermal-energy storage: A critical review on BTES systems, modeling, and system design for higher

system efficiency. Energies 2017. doi:10.3390/en10060743.
[71] Moser M, Gils H-C, Pivaro G. A sensitivity analysis on large-scale electrical energy storage requirements in Europe under consideration of innovative storage technologies. J Clean Prod 2020;269:122261. doi:10.1016/j.jclepro.2020.122261.
[72] Nastasi B, Lo Basso G, Astiaso Garcia D, Cumo F, de Santoli L. Power-to-gas leverage effect on power-to-heat application for urban renewable thermal energy systems. Int J Hydrogen Energy 2018. doi:10.1016/j.ijhydene.2018.08.119.
[73] Hydrogen Council. Path to hydrogen competitiveness A cost perspective 2020.
[74] Global Commission on the Geopolitics of Energy Transformation, IRENA. A New World The Geopolitics of the Energy Transformation 2019.
[75] Pflugmann F, Blasio N De. The Geopolitics of Renewable Hydrogen in Low-Carbon Energy Markets. Geopolit Hist Int Relations 2020;12:7. doi:10.22381/GHIR12120201.
[76] Van de Graaf T, Overland I, Scholten D, Westphal K. The new oil? The geopolitics and international governance of hydrogen. Energy Res Soc Sci 2020. doi:10.1016/j.erss.2020.101667.
[77] PricewaterhouseCoopers (PWC) Australia. Embracing clean hydrogen for Australia - How the journey towards decarbonisation can be fuelled by Hydrogen 2020.
[78] van Wijk A, Chatzimarkakis J. Green Hydrogen for a European Green Deal A 2x40 GW Initiative. Hydrog Eur 2020.
[79] van Wijk A, Wouters F, Rachidi S, Ikken B. A North Africa - Europe Hydrogen Manifesto. Dii Desert Energy 2019.
[80] Tröndle T, Pfenninger S, Lilliestam J. Home-made or imported: On the possibility for renewable electricity autarky on all scales in Europe. Energy Strateg Rev 2019. doi:10.1016/j.esr.2019.100388.
[81] Saadi FH, Lewis NS, McFarland EW. Relative costs of transporting electrical and chemical energy. Energy Environ Sci 2018. doi:10.1039/c7ee01987d.
[82] Vermeulen U. Turning a hydrogen economy into reality. 28th Meet Steer Comm IPHE, Hague, 21 Novemb 2017 2017.
[83] Krieg D. Konzept und Kosten eines Pipelinesystems zur Versorgung des deutschen Straßenverkehrs mit Wasserstoff. Forschungszentrums Jülich 2012.
[84] Taieb A, Shaaban M. Cost Analysis of Electricity Transmission from Offshore Wind Farm by HVDC and Hydrogen Pipeline Systems. 2019 IEEE PES GTD Gd. Int. Conf. Expo. Asia, GTD Asia 2019, 2019. doi:10.1109/GTDAsia.2019.8715900.
[85] James BD, DeSantis DA, Huya-Kouadio JM, Houchins C, Saur G. Analysis of Advanced H2 Production & Delivery Pathways - Project ID: PD102. Strateg Anal (SA), Natl Renew Energy Lab 2018.
[86] Guidehouse. Gas Decarbonisation Pathways 2020–2050. Gas Clim Consort 2020.
[87] Eurostat. Share of energy from renewable sources [nrg_ind_ren]

Renewable energy sources in transport 2020.
[88] European Commission. Road transport: Reducing CO2 emissions from vehicles 2020.
[89] European Parliament. CO2 emissions from cars: facts and figures (infographics) 2019.
[90] Nathaniel Bullard. Electric Car Price Tag Shrinks Along With Battery Cost. BloombergNEF 2019.
[91] Neuhausen J, Andre F, Assmann J, Stürmer C. Staying profitable in the new era of electrification - Powertrain study 2020. Strateg &, PWC 2020.
[92] Nassif GG, Almeida SCA d. Impact of powertrain hybridization on the performance and costs of a fuel cell electric vehicle. Int J Hydrogen Energy 2020. doi:10.1016/j.ijhydene.2020.05.138.
[93] BloombergNEF. Battery Pack Prices Cited Below $100/kWh for the First Time in 2020, While Market Average Sits at $137/kWh 2020.
[94] Boretti A. The Future of the Internal Combustion Engine After "Diesel-Gate." SAE Tech Pap 2017-28-1933 2017. doi:10.4271/2017-28-1933.
[95] Adams J, Houchins C, Ahluwalia R. Onboard Type IV Compressed Hydrogen Storage System —Cost and Performance Status. USA Dep Energy Hydrog Fuel Cells Progr Rec 2019.
[96] Wilson A, Kleen G, Papageorgopoulos D. Fuel Cell System Cost - 2017 - DOE Hydrogen and Fuel Cells Program Record 2017. https://www.hydrogen.energy.gov/pdfs/17007_fuel_cell_system_cost_2017.pdf (accessed August 28, 2019).
[97] Whiston MM, Azevedo IL, Litster S, Whitefoot KS, Samaras C, Whitacre JF. Expert assessments of the cost and expected future performance of proton exchange membrane fuel cells for vehicles. Proc Natl Acad Sci U S A 2019. doi:10.1073/pnas.1804221116.
[98] James BD. Fuel Cell Systems Analysis - Project ID# FC163. 2019 US DOE Hydrog Fuel Cells Progr Rev 2019.
[99] Mohrdieck C, Dehn S. The Intelligent Fuel Cell Plug-in Hybrid Drive System of the Mercedes-Benz GLC F-Cell. ATZelectronics Worldw 2019. doi:10.1007/s38314-019-0019-3.
[100] cH2ange. Prof. Dr. Mohrdieck (Daimler): "The GLC F-CELL has tremendous acceleration, and zero emission." MediumCom 2017.
[101] Harvey J. Platinum's days as fuel cell car component may be numbered. Reuters 2018.
[102] Hao H, Geng Y, Tate JE, Liu F, Sun X, Mu Z, et al. Securing Platinum-Group Metals for Transport Low-Carbon Transition. One Earth 2019. doi:10.1016/j.oneear.2019.08.012.
[103] Robinius M, Kuckertz P, Stolten D, Grube T, Syranidis K, Reuß M, et al. Comparative Analysis of Infrastructures: Hydrogen Fueling and Electric Charging of Vehicles. Jülich, Germany: Forschungszentrum Jülich GmbH Zentralbibliothek, Verlag Jülich; 2018.
[104] Deloitte China, Systems BP. Fueling the Future of Mobility Hydrogen and fuel cell solutions for transportation Volume 1 2020. https://www2.deloitte.com/content/dam/Deloitte/cn/Documents/finance

/deloitte-cn-fueling-the-future-of-mobility-en-200101.pdf (accessed May 4, 2020).
[105] Directorate-General for Research and Innovation Unit F – Bioeconomy. A sustainable bioeconomy for Europe: strengthening the connection between economy, society and the environment - Updated Bioeconomy Strategy. Eur Comm 2018. doi:10.2777/792130.
[106] Burch I, Gilchrist J. Survey of Global Activity to Phase Out Internal Combustion Engine Vehicles - April 2020 Revision. Clim Cent 2020.
[107] Wappelhorst S, Cui H. Growing momentum: Global overview of government targets for phasing out sales of new internal combustion engine vehicles. Int Counc Clean Transp 2020.
[108] European Automobile Manufacturers Association (ACEA), Potsdam Institute for Climate Impact Reasearch (PIK), Scania, Daimler Truck, Volvo Group, CNH Industrial, et al. Joint Statement - The transition to zero-emission road freight transport 2020.
[109] European Commission. REGULATION (EU) 2019/1242 OF THE EUROPEAN PARLIAMENT AND OF THE COUNCIL of 20 June 2019 setting CO2 emission performance standards for new heavy-duty vehicles and amending Regulations (EC) No 595/2009 and (EU) 2018/956 of the European Parliament and of th. Off J Eur Union 2019.
[110] International Energy Agency (IEA). Global EV Outlook 2020 - Entering the decade of electric drive? 2020.
[111] Association of European Automotive and Industrial Battery Manufacturers (EUROBAT). Battery Innovation Roadmap 2030 2020.
[112] Anwar S, Zia MYI, Rashid M, Rubens GZ de, Enevoldsen P. Towards Ferry Electrification in the Maritime Sector. Energies 2020. doi:10.3390/en13246506.
[113] European Maritime Safety Agency (EMSA), DNV GL AS Maritime. Electrical Energy Storage for Ships - EMSA Maritime Battery Study 2020.
[114] (WSDOT) WSD of T. Washington Electric Aircraft Feasibility Study 2020.
[115] Fuel Cells and Hydrogen 2 Joint Undertaking (FCH2JU). Hydrogen roadmap Europe - A sustainable pathway for the European energy transition 2019. doi:https://doi.org/10.2843/341510.
[116] Fuel Cells and Hydrogen 2 Joint Undertaking (FCH2JU). Hydrogen Roadmap Europe - A Sustainable pathway for the European energy transition. 2019.
[117] Ruf Y, Baum M, Zorn T, Menzel A, Rehberger J. Study report Fuel Cells Hydrogen trucks - Heavy-Duty's High Performance Green Solution. Fuel Cell Hydrog 2 Jt Undert (FCH 2 JU) 2020.
[118] Tronstad T, Åstrand HH, Haugom GP, Langfeldt L. Study on the use of fuel cells in shipping. Eur Marit Saf Agency (EMSA), DNV GL Marit 2017.
[119] Ruf Y, Zorn T, De Neve PA, Andrae P, Erofeeva S, Garrison F, et al. Study on the use of fuel cells and hydrogen in the railway environment - Final Study. Rol Berger Shift2Rail Jt Undertaking, Fuel Cells Hydrog Jt Undert 2019. doi:10.2881/495604.
[120] Thomson R, Weichenhain U, Sachdeva N, Kaufmann M. Hydrogen | A future fuel for aviation? Rol Berger 2020.

[121] McKinsey & Company. Hydrogen-powered aviation A fact-based study of hydrogen technology, economics, and climate impact by 2050. Clean Sky 2 JU, Fuel Cells Hydrog 2 JU 2020.
[122] European Federation for Transport and Environment. CO2 Emissions from cars: the facts 2018.
[123] European Environment Agency. Final energy consumption in Europe by mode of transport 2019.
[124] European Alternative Fuels Observatory (EAFO). Road Transport | Passenger cars M1 2020.
[125] Samsun RC, Antoni L, Rex M. Report on Mobile Fuel Cell Application: Tracking Market Trends. Adv Fuel Cells Technol Collab Program Int Energy Agency 2020.
[126] International Energy Agency (IEA). 2015 Technology Roadmap: Hydrogen and Fuel Cells. Paris, France: IEA Publications; 2015.
[127] Teske DS, Sawyer S, Schäfer O, Pregger T, Simon S, Naegler T. energy [r]evolution, a sustainable world energy outlook 2015 - 100% renewable energy for all. Greenpeace Int Glob Wind Energy Counc SolarPowerEurope, DLR Inst Eng Thermodyn n.d.
[128] Schmidt PR, Zittel W, Weindorf W, Raksha T. Renewables in Transport 2050 Empowering a Sustainable Mobility Future with zero emission fuels from renewable electricity - Europe and Germany. Ludwig-Bölkow-Systemtechnik GmbH 2016.
[129] Fridstrøm L. Electrifying the Vehicle Fleet: Projections for Norway 2018-2050. Inst Transp Econ Nor Cent Transp Res 2019.
[130] KPMG. KPMG's 21st consecutive Global Automotive Executive Survey 2020 - Executive Summary 2020.
[131] Element Energy, Cambridge Econometrics. Low-carbon cars in Europe: A socioeconomic assessment. Eur Clim Found 2018. https://www.camecon.com/wp-content/uploads/2018/02/Fuelling-Europes-Future-2018-v1.0.pdf (accessed April 29, 2020).
[132] Henning HM, Palzer A. What will the energy transformation cost - Pathways for Transforming the German Energy System by 2050. Fraunhofer ISE 2015.
[133] Centraal Bureau voor de Statistiek (CBS). Motorbrandstoffen; afzet in petajoule, gewicht en volume. Statline 2020.
[134] Wilke C, Bensmann A, Martin S, Utz A, Hanke-Rauschenbach R. Optimal design of a district energy system including supply for fuel cell electric vehicles. Appl Energy 2018;226:129–44. doi:https://doi.org/10.1016/j.apenergy.2018.05.102.
[135] Nuffel L van, Dedecca JG, Smit T, Rademaekers K. Sector coupling: how can it be enhanced in the EU to foster grid stability and decarbonise? Trinomics BV, Eur Parliam Comm Ind Res Energy 2018.
[136] Blok K, Nieuwlaar E. Introduction to Energy Analysis. Third Edition. | Abingdon, Oxon; New York, NY: Routledge, 2021.: Routledge; 2020. doi:10.4324/9781003003571.
[137] International Renewable Energy Agency (IRENA). Hydrogen from

renewable power: Technology outlook for the energy transition 2018.
[138] Hydrogen Council. How hydrogen empowers the energy transition. Brussels, Belgium: Hydrogen Council; 2017.
[139] Albrecht U, Bünger U, Michalski J, Raksha T, Wurster R, Zerhusen J. International Hydrogen Strategies - A study commissioned by and in cooperation with the World Energy Council Germany. Ludwig-Bölkow-Systemtechnik GmbH, Weltenergierat - Deutschl (World Energy Counc Ger 2020:3.
[140] Bhavnagri K, Henbest S, Izadi-Najafabadi A, Wang X, Tengler M, Callens J, et al. Hydrogen Economy Outlook - Key messages. BloombergNEF 2020.
[141] International Energy Agency (IEA). The Future of Hydrogen - Seizing today's opportunities 2019.
[142] Gielen D, Taibi E, Miranda R. Hydrogen: A renewable energy perspective. Int Renew Energy Agency 2019.
[143] Mathis W, Thornhill J. Hydrogen's Plunging Price Boosts Role as Climate Solution. 2019.
[144] Martinsen A. Hydrogen opens a prolific service industry as coming project spending bakes a $400 billion pie. Rystad Energy 2020.
[145] Hydrogen Council. Hydrogen scaling up 2017.
[146] International Energy Agency (IEA). Capacity of electrolysers for hydrogen production by commissioning year and intended use of hydrogen, 2010-2020 2020.
[147] Farrugio G. Green hydrogen plans already top 60 GW, but less than half is likely to operate by 2035 as costs bite. Rystad Energy 2020.
[148] International Renewable Energy Agency (IRENA). Green Hydrogen Cost Reduction: Scaling up Electrolysers to Meet the 1.5^0C Climate Goal 2020.
[149] Diermann R. Thyssenkrupp increases annual electrolyzer capacity to 1 GW. PV Mag 2020.
[150] Power I. Manufacturing Commences at the ITM Power Gigafactory 2021.
[151] Eurostat. Renewable energy statistics. Stat Explain 2020.
[152] Stappel M, Gerlach A-K, Scholz A, Pape C. The European Power System in 2030: Flexibility Challenges and Integration Benefit. Fraunhofer Institute for Wind Energy and Energy System Technology (IWES): 2015.
[153] Brauner G, Bofinger S, Schwing U, Magin W, Glaunsinger W, Pyc I, et al. Flexibility of thermal power generation for RES supply in Germany until 2020. Elektrotechnik Und Informationstechnik 2014;131:361. doi:10.1007/s00502-014-0234-9.
[154] Union of the Electricity Industry - EURELECTRIC. Flexible Gas Markets for Variable Renewable Generation. 2014.
[155] Hach D, Spinler S. Capacity payment impact on gas-fired generation investments under rising renewable feed-in - A real options analysis. Energy Econ 2016;53:270–80. doi:10.1016/j.eneco.2014.04.022.
[156] Nitsch J, Pregger T, Scholz Y. Langfristszenarien und Strategien für den Ausbau der erneuerbaren Energien in Deutschland bei Berücksichtigung der Entwicklung in Europa und global. Deutsches Zentrum Für Luft- Und Raumfahrt (DLR), Fraunhofer Institute for Wind Energy and Energy System

Technology (IWES): 2012.
[157] Energistyrelsen - Danish Energy Agency (DEA). Energi Balance Model (EMB) public figures background data for Energiscenarier frem mod 2020, 2035 og 2050 2014.
[158] European Climate Foundation. Roadmap 2050 - all data: A Practical Guide to a Prosperous, Low-Carbon Europe 2010:142.
[159] Schlachtberger DP, Brown T, Schramm S, Greiner M. The benefits of cooperation in a highly renewable European electricity network. Energy 2017. doi:10.1016/j.energy.2017.06.004.
[160] Caglayan DG, Heinrichs HU, Stolten D, Robinius M. The Impact of Temporal Complexity Reduction on a 100% Renewable European Energy System with Hydrogen Infrastructure. Preprints 2019;2019100150. doi:10.20944/PREPRINTS201910.0150.V1.
[161] Staffell I, Scamman D, Velazquez Abad A, Balcombe P, Dodds PE, Ekins P, et al. The role of hydrogen and fuel cells in the global energy system. Energy Environ Sci 2019. doi:10.1039/c8ee01157e.
[162] Child M, Kemfert C, Bogdanov D, Breyer C. Flexible electricity generation, grid exchange and storage for the transition to a 100% renewable energy system in Europe. Renew Energy 2019. doi:10.1016/j.renene.2019.02.077.
[163] Victoria M, Zhu K, Brown T, Andresen GB, Greiner M. The role of storage technologies throughout the decarbonisation of the sector-coupled European energy system. ArXiv Prepr ArXiv190606936 2019.
[164] Zappa W, Junginger M, van den Broek M. Is a 100% renewable European power system feasible by 2050? Appl Energy 2019. doi:10.1016/j.apenergy.2018.08.109.
[165] Eurostat. Complete energy balances (nrg_bal_c) - 2018. Energy Stat - Complet Energy Balanc 2020.
[166] Eurostat. Supply, transformation and consumption of gas [nrg_cb_gas] - 2019 2021.
[167] Gas Infrastructure Europe (GIE). AGSI+ Aggregated Gas Storage Inventory - Historical data 2021.
[168] Eurostat. Electricity and heat statistics. Stat Explain 2020.
[169] Council of the European Union. COUNCIL DIRECTIVE 2009/119/EC of 14 September 2009 imposing an obligation on Member States to maintain minimum stocks of crude oil and/or petroleum products. Off J Eur Union 2009.
[170] European Commission. Investment Projects in Energy Infrastructure Accompanying the document COMMUNICATION FROM THE COMMISSION TO THE EUROPEAN PARLIAMENT, THE COUNCIL, THE EUROPEAN ECONOMIC AND SOCIAL COMMITTEE AND THE COMMITTEE OF THE REGIONS Progress towards completing the I. Comm Staff Work Doc 2014:5.
[171] International Energy Agency (IEA). Oil Stocks of IEA Countries Measured in days of net imports - September 2020 2020.
[172] Agence de la transition Ecologique (ADEME), Artelys, ARMINES-PERSEE, Energies Demain. A 100% renewable electricity mix? Analysis and optimization - Exploring the boundaries of renewable power generation in

France by 2050 2016.
[173] Element Energy, Cambridge Econometrics. Towards Fossil-Free Energy in 2050 - Net Zero 2050 -Archetype Modelling Results. Eur Clim Found 2019. http://europeanclimate.org/content/uploads/2019/11/14-03-2019-ffe-2050-dispatch-model-results.xlsx (accessed July 10, 2020).
[174] Element Energy, Cambridge Econometrics. Towards Fossil-Free Energy in 2050 - Net Zero 2050 - Executive Summary. Eur Clim Found 2019.
[175] Pasaoglu G, Fiorello D, Martino A, Zani L, Zubaryeva A, Thiel C. Driving and parking patterns of European car drivers - a mobility survey. Petten, The Netherlands: Joint Research Centre (JRC) – European Commission (EC); 2012.
[176] Kempton W, Tomić J. Vehicle-to-grid power fundamentals: Calculating capacity and net revenue. J Power Sources 2005;144:268–79. doi:10.1016/j.jpowsour.2004.12.025.
[177] Kempton W, Tomić J. Vehicle-to-grid power implementation: From stabilizing the grid to supporting large-scale renewable energy. J Power Sources 2005;144:280. doi:10.1016/j.jpowsour.2004.12.022.
[178] Andrey C, Barberi P, Lacombe L, Nuffel L van, Gérard F, Gorenstein Dedecca J, et al. Study on energy storage Contribution to the security of the electricity supply in Europe - Final report. Artelys, Trinomics, Enerdata, Eur Comm 2020.
[179] Caglayan DG, Weber N, Heinrichs HU, Linßen J, Robinius M, Kukla PA, et al. Technical potential of salt caverns for hydrogen storage in Europe. Int J Hydrogen Energy 2020. doi:10.1016/j.ijhydene.2019.12.161.
[180] Hyundai Motor Company. Hyundai ix35 fuel cell highlights 2013. www.hyundai.com/worldwide/en/eco/ix35-fuelcell/highlights (accessed November 1, 2019).
[181] Toyota Motor Corporation. outline of the Mirai 2014. http://newsroom.toyota.co.jp/en/download/13241306 (accessed August 28, 2019).
[182] Honda Motor Co. Honda begins sales of all-new clarity fuel cell – clarity fuel cell realizes the world's top-class cruising range among zero emission vehicles of approximately 750 km 2016. http://world.honda.com/news/2016/4160310eng.html?fro.
[183] U.S. Department of Energy (DOE). How Do Fuel Cell Electric Vehicles Work Using Hydrogen? - Key Components of a Hydrogen Fuel Cell Electric Car. Energy Effic Renew Energy - Altern Fuels Data Cent n.d.
[184] Luo X, Wang J, Dooner M, Clarke J. Overview of current development in electrical energy storage technologies and the application potential in power system operation. Appl Energy 2015;137:511–36. doi:10.1016/j.apenergy.2014.09.081.
[185] J. Michaelis, Genoese F, Wietschel M. Evaluation of Large-Scale Hydrogen Storage Systems in the German Energy Sector. Fuel Cells 2014;2014:14, 517. doi:10.1002/fuce.201300213.
[186] Rebours Y, Kirschen D. What is spinning reserve. Univ Manchester 2005.
[187] International Energy Agency (IEA). Energy Technology Perspectives 2014:

harnessing electricity's potential. 2014. doi:10.1787/energy_tech-2014-en.
[188] Shariff SM, Iqbal D, Saad Alam M, Ahmad F. A State of the Art Review of Electric Vehicle to Grid (V2G) technology. IOP Conf. Ser. Mater. Sci. Eng., 2019. doi:10.1088/1757-899X/561/1/012103.
[189] Hyundai Motor Company. Hyundai Nexo 2019 Specifications. Hyundai Newsroom n.d.
[190] Reddi K, Elgowainy A, Rustagi N, Gupta E. Impact of hydrogen SAE J2601 fueling methods on fueling time of light-duty fuel cell electric vehicles. Int J Hydrogen Energy 2017. doi:10.1016/j.ijhydene.2017.04.233.
[191] Toyota Motor Corporation. Toyota moves to expand mass-production of fuel cell stacks and hydrogen tanks towards ten-fold increase post-2020. Toyota Eur Newsroom 2018.
[192] Hyundai Motor Group. HMG, a First Mover of the Hydrogen Society 2019.
[193] Navigant a Guidehouse Company. Integration routes North Sea offshore wind 2050. North Sea Wind Power Hub 2020. https://northseawindpowerhub.eu/wp-content/uploads/2020/04/NSWPH-Integration-routes-offshore-wind-2050.pdf (accessed April 29, 2020).
[194] Fuel Cell Technologies Office (FCTO) – U.S. Department of Energy (DOE). Multi-Year Research, Development, and Demonstration (MYRD&D) Plan - Section 3.4 fuel cells 2017:17–30. https://energy.gov/sites/prod/files/2017/05/f34/fcto_myrdd_fuel_cells.pdf (accessed August 28, 2019).
[195] V2G Hub. V2G Around the world: V2G Hub 2020. https://www.v2g-hub.com/insights/map.
[196] Sovacool BK, Kester J, Noel L, Zarazua de Rubens G. Actors, business models, and innovation activity systems for vehicle-to-grid (V2G) technology: A comprehensive review. Renew Sustain Energy Rev 2020. doi:10.1016/j.rser.2020.109963.
[197] Habib S, Kamran M, Rashid U. Impact analysis of vehicle-to-grid technology and charging strategies of electric vehicles on distribution networks - A review. J Power Sources 2015. doi:10.1016/j.jpowsour.2014.12.020.
[198] Mwasilu F, Justo JJ, Kim E-K, Do TD, Jung J-W. Electric vehicles and smart grid interaction: A review on vehicle to grid and renewable energy sources integration. Renew Sustain Energy Rev 2014;34:501–16. doi:10.1016/j.rser.2014.03.031.
[199] Sovacool BK, Axsen J, Kempton W. The Future Promise of Vehicle-to-Grid (V2G) Integration: A Sociotechnical Review and Research Agenda. Annu Rev Environ Resour 2017. doi:10.1146/annurev-environ-030117-020220.
[200] Honda worldwide technology picture book power exporter 9000 2017. http://world.honda.com/powerproducts-technology/PowerExporter9000/ (accessed August 28, 2019).
[201] Engineering the Extreme Capability of the Colorado ZH2 2016. www.gm.com/mol/m-2016-oct-1101-zh2.html (accessed August 28, 2019).
[202] International Energy Agency Hybrid & Electric Vehicle (IEA-HEV). Task 28 "Home Grids and V2X Technologies" 2017.

http://www.ieahev.org/tasks/home-grids-and-v2x-technologies-task-28/ (accessed August 28, 2019).
[203] Zini G, Dalla Rosa A. Hydrogen systems for large-scale photovoltaic plants: Simulation with forecast and real production data. Int J Hydrogen Energy 2014;39:107–18. doi:10.1016/j.ijhydene.2013.10.076.
[204] Parra D, Walker GS, Gillott M. Modeling of PV generation, battery and hydrogen storage to investigate the benefits of energy storage for single dwelling. Sustain Cities Soc 2014;10:1–10. doi:10.1016/j.scs.2013.04.006.
[205] Castañeda M, Cano A, Jurado F, Sánchez H, Fernández LM. Sizing optimization, dynamic modeling and energy management strategies of a stand-alone PV/hydrogen/battery-based hybrid system. Int J Hydrogen Energy 2013;38:3830–45. doi:10.1016/j.ijhydene.2013.01.080.
[206] Wulf C, Linßen J, Zapp P. Review of Power-to-Gas Projects in Europe. Energy Procedia 2018;155:367–78. doi:https://doi.org/10.1016/j.egypro.2018.11.041.
[207] Davies HC, Datardina N. A probabilistic model for 1st stage dimensioning of renewable hydrogen transport micro-economies. Renew Energy 2013;60:355–62. doi:10.1016/j.renene.2013.05.029.
[208] Dispenza G, Sergi F, Napoli G, Randazzo N, Di Novo S, Micari S, et al. Development of a solar powered hydrogen fueling station in smart cities applications. Int J Hydrogen Energy 2017;42:27884–93. doi:10.1016/j.ijhydene.2017.07.047.
[209] Kurtz J, Peters M, Muratori M, Gearhart C. Renewable Hydrogen-Economically Viable: Integration into the U.S. Transportation Sector. IEEE Electrif Mag 2018;6:8–18. doi:10.1109/MELE.2017.2784631.
[210] Rahil A, Gammon R, Brown N. Flexible operation of electrolyser at the garage forecourt to support grid balancing and exploitation of hydrogen as a clean fuel. Res Transp Econ 2018;70:125–38. doi:10.1016/j.retrec.2017.12.001.
[211] Chrysochoidis-Antsos N, Liu C, Wijk A van. On-site wind powered hydrogen refuelling stations - From national level to a case study in Germany. 2018 Int. Conf. Smart Energy Syst. Technol., 2018, p. 1–6. doi:10.1109/SEST.2018.8495693.
[212] Chrysochoidis-Antsos N, Escudé MR, van Wijk AJM. Technical potential of on-site wind powered hydrogen producing refuelling stations in the Netherlands. Int J Hydrogen Energy 2020. doi:https://doi.org/10.1016/j.ijhydene.2020.06.125.
[213] Lipman TE, Edwards JL, Kammen DM. Fuel cell system economics: Comparing the costs of generating power with stationary and motor vehicle PEM fuel cell systems. Energy Policy 2004;32:101–25. doi:10.1016/S0301-4215(02)00286-0.
[214] Kissock J. Combined heat and power for buildings using fuel-cell cars. Proc ASME Int Sol Energy Conf 1998;June 13–18:121–32.
[215] Williams BD, Kurani KS. Commercializing light-duty plug-in/plug-out hydrogen-fuel-cell vehicles: “Mobile Electricity” technologies and opportunities. J Power Sources 2007;166:549–66.

doi:10.1016/j.jpowsour.2006.12.097.
[216] Kempton W, Tomic J, Letendre S, Brooks A, Lipman T. Vehicle-to-grid power: battery, hybrid, and fuel cell vehicles as resources for distributed electric power in California. Davis, CA, United States of Ameria: Institute of Transportation Studies; 2001.
[217] Kempton W, Tomić J. Vehicle-to-grid power fundamentals: Calculating capacity and net revenue. J Power Sources 2005;144:268–79. doi:10.1016/j.jpowsour.2004.12.025.
[218] Garmsiri S, Koohi-Fayegh S, Rosen MA, Smith GR. Integration of transportation energy processes with a net zero energy community using captured waste hydrogen from electrochemical plants. Int J Hydrogen Energy 2016;41:8337–46. doi:10.1016/j.ijhydene.2015.11.191.
[219] Alanne K, Cao S. Zero-energy hydrogen economy (ZEH 2 E) for buildings and communities including personal mobility. Renew Sustain Energy Rev 2017;71:697–711. doi:10.1016/j.rser.2016.12.098.
[220] Cao S. Comparison of the energy and environmental impact by integrating a H2 vehicle and an electric vehicle into a zero-energy building. Energy Convers Manag 2016;123:153–73. doi:10.1016/j.enconman.2016.06.033.
[221] Fernandes A, Woudstra T, Wijk AJM van, Verhoef LA, Aravind PV. Fuel cell electric vehicle as a power plant and SOFC as a natural gas reformer: An exergy analysis of different system designs. Appl Energy 2016;173:13–28. doi:10.1016/j.apenergy.2016.03.107.
[222] Toyota Motor Corporation. Seven-Eleven Japan and Toyota to Launch Joint Next-generation Convenience Store Project in Autumn 2019 toward Greater CO2 Emissions Reduction. Toyota Newsroom 2018. https://newsroom.toyota.co.jp/en/corporate/22833613.html (accessed August 28, 2019).
[223] Cao S, Alanne K. Technical feasibility of a hybrid on-site H2 and renewable energy system for a zero-energy building with a H2 vehicle. Appl Energy 2015;158:568–83. doi:10.1016/j.apenergy.2015.08.009.
[224] Lord AS, Kobos PH, Borns DJ. Geologic storage of hydrogen: Scaling up to meet city transportation demands. Int J Hydrogen Energy 2014;39:15570–82. doi:10.1016/j.ijhydene.2014.07.121.
[225] Mukherjee U, Maroufmashat A, Ranisau J, Barbouti M, Trainor A, Juthani N, et al. Techno-economic, environmental, and safety assessment of hydrogen powered community microgrids; case study in Canada. Int J Hydrogen Energy 2017;42:14333–49. doi:10.1016/j.ijhydene.2017.03.083.
[226] Marchenko O V., Solomin S V. Modeling of hydrogen and electrical energy storages in wind/PV energy system on the Lake Baikal coast. Int J Hydrogen Energy 2017;42:9361–70. doi:10.1016/j.ijhydene.2017.02.076.
[227] Shimizu T, Tsukushi Y, Hasegawa K, Ihara M, Okubo T, Kikuchi Y. A region-specific analysis of technology implementation of hydrogen energy in Japan. Int J Hydrogen Energy 2017;44:19434–51. doi:https://doi.org/10.1016/j.ijhydene.2017.11.128.
[228] European Commission. G. Technology readiness levels (TRL) - General Annexes. Horiz 2020 - Work Program 2016-2017 2017.

[229] Oldenbroek V, Hamoen V, Alva S, Robledo CB, Verhoef LA, Wijk AJM van. Fuel Cell Electric Vehicle-to-Grid: Experimental Feasibility and Operational Performance as Balancing Power Plant. Fuel Cells 2018;18:649–62. doi:https://doi.org/10.1002/fuce.201700192.
[230] European Commission. Energy Roadmap 2050. Communication from the commission to the European parliament, the council, the European economic and social committee and the committee of the regions. 2011.
[231] European Commission. EU Reference Scenario 2016-Energy, transport and GHG emissions Trends to 2050. 2016.
[232] Energistyrelsen - Danish Energy Agency (DEA). Background data from Energiscenarier frem mod 2020, 2035 og 2050. 2014.
[233] ZVEI - German Electrical and Electronic Manufacturers' Association. Voltage Classes for Electric Mobility 2013. https://www.zvei.org/fileadmin/user_upload/Presse_und_Medien/Publikationen/2014/april/Voltage_Classes_for_Electric_Mobility/Voltage_Classes_for_Electric_Mobility.pdf.
[234] Oldenbroek V, Wijtzes S, van Wijk A, Blok K. Fuel cell electric vehicle to grid & H2: Balancing national electricity, heating & transport systems a scenario analysis for Germany in the year 2050. 2017 IEEE Green Energy Smart Syst. Conf., IEEE; 2017, p. 1–6. doi:10.1109/IGESC.2017.8283458.
[235] Oldenbroek V, Verhoef LA, van Wijk AJM. Fuel cell electric vehicle as a power plant: Fully renewable integrated transport and energy system design and analysis for smart city areas. Int J Hydrogen Energy 2017;42:8166–96. doi:10.1016/j.ijhydene.2017.01.155.
[236] Klimstra J, Hotakainen M. Smart Power generation 4th. Helsinki: Avain Publishers; 2011.
[237] Grosshauser R. Power Engineering - Turbines vs. Reciprocating Engines 2016. https://www.power-eng.com/coal/turbines-vs-reciprocating-engines/.
[238] Energistyrelsen - Danish Energy Agency. Technology data for energy plants - Generation of Electricity and District Heating, Energy Storage and Energy Carrier Generation and Conversion (updated 2017). vol. 1. 2012. doi:ISBN: 978-87-7844-940-5.
[239] Parsons Brinckerhoff. Technical assessment of the operation of coal & gas fired plants. 2014.
[240] TU Delta the independent newspaper of TU Delft. Hydrogen car as power backup 2016. https://www.delta.tudelft.nl/article/hydrogen-car-power-backup.
[241] Lim TW, Ahn BK. Hyundai's FCEVs: A Pathway to New Possibilities. ECS Trans 2012;50:3–10. doi:10.1149/05002.0003ecst.
[242] Hyundai Motor Company. ix35 FCEV Emergency Response Guide. 2013.
[243] Pacific Engineering Company. High Voltage Fuse EVFP DC450V 60A Breaking Capacity 2000A 2016. https://www.pecj.co.jp/fuse/files/PEC_Fuse_Catalogue_en.pdf.
[244] Panasonic Corporation. Automotive Relays - EV Relays: AEV18012 2017.
[245] SAE International. SAE Electric Vehicle and Plug in Hybrid Electric Vehicle

Conductive Charge Coupler Standard J1772 2017. https://saemobilus.sae.org/content/j1772_201710 (accessed August 28, 2019).
[246] imc Meßsysteme GmbH. imc BUSDAQ-2 2016. http://www.imc-berlin.com/products/measurement-hardware/imc-busdaq/device-options/.
[247] Ningbo Ginlong Technologies. Three Phase Wind Grid Tie Inverter GCI-10K-W 2014. http://www.ginlong.com/en/Wind_Products/GCI_10K_W.html.
[248] Evans BW. Arduino Programming Notebook - Arduino Playground 2007. https://playground.arduino.cc/uploads/Main/arduino_notebook_v1-1.pdf.
[249] Torquato R, Shi Q, Xu W, Freitas W. A Monte Carlo simulation platform for studying low voltage residential networks. IEEE Trans Smart Grid 2014;5:2766–76. doi:10.1109/TSG.2014.2331175.
[250] Köpf H, Wilkening E, Klosinski C, Kurrat M. Breaking performance of protection devices for automotive dc powertrains with a voltage of 450 V. ICEC 2014; 27th Int. Conf. Electr. Contacts, Dresden, Germany: VDE VERLAG GMBH; 2014, p. 126–31.
[251] Sugawara A, Goso T, Sato T, Tada S, Tanabe K. Direct current interruption on small AC relay using IGBT commutation circuit with surge protection element. 2013 2nd Int. Conf. Electr. Power Equip. - Switch. Technol. ICEPE-ST 2013, 2013. doi:10.1109/ICEPE-ST.2013.6804365.
[252] Team MEV. A Guide to Understanding Battery Specifications. Current 2008:1–3. doi:10.3390/en7084895.
[253] Smets A, Isabella O, Jager K, van Swaaij RACMM, Zeman M. Solar Energy: The Physics and Engineering of Photovoltaic Conversion, Technologies and Systems. Cambridge: UIT Cambridge; 2016. doi:10.1007/SpringerReference_29746.
[254] Lemmon EW, Huber ML, McLinden MO. NIST Standard Reference Database 23. Ref Fluid Thermodyn Transp Prop (REFPROP), Version 91 2013.
[255] General Electric Power. LM6000 Hybrid Electric Gas Turbine (Hybrid EGT) 2017. https://www.gepower.com/services/gas-turbines/upgrades/hybrid-egt.
[256] Jansen B, Binding C, Sundstrom O, Gantenbein D. Architecture and Communication of an Electric Vehicle Virtual Power Plant. 2010 First IEEE Int. Conf. Smart Grid Commun. Gaithersburg, MD, USA, 4-6 Oct. 2010, IEEE; 2010, p. 149–54. doi:10.1109/SMARTGRID.2010.5622033.
[257] Ribberink H, Darcovich K, Pincet F. Battery Life Impact of Vehicle-to-Grid Application of Electric Vehicles. EVS28 Int Electr Veh Symp Exhib 2015:1–11.
[258] Bishop JDK, Axon CJ, Bonilla D, Tran M, Banister D, McCulloch MD. Evaluating the impact of V2G services on the degradation of batteries in PHEV and EV. Appl Energy 2013;111:206–18. doi:10.1016/j.apenergy.2013.04.094.
[259] Wang L, Chen B. Model-Based Analysis of V2G Impact on Battery Degradation, 2017. doi:10.4271/2017-01-1699.
[260] Barnitt R. Analysis of Battery Wear and V2G Benefits Using Real-World

Drive Cycles and Ambient Data 2011. https://energy.gov/sites/prod/files/2014/03/f10/vss044_barnitt_2011_p.pdf (accessed October 24, 2017).
[261] Petit M, Prada E, Sauvant-Moynot V. Development of an empirical aging model for Li-ion batteries and application to assess the impact of Vehicle-to-Grid strategies on battery lifetime. Appl Energy 2016;172:398–407. doi:10.1016/j.apenergy.2016.03.119.
[262] Gough R, Dickerson C, Rowley P, Walsh C. Vehicle-to-grid feasibility: A techno-economic analysis of EV-based energy storage. Appl Energy 2017;192:12–23. doi:10.1016/j.apenergy.2017.01.102.
[263] Yu PT, Gu W, Zhang J, Makharia R, Wagner FT, Gasteiger HA. Carbon-support requirements for highly durable fuel cell operation. Polym. Electrolyte Fuel Cell Durab., 2009, p. 29–53. doi:10.1007/978-0-387-85536-3_3.
[264] De Bruijn FA, Dam VAT, Janssen GJM. Review: Durability and degradation issues of PEM fuel cell components. Fuel Cells 2008;8:3–22. doi:10.1002/fuce.200700053.
[265] Dubau L, Castanheira L, Maillard F, Chatenet M, Lottin O, Maranzana G, et al. A review of PEM fuel cell durability: Materials degradation, local heterogeneities of aging and possible mitigation strategies. Wiley Interdiscip Rev Energy Environ 2014;3:540–60. doi:10.1002/wene.113.
[266] Silva RE, Harel F, Jemeï S, Gouriveau R, Hissel D, Boulon L, et al. Proton Exchange Membrane Fuel Cell Operation and Degradation in Short-Circuit. Fuel Cells 2014;14:894–905. doi:10.1002/fuce.201300216.
[267] Fuel Cell Technologies Office (FCTO) – U.S. Department of Energy (DOE). Multi-Year Research, Development, and Demonstration (MYRD&D) Plan - Section 3.4 Fuel Cells 2017:3.4.1-3.4.58. https://energy.gov/sites/prod/files/2017/05/f34/fcto_myrdd_fuel_cells.pdf (accessed August 28, 2019).
[268] Kim SH. Development of Fuel Cell Electric Vehicle in Hyundai · Kia Motors 2010. http://www.fch.europa.eu/sites/default/files/documents/ga2010/sae-hoon_kim.pdf (accessed October 24, 2017).
[269] Salman P, Wallnöfer-Ogris E, Sartory M, Trattner A, Klell M, Müller H, et al. Hydrogen-Powered Fuel Cell Range Extender Vehicle - Long Driving Range with Zero-Emissions. SAE Tech Pap 2017;2017-March. doi:10.4271/2017-01-1185.
[270] Lee J-Y, Han B-M. A Bidirectional Wireless Power Transfer EV Charger Using Self-Resonant PWM. IEEE Trans Power Electron 2015;30:1784–7. doi:10.1109/TPEL.2014.2346255.
[271] Yu Fang, Songyin Cao, Yong Xie, Wheeler P. Study on bidirectional-charger for electric vehicle applied to power dispatching in smart grid. 2016 IEEE 8th Int. Power Electron. Motion Control Conf. (IPEMC-ECCE Asia), IEEE; 2016, p. 2709–13. doi:10.1109/IPEMC.2016.7512726.
[272] Tachikawa K, Kesler M, Atasoy O. Feasibility Study of Bi-directional Wireless Charging for Vehicle-to-Grid. SAE WCX World Congr. Exp., Detroit,

Michigan, United States of America: SAE International; 2018. doi:10.4271/2018-01-0669.
[273] Kydd PH, Anstrom JR, Heitmann PD, Komara KJ, Crouse ME. Vehicle-Solar-Grid Integration: Concept and Construction. IEEE Power Energy Technol Syst J 2016;3:81–8. doi:10.1109/JPETS.2016.2558471.
[274] Eberle U, Müller B, von Helmolt R. Fuel cell electric vehicles and hydrogen infrastructure: status 2012. Energy Environ Sci 2012;5:8780. doi:10.1039/c2ee22596d.
[275] National Renewable Energy Laboratory - U.S. Department of Energy. Fuel Cell Electric Vehicle Evaluation. Adv Automot Batter Conf 2016. https://www.nrel.gov/docs/fy16osti/66760.pdf (accessed October 24, 2017).
[276] Kim J, Kim S. Obstacles to the Success of Fuel-Cell Electric Vehicles: Are They Truly Impossible to Overcome? IEEE Electrif Mag 2018;6:48–54. doi:10.1109/MELE.2017.2784635.
[277] Wood DL. Impacting Rapid Hydrogen Fuel Cell Electric Vehicle (FCEV) Commercialization: System Cost Reduction and Subcomponent Performance Enhancement. SAE International; 2016.
[278] Ahluwalia RK, Wang X, Rousseau A, Kumar R. Fuel economy of hydrogen fuel cell vehicles. J Power Sources 2004;130:192–201. doi:10.1016/j.jpowsour.2003.12.061.
[279] Yoshida T, Kojima K. Toyota MIRAI Fuel Cell Vehicle and Progress Toward a Future Hydrogen Society. Electrochem Soc Interface 2015;24:45–9. doi:10.1149/2.F03152if.
[280] Robledo CB, Oldenbroek V, Abbruzzese F, van Wijk AJM. Integrating a hydrogen fuel cell electric vehicle with vehicle-to-grid technology, photovoltaic power and a residential building. Appl Energy 2018;215. doi:10.1016/j.apenergy.2018.02.038.
[281] Marignetti F, Minutillo M, Perna A, Jannelli E. Assessment of fuel cell performance under different air stoichiometries and fuel composition. IEEE Trans Ind Electron 2011;58:2420–6. doi:10.1109/TIE.2010.2069073.
[282] Rabbani A, Rokni M, Hosseinzadeh E, Mortensen HH. The start-up analysis of a PEM fuel cell system in vehicles. Int J Green Energy 2014;11:91–111. doi:10.1080/15435075.2013.769882.
[283] Heuer M, Bernstein PA, Wenske M, Styczynski ZA. Results of current density distribution mapping in PEM fuel cells dependent on operation parameters. Energies 2013;6:3841–58. doi:10.3390/en6083841.
[284] Iranzo A, Boillat P, Biesdorf J, Salva A. Investigation of the liquid water distributions in a 50cm2PEM fuel cell: Effects of reactants relative humidity, current density, and cathode stoichiometry. Energy 2015;82:914–21. doi:10.1016/j.energy.2015.01.101.
[285] Kocha SS. Electrochemical Degradation. In: Kumbur EC, Veziroglu TNBT-PEFCD, editors. Polym. Electrolyte Fuel Cell Degrad., Boston: Elsevier; 2012, p. 89–214. doi:10.1016/B978-0-12-386936-4.10003-X.
[286] Büchi FN, Inaba M, Schmidt TJ. Polymer electrolyte fuel cell durability. New York: Springer; 2009.

[287] Iiyama A, Shinohara K, Iguchi S, Daimaru A. Membranes and catalyst performance targets for automotive fuel cells. Handb Fuel Cells 2010:3221–31. doi:doi:10.1002/9780470974001.f500059.
[288] Pei P, Chen H. Main factors affecting the lifetime of Proton Exchange Membrane fuel cells in vehicle applications: A review. Appl Energy 2014;125:60–75. doi:10.1016/j.apenergy.2014.03.048.
[289] Kocha SS. Polymer Electrolyte Membrane (PEM) Fuel Cells, Automotive Applications. In: Kreuer K-D, editor. Fuel Cells, Sel. Entries from Encycl. Sustain. Sci. Technol., Springer; 2013, p. 473–518. doi:https://doi.org/10.1007/978-1-4614-5785-5_15.
[290] Barbir F, Veziroğlu TN, Wang H, Perry ML. PEM Fuel Cells (Second Edition). Boston: Academic Press; 2013. doi:https://doi.org/10.1016/B978-0-12-387710-9.00012-6.
[291] Wang H, Li H, Yuan X-Z. PEM fuel cell failure mode analysis. vol. 1. CRC Press; 2011.
[292] Arboleda J. New Hyundai NEXO FCEV - Hyundai & Fuel Cell Technology. Eur. Hydrog. Energy Conf., 2018, p. 21.
[293] Hochgraf C. APPLICATIONS – TRANSPORTATION | Electric Vehicles: Fuel Cells. In: Garche J, editor. Encycl. Electrochem. Power Sources, Amsterdam: Elsevier; 2009, p. 236–48. doi:https://doi.org/10.1016/B978-044452745-5.00863-7.
[294] California Fuel Cell Partnership (CAFCP). Cost to refill 2015.
[295] Air Products. Air Products' California Fueling Stations Offering Hydrogen Below $10 Per Kilogram 2017.
[296] Clean Energy Partnership (CEP). How much does hydrogen cost at filling stations? - FAQ 2018.
[297] Grube T, Robinius M, Stolten D. Kosten der Wasserstoffbereitstellung in Versorgungssystemen auf Basis erneuerbarer Energien. In: Töpler J, Lehmann J, editors. Wasserst. und Brennstoffzelle Technol. und Marktperspektiven, Berlin, Heidelberg: Springer Berlin Heidelberg; 2017, p. 245–61. doi:10.1007/978-3-662-53360-4_13.
[298] Chardonnet C, Vos L De, Genoese F, Roig G, Bart F, Ha T, et al. Early business cases for H2 in energy storage and more broadly power to H2 applications. Brussels, Belgium: Tractebel, Hinicio, Fuel Cell Hydrogen Joint Undertaking (FCH-JU); 2017.
[299] Fuel Cell Technologies Office (FCTO) – U.S. Department of Energy (DOE). Multi-Year Research, Development, and Demonstration (MYRD&D) Plan - Section 3.1 Hydrogen Production. 2015.
[300] Robinius M, Erdmann G, Stolten D. Strom-und Gasmarktdesign zur Versorgung des deutschen Straßenverkehrs mit Wasserstoff. Forschungszentrum Jülich GmbH, Zentralbibliothek, Verlag, 2015.
[301] Albrecht U, Altmann M, Barth F, Bünger U, Fraile D, Lanoix J-C, et al. Study on hydrogen from renewable resources in the EU Final Report. 2015.
[302] Hildebrandt E, Collins K, Kurlinski R, Avalos R, Blanke A, Castelhano M, et al. 2016 Annual Report on Market Issues and Performance. 2017.
[303] Department of Market Monitoring. Q4 2017 Report on Market Issues and

Performance. 2018.
[304] Tennet. Market Review 2017 - Electricity market inshights. 2018.
[305] Amprion. 2017 Balancing group price - Balancing groups - Energy Market 2018.
[306] Zhang J, Carter RN, Yu PT, Gu W, Wagner FT, Gasteiger HA. FUEL CELLS – PROTON-EXCHANGE MEMBRANE FUEL CELLS | Catalysts: Life-Limiting Considerations. In: Garche J, editor. Encycl. Electrochem. Power Sources, Amsterdam: Elsevier; 2009, p. 626–38. doi:https://doi.org/10.1016/B978-044452745-5.00234-3.
[307] Yu PT, Gu W, Zhang J, Makharia R, Wagner FT, Gasteiger HA. Carbon-Support Requirements for Highly Durable Fuel Cell Operation. In: Büchi FN, Inaba M, Schmidt TJ, editors. Polym. Electrolyte Fuel Cell Durab., New York, NY: Springer New York; 2009, p. 29–53. doi:10.1007/978-0-387-85536-3_3.
[308] Poorte M. Technical and economic feasibility assessment of a Car Park as Power Plant offering frequency reserves. Delft University of Technology, 2017.
[309] Zhou Z, Levin T, Conzelmann G. Survey of U.S. Ancillary Services Markets. United States: 2016. doi:10.2172/1327815.
[310] Khayyam H, Abawajy J, Javadi B, Goscinski A, Stojcevski A, Bab-Hadiashar A. Intelligent battery energy management and control for vehicle-to-grid via cloud computing network. Appl Energy 2013;111:971–81. doi:10.1016/j.apenergy.2013.06.021.
[311] Gerla M, Lee E-K, Pau G, Lee U. Internet of vehicles: From intelligent grid to autonomous cars and vehicular clouds. 2014 IEEE World Forum Internet Things, IEEE; 2014, p. 241–6. doi:10.1109/WF-IoT.2014.6803166.
[312] Oldenbroek V, Alva S, Pyman B, Buning LB, Veenhuizen PA, Van Wijk AJM. Hyundai ix35 fuel cell electric vehicles: Degradation analysis for driving and vehicle-to-grid usage. 30th Int. Electr. Veh. Symp. Exhib. (EVS 2017), Landesmesse Stuttgart GmbH; 2017.
[313] Wilson A, Marcinkoski J, Papageorgopoulos D. On-Road Fuel Cell Stack Durability – 2016 - DOE Hydrogen and Fuel Cell Technologies Program Record 2016. https://www.hydrogen.energy.gov/pdfs/16019_fuel_cell_stack_durability_2016.pdf (accessed March 4, 2021).
[314] Jouin M, Bressel M, Morando S, Gouriveau R, Hissel D, Péra MC, et al. Estimating the end-of-life of PEM fuel cells: Guidelines and metrics. Appl Energy 2016;177:87–97. doi:10.1016/j.apenergy.2016.05.076.
[315] Fletcher T, Thring R, Watkinson M. An Energy Management Strategy to concurrently optimise fuel consumption & PEM fuel cell lifetime in a hybrid vehicle. Int J Hydrogen Energy 2016;41:21503–15. doi:10.1016/j.ijhydene.2016.08.157.
[316] Chen H, Pei P, Song M. Lifetime prediction and the economic lifetime of proton exchange membrane fuel cells. Appl Energy 2015;142:154–63. doi:10.1016/j.apenergy.2014.12.062.
[317] Kurtz J, Wipke K, Sprik S, Saur G. Fuel Cell Technology Status–Voltage

Degradation. Natl Renew Energy Lab 2012. https://www.nrel.gov/docs/fy12osti/54473.pdf (accessed March 4, 2021).
[318] LEM. Automotive current transducer HAH1BV S/06 2017. https://www.lem.com/sites/default/files/products_datasheets/hah1bvw_s06_public_datasheet.pdf (accessed March 4, 2021).
[319] Least-Squares Fitting - MATLAB & Simulink - MathWorks Benelux 2020. https://nl.mathworks.com/help/curvefit/least-squares-fitting.html (accessed March 4, 2021).
[320] Oldenbroek V, Nordin L, Wijk A van. Fuel cell electric vehicle-to-grid: emergency and balancing power for a 100% renewable hospital. 6th Eur. PEFC Electrolyser Forum 2017, 2017.
[321] World Health Organization (WHO). Increasing the health sector's contribution to the reduction of greenhouse gas emissions 2021. https://www.euro.who.int/en/health-topics/environment-and-health/Climate-change/activities/increasing-the-health-sectors-contribution-to-the-reduction-of-greenhouse-gas-emissions.
[322] World Health Organization (WHO). Towards environmentally sustainable health systems in Europe - A review of the evidence 2016.
[323] LCB-HEALTHCARE Consortium. Low Carbon Buildings in the Healthcare Sector 2011.
[324] National Health Service (NHS). Delivering a 'Net Zero' National Health Service 2020.
[325] UNFCCC. Historic Paris Agreement on Climate Change - 195 Nations set path to keep temperature rise well below 2 degrees Celsius. UNFCCC Newsroom 2015;1:1–7. doi:10.1017/CBO9781107415324.004.
[326] Build up - The European Portal for Energy Efficiency in Buildings. RES-HOSPITALS project 2017. https://www.buildup.eu/en/explore/links/res-hospitals-project-0.
[327] Cristalli C. Green@Hospital project Final report 2015.
[328] REHVA, TVVL, Royal HaskoningDHV. REPORT (nearly) Zero Energy Hospital Buildings 2017.
[329] Sleiman HA, Robert S. State-of-the-art of energy-efficient healthcare districts - Deliverable Report D7.9- FINAL. Commis A L'Energie At Aux Energies Altern (CEA), STREAMER Consort 2015.
[330] European Hospital and Healthcare Federation (HOPE). Hospitals in Europe: Healthcare Data 2012.
[331] Eurostat. Hospital beds Per 100 000 inhabitants 2018.
[332] Economidou M, Atanasiu B, Despret C, Economidou M, Maio J, Nolte I, et al. Europe's buildings under the microscope. A country-by-country review of the energy performance of buildings. Build Perform Inst Eur 2011.
[333] European Commission. Commission Recommendation (EU) 2016/1318 of 29 July 2016 on guidelines for the promotion of nearly zero-energy buildings and best practices to ensure that, by 2020, all new buildings are nearly zero-energy buildings. Off J Eur Union 2016.
[334] Traversari R. RES-Hospitals: Towards zero carbon hospitals with renewable energy systems. TNO 2013.

[335] Leach M, Pless S, Torcellini P. Cost Control Best Practices for Net Zero Energy Building Projects. Natl Renew Energy Lab 2014.
[336] Pless S, Torcellini P. Net-Zero Energy Buildings: A Classification System Based on Renewable Energy Supply Options. Natl Renew Energy Lab 2010.
[337] European Parliament. Directive 2010/31/EU of the European Parliament and of the Council of 19 May 2010 on the energy performance of buildings. Off J Eur Union 2010.
[338] Kind R, Lodde H, Deerns. Safe and simple hot water supply system. Int Fed Healthc Eng Dig 2015:44.
[339] Bonnema E, Studer D, Parker A, Pless S, Torcellini P. Large Hospital 50% Energy Savings: Technical Support Document Technical Report NREL/TP-550-47867. Natl Renew Energy Lab 2010.
[340] Schoenmakers I. A systematic approach to obtain energy reduction in the complex HVAC systems of UMCs 2015.
[341] Buonomano A, Calise F, Ferruzzi G, Palombo A. Dynamic energy performance analysis: Case study for energy efficiency retrofits of hospital buildings. Energy 2014;78:555–72. doi:10.1016/j.energy.2014.10.042.
[342] European Parking Association (EPA). Data collection – the scope of parking in Europe. Barcelona, Spain: European Parking Association (EPA); 2013.
[343] Huld T, Müller R, Gambardella A. A new solar radiation database for estimating PV performance in Europe and Africa. Sol Energy 2012;86:1803–15. doi:10.1016/j.solener.2012.03.006.
[344] Huld T, Pinedo-Pascua I. Photovoltaic Solar Electricity Potential in European Countries. Petten, The Netherlands: European Commission - Joint Research Centre; 2012.
[345] International Energy Agency (IEA). Energy Technology Perspectives 2016 - Towards Sustainable Urban Energy Systems. Paris, France: IEA Publications; 2016.
[346] Kantola M, Saari A. Renewable vs. traditional energy management solutions – A Finnish hospital facility case. Renew Energy 2013;57:539–45. doi:10.1016/j.renene.2013.02.023.
[347] Kollmann R, Neugebauer G, Kretschmer F, Truger B, Kindermann H, Stoeglehner G, et al. Renewable energy from wastewater - Practical aspects of integrating a wastewater treatment plant into local energy supply concepts. J Clean Prod 2017;155:119–29. doi:10.1016/j.jclepro.2016.08.168.
[348] Kenway S. How big is the distributed energy opportunity for water and wastewater utilities? Int Water Assoc 2017.
[349] Reinders M, Beckhaus P, Illing F, Misz U, Rißе H, Schröder M, et al. Biogas as a source for producing hydrogen at wastewater treatment plants – EuWaK – A pilot project. Int J Hydrogen Energy 2015;40:8601–6. doi:10.1016/j.ijhydene.2015.05.042.
[350] Gikas P. Towards energy positive wastewater treatment plants. J Environ Manage 2017;203:621–9. doi:10.1016/j.jenvman.2016.05.061.
[351] Chen S, Chen B. Net energy production and emissions mitigation of domestic wastewater treatment system: A comparison of different biogas–

sludge use alternatives. Bioresour Technol 2013;144:296–303. doi:10.1016/j.biortech.2013.06.128.
[352] Shen Y, Linville JL, Urgun-Demirtas M, Mintz MM, Snyder SW. An overview of biogas production and utilization at full-scale wastewater treatment plants (WWTPs) in the United States: Challenges and opportunities towards energy-neutral WWTPs. Renew Sustain Energy Rev 2015;50:346–62. doi:10.1016/j.rser.2015.04.129.
[353] Gude VG. Energy and water autarky of wastewater treatment and power generation systems. Renew Sustain Energy Rev 2015;45:52–68. doi:10.1016/j.rser.2015.01.055.
[354] Gao H, Scherson YD, Wells GF. Towards energy neutral wastewater treatment: methodology and state of the art. Environ Sci Process Impacts 2014;16:1223–46. doi:10.1039/C4EM00069B.
[355] Remy C, Boulestreau M, Lesjean B. Proof of concept for a new energy-positive wastewater treatment scheme. Water Sci Technol 2014;70:1709–16. doi:10.2166/wst.2014.436.
[356] Shoener BD, Bradley IM, Cusick RD, Guest JS. Energy positive domestic wastewater treatment: the roles of anaerobic and phototrophic technologies. Environ Sci Process Impacts 2014;16:1204–22. doi:10.1039/C3EM00711A.
[357] Pronk M, de Kreuk MK, de Bruin B, Kamminga P, Kleerebezem R, van Loosdrecht MCM. Full scale performance of the aerobic granular sludge process for sewage treatment. Water Res 2015;84:207–17. doi:10.1016/j.watres.2015.07.011.
[358] Jenicek P, Kutil J, Benes O, Todt V, Zabranska J, Dohanyos M. Energy self-sufficient sewage wastewater treatment plants: is optimized anaerobic sludge digestion the key? Water Sci Technol 2013;68:1739–44. doi:10.2166/wst.2013.423.
[359] Atlantic County Utilities Authority (ACUA). Jersey-Atlantic Wind Farm 2006. http://acua.com/green-initiatives/renewable-energy/windfarm/ (accessed April 11, 2021).
[360] Yard Energy. OPS | NLD | Vlaardingen 2014. https://yardenergy.com/portfolio/ (accessed April 11, 2021).
[361] International Water Association (IWA). China turns to carbon-neutral treatment plants. Source Mag n.d. https://www.thesourcemagazine.org/china-turns-carbon-neutral-treatment-plants/.
[362] Atlantic County Utilities Authority (ACUA). ACUA Solar Project 2005. http://www.acua.com/green-initiatives/renewable-energy/solar/ (accessed April 11, 2021).
[363] Massachusetts Water Resources Authority (MRWA). Renewable and Sustainable Energy Initiatives at Deer Island 2013. https://www.mwra.com/03sewer/html/renewableenergydi.htm.
[364] Lazarova V. Water-Energy Interactions in Water Reuse. Water Intell Online 2012;11. doi:10.2166/9781780400662.
[365] Spellman FR. Water & Wastewater Infrastructure: Energy Efficiency and

Sustainability. Taylor & Francis; 2013.
[366] Reinier de Graaf Gasthuis. Locaties: Delft 2017. https://rdg-platform.prod.23g.io/locaties/delft (accessed April 11, 2021).
[367] Reinier de Graaf Gasthuis. Bezoekers, Parkeren 2017. https://reinierdegraaf.nl/bezoekers/parkeren/ (accessed April 11, 2021).
[368] EGM Architecten. Reinier de Graaf Gasthuis, ziekenhuis, Delft 2017. https://www.egm.nl/architecten/projecten/reinier-de-graaf-gasthuis-/55 (accessed April 11, 2021).
[369] Carrier Corporation. Global Chiller 30HXC Water-Cooled Liquid Screw Chiller with R-134a refrigerant 2016. https://www.carrier.com/marine-offshore/en/worldwide/products/chillers/30hxc/ (accessed April 11, 2021).
[370] Agora Energiewende. Current and future cost of photovoltaics; long-term scenarios for market development, system prices and LCOE of utility scale PV-systems. Berlin, Germany: Agora Energiewende; 2015.
[371] Koninklijk Nederlands Metereologisch Instituut (KNMI). Uurgegevens van het weer in Nederland - Rotterdam (06344) 2015. https://www.knmi.nl/nederland-nu/klimatologie/uurgegevens (accessed April 11, 2021).
[372] Reda I, Andreas A. Solar position algorithm for solar radiation applications. Sol Energy 2004;76:577–89. doi:10.1016/j.solener.2003.12.003.
[373] Nowak O. Benchmarks for the energy demand of nutrient removal plants. Water Sci Technol 2003;47:125–32. doi:10.2166/wst.2003.0637.
[374] Capodaglio A, Olsson G. Energy Issues in Sustainable Urban Wastewater Management: Use, Demand Reduction and Recovery in the Urban Water Cycle. Sustainability 2019;12:266. doi:10.3390/su12010266.
[375] Bachmann N, Jansen J la C, Baxter D, Bochmann G, Montpart N. Sustainable biogas production in municipal wastewater treatment plants. Int Energy Agency Bioenergy 2015.
[376] Lorenzi E. Società Metropolitana Acque Torino (SMAT) 2015.
[377] Hygear b.v. HGS-L Customer Technical Description 2015.
[378] ITM Power. Inbetriebnahme und betriebserfahrungen der beiden Deutschen PEM P2G Anlagen der Firma ITM Power 2016. https://www.wab.net/fileadmin/media/Forschung_Entwicklung/Wind2Gas/06_Ludwig.pdf (accessed April 11, 2021).
[379] G. Parks, Boyd R, Cornish J, Remick R. Hydrogen station compression, storage, and dispensing technical status and costs 2014:30. https://www.nrel.gov/docs/fy14osti/58564.pdf (accessed August 28, 2019).
[380] Reddi K, Elgowainy A, Sutherland E. Hydrogen refueling station compression and storage optimization with tube-trailer deliveries. Int J Hydrogen Energy 2014;39:19169–81. doi:10.1016/j.ijhydene.2014.09.099.
[381] Elgowainy A, Krishna R, Mintz M, Brown D. H2A delivery scenario analysis model version 3.0* (HDSAM 3.0) user's manual 2015. https://hdsam.es.anl.gov/index.php?content=hdsam (accessed August 28, 2019).
[382] Ringer M. H2A delivery components model version 1.1: user's guide 2006.

https://www.hydrogen.energy.gov/pdfs/h2a_delivery_doc.pdf (accessed August 28, 2019).
[383] Baldwin D. Development of High Pressure Hydrogen Storage Tank for Storage and Gaseous Truck Delivery. Hexag Lincoln 2015.
[384] Baldwin D. Development of High Pressure Hydrogen Storage Tank for Storage and Gaseous Truck Delivery - FY 2015 Annual Progress Report DOE Hydrogen and Fuel Cells Program. Hexag Lincoln 2015.
[385] Bünger U, Michalski J, Crotogino F, Kruck O. Large-scale underground storage of hydrogen for the grid integration of renewable energy and other applications. Compend. Hydrog. Energy, Cambridge, United Kingdom: Elsevier; 2016, p. 133–63. doi:10.1016/B978-1-78242-364-5.00007-5.
[386] Chen T-P. Final report hydrogen delivery infrastructure options analysis, DOE award number: DE-FG36–05GO15032. San Francisco, CA, United States of America: U.S. Department of Energy (DOE), Nexant; 2008.
[387] Feng Z, Wang Y, Lim YC, Chen J, Gibson B. Steel concrete composite vessel for 875 bar stationary hydrogen storage – DOE hydrogen and fuel cells program FY 2016 annual progress report 2016. https://www.hydrogen.energy.gov/pdfs/progress16/iii_5_feng_2016.pdf (accessed August 28, 2019).
[388] Hua TQ, Ahluwalia RK, Peng J-K, Kromer M, Lasher S, McKenney K, et al. Technical assessment of compressed hydrogen storage tank systems for automotive applications. Argonne, IL, USA: Argonne National Laboratory; 2010.
[389] Fuel Cell Technologies Office (FCTO) – U.S. Department of Energy (DOE). Multi-Year Research, Development, and Demonstration (MYRD&D) Plan - Section 3.3 Hydrogen Storage 2015. https://www.energy.gov/sites/prod/files/2015/05/f22/fcto_myrdd_storage.pdf (accessed August 28, 2019).
[390] Koninklijk Nederlands Metereologisch Instituut (KNMI). Uurgegevens van het weer in Nederland - Hoek van Holland (06330) 2015. https://www.knmi.nl/nederland-nu/klimatologie/uurgegevens (accessed April 11, 2021).
[391] Enercon. Technical specifications E-141 EP4 2017. https://www.enercon.de/fileadmin/Redakteur/Medien-Portal/broschueren/pdf/ENERCON_E-141_EP4.pdf (accessed April 11, 2021).
[392] Augustine C, Bain R, Chapman J, Denholm P, Drury E, Hall DG, et al. Renewable Electricity Futures Study - Volume 2: Renewable Electricity Generation and Storage Technologies. Golden, Colorodo, United States of America: National Renewable Energy Laboratory (NREL); 2012.
[393] Steward D, Zuboy J. Community Energy: Analysis of Hydrogen Distributed Energy Systems with Photovoltaics for Load Leveling and Vehicle Refueling. 2014.
[394] Mathiesen B V., Lund H, Connolly D, Wenzel H, Ostergaard PA, Möller B, et al. Smart Energy Systems for coherent 100% renewable energy and transport solutions. Appl Energy 2015;145:139–54.

doi:10.1016/j.apenergy.2015.01.075.
[395] Orecchini F, Santiangeli A. Beyond smart grids - The need of intelligent energy networks for a higher global efficiency through energy vectors integration. Int J Hydrogen Energy 2011;36:8126–33. doi:10.1016/j.ijhydene.2011.01.160.
[396] Barret S. Toshiba starts H2One independent energy supply. Fuel Cells Bull 2015;2015:1. doi:https://doi.org/10.1016/S1464-2859(15)30067-5.
[397] Parra D, Gillott M, Walker GS. Design, testing and evaluation of a community hydrogen storage system for end user applications. Int J Hydrogen Energy 2016;41:5215–29. doi:10.1016/j.ijhydene.2016.01.098.
[398] Mohan V, Shah A, Sheffield JW, Martin KB. Design of a hydrogen community. Int J Hydrogen Energy 2012;37:1214–9. doi:10.1016/j.ijhydene.2011.10.039.
[399] Tzamalis G, Zoulias EI, Stamatakis E, Parissis OS, Stubos A, Lois E. Techno-economic analysis of RES & hydrogen technologies integration in remote island power system. Int. J. Hydrogen Energy, vol. 38, 2013, p. 11646–54. doi:10.1016/j.ijhydene.2013.03.084.
[400] Wu W, Christiana VI, Chen SA, Hwang JJ. Design and techno-economic optimization of a stand-alone PV (photovoltaic)/FC (fuel cell)/battery hybrid power system connected toa wastewater-to-hydrogen processor. Energy 2015;84:462–72. doi:10.1016/j.energy.2015.03.012.
[401] Lacko R, Drobnič B, Mori M, Sekavčnik M, Vidmar M. Stand-alone renewable combined heat and power system with hydrogen technologies for household application. Energy 2014;77:164–70. doi:10.1016/j.energy.2014.05.110.
[402] Uzunoglu M, Onar OC, Alam MS. Modeling, control and simulation of a PV/FC/UC based hybrid power generation system for stand-alone applications. Renew Energy 2009;34:509–20. doi:10.1016/j.renene.2008.06.009.
[403] Ulleberg Ø. Stand-alone power systems for the future: optimal design, operation & control of solar-hydrogen energy systems. NTNU, Trondheim, Norvège 1998:225.
[404] Andrews J, Shabani B. Dimensionless analysis of the global techno-economic feasibility of solar-hydrogen systems for constant year-round power supply. Int J Hydrogen Energy 2012;37:6–18. doi:10.1016/j.ijhydene.2011.09.102.
[405] Little M, Thomson M, Infield D. Electrical integration of renewable energy into stand-alone power supplies incorporating hydrogen storage. Int J Hydrogen Energy 2007;32:1582–8. doi:10.1016/j.ijhydene.2006.10.035.
[406] Shabani B, Andrews J, Watkins S. Energy and cost analysis of a solar-hydrogen combined heat and power system for remote power supply using a computer simulation. Sol Energy 2010;84:144–55. doi:10.1016/j.solener.2009.10.020.
[407] Bernier E, Hamelin J, Agbossou K, Bose TK. Electric round-trip efficiency of hydrogen and oxygen-based energy storage. Int J Hydrogen Energy 2005;30:105–11. doi:10.1016/j.ijhydene.2004.03.039.

[408] Onar OC, Uzunoglu M, Alam MS. Dynamic modeling, design and simulation of a wind/fuel cell/ultra-capacitor-based hybrid power generation system. J Power Sources 2006;161:707–22. doi:10.1016/j.jpowsour.2006.03.055.
[409] Yilanci A, Dincer I, Ozturk HK. A review on solar-hydrogen/fuel cell hybrid energy systems for stationary applications. Prog Energy Combust Sci 2009;35:231–44. doi:10.1016/j.pecs.2008.07.004.
[410] Eroglu M, Dursun E, Sevencan S, Song J, Yazici S, Kilic O. A mobile renewable house using PV/wind/fuel cell hybrid power system. Int J Hydrogen Energy 2011;36:7985–92. doi:10.1016/j.ijhydene.2011.01.046.
[411] Dursun E, Acarkan B, Kilic O. Modeling of hydrogen production with a stand-alone renewable hybrid power system. Int J Hydrogen Energy 2012;37:3098–107. doi:10.1016/j.ijhydene.2011.11.029.
[412] Kalinci Y, Hepbasli A, Dincer I. Techno-economic analysis of a stand-alone hybrid renewable energy system with hydrogen production and storage options. Int J Hydrogen Energy 2015;40:7652–64. doi:10.1016/j.ijhydene.2014.10.147.
[413] Gahleitner G. Hydrogen from renewable electricity: An international review of power-to-gas pilot plants for stationary applications. Int J Hydrogen Energy 2013;38:2039–61. doi:10.1016/j.ijhydene.2012.12.010.
[414] Kriston A, Szabó T, Inzelt G. The marriage of car sharing and hydrogen economy: A possible solution to the main problems of urban living. Int J Hydrogen Energy 2010;35:12697–708. doi:10.1016/j.ijhydene.2010.08.110.
[415] Zhang X, Chan SH, Ho HK, Tan SC, Li M, Li G, et al. Towards a smart energy network: The roles of fuel/electrolysis cells and technological perspectives. Int J Hydrogen Energy 2015;40:6866–919. doi:10.1016/j.ijhydene.2015.03.133.
[416] Gammon R, Roy A, Barton J, Little M. Hydrogen and renewables integration (HARI). Case Study Int Energy Agency Hydrog Implement Agreem 2006.
[417] Newborough M, Peacock AD. Micro-generation systems and electrolysers for refuelling private bi-fuel cars at home. Int J Hydrogen Energy 2009;34:4438–51. doi:10.1016/j.ijhydene.2009.02.050.
[418] Miland H, Ulleberg Ø. Testing of a small-scale stand-alone power system based on solar energy and hydrogen. Sol Energy 2012;86:666–80. doi:10.1016/j.solener.2008.04.013.
[419] Kelly NA, Gibson TL, Ouwerkerk DB. A solar-powered, high-efficiency hydrogen fueling system using high-pressure electrolysis of water: Design and initial results. Int J Hydrogen Energy 2008;33:2747–64. doi:10.1016/j.ijhydene.2008.03.036.
[420] Ulleberg Ø, Nakken T, Eté A. The wind/hydrogen demonstration system at Utsira in Norway: Evaluation of system performance using operational data and updated hydrogen energy system modeling tools. Int J Hydrogen Energy 2010;35:1841–52. doi:10.1016/j.ijhydene.2009.10.077.
[421] Syed F, Fowler M, Wan D, Maniyali Y. An energy demand model for a fleet of plug-in fuel cell vehicles and commercial building interfaced with a clean

energy hub. Int J Hydrogen Energy 2010;35:5154–63. doi:10.1016/j.ijhydene.2009.08.089.
[422] Williams BD. Commercializing Light-duty Plug-in/plug-out Hydrogen-fuel-cell Vehicles: “mobile Electricity” Technologies, Early California Household Markets, and Innovation Management. University of California, Davis; 2007.
[423] Samsun RC. Global Development Status of Fuel Cell Vehicles. Fuel Cells Data, Facts Fig., Wiley-VCH Verlag GmbH & Co. KGaA.; 2016, p. 37–60. doi:10.1002/9783527693924.ch05.
[424] Shinoda K, Lee EP, Nakano M, Lukszo Z. Optimization model for a microgrid with fuel cell vehicles. ICNSC 2016 - 13th IEEE Int. Conf. Networking, Sens. Control, 2016. doi:10.1109/ICNSC.2016.7479027.
[425] Park Lee E, Chappin E, Lukszo Z, Herder P. The Car as Power Plant: Towards socio-technical systems integration. 2015 IEEE Eindhoven PowerTech, IEEE; 2015, p. 1–6. doi:10.1109/PTC.2015.7232756.
[426] Brooker P, Qin N, Mohajeri N. Fuel Cell Vehicles as Back-Up Power Options. Interface Mag 2015;24:57–60. doi:10.1149/2.F05151if.
[427] Nomura N, Fukunaga T, Suzuki J. Cogeneration vehicle system utilizing a fuel cell car, and a mobile unit as a component of the system. U.S. Patent No. 7,040,430, 2006.
[428] Dincer I, Acar C. Review and evaluation of hydrogen production methods for better sustainability. Int J Hydrogen Energy 2014;40:11094–111. doi:10.1016/j.ijhydene.2014.12.035.
[429] Chaubey R, Sahu S, James OO, Maity S. A review on development of industrial processes and emerging techniques for production of hydrogen from renewable and sustainable sources. Renew Sustain Energy Rev 2013;23:443–62. doi:10.1016/j.rser.2013.02.019.
[430] Holladay JD, Hu J, King DL, Wang Y. An overview of hydrogen production technologies. Catal Today 2009;139:244–60. doi:10.1016/j.cattod.2008.08.039.
[431] Promes EJO, Woudstra T, Schoenmakers L, Oldenbroek V, Thallam Thattai A, Aravind PV. Thermodynamic evaluation and experimental validation of 253MW Integrated Coal Gasification Combined Cycle power plant in Buggenum, Netherlands. Appl Energy 2015;155. doi:10.1016/j.apenergy.2015.05.006.
[432] Thallam Thattai A, Oldenbroek V, Schoenmakers L, Woudstra T, Aravind PV. Experimental model validation and thermodynamic assessment on high percentage (up to 70%) biomass co-gasification at the 253 MW<inf>e</inf>integrated gasification combined cycle power plant in Buggenum, The Netherlands. Appl Energy 2016;168. doi:10.1016/j.apenergy.2016.01.131.
[433] Serna Á, Tadeo F. Offshore hydrogen production from wave energy. Int J Hydrogen Energy 2014;39:1549–57. doi:10.1016/j.ijhydene.2013.04.113.
[434] World Health Organization (WHO). Urban Population Growth - Global Health Observatory (GHO) Data 2014. http://www.who.int/gho/urban_health/situation_trends/urban_populatio

n_growth_text/en/ (accessed August 19, 2016).
[435] Meier K. Hydrogen production with sea water electrolysis using Norwegian offshore wind energy potentials: Techno-economic assessment for an offshore-based hydrogen production approach with state-of-the-art technology. Int J Energy Environ Eng 2014;5:1–12. doi:10.1007/s40095-014-0104-6.
[436] Det Norske Veritas Germanischer Lloyd (DNV GL). Offshore production of renewable hydrogen, Summer Project 2015. Høvik, Norway: DNV GL AS; 2015.
[437] International Energy Agency (IEA). Next-Generation Wind and Solar Power - From Cost to Value 2016. http://www.iea.org/publications/freepublications/publication/NextGenerationWindandSolarPower.pdf (accessed October 16, 2016).
[438] Yoshida T, Kojima K. Toyota MIRAI Fuel Cell Vehicle and Progress Toward a Future Hydrogen Society. Interface Mag 2015;24:45–9. doi:10.1149/2.F03152if.
[439] Hyundai Motor Company (HMC). Hyundai ix35 Fuel Cell 2016. http://worldwide.hyundai.com/WW/Showroom/Eco/ix35-Fuel-Cell/PIP/index.html (accessed August 19, 2016).
[440] Daimler AG. Under the Microscope: Mercedes-Benz GLC F-CELL: The Fuel Cell Gets a Plug 2016. http://media.daimler.com/marsMediaSite/en/instance/ko/Under-the-microscope-Mercedes-Benz-GLC-F-CELL-The-fuel-cell-.xhtml?oid=11111320 (accessed August 19, 2016).
[441] Dodds PE, Ekins P. A portfolio of powertrains for the UK: An energy systems analysis. Int. J. Hydrogen Energy, vol. 39, Elsevier Ltd; 2014, p. 13941–53. doi:10.1016/j.ijhydene.2014.06.128.
[442] McKinsey. A portfolio of power-trains for Europe: a fact-based analysis - The role of Battery Electric Vehicles, Plug-in Hybrids and Fuel Cell Electric Vehicles 2010.
[443] The International Zero-Emission Vehicle Alliance. Accelerating the Adoption of Zero-Emission Vehicles 2016. http://www.zevalliance.org/ (accessed August 22, 2016).
[444] Hydrogen Mobility Europe (H2ME). Hydrogen Mobility Europe (H2ME) 2016. http://h2me.eu/ (accessed August 22, 2016).
[445] Hydrogen Link Denmark. National Implementation Plan (NIP) for Hydrogen Refueling Infrastructure, Part of the HIT Project, Denmark 2014. http://www.hydrogenlink.net/download/reports/HIT-NIP-Denmark_3rd-final_June-2014.pdf (accessed August 16, 2016).
[446] UK H2Mobility. Hydrogen: Fuelling Cleaner Motoring 2016. http://www.ukh2mobility.co.uk/ (accessed August 22, 2016).
[447] Air Resources Board (ARB). California Environmental Protection Agency (CalEPA), 2016 Annual Evaluation of Hydrogen Fuel Cell Electric Vehicle Deployment and Hydrogen Fuel Station Network Development 2016. https://www.arb.ca.gov/msprog/zevprog/ab8/ab8_report_2016.pdf (accessed October 17, 2016).

[448] Yang C, Ogden JM. Renewable and low carbon hydrogen for California-Modeling the long term evolution of fuel infrastructure using a quasi-spatial TIMES model. Int J Hydrogen Energy 2013;38:4250–65. doi:10.1016/j.ijhydene.2013.01.195.
[449] Ministry of Economy Trade and Industry (METI). Compilation of the Revised Version of the Strategic Roadmap for Hydrogen and Fuel Cells 2016. http://www.meti.go.jp/english/press/2016/0322_05.html (accessed August 19, 2016).
[450] Clean Energy Partnership (CEP). Clean Energy Partnership (CEP) 2016. https://cleanenergypartnership.de/en/home/ (accessed August 22, 2016).
[451] H2 Mobility. H2 Mobility, Wasserstoff-Tankstellen Infrastruktur 2023≈400 2016. http://h2-mobility.de/en/ (accessed August 22, 2016).
[452] J. Marcinkoski, Spendelow J, Wilson A, Papageorgopoulos D. Fuel Cell System Cost - 2015 - DOE Hydrogen and Fuel Cells Program Record. US Dep Energy 2015. https://www.hydrogen.energy.gov/pdfs/15015_fuel_cell_system_cost_2015.pdf (accessed October 17, 2016).
[453] Rifkin J. The hydrogen economy: The creation of the worldwide energy web and the redistribution of power on earth. Refocus 2003;4:12. doi:10.1016/S1471-0846(03)80112-9.
[454] Ball M, Weeda M. The hydrogen economy - Vision or reality? Int J Hydrogen Energy 2015;40:7903–19. doi:10.1016/j.ijhydene.2015.04.032.
[455] Moliner R, Lázaro MJ, Suelves I. Analysis of the strategies for bridging the gap towards the Hydrogen Economy. Int J Hydrogen Energy 2016;41:19500–8. doi:10.1016/j.ijhydene.2016.06.202.
[456] Kawasaki Heavy Industries. Kawasaki Hydrogen Road - paving the way for a hydrogen-based society 2018. http://global.kawasaki.com/en/stories/hydrogen/.
[457] Toyota Motor Corporation (TMC). Toward Sustainable Energy-Based Society That Use Hydrogen 2016.
[458] Toshiba Corporation. Hydrogen economy envisioned by Toshiba n.d. https://www.toshiba-newenergy.com/en/.
[459] Maroufmashat A, Fowler M, Sattari Khavas S, Elkamel A, Roshandel R, Hajimiragha A. Mixed integer linear programing based approach for optimal planning and operation of a smart urban energy network to support the hydrogen economy. Int J Hydrogen Energy 2016;41:7700–16. doi:10.1016/j.ijhydene.2015.08.038.
[460] Edenhofer O, Pichs-Madruga R, Sokona Y, Seyboth K, Matschoss P, Kadner S, et al. Annex II: Methodology in IPCC special report on renewable energy sources and climate change mitigation 2011. https://www.ipcc.ch/site/assets/uploads/2018/03/SRREN_FD_SPM_final-1.pdf (accessed August 28, 2019).
[461] Wissel S, Rath-Nagel S, Blesl M, Fahl U, Voß A. Stromerzeugungskosten im Vergleich 2008. https://www.ier.uni-stuttgart.de/publikationen/arbeitsberichte/downloads/Arbeitsbericht_04.pdf (accessed August 28, 2019).

[462] Bureau of Labor Statistics (BLS) - U.S. Department of Labor. Inflation Calculator 2016. http://www.bls.gov/data/inflation_calculator.htm (accessed May 9, 2016).
[463] Blok K, Nieuwlaar E. Introduction to Energy Analysis. Abingdon, Oxon ; New York, NY : Routledge, Earthscan,: Routledge; 2016. doi:10.4324/9781315617213.
[464] Eurostat. Simplified energy balances - annual data 2014. ttp://ec.europa.eu/eurostat/en/web/products-datasets/-/NRG_100A (accessed August 22, 2016).
[465] FuelsEurope – division of the European Petroleum Refiners Association. Number of petrol stations in Europe end of 2015. Brussels, Belgium: FuelsEurope; 2016.
[466] Eurostat. Number of private households by household composition, number of children and age of youngest child (1 000) 2014. http://ec.europa.eu/eurostat/en/web/products-datasets/-/LFST_HHNHTYCH (accessed August 22, 2016).
[467] Melaina M, Penev M. Hydrogen station cost estimates: comparing hydrogen station cost calculator results with other recent estimates - NREL/TP-5400-56412. Golden, CO, USA: National Renewable Energy Laboratory (NREL); 2013.
[468] EY, Cambridge Econometrics Ltd, Arcadia International, European Commission. The economic impact of modern retail on choice and innovation in the EU food sector - Final report. Luxembourg, Luxembourg: Publications Office of the European Union; 2014.
[469] Werner S. European space cooling demands. Energy 2016;110:148–56. doi:10.1016/j.energy.2015.11.028.
[470] Enerdata. ODYSSEE database - Transport 2015. http://odyssee.enerdata.net/database/ (accessed August 28, 2019).
[471] Enerdata. ODYSSEE database - Services 2015. http://odyssee.enerdata.net/database/.
[472] Enerdata. ODYSSEE database - Households 2015. http://odyssee.enerdata.net/database/.
[473] Eurostat. Stock of vehicles by category and NUTS 2 regions 2015. http://ec.europa.eu/eurostat/web/products-datasets/-/tran_r_vehst (accessed August 28, 2019).
[474] Eurostat. Population on 1 January 2014.
[475] Danmarks Statistik. BIL6: New Registrations, Sale of Second Hand Vehicles and Stock Etc by Type of Vehicle and Unit 2014. http://www.statbank.dk/BIL6 (accessed August 22, 2016).
[476] Kraftfahrt-Bundesamt. Verkehr in Kilometern der deutschen Kraftfahrzeuge im Jahr 2014 2014. http://www.kba.de/DE/Statistik/Kraftverkehr/VerkehrKilometer/2014/2014_vk_kurzbericht_pdf.pdf?__blob=publicationFile&v=1 (accessed August 22, 2016).
[477] Statline - Centraal Bureau voor de Statistiek (CBS). Verkeersprestaties Motorvoertuigen; Kilometers, Voertuigsoort, Grondgebied 2014.

http://statline.cbs.nl/StatWeb/publication/?VW=T&DM=SLNL&PA=80302NED&LA=NL (accessed August 22, 2016).
[478] Danmarks Statistik. VEJ23: Road Traffic of Dannish Vehicles on Danish Roads by Means of Transport 2014. http://statbank.dk/VEJ23 (accessed August 22, 2016).
[479] UK Department for Transport. Table VEH0101 Licensed Vehicles by Body Type at the End of Quarter: Great Britain and United Kingdom 2014. https://www.gov.uk/government/uploads/system/uploads/attachment_data/file/527186/veh0101.ods (accessed August 22, 2016).
[480] Trafik Analys. Vehicle Statistics - Official Statistics of Sweden 2014. http://www.trafa.se/en/road-traffic/vehicle-statistics/ (accessed August 22, 2016).
[481] Kwanten M. Kilometers afgelegd door Belgische voertuigen in het jaar 2014. Fed Overheidsd Mobil En Vervoer Dir Duurzame Mobil En Spoorbeleid 2015. http://mobilit.belgium.be/sites/default/files/Kilometers_2014_NL.pdf (accessed August 22, 2016).
[482] Sarbu I, Sebarchievici C. General review of ground-source heat pump systems for heating and cooling of buildings. Energy Build 2014. doi:10.1016/j.enbuild.2013.11.068.
[483] Sivasakthivel T, Murugesan K, Thomas HR. Optimization of operating parameters of ground source heat pump system for space heating and cooling by Taguchi method and utility concept. Appl Energy 2014;116:76–85. doi:10.1016/j.apenergy.2013.10.065.
[484] Jung HW, Kang H, Yoon WJ, Kim Y. Performance comparison between a single-stage and a cascade multi-functional heat pump for both air heating and hot water supply. Int J Refrig 2013;36:1431–41. doi:10.1016/j.ijrefrig.2013.03.003.
[485] Girard A, Gago EJ, Muneer T, Caceres G. Higher ground source heat pump COP in a residential building through the use of solar thermal collectors. Renew Energy 2015;80:26–39. doi:10.1016/j.renene.2015.01.063.
[486] U.S. Department of Energy (DOE). Quadrennial technology review – an assessment of energy technologies and research opportunities – Chapter 5 section 5.1. Washington DC, USA: U.S. Department of Energy (DOE); 2015.
[487] International Energy Agency (IEA). Nordic Energy Technology Perspectives 2016: Cities, flexibility and pathways to carbon-neutrality. Oslo, Norway: Nordic Energy Research; 2016. doi:10.1787/9789264257665-en.
[488] Wu X, Xing Z, He Z, Wang X, Chen W. Performance evaluation of a capacity-regulated high temperature heat pump for waste heat recovery in dyeing industry. Appl Therm Eng 2016;93:1193–201. doi:10.1016/j.applthermaleng.2015.10.075.
[489] Olesen MF, Madsen C, Olsen L, Paaske B, Rothuizen ED. High efficient ammonia heat pump system for industrial process water using the ISEC concept. Part 2. Proc. 11th IIR Gustav Lorentzen Conf. Nat. Refrig., Chinese Association of Refrigeration; 2014.
[490] Rothuizen ED, Madsen C, Elmegaard B, Olesen M, Markussen WB. High

efficient ammonia heat pump system for industrial process water using the ISEC concept. Part 1. Proc. 11th IIR Gustav Lorentzen Conf. Nat. Refrig., Chinese Association of Refrigeration; 2014.
[491] Fukuda S, Kondou C, Takata N, Koyama S. Low GWP refrigerants R1234ze(E) and R1234ze(Z) for high temperature heat pumps. Int J Refrig 2014;40:161–73. doi:10.1016/j.ijrefrig.2013.10.014.
[492] Kaiser WH, Van Eldik M. The potential for CO2 heat pumps in the South African industrial sector. Proc. Conf. Ind. Commer. Use Energy, ICUE, vol. 2015- Septe, IEEE Computer Society; 2015, p. 70–5. doi:10.1109/ICUE.2015.7280249.
[493] Directorate-General (DG) for Energy. Communication from the Commission to the European Parliament, the Council, the European Economic and Social Committee and the Committee of the Regions on an EU Strategy for Heating and Cooling. Eur Comm 2016. https://ec.europa.eu/energy/sites/ener/files/documents/1_EN_autre_document_travail_service_part1_v6_0.pdf (accessed August 23, 2016).
[494] Commissariat général au développement durable – Service de l'observation et des statistiques. G – Bilan de La Circulation - Les Comptes Des Transports En 2014 2015. http://www.statistiques.developpement-durable.gouv.fr/fileadmin/documents/Produits_editoriaux/Publications/References/2015/comptes-transports-2014/comptes-transports-fiche-11.pdf (accessed August 22, 2016).
[495] Statline - Centraal Bureau voor de Statistiek (CBS). Motorvoertuigenpark; Inwoners, Type, Regio, 1 Januari 2014. http://statline.cbs.nl/Statweb/publication/?VW=T&DM=SLNL&PA=7374hvv&D1=2-11&D2=0&D3=a&HD=160124-1642&HDR=T&STB=G2,G1 (accessed August 22, 2016).
[496] UK Department for Transport. Table TRA0201 Road Traffic (vehicle Kilometres) by Vehicle Type in Great Britain 2014. https://www.gov.uk/government/uploads/system/uploads/attachment_data/file/523560/tra0201.xls (accessed August 22, 2016).
[497] UK Department for Transport. Table RFS0115 Average Annual Vehicle Kilometres by Vehicle Type 2014. https://www.gov.uk/government/statistical-data-sets/rfs01-goods-lifted-and-distance-hauled (accessed August 22, 2016).
[498] Energy Policy Statistical Support Unit - Sustainable Energy Authority of Ireland (SEAI). Energy in Transport 2014 Report 2014. http://www.seai.ie/Publications/Statistics_Publications/Energy_in_Transport/Energy-in-Transport-2014-report.pdf (accessed August 22, 2016).
[499] Emoss b.v. CM Mission 150e | Elektrische Minibus 2016. http://www.emoss.biz/nl/elektrische-bus/minibus-cm-mission-150e/ (accessed August 23, 2016).
[500] Heiko Ammermann, Ruf Y, Lange S, Fundulea D, Martin A. Fuel Cell Electric Buses – Potential for Sustainable Public Transport in Europe. Rol Berger Fuel Cells Hydrog Jt Undert (FCH JU) 2015.
[501] Sharma AK, Begbie D, Gardner T. Rainwater tank systems for urban water

supply: design, yield, energy, health risks, economics and social perceptions. IWA Publishing; 2015.
[502] Sharma AK, Cook S, Gardner T, Tjandraatmadja G. Rainwater tanks in modern cities: A review of current practices and research. J Water Clim Chang 2016;7:445–66. doi:10.2166/wcc.2016.039.
[503] Siems R, Sahin O. Energy intensity of residential rainwater tank systems: Exploring the economic and environmental impacts. J Clean Prod 2016;113:251–62. doi:10.1016/j.jclepro.2015.11.020.
[504] Gutschner M, Nowak S, Ruoss D, Toggweiler P, Schoen T. Potential for building integrated photovoltaics, IEA-PVPS Task 7. St. Ursen, Switzerland: IEA Photovoltaic Power Systems Programme (PVPS), NET Nowa Energy & Technology Ltd.; 2002.
[505] International Energy Agency (IEA). Energy technology perspectives 2016: towards sustainable urban energy systems, annex H rooftop solar PV potential in cities. Paris, France: IEA Publications; 2016.
[506] Green MA, Emery K, Hishikawa Y, Warta W, Dunlop ED. Solar cell efficiency tables (version 47). Prog Photovoltaics Res Appl 2015;24:n/a-n/a. doi:10.1002/pip.2728.
[507] Defaix PR, van Sark WGJHM, Worrell E, de Visser E. Technical potential for photovoltaics on buildings in the EU-27. Sol Energy 2012;86:2644–53. doi:10.1016/j.solener.2012.06.007.
[508] Breyer C, Gerlach A. Global overview on grid-parity. Prog Photovoltaics Res Appl 2013;21:121–36. doi:10.1002/pip.1254.
[509] Reich NH, Mueller B, Armbruster A, Van Sark WGJHM, Kiefer K, Reise C. Performance ratio revisited: Is PR > 90% realistic? Prog. Photovoltaics Res. Appl., vol. 20, 2012, p. 717–26. doi:10.1002/pip.1219.
[510] Dierauf T, Growitz A, Kurtz S, Hansen C. Weather-Corrected Performance Ratio. NREL Tech Rep NREL/TP-5200-57991 2013:1–16.
[511] Joint Research Center (JRC). PVGIS Photovoltaic Solar Electricity Potential in European Countries - Yearly Global Irradiation Incident on Optimally-Inclined Photovoltaic Modules Placed in Urban Areas of the EU-27 and 6 Candidate Countries. Eur Union 2015. http://re.jrc.ec.europa.eu/pvgis/cmaps/eu_cmsaf_opt/PVGIS-EuropeSolarPotential.pdf (accessed August 23, 2016).
[512] Šúri M, Huld TA, Dunlop ED, Ossenbrink HA. Potential of solar electricity generation in the European Union member states and candidate countries. Sol Energy 2007;81:1295–305. doi:10.1016/j.solener.2006.12.007.
[513] Bertuccioli L, Chan A, Hart D, Lehner F, Madden B, Standen E. Development of water electrolysis in the European union. Final report. Fuel Cells and Hydrogen Joint Undertaking (FCH-JU). Brussels, Belgium: Fuel Cells and Hydrogen Joint Undertaking (FCH-JU); 2014.
[514] Siemens AG. Siemens Silyzer 200 (PEM Electrolysis System) 2015. https://www.industry.siemens.com/topics/global/en/pem-electrolyzer/silyzer/Documents/silyzer-200-en_v1.3_InternetVersion.pdf (accessed August 23, 2016).
[515] SAE International. Hydrogen Fuel Quality for Fuel Cell Vehicles - J2719A.

2015.
[516] Strategic Analysis (SA), National Renewable Energy Laboratory (NREL). PEM electrolysis H2A production case study documentation - Fuel Cell Technologies Office (FCTO) – U.S. Department of Energy (DOE) 2013. https://www.nrel.gov/hydrogen/assets/pdfs/h2a-pem-electrolysis-case-study-documentation.pdf (accessed August 28, 2019).
[517] Carmo M, Fritz DL, Mergel J, Stolten D. A comprehensive review on PEM water electrolysis. Int J Hydrogen Energy 2013;38:4901–34. doi:10.1016/j.ijhydene.2013.01.151.
[518] Götz M, Lefebvre J, Mörs F, McDaniel Koch A, Graf F, Bajohr S, et al. Renewable Power-to-Gas: A technological and economic review. Renew Energy 2016;85:1371–90. doi:10.1016/j.renene.2015.07.066.
[519] Noack C, Burggraf F, Hosseiny SS, Lettenmeier P, Kolb S, Belz S, et al. Studie über die Planung einer Demonstrationsanlage zur Wasserstoff-Kraftstoffgewinnung durch Elektrolyse mit Zwischenspeicherung in Salzkavernen unter Druck. Stuttgart, Germany: German Aerospace Center; 2015.
[520] C. Ainscough, Peterson D, Mille E. DOE Hydrogen and Fuel Cells Program Record 14004: Hydrogen Production Cost From PEM Electrolysis. US Dep Energy 2014. https://www.hydrogen.energy.gov/pdfs/14004_h2_production_cost_pem_electrolysis.pdf (accessed August 23, 2016).
[521] National Renewable Energy Laboratory (NREL). H2A analysis, production case studies: current forecourt hydrogen production from PEM electrolysis version 3.101 2013. https://www.hydrogen.energy.gov/h2a_prod_studies.html (accessed August 28, 2019).
[522] National Renewable Energy Laboratory (NREL). H2A analysis, production case studies: future forecourt hydrogen production from PEM electrolysis version 3.101 2013. https://www.hydrogen.energy.gov/h2a_prod_studies.html (accessed August 28, 2019).
[523] Smolinka T. Cost break down and analysis of PEM electrolysis systems for different industrial and power to gas applications, World of Energy Solutions, Stuttgart (DE), October 12, 2015. 2015.
[524] Mathias MF, Makharia R, Gasteiger HA, Conley JJ, Fuller TJ, Gittleman CJ, et al. Two fuel cell cars in every garage? Interface-Electrochemical Soc 2005;14:24–36.
[525] National Renewable Energy Laboratory (NREL). H2A analysis, production case studies: current forecourt hydrogen production from PEM electrolysis version 3.101 - storage and refueling 2013. https://www.hydrogen.energy.gov/h2a_prod_studies.html (accessed August 28, 2019).
[526] Hirscher M, Hirose K. Handbook of Hydrogen Storage: New Materials for Future Energy Storage. Wiley; 2010.
[527] Klebanoff L. Hydrogen Storage Technology: Materials and Applications.

Taylor & Francis; 2012.
[528] Godula-Jopek A, Jehle W, Wellnitz J. Hydrogen Storage Technologies. Weinheim, Germany: Wiley-VCH Verlag GmbH & Co. KGaA; 2012. doi:10.1002/9783527649921.
[529] Durbin DJ, Malardier-Jugroot C. Review of hydrogen storage techniques for on board vehicle applications. Int J Hydrogen Energy 2013;38:14595–617. doi:10.1016/j.ijhydene.2013.07.058.
[530] Feng Z, Wang Y, Lim YC. Steel Concrete Composite Vessel for 875 Bar Stationary Hydrogen Storage - DOE Hydrogen and Fuel Cells Program FY 2015 Annual Progress Report. Oak Ridge Natl Lab 2015. https://www.hydrogen.energy.gov/pdfs/progress15/iii_8_feng_2015.pdf (accessed August 23, 2016).
[531] Feng Z, Wang Y, Lim YC, Chen J, Anovitz L. Vessel Design and Fabrication Technology for Stationary High- Pressure Hydrogen Storage - FY 2015 Annual Progress Report DOE Hydrogen and Fuel Cells Program. Oak Ridge Natl Lab 2015. https://www.hydrogen.energy.gov/pdfs/review15/pd088_feng_2015_o.pdf (accessed August 23, 2015).
[532] Zhang W, Ren F, Feng Z, Wang J. Manufacturing Cost Analysis of Novel Steel/Concrete Composite Vessel for Stationary Storage of High-Pressure Hydrogen. Oak Ridge Natl Lab 2012. http://info.ornl.gov/sites/publications/files/pub41882.pdf (accessed October 17, 2016).
[533] Teichmann D, Arlt W, Wasserscheid P. Liquid Organic Hydrogen Carriers as an efficient vector for the transport and storage of renewable energy. Int J Hydrogen Energy 2012;37:18118–32. doi:10.1016/j.ijhydene.2012.08.066.
[534] Baldwin D. BULK HAULING EQUIPMENT FOR CHG. Hexag Lincoln 2013. http://energy.gov/eere/fuelcells/downloads/bulk-hauling-equipment-chg (accessed October 17, 2016).
[535] J. Pratt, Terlip D, Ainscough C, Kurtz J, Elgowainy A. H2FIRST reference station design task project deliverable 2-2. Golden, CO, USA: National Renewable Energy Laboratory (NREL); 2015.
[536] Fuel Cell Technologies Office (FCTO) – U.S. Department of Energy (DOE). Multi-Year Research, Development, and Demonstration (MYRD&D) Plan - Section 3.2 hydrogen delivery 2015. https://energy.gov/sites/prod/files/2015/08/f25/fcto_myrdd_delivery.pdf (accessed August 28, 2019).
[537] Elgowainy A, Reddi K. Hydrogen fueling station pre-cooling analysis. Argonne Natl Lab 2016. https://www.hydrogen.energy.gov/pdfs/review16/pd107_elgowainy_2016_o.pdf (accessed August 28, 2019).
[538] Sprik S, Kurtz J, Ainscough C, Saur G, Peters M. Hydrogen Station Data Collection and Analysis 2015. https://www.hydrogen.energy.gov/pdfs/review15/tv017_sprik_2015_o.pdf (accessed October 17, 2016).
[539] Tsotridis G, Pilenga A, Marco GD, Malkow T. EU harmonised test protocols

for PEMFC-MEA testing in single cell configuration for automotive applications. Petten, The Netherlands: Joint Research Centre (JRC); 2015.
[540] Tutuianu M, Bonnel P, Ciuffo B, Haniu T, Ichikawa N, Marotta A, et al. Development of the World-wide harmonized Light duty Test Cycle (WLTC) and a possible pathway for its introduction in the European legislation. Transp Res Part D Transp Environ 2015;40:61–75. doi:10.1016/j.trd.2015.07.011.
[541] de Jager B, van Keulen T, Kessels J. Optimal Control of Hybrid Vehicles. London: Springer London; 2013. doi:10.1007/978-1-4471-5076-3.
[542] Tuominen R, Ihonen J. HyCoRA – Hydrogen Contaminant Risk Assessment grant agreement no: 621223 deliverable 4.2 guidance for the second part of WP1 and WP2 work. Espoo, Finland: VTT Technical Research Centre of Finland; 2015.
[543] Borup R, Meyers J, Pivovar B, Kim YS, Mukundan R, Garland N, et al. Scientific Aspects of Polymer Electrolyte Fuel Cell Durability and Degradation. Chem Rev 2007;107:3904–51. doi:10.1021/cr050182l.
[544] Yousfi-Steiner N, Moçotéguy P, Candusso D, Hissel D. A review on polymer electrolyte membrane fuel cell catalyst degradation and starvation issues: Causes, consequences and diagnostic for mitigation. J Power Sources 2009;194:130–45. doi:10.1016/j.jpowsour.2009.03.060.
[545] Yu Y, Li H, Wang H, Yuan X-Z, Wang G, Pan M. A review on performance degradation of proton exchange membrane fuel cells during startup and shutdown processes: Causes, consequences, and mitigation strategies. J Power Sources 2012;205:10–23. doi:10.1016/j.jpowsour.2012.01.059.
[546] Vieira AS, Beal CD, Ghisi E, Stewart RA. Energy intensity of rainwater harvesting systems: A review. Renew Sustain Energy Rev 2014;34:225–42. doi:10.1016/j.rser.2014.03.012.
[547] Farreny R, Morales-Pinzón T, Guisasola A, Tayà C, Rieradevall J, Gabarrell X. Roof selection for rainwater harvesting: Quantity and quality assessments in Spain. Water Res 2011;45:3245–54. doi:10.1016/j.watres.2011.03.036.
[548] Eurostat. Area by NUTS 3 region 2014. http://ec.europa.eu/eurostat/en/web/products-datasets/-/DEMO_R_D3AREA (accessed August 23, 2016).
[549] Eurostat. Renewable freshwater resources 2014. http://ec.europa.eu/eurostat/en/web/products-datasets/-/ENV_WAT_RES (accessed August 23, 2016).
[550] T.R. Gurung, Umapathi S, Sharma AK. Economics of scale analysis of communal rainwater tanks. Brisbane, Australia: Urban Water Security Research Alliance; 2012.
[551] Barbir F. PEM electrolysis for production of hydrogen from renewable energy sources. Sol Energy 2005;78:661–9. doi:10.1016/j.solener.2004.09.003.
[552] Mistry KH, Lienhard JH. An economics-based second law efficiency. Entropy 2013;15:2736–65. doi:10.3390/e15072736.
[553] Dow Water & Process Solutions. Reverse Osmosis System Analysis (ROSA) for FILMTECTM Membranes, ROSA 9.0.0, ConfigDB u399339_282 2015.

http://www.dow.com/en-us/water-and-process-solutions/resources/design-software/rosa-software (accessed August 23, 2016).
[554] Pérez-González A, Urtiaga AM, Ibáñez R, Ortiz I. State of the art and review on the treatment technologies of water reverse osmosis concentrates. Water Res 2012;46:267–83. doi:10.1016/j.watres.2011.10.046.
[555] Dow water & process solutions. Reverse Osmosis System Analysis (ROSA) for FILMTECTM membranes 2015.
[556] Elimelech M, Phillip WA. The Future of Seawater Desalination: Energy, Technology, and the Environment. Science (80-) 2011;333:712–7. doi:10.1126/science.1200488.
[557] International Renewable Energy Agency (IRENA). Renewable Power Generation Costs in 2014. Abu Dhabi, United Arab Emirates: IRENA; 2015.
[558] International Renewable Energy Agency (IRENA). Renewable energy cost analysis – wind power. Abu Dhabi, United Arab Emirates: IRENA; 2012.
[559] International Energy Agency (IEA). Energy technology perspectives 2012: pathways to a clean energy system. 2012.
[560] Sensfuß F, Pfluger B, Schubert G, Leisentritt J. Tangible ways towards climate protection in the European Union (EU Long-term scenarios 2050). Karslruhe, Germany: Fraunhofer Institute for Systems and Innovation Research ISI; 2011.
[561] Sensfuß F, Pfluger B. Final report optimized pathways towards ambitious climate protection in the European electricity system (EU Long-term scenarios 2050 II). Karslruhe, Germany: Fraunhofer Institute for Systems and Innovation Research ISI; 2014.
[562] Kost C, Mayer JN, Thomsen J, Hartmann N, Senkpiel C, Philipps S, et al. Levelized cost of electricity renewable energy technologies. Karlsruhe, Germany: Fraunhofer Institute for Solar Energy Systems ISE; 2013.
[563] International Energy Agency (IEA). Energy technology perspectives 2014: harnessing electricity's potential. 2014.
[564] International Energy Agency IEA. Technology Roadmap: Solar Photovoltaic Energy. Paris, France: IEA Publications; 2014.
[565] GM marks 50 years of FCEV development, from Electrovan to Chevrolet Colorado ZH2. Fuel Cells Bull 2016;2016:14–5. doi:10.1016/S1464-2859(16)30330-3.
[566] General Motors Company. Mission-Ready Chevrolet Colorado ZH2 Fuel Cell Vehicle Breaks Cover at U.S. Army Show 2016. http://media.gm.com/media/us/en/gm/news.detail.html/content/Pages/news/us/en/2016/oct/1003-zh2.html (accessed December 30, 2016).
[567] Siano P. Demand response and smart grids—A survey. Renew Sustain Energy Rev 2014;30:461–78. doi:10.1016/j.rser.2013.10.022.
[568] Ruback RS. Capital Cash Flows: A Simple Approach to Valuing Risky Cash Flows. Financ Manag 2002;31:85. doi:10.2307/3666224.
[569] Ondraczek J, Komendantova N, Patt A. WACC the dog: The effect of financing costs on the levelized cost of solar PV power. Renew Energy 2015;75:888–98. doi:10.1016/j.renene.2014.10.053.

[570] SCHOOTS K, FERIOLI F, KRAMER G, VANDERZWAAN B. Learning curves for hydrogen production technology: An assessment of observed cost reductions. Int J Hydrogen Energy 2008;33:2630–45. doi:10.1016/j.ijhydene.2008.03.011.
[571] McDowall W. Endogenous technology learning for hydrogen and fuel cell technology in UKSHEC II: Literature review, research questions and data 2012. https://www.ucl.ac.uk/drupal/bartlett/energy/sites/bartlett/files/migrated-files/WP8_McDowall_ETL_1_.pdf (accessed August 22, 2016).
[572] Sørensen B. Fuel cells: Optimism gone – Hard work still there. Int J Hydrogen Energy 2013;38:7578–82. doi:10.1016/j.ijhydene.2012.09.028.
[573] Larminie J, Dicks A. Fuel Cell Systems Explained. West Sussex, England: John Wiley & Sons, Ltd,.; 2003. doi:10.1002/9781118878330.
[574] Barbir F. PEM Fuel Cells: Theory and Practice. Academic Press; 2012.
[575] Weiss M, Junginger HM, Patel MK. Learning energy efficiency: experience curves for household appliances and space heating, cooling, and lighting technologies. Copernicus Institute, Utrecht University; 2008.
[576] Firnkorn J, Müller M. Free-floating electric carsharing-fleets in smart cities: The dawning of a post-private car era in urban environments? Environ Sci Policy 2015;45:30–40. doi:10.1016/j.envsci.2014.09.005.
[577] Pavone M. Autonomous Mobility-on-Demand Systems for Future Urban Mobility. Auton. Driv., Berlin, Heidelberg: Springer Berlin Heidelberg; 2016, p. 387–404. doi:10.1007/978-3-662-48847-8_19.
[578] Burns LD. A vision of our transport future. Nature 2013;497:181–2. doi:10.1038/497181a.
[579] Mathiesen B V., Lund H, Hansen K, Ridjan I, Djørup SR, Nielsen S, et al. IDA's Energy Vision 2050: A Smart Energy System strategy for 100% renewable Denmark. Dep Dev Planning, Aalborg Un 2015. doi:ISBN: 978-87-91404-78-8.
[580] Fuller M. Wireless charging in California: Range, recharge, and vehicle electrification. Transp Res Part C Emerg Technol 2016;67:343–56. doi:10.1016/j.trc.2016.02.013.
[581] Niemi R, Mikkola J, Lund PD. Urban energy systems with smart multi-carrier energy networks and renewable energy generation. Renew Energy 2012;48:524–36. doi:10.1016/j.renene.2012.05.017.
[582] Ebbesen SD, Jensen SH, Hauch A, Mogensen MB. High temperature electrolysis in alkaline cells, solid proton conducting cells, and solid oxide cells. Chem Rev 2014;114:10697–734. doi:10.1021/cr5000865.
[583] Pavel CC, Cecconi F, Emiliani C, Santiccioli S, Scaffidi A, Catanorchi S, et al. Highly Efficient Platinum Group Metal Free Based Membrane-Electrode Assembly for Anion Exchange Membrane Water Electrolysis. Angew Chemie 2014;126:1402–5. doi:10.1002/ange.201308099.
[584] Manolova M, Schoeberl C, Freudenberger R, Ellwein C, Kerres J, Stypka S, et al. Development and testing of an anion exchange membrane electrolyser. Int J Hydrogen Energy 2015;40:11362–9. doi:10.1016/j.ijhydene.2015.04.149.

[585] Leng Y, Chen G, Mendoza AJ, Tighe TB, Hickner MA, Wang CY. Solid-state water electrolysis with an alkaline membrane. J Am Chem Soc 2012;134:9054–7. doi:10.1021/ja302439z.
[586] Joya KS, De Groot HJM. Artificial leaf goes simpler and more efficient for solar fuel generation. ChemSusChem 2014;7:73–6. doi:10.1002/cssc.201300981.
[587] He Y-R, Yan F-F, Yu H-Q, Yuan S-J, Tong Z-H, Sheng G-P. Hydrogen production in a light-driven photoelectrochemical cell. Appl Energy 2014;113:164–8. doi:10.1016/j.apenergy.2013.07.020.
[588] May MM, Lewerenz H-J, Lackner D, Dimroth F, Hannappel T. Efficient direct solar-to-hydrogen conversion by in situ interface transformation of a tandem structure. Nat Commun 2015;6:8286. doi:10.1038/ncomms9286.
[589] Verlage E, Hu S, Liu R, Jones RJR, Sun K, Xiang C, et al. A monolithically integrated, intrinsically safe, 10% efficient, solar-driven water-splitting system based on active, stable earth-abundant electrocatalysts in conjunction with tandem III-V light absorbers protected by amorphous TiO2 films. Energy Environ Sci 2015;8:3166–72. doi:10.1039/c5ee01786f.
[590] Kalisman P, Nakibli Y, Amirav L. Perfect Photon-to-Hydrogen Conversion Efficiency. Nano Lett 2016;16:1776–81. doi:10.1021/acs.nanolett.5b04813.
[591] Pinaud BA, Benck JD, Seitz LC, Forman AJ, Chen Z, Deutsch TG, et al. Technical and economic feasibility of centralized facilities for solar hydrogen production via photocatalysis and photoelectrochemistry. Energy Environ Sci 2013;6:1983–2002. doi:10.1039/c3ee40831k.
[592] Metz S. Linde pioneers hydrogen compression techniques for fuel cell electric vehicles. Fuel Cells Bull 2014;2014:12–5. doi:10.1016/S1464-2859(14)70266-4.
[593] Bouwman P. Fundamentals of Electrochemical Hydrogen Compression. PEM Electrolysis Hydrog. Prod., CRC Press; 2016. doi:10.1201/b19096-14.
[594] Bouwman PJ, Konink J, Semerel D, Raymakers L, Koeman M, Kout W, et al. (Invited) Electrochemical Hydrogen Compression. ECS Trans 2014;64:1009–18. doi:10.1149/06403.1009ecst.
[595] Teichmann D, Stark K, Müller K, Zöttl G, Wasserscheid P, Arlt W. Energy storage in residential and commercial buildings via Liquid Organic Hydrogen Carriers (LOHC). Energy Environ Sci 2012;5:9044–54. doi:10.1039/c2ee22070a.
[596] Teichmann D, Arlt W, Wasserscheid P, Freymann R. A future energy supply based on Liquid Organic Hydrogen Carriers (LOHC). Energy Environ Sci 2011;4:2767–73. doi:10.1039/c1ee01454d.
[597] Geburtig D, Preuster P, Bösmann A, Müller K, Wasserscheid P. Chemical utilization of hydrogen from fluctuating energy sources – Catalytic transfer hydrogenation from charged Liquid Organic Hydrogen Carrier systems. Int J Hydrogen Energy 2016;41:1010–7. doi:10.1016/j.ijhydene.2015.10.013.
[598] Ito H, Miyazaki N, Ishida M, Nakano A. Efficiency of unitized reversible fuel cell systems. Int J Hydrogen Energy 2016;41:5803–15. doi:10.1016/j.ijhydene.2016.01.150.
[599] Lu X, Xuan J, Leung DYC, Zou H, Li J, Wang H, et al. A switchable pH-

differential unitized regenerative fuel cell with high performance. J Power Sources 2016;314:76–84. doi:10.1016/j.jpowsour.2016.02.092.
[600] Wang Y, Leung DYC, Xuan J, Wang H. A review on unitized regenerative fuel cell technologies, part-A: Unitized regenerative proton exchange membrane fuel cells. Renew Sustain Energy Rev 2016;65:961–77. doi:10.1016/j.rser.2016.07.046.
[601] Gabbasa M, Sopian K, Fudholi A, Asim N. A review of unitized regenerative fuel cell stack: Material, design and research achievements. Int J Hydrogen Energy 2014;39:17765–78. doi:10.1016/j.ijhydene.2014.08.121.
[602] Wiser R, Jenni K, Seel J, Baker E, Hand M, Lantz E, et al. Expert elicitation survey on future wind energy costs. Nat Energy 2016;1:16135. doi:10.1038/nenergy.2016.135.
[603] Jacobson MZ, Delucchi MA, Cameron MA, Frew BA. Low-cost solution to the grid reliability problem with 100% penetration of intermittent wind, water, and solar for all purposes. Proc Natl Acad Sci 2015;112:15060–5. doi:10.1073/pnas.1510028112.
[604] International Energy Agency (IEA). Energy and air pollution World energy outlook special report. 2016.
[605] Jones D, Huscher J, Myllyvirta L, Gierens RFJ, Gutmann K, Urbaniak D, et al. Europe's Dark Cloud: how coal-burning countries are making their neighbours sick, Sandbag, Health and Environment Alliance (HEAL), Greenpeace, Climate Action Network (CAN) Europe, WWF European Policy Office, European Climate Foundation (ECF). 2016.
[606] Eising JW, van Onna T, Alkemade F. Towards smart grids: Identifying the risks that arise from the integration of energy and transport supply chains. Appl Energy 2014. doi:10.1016/j.apenergy.2013.12.017.
[607] Hu J, You S, Lind M, Østergaard J. Coordinated charging of electric vehicles for congestion prevention in the distribution grid. IEEE Trans Smart Grid 2014. doi:10.1109/TSG.2013.2279007.
[608] Richardson DB. Electric vehicles and the electric grid: A review of modeling approaches, Impacts, and renewable energy integration. Renew Sustain Energy Rev 2013;19:247–54. doi:10.1016/j.rser.2012.11.042.
[609] You S, Segerberg H. Integration of 100% micro-distributed energy resources in the low voltage distribution network: A Danish case study. Appl Therm Eng 2014. doi:10.1016/j.applthermaleng.2013.11.039.
[610] U.S. Energy Information Administration (EIA). Levelized Cost and Levelized Avoided Cost of New Generation Resources in the Annual Energy Outlook 2016 2016.
[611] U.S. Energy Information Administration (EIA). Assessing the economic value of new utility-scale renewable generation projects using levelized cost of electricity and levelized avoided cost of electricity. 2016.
[612] Oldenbroek V, Smink G, Salet T, van Wijk AJM. Fuel Cell Electric Vehicle as a Power Plant: Techno-Economic Scenario Analysis of a Renewable Integrated Transportation and Energy System for Smart Cities in Two Climates. Appl Sci 2019;10:143. doi:10.3390/app10010143.
[613] Rogelj J, Den Elzen M, Höhne N, Fransen T, Fekete H, Winkler H, et al. Paris

Agreement climate proposals need a boost to keep warming well below 2 °c. Nature 2016;534:631–9. doi:10.1038/nature18307.
[614] Moran D, Kanemoto K, Jiborn M, Wood R, Többen J, Seto KC. Carbon footprints of 13 000 cities. Environ Res Lett 2018;13:064041. doi:10.1088/1748-9326/aac72a.
[615] Moran D, Kanemoto, Keiichiro Jiborn M, Wood R, Többen J, Seto KC. Carbon Footprints of World Cities - Global Gridded Model of Carbon Footprints (GGMCF) 2018. http://citycarbonfootprints.info/ (accessed August 29, 2019).
[616] Hughes S, Chu EK, Mason SG. Introduction. In: Hughes S, Chu EK, Mason SG, editors. Clim. Chang. Cities Innov. Multi-Level Gov., Cham, Switzerland: Springer International Publishing; 2018, p. 1–15. doi:10.1007/978-3-319-65003-6_1.
[617] European Commission. The State of European Cities 2016: Cities leading the way to a better future. Strasbourg, France: European Commission; 2016.
[618] Watts M. Commentary: Cities spearhead climate action. Nat Clim Chang 2017;7:537–8. doi:10.1038/nclimate3358.
[619] International Energy Agency (IEA). Cities lead the way on clean and decentralized energy solutions 2017. https://www.iea.org/newsroom/news/2017/april/cities-lead-the-way-on-clean-and-decentralized-energy-solutions.html (accessed August 29, 2019).
[620] Amann M, Bertok I, Borken-Kleefeld J, Cofala J, Heyes C, Höglund-Isaksson L, et al. Cost-effective control of air quality and greenhouse gases in Europe: Modeling and policy applications. Environ Model Softw 2011;26:1489–501. doi:10.1016/j.envsoft.2011.07.012.
[621] Mundaca L, Busch H, Schwer S. 'Successful' low-carbon energy transitions at the community level? An energy justice perspective. Appl Energy 2018;218:292–303. doi:10.1016/j.apenergy.2018.02.146.
[622] C40 Cities Climate Leadership Group. C40 Cities Climate Leadership Group 2018. http://www.c40.org/about (accessed August 28, 2019).
[623] United Nations. The World's Cities in 2016. New York, United States: United Nations; 2016.
[624] Eurostat. Urban Europe Statistics on cities, towns and suburbs. Luxembourg, Luxembourg: Publications office of the European Union; 2016. doi:10.2785/91120.
[625] De Jong M, Joss S, Schraven D, Zhan C, Weijnen M. Sustainable-smart-resilient-low carbon-eco-knowledge cities; Making sense of a multitude of concepts promoting sustainable urbanization. J Clean Prod 2015;109:25–38. doi:10.1016/j.jclepro.2015.02.004.
[626] International Energy Agency (IEA). Nordic Energy Technology Perspectives 2016: Cities, flexibility and pathways to carbon-neutrality. Oslo, Norway: Nordic Energy Research; 2016. doi:10.1787/9789264257665-en.
[627] Lund PD, Mikkola J, Ypyä J. Smart energy system design for large clean power schemes in urban areas. J Clean Prod 2015;103:437–45. doi:10.1016/j.jclepro.2014.06.005.

[628] Salvi BL, Subramanian KA. Sustainable development of road transportation sector using hydrogen energy system. Renew Sustain Energy Rev 2015;51:1132–55. doi:10.1016/j.rser.2015.07.030.
[629] Sgobbi A, Nijs W, De Miglio R, Chiodi A, Gargiulo M, Thiel C. How far away is hydrogen? Its role in the medium and long-term decarbonisation of the European energy system. Int J Hydrogen Energy 2016;41:19–35. doi:10.1016/j.ijhydene.2015.09.004.
[630] Nastasi B, Lo Basso G. Power-to-Gas integration in the Transition towards Future Urban Energy Systems. Int J Hydrogen Energy 2017;42:23933–51. doi:10.1016/j.ijhydene.2017.07.149.
[631] Kylili A, Fokaides PA. European smart cities: The role of zero energy buildings. Sustain Cities Soc 2015;15:86–95. doi:10.1016/j.scs.2014.12.003.
[632] Parra D, Swierczynski M, Stroe DI, Norman SA, Abdon A, Worlitschek J, et al. An interdisciplinary review of energy storage for communities: Challenges and perspectives. Renew Sustain Energy Rev 2017;79:730–49. doi:10.1016/j.rser.2017.05.003.
[633] Alavi F, Park Lee E, van de Wouw N, De Schutter B, Lukszo Z. Fuel cell cars in a microgrid for synergies between hydrogen and electricity networks. Appl Energy 2017;192:296–304. doi:10.1016/j.apenergy.2016.10.084.
[634] Calvillo CF, Sánchez-Miralles A, Villar J. Energy management and planning in smart cities. Renew Sustain Energy Rev 2016;55:273–87. doi:10.1016/j.rser.2015.10.133.
[635] World Energy Council Netherlands. Bringing North See Energy Ashore Efficiently. Tilburg, The Netherlands: World Energy Council Netherlands; 2017.
[636] Rifkin J. The hydrogen economy: The creation of the worldwide energy web and the redistribution of power on earth. Penguin 2003;4:12. doi:10.1016/S1471-0846(03)80112-9.
[637] Brandon NP, Kurban Z. Clean energy and the hydrogen economy. Philos Trans R Soc A Math Phys Eng Sci 2017;375:20160400. doi:10.1098/rsta.2016.0400.
[638] van Wijk AJM, The Northern Netherlands Innovation Board. The Green Hydrogen Economy in the Northern Netherlands - Full Report. Groningen, the Netherlands: The Northern Netherlands Innovation Board; 2017.
[639] Winkler-Goldstein R, Rastetter A. Power to gas: The final breakthrough for the hydrogen economy? Green 2013;3:69–78. doi:10.1515/green-2013-0001.
[640] Robledo CB, Oldenbroek V, Abbruzzese F, Wijk AJM van. Case study integrating a hydrogen fuel cell electric vehicle with vehicle-to-grid technology, photovoltaic power and a residential building. Appl Energy 2018;215:615–29. doi:https://doi.org/10.1016/j.apenergy.2018.02.038.
[641] Barret S. Hyundai unveils next-gen FCEV NEXO at CES, plus home power. Fuel Cells Bull 2018;2018:2. doi:https://doi.org/10.1016/S1464-2859(18)30002-6.
[642] Peel MC, Finlayson BL, McMahon TA. Updated world map of the Köppen-Geiger climate classification. Hydrol Earth Syst Sci 2007;11:1633–44.

doi:10.5194/hess-11-1633-2007.
[643] Tsikaloudaki K, Laskos K, Bikas D. On the establishment of climatic zones in Europe with regard to the energy performance of buildings. Energies 2012;5:32–44. doi:10.3390/en5010032.
[644] Reda F, Arcuri N, Loiacono P, Mazzeo D. Energy assessment of solar technologies coupled with a ground source heat pump system for residential energy supply in Southern European climates. Energy 2015;91:294–305. doi:10.1016/j.energy.2015.08.040.
[645] Eicker U, Colmenar-Santos A, Teran L, Cotrado M, Borge-Diez D. Economic evaluation of solar thermal and photovoltaic cooling systems through simulation in different climatic conditions: An analysis in three different cities in Europe. Energy Build 2014;70:207–23. doi:10.1016/j.enbuild.2013.11.061.
[646] Dalin P, Nilsson J, Rubenhag A. ECOHEATCOOL, Work package 2, The European Cold Market, final report of WP2 of the project funded within the Intelligent Energy program. Brussels, Belgium: Euroheat & Power; 2006.
[647] Jakubcionis M, Carlsson J. Estimation of European Union service sector space cooling potential. Energy Policy 2018;113:223–31. doi:10.1016/j.enpol.2017.11.012.
[648] Jakubcionis M, Carlsson J. Estimation of European Union residential sector space cooling potential. Energy Policy 2017;101:225–35.
[649] Aebischer B, Catenazzi G, Jakob M. Impact of climate change on thermal comfort, heating and cooling energy demand in Europe. ECEEE Summer Study - Sav ENERGY – JUST DO IT! 2007;2007:859–70.
[650] Eurostat. Household composition statistics 2016. http://ec.europa.eu/eurostat/statistics-explained/index.php/Household_composition_statistics (accessed August 28, 2019).
[651] Troen I, Lundtang Petersen E. European wind atlas. Roskilde, Denmark: Risø National Laboratory; 1989. doi:10.1016/0014-2999(86)90768-5.
[652] Huber M, Dimkova D, Hamacher T. Integration of wind and solar power in Europe: Assessment of flexibility requirements. Energy 2014;69:236–46. doi:10.1016/j.energy.2014.02.109.
[653] Heide D, von Bremen L, Greiner M, Hoffmann C, Speckmann M, Bofinger S. Seasonal optimal mix of wind and solar power in a future, highly renewable Europe. Renew Energy 2010;35:2483–9. doi:10.1016/j.renene.2010.03.012.
[654] Kiviluoma J, Holttinen H, Weir D, Scharff R, Söder L, Menemenlis N, et al. Variability in large-scale wind power generation. Wind Energy 2016;19:1649–65. doi:10.1002/we.1942.
[655] Monforti F, Gaetani M, Vignati E. How synchronous is wind energy production among European countries? Renew Sustain Energy Rev 2016;59:1622–38. doi:10.1016/j.rser.2015.12.318.
[656] Pozo-Vazquez D, Santos-Alamillos FJ, Lara-Fanego V, Ruiz-Arias JA, Tovar-Pescador J. The impact of the NAO on the solar and wind energy resources

in the Mediterranean area. Hydrol. Socioecon. Ecol. Impacts North Atl. Oscil. Mediterr. Reg., Springer; 2011, p. 213–31.
[657] Santos JA, Rochinha C, Liberato MLR, Reyers M, Pinto JG. Projected changes in wind energy potentials over Iberia. Renew Energy 2015;75:68–80. doi:10.1016/j.renene.2014.09.026.
[658] Nuño E, Maule P, Hahmann A, Cutululis N, Sørensen P, Karagali I. Simulation of transcontinental wind and solar PV generation time series. Renew Energy 2018;118:425–36. doi:10.1016/j.renene.2017.11.039.
[659] Bett PE, Thornton HE, Clark RT. Using the Twentieth Century Reanalysis to assess climate variability for the European wind industry. Theor Appl Climatol 2017;127:61–80. doi:10.1007/s00704-015-1591-y.
[660] Kirchner-Bossi N, García-Herrera R, Prieto L, Trigo RM. A long-term perspective of wind power output variability. Int J Climatol 2015;35:2635–46. doi:10.1002/joc.4161.
[661] François B. Influence of winter North-Atlantic Oscillation on Climate-Related-Energy penetration in Europe. Renew Energy 2016;99:602–13. doi:10.1016/j.renene.2016.07.010.
[662] Pfenninger S, Staffell I. Long-term patterns of European PV output using 30 years of validated hourly reanalysis and satellite data. Energy 2016;114:1251–65. doi:10.1016/j.energy.2016.08.060.
[663] Brown TW, Bischof-Niemz T, Blok K, Breyer C, Lund H, Mathiesen B V. Response to “Burden of proof: A comprehensive review of the feasibility of 100% renewable-electricity systems.” ArXiv Prepr ArXiv170905716 2017.
[664] Kılkış B, Kılkış Ş. Hydrogen Economy Model for Nearly Net-Zero Cities with Exergy Rationale and Energy-Water Nexus. Energies 2018;11:1226. doi:10.3390/en11051226.
[665] Rahil A, Gammon R, Brown N. Flexible operation of electrolyser at the garage forecourt to support grid balancing and exploitation of hydrogen as a clean fuel. Res Transp Econ 2018;70:125–38. doi:https://doi.org/10.1016/j.retrec.2017.12.001.
[666] Farahani SS, Veen R van der, Oldenbroek V, Alavi F, Lee EHP, Wouw N van de, et al. A Hydrogen-Based Integrated Energy and Transport System: The Design and Analysis of the Car as Power Plant Concept. IEEE Syst Man, Cybern Mag 2019;5:37–50. doi:10.1109/MSMC.2018.2873408.
[667] Jacobson MZ, Delucchi MA, Cameron MA, Mathiesen B V. Matching demand with supply at low cost in 139 countries among 20 world regions with 100% intermittent wind, water, and sunlight (WWS) for all purposes. Renew Energy 2018;123:236–48. doi:https://doi.org/10.1016/j.renene.2018.02.009.
[668] Eurostat. Population change - Demographic balance and crude rates at national level 2017. http://appsso.eurostat.ec.europa.eu/nui/show.do?dataset=demo_gind (accessed August 28, 2019).
[669] European Environment Agency. Average annual precipitation 1940-1995 Europe 2011. https://www.eea.europa.eu/themes/water/water-resources/figures-and-maps/precipitation/view (accessed August 28,

2019).
[670] Andrews J, Shabani B. Re-envisioning the role of hydrogen in a sustainable energy economy. Int J Hydrogen Energy 2012;37:1184–203. doi:10.1016/j.ijhydene.2011.09.137.
[671] E3MLab. PRIMES MODEL VERSION 6, 2016-2017 Detailed model description - Hydrogen Supply Sub-Model. Athens, Greece: National Technical University of Athens (ICCS/NTUA); 2017.
[672] Maroufmashat A, Elkamel A, Fowler M, Sattari S, Roshandel R, Hajimiragha A, et al. Modeling and optimization of a network of energy hubs to improve economic and emission considerations. Energy 2015;93:2546–58. doi:10.1016/j.energy.2015.10.079.
[673] Hydrogen Hub. Local Hydrogen Hubs 2018. http://www.hydrogenhub.org/#locally (accessed August 28, 2019).
[674] Kostowski W, Lepszy S, Uthke W, Chromik M, Wierciński A, Foltynowicz M, et al. Effectiveness of the Hydrogen Production, Storage and Utilization Chain BT - Renewable Energy Sources: Engineering, Technology, Innovation. In: Mudryk K, Werle S, editors., Cham: Springer International Publishing; 2018, p. 321–31.
[675] Eurostat. Number of private households by household composition, number of children and age of youngest child (1 000) 2015. http://ec.europa.eu/eurostat/en/web/products-datasets/-/LFST_HHNHTYCH (accessed August 28, 2019).
[676] Muratori M, Bush B, Hunter C, Melaina M. Modeling Hydrogen Refueling Infrastructure to Support Passenger Vehicles †. Energies 2018;11:1171. doi:10.3390/en11051171.
[677] Enerdata. ODYSSEE database - Macro 2015. http://odyssee.enerdata.net/database/.
[678] Kraftfahrt-Bundesamt. Verkehr in Kilometern der deutschen Kraftfahrzeuge im Jahr 2015 2016. https://www.kba.de/DE/Statistik/Kraftverkehr/VerkehrKilometer/2015/2015_vk_kurzbericht_pdf.pdf?__blob=publicationFile&v=1 (accessed August 28, 2019).
[679] Kraftfahrt-Bundesamt. Der Fahrzeugbestand im Überblick am 1. Januar 2016 gegenüber 1. Januar 2015 2016. https://www.kba.de/SharedDocs/Pressemitteilungen/DE/2016/pm_08_16_bestand_01_16_pdf.pdf?__blob=publicationFile&v=8 (accessed August 28, 2019).
[680] Enerdata. Definition of data and energy efficiency indicators in ODYSSEE data base 2015. http://www.odyssee-mure.eu/private/definition-indicators.pdf.
[681] Bureau of Labor Statistics (BLS) – U.S. Department of Labor. Inflation calculator 2017. https://www.bls.gov/data/inflation_calculator.htm (accessed August 28, 2019).
[682] Khalilpour KR. Chapter 16 - The Transition From X% to 100% Renewable Future: Perspective and Prospective. In: Khalilpour KRBT-P with P for C and EH, editor. Polygeneration with Polystorage Chem. Energy Hubs,

Cambridge, MA, United States of America: Academic Press; 2019, p. 513–49. doi:https://doi.org/10.1016/B978-0-12-813306-4.00016-1.
[683] Agora Energiewende. Future cost of onshore wind. Recent auction results, long-term outlook and implications for upcoming German auctions. Berlin, Germany: Agora Energiewende; 2017.
[684] Christoph Kost, Shammugamverena S, Jülch V, Nhuyen H-T, Schlegl T. Levelized Cost of Electricity Renewable Energy Technologies. Karlsruhe, Germany: Fraunhofer Institute for Solar Energy Systems ISE; 2018.
[685] National Renewable Energy Laboratory (NREL). H2A analysis, production case studies: Current Distributed Hydrogen Production from Grid PEM Electrolysis version 3.2018 2018. https://www.nrel.gov/hydrogen/assets/docs/current-distributed-pem-electrolysis-v3-2018.xlsm (accessed August 28, 2019).
[686] National Renewable Energy Laboratory (NREL). H2A analysis, production case studies: Current Central Hydrogen Production from Polymer Electrolyte Membrane (PEM) Electrolysis version 3.2018 2018. https://www.nrel.gov/hydrogen/assets/docs/current-central-pem-electrolysis-v3-2018.xlsm (accessed August 28, 2019).
[687] Fuel Cell Technologies Office (FCTO) – U.S. Department of Energy (DOE). Multi-Year Research, Development, and Demonstration (MYRD&D) Plan - Section 3.1 Hydrogen Production 2015. https://www.energy.gov/sites/prod/files/2015/06/f23/fcto_myrdd_production.pdf (accessed August 28, 2019).
[688] Welder L, Stenzel P, Ebersbach N, Markewitz P, Robinius M, Emonts B, et al. Design and evaluation of hydrogen electricity reconversion pathways in national energy systems using spatially and temporally resolved energy system optimization. Int J Hydrogen Energy 2019;44:9594–607. doi:10.1016/j.ijhydene.2018.11.194.
[689] Jacobson MZ, Cameron MA, Hennessy EM, Petkov I, Meyer CB, Gambhir TK, et al. 100% clean and renewable Wind, Water, and Sunlight (WWS) all-sector energy roadmaps for 53 towns and cities in North America. Sustain Cities Soc 2018. doi:10.1016/j.scs.2018.06.031.
[690] Steinberger-Wilckens R, Sampson B. Market, Commercialization, and Deployment—Toward Appreciating Total Owner Cost of Hydrogen Energy Technologies. In: de Miranda PEVBT-S and E of H-BET, editor. Sci. Eng. Hydrog. Energy Technol., Elsevier; 2019, p. 383–403. doi:10.1016/B978-0-12-814251-6.00008-3.
[691] Robinius M, Raje T, Nykamp S, Rott T, Müller M, Grube T, et al. Power-to-Gas: Electrolyzers as an alternative to network expansion – An example from a distribution system operator. Appl Energy 2018;210:182–97. doi:10.1016/j.apenergy.2017.10.117.
[692] Hermkens R, Jansma S, Laan M van der, Laat H de, Pilzer B, Pulles K. Toekomstbestendige gasdistributienetten - Netbeheer Nederland. Kiwa Technol BV 2018.
[693] Sadler D, Cargill A, Crowther M, Rennie A, Watt J, Burton S, et al. H21 Leeds City Gate. Leeds, United Kingdom: Northern Gas Networks; 2016.

[694] Northern Gas Networks. H21 North of England – deep decarbonisation of heat to meet climate change targets 2018. https://www.northerngasnetworks.co.uk/event/h21-launches-national/ (accessed August 28, 2019).
[695] Baufumé S, Grüger F, Grube T, Krieg D, Linssen J, Weber M, et al. GIS-based scenario calculations for a nationwide German hydrogen pipeline infrastructure. Int J Hydrogen Energy 2013;38:3813–29. doi:10.1016/j.ijhydene.2012.12.147.
[696] Johnson N, Ogden J. A spatially-explicit optimization model for long-term hydrogen pipeline planning. Int J Hydrogen Energy 2012;37:5421–33. doi:10.1016/j.ijhydene.2011.08.109.
[697] Brey JJ, Carazo AF, Brey R. Exploring the marketability of fuel cell electric vehicles in terms of infrastructure and hydrogen costs in Spain. Renew Sustain Energy Rev 2018;82:2893–9. doi:10.1016/j.rser.2017.10.042.
[698] Robledo CB, Oldenbroek V, Seiffers J, Seiffers M, Wijk AJM van. Performance of a Lightweight Fuel Cell/Battery Hybrid Electric Vehicle Operating in Vehicle-to-Grid. Fuel Cell Semin Energy Expo 2017. https://pure.tudelft.nl/portal/en/activities/performance-of-a-lightweight-fuel-cellbattery-hybrid-electric-vehicle-operating-in-vehicletogrid(173c09eb-58f8-459a-8631-b11d9bd808ae).html (accessed August 28, 2019).
[699] Kamiya S, Nishimura M, Harada E. Study on Introduction of CO2 Free Energy to Japan with Liquid Hydrogen. Phys Procedia 2015;67:11–9. doi:10.1016/j.phpro.2015.06.004.
[700] Kan S, Shibata Y. Evaluation of the Economics of Renewable Hydrogen Supply in the APEC Region. Tokyo, Japan: The Institute of Energy Economics, Japan (IEEJ); 2018.
[701] Mizuno Y, Ishimoto Y, Sakai S, Sakata K. Economic analysis on internatiol hydrogen energy carrier supply chains. J Japan Soc Energy Resour 2016;38:11–7.
[702] Chapman AJ, Fraser T, Itaoka K. Hydrogen import pathway comparison framework incorporating cost and social preference: Case studies from Australia to Japan. Int J Energy Res 2017;41:2374–91. doi:10.1002/er.3807.
[703] Takaoka Y, Kagaya H, Saeed A, Nishimura M. Introduction to a Liquefied Hydrogen Carrier for a Pilot Hydrogen Energy Supply Chain (HESC) project in Japan - Gastech 2017 Tokyo. Tokyo, Japan: Kawasaki Heavy Industries, Ltd; 2017.
[704] Timmerberg S, Kaltschmitt M. Hydrogen from renewables: Supply from North Africa to Central Europe as blend in existing pipelines – Potentials and costs. Appl Energy 2019;237:795–809. doi:10.1016/j.apenergy.2019.01.030.
[705] Schmidt J, Gruber K, Klingler M, Klöckl C, Camargo LR, Regner P, et al. A new perspective on global renewable energy systems: why trade in energy carriers matters. Energy Environ Sci 2019;12:2022–9.
[706] Blanco-Fernández P, Pérez-Arribas F. Offshore Facilities to Produce Hydrogen. Energies 2017;10:783. doi:10.3390/en10060783.

[707] Jørg Aarnes, Eijgelaar M, Hektor EA. Hydrogen as an energy carrier - An evaluation of emerging hydrogen value chains. Høvik, Norway: DNV GL AS; 2018.
[708] Oceans of Energy. Offshore floating solar 2018. https://oceansofenergy.blue/ (accessed August 28, 2019).
[709] Pouran HM. From collapsed coal mines to floating solar farms, why China's new power stations matter. Energy Policy 2018;123:414–20. doi:10.1016/j.enpol.2018.09.010.
[710] Maekawa K, Takeda M, Hamaura T, Suzuki K, Miyake Y, Matsuno Y, et al. First experiment on liquid hydrogen transportation by ship inside Osaka bay. IOP Conf Ser Mater Sci Eng 2017;278:012066. doi:10.1088/1757-899X/278/1/012066.
[711] Wilhelmsen, Equinor, Moss Maritime, Det Norske Veritas Germanischer Lloyd (DNV GL). New design makes liquefied hydrogen bunker vessels a reality 2019. https://www.wilhelmsen.com/media-news-and-events/press-releases/2019/new-design-makes-liquefied-hydrogen-bunker-vessels-a-reality/ (accessed August 28, 2019).
[712] Budischak C, Sewell D, Thomson H, Mach L, Veron DE, Kempton W. Cost-minimized combinations of wind power, solar power and electrochemical storage, powering the grid up to 99.9% of the time. J Power Sources 2013;225:60–74. doi:10.1016/j.jpowsour.2012.09.054.
[713] Deetjen TA, Martin H, Rhodes JD, Webber ME. Modeling the optimal mix and location of wind and solar with transmission and carbon pricing considerations. Renew Energy 2018;120:35–50. doi:10.1016/j.renene.2017.12.059.
[714] Schaber K, Steinke F, Mühlich P, Hamacher T. Parametric study of variable renewable energy integration in Europe: Advantages and costs of transmission grid extensions. Energy Policy 2012;42:498–508. doi:10.1016/j.enpol.2011.12.016.
[715] Steinke F, Wolfrum P, Hoffmann C. Grid vs. storage in a 100% renewable Europe. Renew Energy 2013;50:826–32. doi:10.1016/j.renene.2012.07.044.
[716] Heide D, Greiner M, von Bremen L, Hoffmann C. Reduced storage and balancing needs in a fully renewable European power system with excess wind and solar power generation. Renew Energy 2011;36:2515–23. doi:10.1016/j.renene.2011.02.009.
[717] Rasmussen MG, Andresen GB, Greiner M. Storage and balancing synergies in a fully or highly renewable pan-European power system. Energy Policy 2012;51:642–51. doi:10.1016/j.enpol.2012.09.009.
[718] Gils HC, Scholz Y, Pregger T, Luca de Tena D, Heide D. Integrated modelling of variable renewable energy-based power supply in Europe. Energy 2017;123:173–88. doi:10.1016/j.energy.2017.01.115.
[719] Pietzcker RC, Ueckerdt F, Carrara S, de Boer HS, Després J, Fujimori S, et al. System integration of wind and solar power in integrated assessment models: A cross-model evaluation of new approaches. Energy Econ 2017;64:583–99. doi:10.1016/j.eneco.2016.11.018.

[720] Jacobson MZ, Delucchi MA, Cameron MA, Mathiesen B V. Appendix A. Supplementary data - Matching demand with supply at low cost in 139 countries among 20 world regions with 100% intermittent wind, water, and sunlight (WWS) for all purposes. Renew Energy 2018;123:236–48, Appendix page 30. doi:10.1016/j.renene.2018.02.009.
[721] Slusarewicz JH, Cohan DS. Assessing solar and wind complementarity in Texas. Renewables Wind Water, Sol 2018;5:7. doi:10.1186/s40807-018-0054-3.
[722] Bucher JD, Bradley TH. Modeling operating modes, energy consumptions, and infrastructure requirements of fuel cell plug in hybrid electric vehicles using longitudinal geographical transportation data. Int J Hydrogen Energy 2018;43:12420–7. doi:10.1016/j.ijhydene.2018.04.159.
[723] Daimler A.G. The GLC F-CELL: First electric vehicle featuring fuel cell and plug-in hybrid technology 2018. https://www.daimler.com/products/passenger-cars/mercedes-benz/glc-f-cell.html (accessed August 28, 2019).
[724] Lane B, Shaffer B, Samuelsen GS. Plug-in fuel cell electric vehicles: A California case study. Int J Hydrogen Energy 2017;42:14294–300. doi:10.1016/j.ijhydene.2017.03.035.
[725] Kikuchi Y, Ichikawa T, Sugiyama M, Koyama M. Battery-assisted low-cost hydrogen production from solar energy: Rational target setting for future technology systems. Int J Hydrogen Energy 2019;44:1451–65. doi:10.1016/j.ijhydene.2018.11.119.
[726] Salet T. Fuel Cell and Battery Electric Vehicles as power plants: a techno-economic scenario analysis in two climates for smart cities. Delft, The Netherlands: Delft University of Technology repository; 2018.
[727] Reddi K, Elgowainy A, Rustagi N, Gupta E. Impact of hydrogen refueling configurations and market parameters on the refueling cost of hydrogen. Int J Hydrogen Energy 2017;42:21855–65. doi:10.1016/j.ijhydene.2017.05.122.
[728] Demir ME, Dincer I. Cost assessment and evaluation of various hydrogen delivery scenarios. Int J Hydrogen Energy 2018;43:10420–30. doi:10.1016/j.ijhydene.2017.08.002.
[729] Reddi K, Mintz M, Elgowainy A, Sutherland E. Challenges and Opportunities of Hydrogen Delivery via Pipeline, Tube-Trailer, LIQUID Tanker and Methanation-Natural Gas Grid. Hydrog. Sci. Eng. Mater. Process. Syst. Technol., Weinheim, Germany: Wiley-VCH Verlag GmbH & Co. KGaA; 2016, p. 849–74. doi:10.1002/9783527674268.ch35.
[730] Yang C, Ogden J. Determining the lowest-cost hydrogen delivery mode. Int J Hydrogen Energy 2007;32:268–86. doi:10.1016/j.ijhydene.2006.05.009.
[731] Cha J, Jo YS, Jeong H, Han J, Nam SW, Song KH, et al. Ammonia as an efficient COX-free hydrogen carrier: Fundamentals and feasibility analyses for fuel cell applications. Appl Energy 2018;224:194–204. doi:10.1016/j.apenergy.2018.04.100.
[732] Aakko-Saksa PT, Cook C, Kiviaho J, Repo T. Liquid organic hydrogen carriers for transportation and storing of renewable energy – Review and

discussion. J Power Sources 2018;396:803–23. doi:10.1016/j.jpowsour.2018.04.011.
[733] Choi EJ, Park JY, Kim MS. A comparison of temperature distribution in PEMFC with single-phase water cooling and two-phase HFE-7100 cooling methods by numerical study. Int J Hydrogen Energy 2018;43:13406–19. doi:10.1016/j.ijhydene.2018.05.056.
[734] Toyota Motor Corporation. Toyota Unveils FC Bus Concept "Sora" 2017. https://newsroom.toyota.co.jp/en/detail/19063778 (accessed August 28, 2019).
[735] Dodds PE, Staffell I, Hawkes AD, Li F, Grünewald P, McDowall W, et al. Hydrogen and fuel cell technologies for heating: A review. Int J Hydrogen Energy 2015;40:2065–83. doi:10.1016/j.ijhydene.2014.11.059.
[736] Ellamla HR, Staffell I, Bujlo P, Pollet BG, Pasupathi S. Current status of fuel cell based combined heat and power systems for residential sector. J Power Sources 2015;293:312–28. doi:10.1016/j.jpowsour.2015.05.050.
[737] Hosseini M, Dincer I, Rosen MA. Hybrid solar–fuel cell combined heat and power systems for residential applications: Energy and exergy analyses. J Power Sources 2013;221:372–80. doi:10.1016/j.jpowsour.2012.08.047.
[738] Cappa F, Facci AL, Ubertini S. Proton exchange membrane fuel cell for cooperating households: A convenient combined heat and power solution for residential applications. Energy 2015;90:1229–38. doi:10.1016/j.energy.2015.06.092.
[739] Adam A, Fraga ES, Brett DJL. Options for residential building services design using fuel cell based micro-CHP and the potential for heat integration. Appl Energy 2015;138:685–94. doi:10.1016/j.apenergy.2014.11.005.
[740] Löbberding L, Madlener R. Techno-economic analysis of micro fuel cell cogeneration and storage in Germany. Appl Energy 2019;235:1603–13. doi:10.1016/j.apenergy.2018.11.023.
[741] Raza MQ, Nadarajah M, Ekanayake C. Demand forecast of PV integrated bioclimatic buildings using ensemble framework. Appl Energy 2017;208:1626–38. doi:10.1016/j.apenergy.2017.08.192.
[742] Mat Daut MA, Hassan MY, Abdullah H, Rahman HA, Abdullah MP, Hussin F. Building electrical energy consumption forecasting analysis using conventional and artificial intelligence methods: A review. Renew Sustain Energy Rev 2017;70:1108–18. doi:10.1016/j.rser.2016.12.015.
[743] Kontokosta CE, Tull C. A data-driven predictive model of city-scale energy use in buildings. Appl Energy 2017;197:303–17. doi:10.1016/j.apenergy.2017.04.005.
[744] Yildiz B, Bilbao JI, Sproul AB. A review and analysis of regression and machine learning models on commercial building electricity load forecasting. Renew Sustain Energy Rev 2017;73:1104–22. doi:10.1016/j.rser.2017.02.023.
[745] Fan C, Xiao F, Wang S. Development of prediction models for next-day building energy consumption and peak power demand using data mining techniques. Appl Energy 2014;127:1–10.

doi:10.1016/j.apenergy.2014.04.016.
[746] Sivaneasan B, Kandasamy NK, Lim ML, Goh KP. A new demand response algorithm for solar PV intermittency management. Appl Energy 2018;218:36–45. doi:10.1016/j.apenergy.2018.02.147.
[747] Chen Y, Xu P, Chu Y, Li W, Wu Y, Ni L, et al. Short-term electrical load forecasting using the Support Vector Regression (SVR) model to calculate the demand response baseline for office buildings. Appl Energy 2017;195:659–70. doi:10.1016/j.apenergy.2017.03.034.
[748] Nge CL, Ranaweera IU, Midtgård O-M, Norum L. A real-time energy management system for smart grid integrated photovoltaic generation with battery storage. Renew Energy 2019;130:774–85. doi:10.1016/j.renene.2018.06.073.
[749] Quddus MA, Shahvari O, Marufuzzaman M, Usher JM, Jaradat R. A collaborative energy sharing optimization model among electric vehicle charging stations, commercial buildings, and power grid. Appl Energy 2018;229:841–57. doi:10.1016/j.apenergy.2018.08.018.
[750] Widén J, Carpman N, Castellucci V, Lingfors D, Olauson J, Remouit F, et al. Variability assessment and forecasting of renewables: A review for solar, wind, wave and tidal resources. Renew Sustain Energy Rev 2015;44:356–75. doi:10.1016/j.rser.2014.12.019.
[751] Saffari M, de Gracia A, Fernández C, Belusko M, Boer D, Cabeza LF. Optimized demand side management (DSM) of peak electricity demand by coupling low temperature thermal energy storage (TES) and solar PV. Appl Energy 2018;211:604–16. doi:10.1016/j.apenergy.2017.11.063.
[752] Müller D, Monti A, Stinner S, Schlösser T, Schütz T, Matthes P, et al. Demand side management for city districts. Build Environ 2015;91:283–93. doi:10.1016/j.buildenv.2015.03.026.
[753] Sehar F, Pipattanasomporn M, Rahman S. An energy management model to study energy and peak power savings from PV and storage in demand responsive buildings. Appl Energy 2016;173:406–17. doi:10.1016/j.apenergy.2016.04.039.
[754] Expósito-Izquierdo C, Expósito-Márquez A, Brito-Santana J. Mobility as a Service. Smart Cities, Hoboken, NJ, USA: John Wiley & Sons, Inc.; 2017, p. 409–35. doi:10.1002/9781119226444.ch15.
[755] Kamargianni M, Li W, Matyas M, Schäfer A. A Critical Review of New Mobility Services for Urban Transport. Transp Res Procedia 2016;14:3294–303. doi:10.1016/j.trpro.2016.05.277.
[756] Jittrapirom P, Caiati V, Feneri A-M, Ebrahimigharehbaghi S, González MJA, Narayan J. Mobility as a Service: A Critical Review of Definitions, Assessments of Schemes, and Key Challenges. Urban Plan 2017;2:13. doi:10.17645/up.v2i2.931.
[757] Park Lee EH, Lukszo Z, Herder P. Conceptualization of Vehicle-to-Grid Contract Types and Their Formalization in Agent-Based Models. Complexity 2018;2018:1–11. doi:10.1155/2018/3569129.
[758] Lee EHP, Lukszo Z, Herder P. Static volume-based and control-based contracts for coordinating vehicle-to-grid supply in a microgrid. 2017 IEEE

PES Innov. Smart Grid Technol. Conf. Eur. (ISGT-Europe), Torino, Italy, 26–29 Sept. 2017, IEEE; 2017, p. 1–6. doi:10.1109/ISGTEurope.2017.8260236.
[759] Robledo CB, Poorte MJ, Mathijssen HHM, van der Veen RAC, van Wijk AJM. Fuel Cell Electric Vehicle-to-Grid Feasibility: A Technical Analysis of Aggregated Units Offering Frequency Reserves. In: Palensky P, Cvetković M, Keviczky T, editors. Intell. Integr. Energy Syst., Cham: Springer International Publishing; 2019, p. 167–94. doi:10.1007/978-3-030-00057-8_8.
[760] Lee EHP, Lukszo Z, Herder P. Aggregated fuel cell vehicles in electricity markets with high wind penetration. 2018 IEEE 15th Int. Conf. Networking, Sens. Control, 2018, p. 1–6. doi:10.1109/ICNSC.2018.8361362.
[761] Nissan Motor Corporation. Wireless Charging System | NISSAN | TECHNOLOGICAL DEVELOPMENT ACTIVITIES 2016. https://www.nissan-global.com/EN/TECHNOLOGY/OVERVIEW/wcs.html (accessed August 28, 2019).
[762] Oldenbroek V, Wijtzes S, Blok K, van Wijk AJM. Fuel cell electric vehicles and hydrogen balancing 100 percent renewable and integrated national transportation and energy systems. Energy Convers Manag X 2021;9:100077. doi:10.1016/j.ecmx.2021.100077.
[763] European Comission. Communication on strengthening Europe's energy networks. COM 718 2017. https://ec.europa.eu/energy/sites/ener/files/documents/communication_on_infrastructure_17.pdf (accessed November 26, 2020).
[764] Joint Research Centre (JRC). Transcontinental and global power grids 2018. https://ses.jrc.ec.europa.eu/transcontinental-and-global-power-grids (accessed November 1, 2019).
[765] PV Magazine. Spain's third interconnection with Morocco could be Europe's chance for African PV – or a boost for coal 2019. https://www.pv-magazine.com/2019/02/20/spains-third-interconnection-with-morocco-could-be-europes-chance-for-african-pv-or-a-boost-for-coal/ (accessed November 1, 2019).
[766] Hansen K, Breyer C, Lund H. Status and perspectives on 100% renewable energy systems. Energy 2019;175:471–80. doi:10.1016/j.energy.2019.03.092.
[767] Guerra OJ, Eichman J, Kurtz J, Hodge B-M. Cost Competitiveness of Electrolytic Hydrogen. Joule 2019. doi:https://doi.org/10.1016/j.joule.2019.07.006.
[768] Energystock b.v. The hydrogen project HyStock 2018. https://www.energystock.com/about-energystock/the-hydrogen-project-hystock (accessed November 1, 2019).
[769] Steward D, Saur G, Penev M, Ramsden T. Lifecycle cost analysis of hydrogen versus other technologies for electrical energy storage. 2009.
[770] HYPOS East Germany. Hydrogen power storage & solutions East Germany 2017. http://www.hypos-eastgermany.de/en (accessed November 1, 2019).
[771] UNDERGROUND.SUN.STORAGE. Underground Sun Storage 2018.

https://www.underground-sun-storage.at/ (accessed November 1, 2019).
[772] Tarkowski R. Underground hydrogen storage: Characteristics and prospects. Renew Sustain Energy Rev 2019. doi:10.1016/j.rser.2019.01.051.
[773] Poorte M. Technical and economic feasibility assessment of a Car Park as Power Plant offering frequency reserves. Delft University of Technology, 2017.
[774] Henning H-M, Palzer A. What Will the Energy Transformation Cost? Pathways for Transforming the German Energy System by 2050. Karlsruhe, Germany: Fraunhofer Institute for Solar Energy Systems ISE; 2015.
[775] Scholz Y, Gils HC, Pietzcker RC. Application of a high-detail energy system model to derive power sector characteristics at high wind and solar shares. Energy Econ 2017;64:568–82. doi:10.1016/j.eneco.2016.06.021.
[776] ACEA. Consolidated Registrations - By Country 2019. https://www.acea.be/statistics/tag/category/by-country-registrations (accessed November 1, 2019).
[777] European Automobile Manufacturers Association (ACEA). ACEA Report Vehicles in use Europe 2018 2018. https://www.acea.be/uploads/statistic_documents/ACEA_Report_Vehicles_in_use-Europe_2018.pdf (accessed April 22, 2020).
[778] Eurostat. Infrastructure - electricity - annual data [nrg_113a] 2018. http://appsso.eurostat.ec.europa.eu/nui/show.do?dataset=nrg_113a (accessed November 1, 2019).
[779] Caglayan D, Heinrichs H, Linßen J, Robinius M, Stolten D. Impact of Different Weather Years on the Design of Hydrogen Supply Pathways for Transport Needs 2019.
[780] Energistyrelsen - Danish Energy Agency (DEA). Energiscenarier frem mod 2020, 2035 og 2050 (full report in danish) 2014.
[781] Energistyrelsen - Danish Energy Agency (DEA). Energy scenarios for 2020, 2035 and 2050 - summary 2014.
[782] National Grid. Future Energy Scenarios 2017 2017.
[783] Ortega JLG, Cantero A. Renewables 2050 - a report on the potential of renewable energies in peninsular spain. Greenpeace 2005.
[784] Jacobson MZ, Delucchi MA, Bauer ZAF, Goodman SC, Chapman WE, Cameron MA, et al. 100% Clean and Renewable Wind, Water, and Sunlight All-Sector Energy Roadmaps for 139 Countries of the World. Joule 2017. doi:10.1016/j.joule.2017.07.005.
[785] Red Eléctrica de España (REE). The Spanish Electricity System 2016 2017.
[786] European Network of Transmission System Operators for Electricity (ENTSO-E). Transparancy platform - load and generation 2017.
[787] Energinet.dk. Production and consumption of electricity data 2014-2017 2017.
[788] Agora Energiewende. Datenpaket 2012-2017 2018.
[789] National Grid. Balancing Data 2017.
[790] Red Eléctrica de España (REE). Temporal analysis generation and consumption. Sist Inf Del Operador Del Sist 2018.

[791] Eurostat. Energy statistics - Energy balances 2017.
[792] Elexon. Elexon Portal 2017.
[793] Réseau de Transport d'Électricité (RTE). RTE customers portal - operational data 2017 2017.
[794] Eurostat. Population on 1 January by age and sex [demo_pjan] - 2015 2017.
[795] Eurostat. Complete energy balances - 2015 [nrg_bal_c] 2017.
[796] StatBank Denmark. Stock of vehicles per 1 January by type of vehicle, region and time - All Denmark - Passenger cars, total - 2014 2017. https://www.statbank.dk/BIL707 (accessed April 23, 2020).
[797] UK Government - Department for Transport. Road traffic estimates in Great Britain: 2015. Natl Stat 2016.
[798] Ministère de la Transition écologique et solidaire - Commissariat général au Développement durable. Comptes transports 2017 - Bilan de la circulation. Les Comptes Des Transp En 2017 – 55e Rapp La Comm Des Comptes Des Transp La Nation 2018.
[799] Nel Hydrogen. Wide Spread Adaption of Competitive Hydrogen Solution, FC Expo 2018 - 14th Int'l Hydrogen & Fuel Cell Expo 2018. http://nelhydrogen.com/assets/uploads/2018/03/2018-03-02-FC-EXPO-Nel_FINAL.pdf (accessed August 28, 2019).
[800] Dow water & process solutions. Reverse Osmosis System Analysis (ROSA) for FILMTECTM membranes, ROSA 9.0.0, ConfigDB u399339_282 2015. https://www.dow.com/en-us/water-and-process-solutions/resources/design-software (accessed August 28, 2019).
[801] Nel Hydrogen. Nel Hydrogen Electrolysers The World's Most Efficient and Reliable Electrolysers. Prod Broch 2020.
[802] Bennoua S, Le Duigou A, Quéméré MM, Dautremont S. Role of hydrogen in resolving electricity grid issues. Int J Hydrogen Energy 2015. doi:10.1016/j.ijhydene.2015.03.137.
[803] Element Energy, Cambridge Econometrics. Fuelling Europe's Future - How the transition from oil strengthens the economy. Eur Clim Found 2018.
[804] Hydrogen Link. NIP Hydrogen Refueling Infrastructure | Denmark National Implementation Plan | 3rd Final edition 2014.
[805] Gas Infrastructure Europe (GIE). GIE Vision 2050 2019. https://www.gie.eu/index.php/gie-media/press-releases/13-news/gie/406-press-release-gas-infrastructure-europe-ready-for-the-green-deal (accessed April 29, 2020).
[806] Hydrogen Europe. Hydrogen Europe Vision on the Role of Hydrogen and Gas Infrastructure on the Road Toward a Climate Neutral Economy – A Contribution to the Transition of the Gas Market 2019.
[807] European Network of Transmission System Operators for Gas (ENTSOG). ENTSOG 2050 Roadmap for Gas Grids 2019.
[808] International Agency Renewable Energy (IRENA). Electric Vehicles: technology brief. Abu Dhabi 2017.
[809] Zero Motorcycles. ZERO MOTORCYCLES – The Electric Motorcycle Company - Official Site 2019.

[810] International Energy Agency (IEA). Global EV Outlook 2019. OECD; 2019. doi:10.1787/35fb60bd-en.
[811] Groupe Renault. Groupe Renault introduces hydrogen into its light commercial vehicles range - Press Kit 2019. https://media.group.renault.com/global/en-gb/groupe-renault/media/pressreleases/21234877/le-groupe-renault-introduit-lhydrogene-dans-sa-gamme-de-vehicules-utilitaires (accessed May 4, 2020).
[812] DHL, Streetscooter, Plugpower. DHL Express & StreetScooter present fuel cell van. Electrive 2019. https://www.electrive.com/2019/05/24/dhl-express-street-scooter-h2-van-with-500km-range/ (accessed May 4, 2020).
[813] Renault Trucks, La Poste. Renault Trucks Corporate - Press releases : The French Post Office and Renault Trucks jointly test a hydrogen-powered truck running on a fuel cell 2015.
[814] Ruf Y, Kaufmann M, Lange S, Heieck F, Endres A, Pfister J. Fuel Cells and Hydrogen Applications for Regions and Cities Vol. 2 - Cost analysis and high-level business case. Rol Berger Fuel Cells Hydrog Jt Undert (FCH2 JU) 2017. https://www.rolandberger.com/publications/publication_pdf/roland_berger_fuel_cell_applications_cost_assessment.pdf (accessed May 4, 2020).
[815] Kane M. Hyundai And H2 Energy To Launch 1,000 Hydrogen Trucks in Switzerland. InsideEVs 2018.
[816] Esoro, Coop, H2 Energy, Powercell, Emoss. The world's first fuel cell heavy goods vehicle able to fulfil Coop's logistics requirements 2017. https://h2energy.ch/wp-content/uploads/2017/06/Brochure-Truck.pdf (accessed May 4, 2020).
[817] Müller KK, Schnitzeler F, Lozanovski A, Skiker S, Ojakovoh M. Clean Hydrogen in European Cities (CHIC) Deliverable No. 5.3 Final Report. Daimler Buses, Air Prod Ned Univ Stuttgart, Elem Energy, 2017.
[818] Reuter B, Faltenbacher M, Schuller O, Whitehouse N, Whitehouse S. New Bus ReFuelling for European Hydrogen Bus Depots - Guidance Document on Large Scale Hydrogen Bus Refuelling. Thinkstep, Fuel Cell Hydrog Jt Undert (FCH JU) 2017.
[819] McKinsey and Company. Urban buses: alternative powertrains for Europe A fact-based analysis of the role of diesel hybrid, hydrogen fuel cell, trolley and battery electric powertrains. Fuel Cell Hydrog Jt Undert (FCH JU) 2012.
[820] Wijtzes S. Fuel cell electric vehicles & hydrogen balancing national 100% renewable integrated transport & energy systems: A scenario analysis for the year 2050. Delft University of Technology, 2017.
[821] Carotenuto A, Figaj RD, Vanoli L. A novel solar-geothermal district heating, cooling and domestic hot water system: Dynamic simulation and energy-economic analysis. Energy 2017. doi:10.1016/j.energy.2017.08.084.
[822] Sayegh MA, Danielewicz J, Nannou T, Miniewicz M, Jadwiszczak P, Piekarska K, et al. Trends of European research and development in district heating technologies. Renew Sustain Energy Rev 2017. doi:10.1016/j.rser.2016.02.023.

[823] European Geothermal Energy Council. Developing geothermal district heating in Europe 2014.
[824] Francisco Pinto J, Carrilho da Graça G. Comparison between geothermal district heating and deep energy refurbishment of residential building districts. Sustain Cities Soc 2018. doi:10.1016/j.scs.2018.01.008.
[825] Möller B, Wiechers E, Persson U, Grundahl L, Lund RS, Mathiesen BV. Heat Roadmap Europe: Towards EU-Wide, local heat supply strategies. Energy 2019. doi:10.1016/j.energy.2019.04.098.
[826] Oprinsen L. The Transition from Natural Gas to 100% Hydrogen in an Existing Distribution Network. Delft Univ Technol 2018.
[827] Hermkes R, Colmer H, Ophoff H. Modern PE pipe enables the transport of hydrogen. Proc 19th Plast Pipes Conf PPXIX, Sept 24-26, 2018, Las Vegas, Nevada 2018. https://www.kiwa.com/globalassets/netherlands/kiwa-technology/downloads/hermkens-et-al---pe-pipes-enable-the-transport-of-hydrogen_ppxix_2018-versie-20180710.pdf (accessed May 5, 2020).
[828] Worcester Bosch. The Future Of Fuel - What the future holds for the UK's mains gas network 2019.
[829] Giacomini. H_2ydroGEM, the hydrogen boiler by Giacomini 2019.
[830] BDR Thermea Group. BDR Thermea Group showcases the world's first hydrogen powered domestic boiler 2019.
[831] Schrier G van der, Besselaar E van den, Schiks C, Verver G. European Climate Assessment & Dataset project. R Netherlands Meteorol Inst 2019.
[832] Day T. TM41: Degree Days: Theory & Application - UK Chartered Institution of Building Services Engineers (CIBSE). London, United Kingdom: CIBSE Publications; 2006.
[833] Ciuffo B, Raposo MA. The future of road transport implications of automated, connected, low-carbon and shared mobility. Eur Comm Jt Res Cent 2019.
[834] International Transport Forum (ITF). ITF Transport Outlook 2019. OECD Publishing; 2019.
[835] National Renewable Energy Laboratory (NREL). H2A analysis, production case studies: current forecourt hydrogen production from PEM electrolysis version 3.101. 2013.
[836] Ekman CK. On the synergy between large electric vehicle fleet and high wind penetration - An analysis of the Danish case. Renew Energy 2011. doi:10.1016/j.renene.2010.08.001.
[837] International Energy Agency (IEA). The Future of Hydrogen, seizing today's opportunities. Paris, France: IEA Publications; 2019.
[838] Wang, Chang, Bai, Liu, Dai, Tang. Mitigation Strategy for Duck Curve in High Photovoltaic Penetration Power System Using Concentrating Solar Power Station. Energies 2019. doi:10.3390/en12183521.
[839] Hou Q, Zhang N, Du E, Miao M, Peng F, Kang C. Probabilistic duck curve in high PV penetration power system: Concept, modeling, and empirical analysis in China. Appl Energy 2019. doi:10.1016/j.apenergy.2019.03.067.
[840] Wang D, Muratori M, Eichman J, Wei M, Saxena S, Zhang C. Quantifying the flexibility of hydrogen production systems to support large-scale

renewable energy integration. J Power Sources 2018. doi:10.1016/j.jpowsour.2018.07.101.
[841] Schoenung SM, Keller JO. Commercial potential for renewable hydrogen in California. Int J Hydrogen Energy 2017. doi:10.1016/j.ijhydene.2017.01.005.
[842] Cheng AJ, Tarroja B, Shaffer B, Samuelsen S. Comparing the emissions benefits of centralized vs. decentralized electric vehicle smart charging approaches: A case study of the year 2030 California electric grid. J Power Sources 2018. doi:10.1016/j.jpowsour.2018.08.092.
[843] Colmenar-Santos A, Muñoz-Gómez AM, Rosales-Asensio E, López-Rey Á. Electric vehicle charging strategy to support renewable energy sources in Europe 2050 low-carbon scenario. Energy 2019. doi:10.1016/j.energy.2019.06.118.
[844] Elnozahy MS, Salama MMA. Technical impacts of grid-connected photovoltaic systems on electrical networks - A review. J Renew Sustain Energy 2013. doi:10.1063/1.4808264.
[845] Obi M, Bass R. Trends and challenges of grid-connected photovoltaic systems - A review. Renew Sustain Energy Rev 2016. doi:10.1016/j.rser.2015.12.289.
[846] Ahmed R, Sreeram V, Mishra Y, Arif MD. A review and evaluation of the state-of-the-art in PV solar power forecasting: Techniques and optimization. Renew Sustain Energy Rev 2020. doi:10.1016/j.rser.2020.109792.
[847] Rahmann C, Mayol C, Haas J. Dynamic control strategy in partially-shaded photovoltaic power plants for improving the frequency of the electricity system. J Clean Prod 2018. doi:10.1016/j.jclepro.2018.07.310.
[848] Barbieri F, Rajakaruna S, Ghosh A. Very short-term photovoltaic power forecasting with cloud modeling: A review. Renew Sustain Energy Rev 2017. doi:10.1016/j.rser.2016.10.068.
[849] Cabrera-Tobar A, Bullich-Massagué E, Aragüés-Peñalba M, Gomis-Bellmunt O. Review of advanced grid requirements for the integration of large scale photovoltaic power plants in the transmission system. Renew Sustain Energy Rev 2016. doi:10.1016/j.rser.2016.05.044.
[850] Nghitevelekwa K, Bansal RC. A review of generation dispatch with large-scale photovoltaic systems. Renew Sustain Energy Rev 2018. doi:10.1016/j.rser.2017.08.035.
[851] Köhler C, Steiner A, Saint-Drenan Y-M, Ernst D, Bergmann-Dick A, Zirkelbach M, et al. Critical weather situations for renewable energies – Part B: Low stratus risk for solar power. Renew Energy 2017;101:794–803. doi:10.1016/j.renene.2016.09.002.
[852] Denholm P, O'Connell M, Brinkman G, Jorgenson J. Overgeneration from Solar Energy in California: A Field Guide to the Duck Chart. Nrel 2015.
[853] Sinden G. Characteristics of the UK wind resource: Long-term patterns and relationship to electricity demand. Energy Policy 2007. doi:10.1016/j.enpol.2005.10.003.
[854] Leahy PG, Foley AM. Wind generation output during cold weather-driven

electricity demand peaks in Ireland. Energy 2012. doi:10.1016/j.energy.2011.07.013.
[855] Steiner A, Köhler C, Metzinger I, Braun A, Zirkelbach M, Ernst D, et al. Critical weather situations for renewable energies – Part A: Cyclone detection for wind power. Renew Energy 2017. doi:10.1016/j.renene.2016.08.013.
[856] Raynaud D, Hingray B, François B, Creutin JD. Energy droughts from variable renewable energy sources in European climates. Renew Energy 2018. doi:10.1016/j.renene.2018.02.130.
[857] Höltinger S, Mikovits C, Schmidt J, Baumgartner J, Arheimer B, Lindström G, et al. The impact of climatic extreme events on the feasibility of fully renewable power systems: A case study for Sweden. Energy 2019. doi:10.1016/j.energy.2019.04.128.
[858] Buttler A, Dinkel F, Franz S, Spliethoff H. Variability of wind and solar power – An assessment of the current situation in the European Union based on the year 2014. Energy 2016. doi:10.1016/j.energy.2016.03.041.
[859] Moral-Carcedo J, Pérez-García J. Integrating long-term economic scenarios into peak load forecasting: An application to Spain. Energy 2017. doi:10.1016/j.energy.2017.08.113.
[860] Moral-Carcedo J, Pérez-García J. Time of day effects of temperature and daylight on short term electricity load. Energy 2019. doi:10.1016/j.energy.2019.02.158.
[861] Sofoklis Makridis. Hydrogen storage and compression. Methane Hydrog. Energy Storage, Institution of Engineering and Technology; 2016, p. 1–28. doi:10.1049/PBPO101E_ch1.
[862] Zakeri B, Syri S. Electrical energy storage systems: A comparative life cycle cost analysis. Renew Sustain Energy Rev 2015;42:569–96. doi:10.1016/j.rser.2014.10.011.
[863] Michalski J, Bünger U, Crotogino F, Donadei S, Schneider G-S, Pregger T, et al. Hydrogen generation by electrolysis and storage in salt caverns: Potentials, economics and systems aspects with regard to the German energy transition. Int J Hydrogen Energy 2017;42:13427–43. doi:10.1016/j.ijhydene.2017.02.102.
[864] Steward D, Saur G, Penev M, Ramsden T. Lifecycle cost analysis of hydrogen versus other technologies for electrical energy storage. Energy Storage Issues Appl., 2011.
[865] Lütkehus I, Salecker H, Adlunger K. Potenzial der Windenergie an Land - Studie zur Ermittlung des bundesweiten Flächen- und Leistungspotenzials der Windenergienutzung an land. Umwelt Bundesamt 2013.
[866] Rose PK, Neumann F. Hydrogen refueling station networks for heavy-duty vehicles in future power systems. Transp Res Part D Transp Environ 2020;83:102358. doi:10.1016/j.trd.2020.102358.
[867] Jensen IG, Wiese F, Bramstoft R, Münster M. Potential role of renewable gas in the transition of electricity and district heating systems. Energy Strateg Rev 2020;27:100446. doi:10.1016/j.esr.2019.100446.
[868] National Grid. Future Energy Scenarios 2019 2019.

[869] Wang A, van der Leun K, Peters D, Buseman M. European Hydrogen Backbone. Guid Enagás, Energinet, Fluxys Belgium, Gasunie, GRTgaz, NET4GAS, OGE, ONTRAS, Snam, Swedegas, Teréga 2020.
[870] Rialland A, Wold KE. Future Studies, Foresight and Scenarios as basis for better strategic decisions. Innov Glob Marit Prod 2020 (IGLO-MP 2020) 2009.
[871] Noel L, Zarazua de Rubens G, Kester J, Sovacool BK. History, Definition, and Status of V2G. Vehicle-to-Grid, Cham: Springer International Publishing; 2019, p. 1–31. doi:10.1007/978-3-030-04864-8_1.
[872] Wipke K, Sprik S, Kurtz J, Ramsden T, Ainscough C, Saur G. National Fuel Cell Electric Vehicle Learning Demonstration Final Report - Technical Report NREL/TP-5600-54860. Natl Renew Energy Lab 2012:2.1.11 Factors Affecting Fuel Cell Durability Figu.
[873] Jacobson MZ, Delucchi MA, Cameron MA, Frew BA. Low-cost solution to the grid reliability problem with 100% penetration of intermittent wind, water, and solar for all purposes. Proc Natl Acad Sci 2015;112:15060–5. doi:10.1073/pnas.1510028112.
[874] Coomans JL. Exploring the operation of a Car Park Power Plant: Formalising the operation of a system innovation with the Actor-Option Framework. TU Delft Repos 2015.
[875] European Automobile Manufacturers Association (ACEA). Vehicles in use Europe - January 2021 2021.
[876] Park Lee EH. A socio-technical exploration of the Car as Power Plant 2019.
[877] Alavi F. Model Predictive Control of fuel-cell-Car-based smart energy systems in the presence of uncertainty 2019.
[878] Fathabadi H. Fuel cell hybrid electric vehicle (FCHEV): Novel fuel cell/SC hybrid power generation system. Energy Convers Manag 2018. doi:10.1016/j.enconman.2017.11.001.
[879] News: Road vehicles: TU Delft team test hydrogen race car on Nürburgring circuit. Fuel Cells Bull 2015. doi:10.1016/s1464-2859(15)30140-1.
[880] Lee EHP, Lukszo Z. Scheduling fuel cell electric vehicles as power plants in a community microgrid. 2016 IEEE PES Innov. Smart Grid Technol. Conf. Eur., 2016, p. 1–6. doi:10.1109/ISGTEurope.2016.7856256.
[881] Eurostat. Population change - Demographic balance and crude rates at regional level (NUTS 3) 2015. http://ec.europa.eu/eurostat/web/products-datasets/-/demo_r_gind3 (accessed August 28, 2019).
[882] Eurostat. Reference Metadata - Population change - Demographic balance and crude rates at regional level (NUTS 3) 2017. http://ec.europa.eu/eurostat/cache/metadata/en/demo_r_gind3_esms.htm (accessed August 28, 2019).
[883] Eurostat. NUTS - Nomenclature of territorial units for statistics Overview 2015. http://ec.europa.eu/eurostat/web/nuts/overview (accessed August 28, 2019).
[884] Peel MC, Finlayson BL, McMahon TA. Updated world map of the Köppen-Geiger climate classification - Supplement. Hydrol Earth Syst Sci 2007;11:1633–44. doi:10.5194/hess-11-1633-2007.

[885] Cunha S, Silva Á, Herráez C, Pires V, Chazarra A, Mestre A, et al. Iberian Climate Atlas Air temperature and precipitation (1971-2000). Madrid, Spain: Agencia Estatal de Metereología (AEMET). Instituto de Meteorologia (IM) de Portugal. Ministerio de Medio Ambiente y Medio Rural y Marino, Gobierno de España.; 2011.
[886] CLIMATE-DATA.org: Hamburg n.d. https://en.climate-data.org/location/69/ (accessed August 28, 2019).
[887] CLIMATE-DATA.org: MURCIA n.d. https://en.climate-data.org/location/3214/ (accessed August 28, 2019).
[888] Deutscher Wetterdienst. Stationsliste der 78 Messstationen (nach Stationsname sortiert) - Hamburg-Fuhlsbüttel - Station ID 1975 2017. ftp://ftp-cdc.dwd.de/pub/CDC/observations_germany/climate/hourly/ (accessed February 14, 2018).
[889] Agencia Estatal de Meteorología (AEMET) - Gobierno de España. El Tiempo. Hoy y últimos días: Murcia - Datos horarios 2018. http://www.aemet.es/es/eltiempo/observacion/ultimosdatos?k=mur&l=7178I (accessed February 14, 2018).
[890] Agencia Estatal de Meteorología (AEMET) - Gobierno de España. Datos historicos horarios meteorologicos Murcia(Murcia) Indicativo climatológico 7178I 2012-2016. Madid, Spain: Agencia Estatal de Meteorología (AEMET); 2017.
[891] Enerdata. Definitions for specific energy indicators and policies | ODYSSEE-MURE 2015. http://www.odyssee-mure.eu/faq/efficiency-indicators-policies-definitions/ (accessed August 28, 2019).
[892] Agencia Estatal de Meteorología (AEMET) - Gobierno de España. Datos historicos horarios meteorologicos Almería Aeropuerto Indicativo climatológico 6325O 2012-2016. Madid, Spain: Agencia Estatal de Meteorología (AEMET); 2017.
[893] Agencia Estatal de Meteorología (AEMET) - Gobierno de España. El Tiempo. Hoy y últimos días: Almería Aeropuerto - Datos horarios 2018. http://www.aemet.es/es/eltiempo/observacion/ultimosdatos?l=6325O (accessed February 14, 2018).
[894] Parra D, Patel MK. Techno-economic implications of the electrolyser technology and size for power-to-gas systems. Int J Hydrogen Energy 2016;41:3748–61. doi:10.1016/j.ijhydene.2015.12.160.
[895] Buttler A, Spliethoff H. Current status of water electrolysis for energy storage, grid balancing and sector coupling via power-to-gas and power-to-liquids: A review. Renew Sustain Energy Rev 2018;82:2440–54. doi:10.1016/j.rser.2017.09.003.
[896] Schmidt O, Gambhir A, Staffell I, Hawkes A, Nelson J, Few S. Future cost and performance of water electrolysis: An expert elicitation study. Int J Hydrogen Energy 2017;42:30470–92. doi:10.1016/j.ijhydene.2017.10.045.
[897] Anvari M, Lohmann G, Wächter M, Milan P, Lorenz E, Heinemann D, et al. Short term fluctuations of wind and solar power systems. New J Phys 2016;18. doi:10.1088/1367-2630/18/6/063027.
[898] Ernst B, Kirby B, Wan Y-H. Short-Term Power Fluctuation of Wind

Turbines : Analyzing Data from the German 250-MW Measurement Program from the Ancillary Services Viewpoint. Golden, CO, USA: National Renewable Energy Laboratory (NREL); 1999.
[899] Wan Y, Bucaneg, D. Short-Term Power Fluctuations of Large Wind Power Plants*. J Sol Energy Eng 2002;124:427–31. doi:10.1115/1.1507762.
[900] Tabar MRR, Anvari M, Lohmann G, Heinemann D, Wächter M, Milan P, et al. Kolmogorov spectrum of renewable wind and solar power fluctuations. Eur Phys J Spec Top 2014;223:2637–44. doi:10.1140/epjst/e2014-02217-8.
[901] Lave M, Reno MJ, Broderick RJ. Characterizing local high-frequency solar variability and its impact to distribution studies. Sol Energy 2015;118:327–37. doi:10.1016/j.solener.2015.05.028.
[902] Hinkelman LM. Differences between along-wind and cross-wind solar irradiance variability on small spatial scales. Sol Energy 2013;88:192–203. doi:10.1016/j.solener.2012.11.011.
[903] Woyte A, Belmans R, Nijs J. Fluctuations in instantaneous clearness index: Analysis and statistics. Sol Energy 2007;81:195–206. doi:10.1016/j.solener.2006.03.001.
[904] McPhy. Electrolyzers for continuous and automated hydrogen production, and/or of large quantity 2018. http://mcphy.com/en/our-products-and-solutions/electrolyzers/large-capacity/ (accessed August 28, 2019).
[905] McPhy. New generation alkaline electrolysis for large-scale platforms (multi MW) 2018. http://mcphy.com/en/our-products-and-solutions/electrolyzers/augmented-mclyzer/ (accessed August 28, 2019).
[906] Gallandat N, Romanowicz K, Züttel A. An Analytical Model for the Electrolyser Performance Derived from Materials Parameters. J Power Energy Eng 2017;05:34–49. doi:10.4236/jpee.2017.510003.
[907] Nel Hydrogen. Electrolyser Product Brochure 2018. http://nelhydrogen.com/assets/uploads/2016/05/Nel-Electrolysers-Brochure-2018-PD-0600-0125-Web.pdf (accessed August 28, 2019).
[908] The Linde Group. Linde raises the bar for hydrogen transport efficiency 2013. https://www.the-linde-group.com/en/news_and_media/press_releases/news_20130925.html (accessed August 28, 2019).
[909] Air Products. Supporting a Growing UK Hydrogen Infrastructure: Air Products' High Pressure Tube Trailer Fleet Expansion and Permanent Fuelling Station Installation 2014. http://www.airproducts.com/Company/news-center/2014/08/0804-air-products-high-pressure-tube-trailer-fleet-expansion-and-permanent-fueling-station.aspx (accessed August 28, 2019).
[910] Elgowainy A, Reddi K, Sutherland E, Joseck F. Tube-trailer consolidation strategy for reducing hydrogen refueling station costs. Int J Hydrogen Energy 2014;39:20197–206. doi:10.1016/j.ijhydene.2014.10.030.
[911] Reddi K, Elgowainy A, Rustagi N, Gupta E. Two-tier pressure consolidation operation method for hydrogen refueling station cost reduction. Int J Hydrogen Energy 2018;43:2919–29. doi:10.1016/j.ijhydene.2017.12.125.
[912] Hong BK, Kim SH. Recent Advances in Fuel Cell Electric Vehicle

Technologies of Hyundai. ECS Trans 2018;86:3–11.
[913] Spinoni J, Vogt J V., Barbosa P, Dosio A, McCormick N, Bigano A, et al. Changes of heating and cooling degree-days in Europe from 1981 to 2100. Int J Climatol 2018;38:e191–208. doi:10.1002/joc.5362.
[914] Kemna R, Acedo JM. Average EU building heat load for HVAC equipment - Final Report of Framework Contract ENER C3 412-2010. Delft, The Netherlands: Van Holsteijn en Kemna B.V., European Commission; 2014.
[915] Traverso M, Donatello S, Moons H, Rodriguez R, Quintero MGC, JRC OW, et al. Revision of the EU Green Public Procurement Criteria for Street Lighting and Traffic Signals. Luxembourg, Luxembourg: Publications Office of the European Union; 2017.
[916] GE Lighting Europe. The Benefits of LED Lighting 2017. http://emea.gelighting.com/LightingWeb/emea/products/technologies/led/lighting/ (accessed August 28, 2019).
[917] Van Heddeghem W, Lambert S, Lannoo B, Colle D, Pickavet M, Demeester P. Trends in worldwide ICT electricity consumption from 2007 to 2012. Comput Commun 2014;50:64–76. doi:10.1016/j.comcom.2014.02.008.
[918] Papachristos G. Household electricity consumption and CO 2 emissions in the Netherlands: A model-based analysis. Energy Build 2015;86:403–14. doi:10.1016/j.enbuild.2014.09.077.
[919] Coroama VC, Hilty LM. Assessing Internet energy intensity: A review of methods and results. Environ Impact Assess Rev 2014;45:63–8. doi:10.1016/j.eiar.2013.12.004.
[920] Gynther L, Lapillone B, Pollier K. Energy efficiency trends and policies in the household and tertiary sectors - An analysis based on the ODYSSEE and MURE databases. Brussels, Belgium: ADEME; 2015.
[921] Liander N.V. Beschikbare data - Dagprofielen gas - G1a 2008. https://www.liander.nl/partners/datadiensten/open-data/data (accessed August 28, 2019).
[922] Liander N.V. Beschikbare data - Dagprofielen gas - G2a 2008. https://www.liander.nl/partners/datadiensten/open-data/data (accessed August 28, 2019).
[923] Vereniging Nederlandse Energie Data Uitwisseling (NEDU). Profielen Elektriciteit 2017 - E1A 2017. http://www.nedu.nl/documenten/verbruiksprofielen/ (accessed August 28, 2019).
[924] Vereniging Nederlandse Energie Data Uitwisseling (NEDU). Profielen Elektriciteit 2017 - E3A 2017. https://www.nedu.nl/documenten/verbruiksprofielen/ (accessed August 29, 2019).
[925] Lorenzo E. Energy Collected and Delivered by PV Modules. In: Luque A, Hegedus S, editors. Handb. Photovolt. Sci. Eng., Chichester, UK: John Wiley & Sons, Ltd; 2011, p. 984–1042. doi:10.1002/9780470974704.ch22.
[926] Diaf S, Notton G, Belhamel M, Haddadi M, Louche A. Design and techno-economical optimization for hybrid PV/wind system under various meteorological conditions. Appl Energy 2008;85:968–87.

doi:10.1016/j.apenergy.2008.02.012.
[927] Green MA, Emery K, Hishikawa Y, Warta W, Dunlop ED. Solar cell efficiency tables (version 47). Prog Photovoltaics Res Appl 2016;24:3–11. doi:10.1002/pip.2728.
[928] Dierauf T, Growitz A, Kurtz S, Hansen C. Weather-Corrected Performance Ratio - NREL Technical Report NREL/TP-5200-57991. Golden, CO, USA: National Renewable Energy Laboratory (NREL); 2013.
[929] European Comission. Photovoltaic Geographical Information System (PVGIS) - Interactive tools 2017. http://re.jrc.ec.europa.eu/pvg_tools/en/tools.html#PVP (accessed August 28, 2019).
[930] Swart RJ, Coppens C, Gordijn H, Piek M, Ruyssenaars P, Schrander JJ, et al. Europe's onshore and offshore wind energy potential - European Environment Agency. Luxembourg, Luxembourg: Office for Official Publications of the European Communities; 2009. doi:10.2800/11373.
[931] Wever N. Quantifying trends in surface roughness and the effect on surface wind speed observations. J Geophys Res Atmos 2012;117. doi:10.1029/2011JD017118.
[932] Hu K, Chen Y. Technological growth of fuel efficiency in european automobile market 1975–2015. Energy Policy 2016;98:142–8. doi:10.1016/j.enpol.2016.08.024.
[933] European Commission. European Commission, Energy, Data & analysis, Weekly Oil Bulletin - Prices over time - 2005 onwards 2017. http://ec.europa.eu/energy/observatory/reports/Oil_Bulletin_Prices_History.xlsx (accessed August 28, 2019).
[934] Eurostat. Electricity prices for household consumers - bi-annual data [nrg_pc_204] 2017. http://appsso.eurostat.ec.europa.eu/nui/show.do?dataset=nrg_pc_204 (accessed August 28, 2019).
[935] Eurostat. Gas prices for household consumers - bi-annual data [nrg_pc_202] 2017. http://appsso.eurostat.ec.europa.eu/nui/show.do?dataset=nrg_pc_202 (accessed August 28, 2019).
[936] International Renewable Energy Agency (IRENA). Renewable Power Generation Costs in 2017. Abu Dhabi, United Arab Emirates: International Renewable Energy Agency (IRENA); 2018.
[937] International Renewable Energy Agency (IRENA). The Power to Change: Solar and Wind Cost Reduction Potential to 2025. Abu Dhabi, United Arab Emirates: International Renewable Energy Agency (IRENA); 2016.
[938] van Wijk AJM, Hellinga C. Hydrogen - the key to the energy transition. Circ – Neemt Dat Al Een Vlucht? n.d. http://profadvanwijk.com/wp-content/uploads/2018/05/Technical-Report-Hydrogen-the-key-to-the-energy-transition.pdf (accessed August 28, 2019).
[939] Feng Z. Vessel design and fabrication technology for stationary high-pressure hydrogen storage – FY 2016 annual progress report DOE hydrogen and fuel cells program 2016.

https://www.hydrogen.energy.gov/pdfs/review16/pd109_feng_2016_o.pdf (accessed August 28, 2019).
[940] Borup R, More K, Weber A. FC-PAD: Fuel Cell Performance and Durability Consortium. Los Alamos, NM, USA: Los Alamos National Laboratory (LANL); 2018.

List of publications

Oldenbroek, V., Wijtzes, S., Blok, K., & van Wijk, A. J. (2021). Fuel cell electric vehicles and hydrogen balancing 100 percent renewable and integrated national transportation and energy systems. Energy Conversion and Management: X, 9, 100077.

Oldenbroek, V., Smink, G., Salet, T., & van Wijk, A. J. (2020). Fuel cell electric vehicle as a power plant: Techno-economic scenario analysis of a renewable integrated transportation and energy system for smart cities in two climates. Applied Sciences, 10(1), 143.

Farahani, S. S., van der Veen, R., **Oldenbroek, V.**, Alavi, F., Lee, E. H. P., van de Wouw, N., ... & Lukszo, Z. (2019). A hydrogen-based integrated energy and transport system: The design and analysis of the car as power plant concept. IEEE Systems, Man, and Cybernetics Magazine, 5(1), 37-50.

Oldenbroek, V., Hamoen, V., Alva, S., Robledo, C. B., Verhoef, L. A., & van Wijk, A. J. M. (2018). Fuel Cell Electric Vehicle-to-Grid: Experimental Feasibility and Operational Performance as Balancing Power Plant. Fuel Cells, 18(5), 649-662.

Robledo, C. B., **Oldenbroek, V.**, Abbruzzese, F., & van Wijk, A. J. (2018). Integrating a hydrogen fuel cell electric vehicle with vehicle-to-grid technology, photovoltaic power and a residential building. Applied energy, 215, 615-629.

Oldenbroek, V., Wijtzes, S., van Wijk, A., & Blok, K. (2017). Fuel cell electric vehicle to grid & H2: Balancing national electricity, heating & transport systems a scenario analysis for Germany in the year 2050. In 2017 IEEE Green Energy and Smart Systems Conference (IGESSC) (pp. 1-6). IEEE.

Oldenbroek, V., Verhoef, L. A., & Van Wijk, A. J. (2017). Fuel cell electric vehicle as a power plant: Fully renewable integrated transport and energy system design and analysis for smart city areas. International Journal of Hydrogen Energy, 42(12), 8166-8196.

Oldenbroek, V., Alva, S., Pyman, B., Buning, L. B., Veenhuizen, P. A., & Van Wijk, A. J. M. (2017). Hyundai ix35 fuel cell electric vehicles: Degradation analysis for driving and vehicle-to-grid usage. In 30th International Electric Vehicle Symposium and Exhibition, EVS 2017 (p. 136982). Landesmesse Stuttgart GmbH.

V. Oldenbroek, L. Nordin, A.J.M. van Wijk (2017). Fuel cell electric vehicle-to-grid: emergency and balancing power for a 100% renewable hospital. 6th European PEFCF & Electrolyser Forum 2017, Lucerne, Switzerland.

Thattai, A. T., **Oldenbroek, V.**, Schoenmakers, L., Woudstra, T., & Aravind, P. V. (2017). Towards retrofitting integrated gasification combined cycle (IGCC) power

plants with solid oxide fuel cells (SOFC) and CO2 capture–A thermodynamic case study. Applied thermal engineering, 114, 170-185.
Thattai, A. T., **Oldenbroek, V.**, Schoenmakers, L., Woudstra, T., & Aravind, P. V. (2016). Experimental model validation and thermodynamic assessment on high percentage (up to 70%) biomass co-gasification at the 253 MWe integrated gasification combined cycle power plant in Buggenum, The Netherlands. Applied energy, 168, 381-393.

J. Boere, **V. Oldenbroek**, A.J.M. van Wijk, F. Oesterholt (2016). The role of water in the hydrogen economy. IWA World Water Congress & Exhibition 2016, Brisbane, Australia.

Promes, E. J. O., Woudstra, T., Schoenmakers, L., **Oldenbroek, V.**, Thattai, A. T., & Aravind, P. V. (2015). Thermodynamic evaluation and experimental validation of 253 MW Integrated Coal Gasification Combined Cycle power plant in Buggenum, Netherlands. Applied Energy, 155, 181-194.

N. Chrysochoidis-Antsos, A.J.M. van Wijk, **V. Oldenbroek**, F. Bisschop (2015). The wind energy potential along highways to fuel a sustainable transport sector. 2015 EWEA Annual Conference and Exhibition, Paris, France.

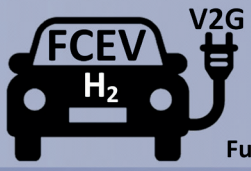

Hydrogen (H_2)
Vehicle to Grid (V2G)
Fuel Cell Electric Vehicle (FCEV)

This thesis presents the design and analysis of future 100% renewable integrated transport and energy systems based on electricity and hydrogen as energy carriers. Passenger cars in Europe are parked on average 97% of the time. So passenger car Fuel Cell Electric Vehicles (FCEVs) can be used for energy balancing and electricity generation when parked and connected to the electricity grid, in the so-called Vehicle-to-Grid (V2G) mode. In Europe around 15.3 million passenger vehicles were sold in 2019. Using the “Our Car as Power Plant” analogy of Van Wijk et al., multiplying each vehicle by 100 kW of future installed electric power in it, this would equal to 1,530 GW of annual sold power capacity in passenger vehicles. This is more than the existing 950 GW installed power generation capacity in Europe in 2019. The goal of this research is to explore the techno-economic potential of hydrogen, FCEVs and V2G in achieving affordable, reliable, scalable and 100% renewable integrated transport and energy systems. In this thesis an experimental, proof of principle approach, is presented to understand and to analyze the current available FCEV and V2G technologies and their limitations. For a European context, 100% renewable integrated transport and energy systems are designed. A hospital, a smart city and 5 countries, having aggregation levels from 500 up to more than 20 million FCEVs.

ISBN 978-94-6384-241-9
9 789463 842419